

# Stereochemistry of Optically Active Transition Metal Compounds



# Stereochemistry of Optically Active Transition Metal Compounds

**Bodie E. Douglas**, EDITOR

*University of Pittsburgh*

**Yoshihiko Saito**, EDITOR

*University of Tokyo*

Based on a symposium  
sponsored by the Division  
of Inorganic Chemistry at  
the ACS/CSJ Chemical  
Congress, Honolulu, Hawaii,  
April 2–6, 1979.

A C S   S Y M P O S I U M   S E R I E S **119**

AMERICAN CHEMICAL SOCIETY  
WASHINGTON, D. C.      1980



Library of Congress  $\square$  Data

Stereochemistry of optically active transition metal compounds.

(ACS Symposium series; 119 ISSN 0097-6156)

Includes bibliographies and index.

1. Stereochemistry—Congresses. 2. Transition metal compounds—Congresses.

I. Douglas, Bodie Eugene, 1924- . II. Saito, Yoshiko, 1920- . III. American Chemical Society. Division of Inorganic Chemistry. IV. Series: American Chemical Society. ACS symposium series; 119.

QD481.S76 541.2'23 80-10816  
ISBN 0-8412-0538-8 ACSMC8 119 1-446 1980

Copyright © 1980

American Chemical Society

All Rights Reserved. The appearance of the code at the bottom of the first page of each article in this volume indicates the copyright owner's consent that reprographic copies of the article may be made for personal or internal use or for the personal or internal use of specific clients. This consent is given on the condition, however, that the copier pay the stated per copy fee through the Copyright Clearance Center, Inc. for copying beyond that permitted by Sections 107 or 108 of the U.S. Copyright Law. This consent does not extend to copying or transmission by any means—graphic or electronic—for any other purpose, such as for general distribution, for advertising or promotional purposes, for creating new collective works, for resale, or for information storage and retrieval systems.

The citation of trade names and/or names of manufacturers in this publication is not to be construed as an endorsement or as approval by ACS of the commercial products or services referenced herein; nor should the mere reference herein to any drawing, specification, chemical process, or other data be regarded as a license or as a conveyance of any right or permission, to the holder, reader, or any other person or corporation, to manufacture, reproduce, use, or sell any patented invention or copyrighted work that may in any way be related thereto.

PRINTED IN THE UNITED STATES OF AMERICA  
**American Chemical  
Society Library**

1155 16th St. N. W.

In Stereochemistry of Optically Active Transition Metal Compounds; Douglas, B., et al.;  
ACS Symposium Series; American Chemical Society: Washington, DC, 1980.

Washington, D. C. 20036

# ACS Symposium Series

**M. Joan Comstock**, *Series Editor*

## *Advisory Board*

|                     |                     |
|---------------------|---------------------|
| David L. Allara     | W. Jeffrey Howe     |
| Kenneth B. Bischoff | James D. Idol, Jr.  |
| Donald G. Crosby    | James P. Lodge      |
| Donald D. Dollberg  | Leon Petrakis       |
| Robert E. Feeney    | F. Sherwood Rowland |
| Jack Halpern        | Alan C. Sartorelli  |
| Brian M. Harney     | Raymond B. Seymour  |
| Robert A. Hofstader | Gunter Zweig        |

## FOREWORD

The ACS SYMPOSIUM SERIES was founded in 1974 to provide a medium for publishing symposia quickly in book form. The format of the Series parallels that of the continuing ADVANCES IN CHEMISTRY SERIES except that in order to save time the papers are not typeset but are reproduced as they are submitted by the authors in camera-ready form. Papers are reviewed under the supervision of the Editors with the assistance of the Series Advisory Board and are selected to maintain the integrity of the symposia; however, verbatim reproductions of previously published papers are not accepted. Both reviews and reports of research are acceptable since symposia may embrace both types of presentation.

## PREFACE

Alfred Werner used the classical approach to prove his intuitive ideas concerning the stereochemistry of coordination compounds. After Werner's death there was little interest in inorganic stereochemistry for a long period. One of the groups which helped to revive interest in this field and to keep it active for many years was that of John C. Bailar, Jr. at the University of Illinois. We are pleased that he consented to write Chapter 1, for this volume as a personal account of his years in research. It is particularly appropriate since he was honored at the ACS/CSJ Meeting in Hawaii in observance of his 75th birthday.

Optical activity was very important in finally convincing Werner's critics of his theories concerning the stereochemistry of coordination compounds. The study of these optically active compounds has yielded increasingly detailed stereochemical information with improvements in theory and instrumentation and a significant increase in the research effort. The developments in ligand field theory, theories of optical activity, the classical Corey-Bailar paper (*see* Chapter 1, Ref. 26) on conformational effects, and the establishment of absolute configurations for a large number of metal complexes (*see* Chapter 2) have been important in stimulating the development of the stereochemistry of metal complexes.

Major activities in the study of inorganic stereochemistry are now spread throughout the world. The first joint ACS/CSJ Chemical Congress in Hawaii provided an opportunity to bring together many active investigators from the United States, Japan, and Australia. It has been 25 years since the absolute configuration of the first metal complex was determined; the contributions to this symposium are representative of the achievements in this field since that time.

The volume begins with some historical background, the opening lectures of the original symposium, and an invited paper on organometallic chemistry. Stereochemical assignments depend on definitive x-ray work and this work provides a basis for linking theory to experiment. Important new theoretical developments should aid our understanding of and stimulate new work in the study of optically active metal compounds. The stereochemical bases for stereoselectivity in square planar and octahedral complexes and in asymmetric hydrogenation are presented as well as other aspects of synthesis and stereoselectivity. Bioinorganic topics include microbial iron transport compounds and metal ion interactions with azoproteins. Various contributions to CD spectra and the effect of

solvent on the spectra are considered. Photoacoustic detection of CD and stereochemical description and notation also are discussed and should be instructive for workers in the field. The volume is representative of current work in the stereochemistry of optically active compounds of transition metals.

We acknowledge the splendid cooperation of the contributors to the symposium and to this volume. Their efforts and those of the ACS Books Department staff in helping to publish the book soon after the symposium were crucial. We hope that this work will be useful to those active in the field and in arousing further interest in inorganic stereochemistry and its applications.

YOSHIHIKO SAITO  
University of Tokyo  
Tokyo 106, Japan  
January 15, 1980

BODIE E. DOUGLAS  
University of Pittsburgh  
Pittsburgh, PA 15260



## Research in the Stereochemistry of Cobalt Complexes

JOHN C. BAILAR, JR.

School of Chemical Sciences, University of Illinois, Urbana, IL 61801

Stereochemistry, long the backbone of coordination chemistry, is still a major area for investigation and discovery. The methods of studying it have changed, and perhaps because of that, the emphasis on the topics under investigation has changed. Synthetic chemistry has been displaced by, or better, augmented by, physical methods. Both approaches are important and both contribute to the growth of our knowledge. It is most appropriate that we should hold a symposium on the stereochemistry of complexes and compare notes on what is being done in the countries which are represented at this meeting. In introducing the symposium, I should like to recount some developments of the nearly fifty years that I have been involved in this field. Most of the work which I shall describe was done by my students -- not that I think that their work is better than that of others, but because I know it better, and it serves to illustrate some interesting aspects of what I think of as the synthetic approach. Space alone would preclude discussing any more.

My entrance into the field of inorganic stereochemistry was brought about in an unusual way. As an organic chemist, my interest lay chiefly in isomerism and isomeric rearrangements. One day in a class in general chemistry which I was teaching, there was a discussion of the hydrolysis of antimony trichloride, which leads to the precipitation of the oxychloride,  $\text{SbOCl}$ . One of the students referred to this as "antimony hypochlorite". While I was correcting his impression that "OCl" always represents a hypochlorite, it occurred to me that the hypochlorite of a metal in the +1 oxidation state would be isomeric with the oxychloride of that metal in the +3 state. This was the first time I had ever imagined that inorganic compounds could exist in isomeric forms, and it was an exciting idea. That very day, I began efforts to prepare the two isomers of  $\text{TlOCl}$ , only to discover that thallos hypochlorite cannot exist, for the cation is easily oxidized and the anion is a strong oxidizing agent. However, the idea of inorganic isomers persisted and my thinking and reading soon led to the postulation of many other cases; for example,

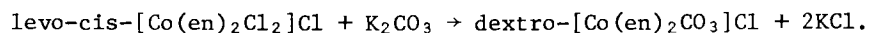
selonosulfate and thioselenate, phosphonium nitrate and ammonium metaphosphate and hydroxylamine nitrite and ammonium nitrate. Of course, one cannot go very far in looking for isomers in inorganic chemistry without discovering the whole, rich field of coordination compounds. And if one can have isomeric rearrangements in organic molecules, why not in the complexes of cobalt, too? It was thus that I became an inorganic chemist.

The stereochemistry of coordination compounds was a part of chemical thinking much earlier than is generally assumed. For example, as early as 1875, van Hoff suggested that compounds containing six groups attached to a central metal atom are at the corners of an octahedron and that geometric isomers should exist for suitably substituted cases (1). However, it was Alfred Werner who demonstrated that this is indeed the case, and also that the four covalent platinum(II) compounds are coplanar. In those early days, the multitude of sophisticated techniques which we now enjoy was not known, and deductions as to structure had to be made mostly on the basis of synthesis and other chemical evidence. Progress was slow, for this kind of structure determination requires a great deal of imagination and more experimental work than determination of structure by modern methods.

Consider, for example, Werner's ingenious determination of the structures of cis- and trans-[Pt(NH<sub>3</sub>)<sub>2</sub>Cl<sub>2</sub>] (2), and his demonstration of the octahedral structure of six-coordinate complexes through the optical resolution of [Co(en)<sub>2</sub>(NH<sub>3</sub>)X]<sup>2+</sup> (X = Cl, Br) (3). We are now able, by modern techniques, not only to perform these demonstrations quickly, but, in the case of chiral complexes, to show the actual configurations of the isomers (4,5).

After Werner's death in 1919, there was little activity in the field of stereochemistry of coordination compounds. An exception is found in the work of Yuji Shibata, who had been one of Werner's students, and who continued with excellent stereochemical work when he returned to Japan. His work on the enzyme-like activity of cobalt complexes furnishes especially interesting examples of stereoselectivity and of the catalytic action of such compounds (6). T. P. McCutcheon and V. L. King, Americans who had done their theses on stereochemical topics under Werner's guidance, did not continue in that field. King, who actually performed the first resolution of an asymmetric complex (7), went into industrial work. McCutcheon became a member of the faculty at the University of Pennsylvania and did research on complex compounds, but not on their stereochemistry.

In a long paper which he published in 1912 (8), Werner described many cis-trans rearrangements which cobalt(III) compounds undergo during replacement reactions. He also described some reactions of optically active complexes, which give optically active products, such as the one shown by the equation

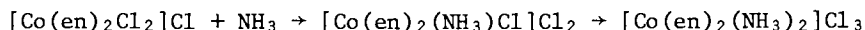


He had no way of knowing whether this reaction involved an inversion of configuration, but on the basis of such studies, he suggested a mechanism for the famous Walden inversion of organic chemistry, postulating that the central atom of a chiral molecule exerts a directive influence.

Some years later, Robert Auten, an undergraduate student at the University of Illinois, achieved an optical inversion in the reaction just mentioned (9). Patterning his work on that of Walden, Auten used silver carbonate instead of potassium carbonate and obtained a levo-rotatory carbonato complex. It was soon found that the choice of carbonate is not the important factor, and Dwyer, Sargeson and Reid, in Australia, showed that the pH of the solution is the deciding factor (10). After his initial success, Auten looked for inversions in the reactions of the dichloro complex with oxalate and nitrite, but did not find them. It is most fortunate that he tried the carbonate reaction first, for otherwise, we would have concluded that optical inversions do not take place in the reactions of cobalt complexes, and probably would not have tried carbonate.

Werner's directions for the resolution of the dichloro complex are very simple and quite specific, but when Auten repeated them, he obtained no crystals of the diastereo isomer at all. Several trials all gave negative results. Upon reflection, Auten realized that laboratories in Europe are not heated as much as ours in America, so he repeated Werner's directions with the solution cooled to 16°. This gave an excellent yield of pure product. Every chemist knows that sometimes repetition of another's work does not give good results; many do not understand, however, that the difficulty may lie in a minor change in conditions.

It was soon found that an inversion takes place also in the reaction



the configuration of the final product depending upon the temperature at which the reaction takes place (11). This seems to be a somewhat more complicated reaction than the one with carbonate, for it proceeds in two distinctly visible steps with sharp changes in color, and in each step the product may have the original configuration, the mirror image one, or the trans configuration. The rotations observed for the diammine were very small, but were confirmed by observations made by several different people and even by secretly having the observers check the same sample repeatedly. The results are shown in Table I.

Table I.  
Reaction of Ammonia with *levo*-[Co(en)<sub>2</sub>Cl<sub>2</sub>]Cl to yield  
[Co(en)<sub>2</sub>(NH<sub>3</sub>)<sub>2</sub>]Cl<sub>3</sub>

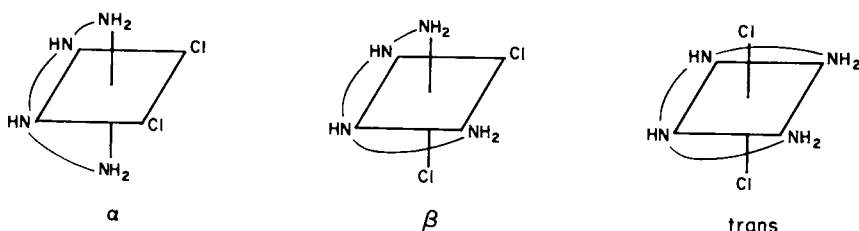
| Reagent                           | Temperature | Ratio cis/trans<br>in product | [α] <sub>D</sub> |
|-----------------------------------|-------------|-------------------------------|------------------|
| Liquid NH <sub>3</sub> (solution) | -77°        | 2.5/1                         | -32°             |
| Liquid NH <sub>3</sub> (solution) | -38°        | 2.85/1                        | -22°             |
| Liquid NH <sub>3</sub> (solution) | +25°        | 3.7/1                         | +18°             |
| Gaseous NH <sub>3</sub>           | +80°        | ∞                             | +38°             |

In the reaction at 80°, the complex remained solid throughout the reaction. Evidently very little rearrangement of any sort took place, for the value of [α]<sub>D</sub> for an authentic sample of dextro [Co(en)<sub>2</sub>(NH<sub>3</sub>)<sub>2</sub>]Cl<sub>3</sub> was +50°. The discovery of inversion in this reaction was somewhat surprising, even to the investigators, for it had been assumed that the two steps would follow the same mechanism, so that any inversion that took place in the first step would be counterbalanced by an inversion in the second. However, Earl Greenwood was not able to get an inversion in the reaction (12)



so it was assumed that inversion takes place only in the replacement of the first chloro group. Ronald Archer later showed that this is, indeed, the case (13).

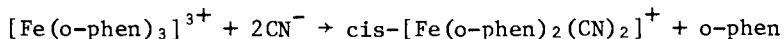
Closely related to this is the much later work of Eishin Kyuno and Laurence Boucher (14), who studied the reactions of the triethylenetetramine complex, [Co(trien)Cl<sub>2</sub>]Cl. The complex cation of this substance exists in three stereoisomeric forms



both the  $\alpha$  and  $\beta$  forms being asymmetric and resolvable. Treatment with base converts the *dextro*- $\alpha$ -form into its *levo*- $\beta$ -isomer.

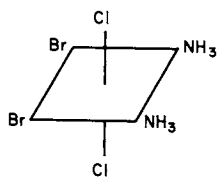
We once thought that all of these rearrangements result from the abstraction of a proton from a coordinated amine and the motion of the resulting negatively charged amine group from

one corner of the octahedron to an adjacent one. This may not be the case, however, for Archer and his students at the University of Massachusetts have observed an inversion in a reaction of an octahedral complex in which there are no acidic protons (15).

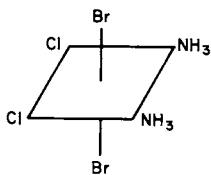


Another stereochemical problem concerns the preparation of octahedral complexes of known configuration.

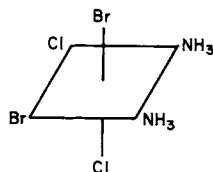
The Russian chemists, who are masters in the manipulation of platinum complexes, have done interesting work in this area. For example, Chernyaev and Krasovskaya (16) prepared all five isomers of  $[\text{Pt}(\text{NH}_3)_2\text{Cl}_2\text{Br}_2]$ :



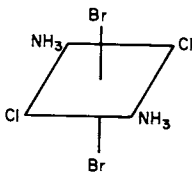
I



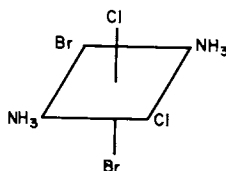
II



III

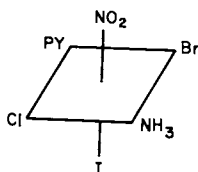


IV



V

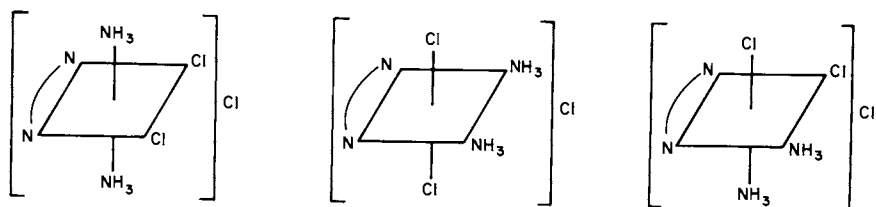
Dr. Anna Gel'man (now usually transliterated as Hel'man) and her colleagues have also done elegant work of this type and have succeeded in making the compound



I

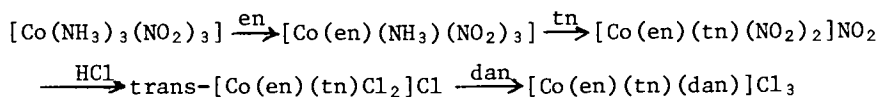
in which the position of each group is firmly established (17). This substance is chiral, but evidently no attempt has been made to resolve it. Platinum lends itself readily to these involved syntheses, for the trans effect in the reactions of planar platinum(II) complexes allows the preparation of isomers which offer good starting places for the formation of the desired octahedral platinum(IV) compounds. It is unfortunate that Dr. Hel'man has not continued her very interesting research on the synthesis of compounds containing a multiplicity of unidentate groups, for it is excellent work. For some years now she has been involved in the chemistry of actinide elements.

The preparation of three isomers of  $[\text{Co}(\text{en})(\text{NH}_3)_2\text{Cl}_2]\text{Cl}$  by Peppard (18), I think, ranks in importance with those just mentioned.



In these syntheses, Peppard had to rely on the very weak trans effect in the cobalt complex  $[\text{Co}(\text{NH}_3)_4(\text{SO}_3)_2]^-$ . The *cis*-dichloro-*cis*-diammineethylenediaminecobalt(III) ion is asymmetric, and Peppard partially resolved it into its enantiomeric forms by adsorption on quartz ground to 100 mesh. This method of resolution is frequently, but not always, effective. Before it can be fully utilized, we will need to learn a great deal more about the principles of adsorption. The preparation of Peppard's isomer's is particularly interesting because cobalt(III) complexes rearrange easily, whereas the platinum compounds do not.

Another case involving cobalt complexes was studied by Work (19), who prepared, among others, a compound containing three different bidentate amines--ethylenediamine, trimethylenediamine, and neopentanediamine,  $[\text{Co}(\text{en})(\text{tn})(\text{dan})]\text{Cl}_3$ , by following and extending a synthesis first described by Werner (20):



The last step was accomplished through the catalytic influence of decolorizing carbon, a method first used by Bjerrum (21) and developed by Work (22). Doubtless, this synthesis now could

be performed more easily through the elegant tris-carbonato method developed by Mori and his colleagues (23).

A great deal could be learned by further synthetic studies of unusual complexes of platinum and cobalt, as well as other metals, but the syntheses are long and multistep and few chemists have the patience to attempt them. Knowledge gained by work on the complexes of one metal can be used only indirectly in studies of another; the chemistries of the complexes of cobalt(III) and chromium(III), for example, are quite different, although these substances closely resemble each other in physical properties.

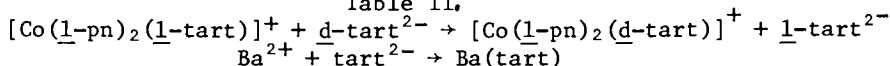
Another topic of interest in the stereochemistry of coordination compounds is that of stereoselective reactions. The first case of this was discovered by Tschugaeff (Chugaev) and Sokoloff in 1907 (24). They prepared the tris-1,2-propanediamine-cobalt(III) complex from racemic propylenediamine and found that the ions obtained contained molecules of only the levo- or only the dextro- base, and that the presence of these in the complex forced an overall asymmetry upon it. Thus, they obtained [D111] and [Lddd] complexes, where the capital letters represent the rotation of the complexes, and the small letters, the rotation of the molecules of coordinated base. Many people have worked in this field since, and a good deal has been learned. Dwyer, Sargeson, and members of their groups have been particularly productive in this field. The subject was discussed in detail by Jaeger (25), who prepared tris-(trans-1,2-cyclopentanediamine) rhodium(III) and cobalt(III) ions, and found that, using the racemic base, only two of the possible isomers, (D111 and Lddd), were formed in each case. Even if only one or two molecules of the optically active base were used along with a symmetrical base, as in  $[\text{Co}(\text{en})_2(\text{cptdin})]^{3+}$  and  $[\text{Co}(\text{en})(\text{cptdin})_2]^{3+}$ , a stereoselective effect was observed. Likewise, efforts to prepare trans- $[\text{Co}(\text{l-cptdin})(\text{d-cptdin})\text{Cl}_2]^+$  were without avail. Jaeger was of the opinion that this stereospecificity was dependent upon the symmetry of the complexes--the more symmetrical the molecule, the greater its stability. It is now generally agreed, however, that the formation of some isomers in preference to others depends upon the conformations of the chelate rings. This concept is largely due to Professor E. J. Corey (26).

The complexes of propylenediamine (1,2-propanediamine) offer a somewhat more complicated picture than those of trans-cyclopentanediamine, for the propylenediamine molecule not only contains an asymmetric carbon atom, but is also unsymmetrical. Werner reported the isolation of all eight of the possible isomers of cis- $[\text{Co}(\text{en})(\text{pn})(\text{NO}_2)_2]^+$ , and this was supported by the work of Cooley and Liu (27), who obtained four isomers of cis- $[\text{Co}(\text{en})(2,3\text{-bn})(\text{NO}_2)_2]^+$  and four cis- $[\text{Co}(\text{en})(\text{iso-bn})(\text{NO}_2)_2]^+$ . (2,3-bn = racemic  $\text{NH}_2\text{CH}(\text{CH}_3)\text{CH}(\text{CH}_3)\text{NH}_2$ ; iso-bn =  $\text{NH}_2\text{C}(\text{CH}_3)_2\text{CH}_2\text{NH}_2$ ). The isomers containing 2,3-butylenediamine proved to be of unequal stability--in fact, in the early experiments, only three

isomers were obtained, and, to isolate the fourth, the experiment had to be repeated, using milder conditions.

In the early belief that these reactions were completely stereospecific, we felt that the reaction of  $[\text{Co}(\underline{1}\text{-pn})_2\text{Cl}_2]^+$  with carbonate could not give an optical inversion under any experimental conditions. This is, of course, not true, as was soon shown by the work of McReynolds (28) and Sister Mary Martinette Hagan (29). In a cobalt complex containing asymmetric ligands, one form is preferred, but both forms can and do exist. In the same belief, we hoped that stereospecific effects could be used in the resolution of racemic potential ligands. This does give partial resolution, as shown by the work of Johnson (30), Jonassen and Gott (31,32) and Hamilton (33). Hamilton's results, shown in Table II, indicate this clearly.

Table II.



| Time of Standing<br>with $\text{Ba}^{2+}$ (hours) | Yield of<br>Ba tart (g) | $[\alpha]_D$ of Recovered<br>Tartaric Acid |
|---|-------------------------|--|
| 0   | 4.7                     | $-6^\circ$                                 |
| 0.2   | 1.5                     | $0^\circ$                                  |
| 0.5   | 0.6                     | $+7.5^\circ$                               |
| 2   | 0.9                     | $+7.5^\circ$                               |
| 4   | 1.6                     | $+7.5^\circ$                               |
| 18  | 0.5                     | $+12^\circ$                                |
| 72  | 0.2                     | $+10^\circ$                                |
| 10.0<br>(theoretical)                             |                         |  |

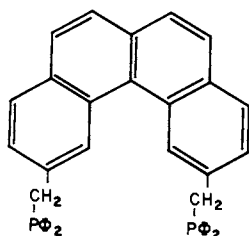
He treated  $[\text{Co}(\underline{1}\text{-pn})_2\text{CO}_3]\text{Cl}$  with a 100% excess of racemic tartaric acid to form the complex  $[\text{Co}(\underline{1}\text{-pn})_2\text{tart}]^+$ . The addition of an excess of barium hydroxide to the solution gave an immediate precipitate of barium tartrate which was removed from the solution, and which was shown to contain an excess of  $\underline{1}$ -tartrate. The filtrate, upon standing, gave more precipitate, which was removed at intervals, and was found to contain tartrate of varying rotatory power, but always dextro. Attempts to improve the stereoselectivity by using very bulky asymmetric ligands, such as phenylethylenediamine, have not improved the situation (34).

The first stereoselective syntheses of coordination compounds were performed by Jonassen and Huffman (35) who treated  $[\text{Co}(\text{en})_2\text{CO}_3]^+$  with  $\underline{d}$ -tartaric acid. This gave a mixture of D- and L- $[\text{Co}(\text{en})_2\underline{d}\text{-tart}]^+$ , which, upon treatment with ethylenediamine at  $50^\circ$ , gave a 70% yield of D- $[\text{Co}(\text{en})_3]^{3+}$ . Either the two tartrato isomers were formed in unequal amounts, or the less

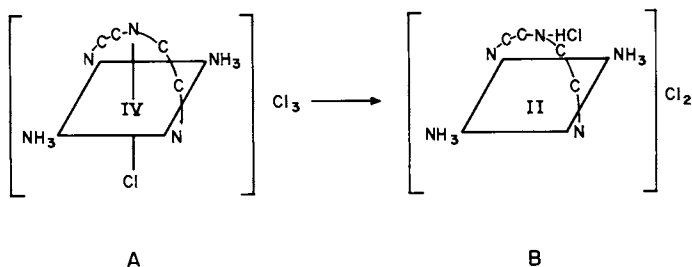


stable one was converted to the more stable one during the reaction with ethylenediamine. Similarly, treatment of the mixed tartrato complexes with hydrochloric acid or with calcium nitrite gave a preponderance of dextro-rotatory-cis-[Co(en)<sub>2</sub>Cl<sub>2</sub>]<sup>+</sup> or dextro-rotatory-cis-[Co(en)<sub>2</sub>(NO<sub>2</sub>)<sub>2</sub>]<sup>+</sup>, respectively.

One other topic should be mentioned--the synthesis of complexes in which a chelating ligand spans trans positions. Werner assumed that a chelating ligand must occupy cis- positions in a complex and for ordinary ligands this is certainly correct. However, several investigators have presented evidence that under some conditions a single chelating group can reach across the trans- positions of a planar complex. Schlesinger (36), and Isslieb and Hohlfield (37) used bidentate ligands which were long enough to reach across the diagonal of a square planar complex of Cu(II) or Ni(II). Venanzi and his students (38,39) synthesized a rigid ligand which can easily adapt itself to the diagonal of a platinum(II) square, but not to the edge:

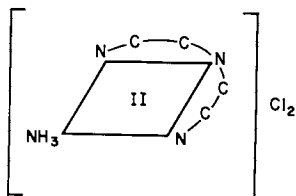


Mattern and Mochida (40) used quite a different approach, attaching a tridentate amine to platinum(IV) and then destroying the bond between the metal and the nitrogen atom in the center of the tridentate ligand by reducing the metal to platinum(II), thus lowering the coordination number from six to four.



Before the experiment was tried, there was no assurance in anyone's mind that the desired bonds would break when the metal was reduced, but it was hoped that the trans effect of the chloride and the secondary nature of the central amine nitrogen

would loosen those atoms from the metal. Happily, that is what occurred. On repeated crystallization from water, the reduced product lost ammonia and chloride, yielding



Compound B, in boiling hypochloric acid, was converted to trans-dichlorodiamine platinum(II). Efforts to place a trans-spanning chelate on each side of the platinum plane have not yet succeeded (41).

There is certainly no dearth of interesting and significant stereochemical problems awaiting solution. Many fundamental questions remain to be answered. Also, the growth of bioinorganic chemistry, the use of metal complexes in cancer chemotherapy, and the widespread concern over pollution have opened up areas which will keep all of us busy for many years to come.

#### Literature Cited

1. van't Hoff, J. H. Maandblad voor Natuurwetenschappen, 1895, 6, 37.
2. Werner, A. Z. anorg. Chem., 1893, 3, 310.
3. Werner, A. Ber., 1911, 44, 1887.
4. Saito, Yoshihiko. Topics in Stereochemistry, Volume 10, pages 95-174, Ernest L. Eliel and Norman L. Allinger, Eds. John Wiley and Sons, New York (1978).
5. Igi, Kozo; Douglas, Bodie E. J. Coordination Chem., 1978, 7, 155-161 and many other earlier articles in the series by Douglas and his students.
6. Shibata, Y.; Yamasaki, Kazuo. J. Chem. Soc. Japan, 1933, 54, 1207, and several preceding articles.
7. King, V. L. J. Chem. Educ., 1942, 19, 345.
8. Werner, Alfred. Ann., 1912, 386, 1.
9. Bailar, John C., Jr.; Auten, Robert W. J. Am. Chem. Soc., 1934, 56, 774.
10. Dwyer, Francis P.; Sargeson, Alan M.; Reid, Ian K. J. Am. Chem. Soc., 1963, 85, 1215.
11. Bailar, John C., Jr.; Haslam, John H.; Jones, Eldon M. J. Am. Chem. Soc., 1936, 58, 2226.
12. Greenwood, Earl L., B. S. Thesis, University of Illinois, 1936.

13. Archer, Ronald D.; Bailar, John C., Jr. J. Am. Chem. Soc., 1961, 83, 812.
14. Kyuno, Eishin; Boucher, L. J.; Bailar, John C., Jr. J. Am. Chem. Soc., 1965, 87, 4458.
15. Archer, Ronald D.; Suydam, L. Jill; Dollberg, Donald D. J. Am. Chem. Soc., 1971, 93, 6837.
16. Chernyaev, I. I.; Krasovskaya, N. N. Russian J. Inorg. Chem., 1959, 4, 455 (in English).
17. Gel'man, A. D.; Essen, L. N. Doklady Akad. Nauk. S.S.S.R., 1950, 75, 693; C. A., 1951, 45, 3279h.
18. Bailar, John C., Jr.; Peppard, D. F. J. Am. Chem. Soc., 1940, 62, 105.
19. Bailar, John C., Jr.; Work, J. B. J. Am. Chem. Soc., 1946, 68, 232.
20. Werner, Alfred. Helv. Chim. Acta, 1918, 1, 10.
21. Bjerrum, J. "Metal Amine Formation in Aqueous Solutions. Theory of Reversible Step Reactions"; P. Hasse and Son: Copenhagen, Denmark, 1941.
22. Bailar, John C., Jr.; Work, J. B. J. Am. Chem. Soc., 1945, 67, 176.
23. Mori, M.; Shibata, M.; Kyuno, E.; Adachi, T. Bull. Chem. Soc. Japan, 1956, 29, 883. See also a review by Shibata, Muraji Proc. Japan Acad., 1974, 50, 779 and the references therein; Bauer, H. F.; Drinkard, W. C. J. Am. Chem. Soc., 1960, 82, 5031.
24. Tschugaeff, L.; Sokoloff, W. Ber., 1907, 40, 177; 1909, 42, 55.
25. Jaeger, F. M. "Optical Activity and High Temperature Measurements"; McGraw-Hill: New York, 1930. This contains references to similar work by Lifschitz and by Smirnoff.
26. Corey, E. J.; Bailar, John C., Jr. J. Am. Chem. Soc., 1959, 81, 2620.
27. Cooley, William E.; Liu, Chui-Fan; Bailar, John C., Jr. J. Am. Chem. Soc., 1959, 81, 4189.
28. Bailar, John C., Jr.; McReynolds, J. P. J. Am. Chem. Soc., 1939, 61, 3199.
29. Sister Mary Martinette, B.V.M.; Bailar, John C., Jr. J. Am. Chem. Soc., 1952, 74, 1054.
30. Johnson, Roy D., Thesis, University of Illinois, 1948.
31. Jonassen, H. B.; Bailar, John C., Jr.; Gott, A. D. J. Am. Chem. Soc., 1952, 74, 3131.
32. Gott, A. D.; Bailar, John C., Jr. Ibid., 1952, 74, 4820.
33. Hamilton, Nathan, Thesis, University of Illinois, 1947.
34. Hryhorczuk, Lew, Thesis, University of Illinois, 1972.
35. Jonassen, Hans B.; Bailar, John C., Jr.; Huffman, E. H. J. Am. Chem. Soc., 1948, 70, 756.
36. Schlessinger, N. Ber., 1925, 58, 1877.
37. Isslieb, K.; Hohlfield, G. Z. anorg. allgem. Chem., 1961, 312, 169.

38. Stefano, N. J.; Johnson, D. K.; Lane, R. M.; Venanzi, L. M. Abst. American Chem. Soc. Meeting (Boston, Mass., April 9-14, 1972) INOR 150.
39. Stefano, N. J.; Johnson, D. K.; Venanzi, L. M. Angew. Chem., Int. Ed. Eng., 1974, 13, 133.
40. Mochida, Isao; Mattern, J. Arthur; Bailar, John C., Jr. J. Am. Chem. Soc., 1975, 97, 3021.
41. Fry, Fred; Bailar, John C., Jr.; unpublished work.

RECEIVED September 11, 1979.

# Absolute Configuration of Transition Metal Complexes

YOSHIHIKO SAITO

The Institute for Solid State Physics, The University of Tokyo, Tokyo, Japan

In this paper an overview will be given on the structural studies of optically active transition metal complexes and their interaction with other fields in coordination chemistry. A quarter of a century has passed away since the first determination of the absolute configuration of a transition metal complex,  $[\text{Co}(\text{en})_3]^{3+}$ , was carried out by anomalous scattering of X-rays (1). Since that time the number of transition metal complexes whose absolute configuration have been determined by X-ray method has been growing at an increasing rate and at this time it has exceeded 130. In addition to this, numerous optically active organometallic compounds have been studied and their absolute configurations established.

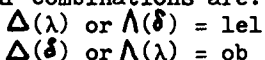
At an early stage of the development, the structural information was rather fragmentary. Nowadays, however, the accumulation of structural data for isomers has enabled us to understand structural principles and the optical properties of chelate complexes in considerable detail. In this connection, column chromatography on SP Sephadex has played an important role in the separation of isomers of coordination compounds (2). In view of the large number of structures, a few basic series of structures will be taken up and discussed.

Among the transition metal complexes, the tris(diamine)metal system, particularly tris(ethylenediamine)cobalt(III) and its analogues, has been studied most extensively from both experimental and theoretical sides.

## Five-Membered Chelate Rings

The cause of the isomerism exhibited by this system may be characterized briefly as a combination of configurational and conformational isomerism, the latter arising from non-planarity of metal-ethylenediamine chelate ring. According to IUPAC nomenclature (3), the designation of the configurational chirality is based upon the edges of the octahedron spanned by the chelate rings. Any two such edges form a pair of skew lines describing a

screw of the same handedness because of the presence of a three-fold axis. The configurational chirality is designated by  $\Lambda$  (left-handed screw) or  $\Delta$  (right-handed screw). The designation of conformation is also based upon the principle of a pair of skew lines. For ethylenediamine one of these lines is defined by the two chelating nitrogen atoms and the other by the two carbon atoms in the chelate ring. This is used to characterize the conformational chirality  $\delta$  (right-handed) or  $\lambda$  (left-handed). The concepts symbolized by  $\Delta$ ,  $\Lambda$  and  $\delta$ ,  $\lambda$  are invariant under proper rotations but are converted into the other under improper rotations. The combination of these symbols, however, gives rise to a characterization of the chelate ring which is chirality invariant. This characterization which is relevant when discussing the complex of unknown absolute configuration, or the conformational energy, is designated by  $lel$  and  $ob$  as proposed by Corey and Bailar (4). Here, the symbols  $lel$  and  $ob$  (parallel and oblique) refer to the direction of the bond between the carbon atoms of the chelate ring relative to the threefold axis defined by the three edges of the octahedron spanned by the ligands. For example,  $\Delta(\lambda)$  means a  $\lambda$  conformation associated with a configuration  $\Delta$  and this is  $lel$ . All the four combinations are:



There are eight possible isomers in the  $[M(en)_3]$  system. They comprise two catoptric series:  $lel_3$ ,  $lel_2ob$ ,  $lelob_2$  and  $ob_3$  with  $\Delta$  and  $\Lambda$  absolute configurations, respectively. Crystal structures have been determined for a number of  $[Co(en)_3]^{3+}$  and  $[Cr(en)_3]^{3+}$  salts. The  $lel_3$  isomers are most frequently recognized in these structures. Table I lists examples of conformers of  $[Co(en)_3]^{3+}$  and  $[Cr(en)_3]^{3+}$  other than  $lel_3$ . It seems that

Table I Compounds containing complex cations with conformations other than  $lel_3$

| Compound                             | Conformation                             | Refs. |
|--------------------------------------|--|-------|
| $[Co(en)_3][SnCl_3]Cl_2$             | $lel_2ob$                                | (5)   |
| $[Co(en)_3][Pb_2Cl_9]Cl \cdot 3H_2O$ | $lel_2ob$                                | (6)   |
| $[Cr(en)_3][Ni(CN)_5] \cdot 1.5H_2O$ | $lel_2ob$ , $lelob_2$                    | (7)   |
| $(-)_589[Cr(en)_3](SCN)_3$           | $lelob_2$                                | (8)   |
| $[Cr(en)_3][Co(CN)_6] \cdot 6H_2O$   | $ob_3$                                   | (9)   |
| $(+)_589[Cr(en)_3]Cl_3 \cdot 2H_2O$  | $lel_3$ , $lel_2$ (60% $lel$ +40% $ob$ ) | (10)  |
| $[Cr(en)_3](SCN)_3 \cdot 0.75H_2O$   | $lel_2$ (70% $lel$ +30% $ob$ )           | (11)  |

the conformers other than  $lel_3$  appear more frequently in Cr(III) complexes than in Co(III) complexes. X-ray evidence always indicates that such isomers are favored because they allow more hydrogen bonding in the crystal. In  $(+)_589-\Lambda-[Cr(en)_3]Cl_3 \cdot 2H_2O$ ,

one of the three chelate rings exhibits conformational disorder and its conformation can be represented as 60%  $\delta$  + 40%  $\lambda$ . In the case of  $[\text{Cr}(\text{en})_3](\text{SCN})_3 \cdot 0.75\text{H}_2\text{O}$  the disorder vanishes and the conformation changes to  $\lambda$  on lowering the temperature to 133K, whereby the unit cell volume contracts by 2.7%, reflecting the more compact  $\lambda$  conformers, but no change is observed in the packing mode (12). Though to less extent, similar conformational disorder was recently detected in crystals of (+)<sub>589</sub>-(3,3'-dimethyl-2,2'-bipyridine)bis(ethylenediamine)cobalt(III) chloride diperchlorate monohydrate. The absolute configuration can be designated as  $\Lambda$ ( $\delta$ -dmbpy,  $\delta$ , 90%  $\lambda$  + 10%  $\delta$ ) (13). In crystals of (+)<sub>589</sub>- $[\text{Co}(\text{en})_3]\text{Cl}_2 \cdot \text{H}_2\text{O}$ , the carbon atoms of the chelate ring that is most loosely packed, appear to oscillate with large amplitudes nearly perpendicular to the C=C bond (14). NMR spectra indicated that the ligands in  $[\text{Co}(\text{en})_3]^{3+}$  undergo rapid inversion between  $\delta$  and  $\lambda$  conformation in solution (15). The barriers to  $\delta \rightleftharpoons \lambda$  interconversion for the five-membered chelate ring in  $[\text{Cr}(\text{CO})_4(\text{Me}_4\text{en})]$ , where  $\text{Me}_4\text{en}$  stands for N,N,N',N'-tetramethylethylenediamine, was determined to be of the order of 39 kJ mol<sup>-1</sup> from a band shape analysis of <sup>13</sup>C NMR spectra of the compound (16). Table II lists the observed geometries of the complex ions,  $[\text{Co}(\text{en})_3]^{3+}$  and  $[\text{Cr}(\text{en})_3]^{3+}$ , together with the result of strain energy minimization (17).

Table II Geometries of the complex ion  $[\text{M}(\text{en})_3]^{3+}$ 

| M        | M-N     | N-C   | C-C   | N-M-N | M-N-C | N-C-C |
|----------|---------|-------|-------|-------|-------|-------|
| Co*      | 1.973 Å | 1.486 | 1.509 | 85.3° | 109.1 | 107.4 |
| Cr**     | 2.067   | 1.493 | 1.514 | 82.9  | 109.6 | 107.9 |
| calc.*** | 2.018   | 1.475 | 1.541 | 86.6  | 106.7 | 107.7 |

\* Average of 13 structures

\*\* Average of six structures

\*\*\* Calculated by strain energy minimization

The Co-N bond is shorter by about 0.1 Å than the Cr-N bond and the N-Co-N angle is greater by 2.3° than the N-Cr-N angle. No appreciable change is observed in the geometry of the coordinated ethylenediamine molecule. The distortion of the  $[\text{MN}_6]$  octahedron in  $[\text{Cr}(\text{en})_3]^{3+}$  is slightly more marked than in the cobalt analogue. Both octahedra are slightly compressed and twisted. The twist angle  $\omega$ , which is zero for a trigonal prismatic and 60° for a regular octahedral arrangement is 55° for  $[\text{Co}(\text{en})_3]^{3+}$  and 53.5° for  $[\text{Cr}(\text{en})_3]^{3+}$ .

In 1959, Corey and Bailar assessed the stabilities of  $[\text{Co}(\text{en})_3]^{3+}$  isomers for the first time by conformational analysis, and calculated that the  $\lambda$  isomer is more stable by 7.6 kJ mol<sup>-1</sup> than the  $\delta$  isomer on the basis of calculation of non-bonded H...H interactions (4). Following this pioneering work, the stability of the M(en) ring was studied by mapping of strain energy

surfaces (18, 19, 20). It turned out that the strain energy is extremely sensitive to the kind of non-bonded potential function. Thus various non-bonded potential functions were evaluated. Recently Niketić and Rasmussen used a fast convergent energy minimization program to calculate equilibrium conformations of  $[M(en)_3]$  conformers (17). Table III shows the strain energies of the four conformers and the calculated equilibrium geometries of the  $lel_3$  isomers are included in Table II.

Table III Strain energies for  $[M(en)_3]$  conformers

|                   | $lel_3$ | $lel_2ob$ | $lelob_2$ | $ob_3$                     |
|-------------------|---------|-----------|-----------|----------------------------|
| Strain energy     | 7.16    | 9.84      | 11.93     | 11.91 kJ mol <sup>-1</sup> |
| Energy difference | 0.00    | 2.68      | 4.77      | 4.75                       |

As seen from Table II, the observed geometries of the complex ions are well reproduced by the selected force field, however, the minimized C-N distances are a little too short and C-C much too long, the M-N-C angle is too small. This is because their force field was originally developed to reproduce the early crystal structure determinations in which the contribution of the hydrogen atoms was neglected (21).

When *trans*-1,2-diaminocyclohexane molecules coordinate to the cobalt atom, the resulting five-membered chelate ring can not exhibit puckering motion owing to fusion with the cyclohexane ring in a chair conformation. All eight possible isomers of  $[Co(\pm chxn)_3]^{3+}$  ions were separated and characterized (22). The absolute configurations of all the isomers have been established by the X-ray method ( $lel_3$ , 23;  $lel_2ob$ , 24;  $lelob_2$ , 25;  $ob_3$ , 26). Figure 1 shows a perspective drawing of  $(-)_589[Co(+chxn)_2(-chxn)]^{3+}$  ion. Two of the C-C bonds in the chelate rings are inclined at a mean angle of 3.9° with respect to the pseudo three-fold axis of the complex ion, while the remaining one is at an angle of 64.4°. Thus the complex ion takes the  $lel_2ob$  conformation.

The energy difference between the  $lel_3$ - and  $ob_3$ -isomers of  $[Co(en)_3]^{3+}$  has not been determined experimentally yet. The difference between  $(-)_589-lel_3$ - and  $(+)_589-ob_3-[Co(R-pn)]^{3+}$  has been determined to be 6.7 kJ mol<sup>-1</sup> (27) and 6.73 kJ mol<sup>-1</sup> (28). Schäffer and his collaborators examined the tris[(+)-*trans*-1,2-diaminocyclohexane]cobalt(III) system (22). Equilibrium between the isomers was established by the presence of charcoal as catalyst at 393K. The equilibrium mixture was separated by column chromatography on a Sephadex ion exchange column and the formation ratios were determined. On the other hand, equilibrium geometries of the four conformers,  $lel_3$ ,  $lel_2ob$ ,  $lelob_2$  and  $ob_3$ , were calculated by Boyd's procedure (29, 30). The strain energies are shown in Table IV. The values do not differ very much from those for



Table IV Strain energies for  $[\text{Co}(\pm\text{chxn})_3]^{3+}$  conformers

|                     | lel <sub>3</sub> | lel <sub>2</sub> ob | lelob <sub>2</sub> | ob <sub>3</sub> |                      |
|---------------------|------------------|---------------------|--------------------|-----------------|----------------------|
| Total strain energy | 67.21            | 69.47               | 71.68              | 72.27           | kJ mol <sup>-1</sup> |
| Energy difference   | 0.00             | 2.26                | 4.65               | 5.06            |                      |
|                     | 0.00             | 0.93                | 3.72               | 8.20*           |                      |

\*Experimental values

$[\text{Co}(\text{en})_3]^{3+}$  conformers, indicating that the presence of the fused cyclohexane ring does not affect the energy differences between the conformers very much. Figure 2 shows a plot of the logarithm of formation percentage vs. minimized strain energy. As can be seen from the figure, a roughly linear relationship exists, suggesting that formation percentages are controlled largely thermodynamically. In constructing this plot, the formation percentage of lel<sub>2</sub>ob and lelob<sub>2</sub> has been divided by 3 to take the statistical factor<sup>2</sup> into account. The calculated strain energies indicate that the preference for the lel conformation is caused largely by N-H...H-C interactions.

The eight isomers of  $[\text{Cr}(\pm\text{chxn})_2]^{3+}$  have also been isolated (31). The absolute configurations were correlated through the X-ray powder patterns of the active racemate containing analogous Co(III) complexes of known absolute configuration.

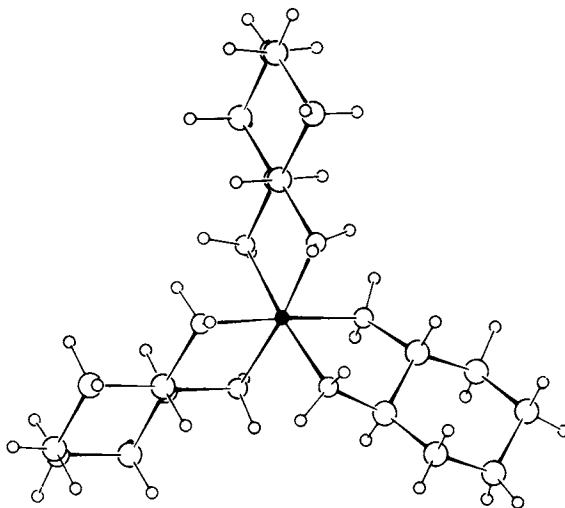
### Six-membered Chelate Rings

Three conformations are possible for a six-membered metal trimethylenediamine ring:

- i) rigid chair form with mirror symmetry
- ii) twist boat form with a twofold axis of rotation
- iii) boat form with mirror symmetry

The twist boat form is chiral and there are two enantiomeric conformations. The chirality can be defined in the same way as a cobalt-ethylenediamine ring and designated as  $\delta$  and  $\lambda$ . The third form, a boat form cannot be accommodated to form a tris(bidentate) complex and, in fact, such a structure has not yet been reported. Niketić and Woldbye showed that there exist 16 possible conformers of the  $[\text{M}(\text{tn})_3]$  system for each of the absolute configurations  $\Delta$  and  $\Lambda$ , in which they adopt the three stable configurations: chair and  $\delta$ - and  $\lambda$ -skew boat forms (32).

(-)<sup>589</sup> $[\text{Co}(\text{tn})_3]^{3+}$  takes the C<sub>3</sub>-chair<sub>3</sub> conformation and its absolute configuration is  $\Lambda$  (33, 34). The shape and the size of the three chelate rings are not exactly identical but differ significantly. The six-membered chelate ring is flexible and is easily deformed by packing forces in the crystal lattice. In one of the chelate rings that is most loosely packed the carbon atoms



Acta Crystallographica

Figure 1. A perspective drawing of the complex ion  $(-)_589\text{-}[\text{Co}(+\text{chxn})_2(-\text{chxn})]^{3+}$  (24)

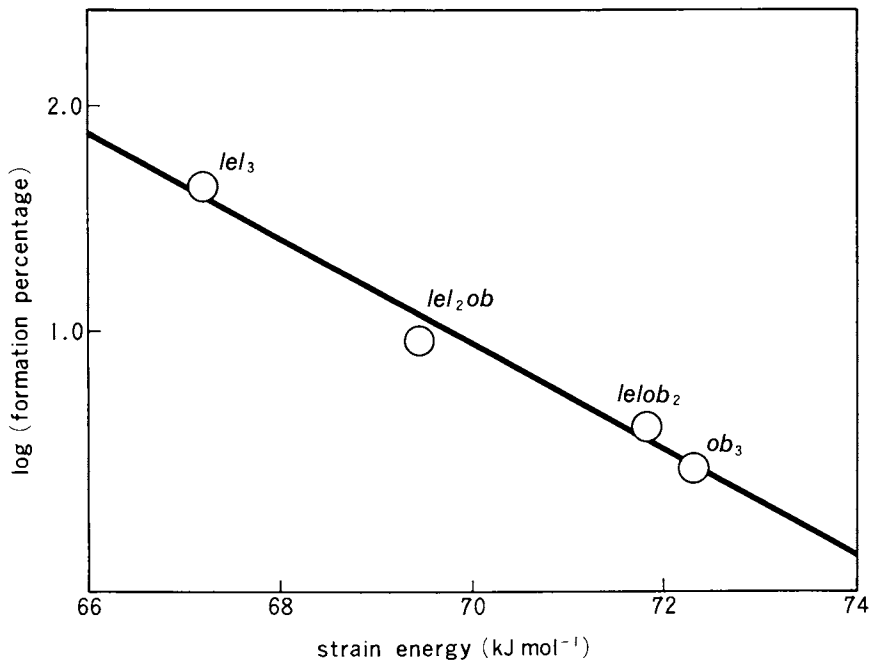


Figure 2. A plot of log of formation percentage vs. minimized strain energy for the  $[\text{Co}(\pm\text{chxn})_3]^{3+}$  system

exhibit much greater thermal motion relative to those in other chelate rings, reflecting the flexibility of the six-membered chelate rings. In crystals of  $[\text{Cr}(\text{tn})_3][\text{Ni}(\text{CN})_5] \cdot 2\text{H}_2\text{O}$  the complex cation takes the syn-chair<sub>2</sub>-1el conformation [ $\Lambda^7(\text{apd}^2)$  and its enantiomer] (35). Recent calculations by consistent force field technique indicated that the C<sub>2</sub>-chair<sub>2</sub> conformer represents the global minimum, supporting the flexibility of the chelate ring. The syn-chair<sub>2</sub>-1el conformer is higher in energy by 10.9 kJ mol<sup>-1</sup>. The observed shape and size of the complex ion,  $[\text{Co}(\text{tn})_3]^{3+}$  can be well reproduced by the strain energy minimization (36).

There are three isomers of 2,4-diaminopentane: R,R, S,S, and R,S. When this molecule forms a six-membered chelate ring, the equatorial preference of the substituted methyl groups fixes the conformation of the chelate ring as follows:

R,S-ptn : chair  
 R,R-ptn : λ-twist-boat  
 S,S-ptn : δ-twist-boat.

The absolute configuration of the 1el<sub>2</sub>- and ob<sub>2</sub>-isomers of  $[\text{Co}(\text{R,R-ptn})_3]^{3+}$  are already known [ $(-)$ <sub>546</sub> 1el<sub>2</sub>- $[\text{Co}(\text{R,R-ptn})_3]^{3+}$ , (37);  $(+)$ <sub>546</sub> ob<sub>2</sub>- $[\text{Co}(\text{R,R-ptn})_3]^{3+}$ , (38)]. There are two possible geometric isomers for  $[\text{Co}(\text{R,S-ptn})_3]^{3+}$ : fac-(C<sub>2</sub>-chair<sub>2</sub>) and mer-(C<sub>2</sub>-chair<sub>2</sub>) forms. The two isomers were separated and resolved into optical isomers (39). The crystal structure of  $(+)$ <sub>589</sub>  $[\text{Co}(\text{R,S-ptn})_3][\text{Co}(\text{CN})_6] \cdot 5\text{H}_2\text{O}$ , the isomer which gave crystals suitable for X-ray work, was determined (40). Figure 3 shows the absolute configuration of the complex ion,  $(+)$ <sub>589</sub>  $[\text{Co}(\text{R,S-ptn})_3]^{3+}$ . This is the facial isomer and the three chelate rings take the chair conformation with the substituted methyl groups in equatorial positions. No unusually large thermal motion of the ring carbon atoms was observed.

The circular dichroism spectra in the region of the first absorption band of the tris-bidentate complex ions having six-membered chelate rings are known to be particularly sensitive to experimental conditions. For example, the CD spectrum of Δ-1el<sub>2</sub>- $[\text{Co}(\text{R,R-ptn})_3]\text{Cl}_3$  in an aqueous solution shows two peaks: Δε<sub>3</sub> = -0.589, 522 nm; Δε = +0.104, 462.5 nm, whereas that of Δ-1el<sub>2</sub>- $[\text{Co}(\text{R,R-ptn})_3](\text{ClO}_4)_3$  in an aqueous solution gives a negative peak (Δε = -0.587)<sub>4</sub> at 518 nm (41). The solid state CD differ from the solution CD and the solution CD are sensitive to the temperature of measurement and are affected by the presence of oxo anions (42, 43, 44). Table V lists the lowest frequency CD spectra of tris-diamine cobalt(III) complexes in the CT region. All the absolute configurations have been established by the X-ray method. Unlike the CD spectra in the first absorption region, those in the CT region are insensitive to the conditions of the measurement described above.

Using all of the recorded CD data for tris-diamine cobalt(III) complexes of known absolute configuration, an empirical rule relating the absolute configuration to CD spectra of tris-diamine cobalt(III) complexes in the charge-transfer region was estab-

Table V The lowest frequency CD band of tris-diamine cobalt(III) complexes in the CT region

|  | $\times 10^3 \text{ cm}^{-1}$ |       | Absolute configuration |
|--|-------------------------------|-------|------------------------|
| (+) $_{589}\text{-[Co(en)}_3\text{]}^{3+}$       | 47.4                          | -31   | $\wedge$ ( <u>45</u> ) |
| (+) $_{589}\text{-[Co(R,R-chxn)}_3\text{]}^{3+}$ | 44.1                          | +48   | $\Delta$ ( <u>22</u> ) |
| (-) $_{589}\text{-[Co(S,S-chxn)}_3\text{]}^{3+}$ | 43.9                          | +17   | $\Delta$ ( <u>22</u> ) |
| (-) $_{589}\text{-[Co(tn)}_3\text{]}^{3+}$       | 40.0                          | -13   | $\wedge$ ( <u>46</u> ) |
| (-) $_{589}\text{-[Co(S-bn)}_3\text{]}^{3+}$     | 40.2                          | -12   | $\wedge$ ( <u>47</u> ) |
| (+) $_{589}\text{-[Co(R,S-ptn)}_3\text{]}^{3+}$  | 39.4                          | -8.7  | $\wedge$ ( <u>48</u> ) |
| (+) $_{546}\text{-[Co(R,R-ptn)}_3\text{]}^{3+}$  | 42.0                          | +6.5  | $\wedge$ ( <u>46</u> ) |
| (-) $_{546}\text{-[Co(R,R-ptn)}_3\text{]}^{3+}$  | 42.2                          | +18   | $\Delta$ ( <u>46</u> ) |
| (-) $_{589}\text{-[Co(tmd)}_3\text{]}^{3+}$      | 43.5                          | -26.2 | $\wedge$ ( <u>49</u> ) |

lished: a tris(diamine)cobalt(III) complex whose sign of the lowest-frequency CD band in the charge-transfer region is negative has absolute configuration  $\wedge$ ; if it is positive, the absolute configuration is  $\Delta$ . In the case of (+)  $_{546}\text{-[Co(R,R-ptn)}_3\text{]}^{3+}$ , the empirical rule is violated, because the positive CD contribution of the optically active ligand itself is superposed in this region.

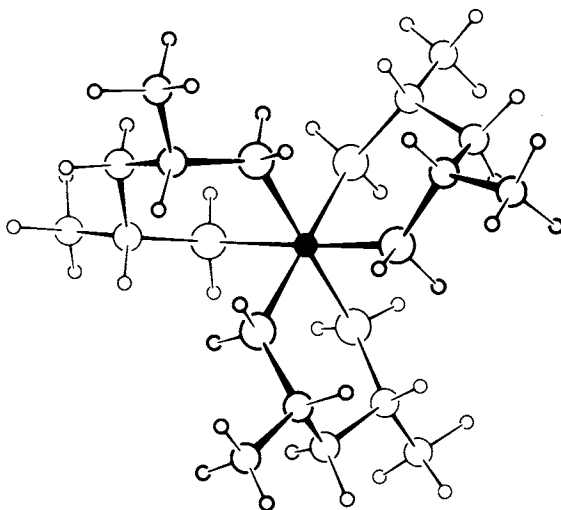
### Seven-Membered Chelate Rings

Only a small number of structures containing seven-membered chelate rings are known (50, 51). Tris(1,4-diaminobutane)cobalt(III) ion is a third member of a basic series of structures:  $[\text{Co}\{\text{H}_2\text{N}-(\text{CH}_2)_n\text{-NH}_2\}_3]^{3+}$ , ( $n=1, 2, 3\dots$ ). This complex ion has seven-membered chelate rings. Figure 4 shows the absolute configuration of (+)  $_{589}\text{-[Co(tmd)}_3\text{]}^{3+}$ . It has  $D_3$  symmetry. Table VI

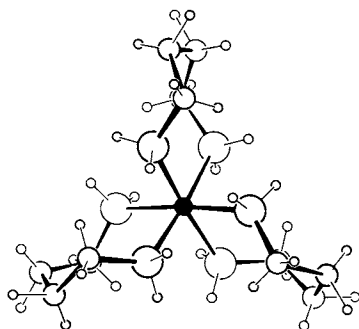
Table VI Geometry of the chelate ring in  $[\text{Co(tmd)}_3]^{3+}$

|          | obs.      | calc. $\text{\AA}$ |
|----------|-----------|--------------------|
| Co-N     | 1.991(5)  | 2.004 $\text{\AA}$ |
| N-C      | 1.506(11) | 1.515              |
| C-C      | 1.512(13) | 1.527              |
| N-Co-N   | 89.2(2)   | 88.4 $^\circ$      |
| Co-N-C   | 122.9(3)  | 120.4              |
| N-C-C    | 113.6(5)  | 113.3              |
| C-C-C    | 111.6(6)  | 113.7              |
| Co-N-C-C | 96.2      | 101.1              |
| N-C-C-C  | 75.9      | 79.0               |
| C-C-C-C  | 56.3      | 56.1               |

compares the observed and calculated geometries of the complex ion

*Acta Crystallographica*

*Figure 3. A perspective drawing of the complex ion  $(+)_{S89}\text{-fac-}[\text{Co}(\text{R,S-ptn})_3]^{3+}$  (40)*

*Acta Crystallographica*

*Figure 4. A perspective drawing of the complex ion  $(+)_{S89}\text{-}[\text{Co}(\text{tmd})_3]^{3+}$  (51)*

(29). The chelate ring takes on a skew conformation and it is strained: all the bond angles in the chelate ring are greater than the normal tetrahedral angle. The minimized structure agrees reasonably well with the observation. The chelate ring is chiral and the conformation can be designated as  $\lambda$  provided that the helicity is defined by the line joining nitrogen atoms and the line joining the two carbon atoms next to the nitrogen atoms. The central C-C bond in the chelate ring is inclined by about  $0.6^\circ$  with respect to the threefold axis of the complex ion. Hence this is the  $1\lambda_3$  isomer and the absolute configuration is  $\Delta(\lambda\lambda\lambda)$ . A marked difference in the geometry of this complex ion from that of  $[\text{Co}(\text{en})_3]^{3+}$  is that three of the six methylene groups bonded to the nitrogen atoms are above the upper trigonal plane of the three nitrogen atoms and the remaining three are below the lower trigonal plane of the nitrogen atoms. The average deviation is  $0.37 \text{ \AA}$ . On the other hand, the ethylene group at the center of the chelate ring is  $3.83 \text{ \AA}$  distant from the threefold axis, compared to  $2.81 \text{ \AA}$  in the case of  $[\text{Co}(\text{en})_3]^{3+}$ . These characteristic features in the arrangement of the non-ligating atoms affect the magnitudes of rotatory strengths  $R(E)$  and  $R(A_2)$ . This point will be discussed in the next section.

#### Circular Dichroism Spectra of Tris(diamine)cobalt(III) Complexes

Tris(diamine)cobalt(III) complexes usually give two circular dichroism bands with opposite sign and different magnitudes in the absorption region around  $20 \times 10^3 \text{ cm}^{-1}$  in aqueous solution (the first absorption region). These bands are ascribed to the  $d$  electron transition from the  $^1A_1$  ground state to the  $^1E_a$  and  $^1A_2$  excited levels of octahedral parentage in a  $D_3$  environment. McCaffery and Mason measured the single crystal circular dichroism spectrum of  $(+)^{589}\text{-}[\text{Co}(\text{en})_3]_2\text{Cl}_6 \cdot \text{NaCl} \cdot 6\text{H}_2\text{O}$  with light propagated parallel to the optic axis, in which all the complex ions are arranged with their threefold axes parallel to the optic axis (45). Under this condition only the E component is excited. This crystal measurement showed that the intrinsic rotatory strength of the  $^1A_1 \rightarrow ^1E_a$  transition is positive and substantially larger than that of solution circular dichroism. This means that the intrinsic rotatory strength of  $^1A_1 \rightarrow ^1A_2$  must be negative and almost as large as that of the E component, since the trigonal splitting is small. Kuroda and Saito showed that the rotatory strengths of the E and  $A_2$  components can be separated by combining the circular dichroism spectra of a single uniaxial crystal and in its microcrystalline state (52). Even if the threefold axis of the complex ion is not oriented parallel to the optic axis, it is possible to resolve the observed solid state CD spectra into the E and  $A_2$  components by making use of the known crystal structure. Jensen and Galsbøl measured the crystal CD spectra of  $(+)^{589}\text{-}[\text{Co}(\text{en})_3]^{3+}$  ion doped in a host crystal of racemic  $[\text{Ir}(\text{en})_3]_2\text{Cl}_6 \cdot \text{NaCl} \cdot 6\text{H}_2\text{O}$  with light propagated both parallel and perpendicular to the three-

fold axis of  $[\text{Co}(\text{en})_3]^{3+}$  (53). This was first achieved by the phase modulation technique in polarized spectroscopy (54). Before then, measurements of CD were restricted to solution, glasses, fine powder and uniaxial crystals with light propagated along the optic axis, since the signal was otherwise distorted by interference from linear birefringence and linear dichroism. Table VII summarizes the observed rotatory strengths of some tris-diamine cobalt(III) complexes. As seen from the table,  $R(E)$  is positive and  $R(A_2)$  is negative for the absolute configuration  $\Lambda$ , while  $R(E)$  is negative and  $R(A_2)$  is positive for  $\Delta$  configuration, in agreement with the well-known empirical rule for the solution CD spectrum. The values listed in Table VII of  $R(E)$  and  $R(A_2)$  are corrected for random orientation factors of  $2/3$  and  $1/3$ , respectively. Thus the net rotatory strength  $R(T_1) = R(E) + R(A_2)$  may be compared directly with the observed values for solution, which are listed in the last column of Table VII. The net rotatory strength  $R(T_1)$  changes sign on going from solid to solution in the case of  $[\text{Co}(\text{S,S-cptn})_3]^{3+}$  and  $[\text{Co}(\text{S,S-ptn})_3]^{3+}$ . This observation may be ascribed to the ion association or conformational change in solution (41). The absolute values of the observed  $R(E)$  and  $R(A_2)$  possess nearly the same magnitudes with opposite signs.  $|R(E)|$  has the major rotatory strength for the complexes with five-membered chelate rings like  $[\text{Co}(\text{en})_3]^{3+}$ ,  $[\text{Co}(\text{pn})_3]^{3+}$ ,  $[\text{Co}(\text{chxn})_3]^{3+}$  and  $[\text{Co}(\text{cptn})_3]^{3+}$ , whereas  $R(A_2)$  possesses the major rotatory strength for the complexes  $[\text{Co}(\text{ptn})_3]^{3+}$  and  $[\text{Co}(\text{tmd})_3]^{3+}$ . This trend appears to be related to the spatial arrangement of the non-ligating atoms around the cobalt atom. Figure 5 shows projections of the chelate rings of these complexes upon a plane through the threefold axis and the twofold axis. As seen from the figure, all the non-ligating atoms are between the trigonal planes formed by the three nitrogen atoms for those complexes whose  $|R(E)|$  is greater than  $|R(A_2)|$ . On the contrary, in the case of the complexes with  $|R(E)| < |R(A_2)|$ , some of the non-ligating atoms are above and below the trigonal planes and those atoms lying between the trigonal planes are smaller in number and located more distant than those in the first group. The  $d-d$  transitions are magnetic dipole-allowed but electric dipole forbidden. If a coulombic correlation between the components of the electric hexadecapole moment of the  ${}^1A_1 \rightarrow {}^1T_1$   $d$  electron transition and a transition dipole moment induced in each ligand group is considered, the correlated dipole moment of the ligand group gives rise to a non-zero scalar product with a component of the magnetic transition moment (55). Thus such a disposition as well as the geometry of the chelate ring system might give a greater  $|R(A_2)|$  than  $|R(E)|$  for the complex ions of the second group.

These  $D_3$  complexes have played a prominent role as model systems in the theoretical studies of natural optical activity, since the high symmetry of the complexes makes tedious calculations more or less feasible and a lot of experimental data are

Table VII. Rotatory strengths of tris(diamine)cobalt(III) complexes ( $10^{-40}$  cgs)  
 Values of R(E) and R(A<sub>2</sub>) are corrected by the fixed orientation  
 factors of 2/3 and 1/3 respectively.

|  | R(E)           | R(A <sub>2</sub> ) | R(T <sub>1</sub> ) | Ref.         | R(T <sub>1</sub> ) <sub>soln</sub> |
|--|----------------|--------------------|--------------------|--------------|------------------------------------|
| Λ-2[Co(en) <sub>3</sub> ]Cl <sub>3</sub> ·NaCl·6H <sub>2</sub> O | +62.9<br>+52.6 | -58.6              | +4.3               | (52)<br>(45) | +4.4                               |
|  | +50.9          |                    |                    | (102)        |                                    |
|  | +43            | -41                | +2                 | (53)         |                                    |
| Λ-[Co(en) <sub>3</sub> ]Br <sub>3</sub> ·H <sub>2</sub> O        | +59.9          | -55.7              | +4.2               | (52)         | +4.4                               |
| Λ-[Co(S-pn) <sub>3</sub> ]Br <sub>3</sub>                        | +38.1          | -36.6              | +1.5               | (52)         | +4.2                               |
|  | +41.5          |                    |                    | (102)        |                                    |
| Λ-[Co(S,S-chxn) <sub>3</sub> ]Cl <sub>3</sub> ·5H <sub>2</sub> O | +56.5          | -51.1              | +5.4               | (52)         | +3.9                               |
| Λ-[Co(S,S-cptn) <sub>3</sub> ]Cl <sub>3</sub> ·4H <sub>2</sub> O | +57.3          | -54.5              | +2.8               | (52)         | -4.3                               |
| Λ-[Co(S,S-ptn) <sub>3</sub> ]Cl <sub>3</sub> ·2H <sub>2</sub> O  | +12.5          | -14.5              | -2.0               | (52)         | +1.9                               |
| Λ-[Co(tmd) <sub>3</sub> ]Br <sub>3</sub>                         | +31.1          | -38.7              | -7.6               | (52)         | -4.9                               |



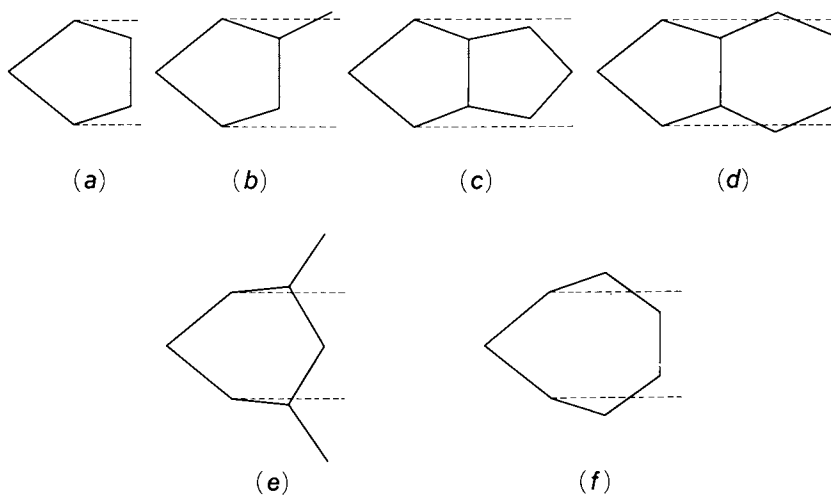


*Figure 5. Projections of a chelate ring upon a plane formed by the threefold axis and a twofold axis for tris(bidentate) complexes: (a)  $[\text{Co}(\text{en})_3]^{3+}$ , (b)  $[\text{Co}(\text{pn})_3]^{3+}$ , (c)  $[\text{Co}(\text{cptn})_3]^{3+}$ , (d)  $[\text{Co}(\text{chxn})_3]^{3+}$ , (e)  $[\text{Co}(\text{ptn})_3]^{3+}$ , (f)  $[\text{Co}(\text{tmd})_3]^{3+}$ .*

available for comparison. The theoretical study was carried out by a number of workers, notably by Richardson (56-61), Evans, Schreiner and Hauser (62) and Mason and Seal (55). Two models are now employed to calculate the optical rotatory strength: one is the crystal field model admitting only static coupling between a metal  $d$ -electron and the charge distribution in the perturbing ligand in the ground state and the other is the dynamic coupling model taking into account of the coupling of the transition in the chromophore with electric dipole transition induced in the ligand by the transition charge distribution. Both models can account for the observed features of the CD spectra with considerable success. For  $[\text{Co}(\text{en})_3]^{3+}$ , the values for observed  $R(E)$ 's in Table VII should be compared with theoretical values of 33.7 and 63.8, the former being based on the crystal field model (62) and the latter on the dynamic coupling model (55). The agreement is good.

### Diethylenetriamine Complexes

There are three different ways of coordinating two diethylenetriamine molecules to a cobalt(III) ion. Among three geometric isomers, the u-facial- and mer-isomers are optically active and have pairs of enantiomers respectively, whereas the s-facial-isomer is optically inactive. All geometric and optical isomers in this system were isolated, and the geometric configurations were assigned for the optically active isomers from the difference in racemization behavior of the optically active u-facial- and mer-isomers (63). All the crystal structures of these isomers were determined. The s-facial isomer has approximately  $C_{2h}$  symmetry. The conformations of the two fused chelate rings are enantiomeric (64). In crystals of  $(-)\text{-}^{589}\text{-u-fac-}[\text{Co}(\text{dien})_2][\text{Co}(\text{CN})_6] \cdot 2\text{H}_2\text{O}$ , there exist two different conformers in an asymmetric unit. They both have a twofold axis and the absolute configuration can be designated as skew chelate pairs  $\Delta \wedge \Delta$ . However, the conformations of the two chelate rings formed by a dien molecule in one complex ion are  $\delta \lambda$ , while those in the other are  $\lambda \lambda$  (65).

The absolute configuration of  $(+)\text{-}^{589}\text{-mer-}[\text{Co}(\text{dien})_2]\text{Br}_3 \cdot 1.6\text{-H}_2\text{O}$  has recently been determined (66). Figure 6 shows a perspective drawing of the complex ion. The complex ion can be designated as trans- $\lambda$ -NH, providing that the chirality is defined by the line joining the two H atoms and the line joining the two secondary nitrogen atoms in trans-positions (3, 60). The two terdentate molecules coordinate to the central cobalt atom in mer positions with three nitrogen atoms forming a distorted octahedral complex. The complex ion has an approximate twofold symmetry. The Co-secondary N bond of 1.940 Å is significantly shorter than the Co-terminal N bond of 1.981 Å. The angle subtended at the central cobalt atom is 187°. The three ligating nitrogen atoms of the ligand and the cobalt atom are nearly copla-

nar and the two planes formed by the cobalt and the three nitrogen atoms make an angle of  $89.6^\circ$ . The five-membered chelate ring takes an envelope form, one of the two methylene carbon atoms that is bonded to the secondary nitrogen atom is shifted by  $0.64 \text{ \AA}$  from the plane formed by the remaining four atoms. The conformations of the two fused chelate rings are  $\delta$  and  $\lambda$ , respectively. The geometry of the complex cation agrees well with the result of conformational analysis (67), as shown in Table VIII.

The net chirality of this complex ion is zero. The optical activity of the complex ion arises from the dissymmetric disposition of the methylene groups with respect to the coordination plane and the chiral arrangement of the two trans N-H bonds. Richardson's sector rule (60) was tested on the basis of the final atomic parameters. In his derivation the perturbation treatment

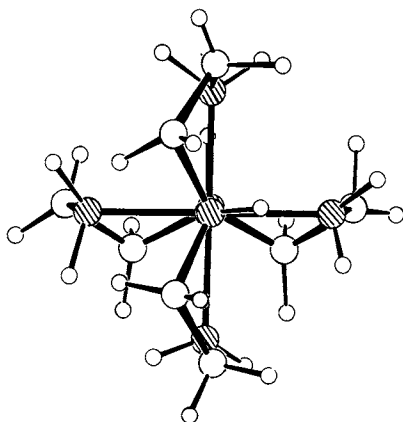
Table VIII Observed and calculated geometries of  
mer-[Co(dien)<sub>2</sub>]<sup>3+</sup>

|                         | obs.  | calc.   |
|-------------------------|-------|---------|
| Co-N(H <sub>2</sub> )   | 1.981 | 1.976 Å |
| Co-N(H)                 | 1.940 | 1.942   |
| C-N(H <sub>2</sub> )    | 1.493 | 1.495   |
| C-N                     | 1.482 | 1.486   |
| N-Co-N                  | 85.1  | 86.0°   |
| C-N-C                   | 116.2 | 114.5   |
| Co-N(H <sub>2</sub> )-C | 109.3 | 109.3   |
| Co-N(H)-C               | 109.5 | 107.8   |
| N(H <sub>2</sub> )-C-C  | 108.7 | 109.1   |
| N(H)-C-C                | 104.7 | 105.9   |

was carried out to the second order in both the wave function and rotatory strength. A negative net rotatory strength in the region of the first absorption,  $A_1 \rightarrow T_1$  was predicted. The CD spectra of the complex ion in aqueous solution agreed with this<sub>3</sub> expectation ( $\Delta\epsilon = +0.096$  at  $19.5 \times 10^3 \text{ cm}^{-1}$ ,  $\Delta\epsilon = -0.181$  at  $21.9 \times 10^3 \text{ cm}^{-1}$ , (68)).

#### Complexes with a Cyclic Terdentate, R-MeTACN

Mason and Peacock synthesized the cyclic terdentate, R(-)-2-methyl-1,4,7-triazacyclononane and its Co(III) complex, [Co(R-MeTACN)<sub>2</sub>]<sup>3+</sup> (69). Figure 7 shows a perspective drawing of the complex ion, (-)<sub>589</sub>-[Co(R-MeTACN)<sub>2</sub>]<sup>3+</sup> in its iodide pentahydrate crystals. The complex ion has D<sub>3</sub> symmetry by the requirement of



Acta Crystallographica

Figure 6. A perspective drawing of the complex ion  $(+)_{S_{89}}\text{-mer-}[\text{Co}(\text{dien})_2]^{3+}$  (66)

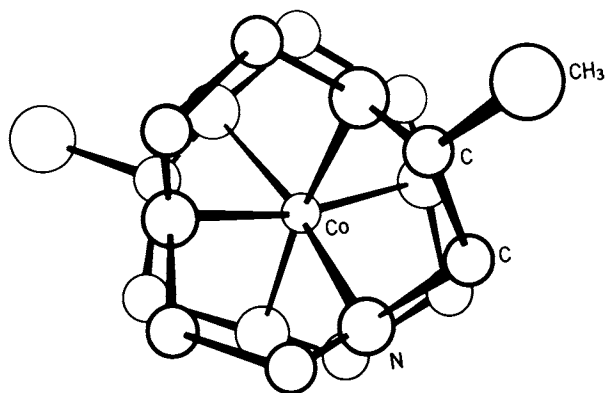


Figure 7. A perspective drawing of the complex ion  $(-)_{S_{89'}}[\text{Co}(\text{R-MeTACN})_2]^{3+}$

the space group. The methyl group is attached to one of the three chelate rings of the cyclic terdentate ligand, so that the complex ion exhibits orientational disorder. The observed electron-density distribution indicates that the methyl group is attached in equatorial positions with respect to the chelate ring. There are three possible geometrical isomers for the complex ion in respect of the positions of the two methyl groups. No conclusion can be drawn concerning the isomerism, due to the orientational disorder, since the X-ray analysis only indicates the average structure. Two molecules of the cyclic terdentate coordinate to the cobalt atom with six secondary nitrogen atoms from above and below the metal atom to form an octahedral complex. A MeTACN molecule spans a face of the octahedron. The six five-membered chelate rings take  $\lambda$  conformation (70). Nonomiya separated the cobalt(III) complex into five components using SP Sephadex column chromatography, although there are nine possible isomers (71). Figure 8 shows two modes of coordination of R-MeTACN. In the mode "b", the ligand is coordinated to the metal atom with the nine-membered ring upside down compared to the mode "a". The absolute configuration of N(1) is S in the mode "a", while it is R in the "b" mode. There are three ways of combining the modes "a" and "b": aa, ab and bb. In addition to this there are three geometrical isomers in respect of the positions of the methyl groups. Accordingly, nine isomers are possible as a whole. The crystal subjected to X-ray structure analysis incorporates three aa type isomers. Nonomiya found that aa and ab type isomers can be separated, respectively, into two components: one isomer and a mixture of the remaining two. On the other hand the bb type isomers were separated as one component by his method. All these complexes show very strong positive CD extremes in the region of the first spin allowed  $d-d$  transition of octahedral parentage.

The geometric array of chelate groups in this complex ion differ from that of  $[\text{Co}(\text{en})_3]^{3+}$  in the same manner as described before. It has the non-ligating atoms above and below the trigonal planes of the ligating nitrogen atoms and none of the non-ligating atoms exists in the equatorial plane. The crystals of  $[\text{Co}(\text{R-MeTACN})_2] \cdot 5\text{H}_2\text{O}$  are optically uniaxial and each complex ion is arranged with the threefold axis parallel to the optic axis. The light propagated along the optic axis can only excite the E component of the transition. The single crystal circular dichroism spectrum shows a single negative peak at 487 nm, while that in aqueous solution has a positive peak at about 487 nm. The solution circular dichroism spectra also reveals  $R(A_2)$ , giving the sum,  $R(T_1) = R(E) + R(A_2)$ . A comparison of the single crystal and the solution CD spectra indicates that R(E) has minor rotatory strength of  $-0.16 \text{ DB}_M$  and  $R(A_2) + 0.32 \text{ DB}_M$  (72). This result supports the observed relation between the relative magnitudes of  $R(E)$  and  $R(A_2)$  and the arrangement of non-ligating atoms in tris-bidentate complexes (Table VII). The polar capping of  $\Lambda - (+)_{589}^-$

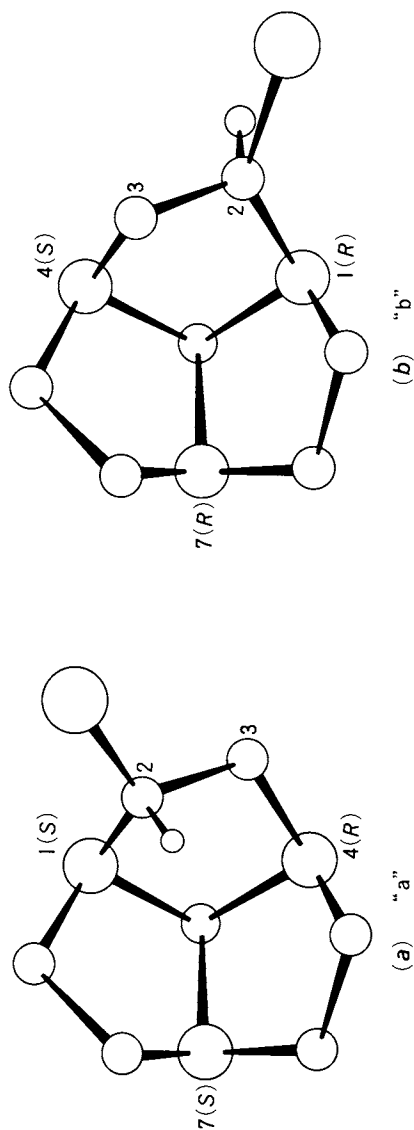


Figure 8. Two modes of coordination of R-MeTACN

$[\text{Co}(\text{en})_3]^{3+}$  with the phosphate ion by hydrogen bonding in solution is known to enhance  $R(A_2)$  at the expense of  $R(E)$  (73, 74). The polar capping of  $(+)^{589}[\text{Co}(\text{en})_3]^{3+}$  by the covalently bonded tris-(methyleneamino) group results in  $(-)^{589}[\text{Co}(1,3,6,8,10,13,16,19\text{-octa-aza-bicyclo}[6.6.6]\text{-eicosane})]^{3+}$  (75). This complex ion gives  $R(T_1)$  of  $-0.068 \text{ D}_{\text{M}}$ , in contrast to  $+0.047$  of  $\Lambda\text{-}[\text{Co}(\text{en})_3]^{3+}$ . These observations illustrate the general enhancement of  $R(A_2)$  at expense of  $R(E)$  by the addition of atoms or atomic groups to the polar region of the  $[\text{CoN}_6]$  chromophore of  $D_3$  symmetry.

### Electron-density Distribution in $D_3$ Complexes

Recent improvements in experimental and computational techniques in X-ray crystallography have made it possible to estimate atomic charge-density in an optically active transition metal complex, based on accurate intensity data. Two examples will be described here. The crystal structures of  $\Lambda\text{-}1\text{el}_3\text{-}[\text{Co}(\text{S},\text{S}\text{-chxn})_3]\text{-}(\text{NO}_2)_3 \cdot 3\text{H}_2\text{O}$  and  $\Delta\text{-ob}_3\text{-}[\text{Co}(\text{S},\text{S}\text{-chxn})_3]\text{-}(\text{NO}_2)_3 \cdot 3\text{H}_2\text{O}$  have been determined (76). The number of electrons within a sphere of radius 1.22 Å (covalent radius of cobalt) are listed in Table IX, together with other related complex ions. The central metal atom is neutralized largely by donation of electrons from the ligating nitrogen atoms, illustrating that Pauling's electroneutrality rule holds for these transition metal complexes. Larsson and his col-

Table IX. Effective charge on the central metal atom

| Complex  | $C(R)^a$ | Effective charge | Ref. |
|--|----------|------------------|------|
| $[\text{Co}(\text{NH}_3)_6]^{3+}$  | 26.3(3)  | +0.7             | (77) |
| $[\text{Co}(\text{CN})_6]^{3+}$  | 26.8(3)  | +0.2             | (77) |
| $[\text{Co}(\text{NO}_2)_6]^{3-}$  | 26.3(1)  | +0.7             | (78) |
| $\Lambda\text{-}1\text{el}_3\text{-}[\text{Co}(\text{S},\text{S}\text{-chxn})_3]^{3+}$ | 26.8(3)  | +0.2             | (76) |
| $\Delta\text{-ob}_3\text{-}[\text{Co}(\text{S},\text{S}\text{-chxn})_3]^{3+}$          | 26.8(3)  | +0.2             | (76) |

a: Number of electrons within a sphere of radius 1.22 Å

laborators estimated the effective charge of cobalt in  $[\text{Co}(\text{en})_3]^{3+}$  and  $[\text{Co}(\text{CN})_6]^{3-}$  by ESCA and obtained the value of  $+0.7(3)$  and  $+0.6(4)$ , respectively (79).

Non-bonding  $d$  electrons in these complex ions show an aspherical distribution, which can be detected in the final difference synthesis. These complexes possess six  $3d$  electrons and they are in the low-spin state. In an  $O_h$  environment, the difference synthesis indicates excess electron-density in the direction of  $t_2$  orbitals and a deficiency in the  $e_g$  orbitals, since the difference synthesis gives the deviation of electron-density from spherical distribution. In the difference synthesis, there exist eight positive peaks arranged at the apices of a cube.

Figure 9 illustrates this situation. A, B, C, ... G, H are the positions of positive peaks due to excess electron-density in  $t_{2g}$  orbitals. One threefold axis of the cube is oriented vertically. As seen from the figure, the six positive peaks are located in such a way that they avoid repulsion from bonding electrons in the cobalt-nitrogen bond. The change in the residual electron-density distribution around the cobalt atom on lowering the symmetry from  $O_h$  to  $D_3$  ( $1e_1$  or  $ob_3$ ) can be described conveniently in terms of Figure 9. A chelate ring with the  $1e_1$  conformation is drawn by a thick, full line. The residual density observed in  $\Lambda$ - $1e_1$ - $[\text{Co}(\text{S,S-chxn})_3]^{3+}$  has a tendency to avoid regions of high  $3^2$  field owing to the chelate rings: there are two lobes at A and H which are more stable than others, because no chelate ring spans across this direction, the remaining six peaks are fused to give three lobes, namely, B and F, C and G, and D and E. The three lobes keep away from the chelate ring plane. It is to be noted that this distribution of the residual electron-density peaks is chiral. The observed residual electron-density in  $\Lambda$ - $1e_1$ - $[\text{Co}(\text{S,S-chxn})_3](\text{NO}_2)_3 \cdot 3\text{H}_2\text{O}$  is shown in Figure 10. The above-mentioned features can be seen clearly in the two sections.

The residual electron-density in the  $ob_3$  isomer has a tendency to avoid the equatorial region, owing to the repulsion from the ethylene groups lying near the equatorial plane, and to accumulate in the polar region around the threefold axis (A and H).

### The Crystal Structure of Active Racemates and Other Diastereoisomers

In 1912 Werner introduced a criterion of least soluble diastereoisomers to correlate the absolute configurations of optically active complexes with the solubility of their diastereoisomers using the same optically active agent (80). Delepine prepared the active racemates and this, in connection with their properties (especially the X-ray diffraction powder patterns), led to a correlation of the absolute configurations for the compounds considered (81, 82). Anderson, Galsbøl and Harnung proposed a method to correlate the unknown absolute configuration of a complex to another of known absolute configuration through a series of powder diffraction patterns of active racemates (83). It is based on the assumption that the compound in question and the active racemate containing the reference complex must be isostructural with the corresponding racemate. Recently, Herpin and his collaborators determined the crystal structures of two active racemates: (+) $_{589}$ - $[\text{Co}(\text{en})_3](-)_{589}$ - $[\text{Cr}(\text{en})_3]\text{Cl}_6 \cdot 6.1\text{H}_2\text{O}$  (84) and (+) $_{589}$ - $[\text{Cr}(\text{en})_3](+)_{589}$ - $[\text{Rh}(\text{en})_3]\text{Cl}_6 \cdot 6\text{H}_2\text{O}$  (85). Both structures are isostructural with the corresponding racemates like  $[\text{Co}(\text{en})_3]\text{Cl}_2 \cdot 2.8\text{H}_2\text{O}$  and  $[\text{Cr}(\text{en})_3]\text{Cl}_2 \cdot 3\text{H}_2\text{O}$  (86), in which the enantiomeric complex ions are stacked alternately with the threefold axis parallel to form a columnar structure. Between the complex ions are the chloride anions. In the active racemates the two complex ions



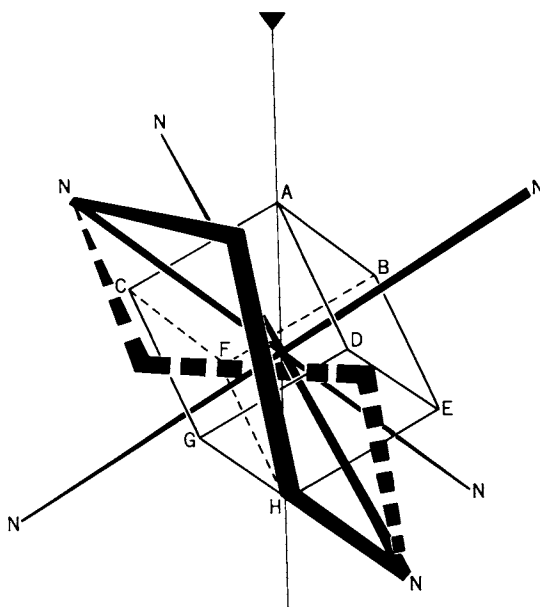


Figure 9. Illustrating the relative arrangements of the residual electron density peaks owing to the excess density in  $t_{2g}$  orbitals and a five-membered chelate ring. A, B, C . . . stand for the peak positions. A *lel* chelate ring is drawn by thick lines and an *ob* ring by broken lines.

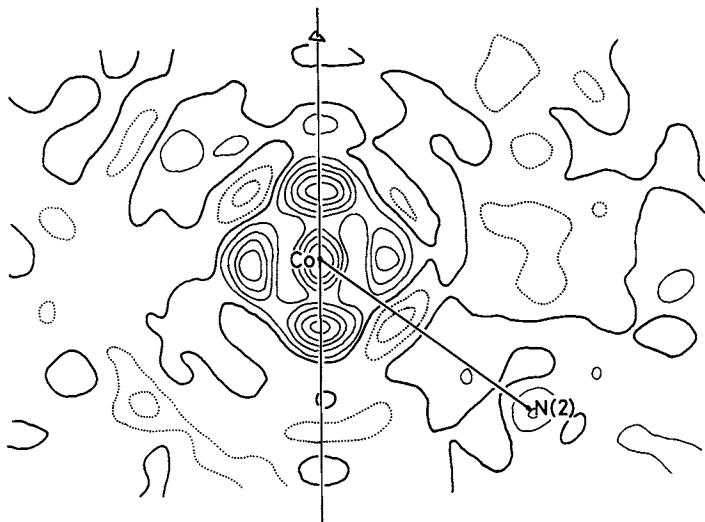


Figure 10a. A section of the difference synthesis  $1e1_3$ - $[\text{Co}(\text{chxn})_3]^{3+}$ . This section is through a threefold axis and a Co-N bond.

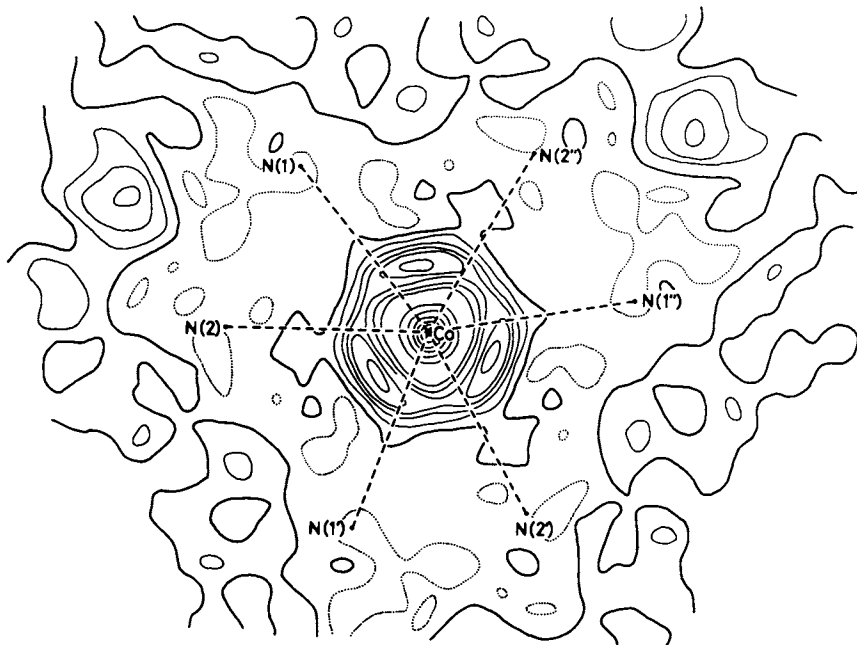


Figure 10b. A section of the difference synthesis  $1e1_3$ - $[\text{Co}(\text{chxn})_3]^{3+}$ . This section is through the Co atom and perpendicular to the threefold axis.

with opposite absolute configurations are arranged alternately like the enantiomeric complex ions in the racemates.

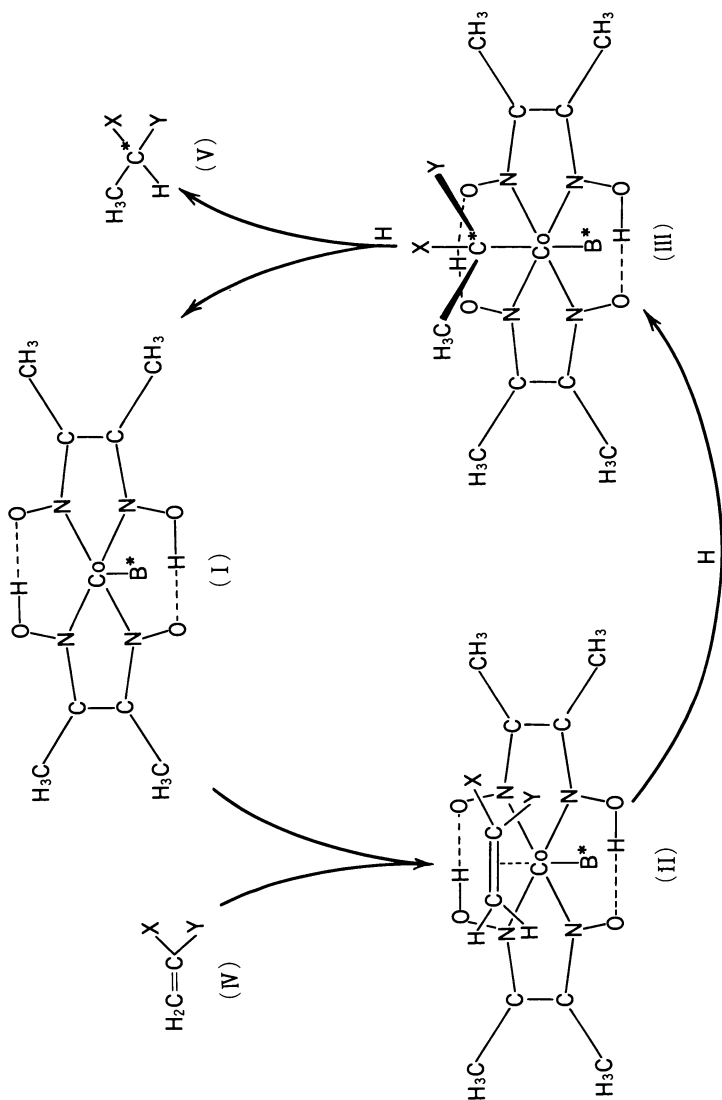
Yoneda and his collaborators determined a number of structures of diastereoisomers that are used for resolution of optical isomers (87, 88, 89, 90, 91). Crystals of  $\Lambda$ -[Co(en)<sub>3</sub>]<sub>2</sub>(d-tartBr)·5H<sub>2</sub>O (87) and Li  $\Lambda$ -[Cr(en)<sub>3</sub>]<sub>2</sub>(d-tart)<sub>2</sub>·H<sub>2</sub>O and (-)<sub>589</sub><sup>3</sup>[Co(ox)(en)<sub>2</sub>]<sub>2</sub>H(d-tart)·2H<sub>2</sub>O (90); <sup>3</sup>trans-(O)<sub>2</sub>(+)<sub>589</sub><sup>3</sup>[Co(gly)<sub>2</sub>(en)]H(d-tart)·3H<sub>2</sub>O and (-)<sub>589</sub><sup>3</sup>[Co(gly)<sub>2</sub>(en)]H(d-tart)·H<sub>2</sub>O (92). More structural information may be needed before a definite conclusion can be drawn on the structural aspects of the resolution mechanism by solubility difference of diastereoisomeric pairs. Broadly speaking, the less soluble diastereoisomer has a more closely packed structure and the complex ions and the counter ions are more firmly held together by hydrogen bonding than for the more soluble isomer. It is certain that various modes of association between a complex ion and a resolving agent revealed in these structure investigations provide important information for the mode of ion association in solution (93).

### Structural Study of Asymmetric Hydrogenation

Ohashi and Sasada have studied comprehensively the structural aspects of asymmetric hydrogenation catalyzed by transition metal complexes (94). These authors studied the crystal structures of the complexes between bis(dimethylglyoximate)cobalt and asymmetric amines and the intermediate complexes with these complexes and substrates (prochiral olefins). They proposed that the asymmetry of the amine is transferred to the reaction products in a transition state through the distortion of the bis(dimethylglyoximate)-cobalt moiety. This proposal was supported by the strain energy calculation of the intermediate complexes. Figure 11 shows the reaction scheme. An olefin molecule (substrate), H<sub>2</sub>C=CXY (IV), coordinates to the catalyst (I) to form an intermediate  $\pi$ -complex, where X is an electron attracting group and Y an electron donating group. It is hydrogenated to a  $\sigma$ -complex (III), which is further converted to the final product (V) and the complex (I) by hydrogenation. At this final stage, the Co-C bond cleavage is known to proceed mainly through inversion of configuration at the carbon atom (95). Table X shows the optical yield of the reaction when

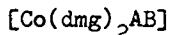
Table X Optical yield of the asymmetric hydrogenation of CH<sub>2</sub>=CXY at room temperature

| X                             | Y  | Optical yield | Absolute configuration |
|-------------------------------|--|---------------|------------------------|
| COOCH <sub>3</sub>            | C <sub>6</sub> H <sub>5</sub>                        | 7%            | S                      |
| COOCH <sub>3</sub>            | NHCOCH <sub>3</sub>                                  | 19            | S                      |
| COOCH <sub>3</sub>            | NHCOCH <sub>2</sub> (C <sub>6</sub> H <sub>5</sub> ) | 7             | S                      |
| C <sub>6</sub> H <sub>5</sub> | COC <sub>6</sub> H <sub>5</sub>                      | 49.2          | S                      |

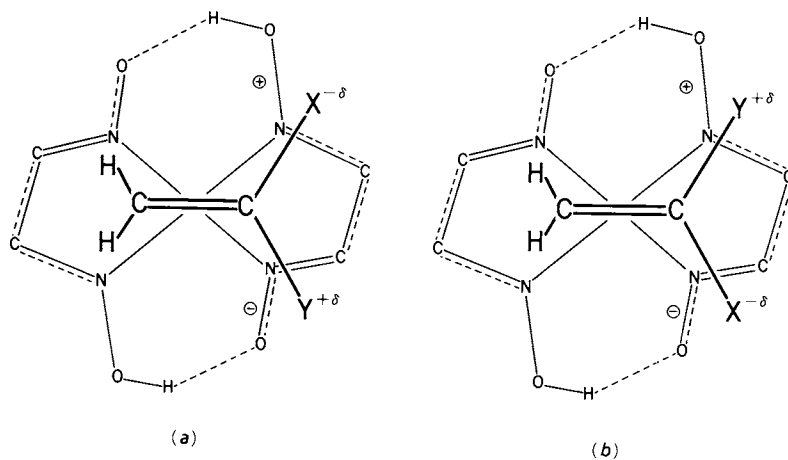


Bulletin of the Chemical Society of Japan  
 Figure 11. A reaction scheme of asymmetric hydrogenation of olefins catalyzed by an optically active transition metal compound (96)

B\* is quinine. In cases of high optical yield it has so far been impossible to isolate the intermediate complex in the crystalline state. Thus some appropriate model compounds were selected and the crystal structures were determined:

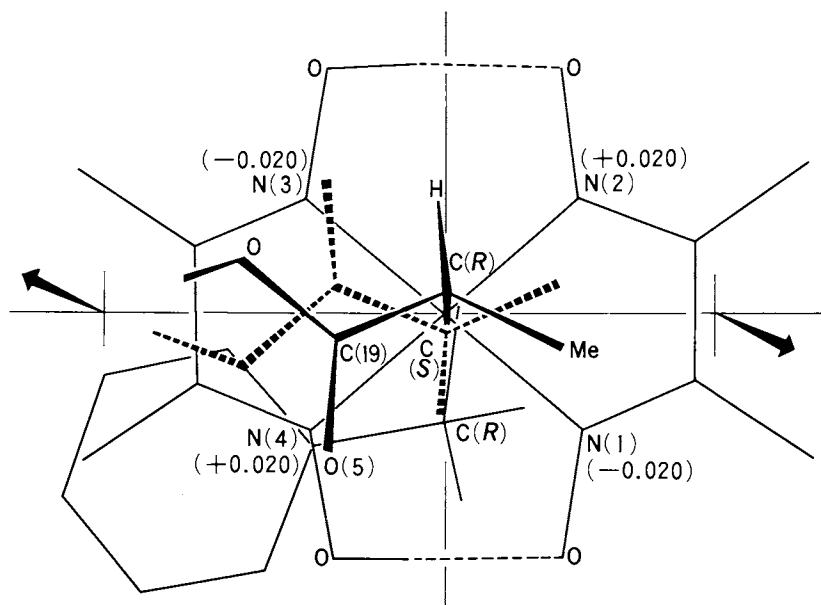


(i) is considered to be a model compound for the catalyst (I), since the small methyl group does not affect the geometry of the cobaloxime moiety. Unlike the cobaloxime complexes with optically inactive amines (98, 99, 100, 101), the symmetry of the cobaloxime moiety in (i) descends from  $D_{2h}$  to  $C_{2h}$ , probably owing to the coordination of optically active base. The observed geometry of the cobaloxime moiety indicates that the electronic structure can be represented by the schematic drawing shown in Figure 12 (a) and (b), which also illustrates the two possible arrangements of a substrate and the cobaloxime moiety. Electrostatic interaction between the substrate and the cobaloxime moiety clearly favors the configuration (a) over (b), indicating that the sides of the plane of the substrate are distinguished on forming a  $\pi$ -complex. Thus this deformation of the cobaloxime moiety from  $D_{2h}$  to  $C_{2h}$  is one factor inducing asymmetry in the reaction stage of  $\pi$ -bond formation. The compound (ii) is a model compound for the  $\sigma$ -complex (III). Figure 13 presents a projection of the molecule upon the average coordination plane. The plane of the cobaloxime moiety is no longer planar but twisted. The line joining N(1) and N(2) and that joining N(3) and N(4) form a  $\lambda$  skew pair. This distortion is partly to alleviate the repulsion between the 1-(methoxycarbonyl)ethyl (mce) group and the cobaloxime moiety and such deformation also stabilizes the coordination of the base moiety. The cobalt atom is displaced upward from the mean plane by 0.04 Å, whereas in (i) it is shifted downward by about 0.04 Å. In Figure 13 a presumed conformation of the  $\sigma$ -complex with the S-1-(methoxycarbonyl)ethyl group is drawn by thick broken lines. In this case the methyl group of the mce group approaches N(2), which is shifted above the mean plane, giving rise to the stronger repulsion. Thus the  $\sigma$ -complex with the S-mce group is energetically less stable than that with the R-mce group. This is another factor inducing the asymmetry at the stage of  $\sigma$ -bond formation. The strain energies were calculated for the diastereoisomeric  $\pi$ - and  $\sigma$ -complexes by Boyd's procedure (30). It turned out that the energy difference between the two alternative configurations (a) and (b) in Figure 12 is in the range 0.8 - 1.7 kJ mol<sup>-1</sup> and that between the diastereoisomers of the  $\sigma$ -complex ranges from 3.3 to 4.6 kJ mol<sup>-1</sup>, which account for the observed optical yield reasonably.



Bulletin of the Chemical Society of Japan

Figure 12. A schematic of a  $\pi$ -complex. Two possible arrangements having minimum nonbonded interactions are shown (96).



Bulletin of the Chemical Society of Japan

Figure 13. The structure of a  $\delta$ -complex. A presumed conformation of the complex with S-mce group is drawn by broken lines (97).

### Conclusion

As a result of the accumulation of structural knowledge on metal chelate complexes, it is now possible to predict with reasonable certainty the conformation and strain energy of an unknown complex. The absolute configuration of the complex can be determined on the basis of its CD spectrum if a reference complex of known absolute configuration is selected appropriately. The cobalt(III) complexes containing nitrogen as ligating atoms have been studied most extensively. It is hoped that complexes containing metals other than cobalt and ligating atoms other than nitrogen will be investigated in similar detail.

The importance of the accurate structure determination of optically active transition metal compounds deserves special emphasis. If the electron-density distribution and geometrical arrangement of the atomic nuclei are well known, it is possible, at least in principle, to predict all the physical and chemical properties of the complex on the basis of quantum mechanical calculations.

Finally a good deal of activity has been apparent in the fields of stereoselective and/or stereospecific reactions and catalysis involving optically active transition metal compounds. The increasing interest in this field will certainly require a much greater knowledge of absolute configurations than has emerged during the past twenty-five years.

### Literature Cited

1. Saito, Y.; Nakatsu, K.; Shiro, M.; Kuroya, H. Acta Crystallogr., (1954), 7, 636; (1955), 8, 729.
2. Yoshikawa, Y.; Yamasaki, K. Inorg. Nucl. Chem. Lett., (1970), 6, 523.
3. "Nomenclature of Inorganic Chemistry"; 2nd Ed.; Butterworths: London, (1970); Inorg. Chem., (1970), 9, 1.
4. Corey, E.J.; Bailer, J.C. Jr. J. Am. Chem. Soc., (1959), 81, 2620.
5. Haupt, H.J.; Huber, F.; Preut, H. Z. Anorg. Allg. Chem., (1978), 422, 31.
6. Haupt, H.J.; Huber, F. Z. Anorg. Allg. Chem., (1978), 442, 31.
7. Raymond, K.N.; Corfield, P.W.R.; Ibers, J.A. Inorg. Chem., (1968), 7, 1362.
8. Brouty, C.; Spinat, P.; Whuler, A. Acta Crystallogr., (1977), B33, 3453.
9. Raymond, K.N.; Ibers, J.A. Inorg. Chem., (1968), 7, 2333.
10. Whuler, A.; Brouty, C.; Spinat, P.; Herpin, P. Acta Crystallogr., (1977), B33, 2877.
11. Brouty, C.; Spinat, P.; Whuler, A.; Herpin, P. Acta Crystallogr., (1977), B33, 1913.
12. Brouty, C.; Spinat, P.; Whuler, A.; Herpin, P. Acta Crystallogr., (1977), B33, 1920.
13. Sato, S.; Saito, Y. Acta Crystallogr., (1978), B34, 3352.
14. Iwata, M.; Nakatsu, K.; Saito, Y. Acta Crystallogr., (1969),

- (1977), 50, 898.
47. Kojima, M.; Fujita, J. Bull. Chem. Soc. Jpn., (1977), 50, 3237.
48. Kojima, M.; Fujita, J. Chem. Lett., (1976), 429.
49. Fujita, J.; Ogino, H. Chem. Lett., (1974), 57.
50. Nakayama, Y.; Matsumoto, K.; Ooi, S.; Kuroya, H. Chem. Commun., (1973), 170.
51. Sato, S.; Saito, Y. Acta Crystallogr., (1975), B31, 1378.
52. Kuroda, R.; Saito, Y. Bull. Chem. Soc. Jpn., (1976), 49, 433.
53. Jensen, H.P.; Galsbøl, F. Inorg. Chem., (1977), 16, 1294.
54. Jensen, H.P.; Schellman, J.A.; Troxell, T. Appl. Spectroscopy, (1978), 32, 192.
55. Mason, S.F.; Seal, R.H. Mol. Phys., (1976), 31, 755.
56. Richardson, F.S. J. Phys. Chem., (1971), 75, 692.
57. Richardson, F.S. J. Chem. Phys., (1971), 54, 2453.
58. Richardson, F.S. J. Chem. Phys., (1972), 57, 589.
59. Richardson, F.S. Inorg. Chem., (1971), 10, 2121.
60. Richardson, F.S. Inorg. Chem., (1972), 11, 2366.
61. Strickland, R.W.; Richardson, F.S. Inorg. Chem., (1973), 12, 1025.
62. Evans, R.S.; Schreiner, A.F.; Hauser, P.J. Inorg. Chem., (1974), 13, 2185.
63. Keene, F.R.; Searle, G.H.; Yoshikawa, Y.; Imai, A.; Yamasaki, K. Chem. Commun., (1970), 784.
64. Kobayashi, M.; Marumo, F.; Saito, Y. Acta Crystallogr., (1972), B28, 470.
65. Konno, M.; Marumo, F.; Saito, Y. Acta Crystallogr., (1973), B29, 739.
66. Okiyama, K.; Sato, S.; Saito, Y. Acta Crystallogr., (1979), B35, in the press.
67. Yoshikawa, Y. Bull. Chem. Soc. Jpn., (1976), 49, 159.
68. Kojima, M.; Iwagaki, M.; Yoshikawa, Y.; Fujita, J. Bull. Chem. Soc. Jpn., (1977), 50, 3216.
69. Mason, S.F.; Peacock, R.D. Inorg. Chim. Acta, (1976), 19, 75.
70. Mikami, M.; Kuroda, R.; Konno, M.; Saito, Y. Acta Crystallogr., (1977), B33, 1485.
71. Nonomiya, M. Inorg. Chim. Acta, (1978), 29, 211.
72. Kuroda, R.; Mason, S.F. Chem. Lett., (1978), 1045.
73. Mason, S.F.; Norman, B.J. J. Chem. Soc., (1966), (A), 307.
74. Duesler, E.N.; Raymond, K.N. Inorg. Chem., (1971), 10, 1486.
75. Creaser, I.I.; Harrowfield, J.McB.; Herlt, A.J.; Sargeson, A.M. A.M.; Springborg, J.; Geue, R.J.; Snow, M.R. J. Am. Chem. Soc. (1977), 99, 3181.
76. Miyamae, H.; Sato, S.; Saito, Y. Acta Crystallogr., To be published.
77. Iwata, M.; Saito, Y. Acta Crystallogr., (1973), B29, 822.
78. Ohba, S.; Toriumi, K.; Sato, S.; Saito, Y. Acta Crystallogr., (1978), B34, 3535.
79. Larson, R.; Folkesson, B. Physica Scripta, (1977), 16, 357.
80. Werner, A. Ber., (1912), 45, 1228.



- B25, 2562.
15. Beattie, J.K. *Acc. Chem. Res.*, (1971), 4, 253.
  16. Hawkins, C.J.; Peachey, R.M.; Szoredi, C.L. *Aust. J. Chem.*, (1978), 31, 973.
  17. Niketić, S.R.; Rasmussen, K. *Acta Chem. Scand.*, (1978), A32, 391.
  18. Gollogly, J.R.; Hawkins, C.J. *Inorg. Chem.*, (1969), 8, 1168.
  19. Gollogly, J.R.; Hawkins, C.J. *Inorg. Chem.*, (1970), 9, 576.
  20. Gollogly, J.R.; Hawkins, C.J.; Beattie, J.R. *Inorg. Chem.*, (1971), 10, 317.
  21. Saito, Y. *Pure and Appl. Chem.*, (1969), 17, 21.
  22. Harnung, S.E.; Søndergaard Sørensen, B.; Creaser, I.; Maegaard, H.; Pfenninger, U.; Schäffer, C.E. *Inorg. Chem.*, (1976), 15, 2123.
  23. Marumo, F.; Utsumi, Y.; Saito, Y. *Acta Crystallogr.*, (1970), B26, 1492.
  24. Sato, S.; Saito, Y. *Acta Crystallogr.*, (1977), B33, 860.
  25. Sato, S.; Shintani, H.; Saito, Y. unpublished work.
  26. Kobayashi, A.; Marumo, F.; Saito, Y. *Acta Crystallogr.*, (1972), B28, 2709.
  27. Dwyer, F.P.; McDermott, T.E.; Sargeson, A.M. *J. Am. Chem. Soc.*, (1963), 85, 2913.
  28. Harnung, S.E.; Kallesøe, S.; Sargeson, A.M.; Schäffer, C.E. *Acta Chem. Scand.*, (1974), A28, 385.
  29. Sato, S.; Saito, Y. unpublished work.
  30. Boyd, R.H. *J. Chem. Phys.*, (1968), 49, 2574.
  31. Harnung, S.E.; Laier, T.R. *Acta Chem. Scand.*, (1978), A32, 41.
  32. Niketić, S.R.; Woldbye, F. *Acta Chem. Scand.*, (1973), 27, 621.
  33. Nomura, T.; Marumo, F.; Saito, Y. *Bull. Chem. Soc. Jpn.*, (1969), 42, 1016.
  34. Nagao, R.; Marumo, F.; Saito, Y. *Acta Crystallogr.*, (1973), B29, 2438.
  35. Journak, F.A.; Raymond, K.N. *Inorg. Chem.*, (1974), 13, 2387.
  36. Niketić, S.R.; Rasmussen, K.; Woldbye, F.; Lifson, S. *Acta Chem. Scand.*, (1976), A30, 485.
  37. Kobayashi, A.; Marumo, F.; Saito, Y. *Acta Crystallogr.*, (1973), B29, 2443.
  38. Kobayashi, A.; Marumo, F.; Saito, Y. *Acta Crystallogr.*, (1972), B28, 3591.
  39. Kojima, M.; Fujita, J. *Chem. Lett.*, (1976), 429.
  40. Sato, S.; Saito, Y. *Acta Crystallogr.*, (1978), B34, 420.
  41. Kuroda, R.; Fujita, J.; Saito, Y. *Chem. Lett.*, (1975), 225.
  42. Beddoe, P.G.; Harding, M.J.; Mason, S.F.; Peart, B.J. *Chem. Commun.*, (1968), 689.
  43. Gollogly, J.R.; Hawkins, C.J. *Chem. Commun.*, (1968), 689.
  44. Beddoe, P.G.; Mason, S.F. *Inorg. Chem.*, (1968), 4, 433.
  45. McCaffery, A.J.; Mason, S.F. *Mol. Phys.*, (1963), 6, 359.
  46. Kojima, M.; Fujita, M.; Fujita, J. *Bull. Chem. Soc. Jpn.*,

81. Delepine, M. Bull. Soc. Chim. France, (1931), 29, 656.
82. Delepine, M.; Charonnat, R. Bull. Soc. Franc. Mineral. Crist., (1930), 53, 73.
83. Andersen, P.; Galsbøl, F.; Harnung, S.E. Acta Chem. Scand., (1969), 23, 3027.
84. Whuler, A.; Brouty, C.; Spinat, P.; Herpin, P. Acta Crystallogr., (1976), B32, 194.
85. Whuler, A.; Brouty, C.; Spinat, P.; Herpin, P. Acta Crystallogr., (1976), B32, 2542.
86. Whuler, A.; Brouty, C.; Spinat, P.; Herpin, P. Acta Crystallogr., (1975), B31, 2069.
87. Kushi, Y.; Kuramoto, M.; Yoneda, H. Chem. Lett., (1976), 135.
88. Kushi, Y.; Kuramoto, M.; Yoneda, H. Chem. Lett., (1976), 339.
89. Kushi, Y.; Kuramoto, M.; Yoneda, H. Chem. Lett., (1976), 663.
90. Kushi, Y.; Kuramoto, M.; Yoneda, H. Chem. Lett., (1976), 1133; Bull. Chem. Soc. Jpn., (1978), 51, 3251.
91. Yoneda, H.; Yoshikawa, T. Chem. Lett., (1976), 707.
92. Kuramoto, M.; Kushi, Y.; Yoneda, H. Bull. Chem. Soc. Jpn., To be published.
93. Private communication from Professor Yoneda.
94. Ohashi, Y. J. Crystallogr. Soc. Jpn., (1977), 19, 303, (in Japanese).
95. Ohgo, Y.; Natori, Y.; Takeuchi, S.; Yoshimura, J. Chem. Lett., (1974), 1327.
96. Ohashi, Y.; Sasada, Y. Bull. Chem. Soc. Jpn., (1977), 50, 1710.
97. Ohashi, Y.; Sasada, Y. Bull. Chem. Soc. Jpn., (1977), 50, 2863.
98. Lenhert, P.G. Chem. Commun., (1967), 980.
99. McFadden, D.L.; McPhail, A.T. J. Chem. Soc. Dalton Trans., (1974), 363.
100. Ginderow, P.O. Acta Crystallogr., (1975), B31, 1092.
101. Bigotto, A.; Zangrand, E.; Randaccio, L. J. Chem. Soc. Dalton Trans., (1976), 96.
102. Judkins, R.R.; Royer, D.J. Inorg. Chem., (1974), 13, 945.

RECEIVED September 13, 1979.

## Circular Dichroic Intensities in the Vibronic Transitions of Chiral Metal Complexes

FREDERICK S. RICHARDSON

Department of Chemistry, University of Virginia, Charlottesville, VA 22901

The chiroptical properties of optically active transition metal complexes have played an enormously influential role in the stereochemical and electronic structural characterization of metal coordination compounds. Werner's early work (1) in resolving the optical isomers of bis- and tris-chelated transition metal complexes containing achiral ligands established the octahedral structure of hexa-coordinated complexes and posed the problems of molecular stereochemistry and absolute configuration of metal coordination compounds. In the 1930's, the optical rotatory properties of Werner's complexes were studied extensively by Jaeger (2), Mathieu (3), and Kuhn (4, 5, 6) with the objective of relating these properties to specific stereochemical features (most notably, the absolute configuration) of the systems. Attempts were also made to construct a theory of optical activity in transition metal complexes which would permit systematic correlation of the observed optical rotatory (and circular dichroic) properties with absolute configuration (4, 5). These latter attempts employed a classical representation of the metal ion and ligand electronic structure (and electronic transitions), and they were restricted to treating only those optical rotatory properties associated with absorptions occurring in the visible region of the spectrum.

The first definitive determination of the absolute configuration of a chiral metal complex was reported by Saito and coworkers (7) in 1955 using the anomalous x-ray scattering method. Saito and coworkers (7) found that the tris(ethylenediamine)-cobalt(III) isomer which is dextrorotatory at the sodium D-line, (+)-[Co(en)<sub>3</sub>]<sup>3+</sup>, has the  $\Lambda$ -configuration (8). This finding was contrary to the configurational assignment predicted according to the Kuhn and Bein (4, 5) classical coupled oscillator model for tris-chelated Co(III) complexes.

Moffitt (9) introduced the first quantum mechanical theory of optical activity in chiral transition metal complexes. He

adopted a crystal field model for representing the spectroscopic states of the metal ion  $d$ -electrons, and used the "one-electron" theory of molecular optical activity proposed by Condon, Alter, and Eyring (10) to develop expressions for the rotatory strengths of the metal ion  $d-d$  (ligand field) transitions. Moffitt's work marked the advent of "modern" developments in the theory of optical activity in transition metal complexes. Many of the theoretical developments in transition metal complex optical activity during the 1960's and early 1970's were based on the fundamental aspects of Moffitt's model. However, several theories and models have been developed and proposed which represent major departures from Moffitt's simple one-electron crystal field model (11, 12). These include theories which represent the wave functions of the spectroscopic states in terms of molecular orbital models (of varying degrees of sophistication and completeness), and independent systems/perturbation models which include both static (point charge crystal field) and dynamic (ligand polarization) metal ion-ligand interactions. Furthermore; theoretical treatments have been expanded to include consideration of the optical activity associated with metal $\leftrightarrow$ ligand charge-transfer transitions and intra-ligand transitions, as well as with the metal  $d-d$  transitions (11, 12).

The primary objectives of nearly all of the theoretical studies carried out on transition metal complex optical activity have been to calculate electronic rotatory strengths and to correlate the signs and magnitudes of these electronic rotatory strengths with specific stereochemical and electronic structural features of a given system. The stereochemical features of primary interest have been absolute configuration, conformational features in the ligand environment (or in chelate rings), and local distortions within the metal ion-donor atom coordination cluster. The electronic structural features of primary interest have been identities (assignments) of electronic transitions and their magnetic dipole versus electric dipole character.

The rotatory strength associated with an electronic transition  $o \rightarrow m$  may be written as

$$R_{om} = \sum_v \sum_\mu R_{ov,m\mu} N_v(T) \quad (1)$$

where  $R_{ov,m\mu}$  is a vibronic rotatory strength defined by

$$R_{ov,m\mu} = \text{Im} \langle \psi_o \phi_{ov} | \hat{\underline{\mu}} | \psi_m \phi_{m\mu} \rangle \cdot \langle \psi_m \phi_{m\mu} | \hat{\underline{m}} | \psi_o \phi_{ov} \rangle \quad (2)$$

and  $N_v(T)$  is a normalized Boltzmann weighting factor reflecting the population of the  $v$ -th vibrational level of the ground electronic state ( $o$ ) at temperature  $T$ . In Eq. (2),  $\hat{\underline{\mu}}$  and  $\hat{\underline{m}}$  are the electric and magnetic dipole moment operators, respectively,  $\phi_{ov}$  and  $\phi_{m\mu}$  are vibrational wave functions, and  $\psi_o$  and  $\psi_m$  are electronic wave functions. In writing Eq. (2), we have assumed the Born-Oppenheimer adiabatic approximation and we take  $\psi_o$  and  $\psi_m$

to be eigenfunctions of the electronic Hamiltonian of the system. In the Born-Oppenheimer adiabatic approximation, electronic motion is fully correlated with the nuclear positions (instantaneous static configurations), but is not correlated with nuclear motion. In this approximation, the vibronic wave functions have well-defined electronic and vibrational quantum numbers.

In cases where the adiabatic Born-Oppenheimer approximation breaks down, Eqs. (1) and (2) are no longer appropriate since the system cannot exist in stationary states with well-defined electronic quantum numbers. In these cases, the system can be viewed as sampling different parts of the electronic configurational space as the nuclei vibrate. These cases can be expected to occur when electron-nuclear vibrational coupling (vibronic coupling) is large and when there are degenerate or nearly degenerate electronic states in the system. A breakdown in the adiabatic Born-Oppenheimer approximation for degenerate states is referred to as the Jahn-Teller (JT) effect, and a breakdown of this approximation in the presence of nearly degenerate states is commonly referred to as the pseudo Jahn-Teller (PJT) effect. In the nonadiabatic approximation, the vibronic wave functions of the system must be expressed as

$$\Psi_j = \sum_n \sum_v C_{j,nv} \psi_n \phi_{nv} \quad (3)$$

where, now, the composite vibronic quantum number  $j$  is the only "good" quantum number for designating molecular states, and the  $\{\psi_n \phi_{nv}\}$  are the adiabatic Born-Oppenheimer vibronic wave functions. The expansion coefficients,  $C_{j,nv}$ , reflect electron-nuclear vibrational coupling.

In cases where the adiabatic approximation breaks down, the only well-defined transitions are vibronic transitions with rotatory strengths given by

$$R_{ij} = \text{Im} \langle \Psi_i | \hat{\underline{m}} | \Psi_j \rangle \cdot \langle \Psi_j | \hat{\underline{m}} | \Psi_i \rangle \quad (4)$$

(for the vibronic transition  $i \rightarrow j$ ). If strong vibronic coupling exists only within a small, well-defined subset of molecular electronic states, then it may be possible to calculate a net electronic rotatory strength for transitions to these states by summing over all the vibronic rotatory strengths associated with vibronic levels falling within the manifold of coupled electronic states. Only in this context does the term, electronic rotatory strength, have any meaning in the presence of very strong vibronic coupling (and a consequent breakdown of the adiabatic Born-Oppenheimer approximation).

This excursion into electronic versus vibronic rotatory strengths and the adiabatic versus the nonadiabatic approximation may be highly relevant to the detailed interpretation of transition metal complex chiroptical spectra. In most optically active transition metal complexes, the symmetry of the metal ion-donor atom cluster remains rather high (nearly  $O_h$  or nearly  $D_{4h}$ ) and, as a result, it is common to find many near-degeneracies (or even exact degeneracies) among the spectroscopic states of interest. Even in

the presence of low-symmetry ligand fields, there remains uncertainty regarding the relative perturbative strengths of vibronic coupling versus low-symmetry ligand field potentials in influencing the detailed nature of the spectroscopic states in a metal complex. In fact, in some cases strong vibronic coupling can serve to quench or moderate ligand field effects, and in other cases it can lead to amplification of ligand field effects (13). Clearly, in dealing with the chiroptical spectra of transition metal complexes it is important to be cognizant of the possible influences of vibronic coupling upon the spectral details. In particular, great care must be exercised in making spectra-structure correlations based on the assignment of specific spectral features to well-defined (pure) electronic transitions.

Concern about the possible influence of vibronic interactions upon the CD spectra of transition metal complexes was first expressed by R.G. Denning (14). Denning proposed that the  $^1T_{1g}$  excited state of  $Co(en)_3^{3+}$  undergoes a strong (tetragonal) Jahn-Teller distortion via coupling to an  $e_g$  vibrational mode of the  $CoN_6$  cluster. This strong tetragonal JT distortion was then presumed to be effective in "quenching" the crystal field induced trigonal splitting of the  $^1T_{1g}$  state (a manifestation of the so-called Ham effect) in  $Co(en)_3^{3+}$ . Denning (14) further suggested that the two CD bands observed in the region of the  $^1A_{1g} \rightarrow ^1T_{1g}$  transition in  $Co(en)_3^{3+}$  arise from two different JT vibronic states derived from  $^1T_{1g}-e_g$  coupling, rather than from the two trigonal components ( $^1E$  and  $^1A_2$ ) of the  $^1T_{1g}$  electronic state. The influence of Jahn-Teller and pseudo Jahn-Teller interactions upon the CD spectra of the d-d transitions in transition metal complexes has been studied in considerable detail (theoretically) by Richardson and coworkers (15, 16, 17, 18, 19). These latter studies included consideration of metal complexes belonging to trigonally symmetric structural classes (16), as well as metal complexes of pseudo-tetragonal symmetry (15, 17, 18). The main conclusion of these studies was that whereas vibronic interactions of the JT and PJT types (within the manifold of d-d excited states) will not, in general, alter the net (or total) d-d rotatory strength for a given system, they can play a dominant role in determining how CD intensity is distributed throughout the d-d transition region. It was found that in the presence of strong JT and PJT interactions among the d-d states, it becomes impossible (or meaningless) to assign specific features in the CD spectra to specific d-d electronic transitions. The individual CD bands, in such cases, will generally reflect "mixed" electronic parentage.

In those cases where the adiabatic approximation can be assumed to hold, the influence of vibronic coupling on the spectroscopic properties of a system can be treated within the Herzberg-Teller (perturbative) formalism (20) for vibronic interactions. This formalism is applicable when the vibronic interaction energies are small compared to the energy spacings between the

coupled electronic states. Vibronic rotatory strengths and circular dichroism spectra, considered within the adiabatic approximation and the Herzberg-Teller (HT) formalism, have been treated in considerable detail by Weigang and coworkers (21, 22, 23). Weigang concentrated primarily on the CD of organic chromophores in his applications of the theory. Vibronically induced coupling of the d-d spectroscopic states to odd-parity (ungerade) electronic states of transition metal complexes plays a significant (and sometimes dominant) role in determining the observed dipole strengths and absorption intensities of d-d transitions. The possible influence of these vibronic interactions upon d-d rotatory strengths has been considered qualitatively by M.J. Harding (24) using Weigang's theory. However, no detailed or quantitative studies have been reported on this problem.

Bray, Ferguson, and Hawkins (25) have applied the vibronic coupling model of Perrin and Gouterman (26) in their interpretation of the CD spectra produced by the coupled ligand→ligand (molecular exciton) transitions in tris complexes of 1,10-phenanthroline and 2,2'-bipyridine with Zn(II) and Ni(II). This problem involving a trimer comprised of three trigonally disposed interacting monomer units (ligand chromophores) is formally analogous to the problem involving a trigonally perturbed  $T_{1g}$  state (treated by Richardson, et al., (16) for  $Co(en)_3^{3+}$ ). In the weak (vibronic) coupling limit, electronic rotatory strengths are well-defined; whereas in the strong (vibronic) coupling limit, one can only speak of vibronic rotatory strengths of mixed electronic composition.

In the present study, we shall re-examine the theory of vibronic coupling in chiral transition metal complexes as it pertains to rotatory strength calculations and to the interpretation of the observed CD spectra for these systems. We shall focus primarily on the d-d (ligand-field) transitions, and shall consider vibronic coupling both within the manifold of d-electron states and between the d-electron states and higher energy charge-transfer, ligand-ligand, and metal ion Rydberg states.

## II. Theory

A. General Aspects. We shall consider as model systems six-coordinate trigonal dihedral ( $D_3$ ) metal complexes in which the metal ion-donor atom cluster ( $ML_6$ ) has near-octahedral ( $O_h$ ) symmetry. Furthermore, we shall restrict our attention to vibronic interactions involving only those vibrational modes which are localized within the  $ML_6$  cluster (the so-called "cluster modes"). The  $ML_6$  cluster has 15 vibrational degrees-of-freedom which, assuming octahedral ( $O_h$ ) symmetry, can be described in terms of six normal coordinates:  $Q_1(a_{1g})$ ,  $Q_2(e_g)$ ,  $Q_3(t_{1u})$ ,  $Q_4(t_{1u})$ ,  $Q_5(t_{2g})$ , and  $Q_6(t_{2u})$ . For a trigonally distorted ( $D_3$ )  $ML_6$  cluster, ten normal coordinates are required to describe the 15 vibrational degrees-of-freedom. We shall denote the normal coordinates of the

American Chemical  
Society Library

1155 16th St. N. W.

In Stereochemistry of Optically Active Transition Metal Compounds; Douglas, B., et al.; ACS Symposium Series; American Chemical Society: Washington, DC, 1980.

Washington, D. C. 20036

trigonally distorted  $ML_6$  system by:  $Q_1(a_1)$ ,  $Q_2(e)$ ,  $Q_{3a}(a_2)$ ,  $Q_{3e}(e)$ ,  $Q_{4a}(a_2)$ ,  $Q_{4e}(e)$ ,  $Q_{5a}(a_1)$ ,  $Q_{5e}(e)$ ,  $Q_{6a}(a_1)$ , and  $Q_{6e}(e)$ . If the trigonal distortion is assumed small, then we can expect the trigonal modes to reflect strong octahedral parentage. Thus, for example, the  $Q_{3a}(a_2)$  and  $Q_{3e}(e)$  trigonal modes are expected to correlate strongly with the  $Q_3(t_{1u})$  octahedral mode.

We shall write the vibrational-electronic (vibronic) Hamiltonian of the system as

$$H(r, Q) = H_e(r, Q) + T_v(Q), \quad (5)$$

where  $T_v(Q)$  is the kinetic energy operator for nuclear vibrational motion within the  $ML_6$  cluster, and  $H_e(r, Q)$  is the electronic Hamiltonian operator defined by

$$H_e(r, Q) = T_e(r) + V(r, Q). \quad (6)$$

In Eq. (6),  $T_e(r)$  is the kinetic energy operator for the electrons and  $V(r, Q)$  is the total potential energy operator for the system. The collection of electron coordinates is denoted by  $\{r\}$  and the collection of normal coordinates for the  $ML_6$  cluster is denoted by  $\{Q\}$ . Expanding  $V(r, Q)$  in the normal coordinates  $\{Q\}$  about the equilibrium nuclear configuration of the  $ML_6$  cluster, we may write

$$V(r, Q) = V^0(r) + \sum_{\alpha} V'_{\alpha} Q_{\alpha} + \left(\frac{1}{2}\right) \sum_{\alpha} \sum_{\beta} V''_{\alpha\beta} Q_{\alpha} Q_{\beta} + \dots, \quad (7)$$

where  $V'_{\alpha} = [\partial V(r, Q)/\partial Q_{\alpha}]_0$ ,  $V''_{\alpha\beta} = [\partial^2 V(r, Q)/\partial Q_{\alpha} \partial Q_{\beta}]_0$ , and  $\alpha$  and  $\beta$  label normal coordinates of the  $ML_6$  system. The term  $V^0(r)$  represents the potential energy of the complete system with the nuclei clamped in their equilibrium positions. The operator  $V^0(r)$  has trigonal dihedral ( $D_3$ ) symmetry and may be written as

$$V^0(r) = V^0_O + V^0_T, \quad (8)$$

where  $V^0_O$  is the octahedral ( $O_h$ ) part of  $V^0(r)$  and  $V^0_T$  is the trigonal dihedral ( $D_3$ ) part of  $V^0(r)$ . The ungerade components of  $V^0_T$  reflect the chirality of the system.

The second and third terms in Eq. (7) are vibronic coupling terms and their influence on the electronic properties of the system will be treated by perturbation techniques. In our perturbation treatment we define the zeroth-order electronic Hamiltonian to be

$$H^0_e(r) = T_e(r) + V^0(r), \quad (9)$$

with eigenfunctions  $\psi_n^0$  obtained as solutions to the Schrödinger equation

$$H^0_e(r) \psi_n^0(r) = E_n^0 \psi_n^0(r). \quad (10)$$



In the so-called "crude adiabatic approximation", the zeroth-order vibronic wave functions may be written as

$$\Psi_{n\nu}^0(\mathbf{r}, Q) = \psi_n^0(\mathbf{r}) \phi_{n\nu}(Q), \quad (11)$$

where the vibrational wave functions  $\phi_{n\nu}(Q)$  are found as solutions to

$$[T_\nu(Q) + V^0(\mathbf{r}) + (\frac{1}{2}) \sum_{\alpha} V''_{\alpha\alpha} Q_{\alpha}^2] \phi_{n\nu}(Q) = W_{n\nu}^0 \phi_{n\nu}(Q). \quad (12)$$

In writing Eq. (12) we have assumed the harmonic approximation for vibrational motions of the  $ML_6$  nuclei.

In our perturbation treatment of vibronic interactions the wave functions defined by Eq. (11) comprise our zeroth-order basis set, and the perturbation Hamiltonian is given by

$$H'(\mathbf{r}, Q) = H_E(\mathbf{r}, Q) - H_E^0(\mathbf{r}) \quad (13)$$

or,

$$H'(\mathbf{r}, Q) = \sum_{\alpha} V'_{\alpha} Q_{\alpha} + (\frac{1}{2}) \sum_{\alpha} \sum_{\beta} V''_{\alpha\beta} Q_{\alpha} Q_{\beta} \quad (14)$$

including terms linear and quadratic in the normal coordinates  $\{Q\}$ . The "perturbed" vibronic wave functions may be expressed as

$$\Psi_j = \sum_{n} \sum_{\nu} C_{j,n\nu} \psi_n^0(\mathbf{r}) \phi_{n\nu}(Q) \quad (15)$$

where the expansion coefficients,  $C_{j,n\nu}$ , are to be found by diagonalizing  $(H_E^0 + H')$  in the basis set  $\{\psi_n^0(\mathbf{r}) \phi_{n\nu}(Q)\}$ .

B. Co(III) Systems. The model described above (in Section II.A.) is applicable to any six-coordinate system of trigonal dihedral ( $D_3$ ) symmetry. To illustrate the applications of the model, we consider here six-coordinate Co(III) complexes of  $D_3$  symmetry in which the Co(III) ion resides in a "strong" crystal field. In this case, the ground state of the complex is non-degenerate with  $A_1(A_{1g})$  symmetry and the  $d$ -electron (singlet) excited states are of symmetry types  $A_2(T_{1g})$ ,  $E(T_{1g})$ ,  $A_1(T_{2g})$  and  $E(T_{2g})$ . A schematic energy level diagram is given in Figure 1 for these  $d$ -electron states and for two additional states of  $T_{1u}$  octahedral parentage,  $A_2(T_{1u})$  and  $E(T_{1u})$ . The latter states may be assumed to be derived either from metal $\leftrightarrow$ ligand charge-transfer excitations or from a  $d^5p$  metal ion configuration. The electric dipole (ED) and magnetic dipole (MD) selection rules governing transitions between the  $A_1(A_{1g})$  ground state and the excited states shown in Figure 1 are summarized as follows:

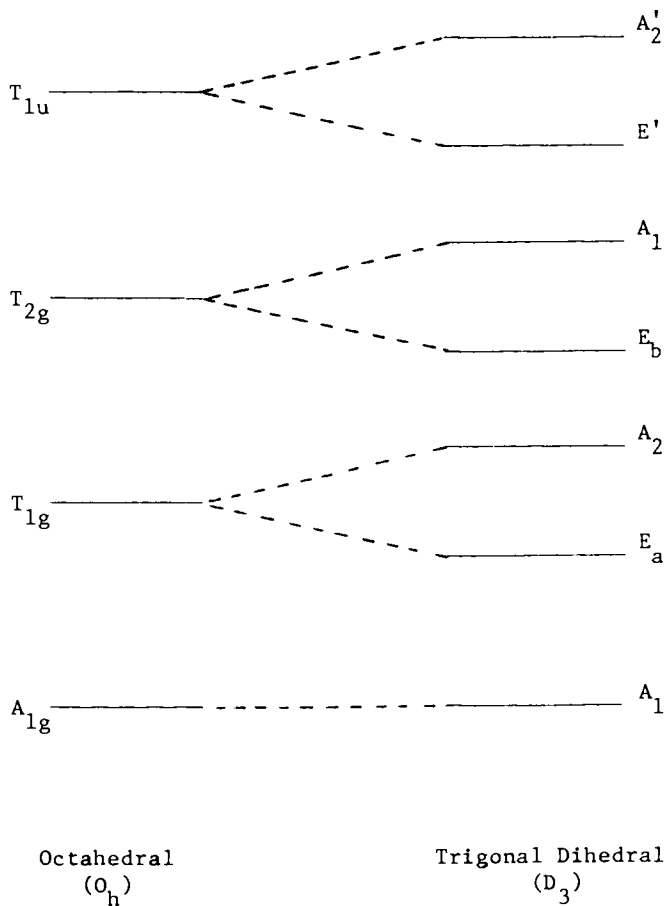


Figure 1. Schematic energy-level diagram for a Co(III) complex

| <u>Excited State</u>              | <u>O<sub>h</sub></u> | <u>D<sub>3</sub></u> |
|-----------------------------------|----------------------|----------------------|
| A <sub>2</sub> (T <sub>1g</sub> ) | MD                   | MD(z), ED(z)         |
| E (T <sub>1g</sub> )              | MD                   | MD(x,y), ED(x,y)     |
| A <sub>1</sub> (T <sub>2g</sub> ) | --                   | --                   |
| E (T <sub>2g</sub> )              | --                   | MD(x,y), ED(x,y)     |
| A <sub>2</sub> (T <sub>1u</sub> ) | ED                   | MD(z), ED(z)         |
| E (T <sub>1u</sub> )              | ED                   | MD(x,y), ED(x,y)     |

where the polarization designations (x,y,z) refer to a trigonal coordinate system (with the z-axis coincident with the C<sub>3</sub> symmetry axis of the system). Assuming strong octahedral parentage, the A<sub>1</sub>(A<sub>1g</sub>)→A<sub>2</sub>(T<sub>1g</sub>) and E(T<sub>1g</sub>) transitions may be expected to exhibit relatively strong optical activity and only weak absorptivity, whereas the A<sub>1</sub>(A<sub>1g</sub>)→A<sub>2</sub>(T<sub>1u</sub>) and E(T<sub>1u</sub>) transitions may be expected to exhibit strong optical activity and strong absorptivity. The A<sub>1</sub>(A<sub>1g</sub>)→A<sub>1</sub>(T<sub>2g</sub>) and E(T<sub>2g</sub>) transitions would be expected to exhibit relatively weak optical activity and weak absorptivity. These expectations based on symmetry selection rules reflecting strong octahedral parentage are generally borne out by experimental observation.

In our analysis of the model Co(III) systems we shall assume strong octahedral parentage for the electronic states and for the CoL<sub>6</sub> vibrational modes. We shall further assume that the ground electronic state A<sub>1</sub>(A<sub>1g</sub>) remains unaffected by vibronic interactions. Given these assumptions, the principal influences of the Q<sub>2</sub>(e<sub>g</sub>) and Q<sub>5</sub>(t<sub>2g</sub>) vibrational modes are to (1) cause Jahn-Teller (JT) and pseudo Jahn-Teller (PJT) distortions within the T<sub>1g</sub>, T<sub>2g</sub>, and T<sub>1u</sub> excited states, and (2) induce mixing between the T<sub>1g</sub> and T<sub>2g</sub> excited states. These effects will be manifested in the intensity distributions within the A<sub>1g</sub>→T<sub>1g</sub> and A<sub>1g</sub>→T<sub>2g</sub> d-d transitions, but they will not significantly alter the net (or total) CD and absorption intensities of these transitions. On the other hand, the Q<sub>3</sub>(t<sub>1u</sub>), Q<sub>4</sub>(t<sub>1u</sub>), and Q<sub>6</sub>(t<sub>2u</sub>) vibrational modes will be effective in mixing the T<sub>1u</sub> excited state with the T<sub>1g</sub> and T<sub>2g</sub> excited states. This will lead to a redistribution of electric dipole intensity out of the A<sub>1g</sub>→T<sub>1u</sub> transition and into the A<sub>1g</sub>→T<sub>1g</sub> and A<sub>1g</sub>→T<sub>2g</sub> d-d transitions.

In what follows, we shall first examine the influence of T<sub>1g</sub>\* (t<sub>2g</sub> + e<sub>g</sub>) coupling on the CD spectrum of the Co(III) A<sub>1g</sub>→T<sub>1g</sub> transition (neglecting all other vibronic interactions). Secondly, we shall examine the influence of the t<sub>2g</sub>(Q<sub>5</sub>) and e<sub>g</sub>(Q<sub>2</sub>) vibrational modes on the A<sub>1g</sub>→T<sub>2g</sub> CD spectrum via vibronically induced T<sub>1g</sub>-T<sub>2g</sub> mixings. Finally, we shall consider T<sub>1g</sub>-T<sub>1u</sub> and T<sub>2g</sub>-T<sub>1u</sub> mixings under the influence of vibronic interactions with the t<sub>1u</sub>(Q<sub>3</sub> and Q<sub>4</sub>) and t<sub>2u</sub>(Q<sub>6</sub>) vibrational modes.

C. T<sub>1g</sub>\* (t<sub>2g</sub>+e<sub>g</sub>) Coupling. To terms linear in Q<sub>α</sub>, the vibronic Hamiltonian for this case may be written as

$$H(r, Q) = H_E^0(r) + (h_2 + h_{5e} + h_{5a}) + (V_{2+}' Q_{2+} + V_{2-}' Q_{2-} + V_{5e+}' Q_{5e+} + V_{5e-}' Q_{5e-} + V_{5a}' Q_{5a}), \quad (16)$$

where  $H_E^0(r)$  is defined by Eq. (9),  $h_\alpha$  is the harmonic oscillator Hamiltonian for the  $\alpha$ -th trigonal vibrational mode, and  $V_\alpha' Q_\alpha$  is the linear vibronic coupling term for the  $Q_\alpha$  mode. The + and - subscripts denote components of the doubly degenerate vibrational modes,  $Q_2$  and  $Q_{5e}$ . It is understood that all of the operators appearing in Eq. (16) are defined for the trigonally distorted  $T_{1g}(A_2 + E)$  electronic state of the Co(III) model system. Having defined our vibrational coordinates with respect to the trigonally distorted equilibrium geometry of the  $CoL_6$  cluster,  $V_{5a}' = 0$  and the linear coupling term  $V_{5a}' Q_{5a}$  vanishes in Eq. (16).

We denote the trigonal components of the  $T_{1g}$  electronic state by  $\psi_0^0(A_2)$ ,  $\psi_+^0(E)$ , and  $\psi_-^0(E)$ . These functions are eigenfunctions of the operator  $H_E^0(r)$ , and they have the symmetry properties  $C_3 \psi_0^0 = \psi_0^0$ ,  $C_3 \psi_+^0 = \omega \psi_+^0$ , and  $C_3 \psi_-^0 = \omega^* \psi_-^0$ , where  $\omega = \exp(2\pi i/3)$  and  $C_3$  is the threefold rotation operator of the  $D_3$  point group. The doubly degenerate vibrational modes may be conveniently expressed in polar coordinate form as

$$Q_{2+} = \rho_2 \exp(i\phi), \quad Q_{2-} = \rho_2 \exp(-i\phi)$$

and,

$$Q_{5e+} = \rho_{5e} \exp(i\phi'), \quad Q_{5e-} = \rho_{5e} \exp(-i\phi')$$

with  $C_3 Q_{2+} = \omega Q_{2+}$ ,  $C_3 Q_{2-} = \omega^* Q_{2-}$ , and similarly for  $Q_{5e+}$  and  $Q_{5e-}$ . The effects of the  $Q_2$  and  $Q_{5e}$  vibrational modes will be to render the  $E(\psi_+^0, \psi_-^0)$  electronic state Jahn-Teller unstable and to couple the  $E(\psi_+^0, \psi_-^0)$  and  $A_2(\psi_0^0)$  states via a pseudo Jahn-Teller mechanism.

The vibronic wave function for the  $T_{1g}^*(t_{2g} + e_g)$  system may be expressed as

$$\Psi = \psi_0^0(\chi_2^{(o)} + \chi_{5e}^{(o)} + \chi_{5a}^{(o)}) + \psi_+^0(\chi_2^{(+)} + \chi_{5e}^{(+)} + \chi_{5a}^{(+)}) + \psi_-^0(\chi_2^{(-)} + \chi_{5e}^{(-)} + \chi_{5a}^{(-)}). \quad (17)$$

The vibronic energy levels and vibrational amplitude functions ( $\chi_\alpha^{(o)}$ ,  $\chi_\alpha^{(+)}$ , and  $\chi_\alpha^{(-)}$ ), where  $\alpha = 2, 5e$ , or  $5a$ ) may be found by solving the secular equation, Eq. (18). In this matrix equation,

$$H_E^0(r) \psi_\pm^0 = E_\pm^0 \psi_\pm^0, \quad (19)$$

$$H_E^0(r) \psi_0^0 = E_0^0 \psi_0^0 \quad (20)$$

and the interaction matrix elements,  $E_{ij}$  and  $T_{ij}$ , are given by

$$E_{ij} = \langle \psi_i^0 | V_{2+}' Q_{2+} + V_{2-}' Q_{2-} | \psi_j^0 \rangle, \quad (21)$$



and,

$$T_{ij} = \langle \psi_i^0 | V_{5e+}^i Q_{5e+} + V_{5e-}^i Q_{5e-} | \psi_j^0 \rangle. \quad (22)$$

Symmetry arguments require that

$$E_{+0} = E_{0-} = E_{-0}^* = E_{0+}^* = \gamma_2 Q_{2+} = \gamma_2 \rho_2 \exp(i\phi), \quad (23)$$

$$T_{+0} = T_{0-} = T_{-0}^* = T_{0+}^* = \gamma_{5e} Q_{5e+} = \gamma_{5e} \rho_{5e} \exp(i\phi'), \quad (24)$$

$$E_{+-} = E_{-+}^* = k_2 Q_{2-} = k_2 \rho_2 \exp(-i\phi), \quad (25)$$

and,

$$T_{+-}^* = T_{-+} = k_{5e} Q_{5e-} = k_{5e} \rho_{5e} \exp(-i\phi'), \quad (26)$$

where the linear coupling constants for the PJT interactions,  $\gamma_\alpha$ , are defined by

$$\gamma_\alpha = \langle \psi_+^0 | (\partial V / \partial Q_{\alpha+})_0 | \psi_0^0 \rangle = \langle \psi_+^0 | V_{\alpha+}^i | \psi_0^0 \rangle, \quad \alpha \equiv 2 \text{ or } 5e. \quad (27)$$

The linear coupling constant for the JT interactions,  $k_\alpha$ , are defined by

$$k_\alpha = \langle \psi_+^0 | (\partial V / \partial Q_{\alpha-})_0 | \psi_0^0 \rangle = \langle \psi_+^0 | V_{\alpha-}^i | \psi_0^0 \rangle, \quad \alpha \equiv 2 \text{ or } 5e. \quad (28)$$

The matrix equation (18) is block-diagonal (as shown) only if the coupling modes,  $\alpha = 2, 5e$ , and  $5a$ , are mutually orthogonal. The two-dimensional harmonic oscillator Hamiltonians for the  $\alpha = 2$  and  $5e$  modes are given by

$$h_\alpha = \left(\frac{1}{2}\right) \omega_\alpha^2 \rho_\alpha^2 - \left(\frac{1}{2}\right) [(\partial^2 / \partial \rho_\alpha^2) + (1/\rho_\alpha)(\partial / \partial \rho_\alpha) + (1/\rho_\alpha)^2 (\partial^2 / \partial \phi^2)]. \quad (29)$$

The eigenfunctions of  $h_\alpha$  may be obtained from solutions to

$$h_\alpha \chi_{\alpha, v\ell} = \epsilon_{\alpha, v\ell} \chi_{\alpha, v\ell} = (v_\alpha + 1) \hbar \omega_\alpha \chi_{\alpha, v\ell} \quad (30)$$

where the quantum numbers  $v$  and  $\ell$  can take on the values,  $v = 0, 1, 2, \dots$  and  $\ell = v, v-2, \dots, -v$ . For  $\alpha = 5a$ , we write

$$h_\alpha \chi_{\alpha, v} = \epsilon_{\alpha, v} \chi_{\alpha, v} = (v_\alpha + \frac{1}{2}) \hbar \omega_\alpha \chi_{\alpha, v} \quad (31)$$

where  $h_\alpha$  is a one-dimensional harmonic oscillator Hamiltonian expressed in terms of  $Q_{5a}$ .

It is now convenient to expand the vibrational amplitude functions ( $\chi_\alpha^{(0)}$ ,  $\chi_\alpha^{(+)}$ , and  $\chi_\alpha^{(-)}$ ) appearing in Eqs. (17) and (18) in terms of basis sets constructed from the eigensolutions of Eqs. (30) and (31). Upon doing this, the eigensolutions of Eq. (18) may be expressed as

$$\begin{aligned}
 \Psi_j = & \psi_o^o \left( \sum_{\nu\lambda} A_{j\nu\lambda}^{(o)} \chi_{2,\nu\lambda}^{(o)} + \sum_{\nu\lambda} B_{j\nu\lambda}^{(o)} \chi_{5e,\nu\lambda}^{(o)} + \sum_{\nu} C_{j\nu}^{(o)} \chi_{5a,\nu}^{(o)} \right) \\
 & + \psi_+^o \left( \sum_{\nu\lambda} A_{j\nu\lambda}^{(+)} \chi_{2,\nu\lambda}^{(+)} + \sum_{\nu\lambda} B_{j\nu\lambda}^{(+)} \chi_{5e,\nu\lambda}^{(+)} + \sum_{\nu} C_{j\nu}^{(+)} \chi_{5a,\nu}^{(+)} \right) \\
 & + \psi_-^o \left( \sum_{\nu\lambda} A_{j\nu\lambda}^{(-)} \chi_{2,\nu\lambda}^{(-)} + \sum_{\nu\lambda} B_{j\nu\lambda}^{(-)} \chi_{5e,\nu\lambda}^{(-)} + \sum_{\nu} C_{j\nu}^{(-)} \chi_{5a,\nu}^{(-)} \right) \quad (32)
 \end{aligned}$$

Eq. (32) gives the vibronic wave functions for the  $T_{1g}^*(t_{2g} + e_g)$  coupled system within the linear coupling approximation. The expansion coefficients  $A_{j\nu\lambda}^{(\lambda)}$ ,  $B_{j\nu\lambda}^{(\lambda)}$ , and  $C_{j\nu}^{(\lambda)}$  (where  $\lambda = o, -, \text{ or } +$  and correspond to electronic states  $\psi_o^o$ ,  $\psi_-^o$ , and  $\psi_+^o$ , respectively) are found by solving Eq. (18). The vibrational functions,  $\chi_{\alpha,\nu\lambda}^{(\lambda)}$  ( $\alpha = 2$  or  $5e$ ), are obtained from Eq. (30) for the appropriate  $\lambda(o, -, \text{ or } +)$  and the vibrational functions,  $\chi_{5a,\nu}^{(\lambda)}$ , are obtained from Eq. (31) for the appropriate  $\lambda$ .

For a more complete description of the vibronic levels associated with the  $T_{1g}(A_2 + E)$  electronic excited state, the wave functions  $\Psi_j$  [Eq. (32)] must be augmented to include vibrational wave functions associated with all of the normal modes other than  $\alpha = 2, 5a$ , and  $5e$ . Here we shall restrict our attention to just those vibronic levels derived from the vibrational modes  $\alpha = 2, 5a$ , and  $5e$ . Assuming no vibronic couplings involving the ground electronic state of our model system, the rotatory strength of a transition between the lowest vibrational level of the ground electronic state and the  $j$ -th vibronic level of the  $T_{1g}^*(t_{2g} + e_g)$  coupled state may be written as

$$R_j = \text{Im} \langle \psi_g^o \phi_{g0} | \hat{\underline{\mu}} | \Psi_j \rangle \cdot \langle \Psi_j | \hat{\underline{m}} | \psi_g^o \phi_{g0} \rangle \quad (33)$$

where  $\psi_g^o$  is the electronic wave function for the  $A_1(A_{1g})$  ground state of our model system and  $\phi_{g0}$  is the vibrational wave function for the ground vibrational level of the ground electronic state. In expanded form, Eq. (33) may be written as

$$\begin{aligned}
 R_j = & \sum_{\lambda} R_{\lambda}^{(e)} \left[ \sum_{\alpha,\nu,\lambda} \sum_{\alpha',\nu',\lambda'} D_{j\nu\lambda}^{(\lambda)} D_{j\nu'\lambda'}^{(\lambda)*} \right. \\
 & \left. \times S_{\alpha}^{(\lambda)}(g0|\nu\lambda) S_{\alpha'}^{(\lambda)}(\nu'\lambda'|g0) \right], \quad (34)
 \end{aligned}$$

where,

$$R_{\lambda}^{(e)} = \text{Im} \langle \psi_g^o | \hat{\underline{\mu}} | \psi_{\lambda}^o \rangle \cdot \langle \psi_{\lambda}^o | \hat{\underline{m}} | \psi_g^o \rangle \quad (35)$$

defines the purely electronic rotatory strength associated with the  $\psi_g^o \rightarrow \psi_{\lambda}^o$  ( $\lambda = o, -, \text{ or } +$ ) transition and

$$S_{\alpha}^{(\lambda)}(g0|\nu\lambda) = \langle \chi_{\alpha,o}^{(g)} | \chi_{\alpha,\nu\lambda}^{(\lambda)} \rangle \quad (36)$$

is a Franck-Condon overlap integral over the ground state vibrational function  $\chi_{\alpha,0}^{(g)}$  and the excited state vibrational function  $\chi_{\alpha,v\ell}^{(\lambda)}$  for the  $\alpha$ -th normal mode ( $\alpha = 2, 5a$ , or  $5e$  and  $\lambda = o, -,$  or  $+$ ). For  $\alpha = 5a$ ,  $\ell = \ell' = 0$  for all values of  $v$ . The coefficients  $D_{jv\ell}^{(\lambda)}(\alpha)$  are defined by:

$$D_{jv\ell}^{(\lambda)}(2) = A_{jv\ell}^{(\lambda)},$$

$$D_{jv\ell}^{(\lambda)}(5e) = B_{jv\ell}^{(\lambda)},$$

and,

$$D_{jv\ell}^{(\lambda)}(5a) = C_{jv}^{(\lambda)},$$

where the coefficients  $A_{jv\ell}^{(\lambda)}$ ,  $B_{jv\ell}^{(\lambda)}$ , and  $C_{jv}^{(\lambda)}$  are as defined in Eq. (32). The complex conjugate of  $D_{jv\ell}^{(\lambda)}(\alpha)$  is denoted by  $D_{jv\ell}^{(\lambda)*}(\alpha)$ .

If we make the simplifying assumption that the vibrational wave functions of the ground(g) and excited( $\lambda$ ) electronic states are identical, then Eq. (34) reduces to

$$\begin{aligned} R_j &= R_o^{(e)} [ |A_{joo}^{(o)}|^2 + |B_{joo}^{(o)}|^2 + |C_{jo}^{(o)}|^2 ] \\ &+ R_+^{(e)} [ |A_{joo}^{(+)}|^2 + |B_{joo}^{(+)}|^2 + |C_{jo}^{(+)}|^2 ] \\ &+ R_-^{(e)} [ |A_{joo}^{(-)}|^2 + |B_{joo}^{(-)}|^2 + |C_{jo}^{(-)}|^2 ] \end{aligned} \quad (37)$$

or,

$$R_j = \sum_{\lambda} R_{\lambda}^{(e)} \sum_{\alpha} |D_{joo(\alpha)}^{(\lambda)}|^2. \quad (38)$$

In trigonally distorted systems,  $T_{1g}^*(t_{2g} + e_g)$  coupling is represented more precisely as  $(A_2 + E)^*(a_1 + 2e)$ , where trigonal splitting of the  $T_{1g}$  electronic state has been taken into account and the trigonal components of the  $t_{1g}$  and  $e_g$  vibrational modes appear explicitly. To our knowledge, a full computational treatment of the  $(A_2 + E)^*(a_1 + 2e)$  coupling problem has never been reported. However, several detailed computational studies on the simpler  $(A_2 + E)^*e$  coupling problem have been reported (27, 28). Two of these studies (16, 28) dealt specifically with the influence of  $(A_2 + E)^*e$  coupling on the chiroptical spectra of trigonal dihedral systems. Richardson, et al., (16) presented a formalism for  $(A_2 + E)^*e$  vibronic rotatory strengths which included both linear and quadratic coupling terms. However, in their numerical calculations of rotatory strength spectra, these workers did not include contributions from the quadratic coupling terms. Zgierski and Pawlikowski (28) adopted the formal model presented by Richardson (16), and carried out numerical calculations of vibronic energy levels and vibronic rotatory strength spectra which included linear  $(A_2 + E)^*e$  pseudo Jahn-



Teller couplings and both linear and quadratic E\*e Jahn-Teller couplings.

According to the restricted model adopted in this section (II.C.), all of the rotatory strength associated with the  $A_{1g}(A_1) \rightarrow T_{1g}(A_2 + E)$  electronic transition is distributed among the vibronic levels derived from  $(A_2 + E) \cdot (a_1 + 2e)$  couplings. The total (or net) rotatory strength of the  $A_{1g} \rightarrow T_{1g}$  transition is, therefore, given by

$$R(A_{1g} \rightarrow T_{1g}) = \sum_j R_j = R_o^{(e)} + R_+^{(e)} + R_-^{(e)}, \quad (39)$$

where  $R_j$  is defined by Eq. (34) and the  $R_\lambda^{(e)}$  ( $\lambda = o, -, \text{ or } +$ ) are defined by Eq. (35). The "static" stereochemical and structural features of the metal complex determine the sign and magnitude of  $R(A_{1g} \rightarrow T_{1g})$  as well as the signs and magnitudes of the electronic rotatory strengths  $R_o^{(e)}$ ,  $R_+^{(e)}$ , and  $R_-^{(e)}$ . The chiral aspects of these "static" structural features are described by the potential energy operator,  $V_T^O(r)$ , of Eq. (8). The total (or net)  $A_{1g} \rightarrow T_{1g}$  rotatory strength is invariant to  $T_{1g} \cdot (t_{2g} + e_g)$  vibronic coupling. Only the distribution of electronic rotatory strength among the component vibronic transitions is affected by the  $T_{1g} \cdot (t_{2g} + e_g)$  couplings.

The vibronic coupling model described in this section (II.C.) is highly restricted insofar as only linear coupling terms have been included explicitly, and only two e-type trigonal modes (those derived from the  $t_{2g}$  and  $e_g$  octahedral  $CoL_6$  cluster modes) have been considered. It is relatively easy to extend our treatment to include quadratic coupling terms. However, the inclusion of additional e-type trigonal modes (e.g., those derived from the  $t_{2u}$  and  $t_{1u}$  octahedral modes) would drastically complicate our model. This latter extension of the model should not prove necessary so long as the  $CoL_6$  cluster retains very nearly octahedral symmetry (i.e.,  $V_T^O \ll V_O$  in Eq. (8)).

D.  $(T_{1g} + T_{2g}) \cdot (t_{2g} + e_g)$  Coupling. By octahedral ( $O_h$ ) selection rules, the  $A_{1g} \rightarrow T_{1g}$  transition in  $CoL_6$  systems is magnetic dipole allowed whereas the  $A_{1g} \rightarrow T_{2g}$  transition is magnetic dipole forbidden. Using the notation of Figure 1, the trigonal ( $D_3$ ) selection rules specify that the  $A_1(A_{1g}) \rightarrow A_2(T_{1g})$ ,  $E_a(T_{1g})$ , and  $E_b(T_{2g})$  trigonal transitions are magnetic dipole allowed, while the  $A_1(A_{1g}) \rightarrow A_1(T_{2g})$  transition remains magnetic dipole forbidden. In the usual perturbation treatments of optical activity in trigonal dihedral  $Co(III)$  complexes, it is assumed that the  $A_1 \rightarrow E_b$  component of the erstwhile  $A_{1g} \rightarrow T_{2g}$  transition "borrows" magnetic dipole character (and, therefore, rotatory strength) from the  $A_1 \rightarrow E_a$  component of the  $A_{1g} \rightarrow T_{1g}$  transition. This is assumed to occur via  $T_{1g} - T_{2g}$  mixing induced by the gerade components of the trigonal field potential,  $V_T^O$ . By this model, the sign and magnitude of the  $A_1(A_{1g}) \rightarrow E_b(T_{2g})$  rotatory strength (and CD) may be correlated directly to that of the

$A_1(A_{1g}) \rightarrow E_a(T_{1g})$  transition. The  $A_{1g} \rightarrow T_{1g}$  CD would not reflect any aspects of the  $A_1 \rightarrow A_2$  component of the  $A_{1g} \rightarrow T_{1g}$  transition. This picture is altered drastically when vibronic coupling effects are taken into account. Vibronic coupling may enter into this problem in several ways. First, both the  $T_{1g}$  and  $T_{2g}$  states are subject to "intra-state" couplings of the types (for example):  $T_{1g}^*(t_{2g} + e_g)$  and  $T_{2g}^*(t_{2g} + e_g)$ . Secondly, "inter-state" coupling of the type  $(T_{1g} + T_{2g})^*(t_{2g} + e_g)$  may become important. We shall examine the possible influence of this latter ("inter-state") type of coupling here.

Trigonal e-type modes (derived, for example, from the  $t_{2g}$  or  $e_g$  octahedral modes) can effect the following "inter-state" couplings of trigonal electronic components:  $(E_a + E_b)^*e$ ,  $(E_a + A_1)^*e$ , and  $(A_2 + E_b)^*e$ . This has the consequence that vibronic components of the  $A_1(A_{1g}) \rightarrow A_1(T_{2g})$  transition can exhibit a non-vanishing CD which has been "borrowed" from the  $A_1(A_{1g}) \rightarrow E_a(T_{1g})$  transition. Furthermore, vibronic components of the  $A_1(A_{1g}) \rightarrow E_b(T_{2g})$  transition may exhibit CD "borrowed" from both the  $A_1 \rightarrow E_a$  and  $A_1 \rightarrow A_2$  trigonal components of the  $A_{1g} \rightarrow T_{1g}$  transition. Heretofore, the appearance of multiple components in the  $A_{1g} \rightarrow T_{2g}$  CD region has always been attributed to the presence of multiple species types or to a reduction of symmetry (from  $D_3$  to  $C_3$ ) in the complex under study. Strong  $T_{1g} - T_{2g}$  mixing under the influence of an e-type trigonal vibrational mode is, perhaps, a more likely cause for the appearance of multiple components in the  $A_{1g} \rightarrow T_{2g}$  CD spectrum.

Detailed studies of  $(T_{1g} + T_{2g})^*(t_{2g} + e_g)$  coupling to octahedral systems and of  $(A_2 + E_a + A_1 + E_b)^*e$  coupling in trigonal systems have not yet been carried out. Such studies including numerical computations would be extremely complex. However, the qualitative consequences of such couplings on the CD spectra of chiral trigonal systems may be discerned readily following the arguments given above. In brief,  $(A_2 + E_a + A_1 + E_b)^*e$  coupling can be expected to lead to CD of mixed sign and mixed polarization in the  $A_{1g} \rightarrow T_{2g}$  transition region, reflecting the sign and polarization properties of the  $A_1(A_{1g}) \rightarrow A_2(T_{1g}) + E_a(T_{1g})$  CD bands.

E.  $(T_{1g}+T_{1u})^*(t_{1u}+t_{2u})$  Coupling. This type of coupling is the basis for the so-called Herzberg-Teller (HT) vibronic theory of d-d intensities in octahedral ( $O_h$ ) transition metal complexes. In this theory applied to  $CoL_6$ , the  $A_{1g} \rightarrow T_{1g}$  transition is assumed to gain electric dipole character via vibronically induced  $T_{1g} - T_{1u}$  mixing under the influence of an ungerade vibrational mode (of either  $t_{1u}$  or  $t_{2u}$  symmetry). (Here we shall ignore vibronically induced mixing of the  $A_{1g}$  ground state with ungerade excited states, and consider only vibronic perturbations on the excited state  $T_{1g}$ .) The low-temperature  $A_{1g} \rightarrow T_{1g}$  electric dipole (absorption) spectrum is, then, predicted to consist of three progressions based on false origins located at  $0-1(\omega_3)$ ,

$0-1(\omega_4)$ , and  $0-1(\omega_6)$ , where  $\omega_3$ ,  $\omega_4$ , and  $\omega_6$  are the fundamental frequencies of the  $Q_3(t_{1u})$ ,  $Q_4(t_{1u})$ , and  $Q_6(t_{2u})$  normal modes, respectively. Strong Jahn-Teller distortions within the  $T_{1g}$  and/or  $T_{1u}$  states would, of course, tend to complicate this simple three-progression spectrum.

In trigonal dihedral complexes of "near" octahedral symmetry:  $T_{1g} \rightarrow A_2 + E_a$  and  $T_{1u} \rightarrow A_2' + E'$  (using the notation of Figure 1). In these systems, the  $A_{1g}(A_1) \rightarrow T_{1g}(A_2 + E_a)$  transition has inherent electric dipole strength due to the ungerade components of the "static" trigonal field potential  $V_T^0$ . However, additional electric dipole character may be introduced into this transition via  $(A_2 + E_a + A_2' + E')$ \*e coupling, where the coupling mode is an e-type trigonal vibration. A complete treatment of  $(A_2 + E_a + A_2' + E')$ \*e coupling would require simultaneous consideration of intra-state vibronic interactions (Jahn-Teller and pseudo Jahn-Teller interactions within both  $T_{1g}$  and  $T_{1u}$ ) and inter-state vibronic interactions (of the Herzberg-Teller type between  $T_{1g}$  and  $T_{1u}$ ). Furthermore, all e-type trigonal modes should be considered independent of their octahedral parentage. In the present treatment, we shall adopt a much more restricted model in which only inter-state ( $T_{1g} - T_{1u}$ ) interactions are considered and in which only those e-type trigonal modes of  $t_{1u}$  or  $t_{2u}$  octahedral ancestry are taken into account. This latter restriction to vibrational modes derived from the  $t_{1u}$  and  $t_{2u}$  octahedral vibrations should be acceptable so long as the  $CoL_6$  cluster remains very nearly octahedral and  $V_T^0 \ll V_O^0$ .

Given the approximations cited above, we take  $|A_2\rangle$ ,  $|E_a\rangle$ ,  $|A_2'\rangle$ , and  $|E'\rangle$  to be eigenfunctions of the trigonally symmetric electronic Hamiltonian defined in Eq. (9),  $H_E^0(r) = T_E(r) + V^0(r)$ . We further define a (linear) vibronic interaction operator

$$H'(r, Q) = \sum_{\alpha} V_{\alpha}' Q_{\alpha} \quad (40)$$

where  $\sum_{\alpha}$  is taken over the e-type trigonal modes derived from the  $Q_3(t_{1u})$ ,  $Q_4(t_{1u})$ , and  $Q_6(t_{2u})$  octahedral modes. That is,  $\alpha = 3e, 4e$ , and  $6e$  (see Section II.A. for notation). Restricting our consideration to  $T_{1g} - T_{1u}$  inter-state mixings and using first-order time-independent perturbation theory, we may express the perturbed wave functions of interest as follows:

$$|A_2\rangle = |A_2\rangle + \sum_{\alpha} \lambda_{\alpha}(E', A_2) |E'\rangle Q_{\alpha} \quad (41)$$

$$|E_a\rangle = |E_a\rangle + \sum_{\alpha} \lambda_{\alpha}(E', E_a) |E'\rangle Q_{\alpha} + \sum_{\alpha} \lambda_{\alpha}(A_2', E_a) |A_2'\rangle Q_{\alpha} \quad (42)$$

where,

$$\lambda_{\alpha}(i, j) = (\psi_i^0 | V_{\alpha}' | \psi_j^0) (E_j^0 - E_i^0)^{-1} \quad (43)$$

is a perturbation expansion coefficient. (Note that the perturbed wave functions are denoted by pointed kets  $|\dot{\phantom{a}}\rangle$ , whereas the unperturbed wave functions are denoted by rounded kets  $|\phantom{a}\rangle$ ). Having restricted our perturbation treatment to  $T_{1g} - T_{1u}$  inter-state interactions, it is easy to see that the wave functions expressed by Eqs. (41) and (42) are actually good to first- and second-order in  $H'$ . We shall ignore all vibronic perturbations on the ground electronic state of our Co(III) model system, so that:

$$|A_1\rangle = |A_1\rangle. \quad (44)$$

Utilizing Eqs. (41), (42), and (44), the electric and magnetic dipole transition moments for the  $A_1 \rightarrow A_2$  and  $E_a$  transitions may be expressed (to second-order) as

$$\langle A_1 | \hat{O} | A_2 \rangle = \langle A_1 | \hat{O} | A_2 \rangle + \sum_{\alpha} \lambda_{\alpha}(E', A_2) Q_{\alpha} \langle A_1 | \hat{O} | E' \rangle \quad (45)$$

and

$$\begin{aligned} \langle A_1 | \hat{O} | E_a \rangle &= \langle A_1 | \hat{O} | E_a \rangle + \sum_{\alpha} \lambda_{\alpha}(E', E_a) Q_{\alpha} \langle A_1 | \hat{O} | E' \rangle \\ &\quad + \sum_{\alpha} \lambda_{\alpha}(A_2', E_a) Q_{\alpha} \langle A_1 | \hat{O} | A_2' \rangle, \end{aligned} \quad (46)$$

where  $\hat{O} = \hat{\underline{\mu}}$  or  $\hat{\underline{m}}$ . The rotatory strengths for these transitions, expressed to second-order, are given by

$$\begin{aligned} R(A_1 \rightarrow A_2) &= R^{(0)}(A_1 \rightarrow A_2) \\ &\quad + R^{(0)}\{A_1 \rightarrow E'\} \sum_{\alpha} \sum_{\alpha'} \lambda_{\alpha}(E', A_2) \lambda_{\alpha'}(E', A_2) Q_{\alpha} Q_{\alpha'}, \end{aligned} \quad (47)$$

and,

$$\begin{aligned} R(A_1 \rightarrow E_a) &= R^{(0)}\{A_1 \rightarrow E_a\} \\ &\quad + R^{(0)}\{A_1 \rightarrow E'\} \sum_{\alpha} \sum_{\alpha'} \lambda_{\alpha}(E', E_a) \lambda_{\alpha'}(E', E_a) Q_{\alpha} Q_{\alpha'}, \\ &\quad + R^{(0)}\{A_1 \rightarrow A_2'\} \sum_{\alpha} \sum_{\alpha'} \lambda_{\alpha}(A_2', E_a) \lambda_{\alpha'}(A_2', E_a) Q_{\alpha} Q_{\alpha'}, \\ &\quad + \text{Im}[(A_a | \hat{\underline{\mu}} | E_a) \cdot (E' | \hat{\underline{m}} | A_1)] \\ &\quad + (A_1 | \hat{\underline{\mu}} | E') \cdot (E_a | \hat{\underline{m}} | A_1) \sum_{\alpha} \lambda_{\alpha}(E', E_a) Q_{\alpha}, \end{aligned} \quad (48)$$

where

$$R^{(0)}\{i \rightarrow j\} = \text{Im}(\psi_i^0 | \hat{\underline{\mu}} | \psi_j^0) \cdot (\psi_j^0 | \hat{\underline{m}} | \psi_i^0). \quad (49)$$

Now let us consider a specific vibronic transition leading from the ground vibrational level of the ground electronic state (go) to the  $\nu(\beta)$  vibrational level of the excited electronic

state  $(e\nu(\beta))$ . In the present context,  $g$  refers to the  $A_1$  electronic ground state and  $e$  may be either the  $A_2$  or  $E_a$  electronic excited state of our Co(III) model system.  $\beta$  denotes the vibrational mode containing the  $\nu$  quanta in the vibronic level  $e\nu(\beta)$ . Denoting the initial and final vibrational wave functions by  $\phi_{g_0}$  and  $\phi_{e\nu(\beta)}$ , respectively, we may write for the vibronic rotatory strengths

$$R_{o,\nu(\beta)}(A_1 \rightarrow A_2) = R^{(o)}(A_1 \rightarrow A_2) |\langle \phi_{g_0} | \phi_{e\nu(\beta)} \rangle|^2 \\ + R^{(o)}(A_1 \rightarrow E') \sum_{\alpha} \sum_{\alpha'} \lambda_{\alpha}(E', A_2) \lambda_{\alpha'}(E', A_2) \\ \times \langle \phi_{g_0} | Q_{\alpha} | \phi_{e\nu(\beta)} \rangle \langle \phi_{e\nu(\beta)} | Q_{\alpha'} | \phi_{g_0} \rangle, \quad (50)$$

and,

$$R_{o,\nu(\beta)}(A_1 \rightarrow E_a) = R^{(o)}(A_1 \rightarrow E_a) |\langle \phi_{g_0} | \phi_{e\nu(\beta)} \rangle|^2 \\ + R^{(o)}(A_1 \rightarrow E') \sum_{\alpha} \sum_{\alpha'} \lambda_{\alpha}(E', E_a) \lambda_{\alpha'}(E', E_a) \\ \times \langle \phi_{g_0} | Q_{\alpha} | \phi_{e\nu(\beta)} \rangle \langle \phi_{e\nu(\beta)} | Q_{\alpha'} | \phi_{g_0} \rangle \\ + R^{(o)}(A_1 \rightarrow A_2') \sum_{\alpha} \sum_{\alpha'} \lambda_{\alpha}(A_2', E_a) \lambda_{\alpha'}(A_2', E_a) \\ \times \langle \phi_{g_0} | Q_{\alpha} | \phi_{e\nu(\beta)} \rangle \langle \phi_{e\nu(\beta)} | Q_{\alpha'} | \phi_{g_0} \rangle \\ + \text{Im}[(A_1 | \hat{\underline{\mu}} | E_a) \cdot (E' | \hat{\underline{m}} | A_1) + (A_1 | \hat{\underline{\mu}} | E') \cdot (E_a | \hat{\underline{m}} | A_1)] \\ \times \sum_{\alpha} \lambda_{\alpha}(E', E_a) \langle \phi_{g_0} | Q_{\alpha} | \phi_{e\nu(\beta)} \rangle \langle \phi_{e\nu(\beta)} | \phi_{g_0} \rangle, \quad (51)$$

where  $\phi_{e\nu(\beta)}$  has been chosen to be real. Choosing the perturbing modes  $\{\alpha\}$  to be nontotally symmetric (e-type trigonal modes) and mutually orthogonal, and assuming identical symmetries in the ground and excited electronic states, Eqs. (50) and (51) may be reduced to the following forms:

$$R_{o,\nu(\beta)}(A_1 \rightarrow A_2) = R^{(o)}(A_1 \rightarrow A_2) |\langle \phi_{g_0} | \phi_{e\nu(\beta)} \rangle|^2 \\ + R^{(o)}(A_1 \rightarrow E') \sum_{\alpha} |\lambda_{\alpha}(E', A_2)|^2 |\langle \phi_{g_0} | Q_{\alpha} | \phi_{e\nu(\beta)} \rangle|^2 \delta_{\alpha\beta}, \quad (52)$$

and,

$$\begin{aligned}
R_{o,v(\beta)}(A_1 \rightarrow E_a) &= R^{(o)}(A_1 \rightarrow E_a) |\langle \phi_{go} | \phi_{ev(\beta)} \rangle|^2 \\
&+ R^{(o)}(A_1 \rightarrow E') \Sigma_{\alpha} |\lambda_{\alpha}(E', E_a)|^2 |\langle \phi_{go} | Q_{\alpha} | \phi_{ev(\beta)} \rangle|^2 \delta_{\alpha\beta} \\
&+ R^{(o)}(A_1 \rightarrow A_2') \Sigma_{\alpha} |\lambda_{\alpha}(A_2', E_a)|^2 |\langle \phi_{go} | Q_{\alpha} | \phi_{ev(\beta)} \rangle|^2 \delta_{\alpha\beta}, \quad (53)
\end{aligned}$$

where  $\delta_{\alpha\beta} = 1$  for  $\alpha = \beta$  and  $\delta_{\alpha\beta} = 0$  for  $\alpha \neq \beta$ . For the case  $\beta = \alpha$ , we have

$$\begin{aligned}
R_{o,v(\alpha)}(A_1 \rightarrow A_2) &= R^{(o)}(A_1 \rightarrow A_2) |\langle \phi_{go} | \phi_{ev(\alpha)} \rangle|^2 \\
&+ R^{(o)}(A_1 \rightarrow E') |\lambda_{\alpha}(E', A_2)|^2 |\langle \phi_{go} | Q_{\alpha} | \phi_{ev(\alpha)} \rangle|^2, \quad (54)
\end{aligned}$$

and,

$$\begin{aligned}
R_{o,v(\alpha)}(A_1 \rightarrow E_a) &= R^{(o)}(A_1 \rightarrow E_a) |\langle \phi_{go} | \phi_{ev(\alpha)} \rangle|^2 \\
&+ [R^{(o)}(A_1 \rightarrow E') |\lambda_{\alpha}(E', E_a)|^2 \\
&+ R^{(o)}(A_1 \rightarrow A_2') |\lambda_{\alpha}(A_2', E_a)|^2] |\langle \phi_{go} | Q_{\alpha} | \phi_{ev(\alpha)} \rangle|^2. \quad (55)
\end{aligned}$$

In the absence of both intra-state and inter-state vibronic couplings, the leading (first) terms in Eqs. (52) and (53), respectively, will govern the vibronic rotatory strengths associated with the  $A_1 \rightarrow A_2$  and  $A_1 \rightarrow E_a$  electronic transitions. Neglecting inter-state couplings (such as, for example, between  $T_{1g}$  and  $T_{1u}$ ), but allowing intra-state coupling within  $T_{1g}$  would lead to vibronic rotatory strength expressions involving a combination of the first terms appearing in Eqs. (52) and (53). This latter case is just that treated previously in Section II.C. Eqs. (52) and (53) are appropriate only when intra-state coupling is neglected and when inter-state coupling is confined to  $T_{1g} - T_{1u}$ .

If we make the additional simplifying assumption that the normal modes of the ground(g) and excited(e) electronic states are identical and can be described by harmonic force fields, then we have for the vibrational integrals of Eqs. (54) and (55):

$$\langle \phi_{go} | \phi_{ev(\alpha)} \rangle = 0, \quad v(\alpha) \neq 0 \quad (56a)$$

$$= 1, \quad v(\alpha) = 0 \quad (56b)$$

and,

$$\langle \phi_{go} | Q_{\alpha} | \phi_{ev(\alpha)} \rangle = 0, \quad v(\alpha) \neq 1(\alpha) \quad (57a)$$

$$= 1, \quad v(\alpha) = 1(\alpha) \quad (57b)$$

where  $Q_\alpha$  has been taken to be dimensionless. In this limiting case, all of the vibronically induced ("borrowed") rotatory strength arising from  $T_{1g} - T_{1u}$  inter-state coupling will appear in the  $0-1(\alpha)$  vibronic lines of the  $A_1 \rightarrow A_2$  and  $A_1 \rightarrow E_a$  electronic transitions ( $\alpha =$  any of the e-type trigonal modes which are effective in promoting  $T_{1g} - T_{1u}$  coupling).

The total (or net) rotatory strengths associated with the  $A_1 \rightarrow A_2$  and  $A_1 \rightarrow E_a$  transitions in the presence of inter-state  $T_{1g} - T_{1u}$  coupling are given by:

$$R_{\text{net}}(A_1 \rightarrow A_2) = \sum_{\beta} \sum_{\nu(\beta)} R_{o,\nu(\beta)}(A_\alpha \rightarrow A_2) = R^{(o)}(A_1 \rightarrow A_2) + R^{(o)}(A_1 \rightarrow E') \sum_{\alpha} |\lambda_{\alpha}(E', A_2)|^2 \langle \phi_{go} | Q_{\alpha}^2 | \phi_{go} \rangle, \quad (58)$$

and,

$$R_{\text{net}}(A_1 \rightarrow E_a) = \sum_{\beta} \sum_{\nu(\beta)} R_{o,\nu(\beta)}(A_1 \rightarrow E_a) = R^{(o)}(A_1 \rightarrow E_a) + R^{(o)}(A_1 \rightarrow E') \sum_{\alpha} |\lambda_{\alpha}(E', E_a)|^2 \langle \phi_{go} | Q_{\alpha}^2 | \phi_{go} \rangle + R^{(o)}(A_1 \rightarrow A_2^!) \sum_{\alpha} |\lambda_{\alpha}(A_2^!, E_a)|^2 \langle \phi_{go} | Q_{\alpha}^2 | \phi_{go} \rangle, \quad (59)$$

where  $\sum_{\beta}$  goes over all vibrational modes and  $\sum_{\alpha}$  goes over all effective coupling (perturbing) modes. Finally, the net rotatory strength associated with the  $A_{1g} \rightarrow T_{1g}$  transition is given by:

$$R_{\text{net}}(A_{1g} \rightarrow T_{1g}) = R_{\text{net}}(A_1 \rightarrow A_2) + R_{\text{net}}(A_1 \rightarrow E_a) = R^{(o)}(A_1 \rightarrow A_2) + R^{(o)}(A_1 \rightarrow E_a) + \sum_{\alpha} [R^{(o)}(A_1 \rightarrow E') |\lambda_{\alpha}(E', A_2)|^2 + R^{(o)}(A_1 \rightarrow E') |\lambda_{\alpha}(E', E_a)|^2 + R^{(o)}(A_1 \rightarrow A_2^!) |\lambda_{\alpha}(A_2^!, E_a)|^2] \langle \phi_{go} | Q_{\alpha}^2 | \phi_{go} \rangle. \quad (60)$$

In the special case where  $R^{(o)}(A_1 \rightarrow A_2) = -R^{(o)}(A_1 \rightarrow E_a)$ , as in Moffitt's theory of  $d-d$  optical activity in trigonal ( $D_3$ ) Co(III) complexes (9, 12), Eq. (60) reduces to

$$R_{\text{net}}(A_{1g} \rightarrow T_{1g}) = \sum_{\alpha} \langle \phi_{go} | Q_{\alpha}^2 | \phi_{go} \rangle \{ R^{(o)}(A_1 \rightarrow E') \times [|\lambda_{\alpha}(E', A_2)|^2 + |\lambda_{\alpha}(E', E_a)|^2] + R^{(o)}(A_1 \rightarrow A_2^!) |\lambda_{\alpha}(A_2^!, E_a)|^2 \}. \quad (61)$$

Making the further assumption (in the spirit of Moffitt's simple model) that  $R^{(O)}\{A_1 \rightarrow E'\} = -R^{(O)}\{A_1 \rightarrow A_2'\}$ , Eq. (61) further reduces to

$$R_{\text{net}}(A_{1g} \rightarrow T_{1g}) = R^{(O)}\{A_1 \rightarrow A_2'\} \sum_{\alpha} \langle \phi_{gO} | Q_{\alpha}^2 | \phi_{gO} \rangle [ |\lambda_{\alpha}(A_2', E_a)|^2 - |\lambda_{\alpha}(E', E_a)|^2 - |\lambda_{\alpha}(E', A_2)|^2 ]. \quad (62)$$

Note that the assumptions made in obtaining Eq. (62) also require that

$$R_{\text{net}}(A_{1g} \rightarrow T_{1g}) + R_{\text{net}}(A_{1g} \rightarrow T_{1u}) = 0 \quad (63)$$

The simple formal analysis outlined above reveals several interesting aspects of the  $A_{1g} \rightarrow T_{1g}$  CD predicted for chiral Co(III) complexes of trigonal dihedral symmetry. First,  $(A_2 + E_a + A_2' + E')$ \*e coupling can lead to mixed polarization within the vibronic CD band envelopes of both the  $A_1 \rightarrow A_2$  and  $A_1 \rightarrow E_a$  transitions. In the absence of vibronic coupling, the  $A_1 \rightarrow A_2$  transition would be polarized parallel to the trigonal axis of the system, whereas the  $A_1 \rightarrow E_a$  transition would be polarized perpendicular to the trigonal axis. In the presence of vibronic coupling, vibronic components of both parallel and perpendicular polarization may appear in both the  $A_1 \rightarrow A_2$  and  $A_1 \rightarrow E_a$  CD bands. Secondly, from Eqs. (61) and (62) we see that the net CD associated with the  $A_{1g} \rightarrow T_{1g}$  transition need not vanish even when the zeroth-order net electronic rotatory strength,  $R^{(O)}\{A_1 \rightarrow A_2\} + R^{(O)}\{A_1 \rightarrow E_a\}$ , is zero.

The analysis given here for the vibronic rotatory strengths associated with the  $A_1 \rightarrow A_2$  and  $A_1 \rightarrow E_a$  transitions has ignored all perturbations of the ground electronic state ( $A_1$ ) due to vibronic coupling. Inclusion of vibronic perturbations involving the ground state, such as  $[A_1(A_{1g}) + E']$ \*e coupling, would not lead to any additional, qualitatively new predictions regarding the  $A_{1g} \rightarrow T_{1g}$  CD spectrum.

**F. Summary of Qualitative Conclusions.** In considering the influence of vibronic coupling in the  $d-d$  CD spectra of trigonal dihedral Co(III) systems, we have examined three general cases. First we examined vibronic interactions within the  $T_{1g}(A_2 + E_a)$  excited state of Co(III). These interactions are of the Jahn-Teller and pseudo Jahn-Teller types and require a non-adiabatic vibronic coupling formalism. The principal effects of these interactions are redistributions of rotatory strength among the vibronic components of the  $A_1 \rightarrow A_2$  and  $E_a$  transitions. Secondly, we examined vibronically induced mixings between the  $T_{1g}(A_2 + E_a)$  and  $T_{2g}(A_1 + E_b)$  excited states. Qualitatively we showed that  $(A_2 + E_a + A_1 + E_b)$ \*e coupling could lead to nonvanishing rotatory strength in both the  $A_1 \rightarrow A_1$  and  $A_1 \rightarrow E_b$  vibronically perturbed trigonal components of the  $A_{1g} \rightarrow T_{2g}$  transitions. Con-



sequently, the  $A_{1g} \rightarrow T_{2g}$  CD could exhibit mixed polarization. Finally, we examined the possible consequences of vibronically induced  $T_{1g}(A_2 + E_a) - T_{1u}(A_2' + E')$  mixing. Here we found that vibronic components of mixed polarization can be expected within both the  $A_1 \rightarrow A_2$  and  $A_1 \rightarrow E_a$  CD bands associated with the  $A_{1g} \rightarrow T_{1g}$  transition. In this case, an adiabatic vibronic coupling formalism was assumed valid since the energy separation between the coupled electronic states could be assumed to be large compared to the vibronic coupling energy.

It is, of course, highly artificial to consider each of the above-mentioned coupling cases in isolation. For example, in considering  $T_{1g} - T_{1u}$  interactions rigorously it would be necessary to take into account simultaneously the likelihood that both  $T_{1g}(A_2 + E_a)$  and  $T_{1u}(A_2' + E')$  are both JT and PJT distorted. The same would hold true for vibronically induced  $T_{1g} - T_{2g}$  interactions. Such considerations would lead to exceedingly tedious and complicated formal manipulations and horrendous computational requirements, if one's objective was to explicate quantitatively the vibronic details of the  $A_{1g} \rightarrow T_{1g} + T_{2g}$  CD spectra of trigonal Co(III) systems. At present it would appear necessary to be content with the qualitative conclusions elicited from the less-than-complete treatments given in this section.

The vibronic coupling analysis given here has a very important implication for spectra-structure correlation studies using CD. The usual practise in such studies is to assign specific features in the CD spectra to specific electronic transitions of well-defined electronic state parentage. The intensities of these features are then assumed to be directly and simply related to pure electronic rotatory strengths, and the signs and magnitudes of these electronic rotatory strengths are then correlated with specific stereochemical features of the system (either by use of various models and theories or according to some set of empirical rules). In the presence of non-negligible vibronic interactions these procedures can, at best, be misleading and, at worst, lead to erroneous structural conclusions. Under conditions of non-negligible vibronic interactions it is not possible, in general, to assign specific CD features to transitions of well-defined electronic parentage.

Is it possible to make clear-cut spectra-structure correlations in the absence of a complete vibronic analysis of the spectra and of the systems under study? It seems likely that the net CD intensity (and net electronic rotatory strength) associated with all of the d-d transitions in a given complex will, in large part, be conserved in the presence of non-negligible vibronic interactions. This assumes, of course, that vibronically induced  $T_{1g} - T_{1u}$  mixing will generally be small. Spectra-structure correlations should be based, then, on net d-d rotatory strengths rather than on the rotatory strengths associated with specific CD bands (of uncertain or mixed electronic parentage).

The vibronic coupling theory presented in this section was developed specifically for chiral six-coordinate systems of trigonal dihedral ( $D_3$ ) symmetry, and it was applied to the  $d-d$  CD spectra of Co(III) complexes. It is, of course, similarly applicable to trigonal dihedral complexes of any transition metal ion. The formalism appropriate for analyzing vibronic coupling in chiral systems of other symmetry types is similar to that given here in all general aspects, although the symmetry-determined features will, of course, be different.

### III. Examples

A number of vibronic CD calculations have been reported in the literature for transition metal complexes. Caliga and Richardson (15) treated the general case of pairs of nearly degenerate electronic transitions coupled by a single nontotally symmetric vibrational mode. Their vibronic interaction model was based on a non-adiabatic coupling representation, and their calculations included a wide range of values for the spectroscopic and vibronic coupling parameters inherent to their model. Richardson and coworkers (17, 18) then extended this model to treat dissymmetric pseudo tetragonal (nearly  $D_{4h}$ ) metal complexes in which three nearly degenerate electronic transitions are coupled via pseudo Jahn-Teller interactions involving either two or three vibrational modes of the system. Again, model CD spectra and vibronic rotatory strengths were calculated for a wide variety of parameter sets reflecting the spectroscopic properties and vibronic coupling details of the system.

Richardson and Hilmes (19) incorporated vibronic effects into their treatment of the Cu(II)  ${}^2E_g \rightarrow {}^2T_{2g}$  CD observed in single crystals of  $ZnSeO_4 \cdot 6H_2O$  doped with Cu(II) ions. In the Cu(II): $ZnSeO_4 \cdot 6H_2O$  doped system, the Cu(II) ions are each coordinated to six water molecules with the  $CuO_6$  clusters being very nearly octahedral ( $O_h$ ). However, the exact site symmetry for each Cu(II) is  $C_2$  so that the  ${}^2E_g$  ground state is split into two nondegenerate orbital components and the  ${}^2T_{2g}$  excited state is split into three nondegenerate orbital components. In calculating the temperature dependence of the net (total) CD intensity associated with the  ${}^2E_g \rightarrow {}^2T_{2g}$  Cu(II) transition, Richardson and Hilmes (19) explicitly included pseudo Jahn-Teller type interactions within the split  ${}^2E_g$  ground state assuming a single perturbing vibrational mode. The experimentally observed temperature dependence of the  ${}^2E_g \rightarrow {}^2T_{2g}$  CD could be accounted for quantitatively only by the inclusion of these vibronic interactions within the  ${}^2E_g$  ground state.

As was mentioned previously, two computational studies of vibronic effects in chiral trigonal systems have been reported (18, 28). Both of these studies were addressed to the general problem of vibronic perturbations on the chiroptical spectra of trigonal metal complexes. However, the calculations reported in

each study were based on parameter sets closely related to the  $A_{1g} \rightarrow T_{1g}$  CD of Co(III) complexes such as  $\text{Co}(\text{en})_3^{3+}$  and  $\text{Co}(\text{ox})_3^{3-}$ . In both studies consideration of vibronic interactions was confined to Jahn-Teller and pseudo Jahn-Teller type couplings within a trigonally split excited state of  $T_{1g}$  (or  $T_{2g}$ ) octahedral parentage. In each study only a single vibrational perturbing mode of e-type trigonal symmetry was included in the computational model. The general aspects of the vibronic coupling models used in these two studies were identical to those described in Sections II.A., II.B., and II.C. of the present paper except that only a single perturbing mode was considered. In the earlier study (by Richardson, *et al.* (16)), only linear Jahn-Teller and pseudo Jahn-Teller couplings were included in the numerical calculations. In the more recent study by Zgierski and Pawlikowski (28), quadratic Jahn-Teller couplings were also included in the calculations.

To demonstrate how the simplest type of  $(A_2 + E)*e$  coupling may influence the  $A_{1g}(A_1) \rightarrow T_{1g}(A_2 + E)$  CD of a chiral trigonal dihedral ( $D_3$ ) metal complex, we shall present some results obtained by actual computations. We shall assume a single perturbing vibrational mode of e-type trigonal symmetry and of fundamental frequency  $\bar{\omega}_p$  (expressed in  $\text{cm}^{-1}$ ). We shall denote the trigonal splitting energy by  $\Delta(\text{cm}^{-1}) = (E_{A_2}^0 - E_E^0)/hc$ . Only the linear JT and PJT coupling terms will be included in the computational model. The linear JT coupling constant,  $k$ , will be defined according to Eq. (28), and the linear PJT coupling constant,  $\gamma$ , will be defined according to Eq. (27). The ratio of pure electronic rotatory strengths will be taken in all cases to be  $R_{\pm}^{(e)}:R_{\underline{0}}^{(e)}:R_{\underline{0}}^{(e)} = 1:1:-1$ , where

$$R_{\pm}^{(e)} = \text{Im}(A_1 | \hat{\underline{\mu}} | E_{\pm}) \cdot (E_{\pm} | \hat{\underline{m}} | A_1) \quad (64a)$$

and,

$$R_{\underline{0}}^{(e)} = \text{Im}(A_1 | \hat{\underline{\mu}} | A_2) \cdot (A_2 | \hat{\underline{m}} | A_1). \quad (64b)$$

The vibronic wave functions for the  $(A_2 + E)*e$  coupled excited states of our model system may be written as

$$\begin{aligned} \psi_j = & \psi_{\underline{0}}^{\underline{0}} \sum_{\underline{v}, \underline{\ell}} A_{j\underline{v}\underline{\ell}}^{(\underline{0})} \chi_{\underline{v}\underline{\ell}}^{(\underline{0})} + \psi_{+}^{\underline{0}} \sum_{\underline{v}, \underline{\ell}} A_{j\underline{v}\underline{\ell}}^{(+)} \chi_{\underline{v}\underline{\ell}}^{(+)} \\ & + \psi_{-}^{\underline{0}} \sum_{\underline{v}, \underline{\ell}} A_{j\underline{v}\underline{\ell}}^{(-)} \chi_{\underline{v}\underline{\ell}}^{(-)}, \end{aligned} \quad (65)$$

where the notation is similar to that used in Eq. (32) of Section II.C. except that here we are considering just one coupling mode (an e-type trigonal mode). The expressions and procedures outlined in Ref. 16 and in Section II.C. of the present paper may now be used to calculate the rotatory strengths of transitions originating in the ground vibrational level of the ground electronic state ( $A_1$ ) and terminating in the  $j$  vibronic levels

derived from the  $(A_2 + E)^*e$  coupled excited states.

In all of the calculations reported here we have assumed identical oscillator frequencies for the perturbing mode in the ground and excited electronic states. Furthermore, in constructing the vibronic wave functions given by Eq. (65) we have employed a harmonic oscillator basis set which included all functions with  $v \leq 10$ .

Assuming Gaussian-shaped vibronic CD bands, the CD spectrum in the vicinity of the  $A_{1g}(A_1) \rightarrow T_{1g}(A_2 + E)$  transition of our model system may be synthesized according to

$$\Delta\epsilon(\bar{\omega}) = C \sum_j (\bar{\omega}_j R_j / \delta) \exp[-(\bar{\omega} - \bar{\omega}_j)^2 / \delta^2] \quad (66)$$

where  $\Delta\epsilon = \epsilon_L - \epsilon_R$ ,  $\bar{\omega}_j$  is the transition frequency (in  $\text{cm}^{-1}$ ) for a transition to the  $j$ -th vibronic level,  $R_j$  is the vibronic rotatory strength defined according to Eq. (33),  $\delta$  is a bandwidth parameter (expressed in  $\text{cm}^{-1}$  units), and  $C$  is a constant factor whose numerical value depends, in part, on the units chosen for  $R_j$ . For our present purposes, it will be more convenient to express Eq. (66) as follows:

$$\Delta\epsilon(\Omega) = C \sum_j (\bar{\omega}_E^0 + \Omega_j) (R_j / \delta) \exp[-(\Omega - \Omega_j)^2 / \delta^2], \quad (67)$$

where  $\Omega(\text{cm}^{-1}) = \bar{\omega} - \bar{\omega}_E^0$ ,  $\Omega_j(\text{cm}^{-1}) = \bar{\omega}_j - \bar{\omega}_E^0$  and  $\bar{\omega}_E^0 = (E_E^0 - E_{A_1}^0) / hc$ . The new frequency variable,  $\Omega$ , is defined to be zero at the resonance frequency of the unperturbed, pure electronic transition  $A_1 \rightarrow E$ . In the calculations reported here we have set  $\bar{\omega}_E^0 = 20,000 \text{ cm}^{-1}$ .

CD spectra for the  $A_1 \rightarrow (A_2 + E)^*e$  transitions of our trigonal dihedral ( $D_3$ ) model system were calculated for a number of parameter sets in which the values of  $\Delta$ ,  $\gamma$ , and  $k$  were varied. These spectra are displayed in Figures 2-5. In these figures, the CD intensity scale ( $\Delta\epsilon$ ) is given in arbitrary units and the frequency scale is expressed in terms of  $\Omega(\text{cm}^{-1})$ .

The calculated spectra shown in Figures 2-5 demonstrate the profound influence which vibronic coupling may have on both the qualitative and quantitative aspects of the CD observed within the  $A_1 \rightarrow A_2 + E$  transition region. Although the net (total) rotatory strength and CD intensity remain invariant to the values of  $\Delta$ ,  $\gamma$ , and  $k$ , the distribution of CD intensity and the sign patterns within the CD spectrum are shown to be very sensitive to these parameters. The values of  $\Delta$ ,  $\gamma$ , and  $k$  will, of course, be determined to some extent by those stereochemical and electronic structural features of a complex which one wishes to elucidate via CD spectral studies. However, in nearly all spectra-structure correlation studies reported to date, the influence of vibronic coupling on the CD spectral features has been ignored or neglected. The spectra shown in Figures 2-5 reflect only the simplest kinds of vibronic interactions (intra-state JT and PJT couplings) which may influence the details of

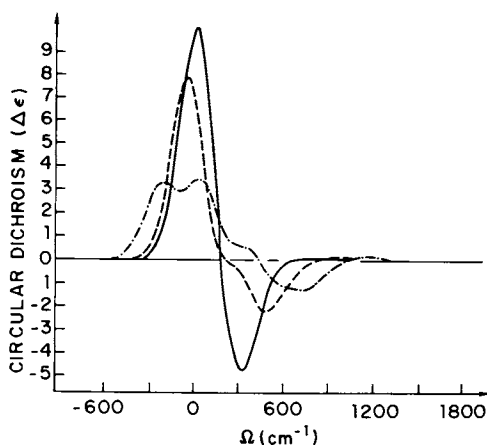


Figure 2. Calculated CD spectra for the  $A_1 \rightarrow (A_2 + E)^*e$  transitions using the parameter sets  $R_+^{(e)}:R_-^{(e)}:R_0^{(e)} = 1:1:-1$  (in arbitrary units),  $\Delta = \bar{\omega}_p = 300 \text{ cm}^{-1}$ ,  $k = 0$  and  $\gamma = 0$  (—),  $\gamma = 0.5 \bar{\omega}_p$  (---), and  $\gamma = 1.0 \bar{\omega}_p$  (- · - ·).  $\Delta\epsilon$  is expressed in arbitrary units and  $\delta$  was taken to be  $0.6 \bar{\omega}_p$ .

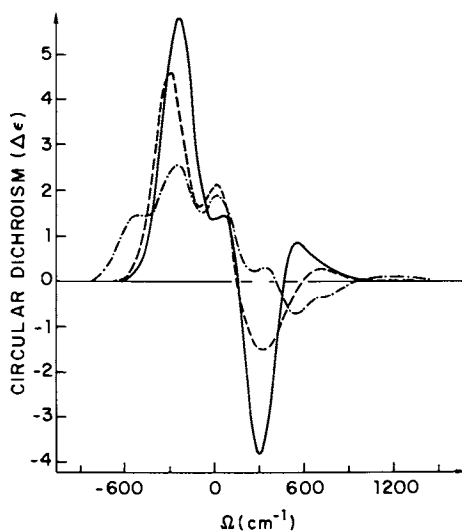


Figure 3. Calculated CD spectra for the  $A_1 \rightarrow (A_2 + E)^*e$  transitions using the parameter sets  $R_+^{(e)}:R_-^{(e)}:R_0^{(e)} = 1:1:-1$  (in arbitrary units),  $\Delta = k = \bar{\omega}_p = 300 \text{ cm}^{-1}$ , and  $\gamma = 0$  (—),  $\gamma = 0.5 \bar{\omega}_p$  (---), and  $\gamma = 1.0 \bar{\omega}_p$  (- · - ·).  $\Delta\epsilon$  is expressed in arbitrary units and  $\delta$  was taken to be  $0.6 \bar{\omega}_p$ .

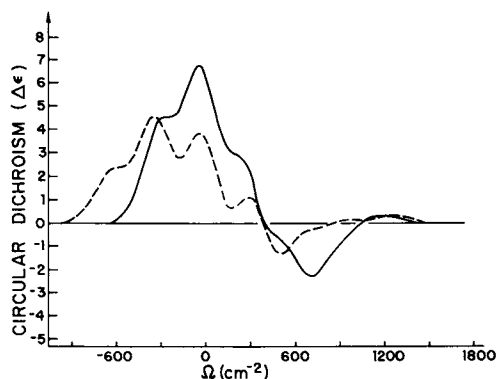


Figure 4. Calculated CD spectra for the  $A_1 \rightarrow (A_2 + E)^*e$  transitions using the parameter sets  $R_c^{(e)}:R_o^{(e)}:R_p^{(e)} = 1:1:-1$  (in arbitrary units),  $\Delta = \gamma = \bar{\omega}_p = 300 \text{ cm}^{-1}$ , and  $k = 0.5 \bar{\omega}_p$  (—) and  $k = 1.25 \bar{\omega}_p$  (---).  $\Delta\epsilon$  is expressed in arbitrary units and  $\delta$  was taken to be  $0.6 \bar{\omega}_p$ .

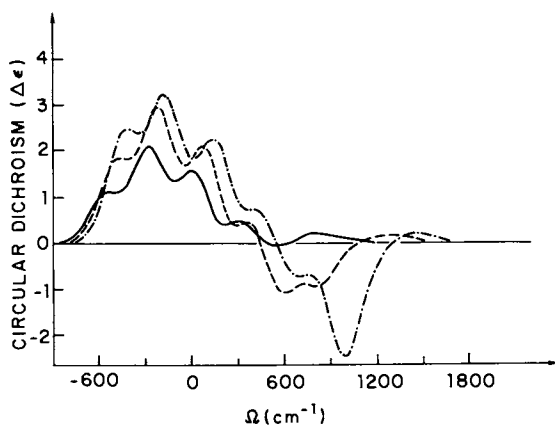


Figure 5. Calculated CD spectra for the  $A_1 \rightarrow (A_2 + E)^*e$  transitions using the parameter sets  $R_c^{(e)}:R_o^{(e)}:R_p^{(e)} = 1:1:-1$  (in arbitrary units),  $\gamma = k = \bar{\omega}_p = 300 \text{ cm}^{-1}$ , and  $\Delta = 0.5 \bar{\omega}_p$  (—),  $\Delta = 1.5 \bar{\omega}_p$  (---), and  $\Delta = 2.5 \bar{\omega}_p$  (- · - ·).  $\Delta\epsilon$  is expressed in arbitrary units and  $\delta$  was taken to be  $0.6 \bar{\omega}_p$ .

the CD spectra associated with chiral transition metal complexes. Multiple mode coupling and inter-state couplings will, in general, introduce additional complications.

#### IV. Conclusions

Modest vibronic coupling strengths in metal complexes may: (1) lead to significant mixings of "fixed-nuclei" electronic states; (2) alter the energy level spacings and orderings within spectroscopic state manifolds; (3) cause significant distortions within degenerate or nearly degenerate spectroscopic states; and, (4) preclude the assignment of transitions to initial and final states of well-defined electronic identities (quantum numbers). The consequences of non-negligible vibronic coupling in chiral metal complexes may be to: (1) produce significant alterations in CD intensity distributions (with regard to sign patterns, relative intensities, and polarization profiles); (2) require that vibronic coupling mechanisms and strengths be taken into account along with stereochemical structural factors in constructing detailed spectra-structure correlation rules; and, (3) abrogate sector (or regional) rules based on the CD observed for specific bands or spectral features.

Vibronic coupling effects on the chiroptical spectra of optically active metal complexes tend to obscure the inherent relationships between the CD observables and structural features such as absolute configuration, ligand conformation, and ligand spatial distributions. For this reason, spectra-structure relationships based on the "fixed-nuclei" approximation and on the assumption of well defined "electronic" transitions must be applied with considerable caution. A great wealth of spectroscopically and structurally important information may be obtained from detailed vibronic analyses of CD spectra. However, very few analyses of this sort have been reported to date.

#### Acknowledgments

This work was supported by the National Science Foundation (Grant CHE77-02150) and by the Camille and Henry Dreyfus Foundation (through a Teacher-Scholar Award to F.R.).

#### Literature Cited

1. "Alfred Werner, 1866-1919", Hevl. Chim. Acta, 1966, Commemoration Volume IX, ICCC, Zurich.
2. Jaeger, F.M., "Spatial Arrangements of Atomic Systems and Optical Activity", George Fisher Baker Lectures, Vol. 7, Cornell University, McGraw-Hill, New York, 1930.
3. Mathieu, J.P., "Les Theories Moleculaires du Pouvoir Rotatoire Naturel", Gauthier-Villars, Paris, 1946.

4. Kuhn, W. and Bein, K., Z. Physik. Chem., 1934, B24, 335.
5. Kuhn, W. and Bein, K., Z. Anorg. Allg. Chem., 1934, 216, 321.
6. Kuhn, W., Naturwissenschaften, 1938, 19, 289.
7. Saito, Y.; Nakatsu, K.; Shiro, M.; and Kuraya, H., Acta Crystallogr., 1955, 8, 729.
8. For the accepted nomenclature and notation regarding absolute configuration designations for coordination compounds, see: (a) "I.U.P.A.C. Information Bulletin No. 33", 1968, p. 68; (b) Inorg. Chem., 1970, 9, 1.
9. Moffitt, W., J. Chem. Phys., 1956, 25, 1189.
10. Condon, E.U.; Alter, W.; and Eyring, H., J. Chem. Phys., 1937, 5, 753.
11. Mason, S.F. in "Fundamental Aspects and Recent Developments in Optical Rotatory Dispersion and Circular Dichroism", edited by J. Ciardelli and P. Salvatore, Heyden and Son, Ltd., New York, 1973; Chapter 3.6.
12. Richardson, F.S., Chem. Rev., 1979, 79, 17.
13. See, for example: (a) Ham, F.S., Phys. Rev., 1965, A138, 1727; (b) Sturge, M.D., Solid State Physics, 1967, 20, 91; (c) Stephens, P.J., J. Chem. Phys., 1969, 51, 1995.
14. Denning, R.G., Chem. Comm., 1967, 120.
15. Caliga, D. and Richardson, F.S., Mol. Phys., 1974, 28, 1145.
16. Richardson, F.S.; Caliga, D.; Hilmes, G.; and Jenkins, J., Mol. Phys., 1975, 30, 257.
17. Richardson, F.S.; Hilmes, G.; and Jenkins, J., Theoret. Chim. Acta (Berl.), 1975, 39, 75.
18. Hilmes, G.; Caliga, D.; and Richardson, F.S., Chem. Phys., 1976, 13, 203.
19. Richardson, F.S. and Hilmes, G., Mol. Phys., 1975, 30, 237.
20. Herzberg, G. and Teller, E., Z. Physik. Chem., 1933, B21, 410.
21. Weigang, O.E., J. Chem. Phys., 1965, 43, 3609.
22. Harnung, S.E.; Ong, E.C.; and Weigang, O.E., J. Chem. Phys., 1971, 55, 5711.
23. Weigang, O.E. and Ong, E.C., Tetrahedron, 1974, 30, 1783.
24. Harding, M.J., J.C.S. Faraday II, 1972, 68, 234.
25. Bray, R.G.; Ferguson, J.; and Hawkins, C.J., Aust. J. Chem., 1969, 22, 2091.
26. Perrin, M.H. and Gouterman, M., J. Chem. Phys., 1967, 46, 1019.
27. See, for example: (a) Englman, R., "The Jahn-Teller Effect in Molecules and Crystals", Wiley-Interscience, New York, 1972, Chapter 3; (b) references 13 and 16 cited above.
28. Zgierski, M.Z. and Pawlikowski, M., J. Chem. Phys., 1979, 70, 3444.

RECEIVED September 13, 1979.



# Stereochemical Correlations in the Circular Dichroism of *d-d* and Charge-Transfer Transitions: Applications to Tris(bidentate) Complexes

PIETER E. SCHIPPER

Department of Theoretical Chemistry, The University of Sydney,  
NSW 2006, Australia

The problem of distinguishing Tweedledum from Tweedledee is not peculiar to Alice (1). Determination of absolute configurations of chiral metal complexes, apart from being of basic chemical significance, has proved an intriguing challenge to a range of techniques. Circular dichroism in particular, because of the ease of measurement, has enjoyed considerable popularity as a stereochemical probe, albeit with incommensurate success. The major difficulty lies in the interpretation of the CD spectrum in terms of some theoretical model of the complex, so that the reliability of the technique is determined largely by the validity or relevance of the theoretical model.

Empirical correlation rules and a complete molecular orbital approach may be considered to constitute the two extremes of the model approach. The many empirical rules (see, e.g. discussions and references in Hawkins' book (2)) cannot be considered model-independent in that they make the implicit assumption that the complexes to which they apply have a similarity of electronic structure and subsequently of CD spectra; the rigorous definition of the nature of the "similarity" would ultimately lead to a well-defined model. Such rules thus require a minimum specification of the model, but also result in a limited predictive power. The other extreme, namely the molecular orbital approach, requires a detailed specification of the model, and the predictive power is restricted theoretically only by computing costs and the transience of the human species.

The most fruitful approach steers the middle course of establishing simple theoretical models of the complex in terms of suitable transferable parameters which may be calculated, or determined empirically by some other technique which is, in itself, independent of the chirality of the complex. The empirical rules may then be assessed theoretically, and the range of their validity defined explicitly in terms of such parameters. The critical discussion of such a simple, unified model in terms of transferable, well-defined parameters is the main aim of this paper.

0-8412-0538-8/80/47-119-073\$05.00/0  
© 1980 American Chemical Society

Separable Chromophore Models. The normal absorption spectra of most metal complexes conveniently comprise three distinct regions: the  $d-d$  region, derived from transitions between perturbed metal  $d$  states; the charge transfer region, comprising transitions involving an electron transfer from a predominantly metal  $d$  state to some linear combination of ligating atom states (or vice versa); and finally, those bands (the chelate region) largely derived from the free ligand transitions. Each such spectral region may be ascribed to emanating from a particular section of the overall complex, called a chromophore, such that a good description (intensity and energies) of the absorption spectrum in that region may be obtained by considering wave functions localized wholly on that chromophore. By defining the chromophores in this way, it becomes possible to parametrize such quantities as electric transition moments and energies unambiguously for each chromophore, as the normal absorption spectrum will simply be that of the totality of non-interacting chromophores.

Such a definition is a crucial assumption in the approach that follows and, somewhat surprisingly, is not commonly exploited in alternative approaches. Consider, for example, the  $d-d$  transitions. If the metal ion is taken as the chromophore, it is generally impossible to get realistic energies and intensities for the normal absorption because of the importance of the metal-ligating atom overlap. Thus it is unlikely to provide a satisfactory basis for a CD model. On the other hand, if the chromophore is taken to include both the metal and the ligating atom system, both the  $d-d$  and charge transfer regions in the normal absorption spectrum may be exploited to parametrize the chromophore as much as possible. The remainder of the complex (the chelate system) then constitutes another chromophoric system.

The importance of this to the development of a CD model arises in the following way. Consider the complex to comprise two chromophores, A and B, such that A is achiral, and B is the chiral perturber. The CD at the transitions of A arises through simple coupling of A and B as described by perturbation theory, yielding expressions containing the transition moments and energies of the unperturbed chromophore. The utility of the perturbation theory therefore depends critically on the definition of the unperturbed chromophores. The dominant terms in the perturbation expansion may then be extracted unambiguously. Thus the aim of a good CD model is to define the chromophores in such a way that, ideally, (i) a single perturbation term dominates, and (ii) the quantities appearing in this term may be calculated realistically or determined empirically (e.g. from the normal absorption spectrum).

Returning to the  $d-d$  transitions as an example, the choice of a metal ion chromophore leads to a number of problems. Firstly, most of the perturbation terms will initially effect adjustments

simply to give closer agreement with the absorption spectrum. Even this will be done inadequately if the  $d-d$  spectra depend directly on the metal-ligand bonding, for then the assumption of a separable metal ion chromophore is, in itself, a bad one. Secondly, those perturbation terms describing the CD will be unnecessarily complex, and in fact those terms arising from metal-ligand bonding (involving, for example, charge transfer states) will not appear in the expressions at all, because they do not appear in the chromophore definitions. The perturbation theory in such a case has to patch up the bad chromophore, before even trying to isolate the limited CD contributions that can arise for that chromophore. The choice of the metal-ligating atom chromophore, on the other hand, leaves the perturbation theory free to isolate the CD directly, as the unperturbed chromophore already should give an adequate description of the normal absorption spectrum.

The art of developing a good CD model thus lies totally in the chromophore definitions, a factor usually swamped by complex perturbation expressions. The importance of this point cannot be overstressed, as the failure of some CD models stems ultimately from an oversimplified chromophore definition, a deficiency that, in most cases, cannot be remedied by any subsequent theoretical refinements (e.g. going to higher order in perturbation theory).

No attempt will be made in this paper to review the large body of literature on CD models of complexes, and the reader is especially referred to a recent, comprehensive review by Richardson (3). The discussion here will be restricted mainly to the approaches developed recently by this author for the CD of charge transfer (4) and  $d-d$  transitions (5), and the specific application to tris(bidentates) and determination of their absolute configuration.

#### Chromophore Definitions: The Model

The complexes which will be considered here are those of  $D_3$  symmetry, such that the chelates and ligating atoms are separately identical. Applications to lower symmetry complexes follow similar lines. The chromophores for such systems may be defined in the following way.

The Achiral Metal-Ligating Atom Chromophore (A). It is unrealistic to ignore metal-ligating atom bonding in the description of either the  $d-d$  or charge transfer (CT) transitions, so that both of these are considered to arise from a single achiral chromophore encapsulating the metal ion and the ligating atoms. The exact specification of the chromophore proceeds through specifying the transition moments and energies of the chromophore transitions. In fact, we will be representing the entire complex by two such moment and energy representations, each representation constituting a single chromophore (A or B).

It should be noted here that this representation is quite distinct from the specification of the wave functions. It may be possible, for example, to get a good estimate of a transition moment and energy from the normal absorption spectrum, without ever explicitly defining a wave function; on the other hand, in some other cases the transition moment may be calculated from an approximate wave function, in which case the moment itself is only as good as the wave function employed. This may, however, be viewed simply as a practical detail of how best to put values to the variables in the moment/energy representation. Any mention of wave functions in this paper should be interpreted in this context (For chemists who are weaned on wave functions, this is not always an easy task.) In order to define the moments appearing in the perturbation expansions, we denote the ground state of A by  $\psi_A^O$ , and let  $\psi_A^d, \psi_A^C$  represent, in a general way, excited *d* and CT configurations, so that  $\psi_A^O \rightarrow \psi_A^d, \psi_A^O \rightarrow \psi_A^C$  constitute a *d-d* and CT transition with respective transition energies (relative to the ground state)  $\epsilon_d, \epsilon_C$ .

Charge transfer transitions are generally electric dipole allowed, with a corresponding electric transition moment

$$\tilde{\mu}^{OC} = \langle \psi_A^O | \tilde{\mu}_A | \psi_A^C \rangle \quad (1)$$

where  $\tilde{\mu}_A$  is the electric dipole operator centred at the symmetry (metal) origin. Under  $D_3$ , this moment will be either z-polarized or x,y-polarized, so that the representation by the totality of CT electric moments is achiral, and may be taken to have  $D_{3d}$  symmetry without any loss of generality. (This illustrates an important feature of moment representations; they may be of higher symmetry than the system they represent. This is because they are an approximation to the system, and an exact representation requires an infinite moment (multipolar) representation. They can never, however, have a lower symmetry.)

The *d-d* transitions may be either magnetic dipole allowed or forbidden, but are generally (by symmetry) electric dipole forbidden. This may seem contradictory as they appear in the normal absorption spectrum with a finite but small intensity, but we shall consider this in detail later. Thus at this stage, the *d-d* transitions are characterized solely by their magnetic transition moments

$$\tilde{m}^{do} = \langle \psi_A^d | \tilde{m}_A | \psi_A^O \rangle \quad (2)$$

where  $\tilde{m}_A$  is the magnetic dipole operator defined at the metal origin. In addition, the moments

$$\tilde{\mu}^{cd} = \langle \psi_A^C | \tilde{\mu}_A | \psi_A^O \rangle \quad (3)$$

connecting the excited CT and *d* configurations appear in the perturbation expansion. All these moments under  $D_3$  again are

either z- or x,y-polarized, constitute an achiral representation, and may be taken without loss of generality to have covering  $D_{3d}$  symmetry.

The above representation is sufficient to describe completely the CT absorption. It might be argued, however, that the  $\bar{d}-\bar{d}$  absorption intensities bear no relation to the moments defined above - and this is perfectly true. That this does not invalidate the representation for the  $\bar{d}-\bar{d}$  region follows from noting that absorption intensities are invariably electric dipole in character, whereas the  $\bar{d}-\bar{d}$  CD predominantly arises from magnetic transition moments which are symmetry allowed. The  $\bar{d}-\bar{d}$  transitions gain intensity in normal absorption through such mechanisms as spin-orbit and vibronic coupling. Taking the latter as an example, it will be mainly the metal-ligating atom system vibrations that control the intensity, so that such effects can be accommodated without expanding the chromophore or, in fact, reducing its symmetry from  $D_{3d}$ . For magnetic dipole forbidden transitions, the moment representation is then simply in terms of the effective dipole moment  $\Delta\mu_{\text{od}}$  as determined from the absorption spectrum. For magnetic dipole allowed  $\bar{d}-\bar{d}$  transitions, this electric moment may be neglected, as discussed later.

The Perturbing Chelate Chromophore System (B). The chelate system B may be considered effectively as three separate chelate chromophores indexed by I such that  $I = 1, 2, 3$ . Each individual chelate is considered to have a ground state  $\phi_I^O$  and two electric dipole allowed (from the ground state) excited states  $\phi_I^R, \phi_I^S$ , so that the moment representation becomes

$$\tilde{\mu}_I^{\text{OR}} = \langle \phi_I^O | \tilde{\mu}_I | \phi_I^R \rangle \quad (4)$$

$$\tilde{\mu}_I^{\text{OS}} = \langle \phi_I^O | \tilde{\mu}_I | \phi_I^S \rangle \quad (5)$$

$$\tilde{\mu}_I^{\text{RS}} = \langle \phi_I^R | \tilde{\mu}_I | \phi_I^S \rangle \quad (6)$$

where  $\tilde{\mu}_I$  is the electric dipole operator defined at the origin of the chelate (which is taken to lie on the  $C_2$  axis of I at the point of the vector  $\tilde{r}_{\text{MI}}$  from the metal origin of A). The transition energies of the excited chelate states are  $\epsilon_R, \epsilon_S$  respectively.

This specification of the B-system is totally adequate for the CD work that follows, and neglects any coupling between the chelates themselves. To explain adequately the energy splitting (though not the intensities) of the chelate system in the complex, it is necessary to consider the interchelate coupling, but this does not necessitate extending the moment representation defining the chromophoric system. It will be shown later that the perturbation of the A chromophore by the B system is independent of this coupling, so that it will not be considered

further.

Assumptions of the Model. There are certain assumptions inherent in these chromophore definitions which explicitly exclude certain CD mechanisms. For example, the higher order transition moments of the metal ion are neglected totally, automatically excluding any contributions to the  $d-d$  CD from first order perturbation theory such as discussed in the dynamic coupling approach of Mason (6), and the static coupling approach initiated by Moffitt (7) and extended by Richardson (8). Furthermore, the chelate system is represented solely by its transition moments, and any chiral effects of the static charge distribution are neglected. The justification for both these assumptions has its source in the high symmetry of the chromophores, and is discussed in detail elsewhere (4,9).

With regard to the CT transitions, the representation by only electric moments at a single origin assumes that the CT chromophore is achiral. This assumption explicitly excludes the mechanism discussed by Mason (10), for reasons discussed in the next section. This is not to imply, however, that the ligating atoms are totally insensitive to the chelate structure; in fact, the chelates perturb the ligating atoms sufficiently to lead to a unique z-direction ( $C_3$  axis) of the achiral chromophore, manifesting as an appreciable energy splitting of the z- and x,y-polarized transitions (which would be degenerate if the achiral chromophore were of octahedral symmetry). This effect on the ligating atoms is not, however, primarily due to the chirality of the chelate system, but to its having a unique  $C_3$  axis. This is of course retained in the  $D_{3d}$  symmetry of A.

This rather exhaustive definition of the chromophores should illustrate the importance of a detailed description of the model, because all the assumptions of the CD model to be described have already been made. Any deficiencies in its description of real systems may be traced directly back to the preceding discussion. We now turn to discussing those perturbation terms which lead to the CD of the CT and  $d-d$  transitions of such chromophores.

### Circular Dichroism of Charge Transfer Transitions

The CD of the CT transitions has attracted little direct interest in the literature. Mason (10) has postulated that it arises from an exciton mechanism in which the CT transition is broken up into three degenerate oscillators or chromophores with different origins. Such a procedure is unjustified quantum mechanically, as each chromophore must have negligible electron exchange with any other chromophore; considering that a common metal  $d$  state is involved in the definition of each such chromophore or oscillator, such a model is, despite its pictorial appeal, theoretically inconsistent. Mason supports his model by noting that the CT CD exhibits the exciton structure characteristic of

the chelate CD, which is determined in an analogous way. It will be shown here, however, that the experimental results (including the characteristic exciton structure of the CT bands) are readily explained by a mechanism that arises purely from the electric moments of the CT states, defined at the natural symmetry origin and of  $D_{3d}$  symmetry, due to perturbation by the chiral chelate system (5).

In describing the CT CD, only the moments  $\mu^{oc}$  and the corresponding transition energies  $\epsilon_c$  of the chromophore A need be considered. Under  $D_{3d}$  symmetry, these moments are either z-polarized (for transitions of  $A_{2u}$  symmetry) or x,y-polarized (for  $E_u$  transitions). The polarization and magnitude of the moments, and the transition energies, are all in principle accessible through normal absorption experiments, so that in this instance the chromophore may be parametrized from absorption data. The CT transitions become CD active simply through coupling with each of the chelate moments  $\mu_I^{or}$ . Only one excited state need be specified in this case, the final CD being summed over all the chelate states. Each chelate I acts independently (any interactions between the chelates being neglected) in giving a coupled-oscillator (Kirkwood-Kuhn) contribution of the form (11)

$$R_I^c = C_\epsilon^c V(\mu^{oc}, \mu_I^{or}) \mu^{oc} \cdot \mu_I^{or} \times r_{MI} \quad (7)$$

where

$$C_\epsilon^c = \frac{\epsilon_c \epsilon_r}{\hbar (\epsilon_r^2 - \epsilon_c^2)} \quad (8)$$

and

$$\begin{aligned} V(\mu^{oc}, \mu_I^{or}) &= \mu^{oc} \cdot (\mu_I^{or} - 3\mu_I^{or} \cdot \hat{r}_{MI}) \hat{r}_{MI} / r_{MI}^3 \\ &= \mu^{oc} \cdot \mu_I^{or} \end{aligned} \quad (9)$$

with the cap denoting the unit vector.

Simplification of this expression may be effected by exploiting the generalized selection rules (9) which we shall use throughout this work. These rules have been formulated in such a way that perturbation expressions such as the above may be reduced to the simplest possible form characteristic of the symmetry of the chromophores involved. In particular, under  $D_{3d}$ , the CT chromophore moment products appearing in the expanded form of equation 7 above, *viz.*,  $\mu^{oc}(\alpha) \mu^{oc}(\beta)$  (where  $\mu^{oc}(\alpha)$  is the  $\alpha$ 'th cartesian component of  $\mu^{oc}$ ), may be replaced by  $P^0 [\mu^{oc}(\alpha) \mu^{oc}(\beta)]$  where  $P^0$  is the totally symmetric projection operator under  $D_{3d}$ , defined as

$$P^0 = \frac{1}{h} \sum_{\xi=1}^h R_\xi \quad (10)$$

The  $R_\xi$  ( $\xi = 1, \dots, h$ ) are the  $h$  symmetry operations of  $D_{3d}$  in this case, and the transformed products become

$$p^0 [\mu^{\text{OC}}(\alpha)\mu^{\text{OC}}(\beta)] = 0 \quad \text{if } \alpha \neq \beta$$

and  $p^0 [\mu^{\text{OC}}(z)]^2 = [\mu^{\text{OC}}(z)]^2 = |\tilde{\mu}^{\text{A}}|^2$  (11)

$$p^0 [\mu^{\text{OC}}(x)]^2 = p^0 [\mu^{\text{OC}}(y)]^2 = \frac{1}{2} [\mu^{\text{OC}}(x)]^2 + \frac{1}{2} [\mu^{\text{OC}}(y)]^2 = |\tilde{\mu}^{\text{E}}|^2.$$

Substitution leads to the complete factorization of the A and I terms, and also leads to a separate contribution for each symmetry:  $R_{\text{I}}^{\text{A}}$  for z-polarized CT transitions, and  $R_{\text{I}}^{\text{E}}$  for x,y-polarized transitions. These have the form

$$R_{\text{I}}^{\text{A}} = C_{\text{E}}^{\text{A}} [\tilde{\mu}^{\text{A}}]^2 [\bar{\mu}_{\text{I}}^{\text{OR}}(z)\mu_{\text{I}}^{\text{OR}}(x)r_{\text{MI}}(y) - \bar{\mu}_{\text{I}}^{\text{OR}}(z)\mu_{\text{I}}^{\text{OR}}(y)r_{\text{MI}}(x)] \quad (12)$$

$$R_{\text{I}}^{\text{E}} = C_{\text{E}}^{\text{E}} [\tilde{\mu}^{\text{E}}]^2 [\bar{\mu}_{\text{I}}^{\text{OR}}(y)\mu_{\text{I}}^{\text{OR}}(z)r_{\text{MI}}(x) - \bar{\mu}_{\text{I}}^{\text{OR}}(x)\mu_{\text{I}}^{\text{OR}}(z)r_{\text{MI}}(y)]. \quad (13)$$

Summation over I and substitution for the geometrical factors (assuming the metal-ligating atom geometry is octahedral) leads to the following expressions for the CD of the CT transitions, with  $r_{\text{ML}}$  being the value of any one of the  $r_{\text{MI}}$ :

$$R_{\text{B}}^{\text{A}} = \frac{2 \epsilon_{\text{A}}}{(\epsilon_{\text{r}}^{\text{z}} - \epsilon_{\text{A}}^{\text{z}})} \frac{|\tilde{\mu}^{\text{A}}|^2}{r_{\text{ML}}^3} R_{\text{B}}^{\text{A}}(r) \quad (14)$$

$$R_{\text{B}}^{\text{E}} = \frac{\epsilon_{\text{E}}}{(\epsilon_{\text{r}}^{\text{z}} - \epsilon_{\text{E}}^{\text{z}})} \frac{|\tilde{\mu}^{\text{E}}|^2}{r_{\text{ML}}^3} R_{\text{B}}^{\text{E}}(r) \quad (15)$$

$R_{\text{B}}^{\text{A}}(r)$ ,  $R_{\text{B}}^{\text{E}}(r)$  are the CD strengths of the  $A_2$ , E bands of the chelate system as derived from Moffitt's exciton modification (12) of the Kirkwood-Kuhn mechanism, applied to tris(bidentates) by Mason (10). For the D configuration, they reduce to

$$R_{\text{B}}^{\text{A}}(r) = -R_{\text{B}}^{\text{E}}(r) = \pm \frac{\epsilon_{\text{r}}}{\sqrt{2}\hbar} r_{\text{ML}} |\tilde{\mu}^{\text{OR}}|^2 \quad (16)$$

with the + sign for long-axis, - for perpendicular axis polarized transitions of the chelate. For the L configuration, all the signs are reversed. Thus the CT CD terms may be interpreted as simply due to stealing of the chelate CD; a CT transition of a given polarization steals its CD from the chelate band of the same polarization, and has the same sign, provided of course that the CT transition lies at lower energies than the chelate bands. The result of this is that a pair of close-lying  $A_{2u}$ ,  $E_u$  transfer states lead to a band system that mimics the exciton shape of the chelate system.

The ratios of the CT CD to that of the chelate system have the value

$$\Delta^{\text{A}} = R_{\text{B}}^{\text{A}}/R_{\text{B}}^{\text{A}}(r) = 2K \frac{\epsilon_{\text{A}}}{(\epsilon_{\text{r}}^{\text{z}} - \epsilon_{\text{A}}^{\text{z}})} |\tilde{\mu}^{\text{A}}|^2 / r_{\text{ML}}^3 \quad (17)$$



$$\Delta^E = R^E/R_B^E(r) = K \frac{\epsilon_E}{(\epsilon_r^2 - \epsilon_r)} |\underline{\mu}^E|^2 / r_{ML}^3 \quad (18)$$

with  $K = 1.6 \times 10^5$ ,  $r_{ML}$  in Å,  $\mu$  in eÅ, and  $\epsilon$  in  $\text{cm}^{-1}$ . For  $\text{Fe}(\text{dipy})_3^{2+}$ , for example, with  $r_{ML} = 3\text{Å}$ ,  $\epsilon_r = 35000 \text{ cm}^{-1}$  and  $\epsilon_A \approx \epsilon_E = 20000 \text{ cm}^{-1}$ , the ratios are

$$\Delta^A \approx 0.6 |\underline{\mu}^A|^2 ; \quad \Delta^E \approx 0.3 |\underline{\mu}^E|^2 ,$$

which, with moments of the order of 0.5 eÅ (quite realistic values for the CT transitions) gives the CT CD being about 15% of that of the chelate system. The agreement with experimental CD intensities (10) using independent polarization data from linear dichroism studies (13) is rather good.

The simplicity of the expression makes the CT CD an excellent probe for determination of the absolute configuration. If the energy, intensity, and polarization of a CT transition are known, then the sign of the CD determines unambiguously the absolute configuration of the chelate system, as it is the same as that of the exciton chelate band of the same polarization. Energy and intensity may be determined directly from the normal absorption spectrum, and the polarization from solid state spectra or, for certain complexes, by linear dichroism (LD). For  $\text{Fe}(\text{dipy})_3^{2+}$ , for example, the polarizations of the CT bands have been determined through LD studies using flow orienting techniques for the complex bound to a DNA substrate (13). Note that the actual parentage of the CT transitions in such complexes is quite immaterial; thus whether the particular transition has a large  $d-d$  component (which is possible in some complexes) is not important, provided it has appreciable electric dipole strength.

In principle, the exciton bands themselves could be used directly in this manner to assign the configuration, but their high energies and intensities make polarization measurements far less accessible. In fact, alternative methods exploiting the chelate CD have been proposed (see, e.g., the work of Mason (10) and the references in Hawkins (2)). Mason's method of calculating directly the exciton splitting to assign the  $A_2$  and E components has led to some ambiguous results. This is probably due to the extreme sensitivity of energy calculations to changes in the metal-ligand bonding. Transition moment criteria developed here are free from any energy calculations, and any variations in the metal-ligand bonding are accommodated directly through parametrization of the moments from the absorption spectrum.

### Circular Dichroism of the $d-d$ Transitions

Magnetic Dipole Forbidden Transitions. If the  $d-d$  transition is magnetic dipole forbidden, it is characterized in this model solely through its weak electric transition moment  $\Delta\mu_{od}$  (defined at the metal origin) arising through such mechanisms as vibronic or spin-orbit coupling. This moment and the corresponding

energy  $\epsilon_d$  may be obtained directly from the absorption spectrum, so that exact mechanism through which the intensity derives is immaterial. The CD of such a transition will arise in our model in a way totally analogous to that of the CT transitions. As  $\Delta\mu^{od}$  is either z- or x,y-polarized, the CD has the same form as equations 14, 15 where the  $\epsilon_A$ ,  $\epsilon_E$ ,  $R^A$ ,  $R^E$  now correspond to the  $d-d$  transition of the appropriate polarization, and  $\mu^z \equiv \Delta\mu^{od}$  (if z-polarized),  $\mu^E \equiv \Delta\mu^{od}$  (if x,y-polarized). Again the CD is stolen directly from the chelate CD, and the ratios of the  $d-d$  CD in this case to that of the chelate system have the values given in equations 17, 18 with the appropriate values of the  $\Delta\mu^{od}$ . Neglecting the energy factors, the ratio of the  $d-d$  CD to that of the CT CD of the same polarizations is equal to

$$|\Delta\mu^{od}|^2 / |\mu^{oc}|^2 .$$

It is interesting to speculate whether the  $d-d$  CD of magnetic dipole forbidden transitions may be used to assign absolute configurations in exactly the same way as suggested for the CT CD. The magnitude of the effect predicted by the above model is in good agreement with the observed bands.

The validity of the direct substitution for  $\Delta\mu^{od}$  into the first-order expression for the CD of electric dipole allowed transitions is verified readily using, for example, a simple vibronic coupling model. The procedure is analogous to that discussed elsewhere for vibronic contributions to DICD (dispersion (dispersion-induced CD) (14)). As  $\Delta\mu^{od}$  is, in itself, first-order in the vibronic perturbation, the CD strength of the  $d-d$  transition is effectively third-order overall (substitution of  $|\Delta\mu^{od}|^2$  into a first-order term). Thus it will be about three orders of magnitude smaller than the chelate CD.

This contribution also arises for magnetic dipole allowed transitions, but in such cases, there is an effectively second-order perturbation term involving the magnetic moment that should therefore be about an order of magnitude stronger, and thus dominate the  $d-d$  CD. This is the mechanism that will be discussed now. (It is interesting to note in passing that for the achiral chromophore, any magnetic dipole allowed transitions must have the magnetic transition moment for a particular vibronic band orthogonal to the small electric moment for the same vibronic transition. It is unlikely that sufficient vibrational resolution is possible for  $d-d$  spectra to exploit this simple relationship for assignment if the polarization of one is known.)

Magnetic Dipole Allowed Transitions. In the previous cases, the CD has arisen essentially through the electric dipole transition moment of the transition, so that the quantities appearing in the CD expressions are the same as those responsible for the normal absorption; complete parametrization based on the normal absorption spectrum is therefore possible. In the case of

magnetic dipole allowed transitions, the CD exploits the magnetic moment of the  $d-d$  transition, a quantity that does not play any role in normal absorption, so that complete parametrization is no longer possible. However, we shall still take the energies from the normal absorption spectrum as characteristic of the chromophore.

The CD strength of a magnetic dipole allowed  $d-d$  transition of the chromophore A as defined earlier arises from second-order perturbation theory, and incorporates the two electric moments involving a CT state (referred to as the intermediate state) of the A chromophore to provide the dipole-dipole coupling to the B chromophore system. The CD arising from a particular chelate I at the  $d-d$  transition energy has the form (5)

$$R_I^d = \text{Im} \{ C_\epsilon^d V(\underline{\mu}^{oc}, \underline{\mu}_I^{rs}) V(\underline{\mu}^{cd}, \underline{\mu}_I^{so}) \} \underline{\mu}_I^m \cdot \underline{m}^{do} \quad (21)$$

where

$$C_\epsilon^d = [\Delta\epsilon_{rd} (\epsilon_{cs} - \epsilon_d)]^{-1}, \quad \Delta\epsilon_{rd} = \epsilon_r - \epsilon_d, \quad \epsilon_{cs} = \epsilon_c + \epsilon_s.$$

The interaction terms are defined in equation 9. The simplest interpretation of this term is that the radiation field interacts directly with the last two moments (it sees the whole molecule effectively as a point) with the quantity in curly brackets providing a strong perturbative glue of dipolar interactions between electric transition moments (each of which is symmetry allowed) on A and B, so that the radiation field sees the two chromophores as a single system. Further discussion of this term is given elsewhere (5).

Simplification of this expression is again effected by exploiting the generalized selection rules (9). Equation 21 is expanded in terms of cartesian components, each having a moment factor pertaining to A of the form  $[\mu(\alpha)\mu(\beta)m(\gamma)]$ . Replacing each such factor by its projection  $P^0[\ ]$  as described earlier under the  $D_{3d}$  symmetry of A, the expression for  $R_I^d$  reduces to a simple product of A and I factors. The exact form depends directly on the symmetries  $\Gamma_d, \Gamma_c$  of the  $d-d$  and CT transitions involved, so that  $R_I^d$  is written in the form

$$R_I^d(\Gamma_d, \Gamma_c) = \frac{1}{2} C_\epsilon^d \text{Im} \Omega_A(\Gamma_d, \Gamma_c) \Lambda_I(\Gamma_d, \Gamma_c) \quad (22)$$

Noting that  $\Gamma_d$  can only be either  $A_{2g}$  or  $E_g$ , and  $\Gamma_c$  either  $A_{2u}$  or  $E_u$ , it follows that three possible contributions may be distinguished. Introducing the notation

$$(\underline{a}, \underline{b}, \underline{c}) = [a(x)b(y) - b(x)a(y)] c(z), \quad (23)$$

these three contributions are those for which

$$\Omega_A(A_{2g}, E_u) = (\underline{\mu}^{oc}, \underline{\mu}^{cd}, \underline{m}^{do}); \quad \Lambda_I(A_{2g}, E_u) = (\underline{\mu}_I^{-rs}, \underline{\mu}_I^{-so}, \underline{\mu}_I^{\text{or}})$$

$$\Omega_A(E_g, E_u) = (\tilde{m}^{do}, \tilde{\mu}^{oc}, \tilde{\mu}^{cd}); \quad \Lambda_I(E_g, E_u) = (\tilde{\mu}_I^{or}, \tilde{\mu}_I^{-rs}, \tilde{\mu}_I^{-so})$$

$$\Omega_A(E_g, A_{2u}) = (\tilde{\mu}^{cd}, \tilde{m}^{do}, \tilde{\mu}^{oc}); \quad \Lambda_I(E_g, A_{2u}) = (\tilde{\mu}_I^{-so}, \tilde{\mu}_I^{or}, \tilde{\mu}_I^{-rs}). \quad (24)$$

As a final formality, it remains to sum over the I to determine the CD strength of a given  $d-d$  transition due to interaction with the entire chelate system. Writing

$$R^d(\Gamma_d, \Gamma_c) = \sum_I R_I^d(\Gamma_d, \Gamma_c) \quad (25)$$

and defining

$$\Lambda_B(\Gamma_d, \Gamma_c) = \sum_I \Lambda_I(\Gamma_d, \Gamma_c),$$

it follows that

$$R^d(\Gamma_d, \Gamma_c) = \frac{1}{2} C_\epsilon^d \text{Im} \Omega_A(\Gamma_d, \Gamma_c) \Lambda_B(\Gamma_d, \Gamma_c). \quad (26)$$

We shall refer in a general way to the A term ( $\Omega_A$ ) as the *inducibility of A*, and to the B term ( $\Lambda_B$ ) as the *inducing power of B*. In principle, this expression should be summed over all CT states of the appropriate symmetry, and over all states  $r, s$  of the chelate system. However, we shall see that there are physical reasons which lead to dominant contributions from particular states.

*The Inducibility of A.* The  $\Omega_A$  are functions purely of the achiral chromophore A. It is impossible to estimate these empirically by other techniques, so that the only approach would seem to be through simple model calculations. These are beyond the scope of this paper, so that the inducibility will be discussed in a general way, with a particular emphasis on its role in establishing CD/stereochemical correlations.

Some insight into the nature of the inducibility may be gained through considering a particular  $d-d$  transition, say  $\psi_A^0 \rightarrow \psi_A^1$  (symmetry  $\Gamma_{d_1}$ ). Supposing for purposes of illustration that all states may be described by single configurations or determinants, then each transition may be considered as a single electron jump between one electron orbitals. The  $d-d$  transition may then be written in the simpler notation  $d \rightarrow d_1$ . Denoting the CT state by  $c_1$ , it follows from the fact that each dipole operator is a one electron operator that the inducibility is only finite if the matrix elements

$$\langle d_0 | \tilde{m}_A | d_1 \rangle \quad \langle d_1 | \tilde{\mu}_A | d_1 \rangle \quad \langle c_1 | \tilde{\mu}_A | d_0 \rangle$$

do not vanish by symmetry. This implies immediately that the charge transfer transition that acts as an intermediate is either an electron transfer from  $d_0 \rightarrow c_1$  or from  $c_1 \rightarrow d_1$ . (See reference

(15) for further details.) This severely restricts the CT intermediate states, so that in most cases only one need be considered. In the one electron picture, CT transitions involving any other  $d$  states cannot contribute to the inducibility of the  $d_0 \rightarrow d_1$  transition. The result of this is that the inducibility of transitions to other  $d$  states will generally be quite different, as quite different CT states are involved, leading to quite different CD strengths for each  $d-d$  transition. There are also extra symmetry restraints inherent in equation 24 restricting the nature of the CT states that can act as intermediates. This leads to a number of important conclusions, which are labelled for each reference in later sections.

C(1) *The value of the inducibility depends critically on the nature of the  $d-d$  transition, and in turn on the nature of the intermediate charge transfer state.*

C(2) *For tris(bidentates), the  $E_g, A_{2g}$   $d-d$  transitions will therefore have quite different inducibilities, because quite different intermediate charge transfer states are involved.*

C(3) *Any changes in the charge transfer states (e.g. through perturbation of the ligating atoms) will lead directly to changes in the inducibility and thus to changes in the  $d-d$  CD.*

C(4) *Any correlations between the inducibilities of two  $d-d$  transitions (e.g. the  $E_g/A_{2g}$  ratio) are transferable from complex to complex only if the achiral chromophore is strictly the same in each case; i.e. such correlations should only be expected for complexes with similar  $d$  electron configurations and similar charge transfer states.*

There is another conclusion that follows from the considerations of the next section, but is best collected here as it relates directly to the inducibility.

C(5) *The relative intensities of the CD of  $d-d$  transitions of  $A_{2g}, E_g$  symmetry is determined largely by the inducibilities, and thus the nature of the achiral chromophore.*

*The Inducing Power.* The inducing power is characteristic of the chelate system, and because of the dependence on transition moments connecting the excited states also cannot strictly be determined empirically. Some conclusions may, however, be drawn immediately.

C(6) *The inducing power is of opposite sign for the D and L configurations of the chelate system.*

C(7) *A series of complexes with the same chelate system will be characterized by the same inducing powers.*

The inducing power may be directly interpreted as a hyperpolarizability term of the chelate system, so that it is unlikely to be much affected by the details of the metal-ligand bonding.

It is actually possible to simplify the form of the inducing power in terms of the moment representations defined earlier. Assuming an octahedral geometry of the metal-ligating atom system, and considering initially extended pi-system chelates for which the transitions are mainly long- or short-axis polarized, the inducing powers are readily shown to reduce to the form

$$\Lambda(A_{2g}, E_u) = -\Lambda(E_g, E_u) = -2\sqrt{2} \mu^{or} \mu^{rs} \mu^{so} / r_{ML}^6;$$

$$\Lambda(E_g, A_{2u}) = 0 \quad (27)$$

if both  $\mu^{or}$ ,  $\mu^{so}$  are long-axis polarized, and

$$\Lambda(A_{2g}, E_u) = -\Lambda(E_g, A_u) = 2\sqrt{2} \mu^{or} \mu^{rs} \mu^{so} / r_{ML}^6; \quad \Lambda(E_g, E_u) = 0 \quad (28)$$

if  $\mu^{or}$  is long-axis,  $\mu^{so}$  short-axis polarized. The above are all defined for the  $D$  configuration. The signs of the transition moments are determined by using the reference directions of Figure 1 as being positive for the dipole operator.

For ligand systems such as dipy, phen, the CD spectra of the chelate systems suggest that the terms of equation 28 should be the dominant factors leading to the  $d-d$  CD. The equality (in magnitude) of the inducing powers in equation 27, and also of those in equation 28, follows from the  $D_3$  symmetry of the chelate system, and may be taken as a general feature of  $D_3$  systems. It is this factor that leads to conclusion C(5) of the previous section.

It is difficult to determine simply from looking at the previous equations how the inducing powers of different ligand systems will be related. However, if the hyperpolarizability type terms are determined largely by arrangement of the pi-systems rather than their internal details (which is quite plausible if one considers somewhat naively that each is really a "sea" of pi-electrons floating around each chelate frame), then it would be most likely that the overall inducibilities would at least be of the same sign for a range of chelate systems. This appears to be the case even for saturated ligand systems. We shall therefore make the following *assumption*, stressing that it need not be strictly true even within the confines of our model (C(1)-C(7) are conclusions based directly on the CD model, and are not assumptions).

A(1) *The sign of the inducing power is independent of the detailed structure of the chelate, and determined only by the overall configuration of the complex.*

*Magnitude of the Second-Order Terms.* Before discussing the applications of these conclusions, it is important to establish that the mechanism discussed here can account for the magnitude of the  $d-d$  CD found experimentally. Using equation 16 and the units discussed for equations 17, 18, the magnitude of the ratio

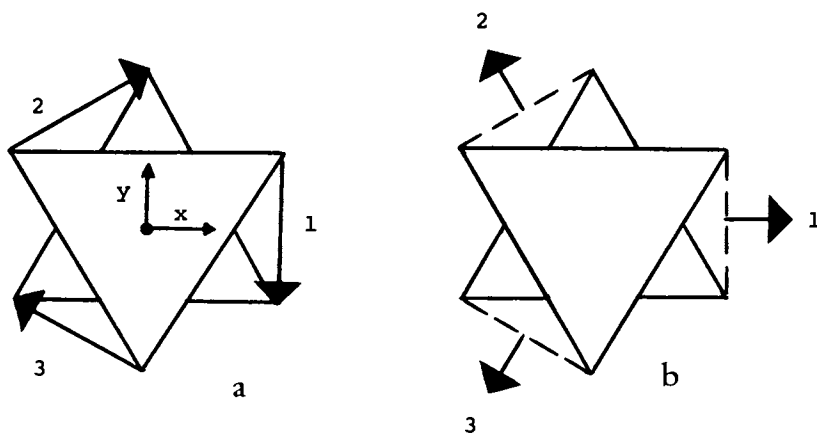


Figure 1. Definition of dipole operator directions and axis system: (a) long-axis chelate transitions; (b) short-axis chelate transitions.

of the  $d-d$  CD (magnetic dipole allowed) to that of the chelate CD has the form (see equation 22)

$$\Delta = 2.1 \times 10^4 C_{\epsilon}^d \frac{\Omega_A(\Gamma_d, \Gamma_c) \Lambda_B(\Gamma_d, \Gamma_c)}{\epsilon_r r_{ML} |\mu^{or}|^2} \quad (29)$$

Putting  $r = 3 \text{ \AA}$ ,  $\Delta \epsilon_{rd} \approx \epsilon_r / 3 \approx (\epsilon_{CS} - \epsilon_d) / 5 = 10^4 \text{ cm}^{-1}$ , and all chelate dipole moments equal to  $1 \text{ e} \text{ \AA}$ , the ratio reduces to

$$\Delta \approx 0.02 \Omega_A(\Gamma_d, \Gamma_c) \quad (30)$$

with  $m$  in BM. Assuming the CT moments for A are of the order of  $1/3 \text{ e} \text{ \AA}$ , and the magnetic moment about 3 BM, the ratio is still about  $10^{-2}$ , in good agreement with the magnitudes found experimentally. Considering that the above values are not unrealistic, such a simplistic calculation should not be dismissed as trivial evidence for the importance of the mechanism. It is questionable whether many other  $d-d$  CD models could meet this rather stringent test of giving an absolute magnitude in the right ballpark for realistic parameter values.

### Applications

It may seem that the previous discussion leads to so many restrictions that one despairs at the use of  $d-d$  CD as a stereochemical probe at all. The source of this apparent dilemma is that the CD is sensitive not only to the absolute configuration of the chelate system, but also to any variations in the achiral chromophore. Such a negative conclusion is readily alleviated, however, if the restrictions are considered together with established empirical rules. In addition, the sensitivity to the achiral chromophore, though a partial hindrance to the establishment of a simple CD-stereochemical correlation to cover all complexes, is actually an appreciable advantage to the study of the effects of, for example, added anions on the metal-ligand bonding. We now illustrate these features with some examples.

The Dominant E Rule. The  $T_{1g}$  band in  $d^3$ ,  $d^8$  and spin-paired  $d^6$  tris(bidentate) complexes is generally split into distinct  $A_{2g}$ ,  $E_g$  components, and it is found empirically that the  $E_{2g}$  band has the stronger CD. The absolute configuration is thus determined directly through the sign of the dominant E band (see e.g. references in Hawkins (2)). This is consistent with A(1), C(2), but should only apply for similar chromophores (C(4)). The relatively wide applicability of this rule must stem from an underlying similarity of the electronic configurations of such chromophores. Perhaps the best example when such a rule should apply rigorously on theoretical grounds are the tris(diamine) complexes, for which the achiral chromophore should not be extensively perturbed by substitutions at the chelate carbons.



This is found to be the case (2).

An illustration of the sensitivity of this rule to changes in the achiral chromophore is that the addition of polarizable oxyanions have a dramatic effect on the CD spectrum (16), the  $A_{2g}$  band gaining intensity at the expense of the  $E_g$  band (17,18), for the diamine complexes discussed above. The effect is only pronounced for those complexes which can lead to hydrogen bonding of the anions to the nitrogen hydrogens. Such effects are frequently rationalized as due to extra perturbations on an achiral chromophore (i.e. they are absorbed into the chiral perturber), but in this model it is probably due to the hydrogen bonding having sufficient effect on the nitrogens that the achiral chromophore definition must incorporate these changes at the outset. The anion effect thus effectively leads to a new achiral chromophore, because of the large effects on the charge transfer states. This has been exploited as a method of isolating the  $A_{2g}$  band, and thus effecting an assignment of the absolute configuration. Such effects serve to illustrate how easily the  $d-d$  CD can be altered through variations in the achiral chromophore (C(s)).

The  $T_{1g}$  Rule. It is tempting to simplify the symmetry of the achiral chromophore, and thus in turn simplify the CD-stereochemical correlations. For example, if the ligating atoms are taken to be isotropic, the symmetry of the achiral chromophore becomes octahedral. The CD should then reduce to that of a single  $T_{1g}$  band. Empirically, the  $T_{1g}$  CD could be approximated as a simple sum of the  $A_{2g}$ ,  $E_g$  bands, leading to a " $T_{1g}$ " rule.

Under such octahedral symmetry of the achiral chromophore, the generalised selection rules reduce the CD strength for the  $T_{1g}$  band to a single contribution for each chelate I:

$$R_I^d(T_{1g}) = \frac{1}{6} C_\epsilon^d \text{Im} [\tilde{\mu}_{\sim}^{oc} \times \tilde{\mu}_{\sim}^{cd} \cdot \tilde{m}_{\sim}^{do}] [\tilde{\mu}_{\sim I}^{-rs} \times \tilde{\mu}_{\sim I}^{-so} \cdot \tilde{\mu}_{\sim I}^{-or}] \quad (31)$$

For achiral chelates, the triple products of chelate moments on a single chelate I is zero, so that

$$R_I^d(T_{1g}) = 0 \quad \text{for each I} \quad (32)$$

for uncoupled chelates. [There is a small contribution if a degree of coupling between the chelates is introduced, but it is at least an order of magnitude smaller than that derived earlier for the split  $A_{2g}$ ,  $E_g$  bands.] Thus, under  $O_h$ , the CD vanishes, so that the  $T_{1g}$  rule would seem to be of little use. In fact, it is a good illustration of how an unrealistic choice of chromophore can lead to a quite misleading result. In these complexes, the  $E_g$ ,  $A_{2g}$  splitting is crucial to getting an appreciable CD, so that the achiral chromophore must accommodate this clear splitting of the  $T_{1g}$  band at the outset. Addition of the CD of the  $E_g$ ,  $A_{2g}$  components cannot (except in special cases perhaps where they

are equal and opposite in sign) be identified as that of the  $T_{1g}$  band.

Additivity Rules. In addition to these direct CD-stereochemical correlation rules, there are a set of empirical additivity rules determined empirically by Douglas (see, e.g., reference (19) and collated references in Hawkins (2)). An example of such a rule is that for cases in which the chelate itself has an asymmetric carbon. The  $d-d$  CD contributions from the asymmetric carbon atom and that of the chelate system as a whole are found to be additive. The theoretical justification for this additivity follows directly from the model discussed in this paper, and has been discussed in some detail elsewhere (4). (It is worth noting that we implicitly used this additivity in considering the  $d-d$  CD as a sum of contributions from each of the chelates I, with the achiral chromophore adapted to  $D_{3d}$  symmetry.)

#### Literature Cited.

1. Carroll, L., "The Annotated Alice", (ed. M. Gardner), Penguin (1977).
2. Hawkins, C.J., "Absolute Configuration of Metal Complexes", Wiley-Interscience, New York, N.Y. (1971).
3. Richardson, F.S., Chem. Reviews (1979) 79 17.
4. Schipper, P.E., J. Am. Chem. Soc. (1978) 100 1433.
5. Schipper, P.E., J. Am. Chem. Soc. (1979) 000 0000.
6. Mason, S.F. and Seal, R.H., Mol. Phys. (1976) 31 755.
7. Moffitt, W., J. Chem. Phys. (1956) 25 1189.
8. Richardson, F.S., J. Phys. Chem. (1971) 75 692.
9. Schipper, P.E., J. Am. Chem. Soc. (1978) 100 3658.
10. Mason, S.F., Inorg. Chim. Acta Revs. (1968) 2 89.
11. Schellman, J.A., Accts. Chem. Res. (1968) 1 144.
12. Moffitt, W., J. Chem. Phys. (1956) 25 467.
13. Norden, B. and Tjerneld, F., F.E.B.S. Letters (1976) 67 368.
14. Schipper, P.E., Chem. Phys. (1976) 12 15.
15. Schipper, P.E., J. Am. Chem. Soc. (1976) 98 7938.
16. Smith, H.L. and Douglas, B.E., Inorg. Chem. (1966) 5 784.
17. Gollogly, J.R. and Hawkins, C.J., Chem. Comm. (1968) 689.
18. Mason, S.F. and Norman, B.J., Chem. Comm. (1964) 339.
19. Douglas, B.E., Inorg. Chem. (1965) 4 1813.

RECEIVED September 13, 1979.

# Circular Dichroism Spectra of Square Planar Complexes Containing Prochiral Olefins and Their Stereoselective Olefin Exchange

KAZUO SAITO

Chemistry Department, Faculty of Science, Tohoku University, Sendai, 980 Japan

The relationship between the absolute configuration and CD spectrum has been widely discussed, but mostly for octahedral complexes. (1) Asymmetric coordination of  $\eta^2$ -olefins was first demonstrated by Cope *et al.* (2) with *trans*-[PtCl<sub>2</sub>(1-phenylethylamine)(*trans*-cyclo-octene)] and extended by Paiaro and Panunzi (3) by the preparation of a pair of diastereoisomers, such as *trans*-dichloro(*R* or *S*- $\alpha$ -phenylethylamine)(*trans*-2-butene)platinum(II), *trans*-[PtCl<sub>2</sub>(1-phenylethylamine)(tbn)]. Since then several complexes with such an asymmetry have been prepared, and the relationship between the absolute configuration and CD pattern has been discussed for platinum(II) complexes. (4) Scott and Wrixon (5) reported that *S,S*- $\eta^2$  and *R,R*- $\eta^2$  configuration give CD peaks with positive and negative signs in the *d-d* transition region at *ca.* 27,000 cm<sup>-1</sup>. Less information is available for the complexes with other metal ions, and only palladium(II) (5) and iron(0) (6) complexes were discussed.

A change in the kind of olefin does not cause significant changes in absorption spectra, so long as the other ligands remain unchanged. Hence the replacement of one olefin ligand by another cannot be detected by absorption spectrometry. Olefin exchange in platinum(II) complexes is an important elementary reaction related to their catalytic action in homogeneous systems, but kinetic studies have not been made because of such experimental difficulty. NMR studies gave only limited information. Measurement of the change in the CD spectrum of the complexes with prochiral olefins in the presence of an excess of free prochiral or non-prochiral olefins enables the estimation of the substitution rate. This method is useful for examining the influence of other ligands upon the rate of olefin exchange. (*e.g.* *trans* effect, (7)), but is also useful for elucidating the stereo-selectivity involved in the olefin exchange.

This paper deals with the relationship between the absolute configuration of  $\eta^2$ -olefins and the CD pattern of new platinum(II)

0-8412-0538-8/80/47-119-091\$06.00/0  
© 1980 American Chemical Society

and rhodium(I) complexes of the types shown in Figure 1, and with the source of stereoselectivity for olefin exchange.

### CD Pattern of Rhodium(I) and Platinum(II) Complexes

*CD of Rhodium(I) Complexes.* Figure 2 shows the visible and UV absorption of  $\eta^2$ -olefin complexes of rhodium(I). The synthesis of these complexes has been reported elsewhere. (8) It is seen that  $\eta^2$ -olefins give absorption peaks or shoulders in the regions 20,000 to 30,000  $\text{cm}^{-1}$  and around 40,000  $\text{cm}^{-1}$ . These are the same regions with those where  $\eta^2$ -olefin platinum(II) complexes give characteristic absorption, which is exemplified in Figure 3. (9) (Table I)

Figure 4 illustrates the CD spectra of a few rhodium(I) complexes. The pattern is very much dependent on the other ligands. Two characteristic and common peaks are seen in the two regions, where the  $\eta^2$ -olefins cause absorption peaks: *i.e.* negative peaks between 20,000 and 30,000  $\text{cm}^{-1}$  and large positive peaks at *ca.* 40,000  $\text{cm}^{-1}$ . The pattern in the region between these two is too complicated and sensitive to the other ligands and no systematic trend is seen. Figure 5 shows the difference in CD pattern between doubly bridged binuclear complexes of platinum(II) and rhodium(I) containing *S,S-trans*-cyclo-octene (coe), which can be coordinated only in this configuration.

Whenever one looks at the peaks at *ca.* 22,000  $\text{cm}^{-1}$ , the peaks have opposite signs. On the other hand, the sign of the peak at around 40,000  $\text{cm}^{-1}$  is the same, although the intensity differs greatly. The molar extinction coefficient in the former region is *ca.*  $10^3 \text{M}^{-1} \text{cm}^{-1}$ , and cannot be reckoned to be a purely *d-d* transition. However, the influence of the central metal ion is remarkable. The  $\epsilon$  value of the peak at *ca.* 40,000  $\text{cm}^{-1}$  is more than  $10^4 \text{M}^{-1} \text{cm}^{-1}$ , and the CD sign is independent of the metal ion. Hence this must reflect the absolute configuration of the prochiral olefin itself.

*CD of Platinum(II) Complexes.* Scott and Wrixon discussed the relationship between the CD and the structure of various olefins including many terpene derivatives, but theirs is limited to the low energy *d-d* transition region. (5) The CD pattern in the region 30,000 to 40,000  $\text{cm}^{-1}$  is very complicated and cannot be understood systematically. We have synthesized various complexes containing *S,S-trans*-2-butene (tbn) or *S*-2-methyl-2-butene (mbn) as a source of asymmetry and other ligands including L-prolinate, 4-substituted anilines and 4-substituted pyridines. Among them [PtCl(*o*-phenylenediamine)(*S*-mbn)] is the first optically active square planar complexes with positive charge. The CD data are given in Table II.

*Importance of the cis Ligand.* Figure 6 shows the CD of the two geometrical isomers of [PtCl(L-prolinate)(*S,S*-tbn)]. Both are rather large negative CD peaks at *ca.* 36,000  $\text{cm}^{-1}$ , but the *cis* isomer has one shoulder at *ca.* 32,500  $\text{cm}^{-1}$ , whereas the *trans*

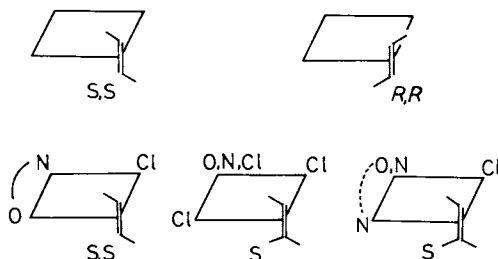


Figure 1. R,R- and S,S-Configuration of prochiral olefins on a square planar complex and the coordinating atoms of studied complexes

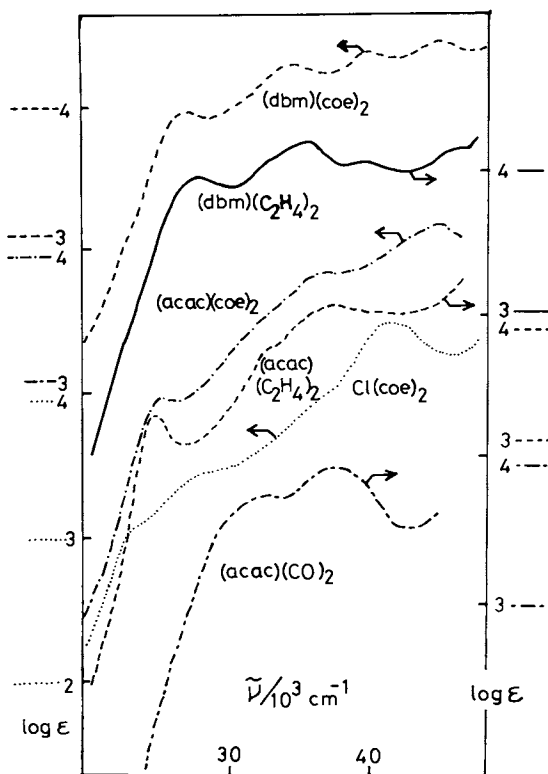


Figure 2. Absorption spectra of rhodium(I) complexes containing olefins and other ligands in hexane: *acac*<sup>-</sup>, enolate anion of acetylacetonone; *coe*, cyclooctene; *dbm*<sup>-</sup>, enolate anion of dibenzoylmethane.

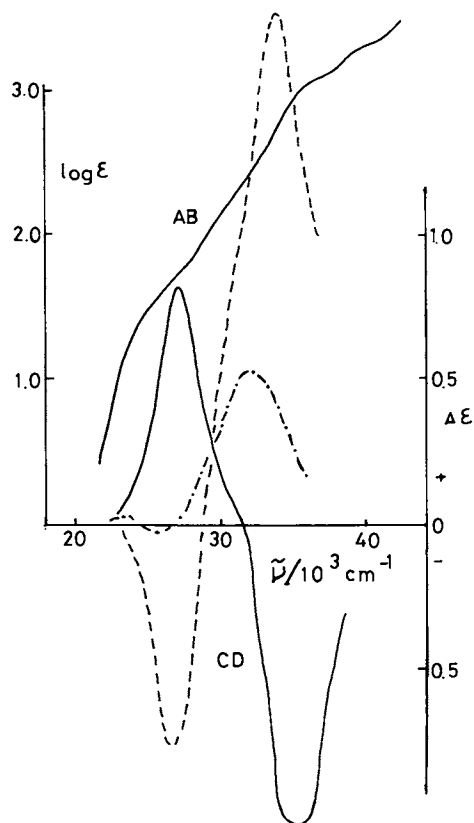


Figure 3. UV absorption and CD spectra of  $[PtCl(L\text{-prolinate})\text{-}(trans\text{-}2\text{-butene})]$ :  
 (—),  $(+)_{ss_0}\Delta\epsilon$ ; (---),  $(-)_{ss_0}\Delta\epsilon$ ; (- · - ·), vincinal effect.

Table I. Absorption Data of Rhodium(I) and Platinum(II) Complexes Containing  $\eta^2$ -Olefins

| Complexes   | $\tilde{\nu}$        | log $\epsilon$ | $\tilde{\nu}$        | log $\epsilon$ |
|---|----------------------|----------------|----------------------|----------------|
|   | $10^3\text{cm}^{-1}$ |                | $10^3\text{cm}^{-1}$ |                |
| [Rh(acac)(CO) <sub>2</sub> ] <sup>a,b</sup>                                       | 25.00                | 1.91           | 41.00                | 3.68           |
| [Rh(acac)(ethylene) <sub>2</sub> ] <sup>c</sup>                                   | 25.00                | 3.31           | 41.32                | 4.00           |
| [Rh(dbm)(ethylene) <sub>2</sub> ] <sup>d</sup>                                    | 27.40                | 3.98           | 40.00                | 4.08           |
| [Rh(acac)( <i>trans</i> -coe) <sub>2</sub> ] <sup>c,e</sup>                       | 25.32                | 2.95           | 40.98*               | 3.94           |
| [Rh(dbm)( <i>trans</i> -coe) <sub>2</sub> ] <sup>c</sup>                          | 27.40                | 3.96           | 40.00                | 4.38           |
| [Rh <sub>2</sub> Cl <sub>2</sub> ( <i>trans</i> -coe) <sub>2</sub> ] <sup>c</sup> | 22.73*               | 2.97           | 40.98                | 4.48           |
| [PtCl(L-pro)( <i>trans</i> -coe)] <sup>f</sup>                                    | 24.8 *               | 1.54           | 40.00                | 3.20           |
| [PtCl(L-pro)( <i>trans</i> -coe)] <sup>g</sup>                                    | 27.03*               | 1.73           | 40.00*               | 3.32           |
| K[PtCl <sub>2</sub> (L-pro)] <sup>h</sup>   | 23.8 *               | 1.37           | 40.00                | 2.62           |

a) in diethylether

c) in hexane

e) cyclooctene

g) in acetonitrile

\*) shoulders

b) enolate anion of acetylacetone

d) enolate anion of dibenzoylmethane

f) L-prolinate, data in Ref.

h) in Ref.

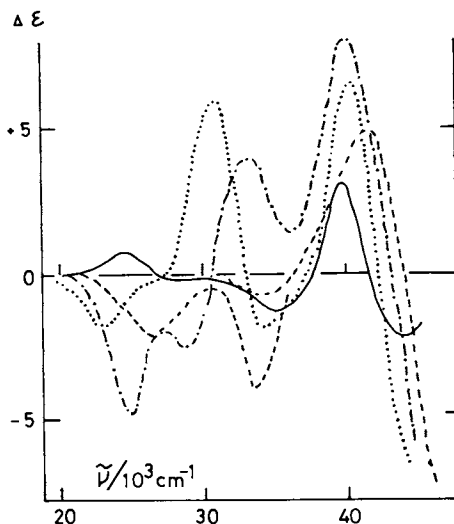


Figure 4. CD spectra of rhodium(I) and platinum(II) complexes containing S,S-trans-2-butene (*tbn*) and S,S-trans-cyclooctene (*coe*) in hexane: (—),  $P(C_6H_5)_2$ -[PtCl<sub>2</sub>(S,S-*tbn*)] in acetonitrile; (· · ·) [Rh<sub>2</sub>Cl<sub>2</sub>(S,S-*coe*)]; (---), [Rh(acac)(S,S-*coe*)<sub>2</sub>]; (- · - ·), [Rh(dbm)(S,S-*coe*)<sub>2</sub>].

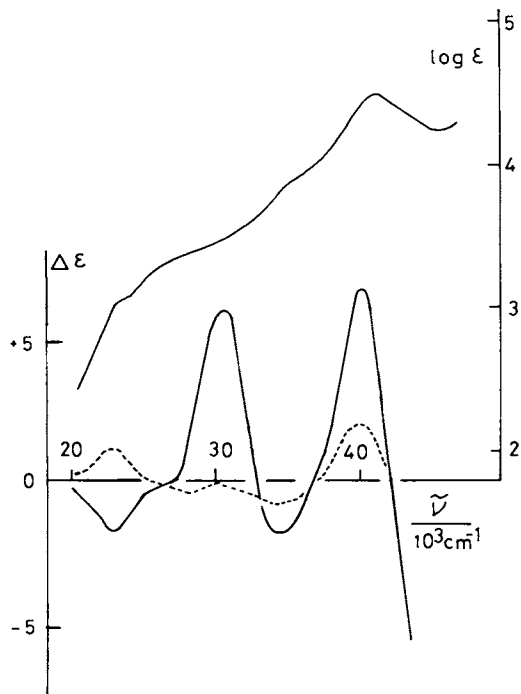


Figure 5. UV absorption and CD spectra of binuclear complexes of platinum(II) and rhodium(I) containing *S,S*-trans-cyclooctene (*coe*): (—),  $[\text{Rh}_2\text{Cl}_2(\text{S,S-coe})_4]$ ; (---),  $[\text{Pt}_2\text{Cl}_4(\text{S,S-coe})_2]$ .



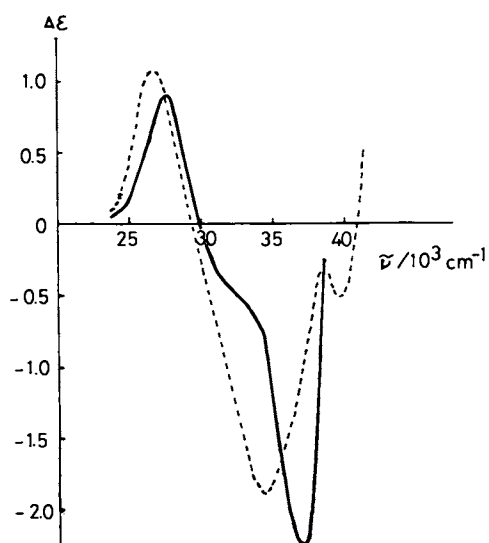


Figure 6. CD spectra of cis- and trans( $N, //$ )-[PtCl(L-prolinate)-(S,S-trans-2-butene)] in acetonitrile: (—), cis isomer; (---), trans isomer.

Table II. Peaks in the Circular Dichroism Spectra of  $\eta^2$ -Olefin complexes of Platinum(II)

| Complexes   | CD peaks    | $\tilde{\nu}/10^3\text{cm}^{-1}$ ( $\Delta\epsilon$ ) |
|---|-------------|---|
| <i>trans</i> ( <i>N</i> ,//)-[PtCl(L-pro)( <i>S</i> , <i>S</i> -tbn)] a,d   | 26.8(+1.08) | 34.3(-1.90) 39.7(-0.54)                               |
| <i>cis</i> ( <i>N</i> ,//)-[PtCl(L-pro)( <i>S</i> , <i>S</i> -tbn)] b,d   | 27.6(+0.92) | ** 33.2(-0.57) 37.0(-2.26)                            |
| P(C <sub>6</sub> H <sub>5</sub> ) <sub>4</sub> [PtCl <sub>3</sub> ( <i>S</i> -mbn)] e   | 22.9(+0.46) | 29.4(+0.13) 34.3(-1.05)                               |
| P(C <sub>6</sub> H <sub>5</sub> ) <sub>4</sub> [PtCl <sub>3</sub> ( <i>S</i> , <i>S</i> -tbn)] d  | 24.0(+0.76) | 28*0(-0.14)   |
| <i>trans</i> -[PtCl <sub>2</sub> ( <i>S</i> -mbn)(4-Cl-anil)] f   | 23.6(+0.51) | 27.0(-0.28)   |
| <i>trans</i> -[PtCl <sub>2</sub> ( <i>S</i> -mbn)(anil)] f  | 23.6(+0.44) | 27.2(-0.30)   |
| <i>trans</i> -[PtCl <sub>2</sub> ( <i>S</i> -mbn)(4-CH <sub>3</sub> -anil)] f   | 23.6(+0.41) | 27.1(-0.26)   |
| [PtCl( <i>S</i> -mbn){ <i>o</i> -C <sub>6</sub> H <sub>4</sub> (NH <sub>2</sub> ) <sub>2</sub> }] [B(C <sub>6</sub> H <sub>5</sub> ) <sub>4</sub> ] g | 28.3(+0.36) | ** 32.8(-0.03) 37.0(-0.59) 40.3(-0.35)                |
| <i>cis</i> -[PtCl <sub>2</sub> ( <i>S</i> , <i>S</i> -tbn)( <i>S</i> -1-PhEtNH <sub>2</sub> )] c h  | 27.3(+1.32) | ** 35.0(-0.72) 37.4(-1.19)                            |

a) Difference spectrum between *trans*(*N*,//)-[PtCl(L-pro)(*S*,*S*-tbn)] and *trans*(*N*,//)-[PtCl(L-pro)(ethylene)]

b) Difference spectrum between *cis*(*N*,//)-[PtCl(L-pro)(*S*,*S*-tbn)] and *cis*(*N*,//)-[PtCl(L-pro)(C<sub>2</sub>H<sub>4</sub>)]

c) Difference spectrum between *cis*-[PtCl<sub>2</sub>(*S*,*S*-tbn)(*S*-1-phenyl-ethylamine)] and *cis*(*N*,//)-[PtCl<sub>2</sub>(ethylene)(*S*-1-phenylethylamine)]

d) in acetonitrile

e) in dichloromethane

f) anil, aniline; in benzene

g) in ethanol

h) *S*-1-phenylethylamine; in acetone

\* peaks are broad

\*\* shoulders

isomer gives one broad peak shifted to longer wave lengths. This fact suggests the importance of other ligands which are *cis* and *trans* to the olefin. Figure 7 illustrates the CD patterns of the *mbn* complexes containing *cis*-dichloro ligands, and a *trans*-chloro or 4-substituted aniline ligand. Despite the difference in basicity and even in the coordinating atom, the negative CD peaks at  $\approx 34,500 \text{ cm}^{-1}$  have almost equal positions and intensities. It seems as if the variation of the *cis* ligand is more important in determining the CD pattern in this region than the *trans* ligand. This consideration is further verified by comparing the CD of those complexes having chlorine and nitrogen in the *cis* position and other donors in the *trans*. (Figure 8) The solvents were chosen in accordance with the solubility and the pattern cannot be compared in one solvent. Here again the location of the negative CD peaks are not very different regardless of the total charge or the presence of another source of asymmetry (*S*-1-phenylethylamine and proline, which have asymmetric nitrogen upon coordination). All these facts suggest that the *cis*-influence is more significant than the *trans*-influence for determining the location of CD peaks around  $35,000 \text{ cm}^{-1}$ . Because of the very strong *trans*-influence of the asymmetric olefin, ligands *trans* to the olefin would have only a small influence on the platinum(II), especially when the *trans* ligands are mere electron pair donors. Figure 9 gives the CD pattern of the complexes *trans*-[PtCl<sub>2</sub>(*S*-mbn)(4-substituted-pyridine)]. The peaks below  $30,000 \text{ cm}^{-1}$  are almost identical, but the negative peaks at  $\approx 35,000 \text{ cm}^{-1}$  shifts as the substituent on the pyridine ring changes. Pyridine derivatives can have  $d_{\pi}-d_{\pi}$  interactions with platinum(II) and may perturb the electronic state.

*Asymmetric Influence from the trans Ligand.* As shown later, when an asymmetric nitrogen is in the *trans* position of the complexes of the type *trans*(*N*,//)-[PtCl(L-am)(ethylene)], asymmetry is introduced by the substitution of *tbn* for the ethylene in organic solvents. (10) L-Alanine, L-phenylalanine, and L-valine fail to introduce asymmetry on the incoming *tbn* in the equilibrated state. However, L-proline, *N*- and *C*-substituted L-proline and even *N*-substituted L-valine induce asymmetry. (Table V) There must be some electronic interaction from the asymmetric nitrogen upon the olefin through platinum(II).

Figure 10 shows the CD pattern of some of these complexes. Complexes without asymmetric nitrogen give only very weak CD in the region from  $20,000$  to  $40,000 \text{ cm}^{-1}$ . Especially between  $27,000$  and  $40,000 \text{ cm}^{-1}$  the CD is much weaker than those with asymmetric nitrogens (Figure 10-D). Since the complexes with L-proline, L-hydroxyproline and *allo*-L-hydroxyproline have very similar patterns to one another, the asymmetric carbon atoms on the pyrrolidine ring do not seem to give significant contributions. (Figure 10-B) On the other hand, introduction of a methyl or benzyl substituent on the nitrogen changes the CD pattern to a

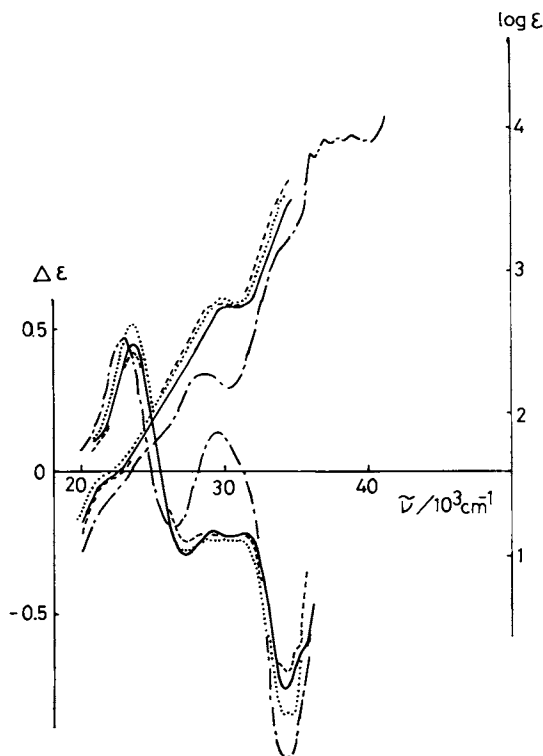


Figure 7. UV absorption and CD spectra of platinum(II) complexes containing *S*-2-methyl-2-butene (*mbn*) and 4-substituted anilines: (—), X = H in *trans*-[PtCl<sub>2</sub>(*S*-*mbn*)(4-X-aniline)] (in benzene); (· · ·), X = Cl in *trans*-[PtCl<sub>2</sub>(*S*-*mbn*)(4-X-aniline)] (in benzene); (---), (X = CH<sub>3</sub>) in *trans*-[PtCl<sub>2</sub>(*S*-*mbn*)(4-X-aniline)] (in benzene); (- · - ·), P(C<sub>6</sub>H<sub>5</sub>)<sub>4</sub>[PtCl<sub>3</sub>(*S*-*mbn*)] in dichloromethane.

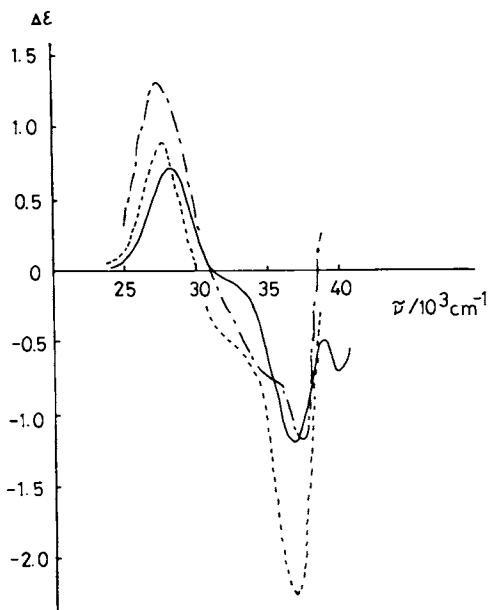


Figure 8. CD spectra of platinum(II) complexes containing *S*-2-methyl-2-butene and various amines on the *cis* site: (—),  $[\text{PtCl}(\text{o-phenylenediamine})(\text{S-mbn})]$  in ethanol; (---),  $\text{cis}(\text{N}_2//)[\text{PtCl}(\text{L-prolinate})(\text{S,S-tbn})]$  in acetonitrile; (-·-·),  $\text{cis}(\text{Cl})[\text{PtCl}_2(\text{S-1-phenylethylamine})(\text{S-mbn})]$  in acetone.

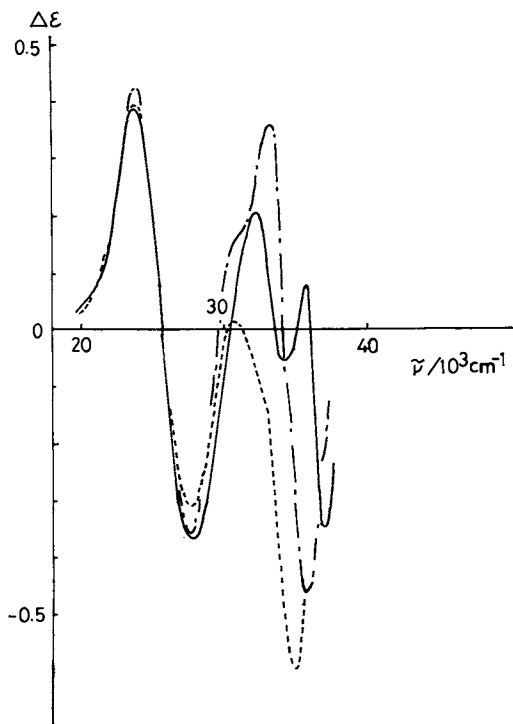


Figure 9. CD spectra of platinum(II) complexes containing *S*-2-methyl-2-butene (*mbn*) and 4-substituted pyridines on the *trans* site in dichloromethane: (---), X = NH<sub>2</sub>; (—), X = H; and (- · - ·), X = CO<sub>2</sub>C<sub>2</sub>H<sub>5</sub> in *trans*-[PtCl<sub>2</sub>(4-X-py)-(S-*mbn*)].

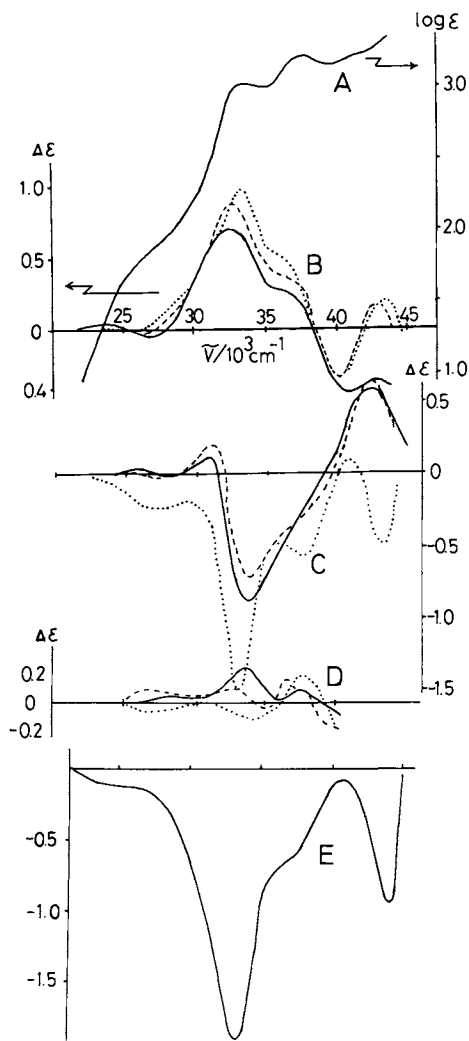


Figure 10. UV absorption (A) and CD spectra of  $\text{trans}(\text{N}, //)\text{-[PtCl(L-aminocarboxylate)(ethylene)]}$  in acetonitrile (10). B: (—), *L*-prolinate; (---), *L*-hydroxyprolinate; (· · ·), *allo-L*-hydroxyprolinate. C: (—), *N*-methyl-*L*-pro; (---), *N*-methyl-*L*-hyp; (· · ·), *N*-benzyl-*L*-pro. D: (—), *L*-alaninate; (---), *L*-phenylalaninate; (· · ·), *L*-valinate. E: (—), *N*-benzyl-*L*-valinate.

marked extent, especially in the region from 25,000 to 40,000  $\text{cm}^{-1}$  (Figure 10-C). In particular *N*-benzyl-L-valinate gives a large negative peak at *ca.* 34,000  $\text{cm}^{-1}$ , which is similar to that of *N*-benzyl-L-prolinate (Figure 10-E). This fact indicates a marked stereoselectivity on coordination of *N*-benzyl-L-valinate. *trans*-(*N*,//)-[PtCl(*N*-bz-L-val)(ethylene)] can exist as a pair of diastereoisomers, *S*(*N*)*S*(*C*) and *R*(*N*)*S*(*C*). Its CD spectrum is very similar to that of *N*-benzyl-L-prolinate complex, which can have only *R*(*N*)*S*(*C*) configuration. The *N*-benzyl-L-valinate complex seems to be formed almost exclusively in the *R*(*N*)*S*(*C*) form, when Zeise's salt undergoes substitution with free *N*-benzyl-L-valine in a slightly acidic solution. The preference for the *R*-configuration around the coordinated nitrogen adjacent to an *S*-carbon is rather common for octahedral complexes. (11) Molecular model studies show that steric hindrance between the substituents on the nitrogen and *S*-carbon would be responsible for the selectivity.

Figures 10-B and -C indicate that the CD curves in the 33,000 and 37,000  $\text{cm}^{-1}$  regions have reversed signs. On the assumption of the additivity law, the differences of CD's between the *N*-benzyl-L-prolinate and L-prolinate, and between *N*-benzyl-L-valinate and L-valinate complexes are plotted against the wave number in Figure 11-A. Similar plots of  $\delta\Delta\epsilon$ 's between *N*-methyl-L-prolinate and L-prolinate, and between *N*-methyl-L-hydroxyprolinate and L-hydroxyprolinate complexes are shown in Figure 11-B. The  $\delta\Delta\epsilon$  curves are very similar to each other regardless of the aminocarboxylate moiety. Hence the additivity law should hold between the contributions of *N*-substituent and of the aminocarboxylate, the former being independent of the chelate framework.

Usefulness of the quadrant rule for the interpretation of the CD signs of  $\eta^2$ -olefin complexes of platinum(II) in 25,000  $\text{cm}^{-1}$  region was demonstrated by Scott and Wrixon (5). We have applied this rule for interpreting the contribution of the asymmetric nitrogen. Figure 12 shows the projection of *trans*-(*N*,//)-[PtCl(*N*-alkyl-L-pro)(ethylene)]. The square plane is represented by the horizontal line, and the Pt-N bond is perpendicular to the paper plane. The asymmetric nitrogen is beneath platinum(II) (large dotted circle). The contribution of the minus quadrant at below left side behind the paper should depend on the size of the substituent on nitrogen (triangle). With an increase in size of this substituent (H, methyl and benzyl) the contribution of this minus component should increase to give the calculated curves shown in Figure 11.

The UV absorption curves of all the present complexes have peaks with  $\epsilon = ca. 10^3 \text{M}^{-1} \text{cm}^{-1}$  from 31,000 to 45,000  $\text{cm}^{-1}$ . Denning, Hartley and Venanzi assigned the absorption bands of Zeise's salt in this region to *d*- $\pi^*$ (ethylene) transition. (12) We have observed CD peaks with  $\Delta\epsilon$ 's -1.3 and +3.3 at *ca.* 35,000 and 39,500  $\text{cm}^{-1}$  for the tetraphenylphosphonium salt of [PtCl<sub>3</sub>(*S*,*S*-tbn)]<sup>-</sup> in acetonitrile. (13) The peak at 35,000  $\text{cm}^{-1}$  must correspond to the same transition as that of the main CD band of Figure 10 (and Figure



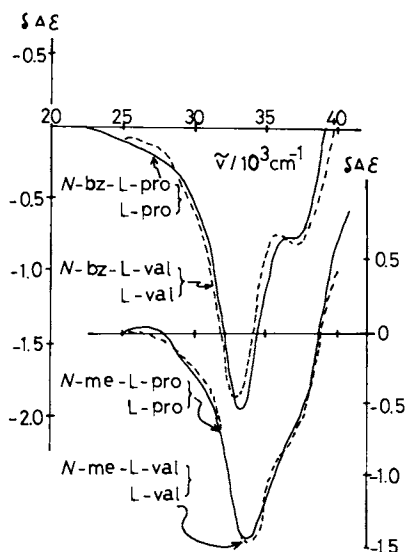


Figure 11. Difference in CD between two complexes of the type  $\text{trans}(\text{N},//)-[\text{PtCl}(\text{L-aminocarboxylate})(\text{ethylene})]$  with and without substituent on the nitrogen (10)

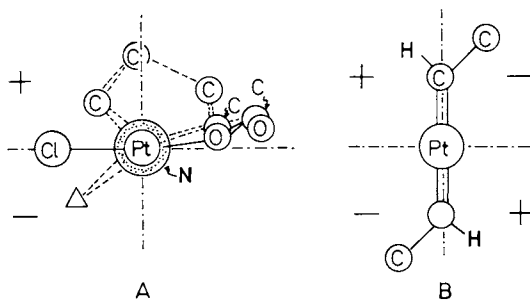


Figure 12. Projection of the square planar complexes (10): A,  $\text{trans}(\text{N},//)-[\text{PtCl}(-\text{substituted L-am})(\text{ethylene})]$ ; B, S,S-*trans*-2-butene moiety.

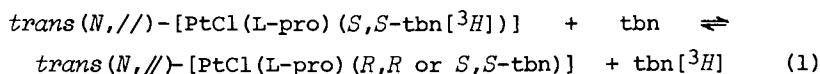
11). Figure 12 also shows the projection of this Zeise-type complex; the C-C moiety is placed across the square plane of platinum(II) behind the paper. A common contribution of the minus region to the lower left behind the paper seems to predominate for the Zeise-type and the present complexes. The  $d-\pi^*$  transition may be perturbed by the asymmetric nitrogen trans to ethylene to give a marked CD peak in this region.

The *cis*-isomer *cis*(*N, //*)-[PtCl(L-pro)(ethylene)] gives only a weak CD in this region (Figure 13).

### Stereo-selectivity on Olefin Exchange

*Selectivity on the Exchange of Prochiral Olefins.* Substitution of olefins for the coordinated  $\eta^2$ -olefin was first studied kinetically by PMR spectroscopy for the complex [PtCl(acac)(C<sub>2</sub>H<sub>4</sub>)] (acac, enolate anion of acetylacetone). (14) Stereo-selectivity in such a reaction was pointed out first by Corradini, Paiaro and Panunzi for the equilibrium of *cis*-[PtCl<sub>2</sub>(*S*-amine)(olefin)] in organic solvent, the *R*-configuration being preferred by 5 to 50 %. (15) Many studies have dealt with the selectivity of reactions of coordinated ligands, (16) but nothing has been reported concerning the stereoselectivity for the substitution of coordinated olefins.

We examined several years ago the rate of the following reactions by use of CD measurements and the isotopic labelling method.



and found a significant selectivity in favor of substitution with retention of configuration (Table III).

Table III. Second Order Rate Constants of the Substitution of 2-Butene for the *S, S*-2-Butene in *trans*(*N, //*)-[PtCl(L-proline)(*S S*-*trans*-2-butene[<sup>3</sup>H])] in Acetone. (17)

| Olefin   | <i>cis</i> -2-butene |          | <i>trans</i> -2-butene* |       |
|--|----------------------|----------|-------------------------|-------|
|  | 8.0                  | -20.0    | 8.0                     | -20.0 |
| Temp/°C  | 8.0                  | -20.0    | 8.0                     | -20.0 |
| $k_{\text{cd}}/10^{-3} \text{M}^{-1} \text{s}^{-1}$  | 347                  | 70.9±7.6 | 6.2                     | 0.9   |
| $k_{\text{iso}}/10^{-3} \text{M}^{-1} \text{s}^{-1}$ |                      | 70.2±4.1 | 32.3                    | 5.6   |

\* The calculated  $k_{[SS]}$  and  $k_{[SR]}$  at 8.0°C are 29.1 and  $3.1 \times 10^{-3} \text{M}^{-1} \text{s}^{-1}$ , respectively, the ratio  $k_{[SS]}/k_{[SR]}$  being 9.4.

The identical rate of substitution of non-prochiral *cis*-2-butene for the coordinated *S,S*-tbn measured by the two methods indicates the absence of other reactions such as local proton exchange between *cis*-2-butene and *trans*-2-butene. The second order rate constants for the tbn substitution measured by the two methods ( $k_{\text{iso}}$  and  $k_{\text{cd}}$ ) are correlated with the rate constants for retention  $k_{[\text{SS}]}$  and inversion of configuration  $k_{[\text{SR}]}$  by Equation (2).

$$k_{\text{cd}} = 2k_{[\text{SR}]} \quad k_{\text{iso}} = k_{[\text{SS}]} + k_{[\text{SR}]} \quad (2)$$

On the basis of the data in Table III it is seen that substitution with retention of configuration is preferred to that with inversion by a factor *ca.* 10 at 8.0°C.

The substrate complex *trans*(*N, //*)-[PtCl(L-pro)(*S,S*-tbn)] has three centers of asymmetry, the coordinated olefin, asymmetric carbon in the L-prolinate, and the nitrogen which becomes asymmetric on coordination. In order to find the actual source of such a significant stereoselectivity on substitution, the L-prolinate complex was converted into [PtCl<sub>3</sub>(*S,S*-tbn)]<sup>-</sup> by the action of hydrochloric acid. The replacement of L-prolinate by chloride proceeded with almost full retention of configuration. (The CD strength is almost equal to that of [PtCl<sub>3</sub>(*S,S*-*trans*-cyclooctene)]<sup>-</sup>.) By use of labelled [PtCl<sub>3</sub>(*S,S*-tbn[<sup>3</sup>H])]<sup>-</sup>, the substitution of tbn for the *S,S*-tbn was measured in acetone by two methods, CD spectroscopy and isotopic exchange. The results are shown in Table IV. Here again a marked stereoselectivity is seen, retention of configuration being preferred. The activation parameters for the  $k_{\text{cd}}$  and  $k_{\text{iso}}$  values indicate that the difference comes mainly from the entropy effect, *i.e.* by a steric reason. Figure 14 illustrates the interaction of the incoming and the coordinated *trans*-2-butene. The coordinated olefin in square planar platinum (II) complexes containing chloride and acetylacetonate (18,19), halide or trifluoroacetate and tertiary phosphines or arsines (20), and halides and tertiary phosphines or phosphites. (21) was found

Table IV. Second Order Rate Constants and Activation Parameters for the Substitution of *trans*-2-butene for [PtCl<sub>3</sub>(*S,S*-*trans*-2-butene[<sup>3</sup>H])]<sup>-</sup> in Acetone (13)

| Temp<br>°C  | $k_{\text{cd}}$                       | $k_{\text{iso}}$                      | $k_{[\text{SS}]}$                     | $k_{[\text{SR}]}$                     | $\frac{k_{[\text{SS}]}}{k_{[\text{SR}]}}$ |
|---|---------------------------------------|---------------------------------------|---------------------------------------|---------------------------------------|---|
|   | $10^{-3} \text{M}^{-1} \text{s}^{-1}$ | $10^{-3} \text{M}^{-1} \text{s}^{-1}$ | $10^{-3} \text{M}^{-1} \text{s}^{-1}$ | $10^{-3} \text{M}^{-1} \text{s}^{-1}$ |   |
| 8.0   | 17.3                                  | 70.6                                  | 62.0                                  | 8.7                                   | 7.2                                       |
| -5.0  | 6.74                                  | 35.1                                  | 31.7                                  | 3.4                                   | 9.3                                       |
| -20.0   | 2.65                                  | 11.4                                  | 10.1                                  | 1.3                                   | 7.8                                       |
| $\Delta H^\ddagger / \text{kJ mol}^{-1}$              |                                       |                                       | 36.3 ± 3.1                            | 37.6 ± 2.7                            |   |
| $\Delta S^\ddagger / \text{J mol}^{-1} \text{K}^{-1}$ |                                       |                                       | -138 ± 12                             | -149 ± 10                             |   |

Figure 13. UV absorption and CD spectra of *cis*(N,/) - [PtCl(L-pro)-(ethylene)] in acetonitrile (10)

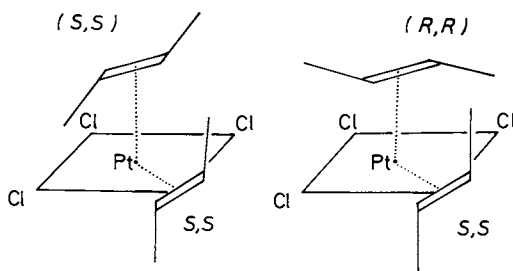
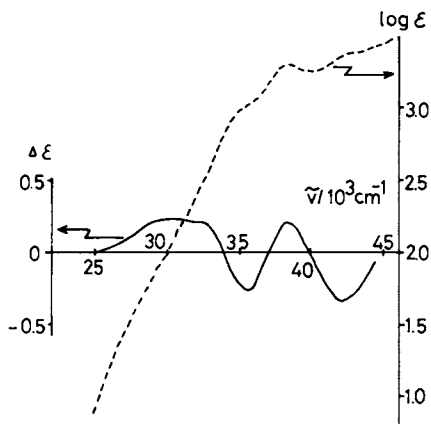
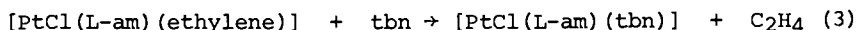


Figure 14. Plausible transition states on the nucleophilic attack of *trans*-2-butene (*tbn*) upon [PtCl<sub>3</sub>(*S,S*-*tbn*)] (13)

to be rotating around the Pt-// axis at room temperature. Even a simple molecular model study discloses that the approach of tbn to form a square pyramidal transition state is easier with retention of configuration (Figure 14-A) than with inversion of configuration (Figure 14-B).

The ratio  $k_{[SS]}/k_{[SR]}$  is slightly but significantly smaller than that for the substitution of tbn for the *S,S*-tbn in *trans*-(*N, //*)-[PtCl(L-pro)(*S,S*-tbn)]. Hence the asymmetric carbon or nitrogen on L-prolinate must play some role in causing the stereoselectivity.

*Induction of Asymmetry on Olefin Exchange.* When an excess of *trans*-2-butene is added to an acetone solution of *trans*-(*N, //*)-[PtCl(L-am)(ethylene)], the UV absorption does not change significantly but the CD pattern changes as shown in Figure 15. (22) The CD strength in the region from 23,000 to 32,000  $\text{cm}^{-1}$  first increases and then decreases, The change in CD strength at 26,300  $\text{cm}^{-1}$  (the maximum of the peak due to the asymmetric coordination of tbn) is plotted against the time in Figure 16. The CD strength increases at the initial stage to reach a maximum ( $\Delta\epsilon_{\text{max}}$ ) (first step). (The UV pattern of the original complex in the region from 32,000 to 45,000  $\text{cm}^{-1}$  changes slightly to approach that of the tbn complex.) This step should involve stereoselective formation of the *S,S*-tbn complex by the following reaction.



Since the tbn overwhelms ethylene, the ethylene should be almost exclusively in free state. (*vide infra*)

In the second step the CD strength at 26,300  $\text{cm}^{-1}$  gradually decreases, while the UV absorption remains unchanged. The second step is much slower than the first step, and both can be kinetically analysed separately. The apparent optical yield in the first step ( $p_{\text{max}}$ ) is calculated by Equation (4),

$$p_{\text{max}} = (\Delta\epsilon_{\text{max}} - \Delta\epsilon_{\text{vic}})/(\Delta\epsilon_{\text{resolv}} - \Delta\epsilon_{\text{vic}}) \quad (4)$$

where  $\Delta\epsilon_{\text{resolv}}$  is the CD peak strength in the region from 26,000 to 27,000  $\text{cm}^{-1}$  of the resolved tbn complex, and  $\Delta\epsilon_{\text{vic}}$  the CD strength due to the vicinal effect of L-aminocarboxylate (L-am) which is represented by the CD strength of the ethylene complex [PtCl(L-am)(ethylene)]. (The CD peak shifts only slightly on the change in the kind of aminocarboxylate in this region.) The  $p_{\text{max}}$  values are listed in Table V.

The second step gives no UV change and is considered to involve the replacement of the asymmetrically coordinated tbn by free tbn towards thermodynamically equilibrated state. The optical yield at equilibrium is calculated by Equation (5)

$$p_{\text{eq}} = (\Delta\epsilon_{\text{eq}} - \Delta\epsilon_{\text{vic}})/(\Delta\epsilon_{\text{resolv}} - \Delta\epsilon_{\text{vic}}) \quad (5)$$

where  $\Delta\epsilon_{\text{eq}}$  is the CD strength in the equilibrated state. The  $p_{\text{eq}}$  values are listed in Table V.

Figure 15. Change in the CD spectrum with time on the reaction between  $\text{trans}(\text{N},//)-[\text{PtCl}(\text{N-me-L-pro})(\text{ethylene})]$  (0.00154M) and  $\text{trans-2-butene}$  (0.279M) in acetone at  $-28.0^\circ\text{C}$  (22): ( $\cdots$ ), original complex; ( $---$ ), 1 min after; ( $-\cdot-\cdot-$ ), 2 min after; ( $---$ ), 4 min after; ( $-\cdot-\cdot-$ ), infinite time.

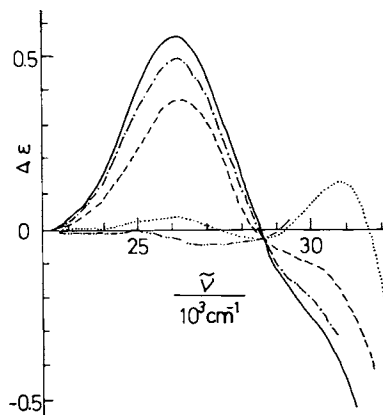


Figure 16. Change in CD strength at  $26,300\text{ cm}^{-1}$  on the reaction given in Figure 15 (22)

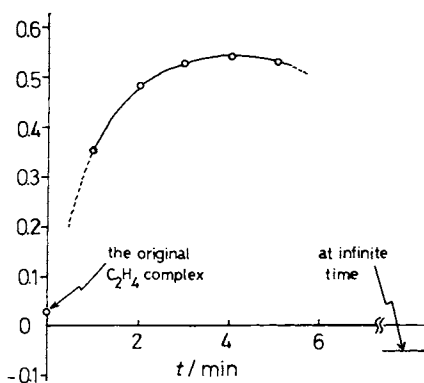


Table V. Kinetic and Thermodynamic Optical Yield of *trans*-(*N*,//)-[PtCl(L-am)(olefin)] on the Reaction of the Corresponding Ethylene Complexes with Olefins (22)

| L-am <sup>a</sup>                | <i>T</i> /°C | Solvent <sup>b</sup> | <i>p</i> <sub>max</sub> /% | <i>p</i> <sub>eq</sub> /% | Olefin |
|----------------------------------|--------------|----------------------|----------------------------|---------------------------|--------|
| L-pro                            | 8.0          | actn                 | 35                         | +12 ( <i>SS</i> )         | tbn    |
|                                  | -27.5        | actn                 | 34                         |                           | tbn    |
| <i>N</i> -me-L-pro               | 8.0          | actn                 | 53                         | -6 ( <i>RR</i> )          | tbn    |
| <i>N</i> -et-L-pro               | 8.0          | actn                 | 50                         | ~0                        | tbn    |
| <i>N</i> -bz-L-pro               | 8.0          | actn                 | 24                         | ~-1 ( <i>RR</i> )         | tbn    |
|                                  | 8.0          | dcm                  | 28                         |                           | tbn    |
| <i>N</i> -bz-L-val               | 8.0          | actn                 | 40                         | -10 ( <i>RR</i> )         | tbn    |
|                                  | 8.0          | an                   | 39                         | -9 ( <i>RR</i> )          | tbn    |
|                                  | 8.0          | L-ma                 | 35                         |                           | tbn    |
| L-val                            | -30.0        | actn                 | 0                          |                           | tbn    |
| L-ala                            | -30.0        | actn                 | 0                          |                           | tbn    |
| L-hyp                            | 8.0          | actn                 | 37                         | +8 ( <i>SS</i> )          | tbn    |
| <i>N</i> -me-L-hyp               | 8.0          | actn                 | 32                         | -7 ( <i>RR</i> )          | tbn    |
| L-ahyp                           | 8.0          | actn                 | 37                         | +6 ( <i>SS</i> )          | tbn    |
| <i>cis</i> ( <i>N</i> ,//)-L-pro | 8.0          | actn                 | 33                         |                           | tbn    |
|                                  | -13.0        | actn                 | 34                         | -27 ( <i>RR</i> )         | tbn    |
| L-pro                            | 8.0          | actn                 | 7                          | +6 ( <i>S</i> )           | mbn    |
| <i>N</i> -me-L-pro               | 8.0          | actn                 | 7                          | ~-1 ( <i>R</i> )          | mbn    |
| L-hyp                            | 8.0          | actn                 | 6                          | ~+3 ( <i>S</i> )          | mbn    |
| <i>N</i> -me-L-hyp               | 8.0          | actn                 | 3                          | ~0                        | mbn    |
| L-ahyp                           | 8.0          | actn                 | 19                         | +7 ( <i>S</i> )           | mbn    |

a) hyp, hydroxyprolinate; ahyp, *allo*-hydroxyprolinate; me, methyl; et, ethyl; bz, benzyl.

b) actn, acetone; dcm, dichloromethane; an, acetonitrile; L-ma, L-methylacetate.

Detailed analysis of the curves exemplified in Figure 16 enables the estimation of individual rate constants for both directions of Equation (3). It was also elucidated that the second step is the exchange of between coordinated and free tbn catalysed by ethylene made free in the first step. However, the detailed kinetic studies have been reported elsewhere (22) and omitted in this review.

The  $p_{eq}$  value is reckoned to reflect the difference in stability between the  $S,S$  and  $R,R$  configurations, and the stability should be related to the structure of complexes. Table V indicates that the *cis*( $N, //$ ) isomers give rather large negative  $p_{eq}$ . Molecular model studies suggest that the  $S,S$ -tbn is subject to a larger steric hindrance with  $R(N)$ -L-proline than  $R,R$ -tbn is, so that the  $R,R$ -configuration is favored. Such a difference in steric hindrance is not seen for *trans*( $N, //$ ) complexes. Among them complexes without asymmetric nitrogen fail to give  $p_{eq}$  values. Those with asymmetric nitrogens give  $p_{max}$  always in favor of the formation of  $S,S$ -configuration. *trans*-2-Butene gives larger  $p_{max}$  than 2-methyl-2-butene does, presumably owing to the presence of two asymmetric carbons. The extent of selectivity for the tbn reaction ranges from 20 to 50 %, and it is rather difficult to find a correlation between the  $p_{max}$  and the structure. The  $p_{max}$  depends on the nature of the  $N$ -substituent, but not on the location of hydroxyl group on the pyrrolidine ring. The incoming tbn should approach platinum(II) from the opposite side to that occupied by pyrrolidine. The bulkiness of the substituent does not increase  $p_{max}$ , but rather decreases it. Studies with molecular models suggest that the approach of tbn to platinum(II) center having asymmetric nitrogen would be easier in  $S,S$ - than in  $R,R$ -configuration, but do not enable more detailed discussion.

The  $p_{eq}$  values have both positive and negative values, and do not seem to be correlated easily with the structure. The sign of  $p_{eq}$  is not always equal to that of  $p_{max}$ . The sequence of magnitude of  $p_{eq}$ 's of the complexes containing various aminocarboxylates is neither parallel to that of  $p_{max}$ 's. Hence, the origin of  $p_{eq}$  does not seem to be in the steric factor. When one compares the sign of  $p_{eq}$ 's with the CD sign in Figure 10 (B and C), one can see a rather distinctive relationship. Positive and negative CD signs in the region around  $35,000\text{ cm}^{-1}$  cause preferential formation of the  $S,S$ -tbn and  $R,R$ -tbn, respectively. We discussed the presence of asymmetric perturbation from the asymmetric nitrogen trans to the olefin on the basis of the quadrant rule. (10) The induction of asymmetry on the reaction of ethylene trans to asymmetric nitrogen with free tbn seems to be due to such an electronic effect. The source of asymmetry has been mostly ascribed to steric origins in various substitution reactions, but the present reaction appears to give a new example of electronic induction of asymmetry.



Summary

$\eta^2$ -Olefins in square planar complexes of platinum(II) and rhodium(I) give absorption peaks or shoulders in the regions from 20,000 to 30,000  $\text{cm}^{-1}$  and ca.40,000  $\text{cm}^{-1}$ . Asymmetrically coordinated olefins give CD peaks corresponding to these peaks; the *S,S*-configuration gives large negative peaks in the latter region for both platinum(II) and rhodium(I) complexes, whereas the CD sign in the former region depends on the central metal ion. In the region from 30,000 to 40,000  $\text{cm}^{-1}$  the CD pattern depends on the variation in ligands other than the olefin. There seems to be a *cis* influence and also some perturbation from the asymmetric nitrogen trans to the olefin.

Prochiral olefins in platinum(II) complexes of the types  $[\text{PtCl}_3(\text{olefin})]^-$  and *cis*- and *trans*(*N, //*)- $[\text{PtCl}(\text{L-am})(\text{olefin})]$  (L-am, L-aminocarboxylate) undergo inter-molecular olefin exchange with an excess of free olefin in organic solvents. Comparison of the rates of CD decrease and the isotopic exchange with labelled ligands exhibited significant stereo-selectivity, retention of configuration being preferred to inversion. On the reaction of  $[\text{PtCl}(\text{L-am})(\text{ethylene})]$  with *trans*-2-butene (tbn) or 2-methyl-2-butene (mbn) appreciable induction of asymmetry was found in the product. Both kinetic and thermodynamic optical yield have been recorded separately. Kinetic selectivity seems to come from a steric factor, but perturbation from asymmetric nitrogen trans to ethylene seems to be responsible for the thermodynamic selectivity.

Abbreviations

|   |   |
|---|---|
| <u>acac</u> <sup>-</sup> , enolate anion of acetylaceton    | <u>am</u> <sup>-</sup> , aminocarboxylate |
| <u>ahyp</u> <sup>-</sup> , <i>allo</i> -hydroxyprolinate    | <u>ala</u> <sup>-</sup> , alaninate       |
| <u>bz</u> , benzyl  | <u>coe</u> , cyclo-octene                 |
| <u>dbm</u> <sup>-</sup> , enolate anion of dibenzoylmethane | <u>CD</u> , circular dichroism            |
| <u>hyp</u> <sup>-</sup> , hydroxyprolinate                  | <u>et</u> , ethyl                         |
| <u>me</u> , methyl  | <u>mbn</u> , 2-methyl-2-butene            |
| <u>pro</u> <sup>-</sup> , prolinate                         | <u>tbn</u> , <i>trans</i> -2-butene       |
| <u>UV</u> , ultraviolet                                     | <u>val</u> <sup>-</sup> , valinate        |

Acknowledgement The expenses were mostly defrayed from a Grant-in-Aid of the Ministry of Education of the Japanese Government, to which deep appreciation is due. The present studies are the result of collaboration of the following chemists. Professor J.Fujita, Dr. K.Kashiwabara (formerly Konya) and Mr. I.Kinoshita who are at Nagoya University now have carried out the difficult synthetic work. Dr. Y.Terai (now in Institute of Physical and Chemical Research) and Messrs H.Kido and S.Miya contributed much in the preparation of some new compounds, and the kinetic studies by CD spectroscopy and isotope labelling method. Thanks are also due to the Chemical Society of Japan for the permission of reproducing Figures 10 to 16 and Tables IV and V from my own papers published in Bulletin of the Chemical Society of Japan.

Literature Cited

1. Hawkins, C.J. "Absolute Configuration of Metal Complexes", Wiley-Interscience, New York, 1971.
2. Cope, A.C.; Ganellin, C.R.; Johnson, H.W., Jr.; van Auken, T. V.; Wilkins, H.J.S. *J. Am. Chem. Soc.*, 1963, 85, 3276.
3. Paiaro, G.; Panunzi, A. *Ibid.*, 1964, 86, 5148 ; 1966, 88, 4843.
4. Paiaro, G. *Organometallic Chem. Rev.*, 1970, A, 6, 319.
5. Scott, A.I.; Wrixon, A.D. *Tetrahedron*, 1970, 27, 2339.
6. Musco, A.; Paiaro, G.; Palumbo, R. *Ricerca Sci.*, 1969, 39, 417
7. Miya, S.; Kashiwabara, K.; Saito, K. in preparation.
8. Kinoshita, I.; Terai, Y.; Kashiwabara, K.; Kido, H.; Saito, K. *J. Organomet. Chem.*, 1977, 127, 237.
9. Konya, K.; Fujita, J.; Nakamoto, K. *Inorg. Chem.*, 1971, 10, 1699.
10. Terai, Y.; Kido, H.; Saito, K. *Bull. Chem. Soc. Jpn.*, 1977, 50, 3265.
11. e. g. Saburi, M.; Yoshikawa, S. *Inorg. Chem.*, 1968, 7, 1890.
12. Denning, R.G.; Hartley, F.R.; Venanzi, L.M. *J. Chem. Soc.*, (A), 1967, 1322.
13. Terai, Y.; Saito, K. *Bull. Chem. Soc. Jpn.*, 1978, 51, 503.
14. Holloway, C.E.; Fogelman, J. *Can. J. Chem.*, 1970, 48, 3802.
15. Corradini, P.; Paiaro, G.; Panunzi, A. *J. Am. Chem. Soc.*, 1966, 88, 2836.
16. Ishii, Y.; Tsutsui, M. Ed. "Organotransition Metal Chemistry", Plenum Press, 1975, p.157 .
17. Terai, Y.; Kido, H.; Fujita, J.; Saito, K. *Bull. Chem. Soc. Jpn.*, 1975, 48, 1233.
18. Holloway, C.E.; Hulley, G.; Johnson, B.F.G.; Lewis, J. *J. Chem. Soc.*, (A) 1969, 53.
19. *Idem.*, *ibid.*, 1970, 1653.
20. Ashley-Smith, J; Douek, I.; Johnson, B.F.G.; Lewis, J. *J. Chem. Soc., Dalton*, 1972, 1776.
21. Ashley-Smith, J.; Douek, Z.; Johnson, B.F.G.; Lewis, J. *ibid.*, 1974, 128.
22. Terai, Y.; Kido, H.; Kashiwabara, K.; Saito, K. *Bull. Chem. Soc. Jpn.*, 1978, 51, 3245.

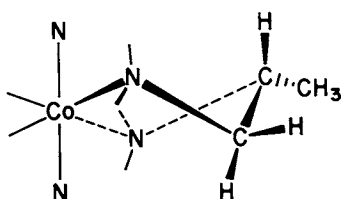
RECEIVED September 13, 1979.

## Chirality Induction in Coordination Complexes

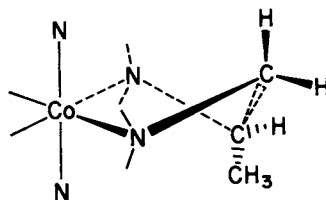
A. M. SARGESON

Research School of Chemistry, The Australian National University,  
P.O. Box 4, Canberra Act 2600, Australia

Over the past twenty years the conformations and steric effects in chelate ring systems have been examined in considerable detail. Structural studies along with equilibrium measurements, some kinetic studies and conformational analyses have given us a better insight into the steric interactions within the chelates and between the chelates (1). For five membered chelates such as coordinated 1,2 diaminopropane



$\lambda$  CoR(-)pn



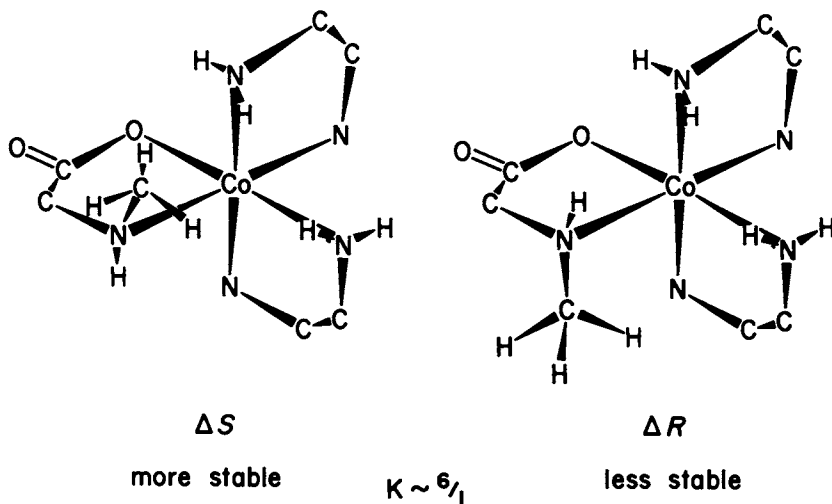
$\delta$  CoR(-)pn

the axial-equatorial nature of the substituents on the C atoms is sufficiently pronounced (2) that the axial methyl groups interact with axial substituents on the metal ion and this conformation is rarely if ever observed (1,2). In this way the conformation of the chelate is controlled as  $\lambda$  for Co(R)(-)pn (1,2). This chelate systems of this type show a marked preference for the isomer where the C-C axes of the individual chelates are near parallel to the  $C_3$  axis of the complex ion, e.g.  $\Delta$ [Co(R)(-)pn<sub>3</sub>]<sup>3+</sup> (1e<sub>3</sub>) is ~15 fold more stable than  $\Lambda$ [Co(R)(-)pn<sub>3</sub>]<sup>3+</sup> (ob<sub>3</sub>) where the C-C axes are oblique to the  $C_3$  axis of the ion (1)<sub>1</sub>

Substituents on the N atoms, however, do not show such a pronounced conformational effect in terms of axial-equatorial orientation but they appear to interact more strongly with the substituents on the metal ion. For example, sarcosinate ion chelates with a substantial specificity in the [Co(en)<sub>2</sub>sarcosinato]<sup>2+</sup> ion (3).

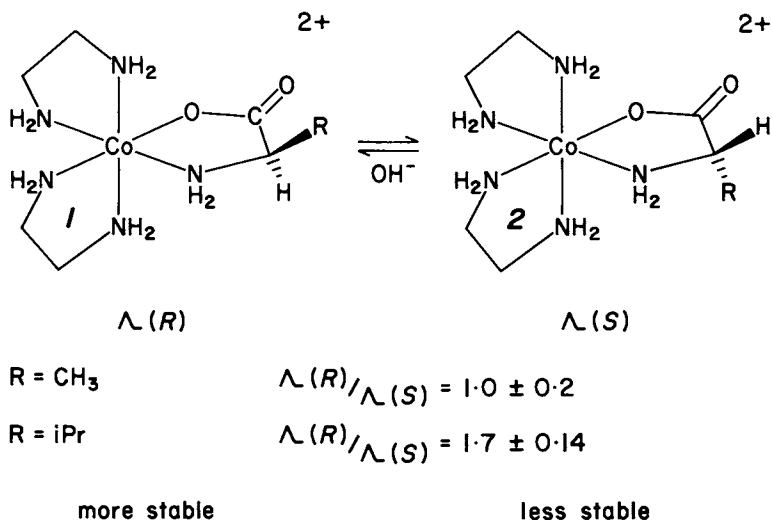
0-8412-0538-8/80/47-119-115\$05.00/0

© 1980 American Chemical Society



In the configuration where the  $\text{CH}_3$  is poised over the ethylenediamine chelate it interacts quite strongly whereas in the alternative configuration the  $\text{CH}_3$  group lies in the space between the two "en" chelates (4). In this situation the conformation of the "en" rings do not seem to be important and the amino acid shows very little conformational character. The equilibration between such ions arises from a base catalyzed removal of the proton at the chiral N center. The  $\text{pK}_a$  of such protons is  $\sim 15-17$ . In acidic solution they are <sup>a</sup> kinetically inert and the chirality at N is therefore preserved.

Substitution on the C atoms of such amino acid chelates does not give such a pronounced effect. Analogous bis(ethylenediamine) amino acid chelate systems show rather little discrimination between the two diastereoisomers. For example, the ratio of the *R* and *S* isomers in the  $\Lambda$  configuration is about equal for alanine and 2:1 for valine(5). It can be argued that the bulk of the R group is important and that the effect of the iso-propyl group is due to its relative orientation in relation to chelate rings 1 and 2. This effect is related to that of the sarcosinato ion except that the substituent is now more distant from the other chelates and the effect is less.

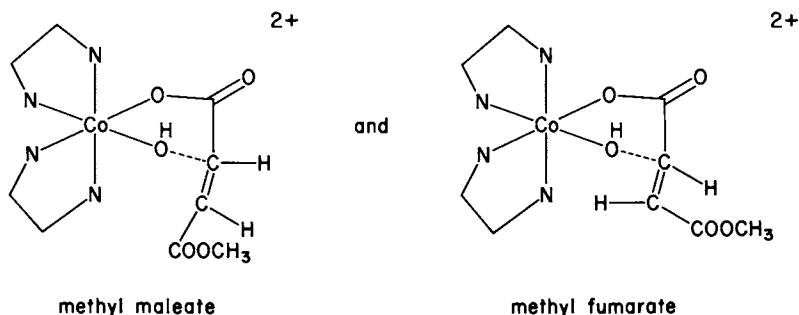


Much of this fact and rationale is fairly old history and it is introduced here to set the scene for some new specificity which is not equilibrium controlled but kinetically controlled. The work has arisen from intramolecular organic reactions promoted by metal ions and the use of coordinated nucleophiles. We have seen, for example, that bound  $\text{OH}^-$  at a metal can provide a high local concentration of the reagent at near neutral pH. The bound nucleophile is still potent even though it is somewhat modified by the metal. The ability of the metal ion to activate and protect organic molecules has also been seen to be substantial. It was logical then that the structural and conformational properties should be put together with the reactivity aspects to design some stereospecific syntheses. Most of the chemistry has been done with Co(III) complexes largely because the ligands do not exchange rapidly with the metal ion and the complexes remain intact for the life times of the reactions considered. In this way the efficacy of the processes can be assessed free from the complication of ligand-metal ion equilibria. The complexes on the whole are cheap to make and the methods are fairly routine and well defined.

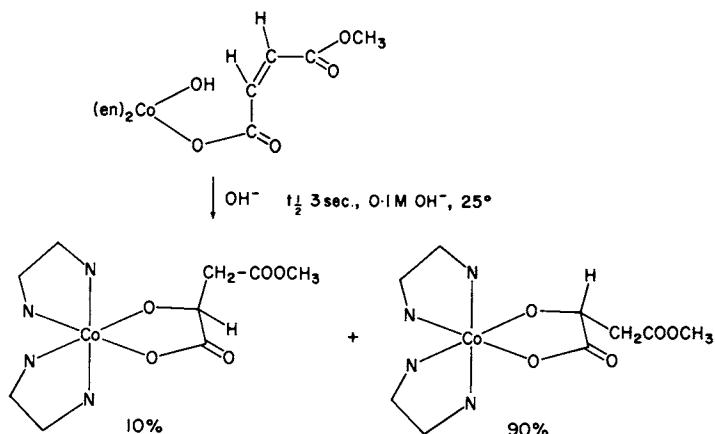
#### Stereospecific hydration of olefins

The efficacy of coordinated nucleophiles has been established for the intramolecular hydrolysis of numerous substrates; for example, coordinated amino acid esters (5), amino nitriles (6,7)

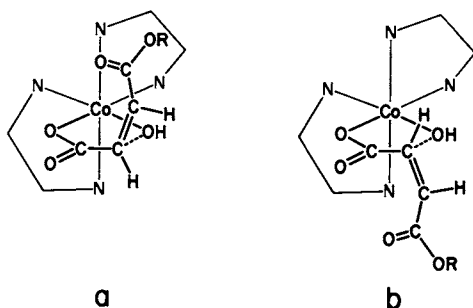
and 2-bromoethylamine (8). The same prospect for cyclization exists with coordinated olefins (9,10) and two systems have been constructed to examine it as follows:



The addition of OH at the olefinic center creates a chiral center at carbon in conjunction with the chiral center at cobalt. Two diastereoisomers are thereby produced. Addition of the bound OH is very rapid for the maleato system and essentially pH independent between pH 8-10. In this range the diastereoisomer ratio is ~2:1 as shown below. However, at higher pH values the rate becomes first order in OH<sup>-</sup> and in 0.1 M NaOH at 25°, the half-life for the production of malate is ~3 sec (at least 10<sup>6</sup>-fold faster than the uncoordinated hydration). Under these conditions the reaction becomes much more stereospecific with a 9:1 ratio of diastereoisomers. While it is clear that in the pH independent region, H<sup>+</sup> addition at the β carbon atom is the rate-determining step, it looks as if in the high base region deprotonation of the CoOH entity and addition of Co-O could be rate-determining.

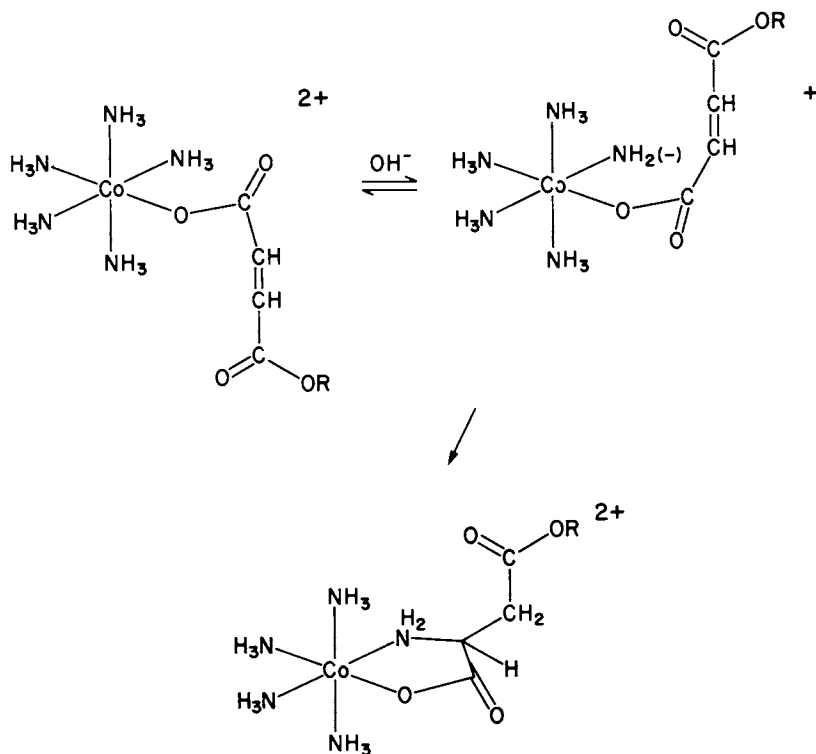


The same pattern was observed for the fumarate complex but the rates were about 1000-fold slower. The increase in specificity is the interesting and surprising feature. For analogous amino systems, the ratio of the diastereoisomers (5) at equilibrium is about 2:1 or less with the same structural relationships as the analogous malate products. It appears, therefore, that the product ratio of the pH independent path resembles the equilibrium situation whereas the path dependent on base is far from that condition. An explanation for the increase could arise if Co-O<sup>-</sup> addition was rate-determining. In the transition states for the generation of the two isomers configuration (a) will be more compressed than that of (b) by virtue of the non-bonded interactions between the substituents on the olefin and adjacent Co(en) chelate. This steric compression will be much more evident in the transition states than in the product malates.



The other specificity feature which is interesting in this reaction is the exclusive formation of the five-membered chelate relative to the possible six-membered chelate. Clearly the ester group *exo* to the chelate is governing the addition and the carboxyl bound to the metal ion has no influence. The stereochemistry for the addition of Co-O<sup>-</sup> or Co-OH requires the olefin and bound carboxyl  $\pi$  orbitals to be essentially orthogonal. It follows therefore that there is a minimal interaction between the two. The same restriction does not hold for the ester group *exo* to the chelate and the olefin is thereby sensitized. This is an interesting restriction placed on the reaction where the metal ion organizes the stereochemistry of the reactants and there will be other examples of such constraints where the metals are involved.

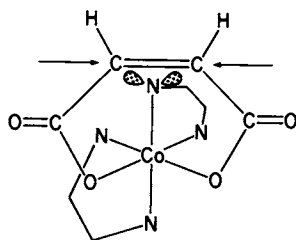
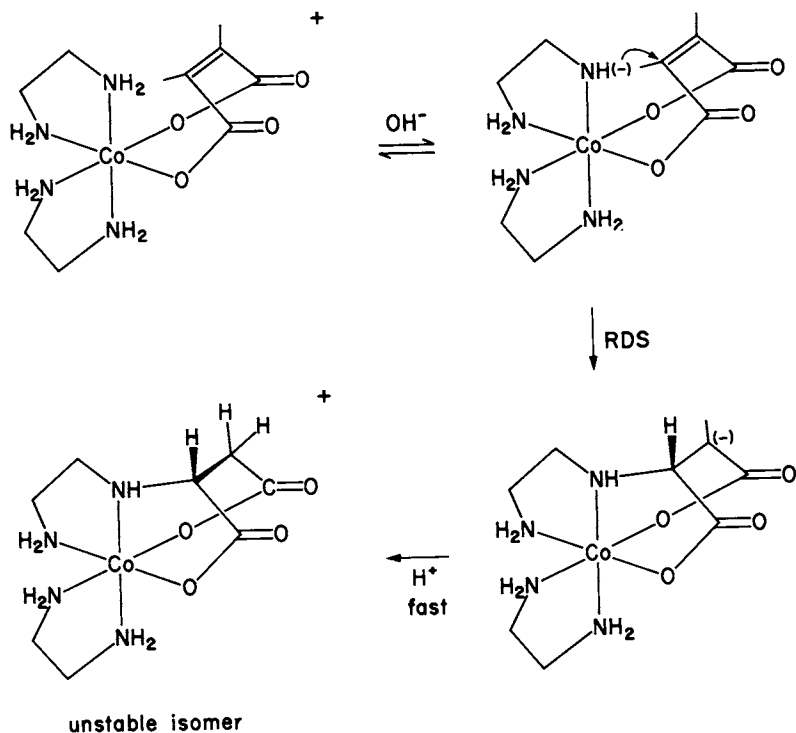
Not only is OH<sup>-</sup> a potent nucleophile in this context but so is NH<sub>2</sub><sup>-</sup> bound to the metal ion. The pentaammine maleatoester complexes of the type Co(NH<sub>3</sub>)<sub>5</sub>OOCCH=CHCOOR<sup>2+</sup> readily react in basic aqueous solution to give the chelated aspartate ester complex (11).



Analogous reactions with the monodentate maleato dianion, however, do not occur and this is not surprising organic chemistry since the terminal anion should deactivate the olefin to nucleophilic attack. It became interesting, therefore, to examine the chelated maleato complex where both carboxylate ions are bound to the metal center and where both should have some ester-like quality.

It transpires that  $[(en)_2Co \text{ maleato}]^+$  reacts rapidly in basic aqueous solutions (12). The rate is first order in hydroxide ion ( $-v = k[\text{maleato complex}][OH^-]$ , where  $k = 0.45 \text{ M}^{-1}\text{s}^{-1}$  at  $25^\circ$ ,  $\mu=1.0 \text{ NaClO}_4$ ). The initial product is a substituted aspartic acid terdentate which subsequently decomposes in the basic medium with cleavage of a carboxylate residue from the Co(III) ion ( $v=k[\text{unstable isomer}][OH^-]$ ,  $k=3.7 \text{ M}^{-1}\text{s}^{-1}$  at  $[OH^-] 25^\circ$ ,  $\mu=1.0 \text{ NaClO}_4$ ). We presume it is the species shown, but this is not certain yet. An interesting aspect of this reaction is not only the speed of the intramolecular addition but the specificity of it. Only the isomer shown appears to be formed. The other isomer possible, where the deprotonated ethylenediamine nucleophile,  $-NH(-)$ , adds at the other carbon atom of the maleate ion, does not seem to be produced in detectable quantities. Superficially there seems no special reason for the discrimination. Moreover the isomer which

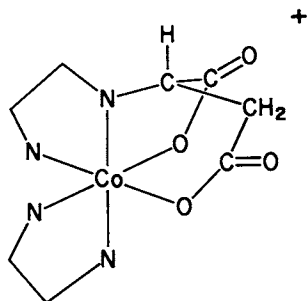




Two sites for addition

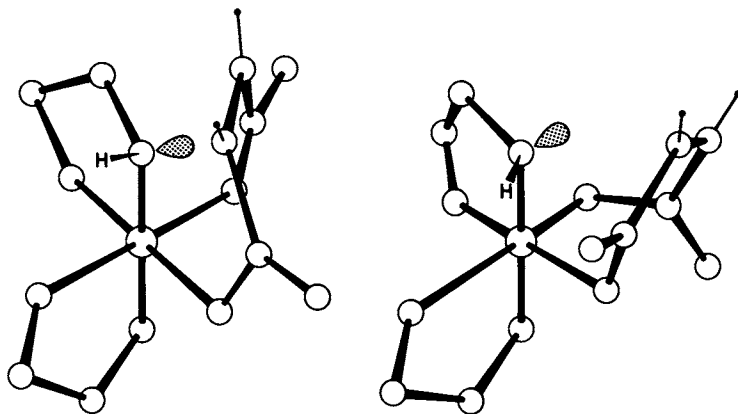
is not observed is by far the most stable. It can be synthesized from Co(II), en and 2-aminoethylaspartate by oxidation with  $O_2$  in the presence of charcoal and the equilibrium position lies heavily in favor of the isomer which is not observed in the kinetic synthesis. So this is an especially interesting instance of chiral induction at a carbon atom where the kinetic route gives, apparently exclusively, the less stable isomer and the equilibrium route leads almost

exclusively to the stable form whose structure has been determined.



Structure of the stable isomer  
(W.L. Steffen)

The apparent reasons for this specificity need some amplification. An examination of the problem using Dreiding models reveals some interesting features for the approach of the olefin to the nucleophile. If there is a requirement for one carboxylate ion to be co-planar and therefore conjugated with the olefin then there are two discrete conformations to be achieved. Both can be realized but one of them is substantially more favorable than the other for the addition of the nucleophile. The two possibilities are depicted,



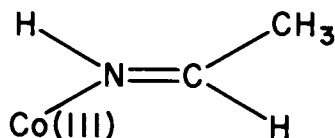
Orientations for the addition of Amido ion to chelated maleate

So the combination of the electronic requirement for activation of the olefin and the restriction which that places on the site for addition of the nucleophile is an interesting aspect of the demands which chelation makes on the reaction. It should be mentioned, of course, that the reaction does not occur at all with

the free maleate ion and ethylenediamine but it does with the diester (13). So the acceleratory effect of chelating the dianion must exceed  $10^6$  and probably is greater than  $10^{10}$ . Not only is the specificity interesting but the reactions conducted in this way are extraordinarily fast. The processes are relevant as models for some enzyme-catalyzed hydration, dehydration and amination-deamination reactions. The specificity was also observed in liquid ammonia and dimethyl sulfoxide.

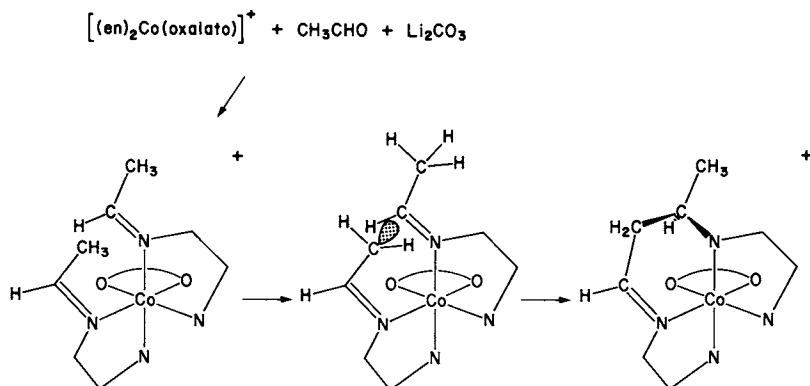
### Stereo Specificity directed by the Chelates

Imine formation in coordinated chelates has been known for a very long time but what has not been all that clear until recently is the stability of the coordinated imine when the imine group is essentially *exo* to the chelate ring. Systems such as



for example, have an extraordinary stability, especially towards concentrated acids (14). They are, however, more vulnerable to bases, presumably because of the ease with which nucleophiles add at the imine carbon center. Acetaldehyde condenses readily with Co(III) amine systems (14) and there is a substantial analogous literature with divalent metal ion amine systems (15). Much of the latter arose from the Curtis complexes formed by dissolving  $[\text{Ni}(\text{en})_3]^{2+}$  in acetone.

In the course of condensing the oxalato complex,  $[\text{Co}(\text{en})_2(\text{C}_2\text{O}_4)]^+$  and  $\text{CH}_3\text{CHO}$ , in basic solution, an acetalimine complex was identified and after prolonged exposure to the aldehyde and base, a complex was isolated where two aldimine residues had condensed together. This self-condensation has to



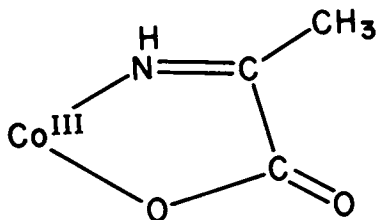
occur on the complex and it appears to be stereospecific in several senses.

The reaction must take place after the condensation of two  $\text{CH}_3\text{CHO}$  molecules adjacent to each other on different ethylenediamine residues. For one, the  $\text{CH}_3$  group has to be *syn* to the  $\text{Co(III)}$  ion and in the other *anti*. The *syn* methyl is deprotonated in the basic medium and the carbanion produced attacks the imine carbon of the other aldimine. The result is a quadridentate where the chiral C center has been formed stereospecifically by the way the imines are oriented through the chelates. Commencing with  $\Delta\text{-[Co(en)}_2\text{ox)]}^+$ , only one isomer should be observed.

The same condensation does not occur with either mesityl oxide or aldol and therefore it is presumed that the only feasible path is the one described. The orientation of the nucleophile is ideal for the intramolecular condensation and it is obvious that deprotonation of the other methyl group would not lead to any reaction. Similarly, condensation of  $\text{CH}_3\text{CHO}$  at the two adjacent N centers both trans to the oxalato group would not lead to the intramolecular reaction. In short, the chelates themselves have directed the specificity. It is tempting to argue that the Curtis condensations with  $[\text{Ni(en)}_3]^{2+}$  in acetone take place by an analogous route and subsequently rearrange to the planar condition about the  $\text{Ni}^{2+}$  ion. So far, attempts to carry out analogous reactions with *trans*- $[\text{Co(en)}_2\text{X}_2]^+$  complexes have not been successful but the negative result does not mean a great deal.

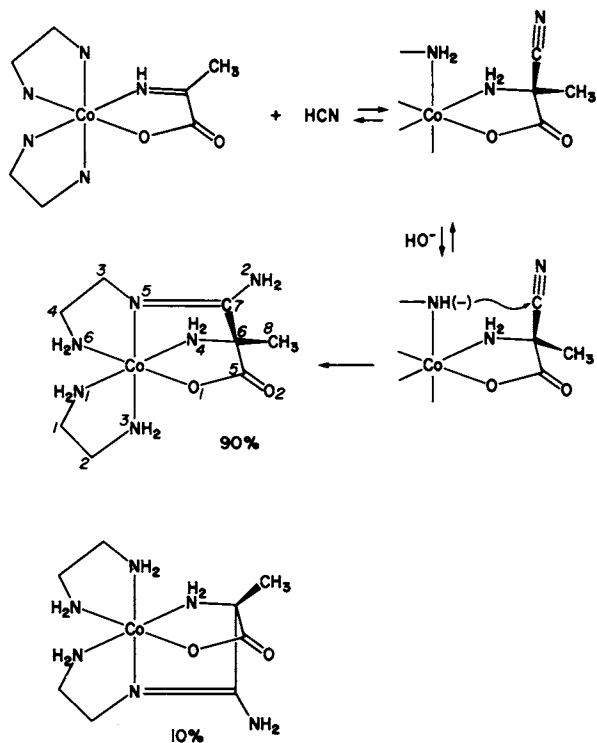
#### Stereospecific addition of $\text{CN}^-$ at a chelated imine - orbital steering

Imines bound to some metal ions are activated to attack by nucleophiles (16, 17) provided the donation from the metal  $d$  electrons to the empty  $\pi^*$  orbitals of the imine is not substantial (18). A good example of an activated chelated imine is that derived from pyruvato-imine bound to the  $\text{Co(III)}$  ion:



In this condition the imine is susceptible to very rapid addition of carbanions such as  $(^-)\text{CH}_2\text{NO}_2$  (16) and  $(^-)\text{CH}(\text{COCH}_3)_2$  (17). Presumably the activity arises because the metal ion imparts some iminium character to the chelate. At the same time the metal prevents protonation of the imine and stabilizes the imine chelate. For example, species of this type are stable in 6 M HCl. Cyanide ion should add in the same manner as the carbanions and we have investigated this reaction using the pyruvato imine bis(ethylene-

diamine)cobalt(III) ion (19) shown below:



It is likely that  $\text{CN}^-$  adds reversibly at the imine center. Other studies would indicate that there is little preference for addition on one side of the planar chelate relative to the other, even though the Co(III) center is chiral. The stabilities of analogous amino acid complexes (5) and the reduction of the chelated imine by the  $\text{BH}_4^-$  ion both show little specificity (20). However, the subsequent reaction of coordinated amide ion with the amino acid nitrile is another matter. Once formed, the amidine quadridentate is stable in dilute acid and base. Moreover, the least stable configuration is the preferred product. The strain in the bound amidine moiety  $-\text{CH}_2-\text{N}=\text{C}(\text{NH}_2)-\text{C}-$  for this isomer is much greater than that in the kinetically less-preferred product where the amidine moiety  $-\text{CH}_2-\text{N}=\text{C}(\text{NH}_2)-\text{C}-$  is close to being planar. The strain difference is reflected in the equilibrium position for the two isomers which lies heavily towards the isomer least favored by the kinetic route.

Both  $\text{CN}^-$  and  $\text{OH}^-$  appear to be involved in the rate law and the involvement of  $\text{CN}^-$  could be accommodated by a pre-equilibrium. After addition of  $\text{CN}^-$  to the imine,  $\text{OH}^-$  abstracts a proton from the amine and the coordinated amide ion attacks the nitrile to generate the amidine. The stereospecificity of the condensation presumably arises from this amide attack and the preference of one site over the other needs some explanation. Dreiding models of the anticipated activated complexes indicate a substantial difference between the two orientations. These are depicted below looking down the  $-\text{CN}$  axis at the orientation of the groups around the bound amide ion. In the orientation which leads to the preferred isomer, the deprotonated orbital points directly at the nitrile C atom. In the orientation which leads to the least abundant isomer, the nitrile is less favorably disposed between the N proton and the deprotonated orbital. We presume it is this "orbital steering" effect which accounts for the stereospecificity. In terms of the energetics, of course, only a difference of about 1.3 kcal/mole in the free energies of activation would be enough to accommodate the results so the effect could be fairly subtle.

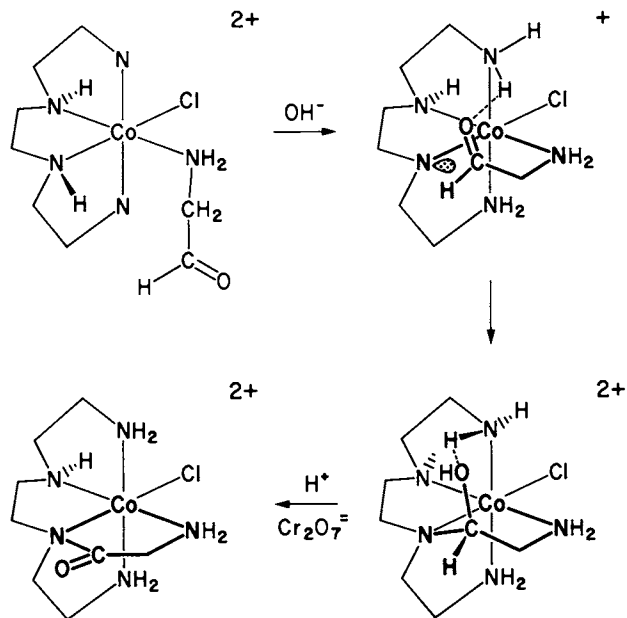


Another interesting facet of this chemistry is the behavior of the most abundant amidine in concentrated  $\text{HCl}$ . Under these conditions the carboxylate group is cleaved and the amino acid amine group undergoes an edge-displacement so that  $\text{Cl}^-$  enters at the site originally occupied by the amine group. The resulting terdentate is meridional and at pH5 in aqueous solution, the chloro complex slowly gives the "less abundant" amidine isomer quantitatively, albeit with an inverted configuration of the ethylenediamine ligands about the cobalt(III) ion. The quantitative edge displacement and the quantitative inversion about cobalt are both unusual facets of cobalt(III) substitution chemistry and merit closer investigation.

#### Stereospecific Carbinolamine Formation

Amino acetaldehyde is a relatively awkward reagent in organic chemistry mainly because it condenses with itself rather readily. The problem can be overcome somewhat by coordinating the amine to a metal ion which renders it less accessible to the aldehyde group.

The amino acetaldehyde protected as the dimethyl acetal reacts readily with  $\alpha$ -[Co trien  $\text{Cl}_2$ ] $^+$  ion to give an aminochloro complex which on treatment with acid yields the coordinated aldehyde shown.



#### Regio- and Stereospecific Aldehyde Condensation

The aldehyde readily undergoes a base catalyzed condensation with a coordinated triethylenetetramine nitrogen center to give a carbinolamine (21). The specificity aspects of this condensation are significant. The coordinated  $\text{Cl}^-$  directs the condensation exclusively to the amine center *trans* to it and the carbinolamine produced is stereospecific in the orientation shown. The regional specificity can be accounted for by the fact that the N-protons *trans* to coordinated  $\text{Cl}^-$  are much more acidic than the others (>100 fold). The specificity of the carbinolamine, however, is more difficult to accommodate. In the structure of the product the OH appears hydrogen bonded to the proximal apical amine group. This attachment may well develop in the transition state and Dreiding models indicate that it is a most favorable configuration. The same opportunity does not occur for the alternative configuration of the carbinolamine moiety.

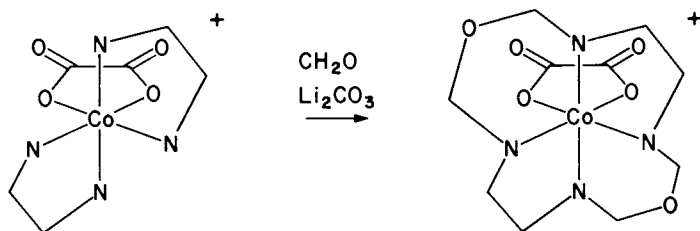
It appears, therefore, that both the substituent effect and intramolecular H-bonding could be powerful aids in determining the specificity at reaction sites.

Chiral metal ion cages

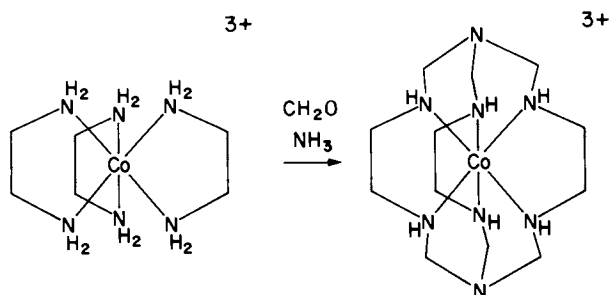
The construction of large fused ring systems like the cryptates (22) requires rather sophisticated organic synthesis and it has occurred to a number of chemists that the problem might be simplified by coordinating a metal ion so that the problem is reduced to linked small ring syntheses. This strategy has now been applied to the synthesis of the nitrogen analogues of the polyether cryptates (24).

The synthesis arose from coordinated imine chemistry of the type described previously (16,17) and the discovery of the synthesis of a dioxacyclam quadridentate on a metal center (25).

*i.e.*



Using a tris(ethylenediamine) complex and ammonia as the base instead of  $\text{OH}^-$ , the prospect of making a trigonal cap was conceived and achieved as follows:

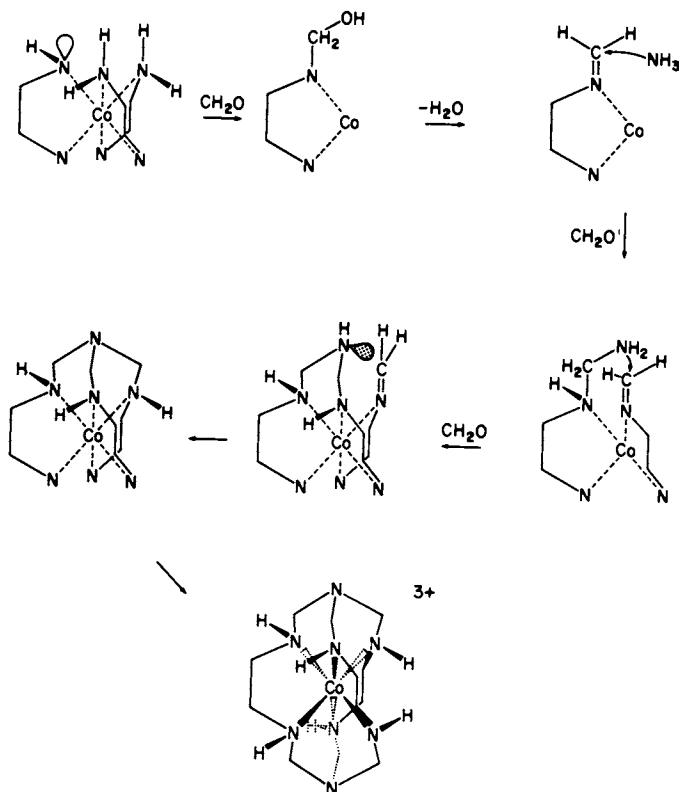


The cage confers interesting properties on the metal compared with the parent tris(ethylenediamine). For example,  $\text{Co}^{2+}$  does not exchange with the  $\text{Co(II)}$  cage in 24 hrs at  $25^\circ$  even though  $\text{Co}^{2+}$  usually exchanges its ligands on the microsecond time scale. Moreover, the  $\text{Co(II)}$  complex retains its chirality at least over



two hours without measurable racemization.

The chirality of the complex is of special interest from the point of view of stereospecificity since it has seven chiral centers, yet if the synthesis is conducted with one chiral form of the tris(ethylenediamine) complex, only one isomer is produced of the 16 possible. This extraordinary specificity needs some examination and to do that the mechanism of synthesis has to be considered in some detail. The first step is obviously the condensation of formaldehyde with the bound ethylenediamine. This requires deprotonation of the bound amine center followed by attack of the coordinated amide ion at the carbonyl center to generate the carbinolamine. Elimination of water leads to the coordinated imine which is then susceptible to addition of ammonia to give the gem-diamine shown. Addition of another  $\text{CH}_2\text{O}$  unit to give another imine is followed by intramolecular attack by the gem-diamine to make the first six-membered ring. Addition of another  $\text{CH}_2\text{O}$  molecule to give another imine group and another intramolecular attack, this time by the ring secondary amine group, leads to the synthesis of the first cap. The process is then



repeated to complete the cage.

Clearly the ammonia-formaldehyde reaction competes with the process but, using an excess of these reagents, the condensation can be made almost quantitative with respect to the tris(ethylenediamine) complex. The specificity is decided by the chirality of the parent tris(ethylenediamine) complex since this decides the orientation of the gem-diamine and subsequent additions of the amino group to the adjacent imine. Unless the gem-diamine is oriented in the apical position, condensation to give the cap is prohibited. The  $\Delta$  or  $\Lambda$  configuration of the ethylenediamine chelates then decides the orientation of the secondary proton if the amino methylene moiety is required to be apical  $\Lambda(S)$  or  $\Delta(R)$ .

These are some of the best examples we have encountered of chirality synthesis organized by metal ions. Further studies will ascertain whether the origins of the specificity are as described but it is clear that substituents on the metal can direct the site of the condensation and that the metal constrains the intramolecular cyclizations to modify the effects anticipated from the regular organic chemistry. The activating effects of the metal ion, the use of coordinated nucleophiles, the possibility of specificity and the protecting and organising capacity of the metal center should all be useful for inorganic and organic synthesis.

#### Literature Cited

1. For examples see Buckingham D.A. and Sargeson A.M., 'Topics in Stereochemistry' (Eds) Allinger N.L. and Eliel E.L. Wiley-Interscience, New York, Vol. 6 p.219, and references therein.
  2. Corey E.J. and Bailar J.C. J. Am. Chem. Soc. (1959) 81, 2620
  3. Fujita M. Yoshikawa Y. and Yamatera H. Bull. Chem. Soc. Japan, (1977) 50, 3209 and references therein.
  4. Halpern B. Turnbull K.R. and Sargeson A.M. J. Am. Chem. Soc. (1966) 88, 4630.
  5. Buckingham D.A. Marzilli L.G. and Sargeson A.M. J. Am. Chem. Soc. (1967) 89, 5133.
  6. Buckingham D.A. Foster D.M. and Sargeson A.M. J. Am. Chem. Soc. (1970) 92, 6151.
  7. Buckingham D.A. Foxman B.M. Sargeson A.M. and Zanella A. J. Am. Chem. Soc. (1970) 94, 6151.
- Buckingham D.A. Sargeson A.M. and Zanella A.  
J. Am. Chem. Soc. (1972) 94, 8246.

8. Buckingham D.A. Davis C.E. and Sargeson A.M.  
*J. Am. Chem. Soc.* (1970) 92, 6159
9. Herlt A.J. Lindoy L.F. Harrowfield J.M. Whimp P.O.  
(unpublished work).
10. Sargeson A.M. *Proc. Royal Australian Chemical Institute*,  
(1976) 229
11. Herlt A.J. (unpublished work).
12. Hammershøj A. and Steffen W. (unpublished work).
13. Phillips A.P. *Chem. Abstracts*, (1962) 57, 1512 8h.
14. Gainsford A.R. Snow M.R. Springborg J. and Taylor D.  
(to be published).
15. Curtis N.F. *Coord. Chem. Rev.* (1968) 3, 3.
16. Harrowfield J.M. and Sargeson A.M. *J. Am. Chem. Soc.* (1974)  
96, 2634.
17. Golding B.T. Harrowfield J.M. Robertson G.B. Sargeson A.M.  
and Whimp P.O. *J. Am. Chem. Soc.* (1974) 96, 3691
18. Evans I.P. Everett G.W. and Sargeson A.M. *J. Am. Chem. Soc.*  
(1976) 98, 8041
19. Geue R. Harrowfield J.M. Sargeson A.M. Springborg J. and  
Taylor D. *Chem. Commun.* (1978) 647.
20. Harrowfield J.M. (unpublished work).
21. Gainsford A.R. Robertson G.B. Sargeson A.M. and  
Whimp P.O. (to be published).
22. Lehn J.M. 'Structure and Bonding', Springer Verlag,  
Berlin (1973) Vol. 16, p. 1.
23. Creaser I. Harrowfield J.M. Herlt A.J. Sargeson A.M. and  
Springborg J. *J. Am. Chem. Soc.* (1977) 99,
24. Sargeson A.M. *Chemistry in Britain*, (1979) 15, 23.
25. Herlt A.J. Sargeson A.M. Springborg J. Taylor D. Geue R. and  
Snow M.R. *J. Chem. Soc. Chem. Comm.* (1976) 285.

RECEIVED October 22, 1979.

# Stereochemistry of Microbial Iron Transport Compounds

KENNETH N. RAYMOND, KAMAL ABU-DARI, and STEPHEN R. SOFEN

Department of Chemistry, University of California, Berkeley, CA 94720

Siderophores are naturally occurring chelate compounds synthesized by microorganisms and used to sequester the biologically essential but sparingly soluble ferric ion from their solution environment (1, 2, 3). The close relationship between microbial pathogenicity and iron metabolism is now well established (4, 5, 6). For example, in salmonellosis (7), infantile enteritis by *E. coli* (8), and mycobacterial infections such as tuberculosis and leprosy (4) a clear-cut effect of iron-binding on pathogenicity has been shown.

The low-molecular-weight siderophores are very powerful chelating agents which typically use hydroxamate, thiohydroxamate, or catecholate groups to encapsulate iron(III) ion in an octahedral, high-spin complex (see Figure 1). These bidentate chelating groups are usually linked to a linear or cyclic peptide of three to six amino acids. The transport of siderophores across cell membranes evidently can be quite conformation dependent, since in some cases the ferric complexes are rapidly passed into the cell while metal-free siderophores are not. The goal of understanding this one-way transport of ferric ion across the cell membrane has led to the results discussed below.

In particular, three questions we would like to answer are:

- 1) Is the intact metal-siderophore complex always transported into the cell (as in the hydroxamate siderophores known as ferrichromes) or is ferric ion alone transferred to a cell-wall-bound transport system?
- 2) How sensitive is the transport process to the exact shape or geometry of the iron-siderophore complex?
- 3) What are the detailed molecular geometries of various kinetically inert metal-siderophore complexes?

Answers to these questions may be obtained by studying the structure (by single crystal x-ray diffraction) and the transport of specific coordination isomers of substitution-inert metal-siderophore complexes. Related work on metal siderophores has been reviewed recently (3, 9). In this paper we summarize our results on studies of the synthesis and characterization of

0-8412-0538-8/80/47-119-133\$09.00/0

© 1980 American Chemical Society

coordination isomers of microbial iron transport compounds and model hydroxamate, thiohydroxamate, and catecholate compounds. Since the ferric ion in these complexes has a high-spin  $d^5$  configuration with no crystal field stabilization, the complexes are quite labile with respect to isomerization in aqueous solution. In addition,  $d^5$  iron(III) ion has no spin-allowed  $d-d$  transitions. Consequently, both absorption and circular dichroism spectra for ferric-siderophores are due to charge transfer transitions. Initially, we felt these characteristics would limit our ability to understand these systems. Later work has shown that the charge transfer based spectra of our ferric complexes are interpretable, since at least some of the ferric siderophore complexes exist as only one isomer in solution. Initially, the use of other metal ions having the same charge and size — yet a  $d$  electron configuration granting significant crystal field stabilization energy (and thus kinetic inertness) as well as ligand field spectra — allowed characterization of the coordination geometry of the metal site in siderophores. Later studies using x-ray crystallography confirmed our initial stereochemical assignments based on solution studies using the  $d^3$  chromium(III) or  $d^6$  rhodium(III) ions in place of iron(III) ion. These ions were chosen because they have almost the same ionic radii as ferric ion yet are usually kinetically inert and exhibit readily interpretable ligand field spectra.

### Hydroxamate Siderophore Complexes

Since hydroxamic acids are unsymmetrical bidentate ligands, both geometrical and optical isomers are possible in tris(hydroxamato)metal complexes. For an octahedral complex formed with three equivalent optically inactive hydroxamate anions, there are two geometric isomers possible, cis and trans. These are also referred to as facial (fac) and meridional (mer), respectively. Each geometrical isomer consists of  $\Delta$  and  $\Lambda$  optical isomers (10), forming a total of four possible isomers;  $\Lambda$ -cis,  $\Delta$ -cis,  $\Lambda$ -trans, and  $\Delta$ -trans (Figure 2). Often the optical isomers of a given geometric isomer are diastereomers because of the ligand optical activity. In such cases the four isomers can be separated theoretically based on differences in their physical properties. In cases of trihydroxamate siderophores, more or fewer isomers are possible depending on the structure and optical activity of the ligand.

### Model Hydroxamate Complexes

The cis- and trans-isomers of several simple tris(hydroxamato)chromium(III) complexes have been separated by thin layer and column chromatographic techniques (11, 12). Both of the corresponding iron(III) and cobalt(III) complexes showed only one band with both techniques. The assignment of geometries for the

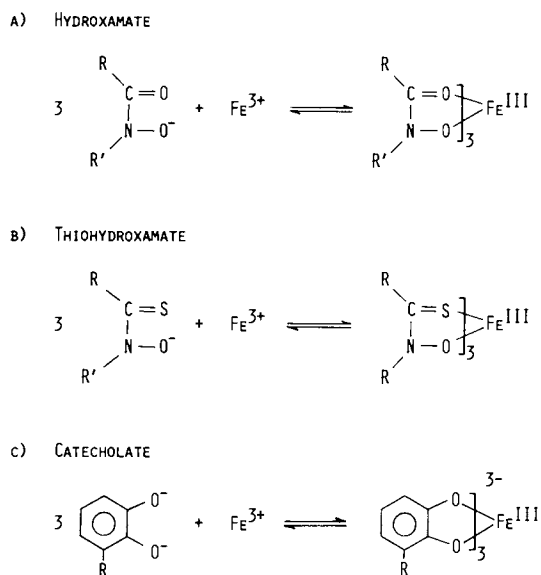


Figure 1. Reaction of simple hydroxamates, thiohydroxamates, and catecholates with Fe(III)

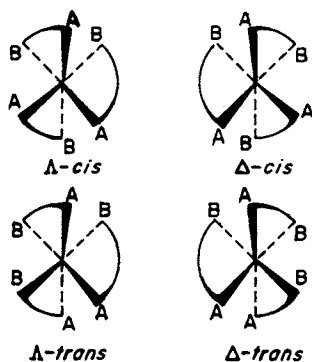


Figure 2. Geometrical and optical isomers of a simple tris(chelate) complex with an unsymmetrical bidentate ligand

Cr(hydroxamate)<sub>3</sub> complexes was originally based on the following criteria:

1) The cis-isomer, which has a higher dipole moment than the trans-isomer, binds more strongly to the sorbent in both thin layer and column chromatographic techniques. Hence, the cis geometry is assigned to the isomer with lower R<sub>f</sub> value. This is parallel to similar results obtained for the geometrical isomers of many compounds including tris(α-amino acid) complexes of cobalt(III) (13, 14, 15) and tris(β-diketonato)cobalt(III) (16, 17, 18) and chromium(III) (18).

2) The cis-isomers of the tris(α-amino acid) complexes of cobalt(III) and chromium(III) have larger extinction coefficients for band maxima of d-d transitions than the corresponding trans-isomers (19-24). Although the difference in the coordination environment between the cis- and trans-tris(hydroxamato)chromium(III) complexes is less than that in the amino acid complexes, differences in the absorption spectra of the cis- and trans-isomers of Cr(hydroxamate)<sub>3</sub> complexes have been found, especially for the extinction coefficients of the high energy transition  ${}^4A_{2g} \rightarrow {}^4T_{1g}$ . Differences are also observed in the energies of the  ${}^4A_{2g} \rightarrow {}^4T_{2g}$  transitions, where the energy of the transitions in the trans-isomers is greater. For example, these transitions for the tris(benzohydroxamato)chromium(III) isomers are λ<sub>max</sub> nm (ε) = 602(83.9) and 400(112) for the trans-isomer and 588(82.1) and 413(127) for the cis-isomers as discussed below.

3) Finally, assignment of geometries was also based on differences in the CD spectra of the cis- and trans-isomers as discussed below.

The pure solid cis- and trans-isomers of tris(benzohydroxamato)chromium(III) have been separated by simple extraction of the cis-isomer into chloroform by adding water to the chloroform/acetone solution of both isomers. The trans-isomer, which is insoluble in chloroform, precipitates out of the solution (25). The cis-isomer is quite stable in dry chloroform solution in the dark and very unstable in wet solvents and polar solvents such as alcohol. In contrast, the trans-isomer is stable in alcohol and was crystallized from isopropanol/heptane mixtures as the dissolved species.

The original assignment of geometry was confirmed by the structure determination of the compound trans-tris(benzohydroxamato)chromium(III) diisopropanol. Figure 3 shows a perspective view of the molecule, and Figure 4 shows a comparison between the coordination geometries of the iron(III) and chromium(III) complexes. As mentioned above, the iron complex shows only one band in its chromatographic behavior and crystallizes in the cis geometry as determined by x-ray crystallography (26). The main difference in the structures of the iron(III) and chromium(III) complexes is the trigonal twist angle (which is the angle between the projections of the trigonal faces of the coordination octahedron). This angle is 47.4° and 35.7° for the chromium(III) and

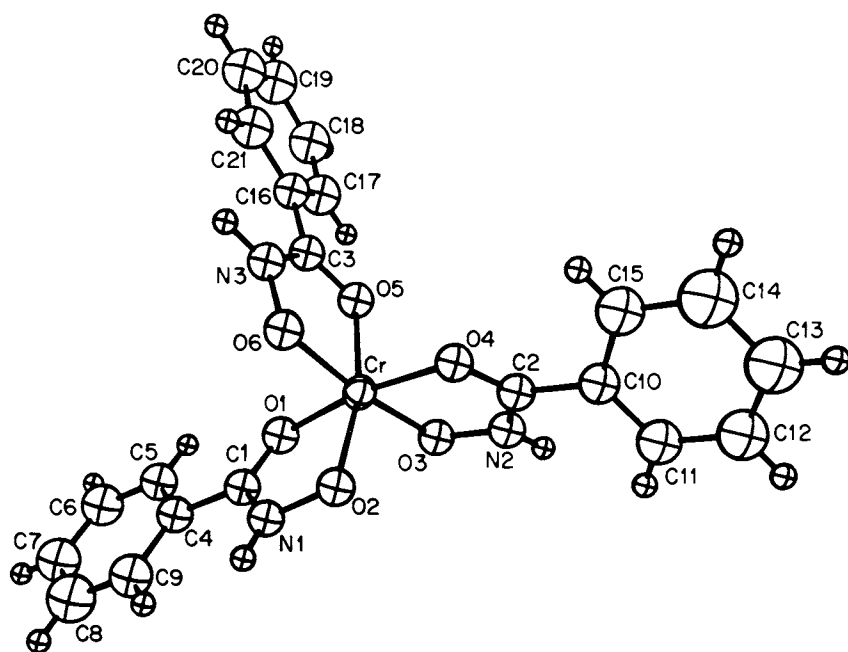


Figure 3. A perspective drawing of *trans*-tris(benzohydroxamato) chromium(III) looking down the molecular (pseudo) threefold axis



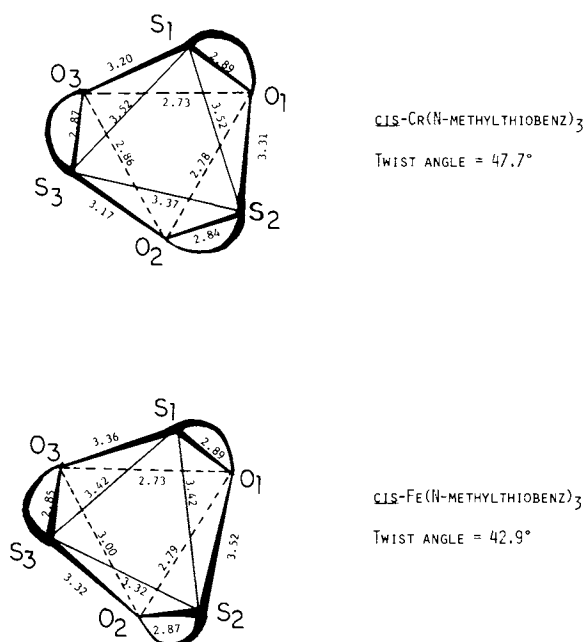


Figure 4. A comparison of the octahedral bonding geometries of *trans*-tris(benzohydroxamato)chromium(III) and *cis*-tris(benzohydroxamato)iron(III)

iron(III) complexes, respectively, and this difference is attributed to the difference in the crystal field stabilization energies of the two compounds.

Recently the salts of the cis- and trans-tris(benzohydroxamate)chromate(III) trianions have been isolated. Their absorption spectra are parallel to those of the neutral species. Figure 5 shows ORTEP plots of these isomers. The corresponding iron complex crystallizes in the cis geometry under the same conditions.

To enhance the separation of the optical isomers of Cr(hydroxamate)<sub>3</sub> complexes, the optically active hydroxamic acid, *l*-menthoxyacethydroxamic acid (men), was prepared as well as its iron(III) and chromium(III) complexes, Fe(men)<sub>3</sub> and Cr(men)<sub>3</sub>. While four diastereomers ( $\Lambda$ -cis,  $\Delta$ -cis,  $\Lambda$ -trans, and  $\Delta$ -trans) are expected for Cr(men)<sub>3</sub>, only three fractions were separated by chromatographic techniques. Two fractions were assigned to be  $\Delta$ -cis and  $\Lambda$ -cis while the partially resolved  $\Lambda$ - and  $\Delta$ -trans mixture separate as one fraction. The geometries of these were assigned based upon the criteria mentioned above. The iron(III) complex gave only one band under the same conditions.

The assignment of the absolute configuration of the Cr(men)<sub>3</sub> isomers was based on their CD spectra, Figure 6. Of particular significance in the assignment are the signs of the CD bands in the low energy transition region (<sup>4</sup>A<sub>2g</sub> → <sup>4</sup>T<sub>2g</sub>). Assuming a D<sub>3</sub> coordination point symmetry, this transition splits into <sup>4</sup>A<sub>2</sub> → <sup>4</sup>A<sub>1</sub> (A<sub>2</sub>) and <sup>4</sup>A<sub>2</sub> → <sup>4</sup>E (E<sub>a</sub>). The two transitions A<sub>2</sub> and E<sub>a</sub> should have CD bands of opposite sign, and based on the widely used empirical rule, the complex has a  $\Lambda$  absolute configuration if the E<sub>a</sub> transition has a positive CD band (27). A difficulty arises in deciding which of the two CD bands in the low energy transition region is the E<sub>a</sub> band. The order of energy of A<sub>2</sub> and E levels varies from one complex to another, and although it is generally accepted that the energy order is A<sub>2</sub> > E<sub>a</sub> for five-membered rings formed by diamine and amino acid complexes (28, 29, 30, 31), the opposite order (E<sub>a</sub> > A<sub>2</sub>) was found for several other complexes (32) including tris(β-diketonato)cobalt(III) (17, 18, 27, 33, 34, 35, 36) and -chromium(III) (18) complexes and tris(oxalato)chromium(III) (33-39). The latter complex is more closely related to the hydroxamate complexes. Based on this and the fact that for most trigonal d<sup>3</sup> and low-spin d<sup>6</sup> complexes, the stronger CD band from the <sup>4</sup>A<sub>2</sub> → <sup>4</sup>T<sub>2</sub> manifold is of E<sub>a</sub> rather than A<sub>2</sub> symmetry (27), the  $\Lambda$ -configuration was assigned to the isomers with positive sign for the dominant low energy band under the T manifold transition. This assignment was later confirmed, as discussed below.

The <sup>4</sup>A<sub>2g</sub> → <sup>4</sup>T<sub>1g</sub> transition is octahedral d<sup>3</sup> and low-spin d<sup>6</sup> complexes factors under point group D<sub>3</sub> into <sup>4</sup>A<sub>2</sub> → <sup>4</sup>A<sub>2</sub> (A<sub>1</sub>) and <sup>4</sup>A<sub>2</sub> → <sup>4</sup>E (E<sub>b</sub>) transitions. The A<sub>1</sub> transition is symmetry forbidden; the CD band in the region of the high energy transition <sup>4</sup>A<sub>2</sub> → <sup>4</sup>T<sub>1</sub> has been assigned to the E<sub>b</sub> transition, as for

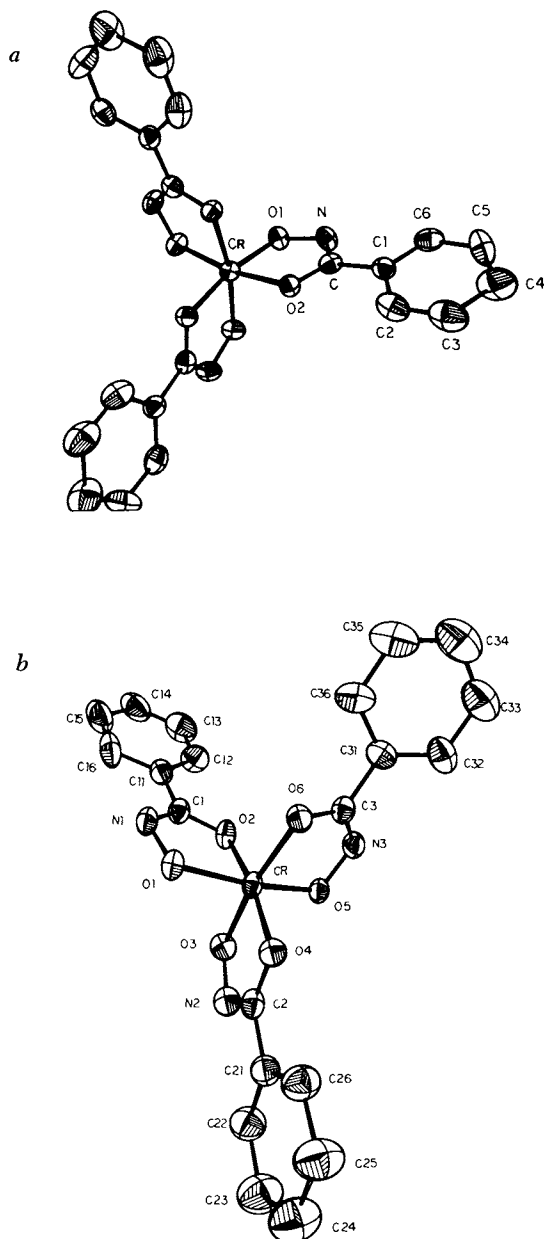


Figure 5. A perspective drawing of the *cis*-tris(benzohydroximato) chromate(III) (5a) and *trans*-tris(benzohydroximato)-chromate(III) (5b) ions, looking down the threefold and pseudofold axes, respectively

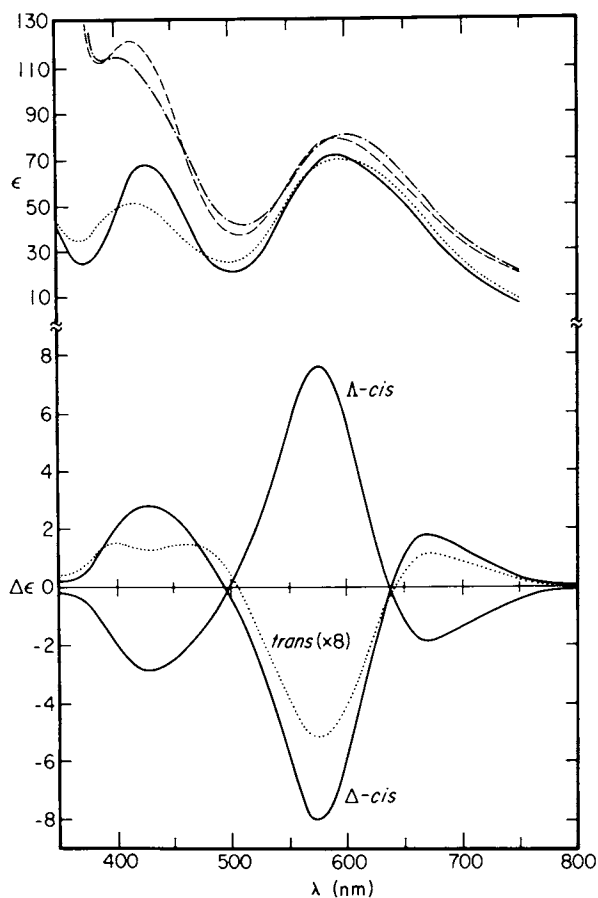
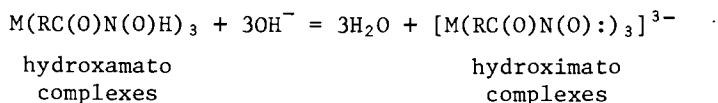


Figure 6. Absorption spectra of  $Cr(benz)_3$  in 17%  $CH_3OH-CHCl_3$  solution, and both absorption and CD spectra of  $Cr(men)_3$  in 3%  $CH_3OH-CHCl_3$ : (---),  $Cis-cr(benz)_3$ ; (- · -),  $trans-Cr(benz)_3$ ; (—),  $cis-Cr(men)_3$ ; and (· · ·),  $trans-Cr(men)_3$ . The CD spectrum of the mixture of  $trans$  isomers has been multiplied by eight (3).

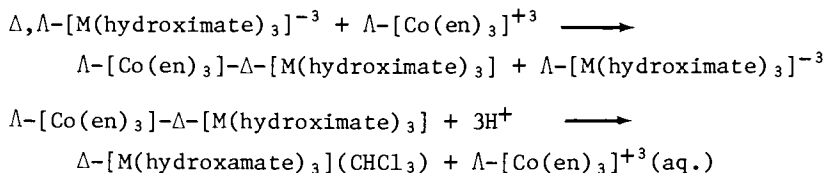
tris(oxalato)- (40) and tris( $\beta$ -diketonato)chromium(III) (27, 35) complexes. Theoretical treatments predict that when the energy order is  $E_a > A_2$ , the signs of  $E_a$  and  $E_b$  transitions are opposite (41). This is consistent with the CD spectra of the hydroxamate complexes. Furthermore, the  $E_b$  transition is split in the lower symmetry trans-isomer, providing an additional criterion for characterizing this isomer.

Tris(benzohydroxamato)iron(III), -cobalt(III), and -chromium(III), as well as other N-unsubstituted hydroxamic and thiohydroxamic acid complexes, can be deprotonated in basic solution to form trianions which are hydroximate complexes. The neutral complexes can be regenerated by neutralization of the hydroximate complexes;



The metal hydroximate complexes have been resolved by forming insoluble diastereomers of one of their optical isomers with the optical isomers of  $[\text{Co}(\text{en})_3]^{+3}$ , leaving the other isomer in solution. The resolved neutral hydroxamate complexes can then be obtained by the acidification of the salts and simultaneous extraction of the neutral compounds.

The four isomers of  $\text{Cr}(\text{benz})_3$  were separated by this method by first separating the  $\Lambda$ -cis,  $\Delta$ -trans mixture from the  $\Delta$ -cis,  $\Lambda$ -trans, followed by the separation of the resolved cis and trans isomers as described earlier. The CD spectra of the resolved  $\text{Cr}(\text{benz})_3$  isomers are similar to those of the  $\text{Cr}(\text{men})_3$  isomers; hence, the absolute configuration of the metal hydroximate anions were assigned to be opposite to that of the  $[\text{Co}(\text{en})_3]^{+3}$  forming the diastereomers. The reactions are summarized below:



The optical isomers of cis- $\text{Cr}(\text{benz})_3$  are quite stable in dry chloroform in the dark, yet isomerize rapidly in methanolic solution. The trans-isomer is moderately stable in alcohols, with a half-life for racemization of a few days. Due to the instability with respect to decomposition of the neutral tris(benzohydroxamato)cobalt(III) complex, only the CD spectrum of the anionic species has been recorded (Figure 7). It resembles that of the cis- $\text{Cr}(\text{hydroxamate})_3$  complexes.

To our surprise, we found that the iron(III) hydroxamate and thiohydroxamate complexes can also be resolved by the method

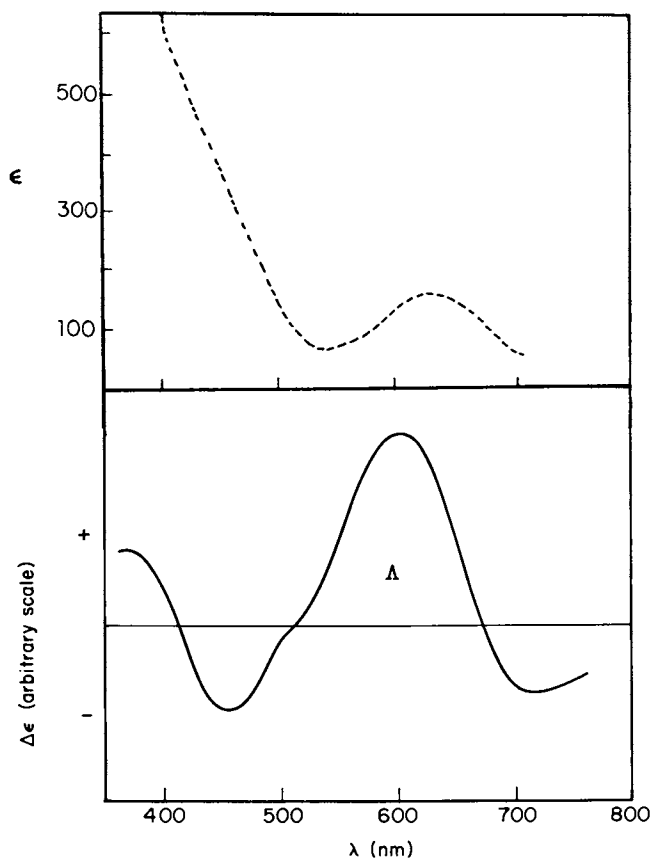


Figure 7. Absorption (---) and CD (—) spectra of  $\Delta$ -tris(benzohydroximato)-cobaltate(III) ion

discussed above and that the  $\text{Fe}(\text{benz})_3$  optical isomers are quite stable in chloroform and acetone solutions, but racemize instantly in methanol and other polar solvents. The CD spectra of the  $\Lambda$  and  $\Delta$  optical isomers of  $\text{Fe}(\text{benz})_3$  are shown in Figure 8. The CD spectrum of the  $\Lambda$ -isomer is quite similar to that of ferrichrome A (Figure 9). [As discussed below, ferrichrome A is the iron(III) complex of a microbe-produced trihydroxamate ligand. Due to the optical activity of the ligand, the compound crystallizes in the  $\Lambda$ -*cis* configuration and apparently exists at least predominantly as this isomer in solution.] This supports our assignment of configuration.

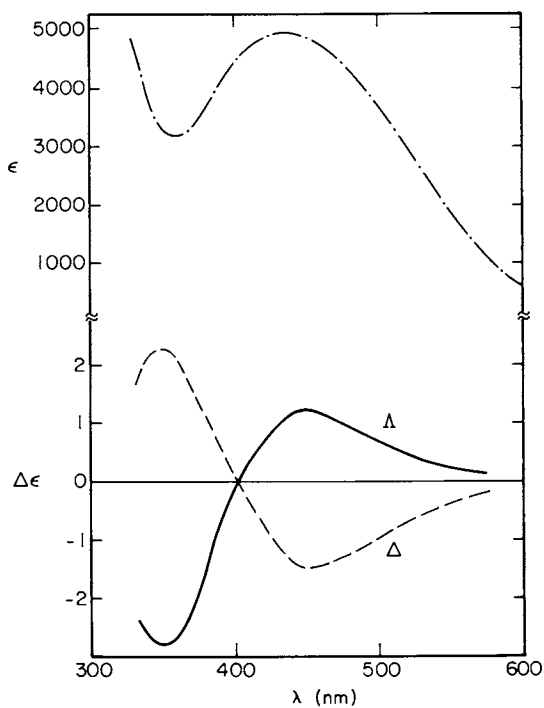
Finally, our assignment of configuration is confirmed by the CD spectra and structure of chromium desferriferrichrome. This compound is found to be isomorphous with ferrichrome (42) which crystallizes in the  $\Lambda$ -*cis* configuration as has been determined by x-ray crystallography (43). In addition, its CD spectrum (Figure 10) is similar to those of the model  $\Lambda$ -*cis*-Cr(hydroxamate)<sub>3</sub> complexes.

### Hydroxamate Siderophore Complexes

Assignment of geometry for the chromic complexes is based on their chromatographic behavior, absorption spectra and the shape of the high energy ( $E_b$ ) CD band. Iron(III) complexes will have the  $\Lambda$  configuration if the CD band in the region of the absorption maximum at 400-500 nm has a positive sign, while chromium(III) complexes have the same configuration if the  $E_a$  transition at 500-600 nm has a positive sign.

The ferrichromes, Figure 11, have natural optical activity associated with the ligand; accordingly, the metal complexes have overall optical activity. An examination of molecular models of the ferrichromes indicates that the *trans*-isomers are improbable due to the cyclic nature of the backbone of the ligand; however, both  $\Lambda$  and  $\Delta$  *cis*-isomers are possible.

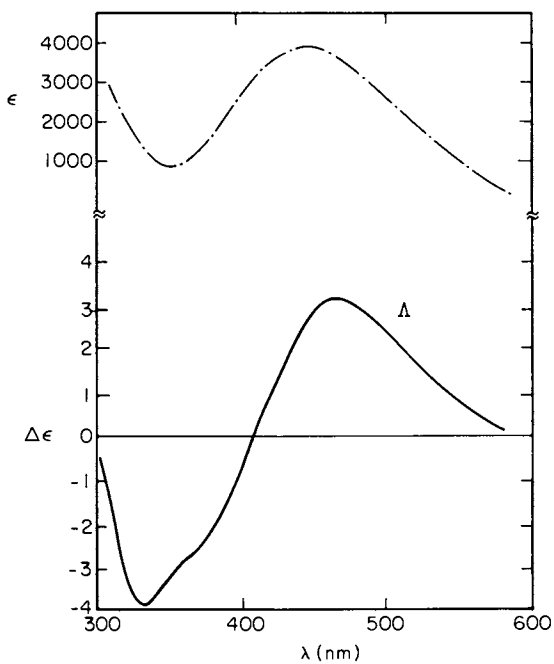
The molecular structure analyses of ferrichrome A (44), ferrichrysin (45), and ferrichrome (43) show that all three complexes exist in the  $\Lambda$ -*cis* configuration. Although crystallization of each member of the series yields only one isomer,  $\Lambda$ -*cis*, it would be possible that both isomers of the labile iron(III) complex coexist in solution, with only the less soluble isomer preferentially crystallizing from the equilibrium mixture. However, the comparable values of  $\Delta\epsilon$  for the CD spectra of ferrichrome A (Figure 9) and  $\Lambda$ -tris(benzohydroxamato)iron(III) (46) (Figure 8), indicate that only the  $\Lambda$ -*cis* isomer of ferrichrome A is present in a measurable amount in solution. The CD spectra of the chromic complexes of desferriferrichrome A and desferriferrichrysin as well as cobalt(III) desferriferrichrome A are similar to that of chromium(III) desferriferrichrome - which crystallizes in the  $\Lambda$ -*cis* configuration, as determined by x-ray crystallography (42).



Journal of the American Chemical Society

Figure 8. Absorption spectrum (- · -) and CD spectra of  $\Delta$  (- - -) and  $\Lambda$  (—) tris(benzohydroxamato)iron(III) in acetone solution (46)





Journal of the American Chemical Society

Figure 9. Absorption (- · -) and CD (—) spectra of Ferrichrome A in aqueous solution (46)

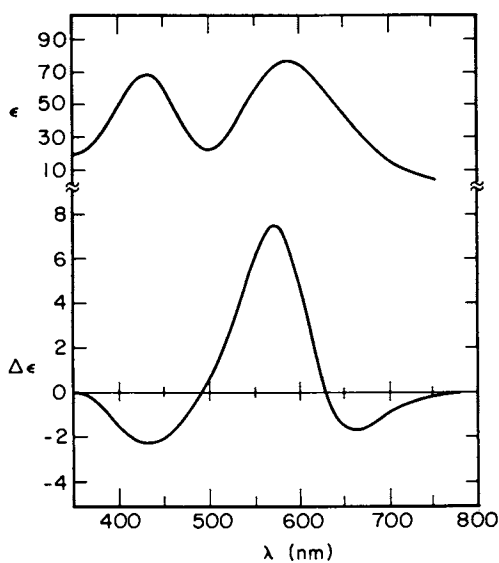


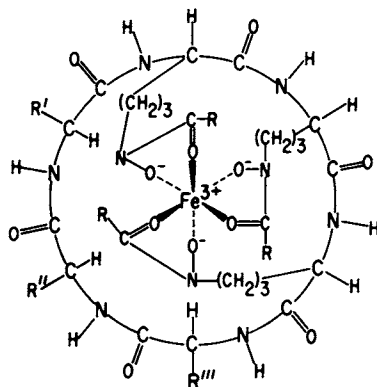
Figure 10. Absorption and CD spectra of chromic deferriferrichrome in aqueous solution (3)

American Chemical  
Society Library

1155 16th St. N. W.

Washington, D. C. 20036

In Stereochemistry of Optically Active Transition Metal Compounds; Douglas, B., et al.; ACS Symposium Series; American Chemical Society: Washington, DC, 1980.



| Siderochrome             | R'                                   | R''                | R'''               | R   |
|--------------------------|--------------------------------------|--------------------|--------------------|---|
| Ferrichrome              | H                                    | H                  | H                  | CH <sub>3</sub>   |
| Ferrichrysin             | CH <sub>2</sub> OH                   | CH <sub>2</sub> OH | "                  | "   |
| Ferricrocin              | H                                    | "                  | "                  | "   |
| Ferrichrome C            | "                                    | CH <sub>3</sub>    | "                  | "   |
| Ferrichrome A            | CH <sub>2</sub> OH                   | CH <sub>2</sub> OH | "                  | -CH=C(CH <sub>3</sub> )-CH <sub>2</sub> CO <sub>2</sub> H ( <i>trans</i> )  |
| Ferrirhodin              | "                                    | "                  | "                  | -CH=C(CH <sub>3</sub> )-CH <sub>2</sub> CH <sub>2</sub> OH ( <i>cis</i> )   |
| Ferrirubin               | "                                    | "                  | "                  | -CH=C(CH <sub>3</sub> )-CH <sub>2</sub> CH <sub>2</sub> OH ( <i>trans</i> ) |
| Albomycin δ <sub>1</sub> | -CH <sub>2</sub> OSO <sub>2</sub> -N | "                  | CH <sub>2</sub> OH | CH <sub>3</sub>   |

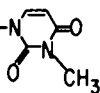


Figure 11. Structure of the ferrichromes. The basic structural feature is a cyclic hexapeptide with the three hydroxamic acid linkages provided by a tripeptide of  $\delta$ N-acetyl- $\delta$ N-hydroxy-l-ornithine. The  $\Delta$ -*cis* coordination iser is shown in each case (3).

Another class of siderophore complexes is the ferrioxamines. In contrast to the ferrichromes, the linear and cyclic ferrioxamines (Figure 12) have the hydroxamate groups as part of a polyamide chain. A second major difference is that the ligands themselves are not optically active; only if a substituent has a chiral center (as in the ferrimycins) is there optical activity for the molecule. Ferrioxamine E, a cyclic ferrioxamine, crystallizes as a racemic mixture of  $\Lambda$ -cis and  $\Delta$ -cis isomers as determined by x-ray crystallography (47). The chromic complexes of ferrioxamine B and D exist in both cis- and trans-forms in a racemic mixture. The cis geometric isomer was separated from one or more of the four possible trans isomers by ion exchange chromatography (48). The absorption spectra of the two fractions are shown in Figure 13. The cis geometry was assigned to the isomer with lower  $R_F$  value and with visible absorption maxima at 583(707) and 419(67.9) nm ( $\epsilon$ ). Both cis- and trans-isomers isomerize with half-lives of several days in aqueous solution at room temperature.

Rhodotorulic acid (RA), Figure 14, is an example of a dihydroxamate siderophore. This sequestering agent forms dimeric complexes with iron, aluminum, and chromium of the stoichiometry  $M_2RA_3$  (49). The CD spectrum of the iron complex, Figure 15, is identical with that of  $\Delta$ -tris(benzohydroxamato)iron(III). Therefore, the complex apparently exists in the  $\Delta$ -cis geometry. This is opposite to that found in all of the other hydroxamate siderophores studied to date. Two fractions corresponding to cis and trans chromium(III) rhodotorulic acid have been separated by chromatographic methods. The CD spectrum of the cis-isomer is similar to the spectra of simple  $\Delta$ -cis-tris(hydroxamato)chromium(III) complexes. The CD spectra of the trans-isomer shows a splitting for the high energy transition ( $E_b$ ) as expected for the chromium hydroxamate complexes with trans geometry.

Another class of dihydroxamate siderophores is represented by aerobactin (Figure 16). The CD spectrum of its iron(III) complex, Figure 17, suggests a  $\Lambda$  configuration for the complex, the same as that assigned to the chromium(III) complex based on its CD spectrum, Figure 18 (50). The close similarity of the CD spectra of iron(III) aerobactin and other iron(III) hydroxamate complexes indicates that the iron is octahedrally coordinated by six oxygen atoms - four hydroxamate oxygens and possibly two from citrate carboxyl and hydroxyl moieties (50).

#### Thiohydroxamate Siderophore Complexes

Tris(thiobenzohydroxamato)chromium(III), -manganese(III), -iron(III), and -cobalt(III), as well as the corresponding complexes with N-methylthiobenzohydroxamic acid, have been found to exist only in the cis geometry as shown by their chromatographic behavior, absorption spectra, and x-ray structural determinations (Figure 19) (51, 52). The same geometry was found for the

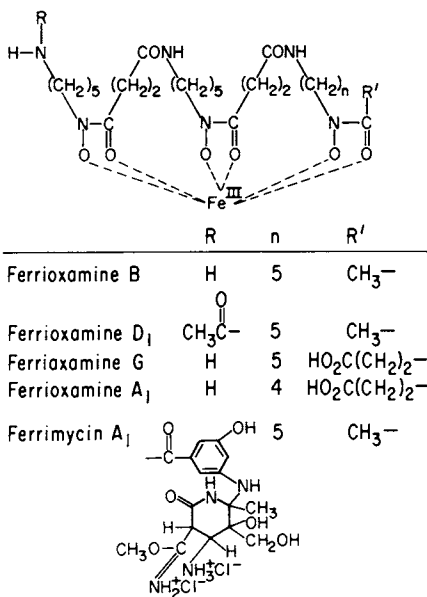


Figure 12. Structure of the linear ferrioxamines. The basic structural feature of the ferrioxamines is repeating units of 1-amino-5-hydroxyaminopentane and succinic acid. Ferrioxamine E is cyclic with  $n = 5$  and an amide linkage such that there are no R or R' substituents, but instead a C-N bond (3)

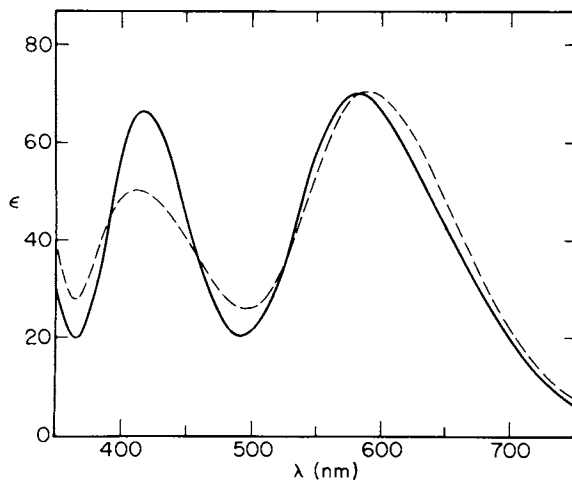


Figure 13. Absorption of the *cis* and *trans* isomers of chromium(III) Deferriferrioxamine B in aqueous solutions: (—), *cis*; (---), *trans* (3).

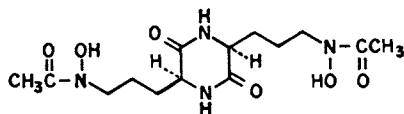


Figure 14. Structure of rhodotorulic acid (49)

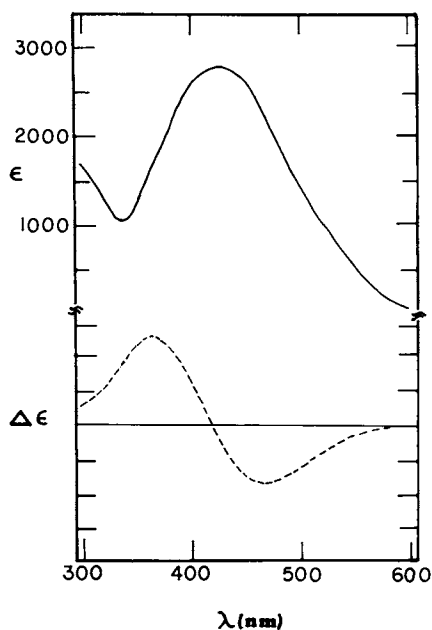


Figure 15. Absorption (—) and CD (---) spectra of the ferric complex of rhodotorulic acid in aqueous solution

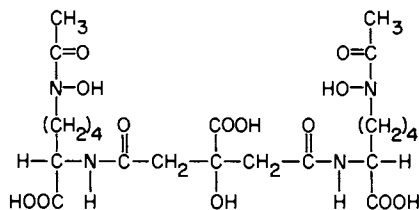


Figure 16. Structure of aerobactin (50)

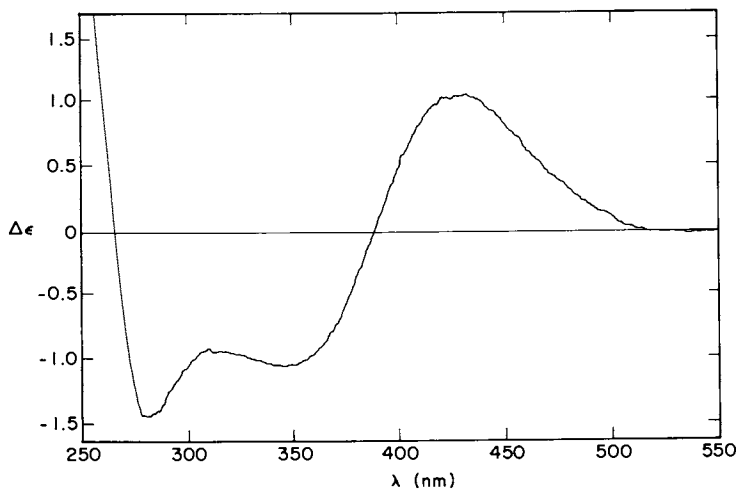


Figure 17. The CD spectrum of iron(III) aerobactin at neutral pH (50)

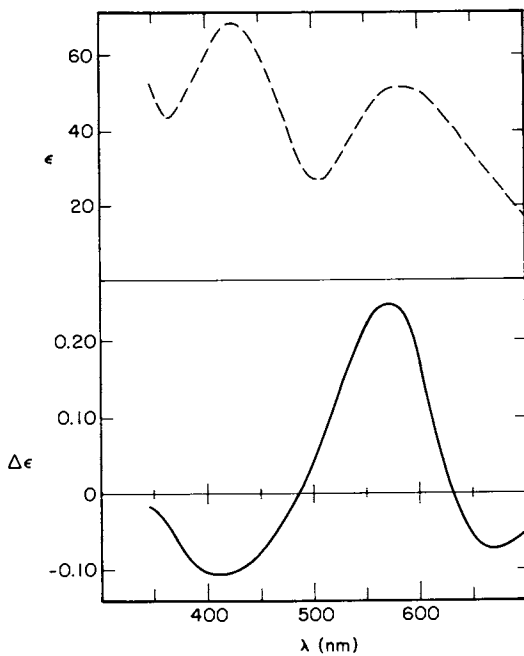


Figure 18. Absorption (---) and CD (—) spectra of chromium(III) aerobactin at neutral pH

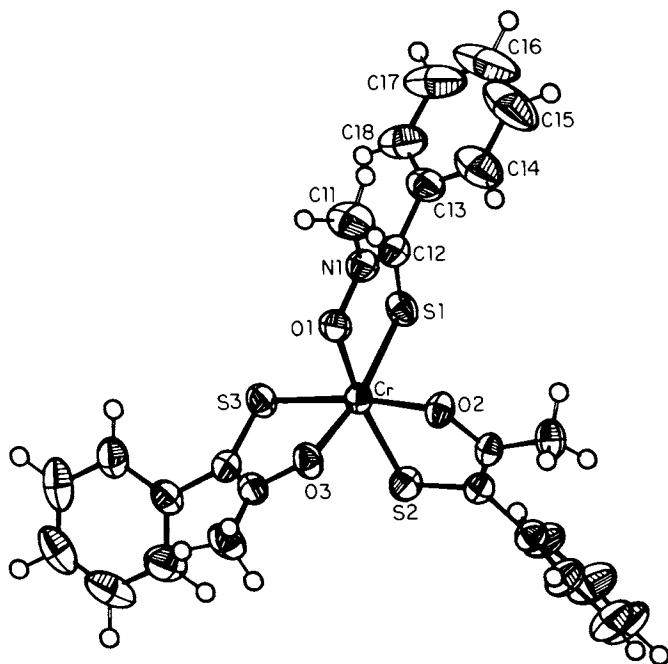


Figure 19. A perspective drawing  $M(N\text{-methylthiobenzohydroxamate})_3$ , where  $M = \text{Cr, Fe, Co, and Mn}$ , as viewed down the molecular threefold axis



tris(thiobenzohydroximato)chromate(III) trianion as shown in Figure 20 (53). The CD spectrum of tris(thiobenzohydroximato)chromium(III), Figure 21, is similar to those of the tris(hydroximato)chromium(III) complexes except for the bands at 425 nm — which probably correspond to a charge transfer transition. The assignment of configuration is based on the sign of the E transition at 600 nm such that the isomer with positive CD band at 600 nm has a  $\Lambda$  configuration. Similar to the case with the hydroximato complexes, diastereomer salts are formed between  $[\text{Co}(\text{en})_3]^{-3}$  and  $[\text{M}(\text{thiohydroximato})_3]^{-3}$  ions with opposite configuration. This was the basis for the assignment of configurations for the tris(thiobenzohydroximato)iron(III) optical isomers, where the  $\Lambda$  configuration is assigned to the isomer with negative and positive CD bands in the regions of the low energy and high energy absorptions at 580 and 490 nm, respectively (Figure 22). It is interesting to compare the CD spectra of the optical isomers of iron(III) complexes of benzohydroxamic and thiobenzohydroxamic acids (Figures 8 and 22, respectively). The thiohydroxamic acid complex has an extra absorption band and an extra CD band, while the rest of the CD bands of the iron(III) thiohydroximato isomers are very similar to those of the iron(III) hydroximato, in position, shape, and sign.

#### Catecholate Siderophore Complexes

In addition to hydroxamic acids, the dihydroxybenzene (catechol) moiety is employed as the chelating unit of some siderophores. In all strains of enteric bacteria studied to date, the natural iron transport agent is the cyclic triester of 2,3-dihydroxy-N-benzoylserine known as enterobactin (Figure 23) (54, 55, 56). In *Bacillus subtilis* 2,3-dihydroxy-N-benzoylglycine has been shown to stimulate iron transport (54, 57). In addition, 2-N,6-N-di(2,3-dihydroxybenzoyl)-L-lysine (58) is a siderophore produced by *Azotobacter vinelandii* which has only two catechol groups. However, of the catecholate siderophores by far the best studied is enterobactin. A major difference between hydroximato and catecholate siderophores occurs in their utilization as transport agents. For the former, the iron complex is taken up by the bacterial cell, the iron released, and the hydroximato siderophore re-secreted for additional iron chelation. In contrast, enterobactin is destroyed by enzymatic hydrolysis within the cell and therefore the ligand is not recycled. This hydrolysis of the amide linkages of the iron(III) enterobactin lowers the redox potential of the chelate complex sufficiently to allow iron reduction — and thus uptake of iron into the cell metabolism (59, 60).

As with the hydroximato siderophores, our initial approach has been to study simple tris(catecholato)metallate(III) complexes as models for the tricatecholate siderophore enterobactin. Unlike hydroximates, catecholate is a symmetric, bidentate ligand.

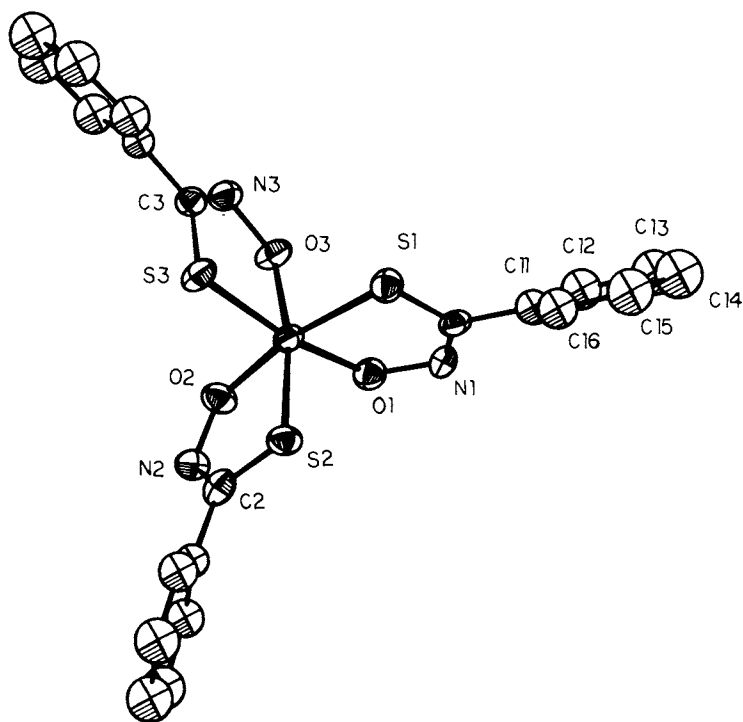
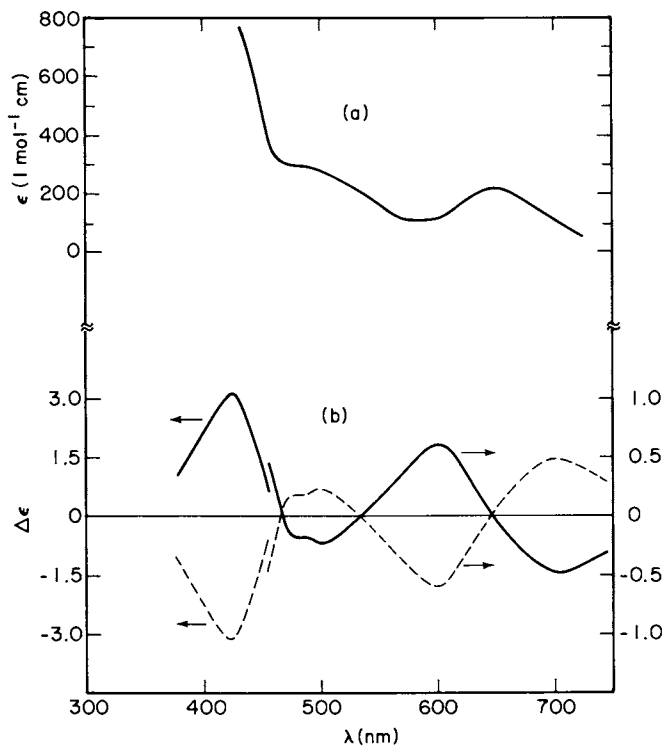
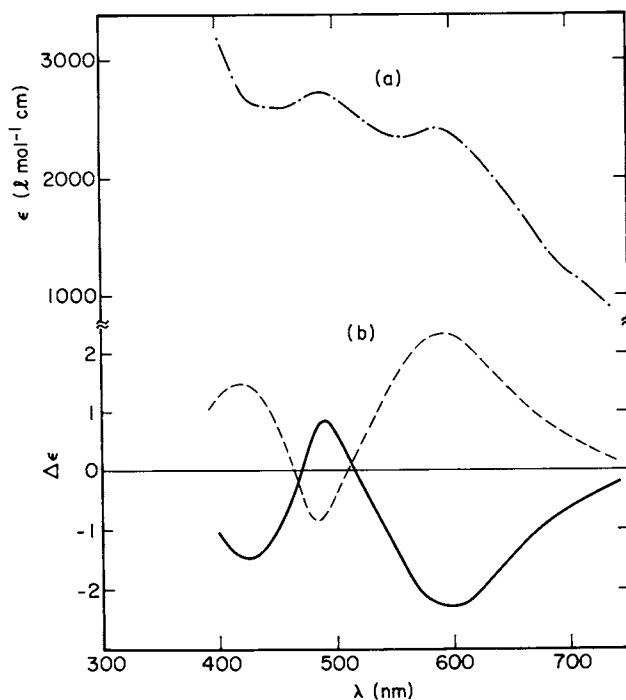


Figure 20. A perspective drawing of tris(thiobenzohydroximato)chromate(III) ion as viewed down the molecular threefold axis



Inorganic Chemistry

Figure 21. (a) Absorption spectrum of tris(thiobenzohydroxamate)chromium in  $\text{CHCl}_3$ ; (b) CD spectra of the  $\Delta$  (---) and  $\Lambda$  (—) form of tris(thiobenzohydroxamate)chromium(III) (51).



Inorganic Chemistry

Figure 22. (a) Absorption spectrum of tris(thiobenzohydroxamato)iron(III); (b) CD spectra of the  $\Delta$  (---) and  $\Lambda$  (—) forms of tris(thiobenzohydroxamato)iron(III) (51).

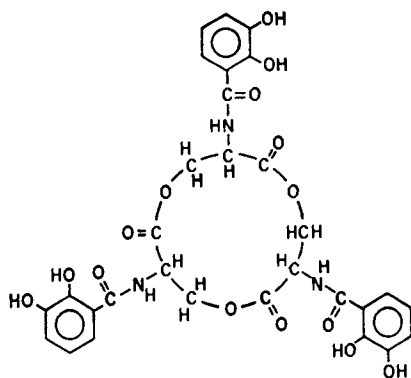


Figure 23. Structural diagram of enterobactin (61)

Consequently, there are no geometrical isomers and only the  $\Lambda$  and  $\Delta$  optical isomers are possible. In catecholates substituted unsymmetrically on the phenyl ring (such as in enterobactin), geometric isomers are possible; however, molecular models of enterobactin argue for the sole existence of the more symmetric (cis) chelate.

### Model Catecholate Complexes

The optical isomers of tris(catecholato)chromate(III) and -rhodate(III) have been separated by selective precipitation of one isomer as the tris(ethylenediamine)cobalt(III) or -chromium(III) double salt in a manner analogous to that discussed above for the hydroxamates (61, 62). As a check on the efficacy of using another metal in place of iron, the molecular structures of tris(catecholato)ferrate(III) and -chromate(III) were determined by single crystal x-ray diffraction (63). As was later found for the benzohydroxamate complexes discussed above, the only significant differences in the structures were the trigonal twist angles. This difference of six degrees is attributed to the crystal field stabilization energy of 12 Dq for  $\text{Cr}^{+3}$  versus 0 Dq for high-spin iron(III) ion. Otherwise, both structures are distorted octahedra with approximate  $D_3$  molecular point symmetry (Figure 24).

While the absolute configuration of transition metal catecholates has not been determined by x-ray diffraction, the assignments are based on several lines of reasoning. In particular, for both the rhodium(III) and chromium(III) complexes, that isomer precipitated by  $\Lambda$ -tris(ethylenediamine)cobalt(III) is assigned the  $\Lambda$  configuration.

For tris(catecholato)chromate(III) the assignment of the absolute configuration from the CD spectrum (Figure 25) is based on the following arguments:

- 1) The CD spectra of  $[\text{Cr}(\text{cat})_3]^{3-}$  and tris(oxalato)chromate(III) may be compared directly. In addition, the spectra may be compared with those of the hydroxamate complexes. The close relationship in chelate ring size and electronic structures of the coordinating portions of the ligands permit direct comparison of the CD spectra.

- 2) The empirical rule for the assignment of absolute configurations of  $D_3$  point group metal complexes of  $d^3$  or  $d^6$  electronic configuration may be applied (27). Accordingly, the low energy E transition will be positive for a  $\Lambda$  complex.

In the case of tris(catecholato)rhodate(III), the assignment of absolute configuration follows similar lines:

- 1) The CD spectra of the catecholate and oxalate complexes are comparable. In the latter a positive CD maximum at 400 nm ( $\Delta\epsilon = +2.85$ ) is assigned to the  $E_a$  transition in the  $\Lambda$ -isomer. As seen in Figure 26 this transition occurs at 420 nm in  $[\text{Rh}(\text{cat})_3]^{3-}$  and is positive for the  $\Lambda$ -isomer ( $\Delta\epsilon = +1.41$ ).

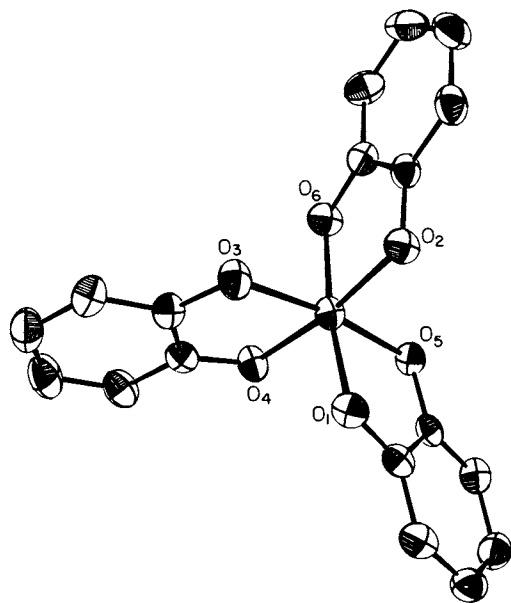


Figure 24. A perspective drawing of the  $[M(\text{catecholate})_3]^{3-}$  anions, where  $M = \text{Cr}$  and  $\text{Fe}$ , as viewed down the molecular threefold axis (63)

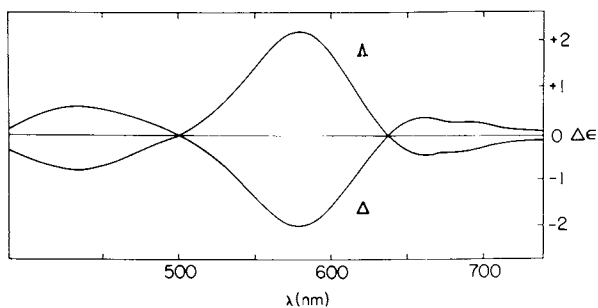
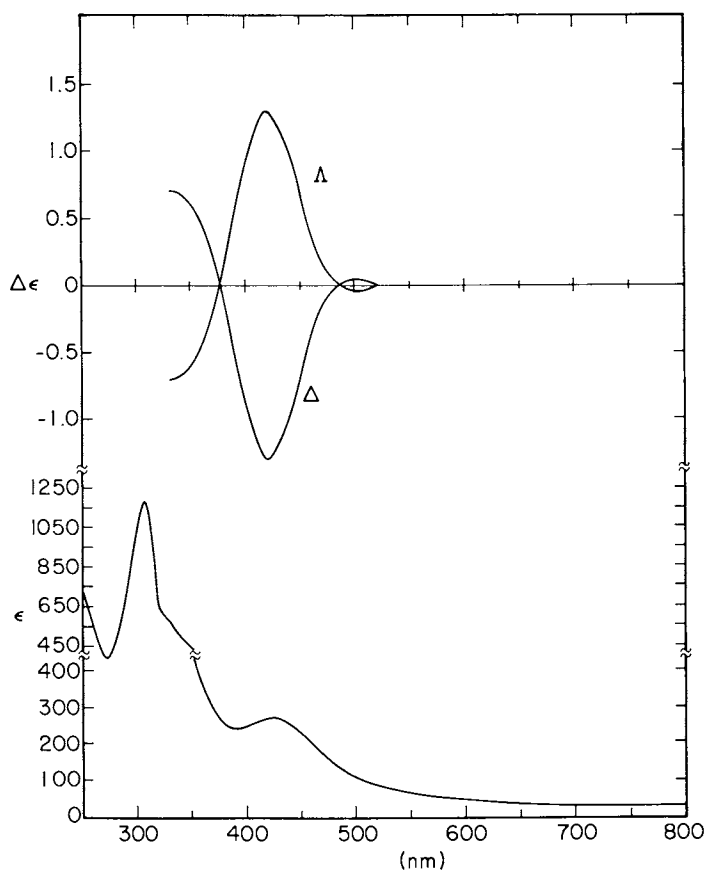


Figure 25. Circular dichroism spectra of  $\Delta$ - and  $\Lambda$ - $\text{K}_3[\text{Cr}(\text{cat})_3]$  in aqueous solutions (61)



Inorganic Chemistry

Figure 26. Absorption and CD spectra of  $\Delta$ - and  $\Lambda$ - $K_3Rh(\text{catecholate})_3$  in aqueous basic solution (62)

2) Again, the empirical rule for  $d^3$  or low-spin  $d^6$  complexes of  $D_3$  symmetry is applicable. For the  $\Lambda$  configuration the transitions with E and  $A_2$  symmetry have positive and negative signs, respectively.

3) Finally, an analogy is drawn between the chromium and rhodium catecholate complexes. The salts  $[\text{Co}(\text{en})_3][\text{M}(\text{cat})_3]$  ( $\text{M} = \text{Rh}, \text{Cr}$ ), prepared from  $\Lambda\text{-}[\text{Co}(\text{en})_3]\text{I}_3\text{H}_2\text{O}$  have been shown by x-ray powder patterns to be isostructural and therefore of the same absolute configuration. Thus the catecholate systems are at least self-consistent.

### Enterobactin

In addition to preparing the model catecholate complexes of rhodium and chromium, the analogous enterobactin complexes were also prepared and their CD spectra recorded (62). From examination of molecular models it is apparent that either the  $\Lambda\text{-cis}$  or  $\Delta\text{-cis}$  diastereomers of a metal enterobactin complex are structurally possible. In theory, these diastereomers should be separable by chromatographic techniques analogous to those used for the hydroxamates (vide supra); however, under a variety of conditions only one chromatographic fraction is obtained. We conclude that one isomer predominates to the exclusion of the other.

The visible spectra of  $d^3$   $\text{Cr}^{3+}$  and  $d^6$   $\text{Rh}^{3+}$  complexes are due to  $d\text{-}d$  transitions (and will be chiefly dependent on the ligands for their ligand field effect) plus some ligand-to-metal charge transfer. Since the ligand field strength of catechol and enterobactin are nearly identical and NMR studies (62, 64) have indicated catecholate coordination for enterobactin, the CD spectra of catecholate and enterobactin complexes may be compared directly. Thus, comparison of the CD spectra of  $[\text{Rh}(\text{enterobactin})]^{-3}$  and  $[\text{Cr}(\text{enterobactin})]^{-3}$  (Figures 27 and 28, respectively) with the analogous catecholate compounds (Figures 26 and 25) leads to the conclusion that the predominant isomer in both cases has a  $\Delta\text{-cis}$  absolute configuration (Figure 29). Finally, the absolute configuration of iron(III) enterobactin is likewise assigned as  $\Delta\text{-cis}$  since:

1) The model  $\text{Cr}^{+3}$  and  $\text{Fe}^{+3}$  catecholates are isostructural and the ionic radii of all three metals are equal to within 0.03 Å.

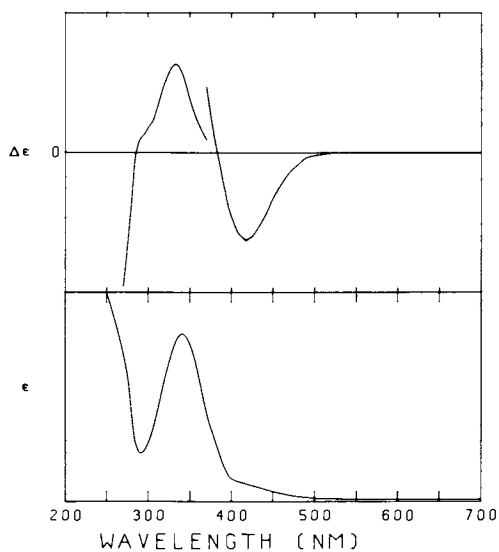
2) All three enterobactin complexes (Fe, Cr, Rh) have identical  $R_f$  values for silica gel TLC in 50% chloroform-methanol solvent.

This  $\Delta\text{-cis}$  absolute configuration for iron(III) enterobactin is opposite to that found for all of the optically active hydroxamate siderophores except rhodotorulic acid.

### Summary

The stereochemistry of microbial iron transport compounds is





Inorganic Chemistry

Figure 27. Absorption spectrum of  $K_3[Rh(ent)_3]$  in aqueous solution (lower curve) and CD spectrum of  $\Delta$ -cis- $K_3[Rh(ent)_3]$  in methanol solution (upper curve). Extinction coefficients are approximate (62).

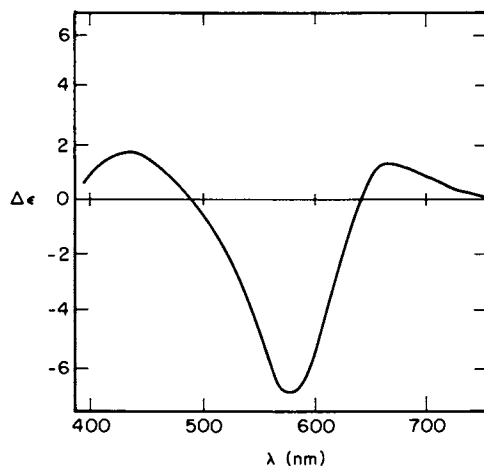


Figure 28. CD spectra of  $[\text{NH}_4]_3[\text{Cr}(\text{ent})]$  (61)

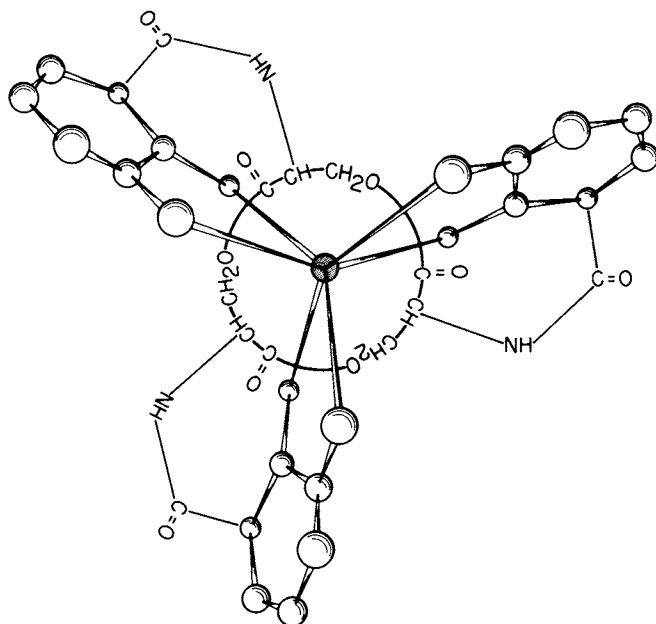


Figure 29. A schematic of the  $\Delta$ -cis isomer of chromium(III) and ferric enterobactin. The metal lies at the center of a distorted octahedron formed by the oxygen atoms of the three catechol dianions (61).

a fascinating composite of coordination chemistry and biochemistry. Results of investigations in this field show that chromic-substituted siderophore complexes are readily prepared and are kinetically inert with respect to isomerization. Furthermore, the spectroscopic properties and single crystal x-ray structures of simple model compounds show that the chromium(III) and iron(III) siderophore complexes are sufficiently similar to regard them as identical for biological systems. Finally, this close similarity permits the use of chromium(III) and rhodium(III) siderophore complexes as chemical probes of the siderophore's metal coordination site. This similarity allows assignment of the geometry and absolute configuration of the metal coordination site by comparison of absorption and circular dichroism spectra with the spectra of model compounds. Thus, the absolute configurations of the biologically relevant isomers of enterobactin, ferrichrome, rhodotorulic acid, and aerobactin have been assigned.

Despite the increase in our understanding of microbial iron transport from these studies, much remains unknown. For example, one of our original queries remains unanswered. Is recognition of the iron(III) siderophore complex and subsequent active transport into the cell dependent on one optical isomer? This and other questions concerning the coordination chemistry of siderophores remain to be answered.

Acknowledgment. This research has resulted from the efforts of several co-workers, past and present, whose names appear in the cited papers. We thank the NIH for research support.

#### Literature Cited

1. Neilands, J. B. "Microbial Iron Metabolism"; Academic Press: San Francisco, 1974.
2. Neilands, J. B. In "Iron Metabolism, Ciba Foundation Symposium: 51"; Elsevier: North Holland, Amsterdam, 1977.
3. Raymond, K. N. Adv. Chem. Ser. (1977), 162, 33-54.
4. Kochan, I. Curr. Top. Microbiol. Immunol. (1973), 60, 1-30.
5. Snow, G. A. Bact. Rev. (1970), 34, 99.
6. Weinberg, E. D. Science (1974), 184, 952-956.
7. Wawskiewicz, E.; Schneider, H. A.; Starcher, B.; Pollack, J.; Neilands, J. B. Proc. Nat. Acad. Sci. USA (1971), 68, 2870-2873.
8. Bullen, J. J.; Rogers, H. J.; Leigh, L. Brit. Med. J., Jan. 8, (1972), 69.
9. Raymond, K. N.; Carrano, C. J. Acc. Chem. Res. (1979), 12, 183-190.
10. Inorg. Chem. (1970), 9, 1-5.
11. Leong, J.; Raymond, K. N. J. Am. Chem. Soc. (1974), 96, 1757-1762.
12. Abu-Dari, K.; Raymond, K. N. Inorg. Chem. submitted for publication.

13. Jursik, F. J. Chromatogr. (1968), 35, 126-128.
14. Jursik, F.; Petru, F.; Hajek, B. J. Chromatogr. (1969), 45, 319-321.
15. Kauffman, G. B.; Pinnell, R. P.; Takahashi, L. T. Inorg. Chem. (1962), 1, 544-550.
16. Palmer, R. A.; Fay, R. C.; Piper, T. S. Inorg. Chem. (1964), 3, 875-881.
17. Springer, C. S., Jr.; Sievers, R. E.; Feibush, B. Inorg. Chem (1971), 10, 1242-1250.
18. King, R. M.; Everett, G. W., Jr. Inorg. Chem (1971), 10, 1237-1242.
19. Shimura, Y.; Tsuchida, R. Bull. Chem. Soc. Jpn. (1956), 29, 311-316.
20. Basolo, F.; Ballhausen, C. J.; Bjerrum, J. Acta Chem. Scand. (1955), 9, 810-814.
21. Mori, M.; Shibata, M.; Kyuno, E.; Kanaya, M. Bull. Chem. Soc. Jpn. (1961), 34, 1837-1842.
22. Dunlop, J. H.; Gillard, R. D. J. Chem. Soc. (1965), 6531-6543.
23. Saraceno, A. J.; Nakagawa, I.; Mizushima, S.; Curran, C.; Quagliano, J. V. J. Am. Chem. Soc. (1958), 80, 5018-5021.
24. Israili, M. N. C.R. Acad. Sci., Ser. C. (1966), 262, 1426-1428.
25. Abu-Dari, K.; Ekstrand, J. D.; Freyberg, D. P.; Raymond, K. N. Inorg. Chem. (1979), 18, 108-112.
26. Lindner, Von H. J.; Goettlicher, S. Acta Crystallogr. (1969), B25, 832-842.
27. McCaffery, A. J.; Mason, S. F.; Ballard, R. E. J. Chem. Soc. (1965), 2883-2892.
28. Larsen, E.; Mason, S. F. J. Chem. Soc. (A) (1966), 313-316.
29. Douglas, B. E.; Yamada, S. Inorg. Chem. (1965), 4, 1561-1565.
30. Denning, R. G.; Piper, T. S. Inorg. Chem. (1966), 5, 1056-1065.
31. McCaffery, A. J.; Mason, S. F.; Norman, B. J. J. Chem. Soc. (1965), 5094-5107.
32. Butler, K. R.; Snow, M. R. J. Chem. Soc., Dalton Trans. (1976), 251-258.
33. Snow, M. R. Acta Crystallogr. (1974), B30, 1850-1856.
34. Dunlop, J. H.; Gillard, R. D.; Ugo, R. J. Chem. Soc., A (1966), 1540-1547.
35. Everett, G. W., Jr.; Chen, Y. T. J. Am. Chem. Soc. (1970), 92, 508-514.
36. Mason, S. F. Quart. Rev., Chem. Soc. (1963), 17, 20-66.
37. Butler, K. R.; Snow, M. R. Chem. Commun. (1971), 550-551.
38. Piper, T. S. J. Chem. Phys. (1962), 36, 2224-2225
39. Piper, T. S.; Carlin, R. L. J. Chem. Phys. (1961), 35, 1809-1815.
40. McCaffery, A. J.; Mason, S. F. Trans. Faraday Soc. (1963), 59, 1-11.

41. Karipides, A. G.; Piper, T. S. J. Chem. Phys. (1964), 40, 674-682.
42. Abu-Dari, K.; Carrano, C. J.; Raymond, K. N. To be published.
43. Loghry, R. A.; Van der Helm, D. Abs. Am. Cryst. Assn., Winter Meeting, March (1978), Abs. PB2.
44. Zalkin, A.; Forrester, J. D.; Templeton, D. H. J. Am. Chem. Soc. (1966), 88, 1810-1814.
45. Norrestam, R.; Stensland, B.; Branden, C. I. J. Mol. Biol. (1975), 99, 501-506.
46. Abu-Dari, K.; Raymond, K. N. J. Am. Chem. Soc. (1977), 99, 2003-2005.
47. Van der Helm, D.; Poling, M. J. Am. Chem. Soc. (1976), 97, 82-86.
48. Leong, J.; Raymond, K. N. J. Am. Chem. Soc. (1975), 97, 293-296.
49. Carrano, C. J.; Raymond, K. N. J. Am. Chem. Soc. (1978), 100, 5371-5374.
50. Harris, W. R.; Carrano, C. J.; Raymond, K. N. J. Am. Chem. Soc. (1979), 101, 2722.
51. Abu-Dari, K.; Raymond, K. N. Inorg. Chem. (1977), 16, 807-812.
52. Freyberg, D. P.; Abu-Dari, K.; Raymond, K. N. Inorg. Chem., submitted for publication.
53. Abu-Dari, K.; Freyberg, D. P.; Raymond, K. N. Inorg. Chem., in press.
54. Ito, Y.; Neilands, J. B. J. Am. Chem. Soc. (1958), 18, 4645-4647.
55. Pollack, J.; Gibson, F. Biochem. Biophys. Res. Commun. (1970), 38, 989-992.
56. O'Brien, I. G.; Gibson, F. Biochem. Biophys. Acta (1970), 215, 393-402.
57. Peters, W. J.; Wanen, R. A. J. Biochem. Biophys. Acta (1968), 165, 225-232.
58. Corbin, J. L.; Bulen, W. A. Biochem. (1969), 8, 757-762.
59. O'Brien, I. G.; Cox, G. B.; Gibson, F. Biochem. Biophys. Acta (1971), 237, 537-549.
60. Cooper, S. R.; McArdle, J. V.; Raymond, K. N. Proc. Nat. Acad. Sci., USA (1978), 75, 3551-3554.
61. Isied, S. S.; Kuo, G.; Raymond, K. N. J. Am. Chem. Soc. (1976), 98, 1763-1766.
62. McArdle, J. V.; Sofen, S. R.; Cooper, S. R.; Raymond, K. N. Inorg. Chem. (1978), 17, 3075-3078.
63. Raymond, K. N.; Isied, S. S.; Brown, L. D.; Fronczek, F. R.; Nibert, J. H. J. Am. Chem. Soc. (1976), 98, 1767-1774.
64. Llinas, M.; Wilson, D. M.; Neilands, J. B. Biochem. (1973), 12, 3836-3843.

RECEIVED September 11, 1979.

## Rational Approaches to Asymmetric Hydrogenation

JOHN M. BROWN, PENNY A. CHALONER, BARRY A. MURRER,  
and DAVID PARKER

Dyson Perrins Laboratory, South Parks Road, Oxford, OX1 3QY, U.K.

Asymmetric catalysis has great potential for synthetic organic chemistry, since optically active molecules may be prepared without the need for resolution. The hydrogenation of prochiral olefins is particularly attractive, since in principle many diverse types of tertiary asymmetric center may be introduced in a single step. Following the discovery of efficient rhodium catalysts for homogeneous hydrogenation by Wilkinson and co-workers, (1), complexes derived from phosphines of the type  $R_1R_2R_3P^*$  were prepared and evaluated. The results were invariably disappointing, and optical yields of hydrogenated products rather poor (2). Two developments led to considerable improvement. First, the use of dehydroamino acids led to efficient and stereoselective reduction (3), and secondly chelating chiral phosphines (4) were found to be effective ligands. Progress between 1971 and 1977 has been reviewed (5,6,7) and now optical yields of more than 90% in the hydrogenation of dehydroamino acids or their derivatives are commonplace.

There have been considerable developments in the last two years. Most of these concern the synthesis and application of new types of chiral chelating biphosphine and will be discussed in context. It is now possible to make some generalizations concerning current knowledge about asymmetric hydrogenation:

- i) Efficient and rapid catalysis of the hydrogenation of dehydroamino acids (enamides) may be effected by a wide variety of rhodium (I) complexes of chelating chiral biphosphines.
- ii) The phosphine may be chiral by virtue of asymmetry at phosphorus or in the inter-phosphine chain. All effective ligands are biarylphosphines, phosphites and aminophosphines. When the asymmetric center is at a remote site the P-aryl groups adopt a preferred conformation which is locally asymmetric.
- iii) Substrates other than dehydroamino acids are normally hydrogenated with lower optical efficiency. Some examples of the reduction of prochiral  $\alpha,\beta$ -unsaturated acids are

0-8412-0538-8/80/47-119-169\$06.50/0

© 1980 American Chemical Society

particularly interesting, and will be discussed later. iv) Optical yields are normally insensitive to reaction conditions (although exceptions are interesting!). Under hydrogenation conditions the catalyst is present as a chelate rhodium(I) cation which binds substrate and hydrogen sequentially. Enamide complexes, which may be observed by phosphorus-31 NMR represent the resting state of the catalyst.

#### Stereoselection in Metal-Olefin Complexation

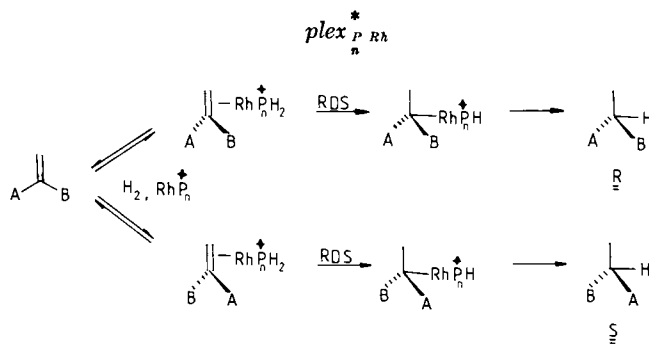
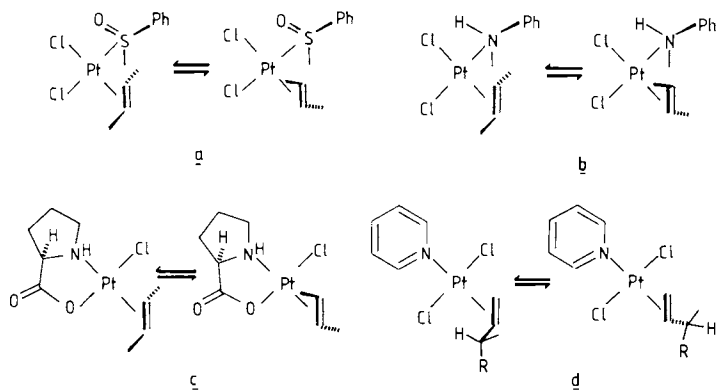
A prerequisite for effective asymmetric hydrogenation is that the prochiral olefin is bound stereoselectively to metal at the rate-determining transition-state (Scheme 1). It is therefore of interest to consider stable metal-olefin complexes which may exist as diastereomers by virtue of alternative modes of prochiral olefin complexation. Most work has been done with comparatively simple asymmetric sulfur or nitrogen ligands, and selectivity is usually low. With simple olefins this is not surprising, since discrimination depends on rather small differences in steric bulk in the absence of polar interactions.

All the examples to be discussed are of square-planar platinum(II) complexes, recorded in Scheme 2. Thus Boucher and Bosnich (8) have prepared a series of olefin complexes derived from (*p*-tolylmethylsulfoxide)dichloroplatinum(II) in which the ligand is *S*-bonded. The *S*-methyl protons provide a convenient and sensitive NMR probe for the determination of diastereomer ratios. In the cases of but-1-ene, 3-methylbut-1-ene, styrene and 3,3-dimethylbut-1-ene crystals of a single diastereomer can be isolated; in all but the last of these, however, there is rapid equilibration between diastereomers in solution, with relatively little discrimination between them (typically 55-75% of the major species). Since several rotamers are possible in the sulfoxide ligand it is not easy to specify the origin of chiral discrimination.

Several workers have studied platinum(II) complexes of olefins containing chiral amine or amino-acid ligands. Panunzi(9) observed stereoselectivity in the reaction between *cis*-(*S*- $\alpha$ -methylbenzylamine)dichloroplatinum (II) and *trans*-2-butene with the major diastereomer formed to the extent of 70% of total complex. More recently (10), it has been shown that the replacement of coordinated *trans*-2-butene by free olefin in (*S*-prolinato)dichloroplatinum (II) complexes takes place more easily with retention than with inversion. Addition of a large excess of *trans*-2-butene to solutions of the corresponding ethylene complexes produced first an increase and then a gradual decrease in their circular dichroism. The kinetic stereoselectivity in this reaction (that is, the differing reaction rates of the two prochiral faces of *trans*-but-2-ene) was 3:1, but at equilibrium the ratio of major and minor diastereomers was 64:36 in the *cis*-isomer and 59:41 in the *trans*-isomer.

Complexation of optically active olefins to achiral



*Scheme 1. Homogeneous hydrogenation catalyzed by an asymmetric com-**Scheme 2. Stereoselection in olefin-platinum complexes*

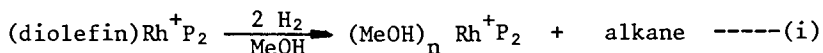
platinum species has been investigated (11). In this latter case, the olefin has two diastereotopic faces, and these give rise to separate diastereomeric complexes. The degree of selectivity depends on the size of the group R (Scheme 2, d), being most for S-3-methyl-4,4-dimethylpent-1-ene. In all cases the complex with opposite configurations at the two chiral centers predominates.

These simple model systems are characterised by low stereoselectivity and since they are flexible, it is difficult to rationalise. The degree of success obtained in asymmetric hydrogenation of enamides suggests a considerably greater degree of discrimination in olefin binding, whose origins form the subject of the following section.

#### Mechanistic Studies on Asymmetric Hydrogenation

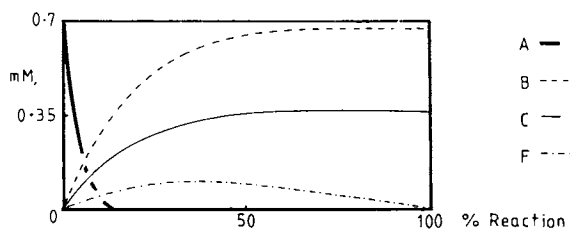
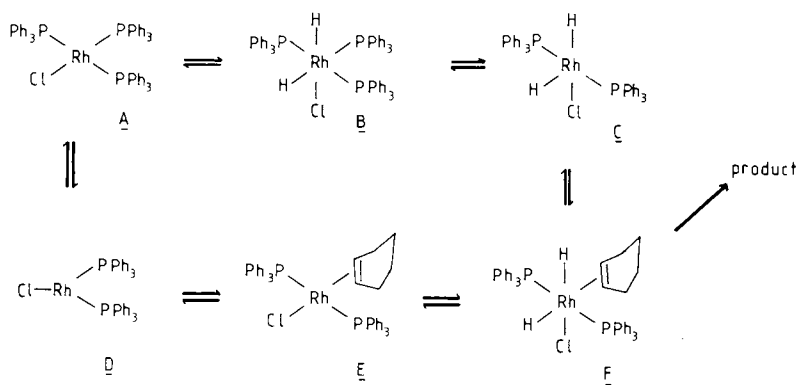
Homogeneous catalysis is generally considered to be a rather empirical branch of chemistry and the instinct or experience of workers in the field is often more useful than mechanistic prediction. This is true of hydrogenation, for which a complete description of the reaction pathway in reductions catalysed by  $(\text{Ph}_3\text{P})_3\text{RhCl}$  is quite recent (12). It had been known for some years, largely as a result of studies conducted by Halpern, Tolman and others (13), that the reaction requires initial hydrogen addition to the catalyst followed by loss of a phosphine trans to hydride and subsequent olefin coordination; the product is then formed by rapid hydride transfer. More recent work of Dutch and French chemists (12) permits an accurate kinetic model to be constructed (Scheme 3) and rules out any role for the "unsaturate" route involving ligand loss prior to olefin coordination.

When our studies commenced it had been assumed that the mechanism of asymmetric hydrogenation by chelating rhodium phosphine complexes followed a similar pathway. It has been demonstrated, however, that the timing is quite different, and that oxidative addition of hydrogen to metal does not occur in the initial stages of reaction. This conclusion follows from studies on the phosphorus-31 NMR spectra of hydrogenated complex solutions made separately by Halpern, Baird and ourselves (14), which demonstrate that the initial hydrogenation follows equation (i).



It was subsequently demonstrated that enamides displace solvent from this adduct, giving new species which are air-sensitive and highly reactive towards hydrogen. These enamide complexes have been characterized spectroscopically (15), and one of the more informative experiments was carried out with the asymmetric ligand DIPAMP and methyl Z- $\alpha$ -benzamidocinnamate (Figure 1). This shows that two diastereomeric enamide complexes are formed in a ratio of 10:1 at room temperature. The two species are related by binding of opposite prochiral faces of

Scheme 3. The mechanism of hydrogenation of cyclohexene catalyzed by  $(PPh_3)_3RhCl$



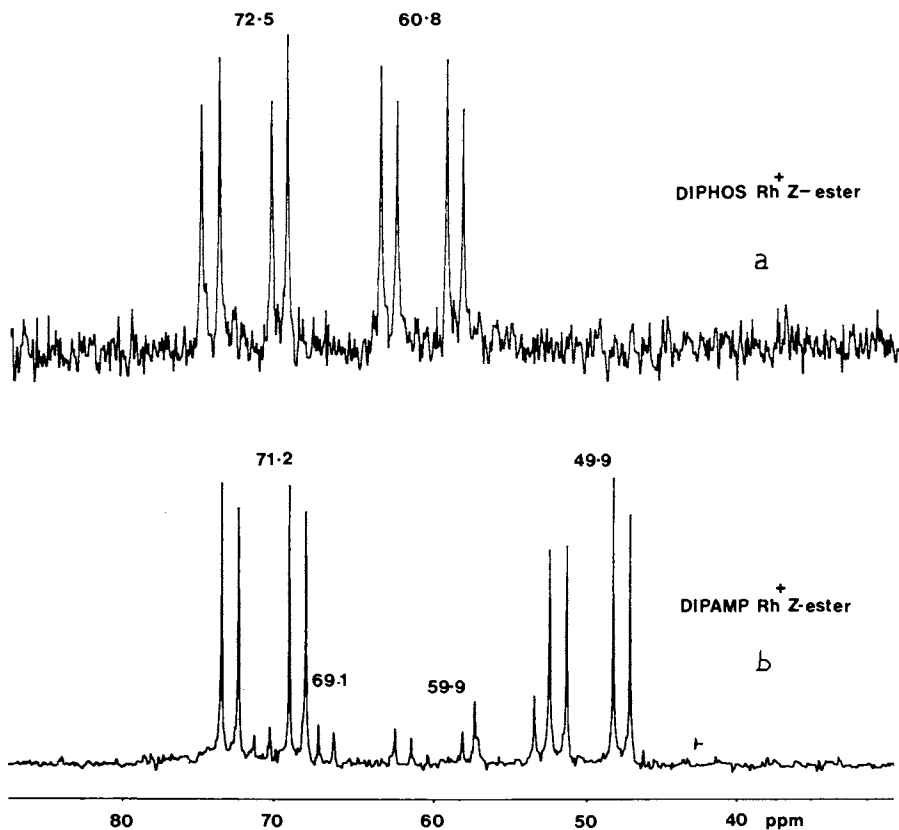


Figure 1. Rhodium enamide complexes derived from (a) bis-diphenylphosphinoethane and (b) DIPAMP with methyl *z*- $\alpha$ -benzamidocinnamate; phosphorus-31 NMR spectra, MeOH, 25°C.

the olefin to rhodium, and the substrate is otherwise coordinated in the same manner. The stereoselectivity in binding is almost as high as the enantiomer excess of 94% observed in hydrogenation of this substrate (18)

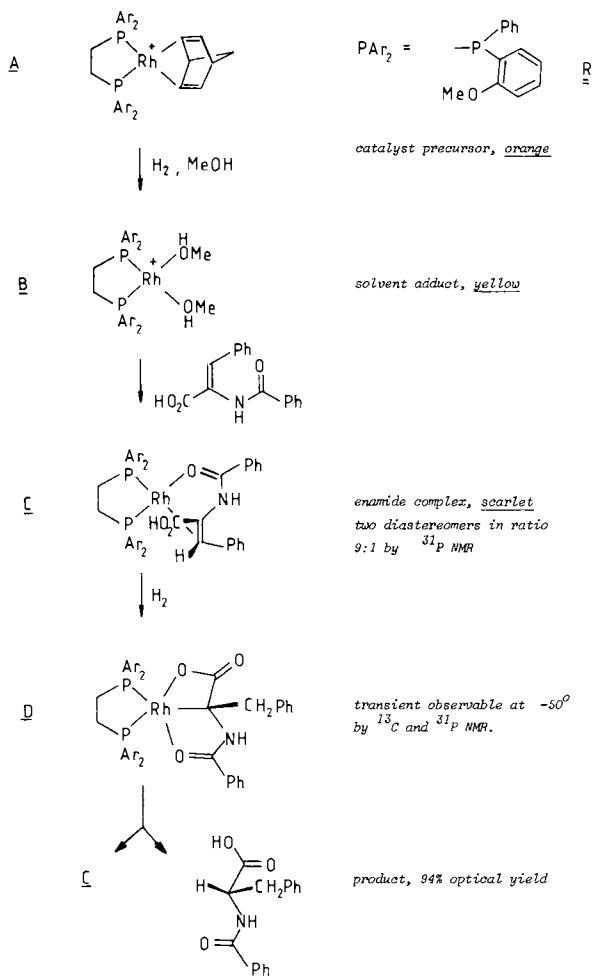
The significance of these NMR experiments lies in the way they are related to the mechanism of hydrogenation. The pathway is as shown in Scheme 4, and although binding of the enamide is reversible, and therefore pre-rate determining, a characteristic red color due to its complex is observed throughout the reaction. The rate-determining step is either addition of hydrogen, or intracomplex hydrogen transfer, and in one case there is evidence for a further transient intermediate (16). Nevertheless, the structure of the rate-determining transition-state is sufficiently close to that of the enamide complex, that the factors causing stereoselectivity in catalysis also stereoselectivity in binding.

In subsequent sections we shall discuss results obtained in asymmetric hydrogenation and rationalize the role of the ligand. The conclusions should be of assistance to the design of new phosphines for catalysis of hydrogenation and several related reactions.

#### Catalysis and Binding by 5-Ring Chelate Biphosphine Rhodium Complexes

Bis-diphenylphosphinoethane complexes are intrinsically chiral and in square-planar chelate complexes the PMP angle is  $82^\circ$  (17) with one methylene group above the co-ordination plane and one below. This enforces a conformation on the chelate ring in which one P-Ph bond is axial and the other equatorial. The phenyl rings are related in pairs by rotation about a  $C_2$  symmetry axis extending from the metal through the  $CH_2-CH_2$  bond. In the absence of other substituents, rapid racemization of individual enantiomeric complexes occurs by pseudorotation of the five-membered ring, which simultaneously exchanges the equatorial and axial phenyl groups. An asymmetric center in the chelate will lead to a preference for one conformer. This may be achieved by aryl-substitution; the only known example of which is RR - DIPAMP (18) (Scheme 5) possessing two *o*-anisyl groups. Biphosphines derived from 1,2-propanediol (19), trans-2,3-butane-diol (20) and 1-phenylethanol (21) are all effective ligands in the asymmetric hydrogenation of enamides. In these cases the conformation of the 5-membered ring is dictated by the preference of the substituent for an equatorial site. This is confirmed by X-ray crystal structures on rhodium olefin complexes of these ligands, all of which show a chiral conformation of the P-phenyl rings (22). Examination of these structures indicates that it is the steric interaction between equatorial P-phenyl groups and vinylic substituents which controls the preferred face of binding to a prochiral olefin. There is one crystal structure of an enamide complex (23). Although this is derived from an achiral biphosphine, it does show that the major steric

## Scheme 4. The mechanism of asymmetric hydrogenation



interaction is between an equatorial phenyl ring and the carbethoxyl group. Simple conformational analysis (see later) enables a correct prediction of the preferred optical sense of asymmetric hydrogenation in catalysis by all these ligands.

When the biphosphine is chiral, but possesses a symmetry axis, there are only two possible diastereomeric modes of binding in an enamide complex in which olefin and amide groups are coordinated to the metal. R-Phenylbis (diphenylphosphino) ethane complexes are disymmetric and consequently there are four possible enamide complexes - either face of the olefin may be cis or trans to Pl. Complexation of methyl  $\alpha$ -acetamidocrylate gives only one of these but complexation of acetamidocinnamic acid or its esters leads to two diastereomeric complexes (21) (Figure 2). A combination of labelling experiments demonstrates that these are regioisomers (same olefin face coordinated to the metal) rather than stereoisomers.

In summary, bis(diphenylphosphino)ethane derivatives form chelates of rigid structure and defined geometry. Their complexes are efficient catalysts (Table I) for reduction of dehydroamino acids, although other prochiral olefins are reduced with low optical efficiency. For comparison purposes, the hydrogenation of dehydrophenylalanines is emphasized in tabulated data.

#### Binding of Enamides and Catalysis by 6-Ring Chelate Rhodium Complexes

The geometry of a chiral 6-membered chelate ring is not conducive to effective asymmetric catalysis. Consider square-planar complexes of d,1-2,3-diphenyl-1,3 bis(diphenylphosphino) propane (24), which are presumed to exist in chair conformation (Scheme 6) with rapid ring inversion. The close approximation to  $\sigma$ -symmetry in the environment of the metal suggests that there will be little discrimination between the diastereomeric modes of binding of a prochiral bidentate ligand, since substituents on the olefin experience similar steric interactions in both isomers. The expectation of low selectivity is borne out in practice, for in some cases enamide complexes derived from this phosphine exist in two diastereomeric forms (Figure 3).

As might be expected, there are few reports of catalytic applications of chiral 6-ring chelates. The homologue of PROPHOS (19) is much less effective in asymmetric hydrogenation of enamides (25). A number of aromatic  $\alpha$ -aminoethylaryl diphenylphosphines have been prepared, but none show promise in catalysis (26).

#### Catalysis and Binding by 7-Ring Chelate Biphosphine Rhodium Complexes

A considerable number of chiral chelates containing a 7-membered ring have been employed in asymmetric hydrogenation. Synthesis of the biphosphine ligand generally involves a naturally occurring chiral precursor, and all examples described have one or more asymmetric centers in the side-chain. Very often, the chelate ring has a  $C_2$  symmetry axis, making the

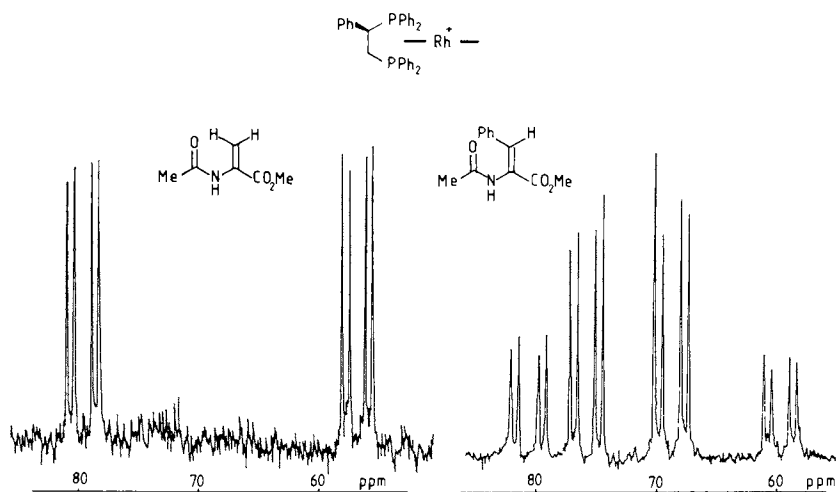
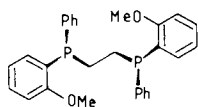


Figure 2. Regioselectivity in enamide complexation; phosphorus-31 NMR spectra, MeOH, 25°C.

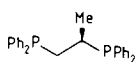


TABLE I. Hydrogenation of enamides by 5-ring chelate biphosphine catalysts

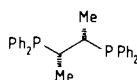
| Entry   | Phosphine | Substrate | Solvent  | Temperature | Pressure, atm | Catalyst/Substrate | Optical yield |
|---------|-----------|-----------|----------|-------------|---------------|--------------------|---------------|
| a, (18) | A         | 1         | MeOH     | 50°         | 3             | 1:1000             | 94 <u>S</u>   |
| b, (18) | A         | 2         | MeOH     | 50°         | 3             | 1:900              | 96 <u>S</u>   |
| c, (19) | B         | 3         | 95% EtOH | 25°         | 1             | 1:250              | 90 <u>S</u>   |
| d, (20) | C         | 1         | EtOH     | 25°         | 1             | 1:100              | 95 <u>R</u>   |
| e, (21) | D         | 2         | MeOH     | 20°         | 1             | 1:50               | 80 <u>S</u>   |
| f, (21) | D         | 4         | MeOH     | 20°         | 1             | 1:50               | 88 <u>S</u>   |
| g, (21) | D         | 5         | MeOH     | 20°         | 1             | 1:50               | 82 <u>S</u>   |
| h, (21) | D         | 6         | MeOH     | 20°         | 1             | 1:50               | 78 <u>S</u>   |



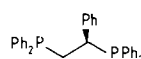
A



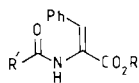
B



C



D

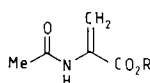


1 R = H R' = Ph

2 R = Me R' = Ph

3 R = H R' = Me

4 R = Me R' = Me



5 R = H

6 R = Me

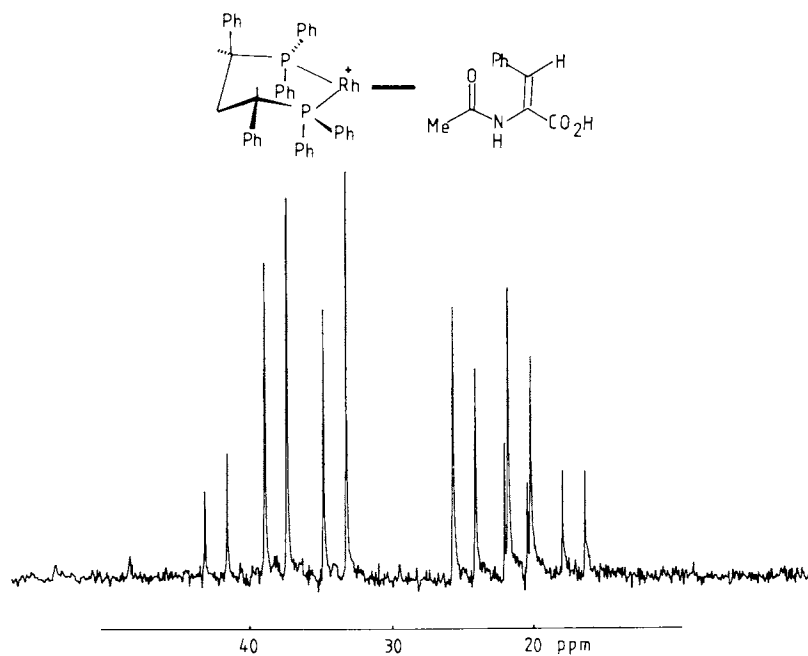


Figure 3. Lack of stereospecificity in enamide binding to a 6-ring chelate; phosphorus-31 NMR spectra, MeOH,  $-35^{\circ}\text{C}$ .

phosphorus atoms equivalent in bicycloheptadiene or cyclooctadiene complexes. The variety of catalysts available, and the apparent capriciousness of optical efficiency with change in ligand structure, is recorded in Table II.

The data may be rationalized. Consider the ligand DIOP, which has been employed more extensively than any other asymmetric biphosphine. Its chelate ring is flexible, and several strain-free conformations are accessible to a complex of square-planar geometry. Many of these may be discounted since they are centrosymmetric and therefore ineffective at inducing asymmetry in the substrate. There are, however, two possible conformations of  $C_2$  symmetry (more correctly, one with a true  $C_2$  axis and another pair of dissymmetric conformations linked by pseudorotation with averaged  $C_2$  symmetry) and these are related to the chair and twist-boat conformations of cycloheptane (Scheme 7) respectively. In the chair conformation, derived as drawn from  $\underline{RR}$  - DIOP, it is the pro- $\underline{R}$  rings which are axial and the pro- $\underline{S}$  phenyl rings equatorial. The situation is reversed in the twist-boat form, and here the pro- $\underline{S}$  phenyl rings are axial and their pro- $\underline{R}$  counterparts equatorial. Inspection of molecular models suggests that the major factor leading to stereoselection in enamide binding and in catalytic hydrogenation is the non-bonded interaction between the P-phenyl ring and the  $\alpha$ -carboxyl or  $\alpha$ -alkoxycarbonyl group. This accords with the general observation that different  $\underline{Z}$ -dehydroamino acids hydrogenate with similar optical efficiency and also that acids and esters tend to give similar optical yields.

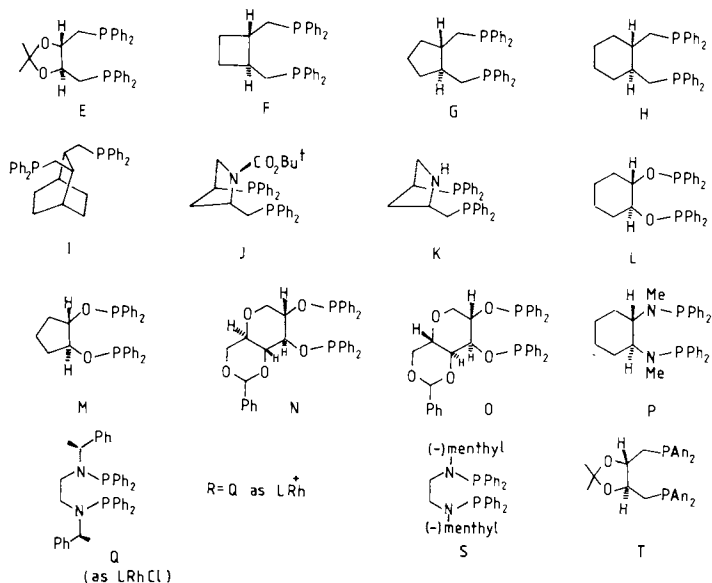
There is a simple empirical rule which is capable of rationalizing all data presently available. This may be stated: "Factors which favor a twist-boat conformation in the chelate when the ligand enantiomer is such that the axial rings are pro- $\underline{S}$  promote the formation of  $\underline{S}$ -amino acid from  $\underline{Z}$ -enamide precursor. Similarly, factors which favor a chair conformation likewise promote the formation of  $\underline{R}$ -amino acid. If the chelate is non-rigid, and neither geometry favored then the optical yield is low".

There are a number of results which may be quoted in support of this hypothesis. Firstly, DIOP and its carbocyclic analogues appear to favor the twist-boat geometry,  $\underline{R}$  - DIOP (from natural tartaric acid) giving  $\underline{R}$ -amino acids. The optical yield depends in the size of the fused ring, decreasing in the sense cyclobutane (91%) > cyclopentane (63%) > cyclohexane (35%), all data referring to hydrogenation of  $\underline{Z}$ -acetamidocinnamic acid. This is precisely the trend which would be expected, for a small trans-fused ring will stabilize the twist-boat conformation whereas a trans-fused cyclohexane will stabilize the chair conformation. A comparison between phosphonites and amino-phosphines is more dramatic. The former (entries l,m,n in Table II) all behave as if they are twist-boat chelates, but the aminophosphine (entry g) behaves as if it is a

TABLE II. Hydrogenation of  $\alpha$ -acetamidocinnamates with 7-ring chelate biphosphines

| Entry      | Phosphine | Substrate              | Solvent                                  | Temperature | Pressure, atm | Catalyst/<br>Substrate | Optical<br>Yield |
|------------|-----------|------------------------|--|-------------|---------------|------------------------|------------------|
| a, (27)    | E         | acid                   | EtOH                                     | ambient     | 1             | 1:100                  | 80 <u>S</u>      |
| b, (27)    | E         | Me ester               | EtOH                                     | ambient     | 1             | 1:100                  | 49 <u>S</u>      |
| c, (28)    | F         | acid                   | EtOH:C <sub>6</sub> H <sub>6</sub> (2:1) | 25°         | 1             | 1:50                   | 86 <u>S</u>      |
| d, (28)    | F         | acid, NEt <sub>3</sub> | EtOH:C <sub>6</sub> H <sub>6</sub> (2:1) | 25°         | 1             | 1:50                   | 91 <u>S</u>      |
| e, (28)    | F         | Me ester               | EtOH:C <sub>6</sub> H <sub>6</sub> (2:1) | 25°         | 1             | 1:25                   | 44 <u>S</u>      |
| f, (28)    | G         | acid                   | EtOH:C <sub>6</sub> H <sub>6</sub> (2:1) | 25°         | 1             | 1:25                   | 63 <u>S</u>      |
| g, (28)    | H         | acid                   | EtOH:C <sub>6</sub> H <sub>6</sub> (2:1) | 25°         | 1             | 1:25                   | 35 <u>S</u>      |
| h, (28)    | H         | Me ester               | EtOH:C <sub>6</sub> H <sub>6</sub> (2:1) | 25°         | 1             | 1:25                   | 01 <u>R</u>      |
| i, (29)    | I         | Me ester               | EtOH:C <sub>6</sub> H <sub>6</sub> (2:1) | 20°         | 1.1           | 1:33                   | 80 <u>S</u>      |
| j, (30)    | J         | acid                   | EtOH                                     | 20°         | 50            | 1:200                  | 30 <u>R</u>      |
| k, (30)    | J         | acid, NEt <sub>3</sub> | EtOH                                     | 20°         | 50            | 1:200                  | 91 <u>R</u>      |
| l, (30)    | K         | acid                   | EtOH                                     | 20°         | 50            | 1:200                  | 6 <u>S</u>       |
| m, (31)    | L         | acid                   | ---                                      | 0°          | 50            | ---                    | 69 <u>S</u>      |
| n, (32)    | M         | Me ester               | ---                                      | 0°          | 50            | ---                    | 12 <u>S</u>      |
| o, (33,34) | N         | acid                   | EtOH                                     | 0°          | 50            | 1:100                  | 75 <u>S</u>      |
| p, (33,34) | N         | Me ester               | EtOH                                     | 0°          | 50            | 1:100                  | 65 <u>S</u>      |
| q, (34)    | O         | acid                   | ---                                      | 25°         | 50            | ---                    | 00               |
| r, (35)    | P         | acid                   | EtOH                                     | 20°         | 1             | 1:100                  | 73 <u>R</u>      |
| s, (36,37) | Q         | acid                   | MeOH                                     | 25°         | 1             | 1:500                  | 66 <u>R</u>      |
| t, (36,37) | R         | acid                   | MeOH                                     | 25°         | 1             | 1:300                  | 80 <u>R</u>      |
| u, (36,37) | S         | acid                   | EtOH                                     | 0°          | 10            | 1:200                  | 93 <u>S</u>      |
| v, (24)    | T         | acid                   | MeOH                                     | 20°         | 1             | 1:100                  | 31 <u>R</u>      |
| w, (24)    | T         | Me ester               | MeOH                                     | 20°         | 1             | 1:100                  | 71 <u>R</u>      |

Optical yields relate to the S-configuration of phosphine



chair chelate. The driving force in the latter case is the extra stability conferred on equatorial N-methyl groups. In a twist-boat conformation one of these is necessarily axial. Further work by Fiorini and co-workers (37) reinforces these observations.

The hydroxyproline-derived biphosphine prepared by Achiwa (44,45,46) and co-workers presents an interesting case. Its rhodium complexes are only effective for asymmetric hydrogenation in the presence of triethylamine, and esters are reduced in poor optical yield. The N-H function coordinates to rhodium, as has been shown by X-ray analysis, and two diastereomers may occur in complexes of N-acyl derivatives which are related by rotation about the amide bond.

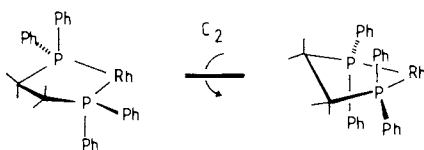
A detailed model for stereoselectivity in catalysis is less certain since the structure of the transition-state in asymmetric hydrogenation is not yet defined. It can, however, be explained in the enamide binding step, as shown in Scheme 8. The approach of the substrate is such as to minimize the proximity strain engendered by interaction between the carboxyl-group and the equatorial phenyl-group. Thus A, where these two substituents are staggered in the intracomplex Newman projection shown, is preferred over B in which these two groups are eclipsed. The transition-state may have a metal-hydride bond or partial bond, and the ligand rotated with respect to the P-Rh-P coordination plane, as in C. This takes account of the possibility that the acid or ester carbonyl group may be involved in stabilizing this hydride.

This model may be an oversimplification, since in some cases (phosphine c(38) Table II) the preferred enamide diastereomer observed by phosphorus-31 NMR magnetic resonance may change with the steric bulk of the ester group. A critical test of the hypothesis will be the optical yield in reduction of primary enamides and enol acetates by deuterium, since no steric effects are operative in these cases.

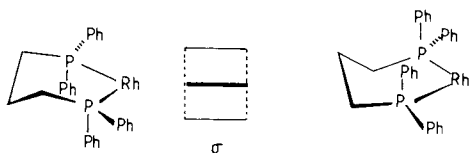
One striking result, which we cannot yet explain adequately, is provided by the comparison between DIOP (entry a,b) and its tetra *o*-methoxy analogue (entry t,u) in which there is a complete reversal of the stereochemical course of reaction. This occurs despite a more generally observed insensitivity of optical yields to alkyl substitution in the aromatic rings of DIOP(39). It is probable that the axial *o*-anisyl groups are weakly coordinated to the metal, as in DIPAMP and that in some way the resulting steric interactions are minimized when the chelate ring has a chair-conformation.

A recent crystallographic study provides striking support for the conformational flexibility of DIOP(40), for Gramlich and Consiglio have determined the structures of its Group VIIC dichlorides. The nickel complex is tetrahedral and has the chelate ring in a chair conformation, distorted so that a pair of phenyl rings is aligned parallel. Both the palladium and

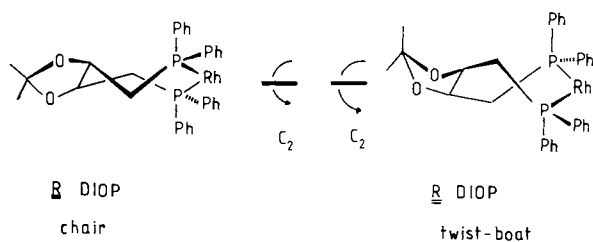
Scheme 5. Chiral conformations in 5-ring chelate biphosphine complexes



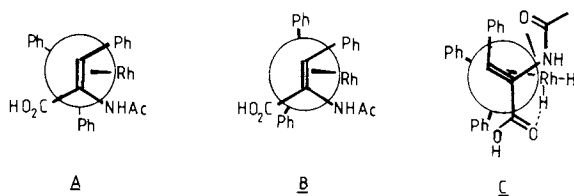
Scheme 6. Conformational isomerism in a 6-ring chelate biphosphine complex



Scheme 7. Chair and twist-boat conformations in a 7-ring chelate biphosphine complex



Scheme 8. Selectivity in enamide binding



platinum complexes are square-planar and they are isostructural, with two conformational isomers alternating. These again possess pairs of parallel phenyl rings, but one isomer is in chair-conformation, and the other in boat-conformation. The flexibility of 7-ring chelates and the likely correlation between ligand geometry and catalytic specificity is clearly demonstrated.

Catalytic Asymmetric Hydrogenation of other Substrates by 7-Ring Chelate Biphosphines

Asymmetric hydrogenation has proved extremely successful in the synthesis of amino-acids from enamides, but it is less effective with other substrates. Most, but not all (48) reported work has been carried out with 7-ring chelates, and some results are recorded in Table III.

The first set of data is concerned with hydrogenation of  $\alpha$ -ethylstyrene (31,32,42). This is the only simple olefin for which reasonable optical yields have been reported, and it is of some interest that all the effective catalysts are phosphonite complexes. Reaction conditions are much more forcing than in the case of enamide hydrogenation, typically requiring high pressures of hydrogen, high catalyst/substrate ratios and protracted reaction times. Since there is no independent mechanistic evidence on intermediates in the catalytic sequence, it is possible that an entirely different pathway is followed here and speculation on the origin of stereoselectivity is not warranted.

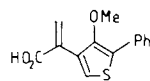
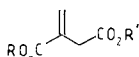
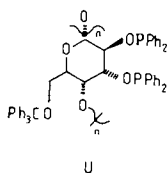
There have been a number of studies of the asymmetric hydrogenation of  $\alpha,\beta$ -unsaturated carboxylic acids, employing either atropic acid or itaconic acid. A very revealing experiment was carried out some time ago by Kagan and co-workers (3) (entry d,e). The optical yield obtained in hydrogenation of atropic acid catalyzed by R-DIOP rhodium complexes in the presence of triethylamine was 63% (S-enantiomer) but its methyl ester reacted in only 7% optical yield to give R-enantiomer. This implies that carboxylate binding is required for stereoselective reaction. The presence of base is not essential, since itaconic acid is hydrogenated by Achiwa's phosphine rhodium complexes to S-methyl succinic acid in 75% optical yield. This increases to 94% in the presence of triethylamine, however, so that the substrate may be bound as a carboxylate anion. As might be expected, dimethyl itaconate gives an inferior optical yield. DIOP is an efficient catalyst for the hydrogenation of the thiophen-substituted acid of entry j which proceeds in 88% optical yield (47). In this case the methoxyl-group may bind to rhodium and thus play a critical part in directing the reaction.

Comparing these results with enamide hydrogenation, it is evident that catalysts effecting R amino acid synthesis from enamides direct S-carboxylic acid formation from unsaturated acids. This implies (Scheme 9) that the preferred carboxyl-group configuration is similar in the two series.

TABLE III. Hydrogenation of non-enamide substrates by 7-ring chelate biphosphines

| Entry   | Phosphine          | Substrate | Solvent                                  | Temperature | Pressure, atm | Catalyst/Substrate | Optical Yield |
|---------|--------------------|-----------|--|-------------|---------------|--------------------|---------------|
| a, (31) | L                  | 7         | -  | 50°         | 50            | --                 | 33 <u>R</u>   |
| b, (32) | M                  | 7         | -  | 50°         | 50            |                    | 60 <u>R</u>   |
| c, (42) | U                  | 7         | C <sub>6</sub> H <sub>6</sub> :EtOH(1:1) | 120°        | --            | 1:80000            | 49 <u>R</u>   |
| d, (3)  | E                  | 8         | C <sub>6</sub> H <sub>6</sub> :EtOH(1:2) | 20°         | 1             | 1:30               | 63 <u>S</u>   |
| e, (3)  | E                  | 9         | C <sub>6</sub> H <sub>6</sub> :EtOH(1:2) | 20°         | 1             | 1:30               | 7 <u>R</u>    |
| f, (43) | E <sub>2</sub> RhH | 8         | C <sub>7</sub> H <sub>8</sub> :BuOH(1:2) | 30°         | 1             | 1:27               | 37 <u>R</u>   |
| g, (44) | J                  | 10        | MeOH <sup>‡</sup>                        | 20°         | 50            | 1:100              | 94 <u>S</u>   |
| h, (45) | J                  | 11        | MeOH <sup>‡</sup>                        | 20°         | 20            | 1:200              | 84 <u>S</u>   |
| i, (46) | J                  | 12        | MeOH <sup>‡</sup>                        | 20°         | 20            | 1:100              | 24 <u>S</u>   |
| j, (47) | E                  | 13        | iPrOH <sup>‡</sup>                       | 20°         | 1             | 1:15               | 88 <u>S</u>   |

<sup>‡</sup> Added NEt<sub>3</sub>





### Coordination of Unsaturated Carboxylic Acids in Rhodium Biphosphine Complexes

Typical square-planar rhodium-olefin complexes such as acetylacetonates (48) have a stoichiometry of two coordinated olefins per metal-atom. Since chelating olefins are bidentate in their cationic rhodium biphosphine complexes, it would be surprising if bis-olefin complexes were never found under hydrogenation conditions. It seems clear, in fact, that they can be the major coordinated species under certain conditions. Thus examples of 2:1 rhodium enamide complexes with bis-diphenylphosphinopropane have been observed (49), although the majority of cases involve  $\alpha\beta$ -unsaturated acids co-complexed with DIOP.

Complexes of unsaturated carboxylic acids generally do not give such sharp and informative phosphorus-31 NMR spectra as those of enamides, and the binding constant of substrate to rhodium is considerably lower (50). With methacrylic acid (Figure 4) the DIOP-rhodium complex formed is dependent on temperature and substrate concentrations—under favourable conditions a 2:1 complex is formed. In the presence of triethylamine, a 1:1 complex is formed which involves binding of the olefin and carboxylate anion. Favouring of this latter species is a general phenomenon, which we have observed for other unsaturated acids in the presence of triethylamine, and for preformed tetramethylammonium salts. The fact that added base promotes the formation of a 1:1 chelate complex at the expense of a 2:1 bis-olefin complex correlates with the enhanced optical yields observed in asymmetric hydrogenation of unsaturated acids in basic media (Table III).

### Rhodium Complexes with Larger-ring Chelates of Chiral Biphosphines

Few complexes of this type have been studied in detail but their behavior suggests that rather different hydrogenation mechanisms are followed. Examples are collected in Table IV. The phosphonite (entry a,b (52)) is of interest in giving much higher optical yields in the hydrogenation of dehydroamino acid esters than with the corresponding acids. Acylaminobiphosphines (entry c,d (53)) give modest optical yields and are of interest because the biotin-derived species may be irreversibly bound to the globular protein avidin. Asymmetric homogeneous hydrogenation may be carried out with the resulting "enzyme co-factor" complex in aqueous solution and although optical yields are modest the experiment illustrates an important concept in catalysis.

Asymmetric ferrocene-derived biphosphines have been utilized in a variety of catalytic asymmetric reactions, but only one application to enamide hydrogenation is reported (54). This is of interest because the acid is reduced in much higher optical yield than its methyl ester, and stereoselectivity is drastically reduced by triethylamine. It implies that hydrogen-bonding between the bound carboxylic acid of the enamide and the

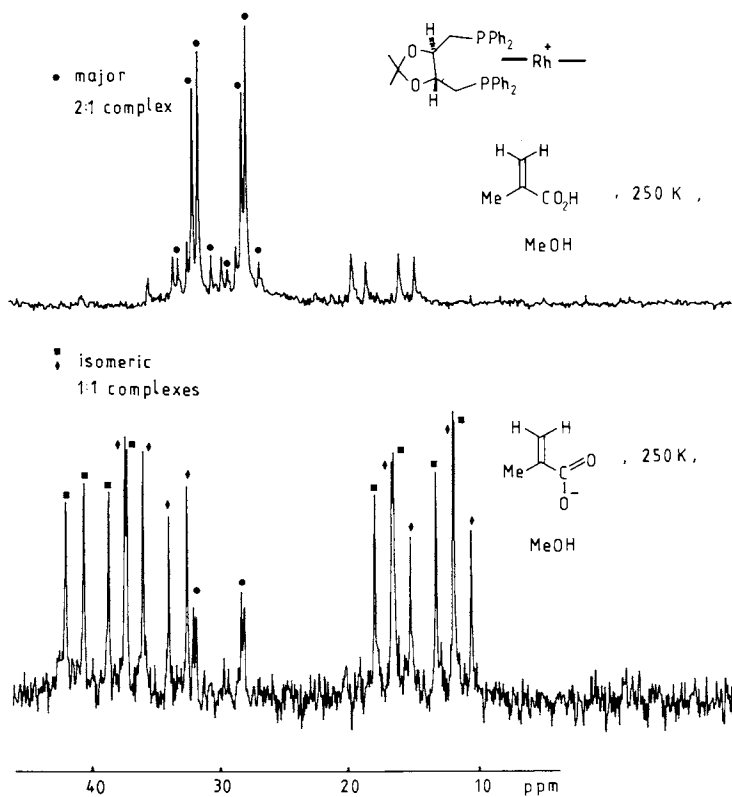
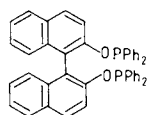


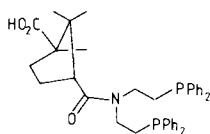
Figure 4. Rhodium biphosphine complexes of unsaturated carboxylic acids and carboxylates; phosphorus-31 NMR spectra, MeOH, conditions as shown.

**TABLE IV.** Hydrogenations catalysed by larger-ring chelate biphosphine complexes

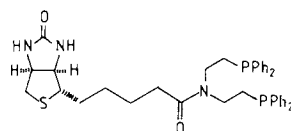
| Entry   | Phosphine         | Substrate | Solvent                       | Temperature | Pressure, atm | Catalyst/Substrate | Optical Yield |
|---------|-------------------|-----------|-------------------------------|-------------|---------------|--------------------|---------------|
| a, (52) | V                 | 4         | C <sub>7</sub> H <sub>8</sub> | 0°          | 95            | 1:50               | 76            |
| b, (52) | V                 | 3         | C <sub>7</sub> H <sub>8</sub> | 25°         | 95            | 1:50               | 9             |
| c, (53) | W                 | 5         | -                             | -           | -             | -                  | 30            |
| d, (53) | X; avidin complex | 5         | H <sub>2</sub> O, pH 7        | 0°          | 1.5           | 1:500              | 42 <u>S</u>   |
| e, (54) | Y                 | 3         | MeOH                          | 25°         | 50            | 1:200              | 93 <u>S</u>   |
| f, (55) | Z                 | 3         |                               | 20°         | 1             | 1:50               | 18 <u>R</u>   |
| g, (55) | AA                | 3         |                               | 20°         | 1             | 1:50               | 13 <u>S</u>   |
| h, (55) | AA                | 3         | , NEt <sub>4</sub>            | 20°         | 1             | 1:50               | 75 <u>S</u>   |
| i, (55) | AA                | 14        | C <sub>6</sub> H <sub>6</sub> | 20°         | 1             | 1:50               | 9 <u>S</u>    |
| j, (55) | AA                | 14        | MeOH, NEt <sub>3</sub>        | 20°         | 1             | 1:50               | 57 <u>S</u>   |



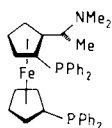
V



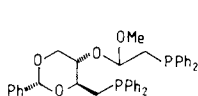
W



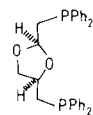
X



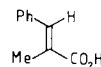
Y



Z



AA



14

tertiary amine is important in determining selectivity.

Monosaccharides have been a prolific source of chiral products and two medium-ring chelating biphosphines are derived from glucose (55). ERYTHROP (entry f) is a poor asymmetric hydrogenation catalyst but DIOXOP is effective, both for enamides and unsaturated acids, in the presence of triethylamine. Our NMR studies (56) show that the course of reaction differs from that with smaller ring chelates, and it is summarized in Scheme 10. The points of particular interest are firstly that a dihydride is produced on hydrogenation of the cyclooctadiene complex, which slowly reverts to a solvent adduct of the type normally observed. Addition of enamide causes slow formation of one diastereomer of a complex whose phosphorus and carbon NMR spectra (the latter on  $^{13}\text{C}$  enriched species) suggest terdentate binding. This step is strongly catalyzed by triethylamine, and an intermediate carboxylate complex may be observed at low temperatures. Hence the role of triethylamine is to catalyze the breakdown of an initially formed dihydride and ensure that enamide binding occurs stereoselectively. The course of reaction is most readily rationalized if ether-oxygen binding occurs at an intermediate stage, and there is precedent for this in simple model systems (57).

The mechanistic divergence in this group of phosphines makes them attractive candidates for further study, particularly in cases where secondary binding sites are available.

#### Rationalization and Summary

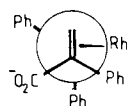
It is now possible to state the minimum requirements for effective asymmetric hydrogenation, using existing rhodium biphosphine complexes. These are as follows:

- i) The substrate must bind tightly and with high asymmetric recognition. This is not easily effected for Z enamides, where the olefin and amide carboxyl groups are bound to rhodium.
- ii) Hydrogen addition should follow rather than precede the substrate binding step.
- iii) The structure of the biphosphine must be sufficiently bulky to effect stereoselection but if it carries substituents which have too high a steric demand then catalysis is inhibited.

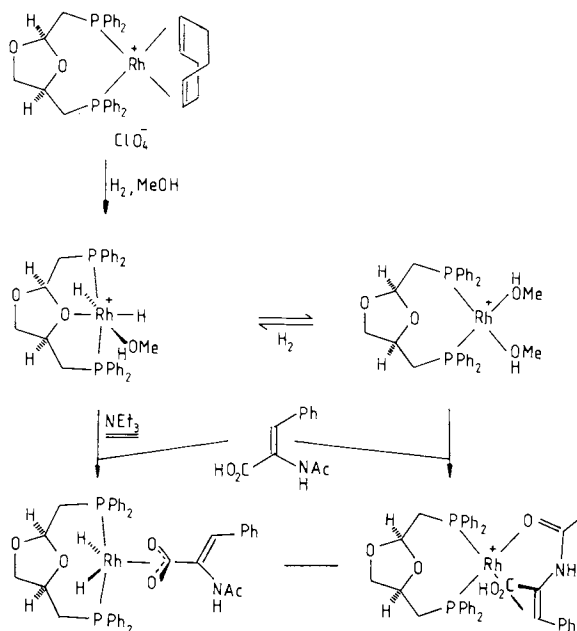
The mechanism followed is as shown in Scheme 4. It is not yet known where the rate-determining transition-state occurs, and either the hydrogen-addition step or intracomplex hydride transfer is a possibility. Experiments in progress should resolve that point.

Asymmetric catalysis by low-valent transition-metal complexes has enormous potential for organic chemistry, but many of its present limitations must be overcome before this can be realized. With existing ligands, hydrogenation of enamides and certain unsaturated carboxylic acids is optically efficient, as is the hydrogenation of  $\alpha$ -amino ketones (58),

*Scheme 9. Preferred orientation in unsaturated carboxylic acid binding to rhodium*



*Scheme 10. Enamide hydrogenation by the asymmetric ligand DIOXOP*



$\alpha$ -keto lactones (59), vinyl esters (18) and the hydrosilylation of  $\alpha$ - or  $\gamma$ -ketoesters (60) with particular catalysts. There are, however, no good examples of asymmetric hydrogenation of less polar organic compounds nor of optically efficient asymmetric catalysis involving carbon-carbon bond formation (61). Extensions to these areas will require the synthesis of new types of phosphine, but it is mechanistic studies of the type described herein which will permit their rational design.

#### Literature Cited

1. Osborn, J.A., Jardine, F.H., Young J.F., and Wilkinson, G., J. Chem. Soc. (A), (1966) 1711.
2. Horner, L., Buthe H. and Siegel, H., Tetrahedron Lett., (1968) 4023; Horner, L., Sieger, H., and Buthe, H., Angew. Chem. Int. Ed. Engl., (1968) 7, 942.
3. Dang, T.P. and Kagan, H.B., J. Chem. Soc., Chem. Commun., (1971) 481.
4. Kagan, H.B. and Dang, T.P., J. Am. Chem. Soc., (1972) 94, 6429.
5. Morrison, J.D., Masler, W.F. and Neuberg, M.K., Adv. Catalysis, (1976) 25, 81.
6. Pearce, R., Chemical Society Specialist Periodical Reports, Catalysis Volume 11, (1979).
7. Valentine, D. Jr. and Scott, J.W., Synthesis, (1978) 329.
8. Boucher, H. and Bosnich, B., J. Am. Chem. Soc., (1977) 99, 6253.
9. Corradini, P., Paiano, G. and Pununzi, A., J. Am. Chem. Soc., (1966) 88, 2863; Pununzi, A. and Paiano, G., J. Am. Chem. Soc., (1966) 88, 4843.
10. Terai, J. and Saito, K. Bull. Chem. Soc. Jap., (1975), 48, 1233, (1978) 51, 503; Terai, Y., Kido, H., Kashiwabara, K. and Saito, K., Bull. Chem. Soc. Jap., (1978) 51, 3254.
11. Lazzaroni, R., Salvadori, P., Bertucci, C. and Veracini, C.A., J. Organomet. Chem., (1975) 99, 475.
12. Rousseau, C., Evard, M and Petit, F., J. Mol. Cat., (1977/8) 3, 309; de Croon, M.H.J.M., van Nisselrooij, P.F.M.T., Kiupers, H.J.A.M. and Coenen, J.W.E., J. Mol. Cat., (1978) 4, 325.
13. Tolman, C.A., Meakin, P.Z., Lindner, D.L. and Jesson, J.P. J. Amer. Chem. Soc., (1974) 96, 2762; Halpern, J., Okamoto, T. and Zakhariev, A., J. Mol. Cat., (1977) 2, 65.
14. Halpern, J. Riley, D.P. Chan, A.S.C. and Pluth, J.J. J. Amer. Chem. Soc., (1977) 99, 8055; Slack, D.A. and Baird, M.C., J. Organomet. Chem., (1977) 142, C69; Brown, J.M. and Chaloner, P.A., J. Chem. Soc., Chem. Commun., (1978) 321; Brown, J.M., Chaloner, P.A. and Nicholson, P.N., J. Chem. Soc., Chem. Commun., (1978) 646.
15. Brown, J.M. and Chaloner, P.A., Tetrahedron Lett., (1978) 1877 and papers in press.

16. Brown, J.M. and Chaloner, P.A. unpublished work.
17. Ball, R.G. and Payne, N.C. Inorg. Chem., (1977) 16, 1187.
18. Vineyard, B.D., Knowles, W.S., Sabacky, M.J., Bachman, G.L. and Weinkauff, D.J., J. Am. Chem. Soc., (1977) 99, 5946.
19. Fryzuk, M.D. and Bosnich, B., J. Am. Chem. Soc., (1978) 100, 5491.
20. Fryzuk, M.D. and Bosnich, B., J. Am. Chem. Soc., (1977) 99, 6262.
21. Brown, J.M. and Murrer, B.A., unpublished work.
22. Payne, N.C., cited as footnote 7 in ref. 19; Ball, R.G. and Payne, N.C., Inorg. Chem., (1977) 16, 1187; Knowles, W.S. private communication.
23. Halpern, J., Trans. Amer. Cryst. Assoc. (1978) 14, 59.
24. Murrer, B.A., unpublished work.
25. Kagan, H.B. private communication.
26. Yamamoto, K. Tomita, A., and Tsuji, J., Chem. Lett., (1978) 3.
27. Gelbard, G., Kagan H.B., and Stern, R., Tetrahedron, (1976) 32, 233; Glaser, R., Geresh, S. and Blumenfeld, J., J. Organomet. Chem., (1976) 112, 355.
28. Glaser, R. Twaik, M. Geresh, S. and Blumenfeld, J., Tetrahedron Lett., (1977) 4635, 4639 and private communication.
29. Dang, T.P. Poulin J.C., and Kagan, H.B., J. Organomet. Chem., (1975) 91, 105.
30. Achiwa, K., J. Am. Chem. Soc., (1976) 98, 8265.
31. Tanaka, M. and Ogata, I. J. Chem. Soc., Chem. Commun. (1975) 735.
32. Hayashi, T. Tanaka, M. and Ogata, I., Tetrahedron Lett., (1977) 295.
33. Cullen, W.R. and Sugi, Y., Tetrahedron Lett., (1978) 1635.
34. Jackson, R. and Thompson, J. Organomet. Chem. (1978) 159, C29.
35. Hanaki, K. Kashiwabara, K. and Fujita, J., Chem. Lett., (1978) 489.
36. Pracejus, G. and Pracejus, H. Tetrahedron Lett. (1977) 3497.
37. Fiorini, M. Marcati, F. and Giongo, G.M., J. Mol. Cat., (1978) 4, 125; Fiorini, M. and Giongo, G.M., ibid (1979) 5, 303.
38. Brown, J.M., Chaloner, P.A., Glaser, R. and Geresh, S., Tetrahedron, in press, 1979.
39. Dang, T.P., Poulin, J.C. and Kagan, H.B., J. Organomet. Chem., (1975) 91, 105.
40. Granlich, V., and Consiglio, G.; Helv. Chim Acta., (1979) 62, 1016.
41. Paiazo G. and Pandolfo, L., Gaz. Chim. Ital., (1977) 107 467; Aguiar, A.M., Morrow, C.J., Morrison, J.D., Burnett, R.E., Masler, W.F. and Bhacca, N.S., J. Org. Chem., (1976) 41, 1545; Fisher, C. and Mosher, H.S., Tetrahedron Lett., (1977) 2487.

42. Kawabata, Y., Tanaka, M. and Ogata, I., Chem. Lett., (1976) 1213.
43. James B.R., and Mahajan, D., Israel J. Chem., (1977) 15, 214.
44. Achiwa, K. Chem. Lett., (1978) 561; Ojima, I., Kogure, T. and Achiwa, K. Chem. Lett., (1978) 567.
45. Achiwa, K., Ohga, Y. and Iitaka, Y. Tetrahedron Lett., (1978) 4683.
46. Achiwa, K., Tetrahedron Lett., (1977) 3735.
47. Stoll, A.P. and Sless, R., Helv. Chim. Acta, (1974) 57, 2487.
48. Jesse, A.C., Meester, M.A.M., Stufkens, D.J. and Vrieze, K., Inorg. Chim. Acta, (1978) 26, 129.
49. Chaloner, P.A., and Murrer, B.A., unpublished work.
50. Parker, D., unpublished work.
51. Ojima, I., and Kogure, T., Chem. Lett., (1978) 1145.
52. Grubbs, R.H., de Vries, R.A., Tetrahedron Lett., (1977) 1879.
53. Wilson, M.E., Nuzzo, R.G., and Whitesides, G.M., J. Am. Chem. Soc., (1978) 100, 2269; Wilson, M.E., and Whitesides, G.M., J. Am. Chem. Soc., (1978) 100, 306.
54. Hayashi, T., Yamamoto, K. and Kumada, M. Tetrahedron Lett., (1976) 1133.
55. Descotes, G., Lafont, D. and Sinou, D., J. Organomet. Chem., (1978) 150, C14; idem, ibid (1979) 169, 87.
56. Brown, J.M., Chaloner, P.A., Descotes, G., Glaser, R., Lafont, D. and Sinou, D., J. Chem. Soc., Chem. Commun., in press.
57. Alcock, N.W., Brown, J.M. and Jeffrey, J.C., J. Chem. Soc. Dalton, (1977) 888.
58. Hayashi, T., Katsumara, A., Konishi, M. and Kumada, M., Tetrahedron Lett., (1979) 425.
59. Achiwa, K. Kogure, T. and Ojima, I., Chem. Lett., (1978) 297; idem, Tetrahedron Lett., (1977) 4431; Ojima, I., Kogure, T., Terasaki, T. and Achiwa, K., J. Org. Chem., (1978) 43, 3444.
60. Ojima, I., Kogure, T. and Kumagai, M., J. Org. Chem. (1977) 42, 1671.
61. Trost, B.M. and Strege, P.E., J. Am. Chem. Soc., (1977) 99, 1649; Felkin H. and Swierczowski, G., Tetrahedron Lett., 31, 2735 (1975) and examples therein.

RECEIVED September 17, 1979.



## Circular Dichroism as a Probe of Metal Ion Interaction with Azoproteins

J. IVAN LEGG, KOZO IGI, GARY J. PIELAK, BRIAN D. WARNER,  
and MICKEY S. URDEA<sup>1</sup>

Department of Chemistry, Washington State University, Pullman, WA 99164

Circular dichroism (CD) has played an important role in our studies on the modification of enzymes and hormones with Co(III). The objective of these studies has been to incorporate selectively substitution inert metal ions at specifically modified sites in proteins as probes of biological function. Significant information concerning the catalytic mechanism of carboxypeptidase A (CPA) (1) has been obtained from a site specific modification of tyrosine 248 with Co(III) (2). The method developed for CPA has been extended to other enzymes and hormones in order to develop an improved method for incorporating stable radioisotopes (<sup>57</sup>Co) into proteins. The substitution-inertness of Co(III) provides the necessary stability in these derivatives (3).

The method involves conversion of tyrosines and histidines on the protein of interest into chelating agents by reaction with a diazonium salt followed by incorporation of cobalt as shown in Figure 1. It has been found that specific incorporation occurs if a ternary complex is formed with ethylenediamine-*N,N'*-diacetate (EDDA), Figure 1. Although there are a number of ways to achieve the desired modification, oxidation of Co(II)-EDDA with H<sub>2</sub>O<sub>2</sub> in the presence of the diazotized protein has given the best results and is most widely applicable. In order to prevent damage to the protein, a free radical scavenger such as phenol must be present during oxidation.

### Azophenol Chelation of Metal Ions as Determined by Ligand Associated Spectral Changes

The azoprotein derivatives are highly chromophoric with spectral properties which are closely mimicked by simple azo compounds such as those shown in Figure 2. These azo derivatives can function as bidentate chelating agents. For example, Eriochrome Black T, an azophenol, is well known as a cheleometric

<sup>1</sup>Current address: Department of Biochemistry and Biophysics, University of California, San Francisco, CA 94143.

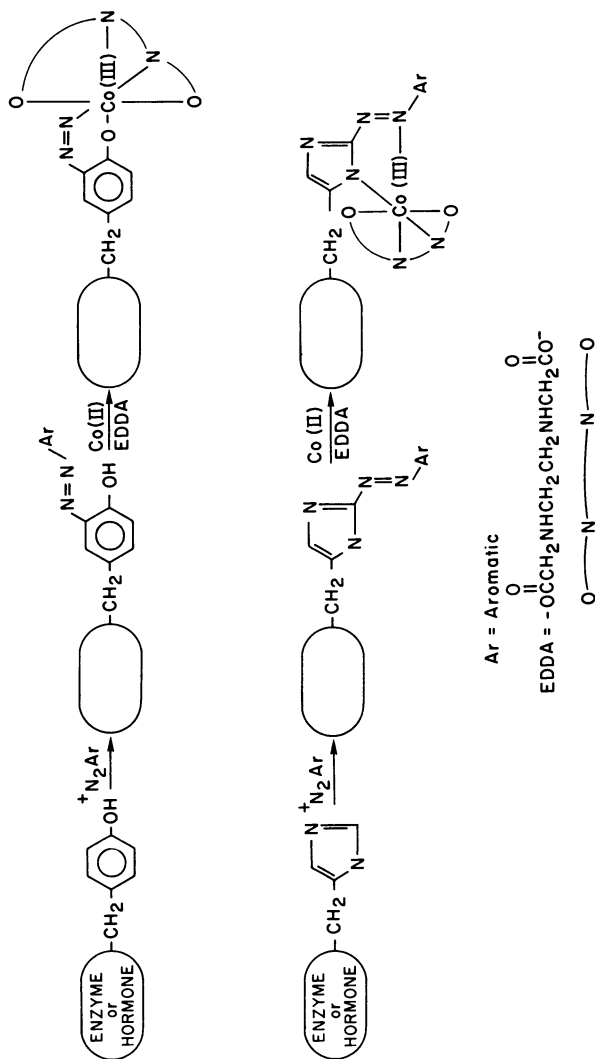


Figure 1. General method for the incorporation of Co(III) into enzymes and hormones

indicator for the titration of  $Mg^{2+}$  with EDTA. The color and associated spectral changes observed upon metal chelation by the azo dyes have played an important role in the characterization of the protein derivatives. Models such as those shown in Figure 2 have been very useful in characterizing the associated spectral properties as well as establishing conditions which lead to Co(III) incorporation into the azoproteins (4,5,6).

Johansen and Vallee were the first to recognize the potential for using an azo chromophore in a protein to monitor the environment of the modified residue with respect to a metal ion (7,8). In their classic study they were able to modify specifically tyrosine 248 in the zinc metalloenzyme, carboxypeptidase A, to give the azotyrosine derivative, arsanilazotyrosine 248 carboxypeptidase A (AA-CPA-Zn), shown in Figure 3A. The native Zn is shown explicitly in order to differentiate it from externally incorporated Co as will be discussed. They found that at intermediate pH's, where the enzyme exhibits maximal activity, the azotyrosine is chelated to the intrinsically bound active site zinc. A distinct red color is associated with zinc chelation in contrast to the yellow and orange colors of the enzyme due to the presence of the free azophenol (low pH) and azophenolate (high pH), respectively (7).

Characteristic absorption spectral changes for AA-CPA-Zn are observed as a function of increasing pH, Figure 4. These changes correspond to the progression from azophenol through chelated azophenolate to free azophenolate (8). Analogous spectral properties have been observed by us and Vallee for Zn azophenol models (4,7).

A much clearer distinction between the various electronic transitions is seen in the CD spectrum, Figure 4, as a result of the differences in sign. A very distinct negative 510 nm band develops upon chelation of the azotyrosine-248 to the active site zinc. This negative band is completely absent when the pH titration is carried out with the apoenzyme (active site Zn removed). These absorption and CD spectral observations confirm those originally made by Johansen and Vallee (7,8).

#### Preparation of Model Azoligand Co(III) Complexes for the Characterization of Co(III) Azoprotein Derivatives

AA-CPA-Zn served as the test system for incorporation of Co(III) into azoproteins as outlined in Figure 3. It was therefore important to distinguish between Co(III) and Zn(II) bound to azophenols. For this purpose model Co(III) complexes of the azophenolate ligands shown in Figure 2 have been prepared and characterized.

The N-acetyl derivatives of tyrosine and histidine were purchased from Vega-Fox and diazotized by the method of Tabachnick and Sobotka (9). These reaction mixtures contained both mono- and bisdiazotized compounds which were separated by preparative TLC

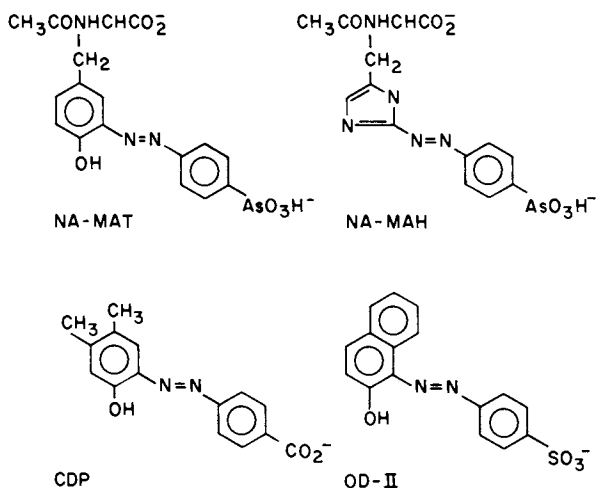


Figure 2. Model azo ligands investigated: NA-MAT (N-acetyl monoarsanilazo-tyrosine); NA-MAH (N-acetyl monoarsanilazohistidine); CDP (2-(4-carboxyphenylazo)-4,5-dimethyl phenol); OD-II (orange dye II, p-(2-hydroxy-1-naphthylazo)-benzene sulfonic acid).

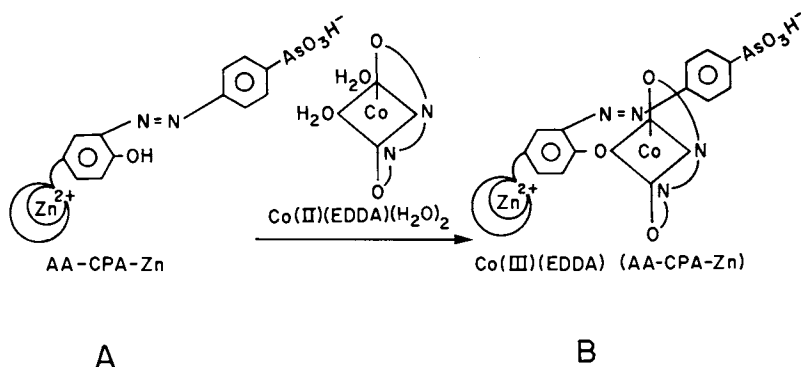


Figure 3. Incorporation of  $\text{Co(III)}$  into arsanilazotyrosine 248 carboxypeptidase A (AA-CPA-Zn).

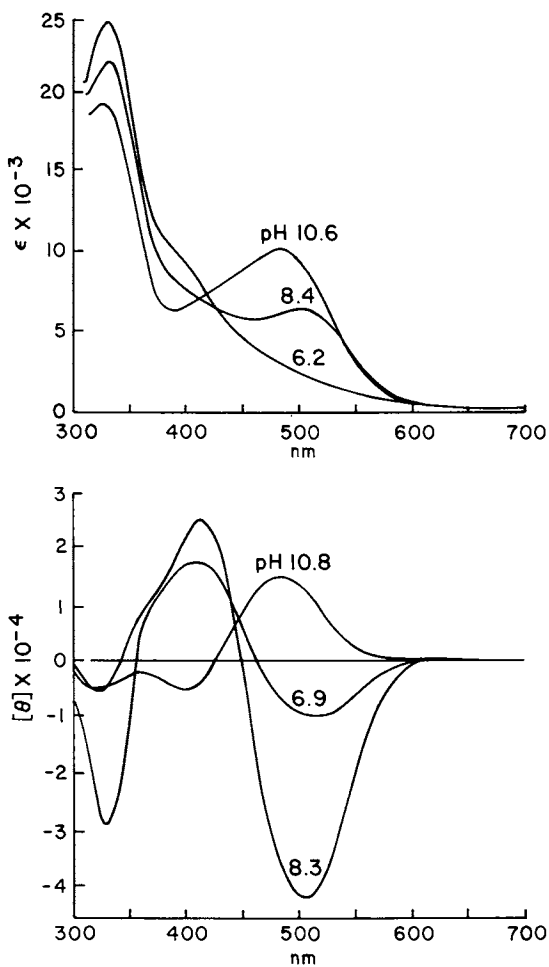


Figure 4. Absorption (upper panel) and circular dichroic (lower panel) spectra of AA-CPA-Zn as a function of pH. Intermediate pH spectra are those associated with complexation of active site zinc by arsanilazotyrosine 248 (see text).

(12). CDP and OD-II were obtained from Alfred Bader Chemical Company and Eastman Chemicals, respectively. The synthesis of Co(III)(EDDA)(azodye) complexes was carried out by the air oxidation of an aqueous solution of 20 mM azodye and 20 mM Co(II)(EDDA)(H<sub>2</sub>O)<sub>2</sub> at pH 9.5. The CDP complex was isolated as previously described (5). The OD-II complex was purified by Sephadex LH-20 chromatography (2). The material was evaporated and dried in a drying pistol. Preparative TLC of Co(III)(EDDA)-(NA-MAT) proved successful (12). The complex was then rechromatographed on LH-20 equilibrated with 80:20, methanol:water, evaporated, and dried. Chemical analyses (C,H,N) of the azoamino acid derivatives and the various Co(III) complexes were in good agreement with the calculated values.

The spectral properties of the complexes are summarized in Figure 5. Unfortunately, absorption spectra analogous to those obtained for the Zn-azophenol enzyme (Figure 4, pH 8.4 spectrum) and models (4,7) were observed for the Co(III) complexes.

#### Circular Dichroic Properties of Model Azophenol and Azonaphthol Complexes

In order to find a more reliable indicator of Co(III)-azophenolate coordination in proteins, the circular dichroic properties of the models were examined. Initially an essentially empirical approach was taken. In the visible absorption spectra of the Co(III)-azophenolate complexes, the ligand associated transitions dominate the spectrum since the molar absorptivities of 4000 - 10,000 are at least an order of magnitude more intense than the configurationally forbidden d-d transitions, Figure 5. For CD transitions the selection rules are not as clearly defined. However, more complex CD spectra were anticipated for the Co(III) azophenols than for the Zn(II) azophenols due to the overlap of d-d and ligand transitions. Since Zn(II) has no d-d transitions a relatively simple CD spectrum is expected in the visible region as is observed for the zinc complex in AA-CPA-Zn, Figure 4 (pH 8.3 spectrum).

In the azoproteins an extrinsic source of optical activity exists in the asymmetric protein environment surrounding the azo derivitized amino acid. Little contribution to the optical activity would be expected from the asymmetric carbon of the diazotized amino acid alone which is considerably removed from the chromophore. This observation is borne out by examining mono-azotyrosine and monoazohistidine where very weak CD spectra were observed.

Complexation of the optically active model ligands to form Co(III)(EDDA)(azo dye) complexes would not necessarily be expected to generate a CD spectrum unless some diastereomeric preference was obtained. Indeed, a CD spectrum is observed for the azo-tyrosine (NA-MAT) complex, Figure 6. The spectrum is substantially more intense than that obtained for the free ligand, but

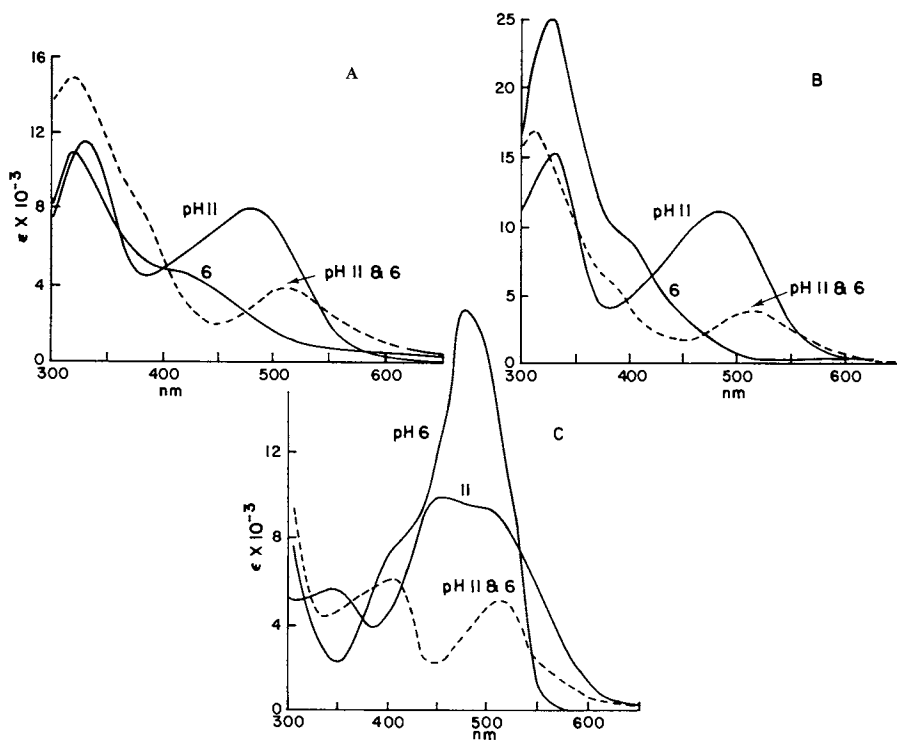


Figure 5. Absorption spectra of azophenol and azonaphthol ligands (—) and corresponding Co(III)-EDDA complexes (---): (A) MAT; (B) CDP; (C) OD-II.

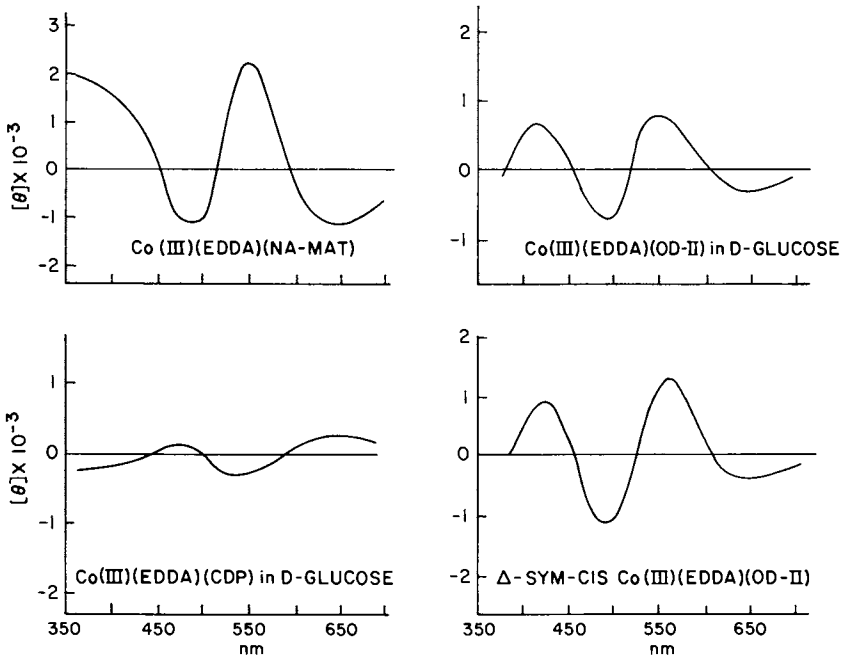


Figure 6. Circular dichroic spectra of azophenol and azonaphthol  $\text{Co(III)}$ -EDDA complexes under various conditions



its specific source (vicinal, configurational) can not be designated without isomer isolation and characterization. Thus far attempts to separate isomers have been unsuccessful. Circular dichroic spectra can also be generated by either dissolving the models in an optically active solvent system or by using resolved Co(III)(EDDA)(H<sub>2</sub>O)<sub>2</sub><sup>+</sup> as starting material. Dissolving the OD-II and CDP complexes in a saturated aqueous D-glucose solution produces the CD spectra shown in Figure 6 (Neither azo ligand contains an intrinsic source of optical activity, Figure 2). Reaction of  $\Lambda$ -s-cis-Co(EDDA)(H<sub>2</sub>O)<sub>2</sub><sup>+</sup> with OD-II results in an optically active dye complex with the CD spectrum shown in Figure 6. If the  $\Delta$  isomer is used, a CD spectrum which is of equal intensity but opposite in sign is produced.

In all cases a characteristic CD spectrum is observed independent of the method employed to obtain the spectrum. Four bands are observed in the visible region whose maxima are very similar among the complexes. The alternating sign pattern of the transitions are also held in common but the absolute signs and intensities differ. It is particularly interesting that despite the fact that the visible spectrum of the azonaphtholate, OD-II, differs significantly from that of the azophenols (Figure 5), the CD generated upon chelation of the dye to Co(III) is nearly identical to the CD spectra obtained for the coordinated azophenolates.

#### Circular Dichroism as a Monitor of Co(III) Chelation by an Azotyrosine in a Protein

Incorporation of Co(III) into AA-CPA-Zn, as outlined in Figure 3B, led to the formation of the desired ternary complex, Co(III)(EDDA)(AA-CPA-Zn), whose absorption spectrum is shown in Figure 7. The characteristic 510 nm absorption band is observed for the red Co(III) complex which is analogous to that observed for the active site Zn complex, Figure 4 (pH 8.4 spectrum). The only indication that a Co(III)-azotyrosine complex has been formed is that the absorption spectrum is invariant with pH as must be the case for a substitution-inert complex. However, the CD spectrum clearly indicates the formation of the Co(III)-azotyrosine complex, Figure 7. The spectrum is very similar to that obtained for the Co(III) model complexes, Figure 6, and is distinctly different from that observed for the active site Zn complex of AA-CPA-Zn, Figure 4 (pH 8.3 spectrum). It is less intense by an order of magnitude and, as expected, more complex than the Zn associated spectrum. Importantly, the distinct negative 510 nm band characteristic of the Zn-azophenol complex (Figure 4) is completely missing.

The band at 630 nm which is also found in the CD spectra of all the Co(III) models (Figure 6) is absent in the absorption spectrum. This very possibly could be a d-d transition which is too weak to be observed in the absorption spectrum. This

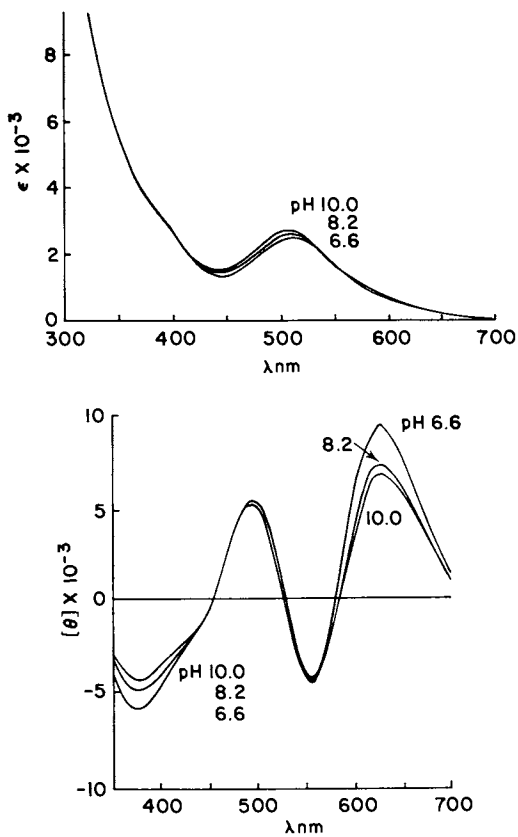


Figure 7. Absorption (upper panel) and circular dichroic (lower panel) spectra of  $\text{Co(III)(EDDA)(AA-CPA-Zn)}$

observation is also consistent with the similarity of the Co(III) azophenolate and azonaphtholate CD spectra since these ligand associated visible spectra differ significantly. Importantly, as with the absorption spectra, the CD spectrum of Co(III)(EDDA)(AA-CPA-Zn) shows little variation with pH due to the substitution-inert nature of the complex.

The Zn can be selectively removed from the azoenzyme derivative without any appreciable change in the absorption and CD spectra confirming coordination of the azophenol to Co(III) (2). The Co(III) modification of AA-CPA-Zn leads to an enzyme derivative which loses all peptidase activity but still maintains esterase activity (1). The modification can be reversed completely by reducing the Co(III) with Fe(II)-EDTA regenerating the original spectral and enzymatic properties observed for AA-CPA-Zn. The return of the original properties confirms the site specific nature of the modification and the lack of damage to the protein (2).

#### Extension to Other Proteins and the Involvement of Azohistidines

We have now extended these studies to other proteins (bovine serum albumin, chymotrypsin, subtilisin, concanavalin A) and hormones (leuteinizing hormone-releasing hormone, glucagon, insulin). These investigations involve the characterization of azohistidine models since diazotization of proteins can also lead to the formation of azohistidines, Figure 1. In the course of these investigations we have found that previously reported azo-amino acid model studies upon which characterization of the azoprotein derivatives is based (10,11) are incorrect due to the lack of purity of the compounds studied (9). A sensitive TLC system we have developed has been used to purify the azotyrosine and azohistidine models (12). The Co(III) complexes of these azohistidine ligands are expected to exhibit CD spectra which will be useful in the characterization of Co(III) incorporated in the various azoenzymes and azohormones.

In addition to offering a unique method for enzyme modification, we expect these studies to result in an improved method for the incorporation of stable radioisotopes into proteins and hormones (<sup>57</sup>Co, <sup>58</sup>Co, <sup>60</sup>Co). Further studies of the CD spectra of the models and azoproteins are expected to lead to a method for the determination of the extent and specificity of Co(III) modification of azoproteins and azohormones.

#### Acknowledgment

Support from the National Institutes of Health (GM-23081) is gratefully acknowledged.

Literature Cited

1. Urdea, M. S.; Legg, J. I. J. Biol. Chem., (1979), submitted for publication.
2. Urdea, M. S.; Legg, J. I. Biochemistry, (1979), submitted for publication.
3. Legg, J. I. Coord. Chem. Rev., (1978), 25, 103.
4. White, W. I.; Legg, J. I. J. Am. Chem. Soc., (1975), 97, 3937.
5. White, W. I.; Legg, J. I. Bioinorg. Chem., (1976), 6, 163.
6. White, W. I.; Legg, J. I. J. Chrom., (1976), 124, 134.
7. Johansen, J. T.; Vallee, B. L. Proc. Nat. Acad. Sci. USA, (1971), 68, 2532.
8. Johansen, J. T.; Vallee, B. L. Proc. Nat. Acad. Sci. USA, (1973), 70, 2006.
9. Tabachnick, M.; Sobotka, H. J. Biol. Chem., (1959), 234, 1726.
10. Tabachnick, M.; Sobotka, H. J. Biol. Chem., (1960), 235, 1051.
11. Riordan, J. R.; Vallee, B. L., Methods in Enz., (1972), XXV(B), 521.
12. Warner, B. D.; Legg, J. I. Inorg. Chem., (1979), in press.

RECEIVED September 24, 1979.

# Preparation and Circular Dichroism Spectra of Cobalt(III) Complexes Containing Chiral Aminophosphine Chelate Ligands

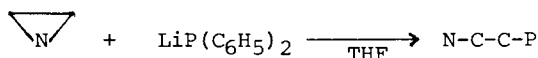
ISAMU KINOSHITA, KAZUO KASHIWABARA, and JUNNOSUKE FUJITA

Department of Chemistry, Faculty of Science, Nagoya University, Nagoya 464 Japan

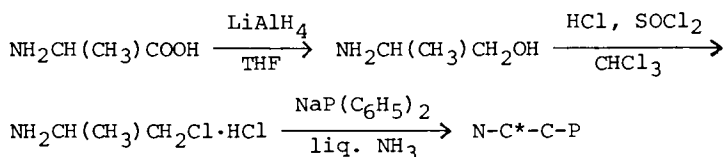
Since Wymore and Bailar (1) first prepared *trans*-[CoX<sub>2</sub>{1,2-bis(diethylphosphino)ethane}<sub>2</sub>]X (X = Cl<sup>-</sup>, Br<sup>-</sup>, and I<sup>-</sup>) in 1960, many cobalt(III)-phosphine complexes have been reported (2). However, no optically active cobalt(III)-phosphine complex has ever been prepared. This paper deals with the preparation, characterization and circular dichroism (CD) spectra of octahedral cobalt(III) complexes containing aminophosphines of the type, NH<sub>2</sub>CH(R)CH<sub>2</sub>PR'R". The aminophosphine is an intermediate ligand between a diamine and a diphosphine. The optical activity of such aminophosphine complexes can be compared with that of diamine complexes studied extensively.

## Preparation of Ligands

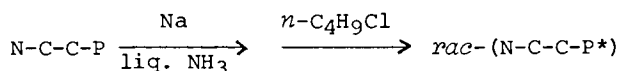
a) NH<sub>2</sub>CH<sub>2</sub>CH<sub>2</sub>P(C<sub>6</sub>H<sub>5</sub>)<sub>2</sub> (N-C-C-P). This ligand was prepared by a modified method of Issleib *et al.* (3).



b) (*S*)-NH<sub>2</sub>CH(CH<sub>3</sub>)CH<sub>2</sub>P(C<sub>6</sub>H<sub>5</sub>)<sub>2</sub> (N-C\*-C-P). This ligand was prepared from (*S*)-alanine by the following method;



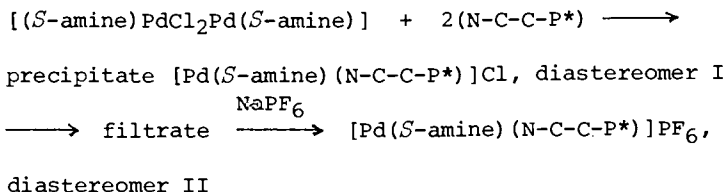
c) (*S*)- or (*R*)-NH<sub>2</sub>CH<sub>2</sub>CH<sub>2</sub>P(*n*-C<sub>4</sub>H<sub>9</sub>)(C<sub>6</sub>H<sub>5</sub>) (N-C-C-P\*). This ligand was prepared from N-C-C-P by the following method;



The resolution was achieved with (+)<sub>D</sub>-di- $\mu$ -chlorobis[(*S*)-*N,N*-dimethyl- $\alpha$ -phenylethylamine-2*C,N*]dipalladium(II) (4,5) ((*S*-amine)PdCl<sub>2</sub>Pd(*S*-amine)) by the following method;

0-8412-0538-8/80/47-119-207\$05.00/0

© 1980 American Chemical Society

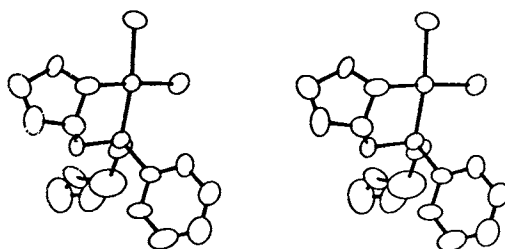


Diastereomer I and II liberated free ligands of (*R*)- and (*S*)-configurations, respectively, on treating with sodium cyanide in water. The notation of absolute configuration of the ligand is reversed upon coordination by the sequence rule (6).

The absolute configuration of N-C-C-P\* was assigned by comparing the CD spectrum of its palladium(II) complex,  $[\text{PdCl}_2(\text{N-C-C-P}^*)]$  with that of  $[\text{PdCl}_2\{\text{CH}_2\text{CH}_2\text{CH}_2\text{NHCHCH}_2\text{P}(n\text{-C}_4\text{H}_9)(\text{C}_6\text{H}_5)\}]$  of known absolute configuration (7). (Figure 1) The  $[\text{PdCl}_2(\text{N-C-C-P}^*)]$  complex, the ligand of which was obtained from the less soluble diastereomer I of  $[\text{Pd}(S\text{-amine})(\text{N-C-C-P}^*)]\text{Cl}$  showed a CD spectrum very similar to the difference CD curve,  $[\Delta\epsilon(\text{I}) - \Delta\epsilon(\text{II})]/2$  derived from the two CD spectra of a diastereomeric pair, I and II of  $[\text{PdCl}_2\{\text{CH}_2\text{CH}_2\text{CH}_2\text{NHCHCH}_2\text{P}(n\text{-C}_4\text{H}_9)(\text{C}_6\text{H}_5)\}]$  (Figure 2). The  $\text{CH}_2\text{CH}_2\text{CH}_2\text{NHCHCH}_2\text{P}(n\text{-C}_4\text{H}_9)(\text{C}_6\text{H}_5)$  ligand was prepared from (*S*)-proline and the complex involves (*S*)-carbon, (*S*)-nitrogen, and (*R*)- or (*S*)-phosphorus atoms. Since the absolute configuration of the phosphorus atom in diastereomer II has been determined to be (*R*) by the X-ray method (7), the difference CD curve would correspond to the vicinal effect curve due to the (*S*)-phosphorus atom in the ligand. Both curves in Figure 2 are very similar, and the absolute configuration of the phosphorus atom in the N-C-C-P\* complex given can be assigned to (*S*)-configuration.

#### Preparation of Complexes

- a) *trans*- $[\text{CoCl}_2(\text{aminophosphine})_2](\text{ClO}_4)$  (aminophosphine = N-C-C-P, N-C\*-C-P, and N-C-C-P\*). To a methanol solution of  $\text{Co}(\text{ClO}_4)_2 \cdot 6\text{H}_2\text{O}$  was added two equivalent moles of an aminophosphine with stirring in an atmosphere of nitrogen. A brown solid  $(\text{Co}(\text{aminophosphine})_2(\text{ClO}_4)_2)$  was obtained by evaporating the methanol under reduced pressure. It was dissolved in  $\text{CH}_2\text{Cl}_2$  and chlorine was bubbled through the solution to oxidize the cobalt-(II) ions. After evaporation to dryness, the crude complex was recrystallized from methanol and water to give green crystals. The complexes are stable in air, insoluble in water, but soluble in most polar organic solvents. Analytical data of all the complexes are in good accord with the calculated values as anhydrous perchlorate salts.
- b)  $[\text{Co}(\text{acac})_2\text{L}](\text{PF}_6 \text{ or } \text{B}(\text{C}_6\text{H}_5)_4)$  (acac = acetylacetonate ion; L = N-C-C-P, N-C\*-C-P, N-C-C-P\*, and  $(\text{C}_6\text{H}_5)_2\text{PCH}_2\text{CH}_2\text{P}(\text{C}_6\text{H}_5)_2$  (P-C-C-P)). A methanol solution containing  $[\text{Co}(\text{acac})_3]$  and the



Bulletin of the Chemical Society of Japan

Figure 1. Stereoscopic view of  $[\text{PdCl}_2\{\overline{\text{CH}_2\text{CH}_2\text{CH}_2\text{NHCHCH}_2\text{P}}(\text{R})(\text{n-C}_4\text{H}_9)(\text{C}_6\text{H}_5)\}]$  (7)

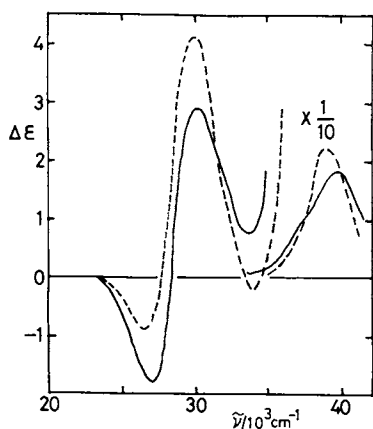


Figure 2. CD spectrum of  $[\text{PdCl}_2\{\text{NH}_2\text{-CH}_2\text{CH}_2\text{P}^*(\text{n-C}_4\text{H}_9)(\text{C}_6\text{H}_5)\}]$  (—) and the calculated CD curve ( $[\Delta\epsilon(\text{I})-\Delta\epsilon(\text{II})]/2$ ) (---) obtained from the CD spectra of a pair of diastereomers, I(S) and II(R) of  $[\text{PdCl}_2\{\overline{\text{CH}_2\text{CH}_2\text{CH}_2\text{NHCHCH}_2\text{P}}(\text{n-C}_4\text{H}_9)(\text{C}_6\text{H}_5)\}]$ .

ligand L (1:1) was stirred with active charcoal overnight at room temperature. The resulting dark red solution was filtered, diluted with water, and chromatographed by use of a column of SP-Sephadex C-25 and an eluent, 0.02M Na<sub>2</sub>SO<sub>4</sub>. The red eluate was saturated with sodium chloride and shaken with chloroform in a separatory funnel, extracting the complex into the chloroform layer. The chloroform was evaporated and the residue was dissolved in water. The complex [Co(acac)<sub>2</sub>L](PF<sub>6</sub> or B(C<sub>6</sub>H<sub>5</sub>)<sub>4</sub>) was precipitated by the addition of NaPF<sub>6</sub> or NaB(C<sub>6</sub>H<sub>5</sub>)<sub>4</sub>.

Resolution (or separation) of optical isomers was achieved by SP-Sephadex column chromatography using 0.02M Na<sub>2</sub>[Sb<sub>2</sub>(L-tart)<sub>2</sub>]. For the N-C-C-P and the P-C-C-P complexes, the bands of optical isomers were separated incompletely, so that the chromatography was repeated until no further increase in Δε/ε values was observed. From the eluates, the optical isomers were isolated by a method similar to that for the racemates.

#### Structure of [CoCl<sub>2</sub>(aminophosphine)<sub>2</sub>](ClO<sub>4</sub>)

Figure 3 shows absorption spectra of the green [CoCl<sub>2</sub>(aminophosphine)<sub>2</sub>](ClO<sub>4</sub>) complexes in methanol. Each of the complexes exhibits a medium intensity band around 16,000 cm<sup>-1</sup>. These bands may correspond to the split component, 1a (1A<sub>1g</sub> → 1E<sub>g</sub>) of the first absorption band of a *trans*-[CoCl<sub>2</sub>(diamine)<sub>2</sub>]<sup>+</sup> complex (8). In Figure 3 is given the spectrum of *trans*-[CoCl<sub>2</sub>(pn)<sub>2</sub>]<sup>+</sup> (pn = 1,2-propanediamine) for comparison. The complexes also show shoulder absorptions around 21,000 cm<sup>-1</sup>, corresponding to the Ib band (1A<sub>1g</sub> → 1A<sub>2g</sub>), another split component of the first absorption band. Therefore, the complexes can be assigned to a *trans*-dichloro structure. This structure is supported by <sup>13</sup>C-NMR spectroscopy. As Figure 4 shows, [CoCl<sub>2</sub>(N-C\*-C-P)<sub>2</sub>]<sup>+</sup> in CHCl<sub>3</sub> exhibits a spectrum assignable to an ABX type. Such a type will be caused by strong coupling with the phosphorus atoms in the *trans* positions. Therefore, the complexes were assigned to a *trans*-dichloro, *trans*-diphosphorus structure. Molecular models also suggest that this structure has the least inter-ligand interactions among other possible structures.

#### Absorption and Circular Dichroism Spectra

##### a) *trans*-[CoCl<sub>2</sub>(aminophosphine)<sub>2</sub>]<sup>+</sup>

Figure 5 shows the CD spectra of *trans*-dichloro complexes of (*S*)-N-C\*-C-P and (*S*)-N-C-C-P\* in methanol. The complexes give two CD components in the Ia band (doubly degenerate) region. The appearance of the two CD components may result from symmetry lowering of the complex ions. However, the sign of the main CD band of the (*S*)-N-C\*-C-P complex is positive opposite to that of the corresponding *S*-pn ((*S*)-N-C\*-C-N) complex as shown in Figure 6.

The chelate rings in these complexes will be stabilized in the δ-gauche form with equatorially disposed methyl groups. In general, *trans*-[CoCl<sub>2</sub>(diamine)<sub>2</sub>]<sup>+</sup> with a δ-gauche form is known to show a negative CD band in the Ia band region, unless the



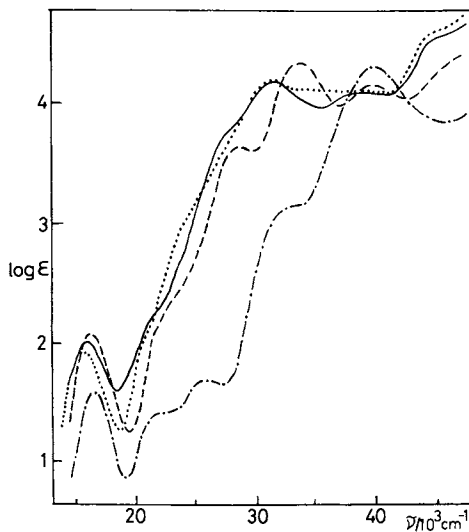


Figure 3. Absorption spectra of trans-dichloro cobalt(III) complexes of  $\text{NH}_2\text{CH}_2\text{-CH}_2\text{P}(\text{C}_6\text{H}_5)_2$  (—);  $\text{NH}_2\text{CH}(\text{CH}_3)\text{CH}_2\text{P}(\text{C}_6\text{H}_5)_2$  (· · ·),  $\text{NH}_2\text{CH}_2\text{CH}_2\text{P}(\text{n-C}_4\text{H}_9)(\text{C}_6\text{H}_5)$  (---), and  $\text{NH}_2\text{CH}(\text{CH}_3)\text{CH}_2\text{NH}_2$  (- · - ·) in methanol

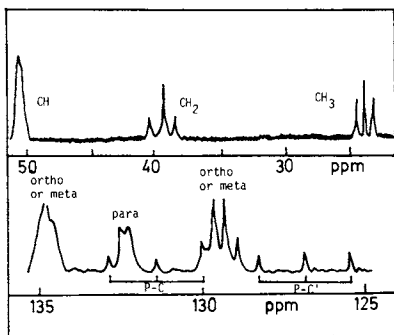


Figure 4.  $\text{C-13}$  NMR spectrum of trans- $[\text{CoCl}_2\{\text{NH}_2\text{CH}(\text{CH}_3)\text{CH}_2\text{P}(\text{C}_6\text{H}_5)_2\}_2]$  ( $\text{ClO}_4$ ) in  $\text{CHCl}_3$  (15.04 MHz, ppm downfield from TMS).

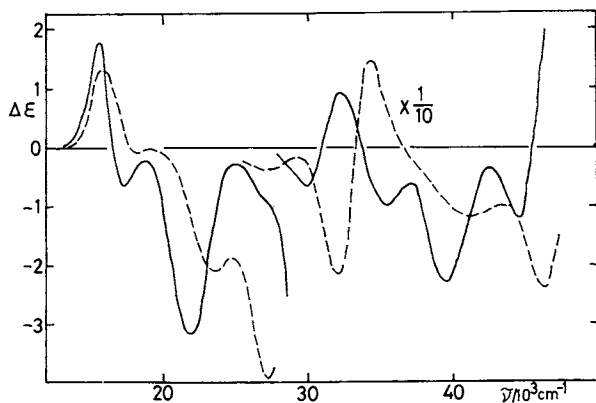


Figure 5. CD spectra of  $\text{trans-[CoCl}_2\{(\text{S})\text{-NH}_2\text{CH}(\text{CH}_3)\text{CH}_2\text{P}(\text{C}_6\text{H}_5)_2\}_2]^+$  (—) and  $\text{trans-[CoCl}_2\{(\text{S})\text{-NH}_2\text{CH}_2\text{CH}_2\text{CH}_2\text{P}(\text{n-C}_4\text{H}_9)(\text{C}_6\text{H}_5)_2\}_2]^+$  (---) in methanol

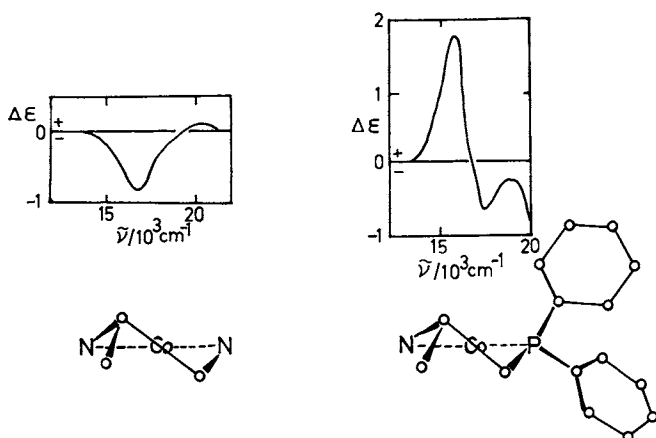


Figure 6. CD spectra of  $\text{trans-dichloro cobalt(III) complexes of } (\text{S})\text{-NH}_2\text{CH}(\text{CH}_3)\text{CH}_2\text{NH}_2$  and  $(\text{S})\text{-NH}_2\text{CH}(\text{CH}_3)\text{CH}_2\text{P}(\text{C}_6\text{H}_5)_2$  in the first absorption band region

ligating nitrogen atom is chiral (9). Although the reason why the (*S*)-N-C\*-C-P complex gives the positive CD band is not clear at present, it may be caused by the two bulky phenyl groups in the ligand. These phenyl groups in the complex are not equivalent because one is equatorial, and the other axial. Therefore, the ligating phosphorus atom becomes chiral and contributes to the CD as a new source of optical activity. The amino hydrogens in the (*S*)-N-C\*-C-N complex are in the same situation as these phenyl groups. However, they are small and may not contribute explicitly to the CD spectrum.

Figure 7 compares the CD spectrum of the (*S*)-N-C-C-P\* complex with that of the corresponding (*R*)-*N*-methyl-ethylenediamine ((*R*)-N\*-C-C-N) complex (9). According to the X-ray analysis (10), the chelate rings in *trans*-[CoCl<sub>2</sub>{(*R*)-N\*-C-C-N}<sub>2</sub>]<sup>+</sup> are in the δ-gauche form and the methyl group is disposed equatorially. The δ-chirality of the (*R*)-N\*-C-C-N chelate ring is the same as that of *trans*-[CoCl<sub>2</sub>(*S*-pn)<sub>2</sub>]<sup>+</sup>, but the CD patterns of these two complexes are almost enantiomeric to each other. Such a difference in the CD has been interpreted by the regional rule proposed by Mason (11). The CD pattern of the (*S*)-N-C-C-P\* complex resembles that of the (*R*)-N\*-C-C-N complex. If it is assumed that the similarity in these CD patterns results from the chelate rings in the same conformational chirality (δ), the phenyl group of the (*S*)-N-C-C-P\* chelate ring becomes equatorial and the *n*-butyl group axial. Thus the axial groups at the chiral nitrogen and phosphorus atoms in the complexes are hydrogen and the *n*-butyl group, respectively, and each of them is the smallest group attached to the chiral atom and the least priority defined by the sequence rule.

#### b) [Co(acac)<sub>2</sub>L]<sup>+</sup>

Figure 8 shows absorption spectra of the bis(acetylacetonato) complexes of ethylenediamine (en, N-C-C-N) (12), N-C-C-P, and P-C-C-P in ethanol. The band around 20,000 cm<sup>-1</sup> of each complex can be assigned to the first *d-d* absorption band, although the intensities increase remarkably with an increase in the number of the ligating phosphorus atoms. From the shift of the band maxima, it is concluded that phosphorus stands at a higher position than nitrogen in the spectrochemical series.

Figure 9 shows CD spectra of these three complexes in ethanol. In the first absorption band region, the N-C-C-N complex gives two negative CD bands, while the phosphorus complexes three CD bands with minus, plus, and minus signs from the longer wavelength side. However, the change of the CD patterns seems to be gradual, and these complexes would have the same absolute configuration. Since the N-C-C-N complex with the negative CD sign has been assigned to Δ-configuration (13), the phosphine complexes in the figure can also be assigned to the same Δ-configuration. This assignment is supported by <sup>1</sup>H-NMR studies of a pair of the diastereomeric (*S*)-N-C-C-P\* complexes.

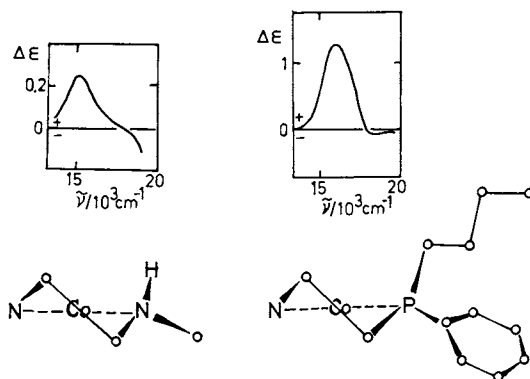


Figure 7. CD spectra of trans-dichloro cobalt(III) complexes of (S)-(CH<sub>3</sub>)NH-CH<sub>2</sub>CH<sub>2</sub>NH<sub>2</sub> and (S)-NH<sub>2</sub>CH<sub>2</sub>CH<sub>2</sub>P(n-C<sub>4</sub>H<sub>9</sub>)(C<sub>6</sub>H<sub>5</sub>) in the first absorption band region

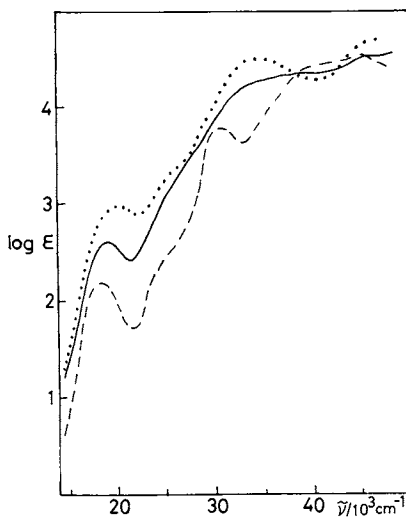


Figure 8. Absorption spectra of bis-(acetylacetonato)cobalt(III) complexes of NH<sub>2</sub>CH<sub>2</sub>CH<sub>2</sub>NH<sub>2</sub> (---), NH<sub>2</sub>CH<sub>2</sub>-CH<sub>2</sub>P(C<sub>6</sub>H<sub>5</sub>)<sub>2</sub> (—), and (C<sub>6</sub>H<sub>5</sub>)<sub>2</sub>PCH<sub>2</sub>-CH<sub>2</sub>P(C<sub>6</sub>H<sub>5</sub>)<sub>2</sub> (· · ·) in ethanol

One diastereomer of  $[\text{Co}(\text{acac})_2((S)\text{-N-C-C-P}^*)]^+$  gives the methine signals of the acetylacetonate ligand at 4.87 and 5.57 ppm with considerably different chemical shifts. On the other hand, the other diastereomer shows these signals at similar frequencies, 5.47 and 5.52 ppm. The big shift to the high field of one methine signal in the former should be caused by the relative location of the phenyl group to the acetylacetonate ring. Figure 10 shows the structures of the two diastereomers. In the  $\Delta$ -configuration, the phenyl ring of the phosphine ligand is located almost parallel to one acetylacetonate ring so that the methine proton should be shielded by the phenyl group to resonate at a high field. In the  $\Lambda$ -configuration, on the other hand, the *n*-butyl group is placed above one acetylacetonate ring and the phenyl group is oriented far from both acetylacetonate rings, two methine protons being not affected by the phenyl group to resonate at similar frequencies. In fact, the P-C-C-P and N-C-C-N complexes show the methine signals at 4.93 and 5.80 ppm, respectively. Thus the diastereomer which gives one of the methine signals at remarkably high field can be assigned to  $\Delta$ -configuration. The CD spectrum of  $\Delta$ - $[\text{Co}(\text{acac})_2((S)\text{-N-C-C-P}^*)]^+$  thus assigned is very similar to that of  $\Delta$ - $[\text{Co}(\text{acac})_2(\text{N-C-C-P})]^+$  assigned on the basis of the CD sign in the first absorption band region.

Figure 11 shows CD spectra of two diastereomeric pairs of the  $(S)\text{-N-C}^*\text{-C-P}$  and  $(S)\text{-N-C-C-P}^*$  complexes in ethanol. The spectra of each pair of diastereomers are nearly enantiomeric to each other, and the patterns are similar to that of the N-C-C-P complex. The results indicate that the vicinal effects of both the chiral ligands are small compared with the configurational effect. From these spectra, the  $\Delta$ -configurational effect curves are obtained for each complex as shown in Figure 12. The curves are very similar to each other and to the CD spectrum of  $\Delta$ - $[\text{Co}(\text{acac})_2(\text{N-C-C-P})]^+$ , indicating that the additivity rule (14) for the configurational and vicinal effects can be applied to the present aminophosphine complexes. Figure 13 shows the vicinal effect curves of the chiral ligands obtained similarly from the observed spectra. The  $(S)\text{-N-C}^*\text{-C-P}$  ligand gives the vicinal effect with a negative CD band in the first absorption band region. This ligand would form a  $\delta$ -gauche chelate ring with the methyl group disposed equatorially. The vicinal effect of a  $\delta$ -gauche chelate ligand gives generally a main CD band with negative sign in this region. Thus the vicinal effect of the  $(S)\text{-N-C}^*\text{-C-P}$  ligand agrees with this general trend. On the other hand, the vicinal effect curve of the  $(S)\text{-N-C-C-P}^*$  ligand shows two CD components of almost equal strength with different signs in the first absorption band region. At present  $[\text{Co}(\text{acac})_2((S)\text{-N-C-C-P}^*)]^+$  and *trans*- $[\text{CoCl}_2((S)\text{-N-C-C-P}^*)]^+$  are the only examples of cobalt(III) complexes containing a chiral phosphorus atom. In order to discuss the optical activity of cobalt(III) phosphine complexes, more CD data will be needed.

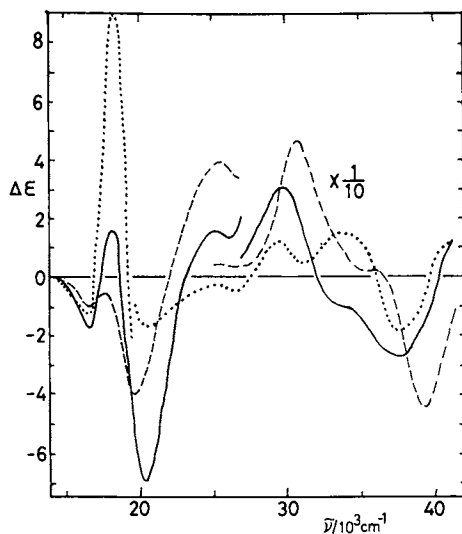
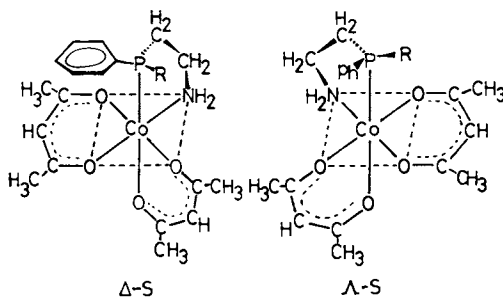


Figure 9. CD spectra of bis(acetylacetonato)cobalt(III) complexes of  $\text{NH}_2\text{CH}_2\text{CH}_2\text{NH}_2$  (---),  $\text{NH}_2\text{CH}_2\text{CH}_2\text{P}(\text{C}_6\text{H}_5)_2$  (—), and  $(\text{C}_6\text{H}_5)_2\text{PCH}_2\text{CH}_2\text{P}(\text{C}_6\text{H}_5)_2$  (···) in ethanol



Chemistry Letters

Figure 10. Structures of  $\Delta(S)$ - and  $\Lambda(S)$ - $[\text{Co}(\text{acac})_2\{\text{NH}_2\text{CH}_2\text{CH}_2\text{P}(\text{n-C}_4\text{H}_9)(\text{C}_6\text{H}_5)\}]^+$  (5)

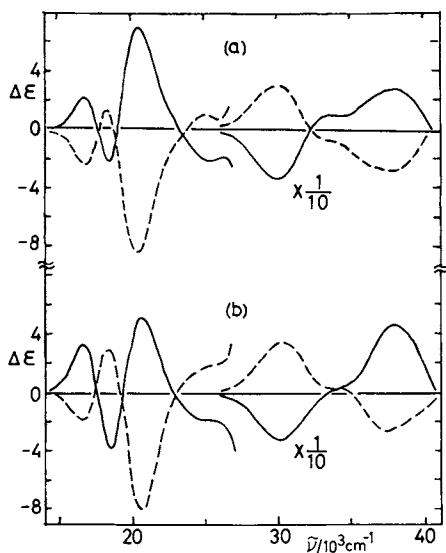


Figure 11. CD spectra of diastereomeric pairs of (a)  $[\text{Co}(\text{acac})_2\{(\text{S})\text{-NH}_2\text{CH}(\text{CH}_3)\text{CH}_2\text{P}(\text{C}_6\text{H}_5)_2\}]^+$  and (b)  $[\text{Co}(\text{acac})_2\{(\text{S})\text{-NH}_2\text{CH}_2\text{CH}_2\text{P}(\text{n-C}_4\text{H}_9)(\text{C}_6\text{H}_5)\}]^+$  in ethanol

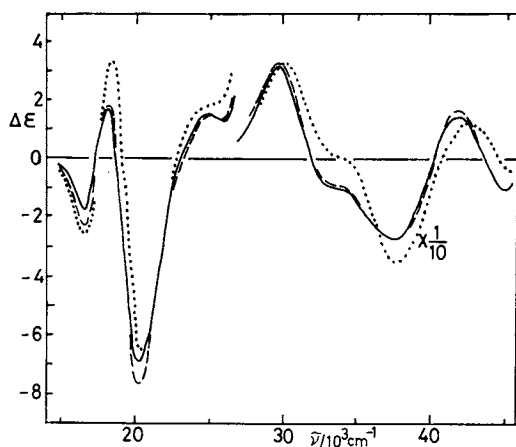
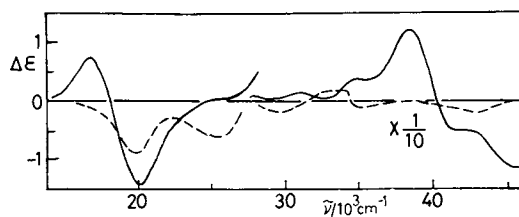


Figure 12. Calculated configurational CD curves of bis(acetylacetonato)cobalt(III) complexes of (S)- $\text{NH}_2\text{CH}(\text{CH}_3)\text{CH}_2\text{P}(\text{C}_6\text{H}_5)_2$  (---) and (S)- $\text{NH}_2\text{CH}_2\text{CH}_2\text{P}(\text{n-C}_4\text{H}_9)(\text{C}_6\text{H}_5)$  (···), and CD spectrum of  $\Delta\text{-}[\text{Co}(\text{acac})_2\{\text{NH}_2\text{CH}_2\text{CH}_2\text{P}(\text{C}_6\text{H}_5)_2\}]^+$  (—).



Chemistry Letters

Figure 13. Calculated vicinal CD curves of bis(acetylacetonato)cobalt(III) complexes of (S)-NH<sub>2</sub>CH(CH<sub>3</sub>)CH<sub>2</sub>P(C<sub>6</sub>H<sub>5</sub>)<sub>2</sub> (---) and (S)-NH<sub>2</sub>CH<sub>2</sub>CH<sub>2</sub>P(n-C<sub>4</sub>H<sub>9</sub>)(C<sub>6</sub>H<sub>5</sub>) (5)



Literature Cited

1. Wymore, C.E.; Bailar, Jr., J.C. J. Inorg. Nucl. Chem., 1960, 14, 42.
2. For example; Shrauzer, G.N.; Windgassen, R.J. J. Am. Chem. Soc., 1967, 89, 1999; Costa, G.; Tanzher, G.; Puxeddu, A. Inorg. Chim. Acta, 1969, 3, 41; Hill, H.A.D.; Morallee, K.G. J. Organomet. Chem., 1968, 11, 167; Tanzher, G.; Mestroni, G.; Puxeddu, A.; Costanzo, R.; Costa, G. J. Chem. Soc. (A), 1971, 2504; Camus, A.; Cocevar, C.; Mestroni, G. J. Organomet. Chem., 1972, 39, 355; Nishikawa, H.; Konya, K.; Shibata, M. Bull. Chem. Soc. Jpn., 1968, 41, 1492; Watanabe, K.; Nishikawa, H.; Shibata, M. *ibid.*, 1969, 42, 1150; Cloyd, Jr., J.C.; Meek, D. W. Inorg. Chim. Acta, 1972, 6, 480; Miskowski, V.M.; Robbins, J.L.; Hammond, G.S.; Gray, H.B. J. Am. Chem. Soc., 1976, 98, 2477; Rigo, P.; Longato, B.; Favero, G. Inorg. Chem., 1972, 11, 300.
3. Issleib, K.; Haferburg, D. Z. Naturforsch., 1965, 20b, 916.
4. Tani, K.; Brown, L.D.; Ahmed, J.; Ibers, J.A.; Yokota, M.; Nakamura, A.; Otsuka, S. J. Am. Chem. Soc., 1977, 99, 7876.
5. Kashiwabara, K.; Kinoshita, I.; Fujita, J. Chem. Lett., 1978, 673.
6. Cahn, R.S.; Ingold, C.K.; Prelog, V. Angew. Chem., Int. Ed. Engl., 1966, 5, 385.
7. Kinoshita, I.; Kashiwabara, K.; Fujita, J.; Yamane, T.; Ukai, H.; Ashida, T. Bull. Chem. Soc. Jpn., 1979, 52, 1413.
8. Yamatera, H. Bull. Chem. Soc. Jpn., 1958, 31, 95.
9. Buckingham, D.A.; Marzilli, L.G.; Sargeson, A.M. Inorg. Chem., 1968, 7, 915.
10. Robinson, W.T.; Buckingham, D.A.; Chandler, G.; Marzilli, L.G.; Sargeson, A.M. Chem. Commun., 1969, 539.
11. Mason, S.F. J. Chem. Soc. (A), 1971, 667.
12. Archer, R.D.; Costradis, B.P. Inorg. Chem., 1965, 4, 1584.
13. Kashiwabara, K.; Igi, K.; Douglas, B.E. Bull. Chem. Soc. Jpn., 1976, 49, 1573.
14. Liu, C.T.; Douglas, B.E. Inorg. Chem., 1964, 3, 1356; Ogino, K.; Murano, K.; Fujita, J. Inorg. Nucl. Chem. Lett., 1968, 4, 351.

RECEIVED September 13, 1979.

## Effect of Solvent on the Circular Dichroism of Metal Complexes

TREVOR D. BAILEY and CLIFFORD J. HAWKINS

Department of Chemistry, University of Queensland, Brisbane, Australia 4067

Since before the turn of the century it has been known that the optical activity of some chiral compounds is solvent dependent (1). For example, in 1877 Landolt (2) reported that the specific rotations of (+)-camphor, (-)-nicotine, (+)-diethyl tartrate, and (-)-turpentine varied with solvent and concentration. In the last decade there has been renewed interest in this solvent dependence. A number of different types of organic compounds has been investigated and the results have been interpreted in terms of variations in conformer populations that have resulted from either the effect of the dielectric on coulombic interactions between dipolar groups in the molecule (3), or from hydrogen-bond interactions between the solvent and the chiral solute (4).

Recently papers have appeared dealing specifically with the effects of solvents on the CD of metal complexes (5,6). Work in this field in our laboratory has been directed at elucidating the particular solvent-solute interactions that are responsible for the changes in the CD of complexes. Four general types of interactions have been recognized:

- (i) stereoselective solvation of the chiral ligand;
- (ii) solvation of the non-chiral ligand;
- (iii) ion association between a chiral ion and the counter ion; and
- (iv) coulombic or hydrogen-bond interactions that change conformer populations.

### Stereoselective Solvation of the Chiral Ligand

As Bosnich and Harrowfield first pointed out, the CD of *trans*-[Co{(R)-pn}<sub>2</sub>Cl<sub>2</sub>]<sup>+</sup>, where pn is 1,2-propanediamine, is particularly sensitive to solvent (5,6). The <sup>1</sup>A<sub>1g</sub> → <sup>1</sup>A<sub>2g</sub> tetragonal component of the lowest energy spin-allowed cubic d-d absorption band (<sup>1</sup>A<sub>1g</sub> → <sup>1</sup>T<sub>1g</sub>) was observed to have a positive Cotton effect in some solvents and a negative in others. Although the <sup>1</sup>A<sub>1g</sub> → <sup>1</sup>E<sub>g</sub> component was positive in each of the solvents

0-8412-0538-8/80/47-119-221\$05.00/0

© 1980 American Chemical Society

studied, significant variations were observed in its rotational strength (6) (Figure 1).

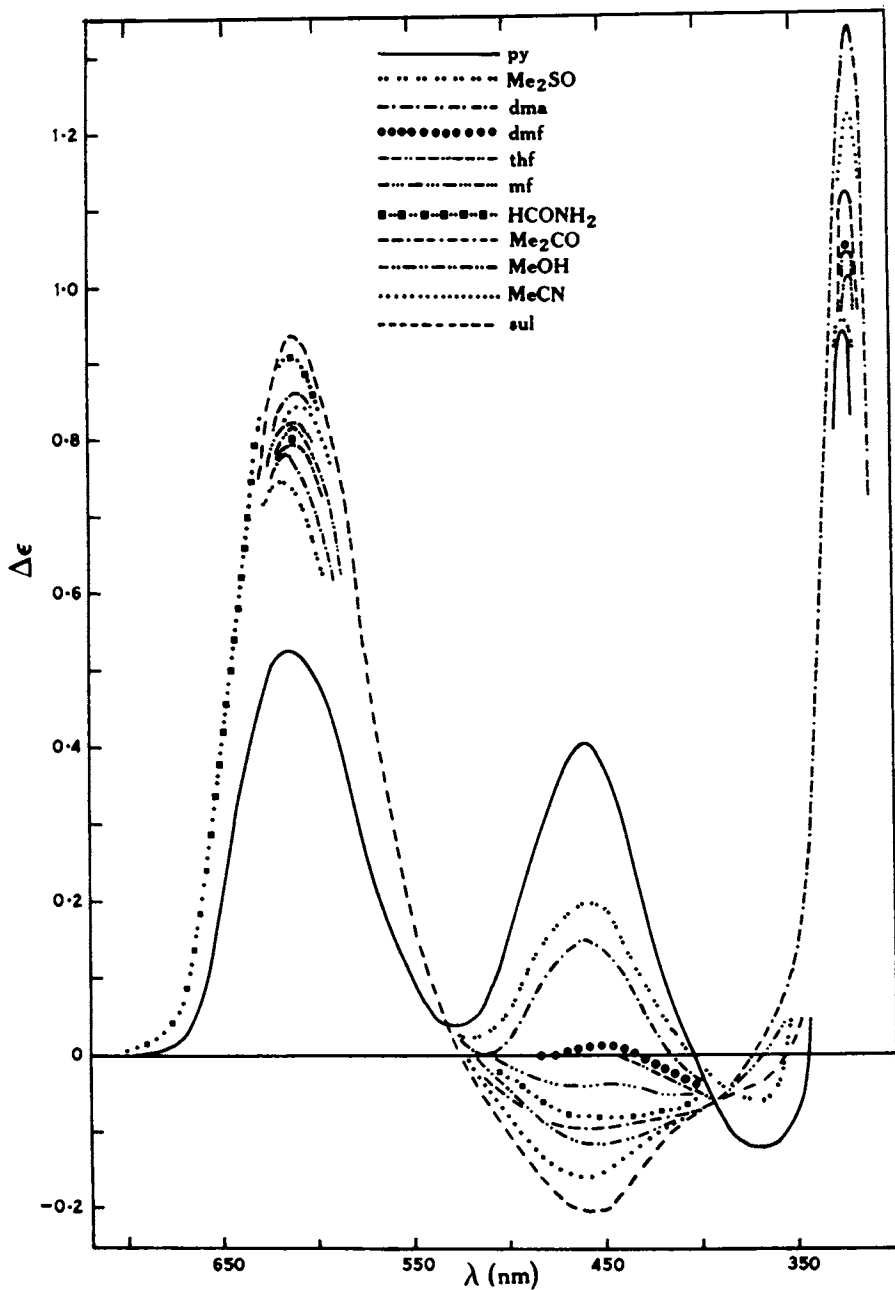
A  $^1\text{H}$  NMR study (6) found that the chemical shifts of the N-H protons were very sensitive to solvent with the shifts being related to the donor number (7) of the solvent, i.e. the ability of the solvent to donate electrons to form a hydrogen bond with the N-H protons. Further, the N-H protons that were essentially equatorial in the puckered five-membered chelate ring showed larger variations in their  $\delta$  values than the axial protons. The differences in the  $\delta$  values for the equatorial and axial protons for the  $\text{NH}_2$  groups were in the order:

$\text{py} > \text{dma} \approx \text{Me}_2\text{SO} > \text{dmf} > \text{MeOH} > \text{thf} \approx \text{Me}_2\text{CO} > \text{sul} \approx \text{MeCN}$ ,  
where py is pyridine, dma dimethylacetamide, dmf dimethylformamide, thf tetrahydrofuran, and sul sulfolane. The difference in the strength of the hydrogen bond formed between the solvent and the equatorial and axial N-H protons makes the  $\text{NH}_2$  group asymmetric, and the degree of asymmetry is solvent dependent.

The rank order of the solvents based on the degree of asymmetry introduced in the  $\text{NH}_2$  groups was found to correspond closely with the rank order based on the values of  $\Delta\epsilon$  for the tetragonal components of the  $^1\text{A}_{1g} \rightarrow ^1\text{T}_{1g}$  absorption band. As the degree of asymmetry induced by solvation increased, the  $^1\text{A}_{1g} \rightarrow ^1\text{E}_g$  Cotton effect became less positive and the  $^1\text{A}_{1g} \rightarrow ^1\text{A}_{2g}$  Cotton effect changed from negative to positive.

The degree of stereoselectivity in the solvation at the  $\text{NH}_2$  groups of a diamine or amino alcohol complex depends on the preference of the chelate ring to exist in one particular conformer, and on the non-bonded interactions between the hydrogen-bonded solvent molecule in the axial or equatorial orientations with the groups on the adjacent carbon and, more importantly, with the apical ligands in an octahedral complex. In complexes such as  $[\text{Mo}\{(\text{R})\text{-pn}\}(\text{CO})_4]$  where the  $\lambda$  and  $\delta$  conformations are equally populated (8), solvation of the N-H protons does not result in the preponderance of an asymmetric  $\text{NH}_2$  group of one configuration as shown by the  $^1\text{H}$  NMR spectrum (9). The CD spectrum correspondingly does not exhibit a marked solvent dependence.

In support of this theory relating the solvent dependence of the CD of complexes of chiral diamines with stereoselective solvation at the  $\text{NH}_2$  group, the rotational strengths of the tetragonal components of the  $^1\text{A}_{1g} \rightarrow ^1\text{T}_{1g}$  absorption band for  $[\text{Co}\{(\text{R})\text{-tmpn}\}(\text{CN})_4]^-$ , where tmpn is  $\underline{\text{N}}, \underline{\text{N}}, \underline{\text{N}}', \underline{\text{N}}'$ -tetramethyl-1,2-propanediamine, do not show any marked solvent dependence although, as will be discussed later, the positions of the CD bands do vary with solvent (9). For the analogous (R)-pn complex, the  $^1\text{A}_{1g} \rightarrow ^1\text{A}_{2g}$  and  $^1\text{A}_{1g} \rightarrow ^1\text{E}_g$  Cotton effects became less negative and less positive, respectively, as the donor number of the solvent increased (9), as was found for *trans*- $[\text{Co}\{(\text{R})\text{-pn}\}_2\text{Cl}_2]^+$  (6). Changes in CD with solvent of a similar order of magnitude have been observed for other related systems (5,10,11).



Australian Journal of Chemistry

Figure 1. CD spectrum of  $\text{trans-[Co}\{(R)\text{-pn}\}_2\text{Cl}_2\text{]BPh}_4$  in various solvents. Abbreviations are as follows: py, pyridine; dma, N,N-dimethylacetamide; dmf, N,N-dimethylformamide; thf, tetrahydrofuran; mf, N-methylformamide; sul, sulfolane (6).

### Solvation of the Non-Chiral Ligand

Changes in the observed CD of a complex with solvent have been observed where solvation of the chiral ligand is unimportant, but where NMR and, in some cases, Raman spectroscopic evidence shows that the non-chiral ligands in the complex are being solvated to varying degrees. Two general effects of this have been observed:

- (i) the spectrochemical parameter,  $\Delta$ , is changed by solvation causing a shift in the absorption and CD spectra, and a change in the tetragonal or rhombic splitting of the cubic absorption bands, and
- (ii) the energy of the charge transfer absorption bands that are involved in the induction of CD in the  $\underline{d-d}$  bands changes significantly.

Solvation of a coordinated  $\text{NH}_3$  ligand, which can be followed by  $^1\text{H}$  NMR, does not cause a marked change in the  $\Delta$  value for that ligand. However, protonation of some ligands, for example  $\text{CN}^-$ , by a protic solvent causes a significant change in the energy of the  $\underline{d-d}$  absorption bands of the metal and, in the case of  $\text{CN}^-$ , an increase in the  $\Delta$  value (12,13). The absorption bands and the associated Cotton effects move with the acceptor number (A.N.) (7) of the solvent, i.e. the ability of the protic solvent to accept electrons from a solute to form a hydrogen bond. For  $[\text{Co}\{(\text{R})\text{-pn}\}(\text{CN})_4]^-$ ,  $\lambda_{\text{max}}$  for the  $^1\text{A}_{1g} \rightarrow ^1\text{T}_{1g}$  absorption band varies as follows: hmpa (hexamethylphosphortriamide) A.N. 10.6,  $\lambda$  368 nm;  $\text{Me}_2\text{SO}$ , A.N. 19.3,  $\lambda$  363 nm;  $\text{MeOH}$ , A.N. 41.3,  $\lambda$  356 nm;  $\text{H}_2\text{O}$ , A.N. 54.8,  $\lambda$  353 nm (9).

Complexes with a tetragonal chromophore, i.e.  $\Sigma\Delta_x = \Sigma\Delta_y \neq \Sigma\Delta_z$ , for example  $[\text{Co}\{(\text{R})\text{-pn}\}(\text{CN})_4]^-$ , have the  $^1\text{A}_{1g} \rightarrow ^1\text{T}_{1g}$  absorption split into two components, with the separation related to the difference in the spectrochemical parameters,  $\Delta$ , for the ligands (14,15):

$$\Delta E_{\text{tet}} = -0.5(0.25\Sigma\Delta_{xy} - 0.5\Sigma\Delta_z) \quad (1)$$

For the above tetracyanide complex, the tetragonal splitting is given by  $0.25(\Delta_{\text{CN}} - \Delta_{\text{pn}})$ . As  $\Delta_{\text{CN}}$  changes with solvent, the tetragonal splitting varies, and therefore, the observed CD will change even though the rotational strength of the individual Cotton effects might not alter.

Although the ligand-field bands of ammine complexes are not very sensitive to solvent, the charge-transfer bands do shift with solvent. For example, the  $\sigma_{\text{L}} \rightarrow \text{M}$  band in  $[\text{Co}(\text{NH}_3)_6]^{3+}$  occurs at 197 nm in water but at 240 nm in  $\text{Me}_2\text{SO}$  (9). The charge transfer transition generates positive charge on the  $\text{NH}_3$  ligands. Therefore, in the excited state, the ligands would be able to form stronger hydrogen bonds with a proton-acceptor solvent than in the ground state, and hence the energy separation between the ground and excited states would decrease for these solvents. Since the

rotational strength induced in an electric dipole forbidden  $d-d$  band via the charge-transfer transition depends on the energy separation between them (16), the observed CD will change with the ability of a solvent to vary the energy of the charge-transfer band. An example where this appears to be important will be discussed later in the paper.

### Ion Association

It has been clearly shown that ion association can markedly alter the CD of an ionic chiral solute. For example, oxyanions such as phosphate form contact ion pairs with tris(diamine)-cobalt(III) complexes, resulting in an increase and a decrease in the sizes of the  ${}^1A_1 \rightarrow {}^1A_2$  and  ${}^1A_1 \rightarrow {}^1E (D_3)$  components, respectively, of the  ${}^1A_{1g} \rightarrow {}^1T_{1g}$  absorption band (17-22). This effect has been ascribed to the generation of asymmetry at the N donors via hydrogen bonding to the anion(23).

The donor and acceptor properties of the solvent as well as its dielectric control the degree of ion association. If this effect needs to be minimized for a cationic solute, anions such as perchlorate or tetraphenylborate should be used with solvents that possess a dielectric greater than, say, 15. For an anionic complex in a polar solvent, lithium could be used as a counter ion. Effects of ion association are more noticeable for complexes that carry a high charge, for example 3+, than for ions that carry a single charge.

### Conformer Population Change

The free energy differences between conformers of a solute are in some cases solvent dependent, especially where

- (a) one conformer of the solute possesses stronger intramolecular hydrogen-bonding properties than others, and the hydrogen-bonding capabilities of the solvents can modify the degree of intramolecular hydrogen bonding and thus change the conformational energy differences (4). Alternatively, the various conformers may differ in their ability to hydrogen bond to the solvent, and the conformer populations will vary depending on the hydrogen-bonding character of the solvent.
- (b) the molecule possesses two neighboring dipoles that are at different orientations to one another in the various conformers (3). The dipolar interactions, which contribute to the conformational free energy differences, depend on the dielectric of the medium, being attenuated in high dielectric media, and enhanced in low dielectric media.

For systems where hydrogen-bonding interactions are not of great importance as far as the CD is concerned, but dipolar interactions are important, it is theoretically possible to determine the strain-energy difference and the dipolar-interaction

energy difference for two conformers in equilibrium via a study of the solvent dependence of the CD. The observed rotational strength is related to these two energy terms by equation 2 (3):

$$RT \ln \left\{ \frac{(\underline{R}_{\text{Obs}} - \underline{R}_{\text{II}})}{(\underline{R}_{\text{I}} - \underline{R}_{\text{Obs}})} \right\} = \Delta G_{\text{S}} + \Delta V/D \quad (2)$$

where  $\underline{R}$  is the rotational strength for a particular transition,  $\Delta G_{\text{S}}$  is the strain-energy difference,  $\Delta V$  is the dipolar-interaction energy difference, and  $D$  is the dielectric constant. If both  $\underline{R}_{\text{I}}$  and  $\underline{R}_{\text{II}}$  are known,  $\Delta G_{\text{S}}$  and  $\Delta V$  can be determined by plotting the left-hand side of equation 2 against  $1/D$ . This should be a straight line with slope  $\Delta V$  and intercept  $\Delta G_{\text{S}}$ . If only  $\underline{R}_{\text{I}}$  is known, the above plot is repeated for various values of  $\underline{R}_{\text{II}}$ . The value that gives the best straight line relationship is chosen for  $\underline{R}_{\text{II}}$ .

In the remainder of this paper the solvent-dependent CD of a particular complex will be considered in some detail. The example has been chosen because the variation in CD with solvent is related to a solvent-induced change in the conformer populations of a chiral ligand.

#### Solvent Dependent CD of Pentaamminecobalt(III) Complexes of Chiral Carboxylates

The CD spectra of carboxylic acids and esters have been studied extensively (24-35). In the region of the  $n \rightarrow \pi^*$  transition of the carboxylate group, two Cotton effects of opposite sign have been observed, the intensities of which vary inversely with one another as the solvent and/or the temperature are changed. These two Cotton effects have been associated with two rotamers of the carboxylates, the populations of which are solvent and temperature dependent (28-31). For a 2-substituted propionic acid or its ester the most stable rotamers are shown in Figure 2. Rotamer III is generally considered not to make a major contribution to the observed CD spectra because of the potentially low rotational strength of its transitions and because of its postulated low relative concentration.

The CD spectra of pentaamminecobalt(III) complexes of (S)- $\alpha$ -amino acids binding through the carboxylate group, and of (S)-2-substituted propionates have either a positive or a negative Cotton effect or both in the region of the  ${}^1A_{1g} \rightarrow {}^1E_g$  ( $D_{4h}$ ) component of the  ${}^1A_{1g} \rightarrow {}^1T_{1g}$  absorption. Previously these two bands have been ascribed to the two components of the transition rendered nondegenerate by the low symmetry of the overall molecule (36,37,38). However, it has been observed that the changes in the sizes of these positive and negative Cotton effects with solvent and temperature are similar to those changes found for the free acids or their esters, and these changes can also be rationalized, at least in part, in terms of changes in rotamer populations. As an example of this, the CD spectrum of pentaamine{(S)-2-chloropropionato}cobalt(III) will be considered in some detail.

From the  $^1\text{H}$  NMR work of Karabatsos and coworkers on substituted acetaldehydes (39,40), and from the infrared studies of Brown (41) and Laato and Isotalo (42) with  $\alpha$ -substituted carboxylic acid esters, it can be concluded that in solution the equilibrium between the rotamers in Figure 2 where R is  $\text{CH}_3$  and X is Cl favours rotamer II in solvents of low dielectric with rotamer III least favoured, and favors rotamer I in solvents of high dielectric. The solvents with high dielectric attenuate the dipole-dipole repulsion between the C-Cl and C=O groups, which is maximized in rotamer I, and hence shift the equilibrium towards rotamer I. If the temperature of the solution is decreased, the associated increase in dielectric would tend to shift the equilibrium towards rotamer I.

As found for similar chiral carboxylates, the CD spectra of 2-chloropropionic acid and other 2-chloro carboxylic acids in the region of the  $n \rightarrow \pi^*$  absorption have a positive and a negative Cotton effect with the positive at lower wavelength for the (S) configuration (28). The low wavelength band was associated with rotamer I and the high wavelength band with II (28). Gaffield and Galetto studied the solvent-induced changes in the  $n \rightarrow \pi^*$  region of the CD spectrum of (S)-2-chlorovaleric acid, and found the general trend that, as the dielectric of the solvent increased, the positive Cotton effect increased in size, and the negative decreased (28). This is consistent with the above proposal that the equilibrium shifts towards I as the dielectric is increased. The variable temperature CD spectra for this compound were also reported with EPA (ether: isopentane: ethanol in a volume ratio of 5:5:2) as solvent. Both the negative and positive Cotton effects increased in size as the temperature was lowered. Since the dielectric increases with decreasing temperature, a decrease in the negative band might have been expected if the dielectric effect was dominant. This was in fact observed for the analogous (S)- $\alpha$ -chloro carboxylic acids with isopropyl and tert-butyl groups on the  $\alpha$ -carbon: the positive Cotton effect increased whereas the negative became diminishingly small at  $-185^\circ\text{C}$ .

Richardson and Strickland (43) have estimated the rotational strengths of the transitions of the carboxylate chromophore for 2-chloropropionic acid directly from molecular orbitals calculated using INDO and CNDO semi-empirical MO models, and excited-state wave functions constructed in the virtual orbital-configuration interaction approximation. Their calculations, which, of course, do not take into account solvent effects, resulted in binding energies for the rotamers increasing in the order  $\text{II} < \text{III} < \text{I}$  which is in disagreement with the order of stabilities concluded from the NMR and infrared work. Further, the calculations yielded rotational strengths of the  $n \rightarrow \pi^*$  transition for rotamers I, II, and III of  $-7.92$ ,  $+13.98$ , and  $-17.5$ , respectively, in conflict with the above conclusions of Gaffield and Galetto (28). Richardson and Strickland (43) questioned the assignment of the high wavelength negative band to the  $n \rightarrow \pi^*$  transition (28)



because their calculations had yielded two almost degenerate transitions, one localized on the Cl atom, and one involving Cl  $\rightarrow$  COOH charge transfer, that were below the  $n \rightarrow \pi^*$  transition in energy occurring at about 260 nm. However, Richardson and Strickland acknowledged that their theoretical model had difficulties with molecules containing second row atoms such as Cl. For the other molecules they studied, the results were in good agreement with the CD spectra.

One structure of pentaammine{(S)-2-chloropropionato}cobalt(III) is given in Figure 3. The ligand is shown as the rotamer I, with the carboxylate group in a plane bisecting  $\angle\text{NCoN}$  as was found in the X-ray determined structure (44) of acetatopentaamminecobalt(III). The energy level diagram is presented in Figure 4, and the absorption spectrum of the complex for a range of solvents in Figure 5. Four bands are observed at the following approximate positions:  ${}^1A_{1g} \rightarrow {}^1T_{1g}$  ( $O_h$ ), 505 nm;  ${}^1A_{1g} \rightarrow {}^1T_{2g}$  ( $O_h$ ), 350 nm;  $\pi_p(0) \rightarrow d_z^2$  charge transfer, 240 nm; and  $\sigma_L \rightarrow d_z^2$  charge transfer, 200 nm. The  $\sigma_z \rightarrow d_{x^2-y^2}$  charge transfer has  $A_2$  symmetry that is electric-dipole forbidden. The tetragonal ligand field splits the  ${}^1A_{1g} \rightarrow {}^1T_{1g}$   $\underline{d-d}$  band into  ${}^1A_{1g} \rightarrow {}^1E_g$  and  ${}^1A_{1g} \rightarrow {}^1A_{2g}$  components, which have been estimated to occur at about 507 nm and 457 nm, respectively (37). The  $\pi$ -interaction removes the degeneracy of the  ${}^1A_{1g} \rightarrow {}^1E_g$  transition to give components of  $B_2$  and  $B_1$  symmetry. In solvents of relatively low dielectric that are also poor donors, some interaction appears to occur between the complex and the tetraphenylborate counter-ion as evidenced by the increased absorption in the region about 300 nm. The effect is most marked for the tetrahydrofuran solution that has the lowest dielectric of the solvents studied.

According to Schipper's AICD theory (16), the  $\underline{d-d}$  transition with  $B_2$  symmetry gains its rotational strength via the charge-transfer transitions with  $B_2$  ( $\pi_p(0) \rightarrow d_z^2$  and  $\sigma_{x-y} \rightarrow d_z^2$ ) and  $A_1$  symmetry, and the  $\underline{d-d}$  transition with  $B_1$  symmetry via the  $B_1$  ( $\sigma_{x+y} \rightarrow d_z^2$ ) and  $A_1$  charge-transfer transitions, whereas the  $\underline{d-d}$  transition with  $A_2$  symmetry is inactive. This is consistent with the observed CD spectra of this type of complex as the components with  $E_g$  parentage dominate the CD spectra (36,37,38). According to the AICD theory, the inducibilities of the  ${}^1A_1 \rightarrow {}^1B_1$  and the  ${}^1A_1 \rightarrow {}^1B_2$  components via the  $\sigma_L \rightarrow d_z^2$  charge-transfer transitions are of the same sign (45), but more work is required before it will be known whether the AICD theory predicts that the two components have the same sign for their rotational strengths because the contribution from the  $\pi_p(0) \rightarrow d_z^2$  charge transfer with  $B_2$  symmetry has to be determined and the orientations of the transitions with respect to the inducing moments must be evaluated.

The CD spectra of the complex under the  ${}^1A_{1g} \rightarrow {}^1T_{1g}$  absorption at 293 K in a range of solvents are presented in Figure 6, and the relationship between the total rotational strength and the dielectric constant of the solvent is plotted in Figure 7. As expected from the work with the carboxylic acids and esters, the

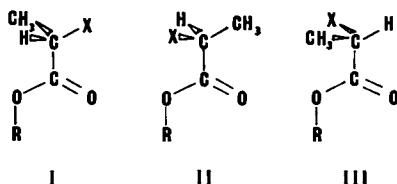


Figure 2. Rotamers of 2-substituted propionic acid ( $R = H$ ) and O-substituted derivatives

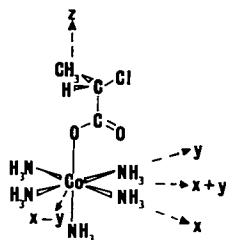


Figure 3. Pentaammine{(S)-2-chloropropionato}cobalt(III)

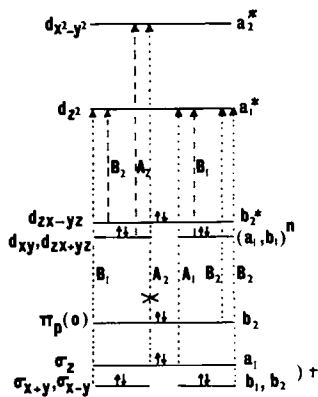


Figure 4. Partial molecular orbital diagram for pentaamminecobalt(III) complexes of carboxylates showing low symmetry components for the  ${}^1A_{1g} \rightarrow {}^1T_{1g}$  d-d transition (---) and the charge-transfer transitions ( $\cdot \cdot \cdot$ ). The charge-transfer transition with  $A_2$  symmetry is electric-dipole forbidden. \*Bonding molecular orbitals formed from ligand group orbitals and p orbitals of cobalt.

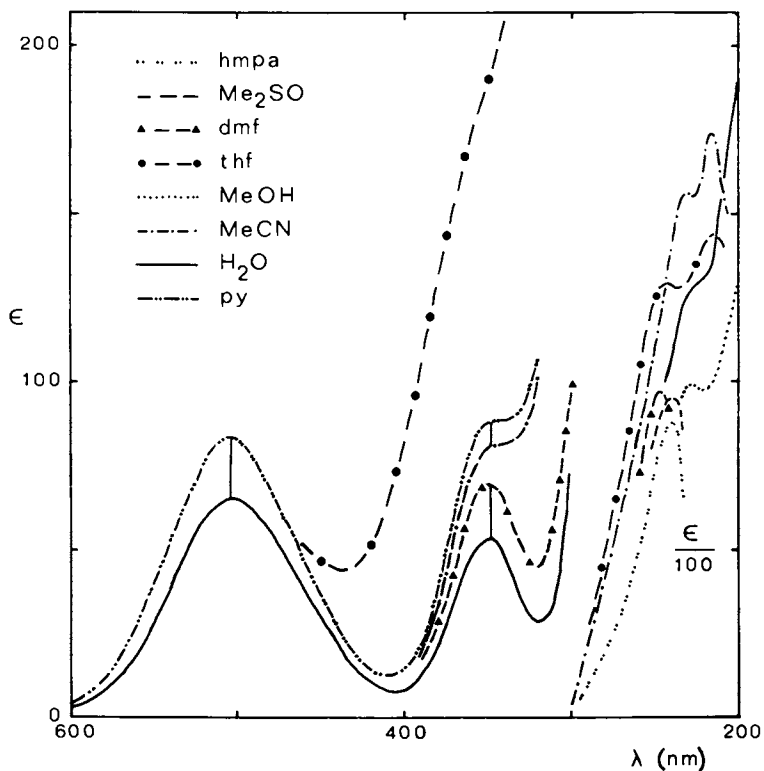


Figure 5. Absorption spectrum of pentaammine{(S)-2-chloropropionato}cobalt(III) tetraphenylborate in (lower set) water (as  $\text{ClO}_4^-$  salt), hexamethylphosphor-triamide (hmpa), dimethyl sulfoxide, N-methylformamide (nmf), N,N-dimethyl-formamide (dmf); (upper set) acetonitrile, methanol, ethanol, acetone, pyridine (py); and tetrahydrofuran (thf). The reference contained tetraphenylborate (as  $\text{Na}^+$  salt) at the same concentration as the solution of the complex.

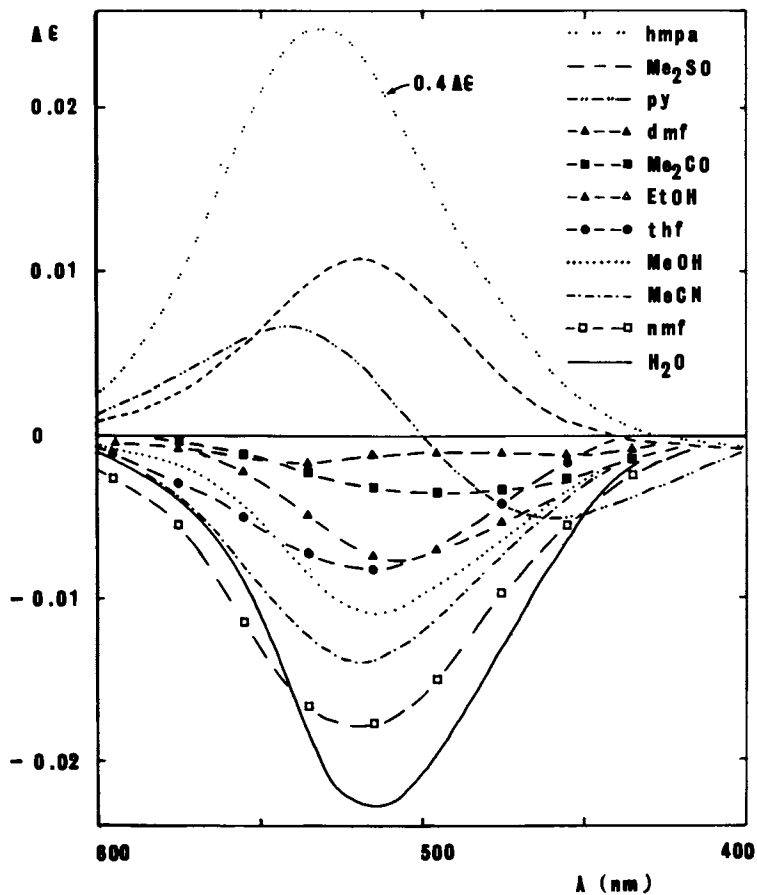


Figure 6. CD spectrum of pentaammine{(S)-2-chloropropionato}-cobalt(III) tetraphenylborate in various solvents. Abbreviations are as for Figure 5. In water, the perchlorate salt was used.

observed rotational strength varies with dielectric. For those solvents that were found by NMR not to solvate the complex strongly at 293 K, the rotational strength becomes less negative and eventually positive as the dielectric decreases. Because the mole fraction of rotamer II increases with decreasing dielectric due to the repulsions between the C=O and C-Cl dipoles, rotamer II must have a positive and rotamer I a negative rotational strength. The reverse trend would be expected for (S)-alaninepentaamminecobalt-(III) in which X is  $\text{NH}_3^+$  since the coulombic interaction of this group with the C=O dipole is attractive. As expected, the rotational strength under the  $^1\text{A}_{1g} \rightarrow ^1\text{T}_{1g}$  absorption for this complex becomes more negative as the dielectric decreases and the equilibrium shifts more towards I (Figure 8).

For a solvent such as acetonitrile that is a poor donor (D.N. = 14.1) (7), the variable temperature CD spectra of the (S)-2-chloropropionate complex (Figure 9) can be understood in terms of the shift in the equilibrium towards the energetically preferred rotamer I at low temperature. This shift in the equilibrium is heightened by the increase in the dielectric as the temperature is lowered. The CD spectra in water and methanol also become more negative as the temperature is lowered.

$^1\text{H}$  and  $^{13}\text{C}$  NMR studies have shown that the major sites for specific solvation are the C=O group with acceptor solvents, and the  $\text{NH}_3$  groups with donor solvents. There seems to be no relationship between the observed rotational strength and the degree of solvation at the C=O group. On the other hand, solvation at the  $\text{NH}_3$  group appears to have a marked effect on the CD. For example, the rotational strengths in hmpa and  $\text{Me}_2\text{SO}$  that are strong donor solvents are much more positive than would have been predicted from their dielectric constant.

As stated above, solvation at  $\text{NH}_3$  does not significantly affect  $\Delta(\text{NH}_3)$  but it does change the energy and intensity of the charge transfer transitions. Unfortunately, solvent absorption in the vicinity of the charge transfer transitions has prevented an experimental analysis of the effects of solvation on the charge transfers. However, the  $\sigma_L \rightarrow d_z^2$  charge transfer transitions would certainly be affected differently to the  $\pi_p(0) \rightarrow d_z^2$ . If, for example, these transitions induce Cotton effects of opposite sign in the  $\underline{d-d}$  bands, the change in the relative positions and intensities of the charge transfers with solvation would give rise to significant changes in the observed CD. This could explain the observed trend to more positive rotational strengths in solvents of high donicity such as hmpa (D.N. = 38.8) and  $\text{Me}_2\text{SO}$  (D.N. = 29.8) and also the trend to more positive rotational strengths in the donor solvents as the temperature is lowered (Figure 10). For the hmpa and  $\text{Me}_2\text{SO}$  solutions, the rotational strength of the positive band increases as the temperature is lowered and the degree of solvation increases. The variable temperature results for methanol and ethanol are in marked contrast to each other. For methanol, as the temperature is lowered, the

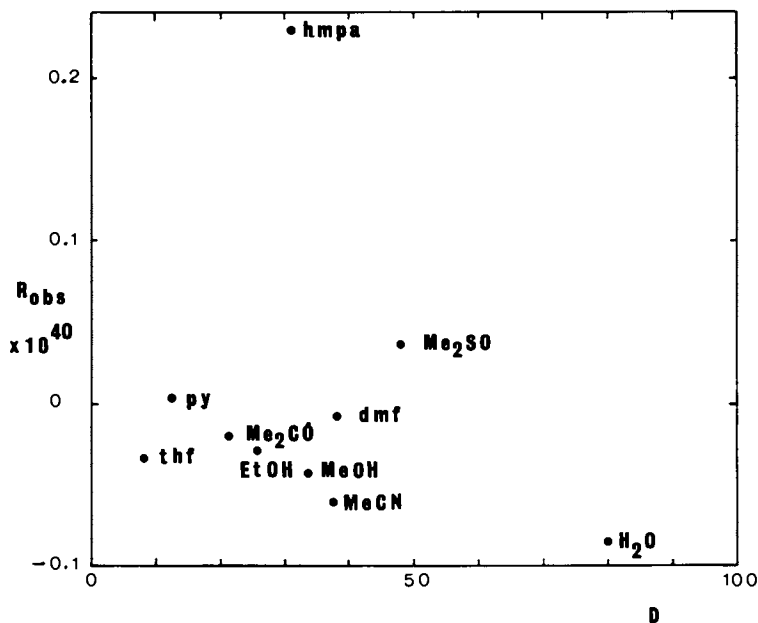


Figure 7. A plot of the observed rotational strength under the  ${}^1A_{1g} \rightarrow {}^1T_{1g}$  absorption band (in cgs units) of pentaamine{(S)-2-chloropropionato}cobalt(III) as a function of the dielectric constant of the solvent

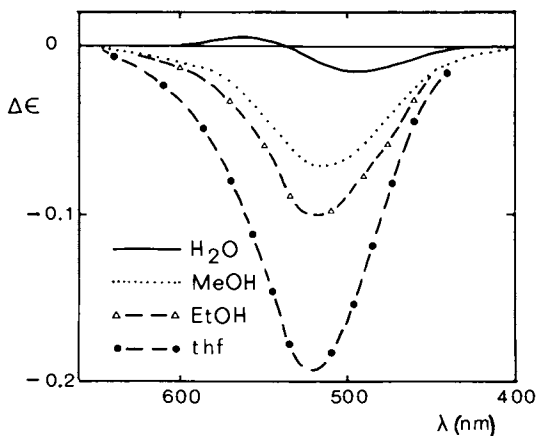


Figure 8. CD spectrum of (S)-alaninepentaamminecobalt(III) as the perchlorate salt in water and as the tetraphenylborate salt in methanol, ethanol, and thf.

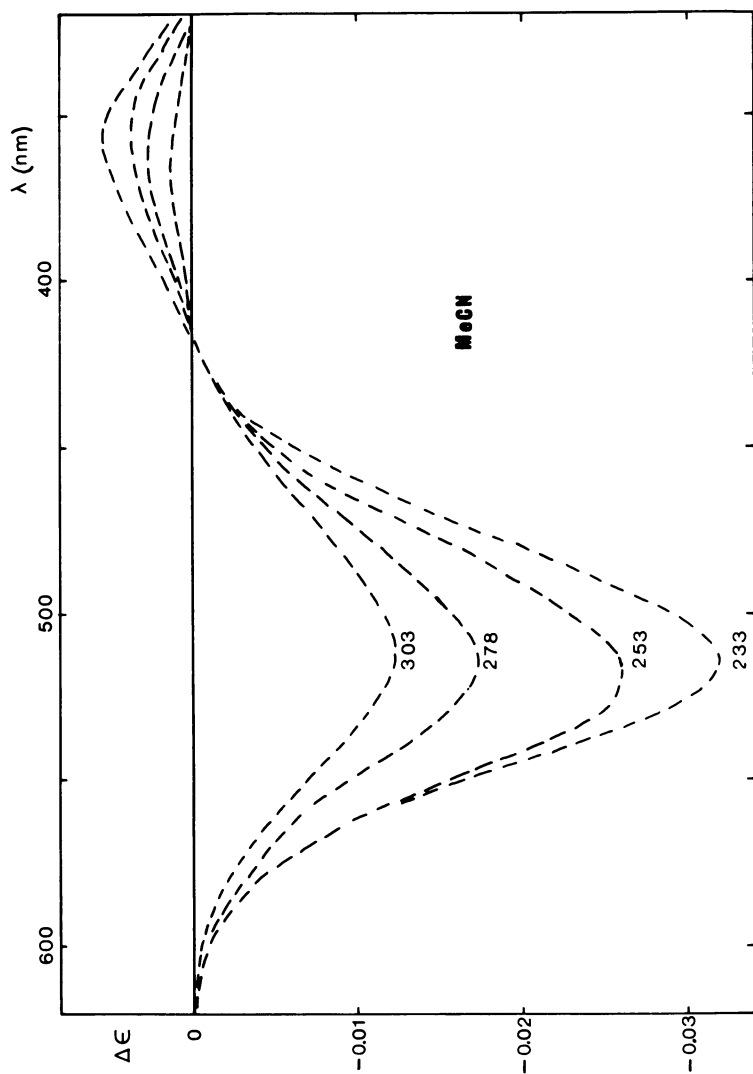


Figure 9. CD spectrum of pentammine{(S)-2-chloropropionato}cobalt(III) tetraphenylborate as a function of temperature in acetonitrile

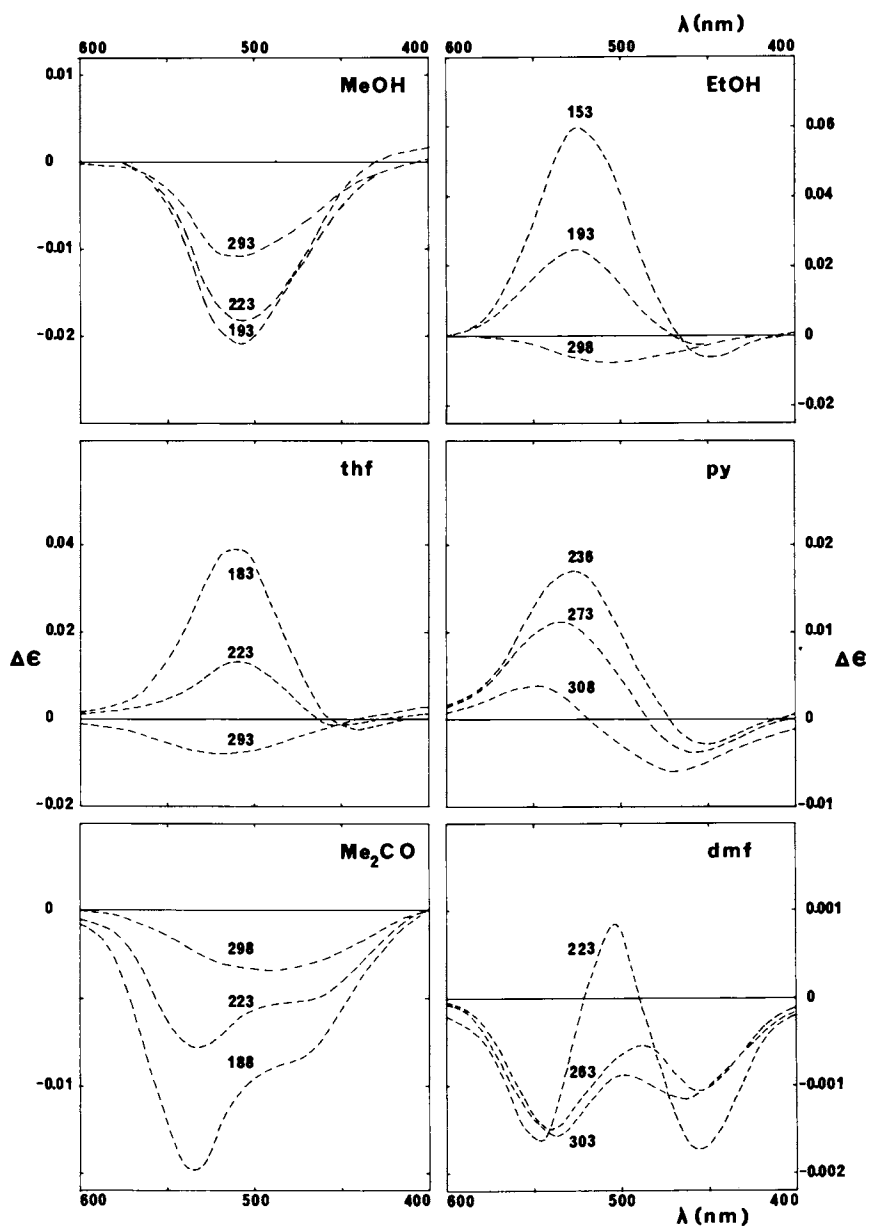


Figure 10. CD spectrum of pentaammine((S)-2-chloropropionato)cobalt(III) tetraphenylborate in various solvents as a function of temperature



rotational strength becomes more negative as would be expected from the increased dielectric at low temperature and the associated shift in the equilibrium towards rotamer I. For ethanol, which has a lower dielectric constant, the equilibrium is shifted further towards rotamer II than for methanol. At low temperatures the CD changes to give a positive band under the  ${}^1A_{1g} \rightarrow {}^1T_{1g}$  absorption. This is not because the equilibrium is shifting towards rotamer II as the temperature is lowered because the dielectric constant for ethanol increases as the temperature is lowered and would shift the equilibrium towards rotamer I. It is felt that the changes in the CD with temperature observed for ethanol and also for tetrahydrofuran and pyridine are due to the positions of the equilibrium in these solvents that have relatively low dielectric constants together with an increase in the degree of solvation. For dmf, which is a relatively good donor solvent (D.N. = 26.6), the effect of solvation is observed at room temperature and this becomes more manifest as the temperature is lowered. Acetone on the other hand is a relatively poor donor (D.N. = 17.0) and the rotational strength becomes more negative as the temperature is lowered in line with the shift in the equilibrium towards rotamer I. A slight positive contribution from solvation is superimposed on this negative band.

#### Acknowledgement

The authors wish to acknowledge financial support from the Australian Research Grants Committee.

#### Literature Cited

1. Lowry, T.M. "Optical Rotatory Power"; Dover Publications Inc.: New York, (1964); pp93-100, 349-356.
2. Landolt, H. Ann., (1877), 189, 241.
3. Kuriyama, K.; Iwata, T.; Moriyama, M.; Ishikawa, M.; Minato, H.; Takeda, K. J. Chem. Soc. C, (1967), 420.
4. Wellman, K.M.; Briggs, W.S.; Djerassi, C. J. Am. Chem. Soc., (1965), 87, 73.
5. Bosnich, B.; Harrowfield, J. MacB. J. Am. Chem. Soc., (1972), 94, 989, 3425.
6. Hawkins, C.J.; Lawrance, G.A.; Peachey, R.M. Aust. J. Chem., (1977), 30, 2115.
7. Mayer, U.; Gutmann, V. Struct. Bonding (Berlin), (1972), 12, 113.
8. Hawkins, C.J.; Peachey, R.M. Aust. J. Chem., (1976), 29, 33.
9. Bailey, T.D.; Hawkins, C.J. unpublished data.
10. Arakawa, S.; Kashiwabara, K.; Fujita, J.; Saito, K. Bull. Chem. Soc. Japan, (1977), 50, 2331.
11. Hawkins, C.J.; McEniery, M.L. Aust. J. Chem., (1979), 32, in press.
12. Shriver, D.F.; Posner, J. J. Am. Chem. Soc., (1966), 88, 1672.

13. Alexander, J.A.; Gray, H.B. J. Am. Chem. Soc., (1968), 90, 4260.
14. Yamatera, H. Bull. Chem. Soc. Japan, (1958), 31, 95.
15. Schäffer, C.E.; Jørgensen, C.K. K. danske Vidensk. Selsk. Skr., Mat.-fys. Medd., (1965), 34(13), 1.
16. Schipper, P.E. J. Am. Chem. Soc., (1978), 100, 1433.
17. Smith, H.L.; Douglas, B.E. J. Am. Chem. Soc., (1964), 86, 3885.
18. Smith, H.L.; Douglas, B.E. Inorg. Chem., (1966), 5, 784.
19. Mason, S.F.; Norman, B.J. Chem. Commun., (1965), 73.
20. Larsson, R.; Mason, S.F.; Norman, B.J. J. Chem. Soc. A, (1966), 301.
21. Mason, S.F.; Norman, B. J. Chem. Soc. A, (1966), 307.
22. Gollogly, J.R.; Hawkins, C.J. Chem. Commun., (1968), 689.
23. Sarneski, J.E.; Urbach, F.L. J. Am. Chem. Soc., (1971), 93, 884.
24. Polonski, T. Tetrahedron, (1975), 31, 347.
25. Gacek, M.; Undheim, K. Tetrahedron, (1973), 29, 863.
26. Hawkins, C.J.; Lawrance, G.A. Aust. J. Chem., (1973), 26, 1801.
27. Scopes, P.M.; Thomas, R.N.; Rahman, M.B. J. Chem. Soc. C, (1971), 1671.
28. Gaffield, W.; Galetto, W. Tetrahedron, (1971), 27, 915.
29. Listowsky, I.; Avigad, G.; England, S. J. Org. Chem., (1970), 35, 1080.
30. Barth, G.; Voelter, W.; Bunnenberg, E.; Djerassi, C. J. Am. Chem. Soc., (1970), 92, 875.
31. Barth, G.; Voelter, W.; Bunnenberg, E.; Djerassi, C. Chem. Commun., (1969), 355.
32. Anand, R.D.; Hargreaves, M.K. Chem. Commun., (1967), 421.
33. Craig, J.C.; Pereira, W.E. Tetrahedron, (1970), 26, 3457.
34. Jørgensen, E.C. Tetrahedron Lett., (1971), 863.
35. Fowden, L.; Scopes, P.M.; Thomas, R.N. J. Chem. Soc. C, (1971), 833.
36. Hawkins, C.J.; Lawson, P.J. Chem. Commun., (1968), 177.
37. Hawkins, C.J.; Lawson, P.J. Inorg. Chem., (1970), 9, 6.
38. Hawkins, C.J.; Lawrance, G.A. Aust. J. Chem., (1971), 24, 2275.
39. Karabatsos, G.J.; Hsi, N. J. Am. Chem. Soc., (1965), 87, 2864.
40. Karabatsos, G.J.; Fenoglio, D.J. J. Am. Chem. Soc., (1969), 91, 1124.
41. Brown, T.L. Spectrochim. Acta, (1962), 18, 1615.
42. Laato, H.; Isotalo, R. Acta Chem. Scand., (1967), 21, 2119.
43. Richardson, F.S.; Strickland, R.W. Tetrahedron, (1975), 31, 2309.
44. Fleischer, E.B.; Frost, R. J. Am. Chem. Soc., (1965), 87, 3998.
45. Schipper, P.E. Personal communication, (1978).

RECEIVED September 13, 1979.

# The Nature of the Equilibrium Displacement Mechanism for the Pfeiffer Effect in Inorganic Chemistry

STANLEY KIRSCHNER and PAUL SERDIUK

Department of Chemistry, Wayne State University, Detroit, MI 48202

The Pfeiffer Effect (1) is defined as the change in optical rotation of an optically active system (usually a solution of one enantiomer of an optically active compound, called the "environment substance", dissolved in an optically inactive solvent) upon the addition of a racemic mixture of a dissymmetric, optically labile coordination compound. Much work has been done on this Effect (2 - 8) and several mechanisms have been proposed to explain it, which are described in a review by Schipper (9). It is of interest to note that the Effect can occur with racemic mixtures of certain optically labile complex cations (e.g., D,L-[Zn(o-phen)<sub>3</sub>]<sup>2+</sup>) whether the environment substance is anionic (d-α-bromo-camphor-π-sulfonate), neutral (levo-nicotine), or cationic (d-cinchoninium). The most frequently used solvent for the Pfeiffer Effect is water (10), although the Effect is known to occur in other solvents as well (3,4,6).

Since the magnitude of the Effect is proportional to the concentrations of both the environment substance and the complex, a series of equations have been developed for observed Pfeiffer rotation, specific Pfeiffer rotation, and molar Pfeiffer rotation which are analagous to those for observed optical rotation, specific optical rotation, and molar optical rotation (3,4,6,10). These are

$$P_{\text{obs.}} = \alpha_{\text{e+c}} - \alpha_{\text{e}} \quad (1)$$

$$[P]_{\lambda}^{\text{t}} = P_{\text{obs.}} / (c)(e)(d) \quad (2)$$

$$[P_{\text{M}}]_{\lambda}^{\text{t}} = P_{\text{obs.}} / [c][e](d_{\text{m}}) \quad (3)$$

0-8412-0538-8/80/47-119-239\$05.00/0

© 1980 American Chemical Society

where  $P_{\text{obs}}$  is the observed Pfeiffer rotation (in degrees),  $\alpha_{e+c}$  is the observed rotation of the solution containing the racemic complex and the environment substance,  $\alpha_e$  is the observed rotation of the solution containing the environment substance only,  $[P]$  is the specific Pfeiffer rotation,  $(c)$  is the concentration of the complex in g/ml,  $(e)$  is the concentration of the environment substance in g/ml,  $d$  is the path length in dm,  $[P_M]$  is the molar Pfeiffer rotation,  $[c]$  is the molar concentration of the complex,  $[e]$  is the molar concentration of the environment substance, and  $d_m$  is the path length in meters.

### The Equilibrium Displacement Mechanism

Dwyer and co-workers (2) and Kirschner and co-workers (3) have proposed that the enantiomers of racemic mixtures of optically labile, dissymmetric complexes are in equilibrium in solutions containing no environment substance, and that the equilibrium constant in such systems is equal to 1. However, in the presence of one enantiomer of an optically active environment substance, this equilibrium is shifted, with a consequent enrichment of one of the enantiomers of the complex, thereby changing the equilibrium constant to something greater or less than 1. An equation which represents a typical Pfeiffer Effect equilibrium is:

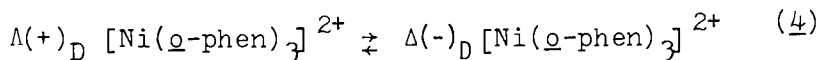


Figure 1 shows the Pfeiffer Effect for the racemic complex  $[\text{Cr}(\text{C}_2\text{O}_4)_3]^{3-}$  in the presence of  $\underline{d}$ -cinchoninium chloride, and this figure also provides strong support for the equilibrium displacement mechanism described above. It should be noticed that the optical rotatory dispersion (ORD) of the complex in the Pfeiffer Effect (Figure 1) is essentially the same as that of the pure enantiomer resolved by conventional means, and it shows a marked Cotton Effect. Since the environment substance itself shows only a plain or normal optical rotatory dispersion in the visible region, the ORD in the Pfeiffer experiment must be due to an excess of one enantiomer of the complex over the other - which is what is postulated to occur in the equilibrium displacement mechanism.

It should be mentioned at this point that Yoneda and co-workers (11) present evidence in favor

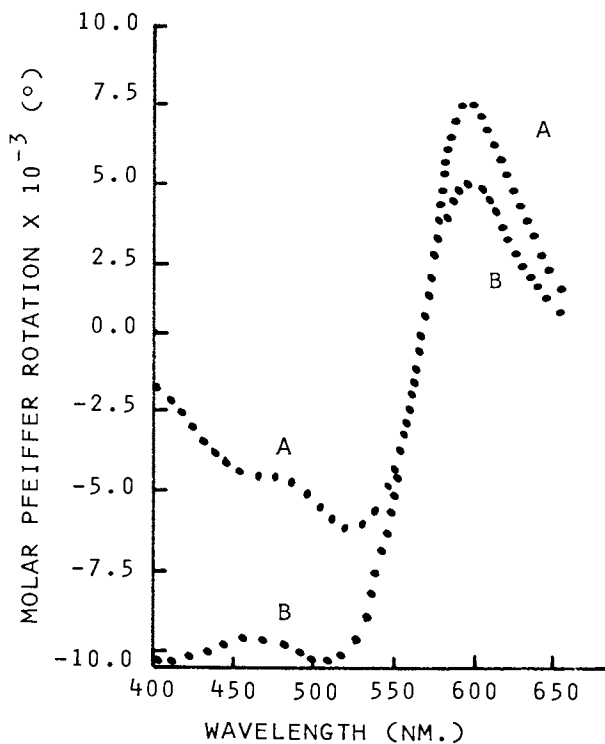


Figure 1. (A) Optical rotatory dispersion of (+)<sub>D</sub>-[Cr(C<sub>2</sub>O<sub>4</sub>)<sub>3</sub>]<sup>3-</sup> in water at 23°C; (B) Pfeiffer rotatory dispersion of D,L-[Cr(C<sub>2</sub>O<sub>4</sub>)<sub>3</sub>]<sup>3-</sup> in water at 23°C with d-cinchoninium chloride.

of a different mechanism for the Effect when cinchoninium cation is used as the environment substance for a complex of the same charge sign as the environment substance. This indicates that the mechanism of the Effect may be different when the environment substance and the complex both have charges of the same sign.

### The Time and Racemization Experiments

In support of the equilibrium displacement mechanism, a study of the Pfeiffer rotation of the system  $\underline{D,L}$ -[Ni(o-phen)<sub>3</sub>]<sup>2+</sup> with levo-malic acid as an environment substance in water produces some interesting results (Figure 2). The Pfeiffer Effect reaches its maximum in just over 4 days, and if, at that time, exactly as much dextro-malic acid is added to the system as the levo enantiomer already present, then this has the effect of removing (deactivating) the environment substance, so that the excess of the complex enantiomer has no alternative but to undergo racemization. It should be noted (Figure 3) that the rate of this racemization is identical to the racemization rate of the optically pure complex which has been resolved by conventional means.

It is also important to note that the Pfeiffer Rotatory Dispersion and the Pfeiffer Circular Dichroism of a given complex enantiomer (e.g.,  $\underline{L}$ -[Co(C<sub>2</sub>O<sub>4</sub>)<sub>3</sub>]<sup>3-</sup>), are the same as the ORD and CD of this complex resolved by conventional means (8).

### Absolute Configuration and Equilibrium Displacement

Further support for the equilibrium displacement mechanism arises from a study of the Pfeiffer Effect and the absolute configurations of the environment substances vs. the absolute configurations of those enantiomers of the complexes which are enriched during the appearance of the Pfeiffer Effect. Table 1 shows the sign of the optical rotation of the enriched enantiomer of the complex as a function of the absolute configuration of the environment substance. It can be seen from Table I that the same enantiomer (D-line) of the tris(bidentate) complex is enriched whenever the environment substance has the same absolute configuration, regardless of the sign of rotation of that environment substance. This indicates that whenever a racemic mixture of an optically labile complex "senses" an environment of a given absolute configuration, the equilibrium between the enantiomers

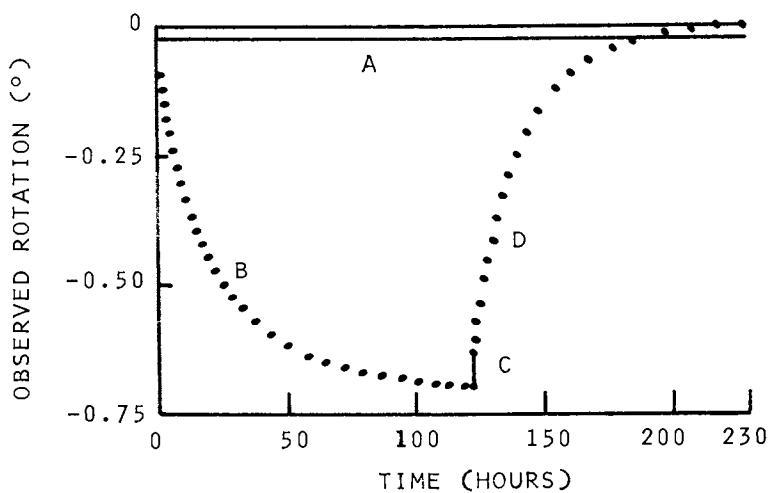


Figure 2. Pfeiffer Effect and the racemization of  $[\text{Ni}(\text{o-phen})_3]\text{Cl}_2$  in water with malic acid as the environment substance. Optical rotation as a function of time is given for: (A) l-malic acid; (B) l-malic acid +  $\text{D,L-}[\text{Ni}(\text{o-phen})_3]\text{Cl}_2$ ; (C) System B + d-malic acid; (D) racemization of the excess L- $[\text{Ni}(\text{o-phen})_3]\text{Cl}_2$  produced by the Pfeiffer Effect (System C allowed to decay).

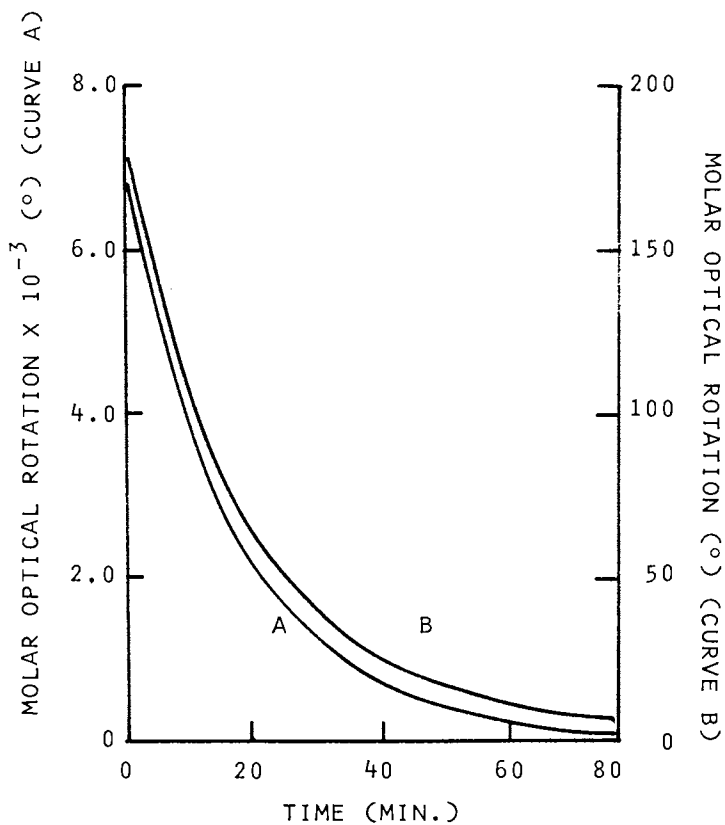


Figure 3. The racemization of the (+)<sub>D</sub> enantiomer of  $[\text{Cr}(\text{C}_2\text{O}_4)_3]^{3-}$  in water at 23°C: (A) the optically pure complex resolved by conventional techniques; (B) the complex partially resolved via the Pfeiffer Effect technique.



of the complex shifts in the same direction, regardless of the sign of rotation of the environment substance (12).

In addition, whenever an environment substance of a given absolute configuration is utilized in the Pfeiffer Effect, the absolute configuration of the complex enantiomer which is enriched during the Effect is fixed. Table II shows the absolute configurations of the enriched enantiomer of the complexes which are produced during the Pfeiffer Effect with enantiomers of environment substances of a given absolute configuration.

Table I.

The Pfeiffer Effect on  $D,L-[Co(\underline{o}\text{-phen})_3]Cl_2$  with Various Environment Substances

| Environment Substance          | Absolute Configuration of Environment | Sign of Rotation of Enriched Complex |
|--------------------------------|---------------------------------------|--------------------------------------|
| (+) <sub>D</sub> Tartaric Acid | RR                                    | Dextro                               |
| (-) <sub>D</sub> Mandelic Acid | R                                     | Dextro                               |
| (+) <sub>D</sub> Malic Acid    | R                                     | Dextro                               |
| (-) <sub>D</sub> Tartaric Acid | SS                                    | Levo                                 |
| (-) <sub>D</sub> Malic Acid    | S                                     | Levo                                 |
| (+) <sub>D</sub> Aspartic Acid | S                                     | Levo                                 |
| (+) <sub>D</sub> Alanine       | S                                     | Levo                                 |

Table II.

Absolute Configurations of Complexes in Pfeiffer Systems

| Environment Substance           | Enriched Complex Enantiomer                       | Predicted Absolute Configuration | Observed Absolute Configuration |
|---------------------------------|---|----------------------------------|---------------------------------|
| S(+) <sub>D</sub> aspartic acid | (-) <sub>D</sub> Ni( <u>o</u> -phen) <sub>3</sub> | 2+ $\Delta$                      | $\Delta$                        |
| S(+) <sub>D</sub> aspartic acid | (+) <sub>D</sub> Fe( <u>o</u> -phen) <sub>3</sub> | 2+ $\Delta$                      | $\Delta$                        |
| S(-) <sub>D</sub> malic acid    | (-) <sub>D</sub> Ni( <u>o</u> -phen) <sub>3</sub> | 2+ $\Delta$                      | $\Delta$                        |
| S(-) <sub>D</sub> malic acid    | (+) <sub>D</sub> Fe( <u>o</u> -phen) <sub>3</sub> | 2+ $\Delta$                      | $\Delta$                        |

This observation appears to be general for the Pfeiffer Effect with tris(bidentate) complexes and environment substances which are organic compounds capable of undergoing hydrogen bonding (12), and it provides a technique for predicting the absolute configurations of dissymmetric, optically labile complexes, as well as of organic acids capable of acting as environment substances in the Pfeiffer Effect. Yoneda and co-workers (11) have pointed out that this observation does not hold when the environment substance is d-cinchoninium cation, in support of a different mechanism for the Pfeiffer Effect in this case.

### Hydrogen Bonding and the Pfeiffer Effect

Several papers have appeared in the literature (13,14) describing hydrogen bonding to the  $\pi$ -electron clouds of aromatic systems, and they point out that the hydrogen bond is in a line perpendicular to the plane of the  $\pi$ -electron cloud. It is proposed that the fundamental nature of the Pfeiffer Interaction between the environment substance and the complex (which is operative in the equilibrium displacement mechanism) is hydrogen bonding between OH groups of the environment compound and the  $\pi$ -electron clouds of the ligands of the complex. Figure 4 shows schematically the "head-on" type of hydrogen bonding which occurs with aromatic systems and which is proposed to occur for the Pfeiffer systems described herein.

Support for this proposal comes from a study of the pH dependence of the Pfeiffer Effect. It can be seen from Table III that an increase in pH results in a marked diminution of the magnitude of the Pfeiffer Effect—a result which would not be expected on the basis of an ionic attraction between the complex and the environment substance. This is due to the fact that an increase in pH of a system where malic acid is the environment substance, for example, would result in the formation of the hydrogen malate or malate anions, which might be expected to be more strongly attracted to the complex cation than malic acid itself. This is clearly not the case, as can be seen from Table III, since the Pfeiffer Effect decreases in magnitude with increasing pH.

Rather, this decrease in magnitude of the Pfeiffer Effect with increasing pH may now be explained as a result of the markedly decreased ability of the malic acid to undergo hydrogen bonding to the aromatic electron cloud, since the hydrogens necessary for this hydrogen bonding are removed as the pH of the system increases.

Table III.

The Pfeiffer Effect and pH for the System Levo-Malic Acid and D,L-[Ni(o-phen)<sub>3</sub>]Cl<sub>2</sub>

| pH  | [P <sub>M</sub> ] <sub>D</sub> <sup>25°</sup> (°) |
|-----|---|
| 1.0 | 2680  |
| 2.0 | 2660  |
| 3.0 | 1980  |
| 4.0 | 820   |
| 5.0 | 380   |
| 6.0 | 320   |
| 7.0 | 340   |
| 8.0 | 80  |
| 9.0 | 120   |

#### Environment Compounds With No Available Hydrogen for Hydrogen Bonding

In order to provide additional tests for the hydrogen bonding proposal, it was decided to study the Pfeiffer Effect with environment substances having reduced (and zero) capacity for hydrogen bonding to the aromatic electron clouds of the ligands of the complexes. Figure 5 shows the formulae of tartaric acid and several of its derivatives which have been utilized in this study. It should be noted that the 2-methoxy-2-hydroxy derivative provides some opportunity for hydrogen bonding, whereas the other two succinate derivatives provide no such opportunity.

Tables IV-VIII describe the Pfeiffer Effect on the D,L-[Ni(o-phen)<sub>3</sub>]<sup>2+</sup> with (+)<sub>D</sub>-tartaric acid, sodium hydrogen (+)-tartrate, the diethyl-2-methoxy-3-hydroxy derivative, the diethyl-2,3-dimethoxy derivative, and the dimethyl-2-3-dimethoxy derivative. As can be seen from their structures, the first three of these compounds have the ability to undergo hydrogen bonding, while the last two do not. Tables IV, V, and VI clearly indicate that significant Pfeiffer Effects occur in the systems containing those environment substances capable of undergoing hydrogen bonding, whereas Tables VII and VIII show that no significant Pfeiffer Effect occurs in those systems containing environment substances which are incapable of undergoing hydrogen bonding. This provides additional evidence in support of the proposed hydrogen bonding mechanism mentioned above.

**American Chemical  
Society Library**

1155 16th St. N. W.

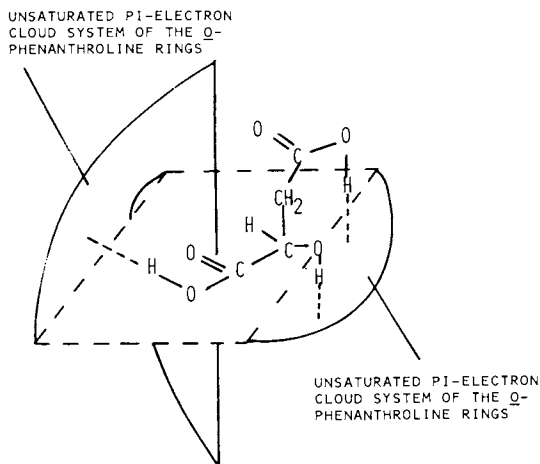


Figure 4. Hydrogen bonding mechanism. Proposed for the Pfeiffer Effect. "Head-on" hydrogen bonding to  $\pi$ -electron clouds of ligand ring systems;  $\Delta(-)$ - $[\text{Ni}(\alpha\text{-phen})_2]^{2+}$  with  $S(-)_D$ -malic acid.

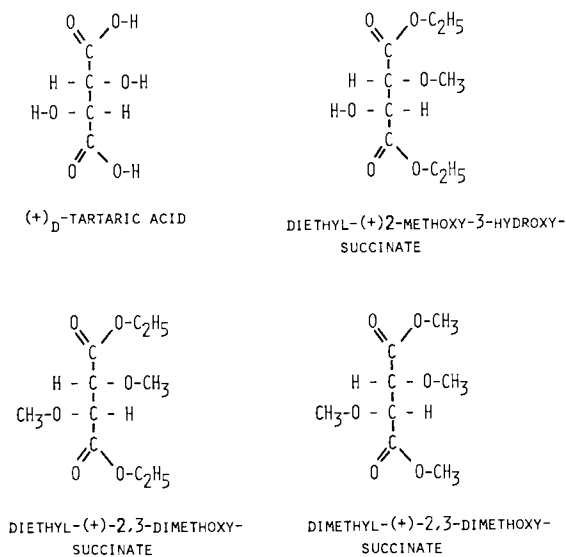


Figure 5. Tartaric acid and substituted tartaric acids

TABLE IV.  
 THE PFEIFFER EFFECT WITH (+)<sub>D</sub>-TARTARIC ACID  
 OBSERVED OPTICAL ROTATION IN DEGREES

| $\lambda$ (NM.) $\rightarrow$ | <u>589</u> | <u>578</u> | <u>546</u> | <u>436</u> |
|-------------------------------|------------|------------|------------|------------|
| <u>TIME</u>                   |            |            |            |            |
| 4 MIN.                        | 0.101      | 0.120      | 0.140      | 0.209      |
| 1 HOUR                        | 0.127      | 0.139      | 0.159      | 0.252      |
| 2 HOURS                       | 0.140      | 0.152      | 0.175      | 0.286      |
| 3.66 "                        | 0.159      | 0.172      | 0.196      | 0.328      |
| 5.33 "                        | 0.181      | 0.191      | 0.220      | 0.379      |
| 7.33 "                        | 0.198      | 0.211      | 0.242      | 0.428      |
| 27.0 "                        | 0.352      | 0.372      | 0.431      | 0.830      |
| 53.3 "                        | 0.440      | 0.465      | 0.538      | 1.055      |
| 75.2 "                        | 0.475      | 0.500      | 0.579      | 1.136      |
| 98.0 "                        | 0.488      | 0.513      | 0.593      | 1.165      |

COMPLEX: TRI(ORTHO-PHENANTHROLINE)NICKEL(II)

PATH LENGTH: 1 DECIMETER

SOLVENT: WATER; TEMPERATURE: 23<sup>o</sup> C.

CONCENTRATIONS: COMPLEX - 0.02 MOLAR

ENVIRONMENT - 0.04 MOLAR

TABLE V.  
 THE PFEIFFER EFFECT WITH  
 SODIUM HYDROGEN (+)<sub>D</sub>-TARTRATE.  
 OBSERVED OPTICAL ROTATION IN DEGREES

| $\lambda$ (NM.) $\rightarrow$ | <u>589</u> | <u>578</u> | <u>546</u> | <u>436</u> |
|-------------------------------|------------|------------|------------|------------|
| <u>TIME</u>                   |            |            |            |            |
| 2 MINUTES                     | 0.185      | 0.195      | 0.221      | 0.340      |
| 1.33 HOURS                    | 0.189      | 0.201      | 0.226      | 0.348      |
| 3.33 "                        | 0.194      | 0.205      | 0.232      | 0.362      |
| 5.17 "                        | 0.205      | 0.215      | 0.242      | 0.386      |
| 25.0 "                        | 0.261      | 0.275      | 0.313      | 0.536      |
| 47.8 "                        | 0.288      | 0.301      | 0.345      | 0.595      |
| 73.0 "                        | 0.300      | 0.314      | 0.357      | 0.632      |
| 99.7 "                        | 0.303      | 0.318      | 0.360      | 0.641      |

COMPLEX: TRI(ORTHO-PHENANTHROLINE)NICKEL(II)

PATH LENGTH: 1 DECIMETER

SOLVENT: WATER; TEMPERATURE: 23<sup>o</sup> C.

CONCENTRATIONS: COMPLEX - 0.02 MOLAR

ENVIRONMENT - 0.04 MOLAR

TABLE VI.  
THE PFEIFFER EFFECT WITH  
DIETHYL-(+)-2-METHOXY-3-HYDROXYSUCCINATE  
OBSERVED OPTICAL ROTATION IN DEGREES

| $\lambda$ (NM.) $\rightarrow$ | <u>589</u> | <u>578</u> | <u>546</u> | <u>436</u> |
|-------------------------------|------------|------------|------------|------------|
| <u>TIME</u>                   |            |            |            |            |
| 5 MINUTES                     | 0.497      | 0.513      | 0.578      | 0.909      |
| 1 HOUR                        | 0.501      | 0.521      | 0.586      | 0.919      |
| 2 HOURS                       | 0.505      | 0.531      | 0.594      | 0.938      |
| 3 "                           | 0.510      | 0.532      | 0.599      | 0.950      |
| 4 "                           | 0.518      | 0.540      | 0.609      | 0.967      |

COMPLEX: TRI(ORTHO-PHENANTHROLINE)NICKEL(II)

PATH LENGTH: 1 DECIMETER

SOLVENT: WATER; TEMPERATURE: 23° C.

CONCENTRATIONS: COMPLEX - 0.02 MOLAR

ENVIRONMENT - 0.04 MOLAR

TABLE VII.

THE PFEIFFER EFFECT WITH  
DIETHYL-(+)-2,3-DIMETHOXYSUCCINATE  
OBSERVED OPTICAL ROTATION IN DEGREES

| $\lambda$ (NM.) $\rightarrow$ | <u>589</u> | <u>578</u> | <u>546</u> | <u>436</u> |
|-------------------------------|------------|------------|------------|------------|
| <u>TIME</u>                   |            |            |            |            |
| 5 MINUTES                     | 0.854      | 0.887      | 1.000      | 1.608      |
| 4 HOURS                       | 0.861      | 0.894      | 1.008      | 1.608      |

COMPLEX; TRI(ORTHO-PHENANTHROLINE)NICKEL(II)  
PATH LENGTH: 1 DECIMETER  
SOLVENT: WATER; TEMPERATURE: 23° C.  
CONCENTRATIONS: COMPLEX - 0.02 MOLAR  
ENVIRONMENT - 0.04 MOLAR

TABLE VIII.

THE PFEIFFER EFFECT WITH  
DIMETHYL-(+)-2,3-DIMETHOXYSUCCINATE  
OBSERVED OPTICAL ROTATION IN DEGREES

| $\lambda$ (NM.) $\rightarrow$ | <u>589</u> | <u>578</u> | <u>546</u> | <u>436</u> |
|-------------------------------|------------|------------|------------|------------|
| <u>TIME</u>                   |            |            |            |            |
| 5 MINUTES                     | 0.219      | 0.226      | 0.256      | 0.400      |
| 1.5 HOURS                     | 0.218      | 0.226      | 0.256      | 0.401      |
| 3.3 "                         | 0.217      | 0.224      | 0.252      | 0.399      |
| 4.2 "                         | 0.215      | 0.223      | 0.248      | 0.396      |

COMPLEX: TRI(ORTHO-PHENANTHROLINE)NICKEL(II)  
PATH LENGTH: 1 DECIMETER  
SOLVENT: WATER; TEMPERATURE: 23° C.  
CONCENTRATIONS: COMPLEX - 0.02 MOLAR  
ENVIRONMENT - 0.04 MOLAR



### Experimental

All optical rotation measurements, optical rotatory dispersions, and circular dichroism spectra were determined on a Cary-60 spectropolarimeter with circular dichroism attachment. In addition, some optical rotations were determined on a Perkin-Elmer Model 141 photoelectric polarimeter. Only reagent grade chemicals were used in the syntheses mentioned below.

The succinate derivatives described in Figure 5 were prepared by the methods of Purdie, Irvine, and Gillis (15). All Pfeiffer Effect studies with these environment compounds were carried out in water under the conditions described in Tables IV-VIII.

### Acknowledgement

The authors wish to express their sincere appreciation to the National Science Foundation for a research grant which contributed significantly to the progress of this investigation.

### Literature Cited

1. Pfeiffer, P. and Quehl, K., *Ber.* (1931) 64, 2667; (1932) 65, 560.
2. Dwyer, F. P., Gyarfás, E. G., and O'Dwyer, M. F., *Nature* (1951) 167, 1036; *J. Proc. Roy. Soc. N.S.W.* (1955) 89, 146.
3. Kirschner, S. and Ahmad, N., *J. Am. Chem. Soc.* (1968) 90, 1910; *Inorg. Chim. Acta.* (1975) 14, 215; Pollock, R. J., Kirschner, S., and Pollice, S., *Inorg. Chem.* (1977) 16, 522.
4. Kirschner, S. and Ahmad, N. in "Coordination Chemistry", Proceedings of the John C. Bailar, Jr. Symposium, Kirschner, S., Ed., Plenum Publishing Corp., New York, (1969).
5. Gyarfás, E. C., *Rev. Pure and Applied Chem.* (1954) 4, 73; Gunter, J. D. and Schreiner, A. F., *Inorg. Chim. Acta.* (1975) 15, 117.
6. Kirschner, S. and Ahmad, N., in "Progress in Coordination Chemistry", Cais, M., ed., Elsevier (1968); *Rec. Chem. Progr.* (1971) 32, 29; Ahmad, N., Ph.D. Dissertation, Wayne State University, 1969.

7. Turner, E. E. and Harris, M. M., Quart. Revs. (1948) 1, 299.
8. Brasted, R. C., Landis, Kuhajek, E. J., Nordquist, P. E. R. and Mayer, L., in "Coordination Chemistry", Kirschner, S., ed., Plenum Press, N. Y. (1969).
9. Schipper, P. E., Inorg. Chim Acta (1975) 12, 199.
10. Kirschner, S. and Magnell, K. R., in "Werner Centennial", Advances in Chemistry Series No. 62, pp. 366 ff. (1966).
11. Mijoshi, K., Kuroda, Y., Takeda, J., Yoneda, H., and Takagi, I., in press; Miyoshi, K., Sakata, K., and Yoneda, H., J. Phys. Chem., (1976) 80, 649; (1975) 79, 1622; Miyoshi, K., Kuroda, Y., and Yoneda, H., Ibid, (1976) 80, 270 649.
12. Kirschner, S., Ahmad, N., Munir, C., Pollock, Pure and Applied Chemistry (1979) 51, 913.
13. Iwamura, H., Tetrahedron Letters, (1970) 2227; Yoshida, Z. and Osawa, E. O., J. Am. Chem. Soc. (1966) 88, 4019.
14. Krueger, P. J. and Mette, H. D., Tetrahedron Letters, (1966) 1587; Oki, M. and Iwamura, H., J. Am. Chem. Soc., (1967) 89, 576.
15. Gillis, R. G., Tetrahedron Letters (1968) No. 12, 1413.

RECEIVED September 13, 1979.

# Phenyl Substituent Contributions in Circular Dichroism Spectra of Cobalt(III) Complexes of Ethylenediamine-*N,N'*-diacetate Ion

GARY G. HAWN<sup>1</sup>, CHRIS MARICONDI<sup>2</sup>, and BODIE E. DOUGLAS

Department of Chemistry, University of Pittsburgh, Pittsburgh, PA 15260

## Additivity of Circular Dichroism Contributions

The major contribution to the rotational strength of optically active complexes of transition metals is usually the chiral arrangement of chelate rings. The additivity of the contributions to the rotational strength was demonstrated (1) for complexes of the type  $[\text{Co}(\text{en})_2(\text{aa})]^{2+}$  (aa = amino acid anion). The  $\Delta$ - and  $\Lambda$ - isomers of  $[\text{Co}(\text{en})_2(\text{S-pala})]^{2+}$  are diastereoisomers, not enantiomers. The CD curves (Figure 1) are not mirror images. The sum of the 2 CD curves is the same as the CD curve for the unresolved complex, an active racemate. The contributions for the  $\Delta$  and  $\Lambda$  arrangements of the chelate rings should cancel for this "vicinal effect" curve, giving twice the contribution of the coordinated S-phenylalaninate ligand. Subtraction of one-half of this CD curve from the curve for either  $\Delta$ - or  $\Lambda$ -  $[\text{Co}(\text{en})_2(\text{S-pala})]^{2+}$  gives a curve which agrees well with the CD curve of one of the isomers of  $[\text{Co}(\text{en})_2(\text{gly})]^{2+}$ . Since the chelate rings of the amino acid ligands are nearly planar, the contribution of an optically active amino acid ligand is expected to be primarily that of the asymmetric center, with little conformational contribution. Yasui, Hidaka, and Shimura (2) found that the CD curve in the  ${}^1\text{T}_{1g}(\text{O}_h)$  band region for a series of "typical" optically active amino acid complex ions of the type  $[\text{Co}(\text{NH}_3)_4(\text{aa})]^{2+}$  are similar to the "vicinal effect" CD curves of optically active amino acids in complex ions of the type  $[\text{Co}(\text{en})_2(\text{aa})]^{2+}$ . Earlier Shimura (3) had observed the Cotton effect caused by the optically active ligand in the complex ion  $[\text{Co}(\text{NH}_3)_4(\text{S-leucinato})]^{2+}$  and referred to this as a "vicinal" effect. Pfeiffer (4) introduced the term "vicinal" effect for Cotton effects caused by optically active ligands.

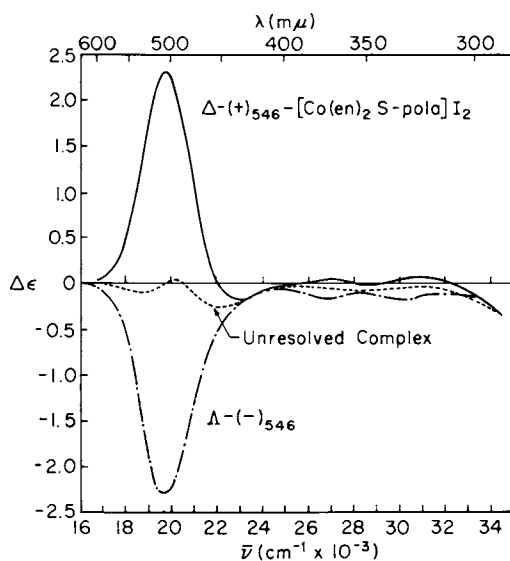
In the case of S-propylenediamine, the methyl substituent causes the conformation of coordinated S-pn ( $\underline{\ell}$ -pn) to be fixed so that the chiral conformation would make a contribution to the rotational strength also. The CD curves for (+)- $[\text{Co}(\text{en})(\underline{\ell}\text{-pn})_2]^{3+}$  (5) has a single broad peak in the  ${}^1\text{T}_{1g}(\text{O}_h)$  region while that for

<sup>1</sup> Current address: Alcolac Inc., 3440 Fairfield Rd., Baltimore, MD 21226

<sup>2</sup> Current address: Pennsylvania State University, McKeesport, PA 15123

0-8412-0538-8/80/47-119-255\$05.00/0

© 1980 American Chemical Society



Inorganic Chemistry

Figure 1. CD curves for the two isomers of  $[Co(en)_2S-pala]^+$  and the unresolved complex (1)

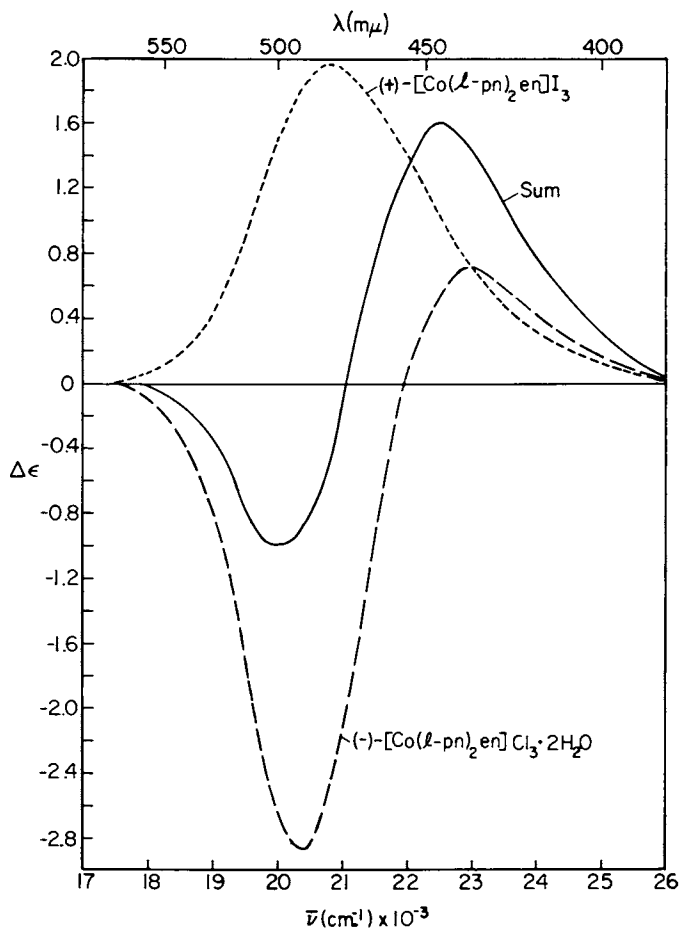
(-)-[Co(en)( $\underline{\ell}$ -pn) $_2$ ] $^{3+}$  shows two distinct components (Figure 2). The contribution from  $\underline{\ell}$ -pn, obtained by adding these curves, shows a stronger contribution to the  $^1A_2(D_3)$  component than to the  $^1E(D_3)$  component. The  $^1E$  component is much more intense than the  $^1A_2$  component for [Co(en) $_3$ ] $^{3+}$ . Subtraction of the contribution from  $\underline{\ell}$ -pn gives "configurational effect" curves for both isomers of [Co(en)( $\underline{\ell}$ -pn) $_2$ ] $^{3+}$  (Figure 3) which are similar to the CD curves of the corresponding isomers of [Co(en) $_3$ ] $^{3+}$ . The same contribution per  $\underline{\ell}$ -pn can be used for [Co(en) $_2$ ( $\underline{\ell}$ -pn) $^{3+}$  and [Co( $\underline{\ell}$ -pn) $_3$ ] $^{3+}$  to show that the effects are approximately additive. One might expect the contributions from  $\underline{\ell}$ -pn to differ somewhat depending on the number of  $\underline{\ell}$ -pn ligands present because of steric effects. Ogino, Murano, and Fujita (6) showed that the contribution of  $\underline{\ell}$ -pn in the tris(propylenediamine) complex is remarkably similar to the CD curve of [Co(NH $_3$ ) $_4$ ( $\underline{\ell}$ -pn)] $^{3+}$ .

Additivity of the various contributions has been demonstrated for many complexes. The contributions are from the chiral configuration of chelate rings (configurational effect), the chiral chelate conformation (conformational effect), and the presence of asymmetric centers in the ligands. As expected, the contributions are considerably greater for asymmetric atoms which are coordinated to the chromophore than for others (see below). The contributions from chiral ring conformations and from asymmetric centers on the ligands often are inseparable. Complexes of 2,2'-diaminobiphenyl (dabp) of the type [Co(dabp)(en) $_2$ ] $^{3+}$  have been of interest (7, 8) since the coordinated non-planar dabp is chiral without an asymmetric center.

### Circular Dichroism of Ethylenediaminediacetic Acid Complexes

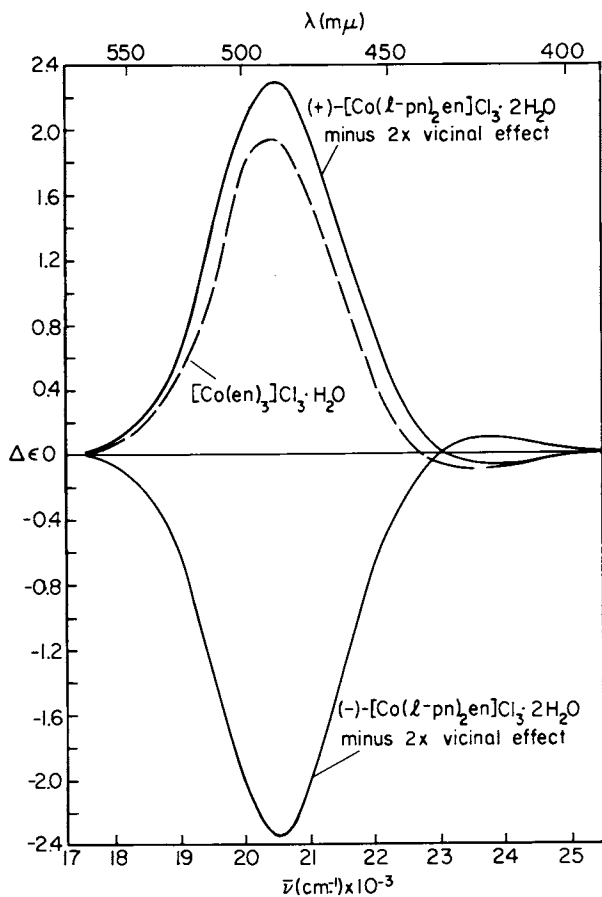
In general the rotational strength of a metal complex depends on the number of chelate rings as well as the size and rigidity of the rings. Ethylenediaminediacetate (edda) is a quadridentate ligand which can form two isomers (Figure 4) with the other two coordination sites cis. The sym-cis isomer is the one easily obtained. In the case of the sym-cis-[Co(edda)X $_2$ ] $^{n+}$  complexes the CD spectra are remarkably insensitive to the nature of the two X groups (9, 10, 11). They can be unidentate (NH $_3$ ), or bidentate with varying ring size (ethylenediamine or trimethylenediamine) (Figure 5) (11), or even the bidentate oxygen ligands CO $_3^{2-}$ , C $_2$ O $_4^{2-}$ , and O $_2$ CCH $_2$ CO $_2^{2-}$  (10), or amino acids (9).

The high CD intensities for sym-cis-[Co(edda)en] $^{+}$  and related complexes might be attributed to the rigid edda backbone, but also the coordinated N atoms are asymmetric. If one replaces the H substituents on the N atoms by methyl groups, the intensity of the major CD peak decreases by more than a factor of two (12) (Figure 6). Replacement of the methyl groups by ethyl groups causes a further slight decrease. It appears that there is a large contribution from the coordinated asymmetric nitrogens in



Inorganic Chemistry

Figure 2. CD curves for (+)- and (-)- $[Co(l-pn)_2en]^{3+}$  and the sum of the two curves (5)



Inorganic Chemistry

Figure 3. The configurational effect curves for (+)- and (-)- $[\text{Co}(l\text{-}pn)_2en]^{3+}$  obtained by subtracting the vicinal contribution of 2  $l\text{-}pn$ . The CD curve for (+)- $[\text{Co}(en)_3]^{3+}$  is shown for comparison (5).

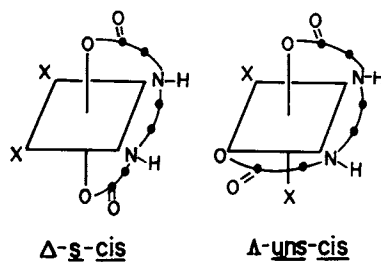
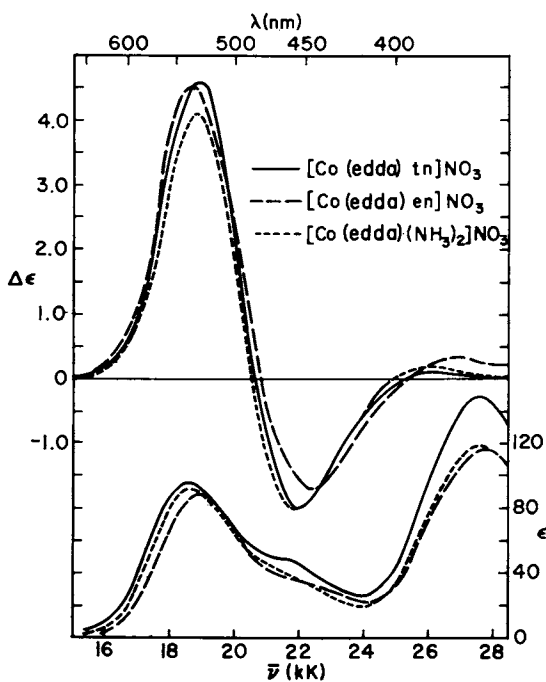


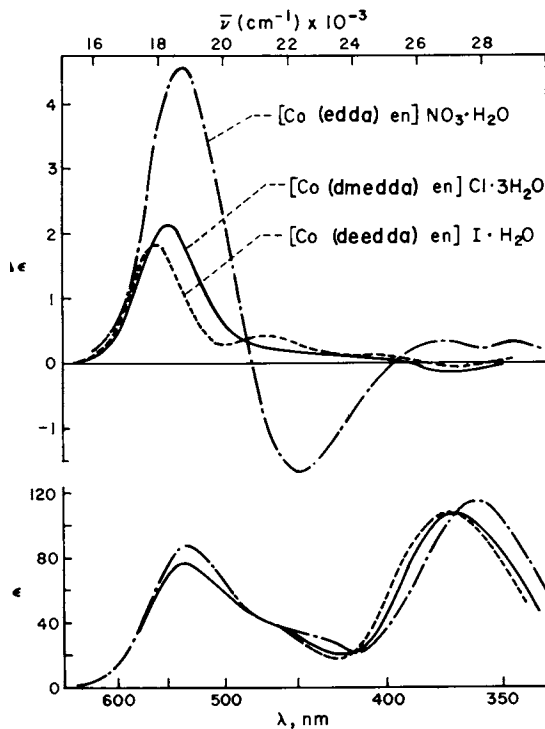
Figure 4. Structures of the *s*-cis and *uns*-cis isomers of  $[\text{Co}(\text{edda})\text{X}_2]$



Inorganic Chemistry

Figure 5. Absorption and CD spectra of *s*-cis- $[\text{Co}(\text{edda})\text{en}]\text{NO}_3$ , *s*-cis- $[\text{Co}(\text{edda})\text{tn}]\text{NO}_3$ , and *s*-cis- $[\text{Co}(\text{edda})(\text{NH}_3)_2]\text{NO}_3$  (11)





Inorganic Chemistry

Figure 6. Absorption and CD spectra of *s-cis*-[Co(edda)en]NO<sub>3</sub> · H<sub>2</sub>O and the corresponding complexes of *N,N'*-dimethyl and *N,N'*-diethyl ethylenediamine-*N,N'*-diacetic acid (12)

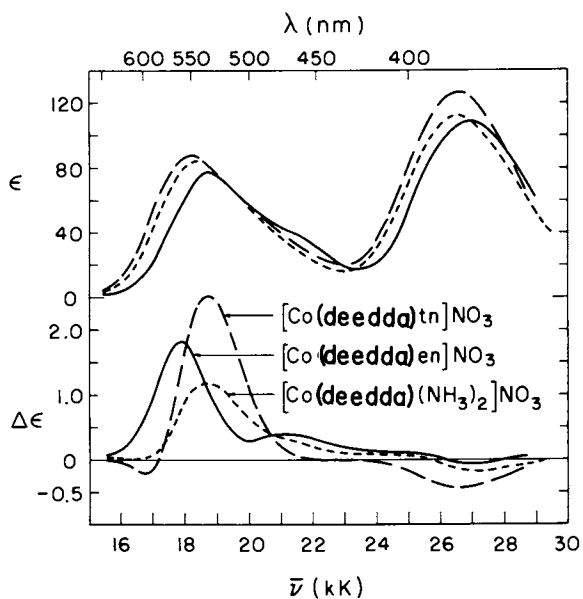
the unsubstituted edda complexes where one of the substituents (H) on N is much different from the other two first neighbor substituent atoms (both CH<sub>2</sub> or one CH<sub>2</sub> and one CH<sub>3</sub>). In the case of alkyl substituted edda complexes (Figure 7), the CD spectra show the usual dependence on the nature of the other ligand(s) (11).

Maricondi and Maricondi (13) showed that benzyl substituents on the N atoms of edda caused a significant change in CD intensities in comparison to methyl substituents (Figure 8) and the "vicinal" contributions of -CH<sub>2</sub>C<sub>6</sub>H<sub>5</sub> and -H substituents are of reversed signs in comparison to -CH<sub>3</sub> substituents (Figure 9). The comparison is even more striking in the case of [Co(ed3a)NO<sub>2</sub>]<sup>-</sup> (ed3a = N,N,N'-ethylenediaminetriacetate ion) and the methyl and benzyl substituted ed3a complexes (Figure 10).

Contributions of Stilbenediamine. The complex [Co(edda)(l-stien)]<sup>+</sup> (l-stien = l-stilbenediamine) was prepared (14) to estimate the contribution from the asymmetric carbons of stilbenediamine. There has been some controversy (15, 16, 17, 18) over the assignment of absolute configuration for l-stien, but a recent X-ray determination (19) established that l-stien has the SS configuration and adopts the  $\delta$  conformation in the tris complex. The formation of [Co(edda)(l-stien)]<sup>+</sup> was stereoselective, favoring the formation of the isomer (70% of product) having a dominant negative CD peak (Figure 11). This isomer is assigned the  $\Delta$ -configuration based on the close similarities to the CD spectra of other edda-diamine complexes (9, 10, 11, 12). This is also the isomer with more favorable steric interactions as revealed by examination of models. The contribution of l-stien to the CD curve is negative (14) throughout the visible range, with a maximum contribution of about 0.6 ( $\Delta\epsilon$ ). The edda ligand still dominates the CD spectrum.

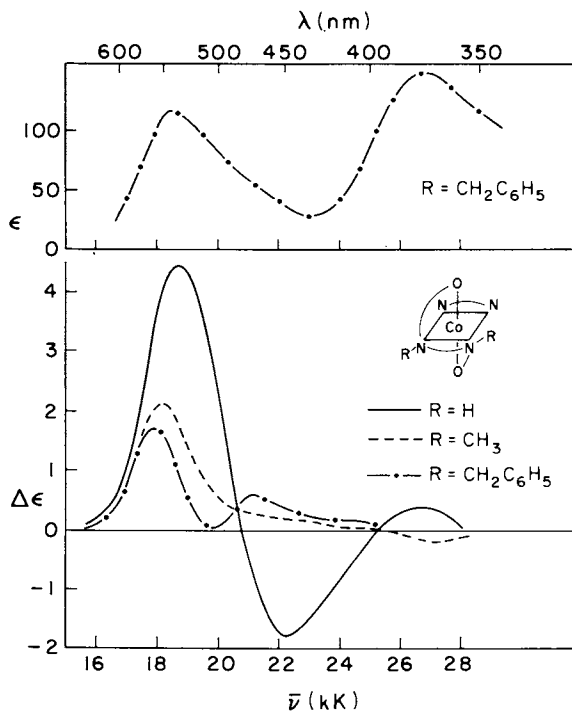
The complex [Co(l-sdda)en]<sup>+</sup> (l-sdda = l-stilbenediaminediacetate ion) contains the l-stilbenediamine backbone, but each nitrogen has as substituents -CH<sub>2</sub>CO<sub>2</sub>, -H, and -CHC<sub>6</sub>H<sub>5</sub>). Only one isomer of [Co(l-sdda)en]<sup>+</sup> was obtained. Both [Co(edda)-(l-stien)]<sup>+</sup> and [Co(l-sdda)en]<sup>+</sup> were shown (14) to have s-cis geometry from their absorption spectra and simple <sup>13</sup>C NMR spectra. In each case the absorption spectrum shows a shoulder in the <sup>1</sup>T<sub>1g</sub>(O<sub>h</sub>) band region, indicating two tetragonal (effective D<sub>4h</sub>) components (<sup>1</sup>E and <sup>1</sup>A<sub>2</sub>). The stereospecificity of [Co(l-sdda)en]<sup>+</sup> is not surprising since the preferred  $\delta$ -conformation permits the two large phenyl substituents of l-sdda to occupy equatorial positions.

Since the CD spectrum of the one isomer of the [Co(l-sdda)-en]<sup>+</sup> (Figure 12) shows a positive dominant CD peak and an overall CD curve similar to that of (+)-s-cis-[Co(edda)(l-stien)]<sup>+</sup>, it might be expected to have the  $\Lambda$ -configuration. However, the  $\Lambda$ -s-cis-configuration would require the l-stilbenediamine backbone to have the  $\lambda$ -conformation, forcing the large



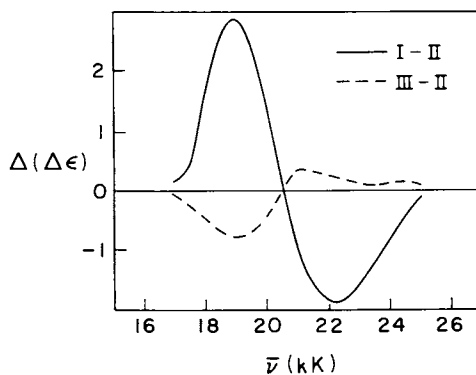
Inorganic Chemistry

Figure 7. Absorption and CD spectra of *s-cis*- $[\text{Co}(\text{deedda})\text{tn}]\text{NO}_3$ , *s-cis*- $[\text{Co}(\text{deedda})\text{en}]\text{NO}_3$ , and *s-cis*- $[\text{Co}(\text{deedda})(\text{NH}_3)_2]\text{NO}_3$  (11)



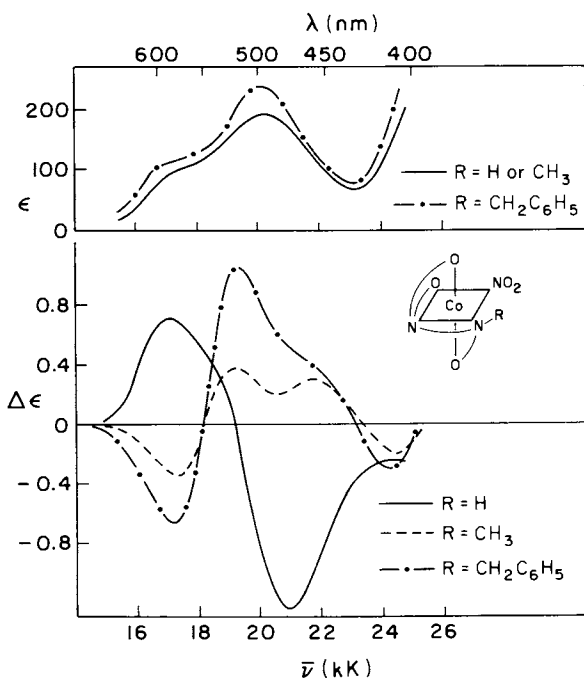
Inorganic Chemistry

Figure 8. Absorption and CD spectra of  $[\text{Co}(\text{dbdda})\text{en}]^+$  and CD spectra of  $[\text{Co}(\text{edda})\text{en}]^+$  and  $[\text{Co}(\text{dmdda})\text{en}]^+$  (13)



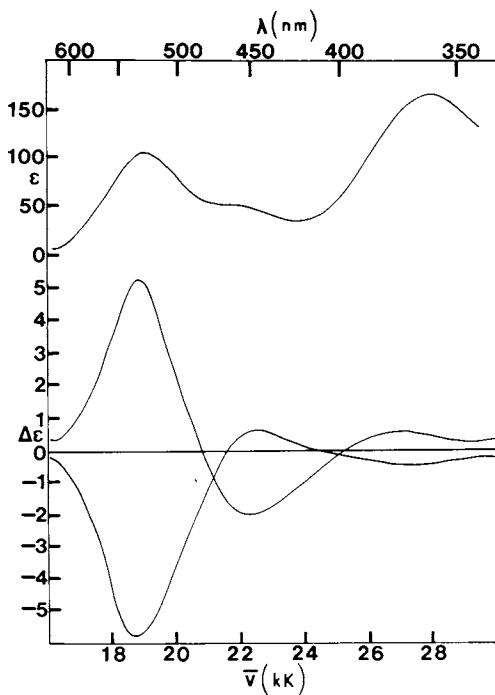
Inorganic Chemistry

Figure 9. Difference CD curves:  $\Delta\epsilon[\text{Co}(\text{edda})\text{en}]^+ - \Delta\epsilon[\text{Co}(\text{dmedda})\text{en}]^+$  (—) and  $\Delta\epsilon[\text{Co}(\text{dbedda})\text{en}]^+ - \Delta\epsilon[\text{Co}(\text{dmedda})\text{en}]^+$  (---) (13)



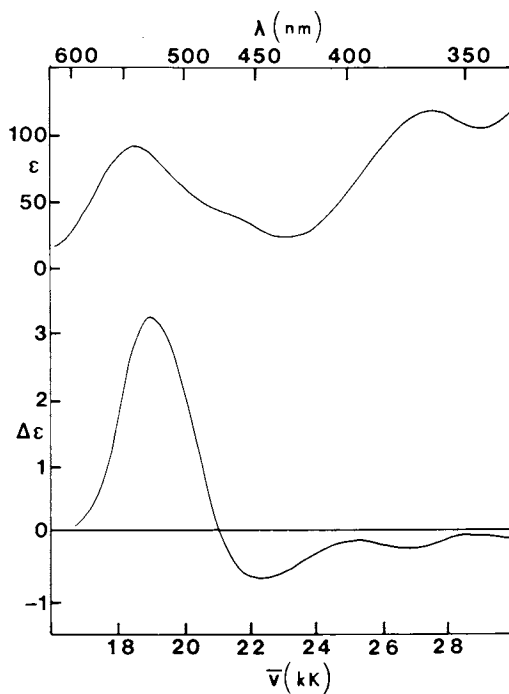
Inorganic Chemistry

Figure 10. Absorption and CD spectra for the  $(-)$ <sub>516</sub> isomers of  $[\text{Co}(\text{ed3a})\text{NO}_2]^-$  and  $[\text{Co}(\text{med3a})\text{NO}_2]^-$  (13)



Inorganic Chemistry

Figure 11. Absorption and CD spectra for the isomers of *s-cis*-[Co(edda)(1-stien)]<sup>+</sup> (14)



Inorganic Chemistry

Figure 12. Absorption and CD spectra for the one isomer of *s-cis*-[Co(1-*sdda*)-en]<sup>+</sup> obtained (14)

substituents into unfavorable axial positions. The favored  $\delta$ -conformation is expected, requiring that the isomer of  $[\text{Co}(\ell\text{-sdda})\text{en}]^+$  have the  $\Delta$ -configuration. Previous studies (10, 11) have shown that the unsubstituted chiral ring pattern for  $\Delta\text{-}[\text{Co}(\text{edda})\text{en}]^+$  contributes approximately -2.5 to the CD intensity of the dominant peak. Furthermore, it was seen that the contribution from  $\ell$ -stien is small, but negative. The maximum CD values for  $\Delta\text{-}[\text{Co}(\ell\text{-sdda})\text{en}]^+$  is +3.22. The additional contribution to the rotational strength in this case must be from the asymmetric nitrogen atoms. In  $[\text{Co}(\ell\text{-sdda})\text{en}]^+$  the asymmetric nitrogens must make very large positive contributions to the rotational strength for the E transition.

Contributions of Asymmetric Nitrogens. The homogeneity of the chemical environment of the asymmetric nitrogen is important in determining the contribution to the rotational strength (12, 13). The substituents on the asymmetric nitrogens of  $[\text{Co}(\ell\text{-sdda})\text{en}]^+$  (methylene of the glycinate ring, hydrogen, and benzyl) are more dissimilar than in the case of complexes of edda, dmedda, dedda, or dbedda and this great dissimilarity might cause the large contribution. It should be noted that the formal designations of absolute configurations for nitrogens with the same overall arrangements of substituents are (R,R) for the s-cis isomers of  $\Delta\text{-}[\text{Co}(\text{edda})\text{en}]^+$  and (S,S) for  $\Delta\text{-}[\text{Co}(\text{dbedda})\text{en}]^+$  and  $\Delta\text{-}[\text{Co}(\ell\text{-sdda})\text{en}]^+$ . The differences result from changes in priorities of substituents on N.

The examination of additive contributions (1, 3, 5, 6,) such as configurational, conformational, and vicinal effects of optically active ligands has been useful in the correlation of stereochemical effects and CD spectra. The ligand-polarization model (20, 21, 22, 24) of optical activity depends upon the polarizability of the perturbing groups which constitute the dissymmetric environment around the symmetric chromophore. Phenyl substituents which have large anisotropic polarizability can make contributions with signs reversed from those expected (20).

The optical activity induced by substituents on the ligand can be significant, and many empirical and theoretical treatments have been developed which relate stereochemical configuration with the signs and magnitude of CD curves. These are commonly referred to as regional or sector rules (15, 24-29). The major difficulty with applying regional rules results from assumptions which must be made about the electrostatic or polarizable nature of the perturbing groups. Bosnich and Harrowfield (15) have pointed out the uncertainty concerning the sign of the potential of hydrogen atoms which are bonded to donor nitrogens. Also, anisotropic perturbing groups, such as benzene rings, can make contributions which are not readily predictable (20).

Maricondi and Maricondi (13) have shown that Mason's hexadecadal regional rule can be applied to predict the experimentally observed sign of the low energy CD transition for

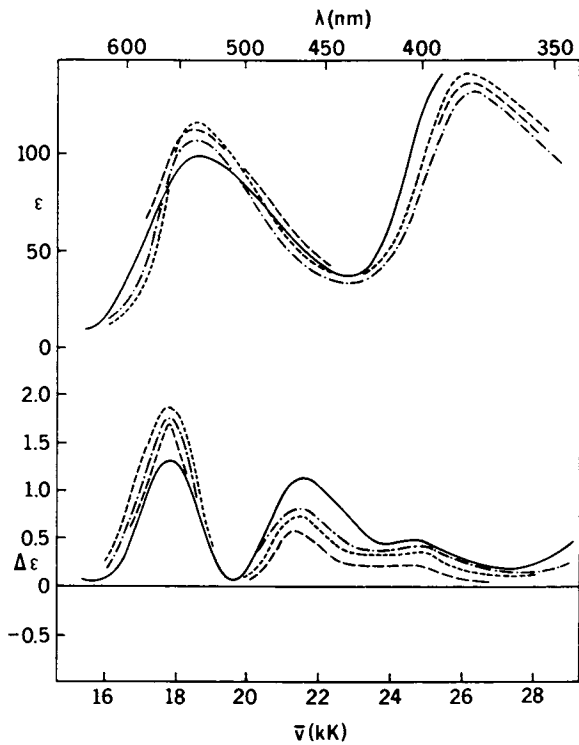


s-cis-[Co(dbedda)en]<sup>+</sup> where the nitrogens are substituted with benzyl groups. Mason (29) assumed that the effect on the sign and magnitude of the rotational strength produced by N-substitution is large, while the effect from C-alkyl substitution is small. The theoretical treatments of Schipper (30, 31) and Richardson (32) show promise of adding to our understanding of the correlation of CD spectra and stereochemistry and the additivity of chiral contributions.

The signs and magnitude of the CD curve of [Co(edda)-(l-stien)]<sup>+</sup> agree with previously studied Co(III)-edda complexes (11, 12, 13), indicating that the edda portion of the complex dominates and that the benzene substitution on the carbons has little effect. However, for [Co(l-sdda)en]<sup>+</sup>, the sign of the low energy peak in the CD spectrum is opposite to what is expected. Either the asymmetric nitrogens make a large contribution, opposite to that from the chiral arrangement of chelate rings to the rotational strength, or, contrary to the case for [Co(edda)(l-stien)]<sup>+</sup>, the benzene substituents on the carbons are making a significant contribution to the rotational strength. The other possibility requires the opposite ( $\Lambda$ ) configuration with the large phenyl substituents in unfavorable axial positions.

Stereospecificity of [Co(l-sdta)]<sup>-</sup>. The complex [Co(l-sdta)]<sup>-</sup> (l-sdta = l-stilbenediaminetetraacetate ion) is formed stereospecifically. The one isomer obtained (33) has a CD curve of the same form as those of the (-)<sub>546</sub>-isomers of [Co(edta)]<sup>-</sup> and [Co(1,3-pdta)]<sup>-</sup> (1,3-pdta = 1,3-propanediaminetetraacetate ion). The absolute configurations of both of these complexes are known to be ( $\Lambda\Lambda\Lambda$ ) (34, 35). The  $\Lambda\Lambda\Lambda$  isomer of [Co(l-sdta)]<sup>-</sup> permits the S,S-stilbenediamine backbone ring to adopt the stable  $\delta$  conformation with both phenyl groups equatorial. If one removes the two "in plane" or G acetate rings to give a sym-sdda complex, the absolute configuration is  $\Delta$  (the rings retained are those which give the  $\Delta$  chiral pair for  $\Lambda\Lambda\Lambda$ -[Co(l-sdta)]<sup>-</sup>). This gives support to the  $\Delta$  absolute configuration assigned above for [Co(l-sdda)en]<sup>+</sup>, which was unexpected from the CD curve in the low energy region, and consequently it supports the overwhelming contribution from the coordinated asymmetric N atoms of l-sdda.

Substituted dibenzylethylenediaminediacetic Acid Complexes. A series of para substituted dbedda analogs was prepared to study any possible electronic effects on asymmetric nitrogens which might be manifested in the CD spectra (14). The substituted dbedda complexes which were prepared were the para methyl, chloro and nitro derivatives. These were compared to the dbedda complex (13) which contains a hydrogen in the para position. As seen from the absorption and CD data shown in Figure 13, substitution of different groups in the para position of the benzene ring has no effect on the position of the maxima



Inorganic Chemistry

Figure 13. Absorption and CD spectra of *s-cis*-[Co(*dbedda*)en]<sup>+</sup> (---) *s-cis*-[Co(*dNO<sub>2</sub>bedda*)en]<sup>+</sup> (—), *s-cis*-[Co(*dClbedda*)en]<sup>+</sup> (- · -), and *s-cis*-[Co(*dmbedda*)en]<sup>+</sup> (· · ·) (14)

for the low energy (E) component and very little effect on the intensities. Only the nitro substituted dbedda complex has a maximum which can be considered to be significantly different. However, small shifts in the positions of two adjacent CD peaks can result in changes in peak intensities. Although the extent of overlap of peaks is difficult or impossible to evaluate, it may be reasonable that the nitro substituted dbedda complex may show a larger tetragonal splitting than the other complexes. Generally, substitution at the para position is probably too far removed from the chromophore to produce any significant changes. The para position was selected to avoid steric effects.

#### Literature Cited

1. Liu, C. T. and Douglas, B. E., Inorg. Chem. (1964), 3, 1356.
2. Yasui, T., Hidaka, J., and Shimura, Y., Bull. Chem. Soc. Japan (1966), 39, 2417.
3. Shimura, Y., Bull. Chem. Soc. Japan (1958), 31, 315.
4. Pfeiffer, P., Christeleit, W., Hesse, T., Pfitzner, H., and Thielert, H., J. Prakt. Chem. (1938), 150, 261.
5. Douglas, B. E., Inorg. Chem. (1965), 4, 1813.
6. Ogino, K., Murano, K., and Fujita, J., Inorg. Nucl. Chem. Letters (1968), 4, 351.
7. Tanimura, T., Ito, H., Fujita, J., Saito, K., Hirai, S., and Yamasaki, K., J. Coord. Chem. (1973), 3, 161.
8. Jordan, W. T., Lin, C.-Y., and Douglas, B. E., J. Coord. Chem. (1973), 3, 1.
9. Legg, J. I., Cooke, D. W., and Douglas, B. E., Inorg. Chem. (1967), 6, 700.
10. Van Saun, C. W. and Douglas, B. E., Inorg. Chem. (1969), 8, 115.
11. Jordan, W. T. and Douglas, B. E., Inorg. Chem. (1973), 12, 403.
12. Maricondi, C. W. and Douglas, B. E., Inorg. Chem. (1972), 11, 688.
13. Maricondi, C. W. and Maricondi, C., Inorg. Chem. (1973), 12, 1524.
14. Hawn, G. G., Maricondi, C., and Douglas, B. E., Inorg. Chem. (1979), 18, in press.
15. Bosnich, B. and Harrowfield, J., J. Am. Chem. Soc. (1972), 94, 3425.
16. Gillard, R. D., Tetrahedron (1965), 21, 503.
17. Fereday, R. L. and Mason, S. F., Chem. Commun. (1971), 1314.
18. Mason, S. F. and Seal, R. H., Chem. Commun. (1973), 422.
19. Kuroda, R. and Mason, S. F., J. Chem. Soc. Dalton (1977), 1016.
20. Hahn, E. G. and Weigang, O. E., Jr., J. Chem. Phys. (1968), 48, 1127.
21. Kirkwood, J. G., J. Chem. Phys. (1937), 5, 479.
22. Mason, S. F. and Seal, R. H., Chem. Commun. (1975), 331.

23. Mason, S. F. and Seal, R. H., Mol. Phys. (1976), 31, 755.
24. Hawkins, G. J. and Larsen, E., Acta. Chem. Scand. (1965), 19, 185, 1969.
25. Schellman, J. A., Acc. Chem. Res. (1968), 1, 144.
26. Schaffer, C. E., Pure Appl. Chem. (1970), 24, 361.
27. Mason, S. F., J. Chem. Soc. A (1971), 667.
28. Richardson, F. S., Inorg. Chem. (1972), 11, 2366.
29. Hearson, J. A., Mason, S. F., and Seal, R. H., J. Chem. Soc. (Dalton) (1977), 1026.
30. Schipper, P. E., J. Am. Chem. Soc. (1978), 100, 1433.
31. Schipper, P. E., This volume.
32. Richardson, F. S., This volume.
33. Hawn, G. G., Chang, C. A., and Douglas, B. E., Inorg. Chem. (1979), 18, 1266.
34. Okamoto, K., Tsukihara, T., Hidaka, J., and Shimura, Y., Chem. Lett. Japan (1973), 145.
35. Nagao, R., Marumo, F., and Saito, Y., Acta. Cryst. (1972), B28, 1852.

RECEIVED September 13, 1979.

# Additivity of Circular Dichroism of $d-d$ Transitions: The Vicinal Effect in a Homologous Series of Triethylenetetraaminecobalt(III) Amino Acid Complexes

ROBERT JOB

Department of Chemistry, Colorado State University, Fort Collins, CO 80523

Sources of dissymmetry in optically active metal complexes can be classified as: (a) inherent dissymmetry within the metal-donor atom coordination cluster, (b) configurational dissymmetry due to the chirality of the chelate system, (c) conformational dissymmetry due to the individual chelate ring conformations, and (d) vicinal dissymmetry due to asymmetric sites upon the ligands (1). For many complexes this set of contributions to the CD spectrum can be reduced to the configurational effect, the conformational effect and the vicinal effect (2,3). The most pragmatic approach to follow generally is to assume that the CD spectrum of a metal chelate complex is simply a summation of a vicinal effect and a configurational effect where the term vicinal effect retains its meaning as before and the other contributions are included in the configurational term (4,5,6,7).

The independent systems/perturbation model, as carried to second order in perturbation theory in Schipper's AICD (associate-induced circular dichroism) theory, makes the following prediction (8). In the case of the complexes  $AB_iB_j\dots$  (a composite complex) and  $A'B_i$  and  $A''B_j$  (substituent complexes) where  $A$ ,  $A'$  and  $A''$  is the same achiral chromophore and  $B_i$  and  $B_j$  have the same configurational relationship to  $A$  in the composite complex as in their respective substituent complexes, the circular dichroism of  $AB_iB_j\dots$  is simply the summation of the CD's of  $A'B_i$ ,  $A''B_j$ , etc. The purpose of this effort is to exhibit an achiral chromophore upon which exchange of chiral ligands induces negligible perturbation in the configurational relationship of the chelating ligands, and thus to allow the utility of the predicted additivity to be demonstrated experimentally.

The compounds studied are the substituted triethylenetetraaminecobalt(III) amino acid complexes depicted in Figure 1. Formally the  $A'B_i$  chromophore will be the triethylenetetraaminecobalt(III) glycinato moiety (compounds 1 and 7, identified in Figure 1) (with an associated configurational effect) and the optically active ( $B_j$ ) chromophores will be represented by the various  $R_2$  substituents at the  $\alpha$ -carbon of the chelated glycine

0-8412-0538-8/80/47-119-273\$05.00/0  
© 1980 American Chemical Society

(with an associated vicinal effect).

## Results

The compounds were synthesized at 45° from the dichlorotriethylenetetraamine moiety and the appropriate amino acid in aqueous solution with pH maintained at  $7.0 \pm 0.1$  by pH-stat (9). In the case where  $R_1 = -CH_3$  or  $-CH(CH_3)_2$ , only  $\Lambda$ - $\beta_2$  and  $\Delta$ - $\beta_1$  products were formed (Figure 2). The circular dichroism spectra were obtained on the perchlorate salts dissolved in 1 M HCl. Typical spectra for an S-amino acid complex (subscript S) and an R-amino acid complex (subscript R) are shown in Figure 3. A characteristic of these spectra is that they can be quite precisely deconvoluted into a minimal number of Gaussian components as shown by the dotted lines in Figure 3. This facilitates storage and manipulation of the experimental data. This deconvolution serves to emphasize the difference between CD spectra of R & S amino acid complexes. It can be seen from Figure 3 that two of the Gaussian peaks have changed sign upon going from an S-amino acid complex to an R-amino acid complex.

One way to obtain the vicinal effect of an amino acid is to prepare both the  $\Delta$  and  $\Lambda$ -tetraaminocobalt(III) complexes of the S-amino acid and average the CD spectra. One drawback to this method is that a resolution procedure is generally necessary in order to obtain the pure compound (10). Our preferred method is to prepare only  $\Lambda$  complexes of the  $\bar{R}$  then S-amino acid in separate reactions then purify by simple recrystallization. Then, since the vicinal effect of an S-amino acid is identically the negative of that for an R-amino acid, the vicinal effect may then be computed by the simple algebraic manipulations outlined in Figure 4. The vicinal effects calculated in this manner for alanine, valine and phenylalanine are shown in Figure 5. The data used for calculate these vicinal effects are taken from measurements on compounds prepared as in literature sources (11) or from Table I. Compound 10 is the  $\beta_1$ -alanine complex of the tetraaminocobalt(III) moiety with  $R_1 = CH_3$ . Since glycine does not have an enantiomer, the vicinal effect for  $\lambda$  and  $\bar{\lambda}$  is zero. The CD of these two complexes (shown in Figure 6) then by definition becomes the configurational effect to which the vicinal effects of Figure 5 should be added. In Figure 7 these additions are made. The dotted lines represent the sum of the configurational and vicinal effects for S-amino acid complexes and the solid lines represent the experimental spectra. Figure 8 shows the results for the R-alanine and R-phenylalanine complexes.

## Discussion

The summation appears to be most nearly perfect for the least sterically hindered cases [ $R_1 = -CH_3$ ,  $R_2 = -CH_3$ ,  $-CH(CH_3)_2$ ], but does not deviate much even for the case where  $R_1 = -CH(CH_3)_2$

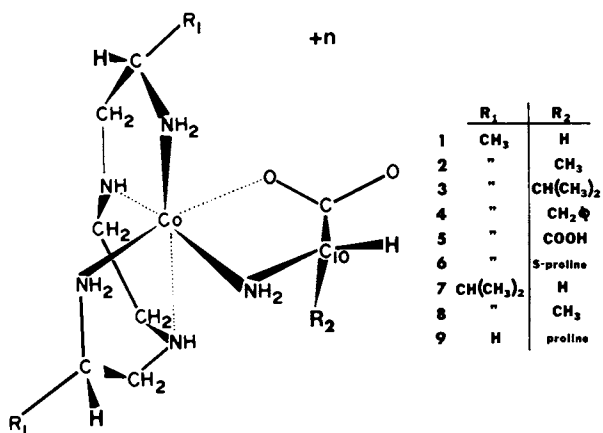


Figure 1. The  $\Lambda$ - $\beta$  compounds studied

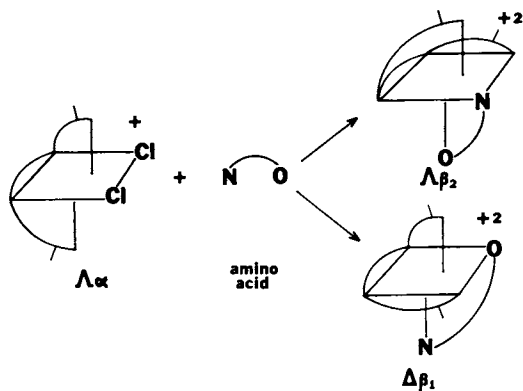


Figure 2. Reaction scheme to form the compounds depicted in Figure 1

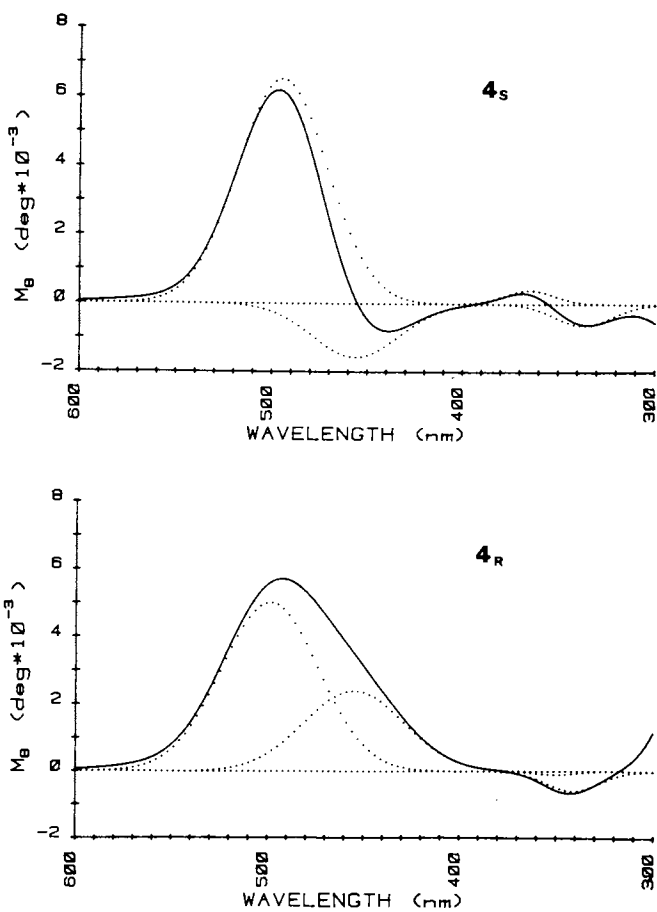


Figure 3. The CD spectra and component Gaussians of Compounds  $4_R$  and  $4_S$  which are typical of all compounds in Figure 1



$$C D (\Lambda-S) = C D (\Lambda) + C D (S\text{-acid})$$

$$C D (\Lambda-R) = C D (\Lambda) + C D (R\text{-acid})$$

$$\equiv C D (\Lambda) - C D (S\text{-acid})$$

Then:

$$C D (S\text{-acid}) = \frac{1}{2}[C.D.(\Lambda-S) - C.D.(\Lambda-R)]$$

Figure 4. Algebra involved in calculating vicinal effects

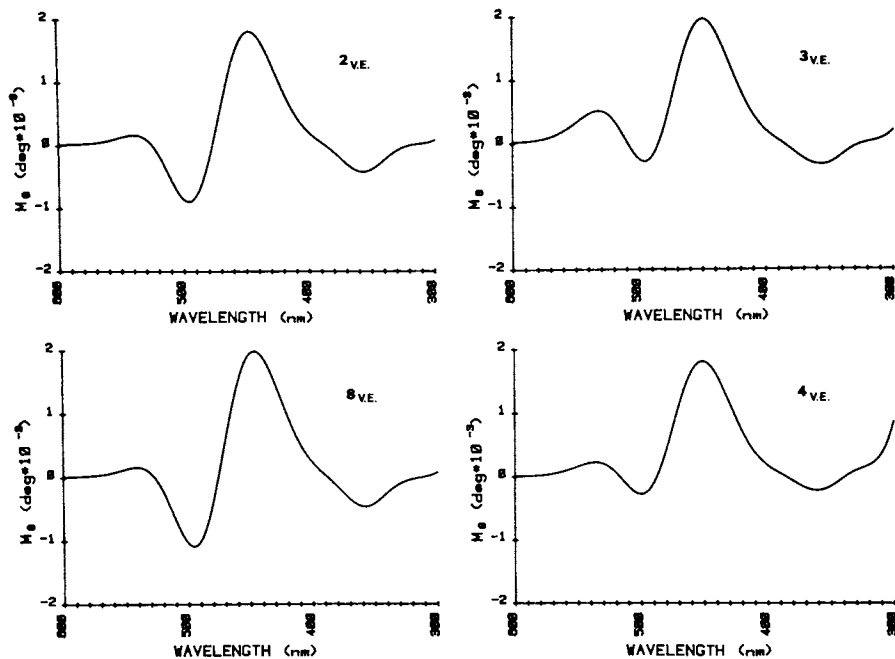


Figure 5. The average vicinal effects calculated for Compounds 2, 3, 4, and 8 of Figure 1

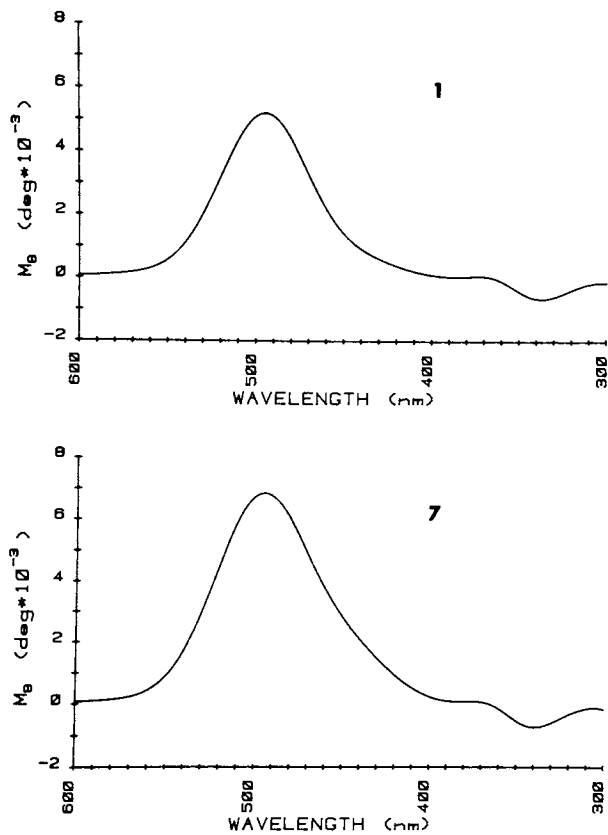


Figure 6. The CD of the glycine Complexes 1 and 7 depicted in Figure 1

Table I. Parameters of the Gaussian Components (i-vii) For the CD Spectra of Amino Acid Complexes.

| Complex* +      |   | i     | ii    | iii  | iv   | v     | vi    | vii   |
|-----------------|---|-------|-------|------|------|-------|-------|-------|
| 1               | a | 495.7 | 440   | 362  | 340  | 259   | 560   |       |
|                 | b | 35    | 32.0  | 18.0 | 24.0 | 23.5  | 42    |       |
|                 | c | 5215  | 525   | 265  | -685 | -1390 | 130   |       |
| 7               | a | 495   | 442   | 363  | 343  | 578   | 261   |       |
|                 | b | 38    | 32    | 17.5 | 24   | 40    | 21    |       |
|                 | c | 6100  | 1170  | 315  | -730 | 90    | -3420 |       |
| 10 <sub>R</sub> | a | 496   | --    | 430  | 384  | 345   | 560   | 263   |
|                 | b | 42.2  | --    | 19   | 19   | 21    | 40    | 26    |
|                 | c | -8111 | --    | -118 | -235 | 823   | -267  | 1390  |
| 10 <sub>S</sub> | a | 513.4 | 464   | 415  | 383  | 349   | 571   | 235   |
|                 | b | 36    | 36    | 19   | 17.5 | 18    | 35    | 28    |
|                 | c | -6656 | -4057 | -236 | -411 | 565   | -277  | 15400 |

\*The constants a, b, c are parameters of the Gaussian  $M_{\theta} = c \exp[-(x-a)^2/b^2]$  with a the location of the peak, b the half width at 1/e of the maximum peak height and c the peak height.

\*Complex 1 and 7 are defined in Figure 1. Complex 10 is the  $\Delta$ - $\beta_1$ -diastereomer of compound 2 depicted in Figure 1.

and  $R_2 = -CH_3$  or where  $R_1 = -CH_3$  and  $R_2 = \text{benzyl}$ . This intimates that these vicinal effects may be of significant synthetic utility both for confirmation of structure and for prediction of CD spectra.

As examples consider the reaction in Figure 2 carried out with the prochiral amino acid I (shown in the insert to Figure 5). This compound may bind in a bidentate fashion through the amino group and one of the carboxyl groups to give either an R or an S-amino acid complex depending on which carboxyl group binds to the metal. The CD spectrum ( $\times 1.5$ ) of this complex is shown in Figure 9 along with the vicinal effect gotten by subtracting the CD of I from it. This effect is clearly that of an R-amino acid, therefore the prochiral compound has bound stereospecifically in an R-fashion (12). Average CD's of a  $\Delta$ - $\Lambda$  mixture have revealed a difference between the vicinal effects of  $\beta_1$  and  $\beta_2$ -amino acid complexes (10). The vicinal effect of  $\beta_1$ -alanine gotten by treating the CD spectrum of compound 10 (the  $\Delta$ -diastereomer of compound 2 with the alanine bound as  $\beta_1$ ) by the equation in Figure 4 is shown in Figure 10. It is seen that the significant difference between the  $\beta_1$  and  $\beta_2$  vicinal effects allows us to peg further our prochiral amino acid as not only bound in an R-configuration but also to be bound in a  $\beta_2$  fashion (as confirmed by X-ray diffraction (11)). The same analysis carried out on the CD spectrum of this ligand in a similar reaction has revealed it to be bound also in an R- $\beta_2$  fashion (13).

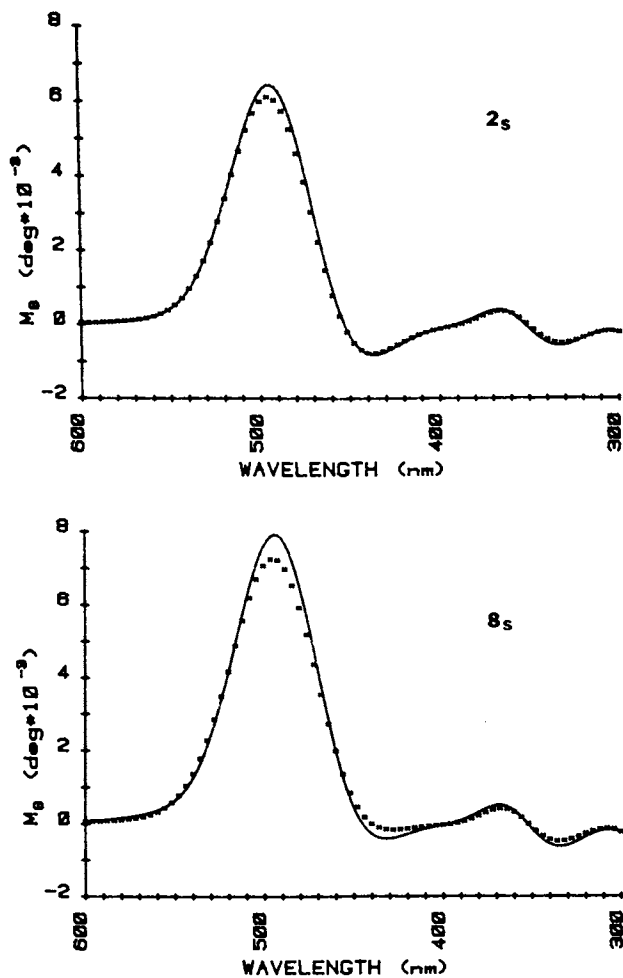
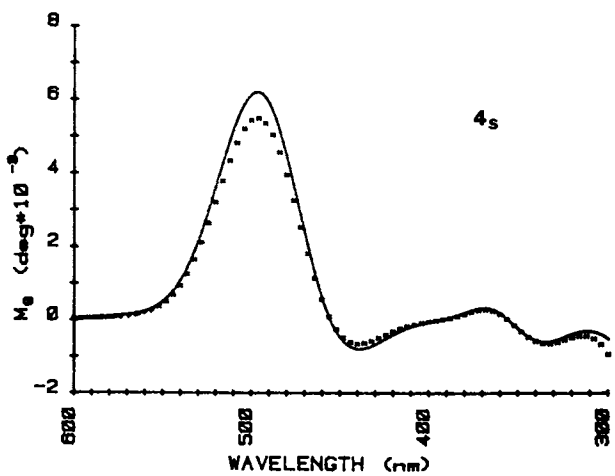
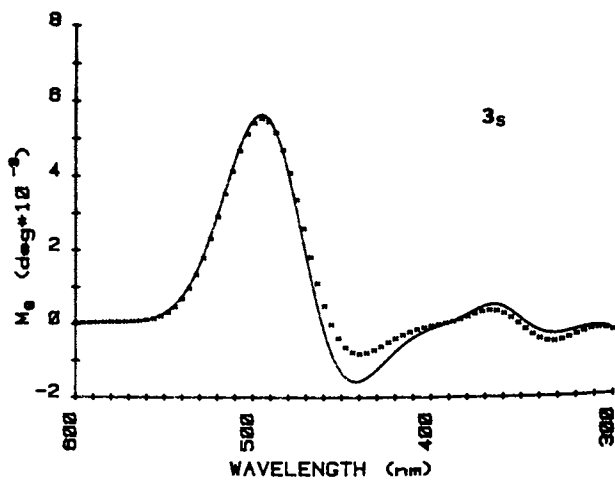


Figure 7. Sum of vicinal plus configuration effects (---) compared with experimental CD spectra for the S-amino acid complexes of 2, 3, 4, and 8 depicted in Figure 1 (—)

*Figure 7 (continued)*

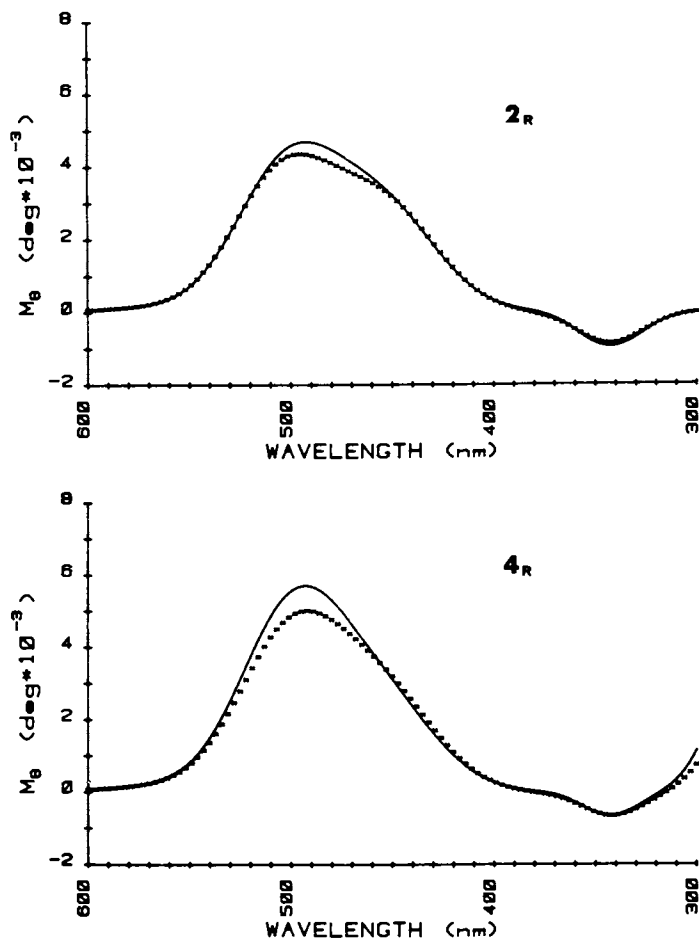


Figure 8. Sum of vicinal plus configuration effects (---) compared with experimental CD spectra for the R-amino acid complexes 2 and 4 depicted in Figure 1 (—)

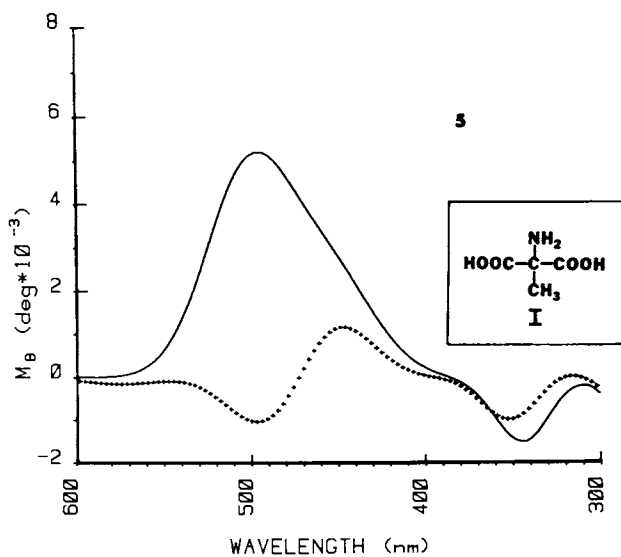


Figure 9. The CD spectrum of Compound 5 (—) and the vincinal effect for the prochiral amino acid I, shown in the insert (---)

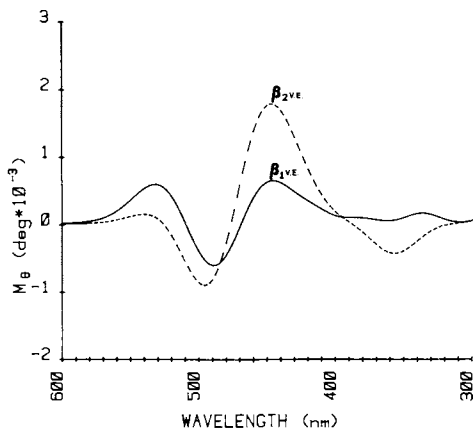


Figure 10. Vicinal effect for  $\beta_1$ -bound (—) alanine derived from the CD spectra of Compounds  $10_R$  and  $10_S$  which are the  $\Delta$ - $\beta_1$  diastereomers of Compound 2 depicted in Figure 1. Vicinal effect for  $\beta_2$ -bound (---) alanine for comparison (from Figure 5).

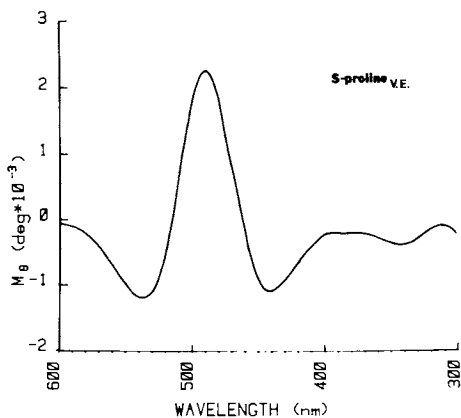


Figure 11. Vicinal effect for  $\beta_2$ -S-proline derived from Complexes  $9_S$  and  $9_R$  depicted in Figure 1



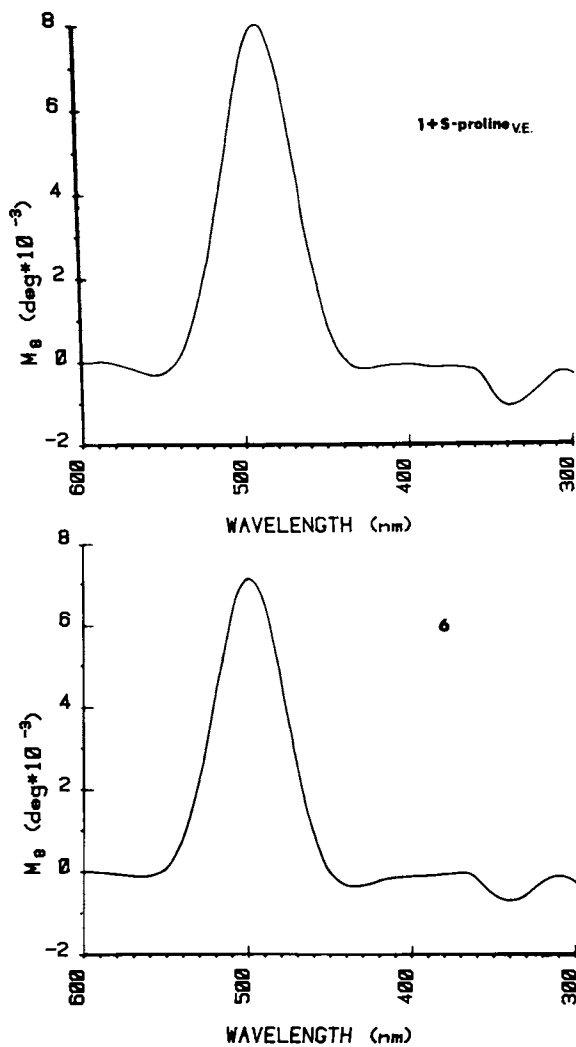


Figure 12. Predicted CD of the  $\beta_2$ -S-proline complex (top) compared with the experimental CD of Compound 9 depicted in Figure 1 (bottom)

In order to predict the CD spectrum of the  $\Lambda\beta_2$  product from the reaction of S-proline as the amino acid in Figure 2, the vicinal effect in Figure 11 for  $\beta_2$ S-proline was determined (from measurements in our laboratory upon complex 9, which had been previously synthesized (11) and characterized by X-ray diffraction (14,15)) and added to the CD of the glycine complex 1 to obtain the CD spectrum shown in the top half of Figure 12. This compares quite favorably with the CD of the principal product (65%) of the reaction (bottom half of Figure 12). Since the proline does not conform precisely to the glycinate skeleton the achiral chromophore is altered and additivity is not required to hold precisely. However the results are sufficiently quantitative to allow for unambiguous product identification. Note that the vicinal effect for  $\beta_2$ S-proline depicts a situation observed by others, i.e., it strongly resembles the vicinal effect for the  $\beta_1$  complexes of other amino acids.

### Conclusion

Although additivity in a tetraaminocobalt(III) amino acid complexes has been previously demonstrated (6,16), the current work has demonstrated a high additivity in a carefully chosen system. However, treatment of these results has not taken into account the charge transfer bands which, being of proper symmetry, must have some nontrivial effect on the d-d transitions. The relevance of the steric contribution to the deviations from perfect additivity will be discussed in a forthcoming publication.

### Summary

This report describes a method of experimentally obtaining the vicinal effects of amino acid anions bound to a tetraaminocobalt(III) moiety by dealing exclusively with  $\Lambda\beta_2$  complexes of both R and S-amino acids. Additivity of circular dichroism of both the configurational and vicinal effects for d-d transitions is verified experimentally. It is demonstrated that the vicinal effect not only contains information as to the chirality of the bound amino acid but also as to the mode of binding, i.e.,  $\beta_1$  vs.  $\beta_2$ .

### Literature Cited

1. Richardson, F. S., Chem. Revs., (1979) 79, 17.
2. Hawkins, C. J., "Absolute Configuration of Metal Complexes", Wiley-Interscience: New York, N.Y. (1971) Chap. 5.
3. Bosnich, B.; Harrowfield, J. M., J. Am. Chem. Soc. (1972) 94, 3425.
4. Liu, C. T.; Douglas, B. E., Inorg. Chem. (1964) 3, 1356.
5. Douglas, B. E.; Yamada, S., ibid. (1965) 4, 1561.
6. Douglas, B. E., ibid. (1965) 4, 1813.

7. Yano, S.; Saburi, M.; Yoshikawa, S.; Fujita, J., Bull. Chem. Soc. Japan, (1976) 49, 101.
8. Schipper, P. E., J. Am. Chem. Soc., (1978) 100, 1433.
9. Job, R.; Freeland, S., Analyt. Biochem., (1977) 79, 575.
10. Lin, C. Y.; Douglas, B. E., Inorg. Chim. Acta (1970) 4, 3.
11. Glusker, J. P.; Carrel, H. L.; Job, R.; Bruice, T. C., J. Am. Chem. Soc. (1974) 96, 5741.
12. Job, R.; Bruice, T. C., J. Am. Chem. Soc., (1974) 96, 809.
13. Job, R. C., J. Am. Chem. Soc., (1978) 100, 5089.
14. Buckingham, D. A.; Marzilli, L. G.; Maxwell, I. E.; Sargeson, A. M.; Freeman, H. C., Chem. Commun., (1969) 583.
15. Freeman, H. C.; Marzilli, L. G.; Maxwell, I. E., Inorg. Chem., (1970) 9, 2408.
16. Hall, S. K.; Douglas, B. E., ibid., (1969) 8, 372.

RECEIVED September 13, 1979.

# Circular Dichroism Spectra of Cobalt(III) Complexes Having Optical Activity Owing to the Arrangement of Unidentate Ligands

M. SHIBATA, S. FUJINAMI, and S. SHIMBA

Department of Chemistry, Faculty of Science, Kanazawa University,  
Kanazawa 920, Japan

Most CD spectral studies of cobalt(III) complexes have been undertaken to investigate various sources of optical activity such as distribution of chelate rings, conformation of chelate rings, vicinal effect due to asymmetric carbon in an optically active ligand, and vicinal effect due to an asymmetric donor atom. Extensive reviews on these subjects have been written by Fujita and Shimura (1), Hawkins (2), and Mason (3).

In contrast to those investigations, much less work has been reported on complexes whose optical activity results from a certain arrangement of unidentate ligands. The reason for the delay in work is considered to be the lack of useful syntheses for such chiral complexes.

The cis-cis-cis-isomer of the  $[Coa_2b_2c_2]$ -type, where a, b and c denote unidentate ligands, is asymmetric and exhibits two enantiomeric forms I and II in Figure 1. The cis-cis-isomer of the  $[Coa_2b_2CC]$ -type, III in Figure 1, also belongs to the same category based on the origin of optical activity, if the CC is an achiral chelate ligand, two enantiomeric forms being possible to exist. The complex of fac(a)- $[Co_3bcd]$ -type, IV in Figure 1, has optical activity due to the arrangement of the unidentates b, c and d about cobalt(III), and hence exists in two enantiomeric forms. Similarly, the complexes of such types as fac(A)- $[Co(A_3)bcd]$  and fac(A)- $[Co(A_3)(BC)d]$ , V and VI in Figure 1, have the same origin of optical activity, which makes it possible to resolve the complexes into optically active forms.

In the present paper some aspects of chiral complexes of these types are dealt with and recent developments in preparative methods and CD spectra are described.

## Syntheses and Optical Resolutions of Complexes with cis-cis Distribution of Unidentates

Cis-cis- $[CoCl_2(NH_3)_2(en)]^+$  — The complex (+)<sub>589</sub>-cis-cis- $[CoCl_2(NH_3)_2(en)]^+$  has been prepared by Hawkins et al. (4). The starting material cis- $[Co(CO_3)(NH_3)_2(en)]ClO_4$  was prepared

0-8412-0538-8/80/47-119-289\$06.50/0

© 1980 American Chemical Society

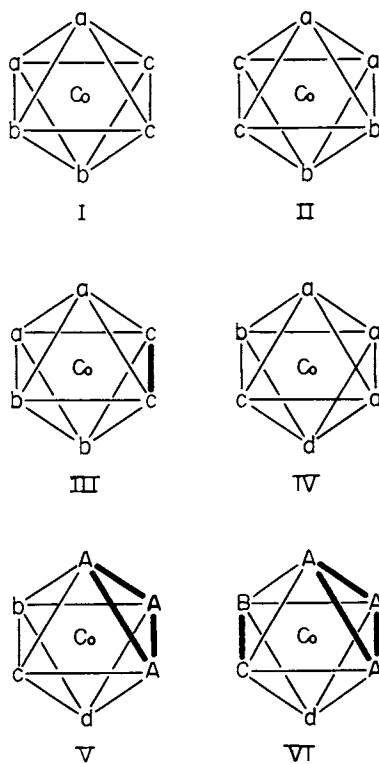


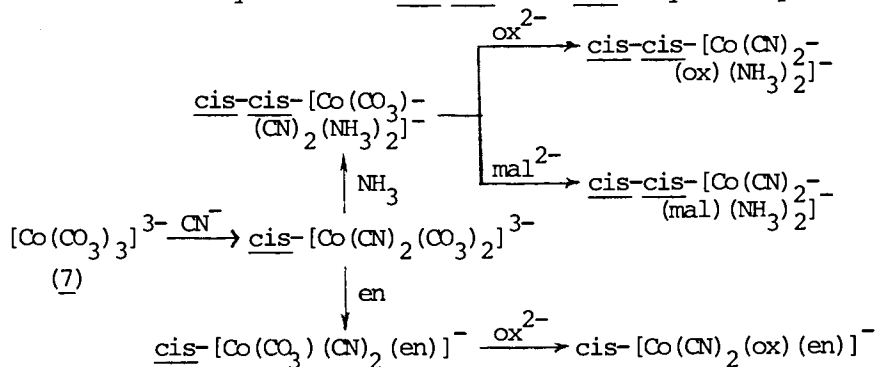
Figure 1. Various types of complexes concerned

according to the method of Bailar and Peppard (5). The racemate was then resolved using ammonium trans-diammine(R-1,2-propanediamine)bis(sulfito)cobaltate(III) as the resolving agent. The diastereoisomeric salt formed was treated with an anion exchange column (BioRad AGL-X2 in  $\text{ClO}_4^-$  form) in order to obtain (+)<sup>589</sup>- $[\text{Co}(\text{CO}_3)(\text{NH}_3)_2(\text{en})]\text{ClO}_4^-$ . Dry hydrogen chloride was passed over the finely ground (+)<sup>589</sup>-compound under anhydrous conditions to produce a bluish purple product, cis-cis- $[\text{CoCl}_2(\text{NH}_3)_2(\text{en})]\text{ClO}_4^-$  which was obtained quantitatively. The related compound, racemic-cis-cis- $[\text{CoCl}_2(\text{NH}_3)_2(\text{R-pn})]\text{Cl}$ , was obtained by passing dry hydrogen chloride over the cis- $[\text{Co}(\text{CO}_3)(\text{NH}_3)_2(\text{R-pn})]\text{CO}_3 \cdot 4\text{H}_2\text{O}$  prepared by the method for the ethylenediamine analogue.

Cis-cis- $[\text{Co}(\text{CN})_2(\text{O},\text{O})(\text{NH}_3)_2]^-$  and related complexes —

Complexes of this type, where O,O represents carbonate ( $\text{CO}_3^{2-}$ ), oxalate ( $\text{ox}^{2-}$ ) and malonate ( $\text{mal}^{2-}$ ), have been synthesized by Ito and Shibata (6). The synthesis depends essentially on the fact that the tricarbonatocobaltate(III) species,  $[\text{Co}(\text{CO}_3)_3]^{3-}$ , prefers successive cis-substitutions by the desired unidentates. Scheme 1 represents the pathways of the syntheses, the syntheses of closely related cis- $[\text{Co}(\text{CN})_2(\text{O},\text{O})(\text{en})]^-$  complexes being illustrated.

Scheme 1. Syntheses of cis-cis- and cis-Dicyano Complexes

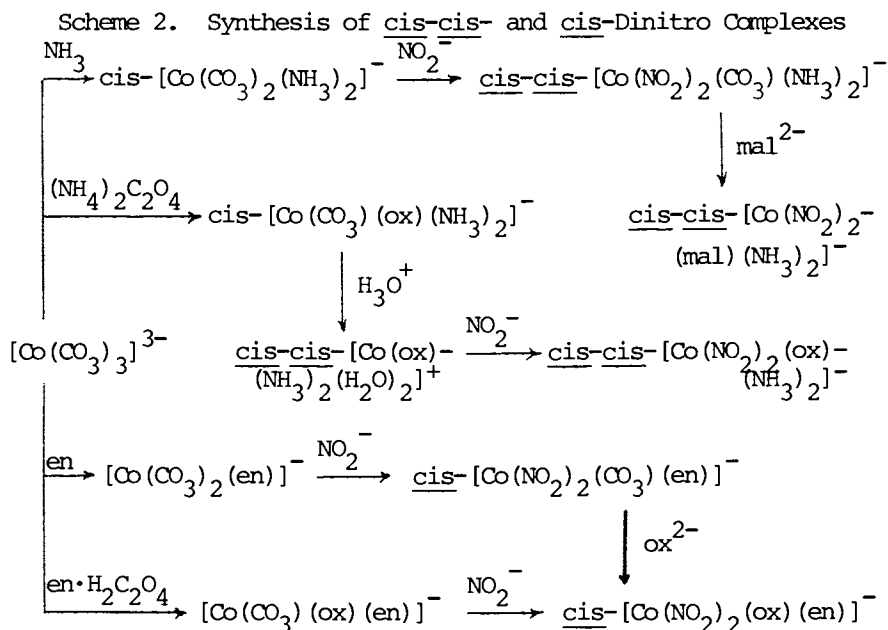


The optical resolutions of all the complexes synthesized have been achieved by the use of either (-)<sup>589</sup>- $[\text{Co}(\text{NO}_2)_2(\text{en})_2]^-$  ( $\text{C}_2\text{H}_3\text{O}_2$ ) or (-)<sup>589</sup>- $[\text{Co}(\text{ox})(\text{en})_2]^-$  ( $\text{C}_2\text{H}_3\text{O}_2$ ), where a half-equivalent amount of the resolving agent, compared to the amount of the racemate, was used for effective resolution.

Cis-cis- $[\text{Co}(\text{NO}_2)_2(\text{O},\text{O})(\text{NH}_3)_2]^-$  and related complexes —

The idea of "cis-substitution" in the carbonato complex has been utilized in the complexes of this series. The pathways are shown in Scheme 2.

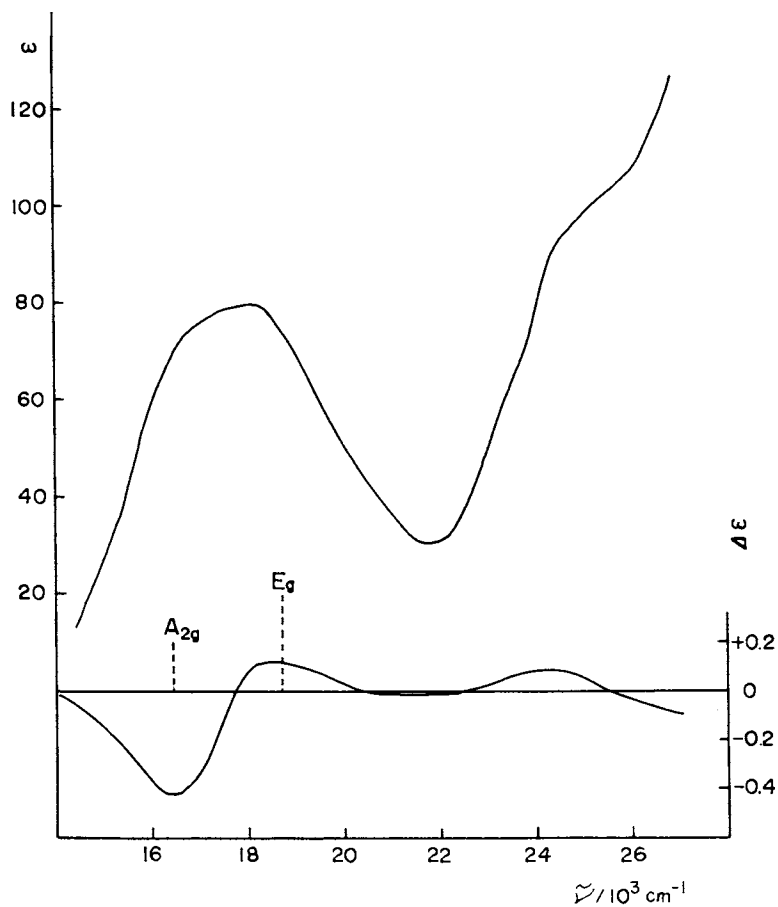
More remarkable was the success in obtaining cis-cis- $\text{K}[\text{Co}(\text{NO}_2)_2(\text{ox})(\text{NH}_3)_2] \cdot 0.5\text{H}_2\text{O}$ . During the period 1917-1937 several groups of workers (8, 9, 10, 11) intended to determine the geometrical structure of Erdmann's salt,  $\text{NH}_4[\text{Co}(\text{NO}_2)_4(\text{NH}_3)_2]$ ,



and contradictory conclusions were drawn regarding whether an oxalate derivative could be resolved into enantiomers or not. Later, X-ray studies showed that the two ammonia groups were in the trans position in the salts with silver (12, 13), potassium (14) and ammonium (15) as counter ions. However, in aqueous solution of Erdmann's salt there is the possibility of equilibrium between trans- and cis-diammine species. Thus, the problem remained unresolved for a long time until the Shibata group succeeded in preparing all three isomers of  $[\text{Co}(\text{NO}_2)_2(\text{ox})(\text{NH}_3)_2]^-$  (16). The cis-cis-isomer and trans-( $\text{NO}_2$ )-isomer were obtained from the reaction mixture of the cis-cis- $[\text{Co}(\text{ox})(\text{NH}_3)_2(\text{H}_2\text{O})_2]^+$  complex and  $\text{KNO}_2$ , the remaining trans-( $\text{NH}_3$ )-isomer from that of the trans- $[\text{Co}(\text{NO}_2)_4(\text{NH}_3)_2]^-$  complex and oxalic acid.

#### CD Spectra for cis-cis-Complexes and their Absolute Configurations

Cis-cis- $[\text{CoCl}_2(\text{NH}_3)_2(\text{en})]^+$  — The absorption and CD spectra in DMSO for the isomer derived from (+) $^{589}$ - $[\text{Co}(\text{CO}_3)(\text{NH}_3)_2(\text{en})]^+$  are shown in Figure 2, where the vertical lines represent the results of the Gaussian analysis of the absorption spectrum, with labels specifying the excited states of the tetragonal components. The CD spectrum shows dominant negative peak at  $16,230 \text{ cm}^{-1}$ , which corresponds closely to the position of the  $^1\text{A}_{1g} \rightarrow ^1\text{A}_{2g}$  ( $D_{4h}$ ) absorption maximum. Another minor positive peak is observed at  $18,350 \text{ cm}^{-1}$ , which is lower in energy by  $350 \text{ cm}^{-1}$  than the position of the  $^1\text{A}_{1g} \rightarrow ^1\text{E}_g$  ( $D_{4h}$ ) absorption.



Australian Journal of Chemistry

Figure 2. Absorption and CD spectra of an isomer of  $\text{cis-}[\text{CoCl}_2(\text{NH}_3)_2(\text{en})]^+$  (4)



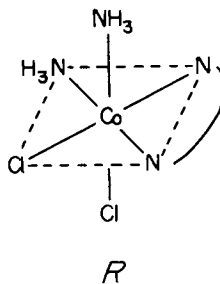
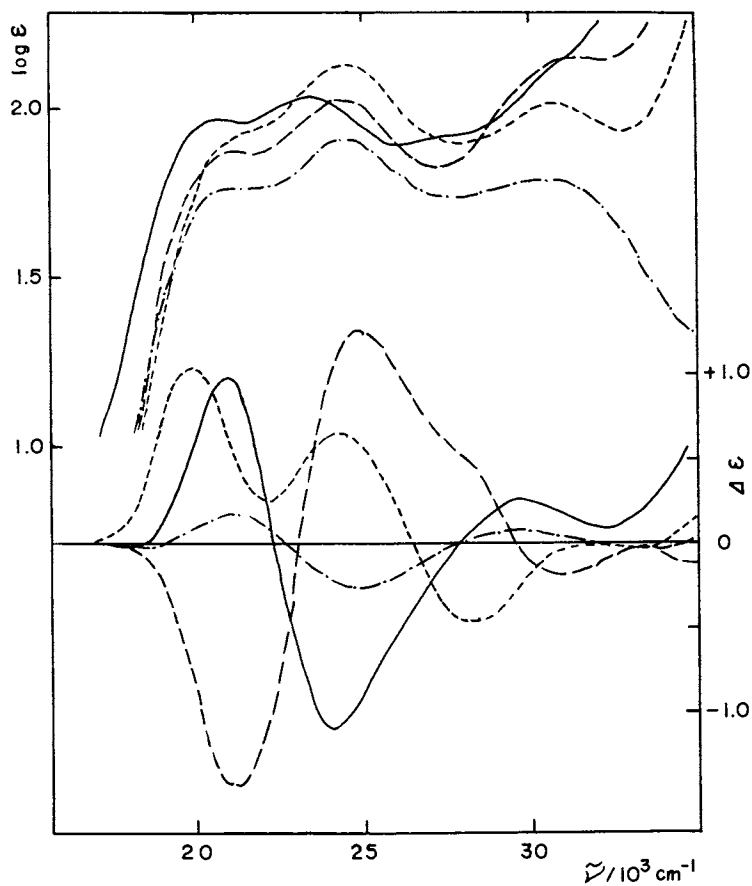
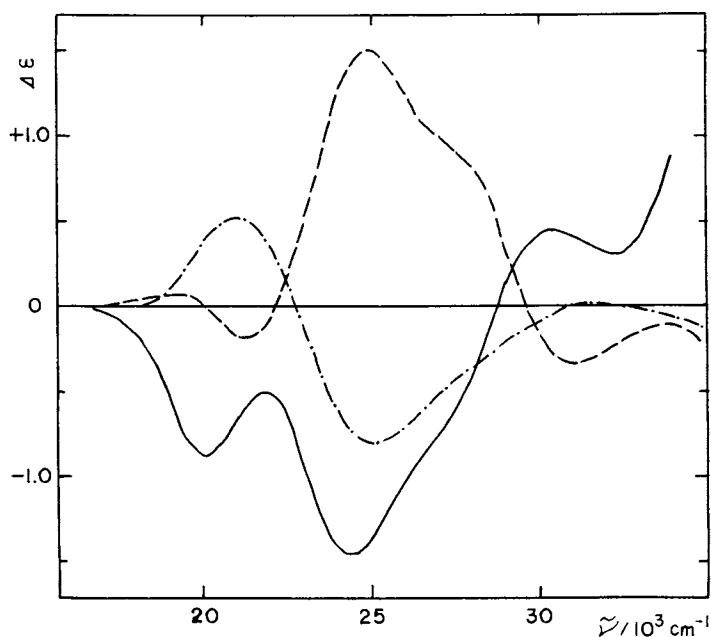


Figure 3. Absolute configuration of the  $\text{cis-}[\text{CoCl}_2(\text{NH}_3)_2(\text{en})]^+$  isomer



Inorganic Chemistry

Figure 4. Absorption and CD spectra of: (—),  $\text{cis-cis-}[\text{Co}(\text{CN})_2(\text{CO}_3)(\text{NH}_3)_2]^-$ ; (- · - ·),  $\text{cis-cis-cis-}[\text{Co}(\text{CN})_2(\text{NH}_3)_2(\text{H}_2\text{O})_2]^+$ ; (---),  $\text{cis-cis-}[\text{Co}(\text{CN})_2(\text{ox})(\text{NH}_3)_2]^-$ ; (· · · ·),  $\text{cis-cis-}[\text{Co}(\text{CN})_2(\text{mal})(\text{NH}_3)_2]^-$  (6).



## Inorganic Chemistry

Figure 5. CD spectra of (—),  $(-)_{589} [Co(CN)_2(CO_3)(en)]^-$ ; (- · - ·),  $(-)_{589} [Co(CN)_2(en)(H_2O)_2]^+$ ; (---),  $(+)_{589} [Co(CN)_2(ox)(en)]^-$  (6).

Since the CD spectrum of the parent complex,  $(+)\text{ }_{589}\text{-}[\text{Co}(\text{CO}_3)_2(\text{NH}_3)_2(\text{en})]^+$  was very similar to that of  $(+)\text{ }_{589}\text{-}[\text{Co}(\text{CO}_3)_2(\text{en})]^+$  whose absolute configuration had been assigned as  $\Lambda$  (17), Hawkins et al. (4) assigned the same absolute configuration  $\Lambda$  to the parent monocarbonato complex. On the basis of the fact that the dichloro complex was derived from the  $(+)\text{ }_{589}\text{-}$ carbonato complex by a solid state reaction without isomerization, they assigned the  $R$  absolute configuration (Figure 3) according to the method of Cahn et al. (18). When the CD spectrum of this  $R$  isomer was compared with that of  $(+)\text{ }_{589}\text{-}[\text{CoCl}_2(\text{en})_2]^+$ , the same sign of Cotton effect was found. For this, Hawkins et al. (1, 4) have stated that there is no *a priori* reason for suggesting that the two should have the same sign of Cotton effect for the comparable transitions, because the two complexes attain their dissymmetry in different ways, namely, the bis(ethylenediamine) complex gain dissymmetry from the distribution of en rings, and the *cis-cis*-diamminedichloro complex, from the arrangement of the donor groups about the central cobalt.

$\text{Cis-cis-}[\text{Co}(\text{CN})_2(\text{O},\text{O})(\text{NH}_3)_2]^-$  and a related complex — The absorption and CD spectra are shown in Figure 4, including the spectra of *cis-cis-cis*- $[\text{Co}(\text{CN})_2(\text{NH}_3)_2(\text{H}_2\text{O})_2]^+$  derived by the acid-hydrolysis of resolved *cis-cis*- $[\text{Co}(\text{CN})_2(\text{CO}_3)(\text{NH}_3)_2]^-$  with  $\text{HClO}_4$ . The CD spectra of the related  $[\text{Co}(\text{CN})_2(\text{O},\text{O})(\text{en})]^-$  complexes are shown in Figure 5. When attention is given to the CD curves in the  $T_{1g}$  band region, marked changes in the CD patterns are seen in contrast to the similarity of the absorption curves; the curve for the  $[\text{Co}(\text{CN})_2(\text{CO}_3)(\text{NH}_3)_2]^-$  shows a (+, -) pattern, while that for the en analogue shows a (-, -) pattern. The curves for the diaqua derivatives from those carbonato complexes show the same (+, -) patterns. The patterns for the  $[\text{Co}(\text{CN})_2(\text{ox})(\text{NH}_3)_2]^-$  and the en analogue are (-, +) and (+, -, +), respectively. The remaining  $[\text{Co}(\text{CN})_2(\text{mal})(\text{NH}_3)_2]^-$  exhibits the CD curve with a (+, +) pattern. The  $\Delta\epsilon_{\text{max}}$  values of the dominant peaks are in the range of 0.5-1.5 for all the complexes except for *cis-cis-cis*- $[\text{Co}(\text{CN})_2(\text{NH}_3)_2(\text{H}_2\text{O})_2]^+$  complex ( $\Delta\epsilon_{\text{max}} = -0.27$ ).

The absolute configuration has been studied by X-ray diffraction method for  $K(+)\text{ }_{589}\text{-}[\text{Co}(\text{CN})_2(\text{mal})(\text{NH}_3)_2]\cdot\text{H}_2\text{O}$  (19) and the configuration of the complex anion has been determined to  $S$  (Figure 6). The absolute configurations of the other complexes have been determined tentatively by comparing the CD spectra in the  $T_{1g}$  band region with that of the standard.

The  $S(+)\text{ }_{589}\text{-}[\text{Co}(\text{CN})_2(\text{mal})(\text{NH}_3)_2]^-$  complex shows a (+, +) pattern, while the  $(-)\text{ }_{589}\text{-}[\text{Co}(\text{CN})_2(\text{CO}_3)(\text{en})]^-$  complex shows a (-, -) pattern, hence the latter is assigned the  $R$  configuration. The  $(-)\text{ }_{589}\text{-}[\text{Co}(\text{CN})_2(\text{en})(\text{H}_2\text{O})_2]^+$  species is also regarded as having the same configuration as the parent carbonato complex, because acid-hydrolysis proceeds with retention of configuration. The CD pattern of  $(+)\text{ }_{589}\text{-}[\text{Co}(\text{CN})_2(\text{CO}_3)(\text{NH}_3)_2]^-$  resembles that of  $R(-)\text{ }_{589}\text{-}[\text{Co}(\text{CN})_2(\text{en})(\text{H}_2\text{O})_2]^+$  if the first very weak peak of negative sign is ignored, leading to the  $R$  configuration for the

carbonato complex. The (+)<sub>589</sub>-[Co(CN)<sub>2</sub>(NH<sub>3</sub>)<sub>2</sub>(H<sub>2</sub>O)<sub>2</sub>]<sup>+</sup> species derived from the R-carbonato complex should be R because of retention of configuration. The (-)<sub>589</sub>-[Co(CN)<sub>2</sub>(ox)(NH<sub>3</sub>)<sub>2</sub>]<sup>-</sup> complex exhibits almost the reverse pattern of R-[Co(CN)<sub>2</sub>(CO<sub>3</sub>)(NH<sub>3</sub>)<sub>2</sub>]<sup>-</sup> so it is regarded as S. The CD signs with respect to the (+)<sub>589</sub>-[Co(CN)<sub>2</sub>(ox)(en)]<sup>-</sup> complex are identical with those of the S-[Co(CN)<sub>2</sub>(mal)<sub>2</sub>(NH<sub>3</sub>)<sub>2</sub>]<sup>-</sup> complex and opposite to those of the R-[Co(CN)<sub>2</sub>(CO<sub>3</sub>)(NH<sub>3</sub>)<sub>2</sub>]<sup>-</sup> complex, and the features of the CD curve are the reverse of those for the R-[Co(CN)<sub>2</sub>(CO<sub>3</sub>)(en)]<sup>-</sup> complex. Consequently, this oxalato-complex is regarded as having the S configuration.

It will be noted that when an en chelate ring is replaced by the coordination of two NH<sub>3</sub>, or an O,O-chelate is replaced by another one, the signs of the CD peaks on the higher frequency sides in the T<sub>1g</sub> band regions never change for fixed absolute configurations,<sup>1g</sup> that is, the (+) sign corresponds to S for the cis-cis-complexes, and Δ for the cis-complexes. The solubility rule (20) has been found to hold when (-)<sub>589</sub>-[Co(NO<sub>2</sub>)<sub>2</sub>(en)<sub>2</sub>]<sup>+</sup> is used as the resolving agent.

Cis-cis-[Co(NO<sub>2</sub>)<sub>2</sub>(O,O)(NH<sub>3</sub>)<sub>2</sub>]<sup>-</sup> and related complexes — The CD spectra of these complexes are shown in Figures 7 and 8. The CD spectra for the cis-cis-[Co(NO<sub>2</sub>)<sub>2</sub>(O,O)(NH<sub>3</sub>)<sub>2</sub>]<sup>-</sup> complexes show two or three peaks of alternating sign, and the Δε<sub>max</sub> values of dominant peaks are in the range of 0.33-1.47. On the other hand, each of the two cis-[Co(NO<sub>2</sub>)<sub>2</sub>(O,O)(en)]<sup>-</sup> complexes shows a single positive peak with larger Δε<sub>max</sub> values. With respect to the corresponding cis-cis-cis and cis-cis-diaqua complexes, there are (-, +) patterns with much lower intensities.

X-ray studies have been carried out with (-)<sub>589</sub>-[Co(NO<sub>2</sub>)<sub>2</sub>(en)<sub>2</sub>]<sup>-</sup> and (-)<sub>589</sub>-[Co(NO<sub>2</sub>)<sub>2</sub>(ox)(NH<sub>3</sub>)<sub>2</sub>]<sup>-</sup> (21) and the absolute configuration of the complex anion has been determined to be R (Figure 9). By comparing the CD patterns in turn, the absolute configurations of the other complexes have been assigned tentatively. The absolute configurations of the diaqua complexes have been considered to be the same as those for the parent carbonato complexes. It is noted again that the positive signs of the peaks on the higher frequency sides of the T<sub>1g</sub> bands correspond to the R configuration with the exceptions of the two diaqua complexes. The solubility rule holds in the same manner as the previous case.

Besides the complexes belonging to the two above-mentioned types, cis-cis-[Co(ox)(NH<sub>3</sub>)<sub>2</sub>(H<sub>2</sub>O)<sub>2</sub>]NO<sub>3</sub> has been prepared by the acid-hydrolysis of the cis-[Co(CO<sub>3</sub>)(ox)(NH<sub>3</sub>)<sub>2</sub>]<sup>-</sup> complex and resolved with (+)<sub>546</sub>-[Co(edta)]<sup>-</sup> (22). Figure 10 shows absorption and CD spectra for the less soluble isomer. It has been confirmed that the conversion between the resolved diaqua complex and an active-[Co(CO<sub>3</sub>)(ox)(NH<sub>3</sub>)<sub>2</sub>]<sup>-</sup> species in solution takes place with retention of configuration, the spectra for the carbonato complex species being included in Figure 10. The diaqua complex exhibits a (-, +) pattern and the carbonato

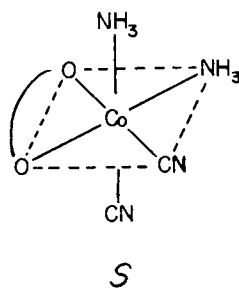
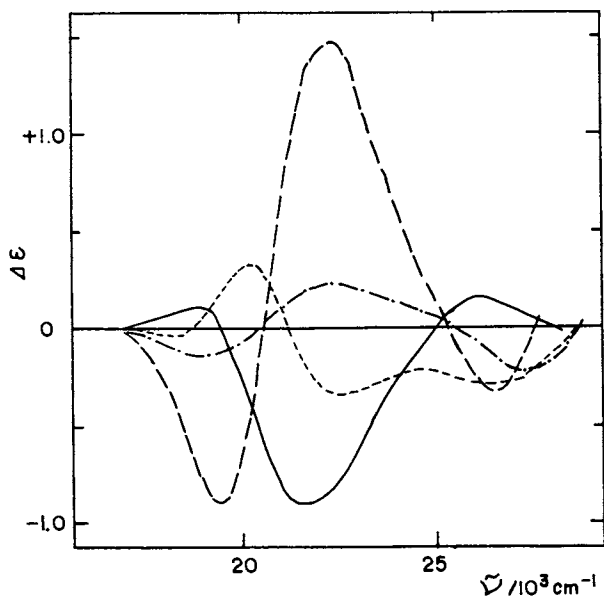
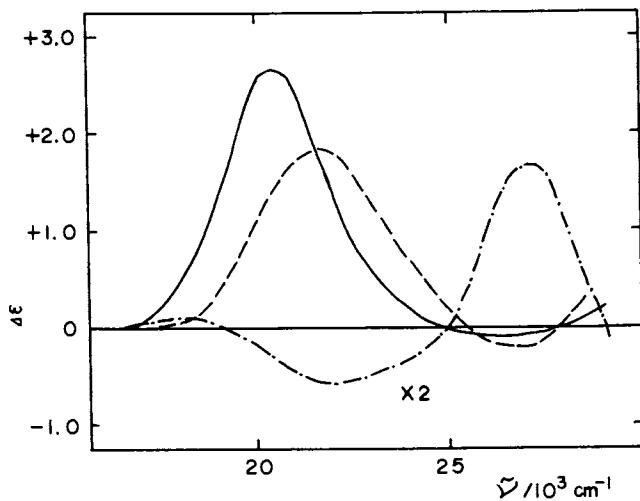


Figure 6. Absolute configuration of  $(+)_{S98}^{-}[Co(CN)_2(mal)(NH_3)_2]^{-}$



Inorganic Chemistry

Figure 7. CD spectra of (—),  $(-)_{S98}^{-}[Co(NO_2)_2(CO_3)(NH_3)_2]^{-}$ ; (- · - ·),  $(+)_{S89}^{-}[Co(NO_2)_2(NH_3)_2(H_2O)_2]^{-}$ ; (- - -),  $(-)_{S98}^{-}[Co(NO_2)_2(ox)(NH_3)_2]^{-}$ ; (· · ·),  $(+)_{S89}^{-}[Co(NO_2)_2(mal)(NH_3)_2]^{-}$  (6).



## Inorganic Chemistry

Figure 8. CD spectra of (—),  $(+)^{599-}[\text{Co}(\text{NO}_2)_2(\text{CO}_3)(\text{en})]$ ; (- · - ·),  $(+)^{598-}[\text{Co}(\text{NO}_2)_2(\text{en})(\text{H}_2\text{O})_2]$ ; (- - -),  $(+)^{589-}[\text{Co}(\text{NO}_2)_2(\text{ox})(\text{en})]^-$  (6).

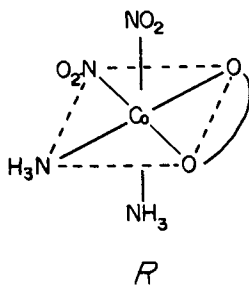
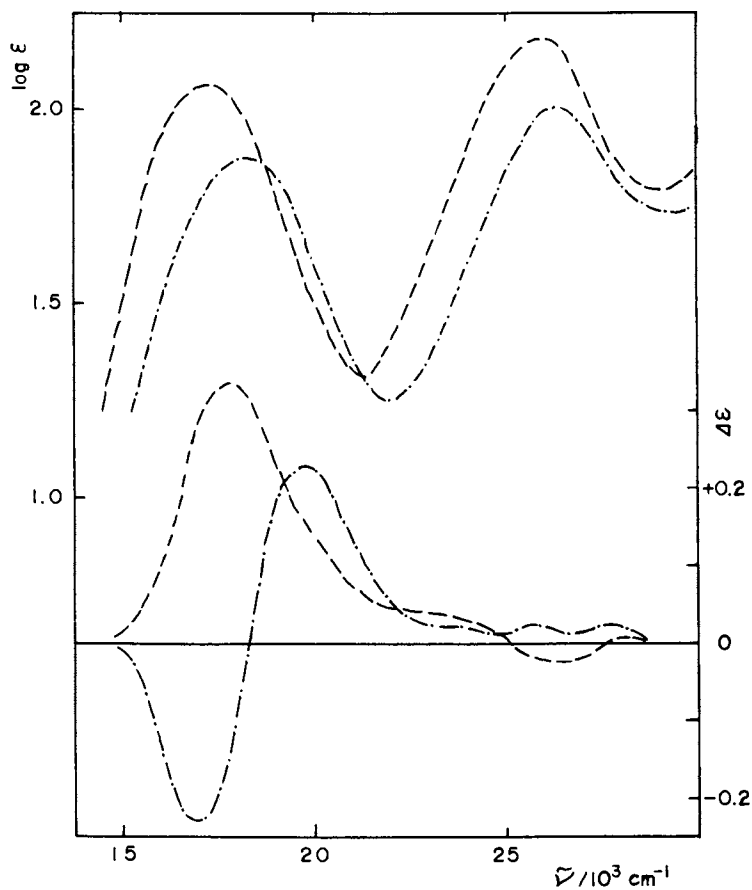


Figure 9. Absolute configuration of  $(-)^{589-}[\text{Co}(\text{NO}_2)_2(\text{ox})(\text{NH}_3)_2]^-$



Chemistry Letters

Figure 10. Absorption and CD spectra of (- · · ·),  $[\text{Co}(\text{ox})(\text{NH}_3)_2(\text{H}_2\text{O})_2]^+$  and (---),  $[\text{Co}(\text{CO}_3)(\text{ox})(\text{NH}_3)_2]^-$  (22)

complex species exhibits a single positive peak. Very recently,  $(-)^{589}\text{-}[\text{Co}(\text{CO}_3)(\text{ox})(\text{NH}_3)_2]^-$  was isolated and its absolute configuration was assigned as  $\Delta$  by means of the CD comparison (23). On this basis, the above-mentioned diaqua complex is now regarded as R. It has also been reported that the acid-hydrolysis of  $\Delta(+)^{589}\text{-}[\text{Co}(\text{CO}_3)(\text{mal})(\text{NH}_3)_2]^-$  to give  $(-)^{589}\text{-}[\text{Co}(\text{mal})(\text{NH}_3)_2(\text{H}_2\text{O})_2]^+$  brings a reversal of the signs of two CD peaks in the  $T_{1g}$  band region, i.e.  $(-, +)$  pattern  $\rightarrow (+, -)$  pattern (23). In view of these facts, it seems most likely that the replacement of two  $\text{H}_2\text{O}$  for a  $\text{CO}_3^{2-}$  in a carbonato enantiomeric complex results in a decrease of the rotational strength, sometimes giving a reversed CD pattern in the  $T_{1g}$  band region.

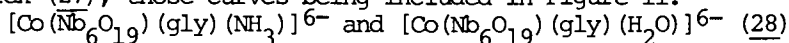
Very recently, Mason (24) investigated the optical activity of  $R(+)\text{-cis-cis-cis-}[\text{Co}(\text{CN})_2(\text{NH}_3)_2(\text{H}_2\text{O})_2]^+$  and  $S(+)\text{-cis-cis-cis-}[\text{Co}(\text{NO}_2)_2(\text{NH}_3)_2(\text{H}_2\text{O})_2]^+$ , which had been reported by Ito and Shibata, theoretically, employing a third-order and a fourth-order ligand-polarization model, and it was concluded that both ligand-polarization mechanisms contribute significantly, but not exclusively, to the d-electron optical activity of chiral unidentate complexes of the all-cis- $[\text{Co}a_2b_2c_2]$  type.

#### Synthesis and CD Spectra of Complexes Containing 1,1,1-Tris(aminomethyl)ethane or Hexaniobate Ion as a Terdentate Ligand

The ligand, 1,1,1-tris(aminomethyl)ethane (tame) is a typical tripod ligand and coordinates facially to a Co(III) ion. Hexaniobate ion,  $\text{Nb}_6\text{O}_{19}^{8-}$ , is known to function as a bulky terdentate ligand (25, 26). Shimura and his coworkers (27, 28) have prepared a few complexes of the  $\text{fac}(A)\text{-}[\text{Co}(A_3)(BC)d]$  type, where  $A_3$  represents those terdentate ligands.

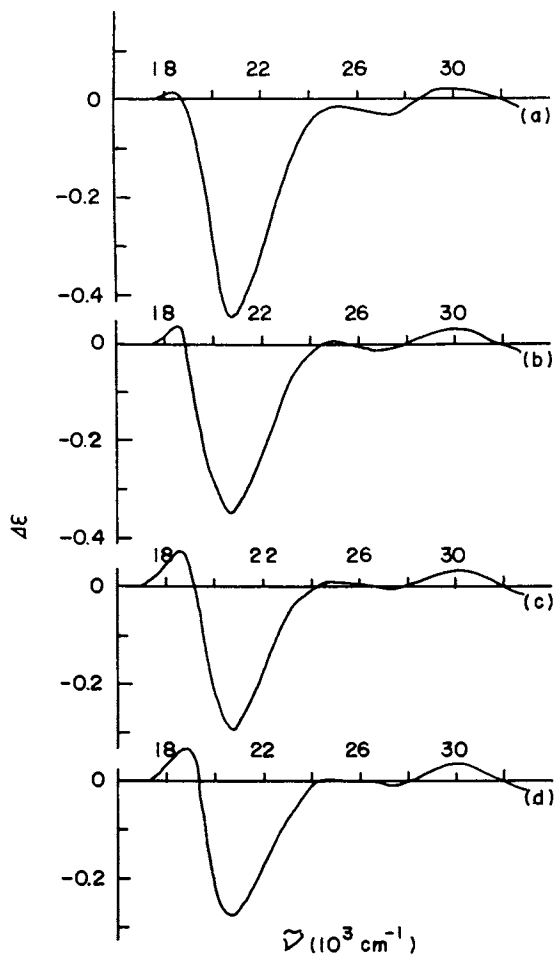
$[\text{Co}(\text{gly})(\text{NH}_3)(\text{tame})]^{2-}$  (27) — The terdentate ligand was prepared in the form of trihydrochloride ( $\text{tame}\cdot 3\text{HCl}$ ). As the starting material for the preparation of the complex they used  $\text{Kcis-}[\text{Co}(\text{CO}_3)_2(\text{NH}_3)_2]\cdot\text{H}_2\text{O}$  (7). The isolated  $[\text{Co}(\text{gly})(\text{NH}_3)(\text{tame})]\text{Cl}_2$  was resolved by using  $\text{K}_2[\text{Sb}_2(\text{d-tart})_2]\cdot 3\text{H}_2\text{O}$  as resolving agent. Other related complexes containing an optically active amino acid instead of glycine have been prepared and separated chromatographically into diastereoisomeric pairs.

The CD spectrum of the  $(-)^{589}\text{-glycinato}$  complex is shown in Figure 11. It is seen that the configurational CD contribution which arises from the chirality due to the arrangement of glycinate and  $\text{NH}_3$  is quite small. On the basis of the so-called additivity rule of the configurational and vicinal contributions, it was found that the configurational curves for the diastereomeric complexes are similar to the CD curve for the enantiomeric complex (27), those curves being included in Figure 11.



— As a reagent for the terdentate ligand sodium hydrogenhexaniobate  $\text{Na}_4\text{HNb}_6\text{O}_{19}\cdot 15\text{H}_2\text{O}$  was used. The action of this previously neutralized reagent on  $\text{Kcis-}[\text{Co}(\text{CO}_3)_2(\text{NH}_3)_2]\cdot\text{H}_2\text{O}$  in aqueous solu-





Bulletin of the Chemical Society of Japan

Figure 11. CD curve of  $(-)\text{-}_{589}[\text{Co}(\text{gly})(\text{NH}_3)(\text{tame})]\text{Cl}_2 \cdot 3\text{H}_2\text{O}$  (a) and calculated configurational curves of  $[\text{Co}(\text{L-ala})(\text{NH}_3)(\text{tame})]^{2+}$  (b),  $[\text{Co}(\text{L-val})(\text{NH}_3)(\text{tame})]^{2+}$  (c), and  $[\text{Co}(\text{L-ileu})(\text{NH}_3)(\text{tame})]^{2+}$  (d) (27)

tion resulted in the isolation of  $K_7[Co(Nb_6O_{19})(CO_3)(NH_3)]$ . Using this intermediate, two complexes of  $[Co(Nb_6O_{19})(gly)-(NH_3)]^{6-}$  and  $[Co(Nb_6O_{19})(gly)(H_2O)]^{6-}$  were isolated as lithium salts. Optical resolutions of these complexes were carried out by the use of (+) $_{589}-[Co(en)_3]Br_3$  as resolving agent.

The other related complexes containing an optically active amino acid instead of glycine have been prepared in a similar manner and chromatographically separated into diastereoisomers.

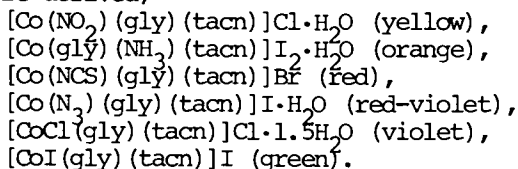
The CD spectra for the less soluble forms of the complexes are shown in Figure 12, in which the calculated configurational curve of an active form of  $[Co(Nb_6O_{19})(L-val)(NH_3)]^{6-}$  is included. In contrast to the CD spectrum of the same complexes, the CD spectra of the hexaniobato complexes deviate considerably from the additivity rule, the reason for such difference between the  $[CoCN_5]$  and the  $[CoO_4N_2]$  types being unknown.

#### Synthesis and CD Spectra of a Series of Complexes Containing 1,4,7-Triazacyclononane

Since the titled cyclic triamine,  $\overline{NHCH_2CH_2NHCH_2CH_2NHCH_2CH_2}$  (tacn) coordinates facially in an octahedral complex, it is available for the preparation of the *fac*(A) $_3$ -[Co(A) $_3$ (BC)d]-type complexes. Using this ligand, glycinate and a variety of unidentates, various complexes of this type were now synthesized by the present authors, their CD spectral studies being carried out.

Synthesis and resolution of the [Coa(gly)(tacn)]-type complexes — The terdentate ligand was prepared as its trihydrochloride by the method of Richman and Atkins (29). Equimolar amounts of *mer*(N)-*trans*(NH $_3$ )-[Co(CO $_3$ )(gly)(NH $_3$ ) $_2$ ] (30) and tacn·3HCl were dissolved in water, and the solution was adjusted to pH 2 with HClO $_4$  (60%) and then adjusted to pH 9 with aqueous KOH solution, whereupon the color of the solution changed from violet to red, indicating the formation of [Co(gly)(tacn)-(H $_2$ O)] $^{2+}$ . The purification of the desired complex species was carried out by means of ion-exchange chromatography (SP-Sephadex C-25 in Na $^+$  form and 0.1 M NaClO $_4$ ). Finally, from an ethanolic solution of the concentrated eluate, red crystals of the aqua complex compound, [Co(gly)(tacn)(H $_2$ O)](ClO $_4$ ) $_2$ , was obtained.

Using this aqua complex as an intermediate, the following compounds were derived;



The reaction of the aqua complex and KCN in aqueous solution gave no cyano complex, unidentified materials being formed in the reaction mixture. Instead the action of KCN on [CoCl(gly)(tacn)]NO $_3$  in dimethylsulfoxide resulted in the substitution of coordinated chloride ion by cyanide ion. From the reaction

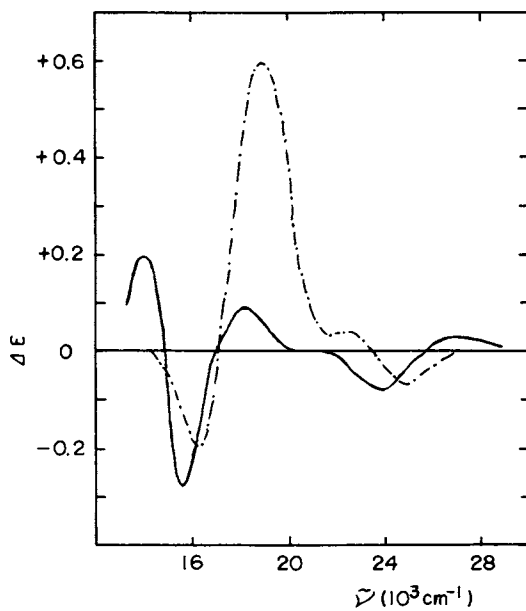


Figure 12. CD spectra of (---),  $(+)^{546}_{CD}\text{-[Co(Nb}_6\text{O}_{19})(\text{gly})(\text{NH}_3)]^{6-}$  and (—),  $(+)^{546}_{CD}\text{-[Co(Nb}_6\text{O}_{19})(\text{gly})(\text{H}_2\text{O})]^{6-}$  (28)

mixture yellow crystals,  $[\text{Co}(\text{CN})(\text{gly})(\text{tacn})]\text{Br}$ , were obtained after ion-exchange purification.

Optical resolutions of the cyano, nitro and ammine complexes were carried out by column chromatography of SP-Sephadex C-25 in the  $\text{Na}^+$  form. Complete separation of the two enantiomers was achieved by using 0.05 M  $\text{Na}_2[\text{Sb}_2(\text{d-tart})_2] \cdot 2\text{H}_2\text{O}$  as eluent. The isothiocyanato, aqua, azido and dichloro complexes were resolved completely on columns of Dowex 50W-X8 resin in  $\text{Na}^+$  form by eluting with 0.3 M  $\text{Na}_2[\text{Sb}_2(\text{d-tart})_2] \cdot 2\text{H}_2\text{O}$ . It is worth noting that ion-exchange resin is used very effectively for such a complex for which resolution is achieved only partially on the Sephadex column. Resolution of the iodo complex was unsuccessful because of a great lability of the ligating iodide for ligand substitutions.

Absorption and CD spectra of the  $[\text{Co}(\text{gly})(\text{tacn})]$ -type complexes — The absorption spectrum of the racemic ammine complex and the CD spectra of the resolved isomers are shown in Figure 13, showing that the CD curves are mirror images of each other. Since the same situation is encountered in the resolved pairs of other complexes, the CD spectra for only the isomers obtained from the earlier eluates are illustrated together with the absorption spectra in Figures 14-17. The spectra for the hydroxo complex,  $[\text{Co}(\text{OH})(\text{gly})(\text{tacn})]^+$ , were those measured with an aqueous solution of the aqua complex at pH 9.0.

A striking characteristic in common for all of the CD spectra for the earlier eluted enantiomers, except for the  $\text{CN}^-$ -containing isomer, is that a major CD peak of negative sign is observed on the higher-frequency-side in the first absorption band region. The CD curve of the  $\text{CN}^-$ -containing isomer shows one peak with a shoulder at higher frequency.

Experiments were tried to obtain optically active complexes directly from the  $(-)^{589}[\text{Co}(\text{gly})(\text{tacn})(\text{H}_2\text{O})]^{2+}$  complex. The conversions were successful to give the corresponding  $(-)^{589}$ -nitro,  $(-)^{589}$ -isothiocyanato,  $(+)^{589}$ -azido and  $(-)^{589}$ -chloro complexes. On the other hand, the oxidation of the  $(-)^{589}[\text{Co}(\text{NCS})(\text{gly})(\text{tacn})]^+$  complex by aqueous  $\text{H}_2\text{O}_2$  at pH ca. 3 produced  $(-)^{589}$ -ammine,  $(-)^{589}$ -cyano and  $(-)^{589}$ -aqua complexes, all being separated chromatographically. Similar oxidative degradation reactions have been reported by Gillard and Maskill (31); they found that  $(-)-[\text{Co}(\text{NCS})_2(\text{en})]^{+}$  was converted into  $(-)-[\text{Co}(\text{NH}_3)_2(\text{en})]^{3+}$  and also to  $L(-)-[\text{Co}(\text{CN})_2(\text{en})]^{+}$ , and that these three complexes have the same absolute configuration.

On the basis of the above results, it is assumed that the earlier eluted enantiomers, whose major CD peaks have negative sign, have the same arrangement with respect to the glycinate and an unidentate ( $\text{CN}^-$ ,  $\text{NO}_2^-$ ,  $\text{NH}_3$ ,  $\text{NCS}^-$ ,  $\text{H}_2\text{O}$ ,  $\text{OH}^-$ ,  $\text{N}_3^-$ , or  $\text{Cl}^-$ ). An X-ray analysis has been carried out for  $(-)^{589}[\text{Co}(\text{gly})(\text{NH}_3)(\text{tacn})]\text{I}_2 \cdot \text{H}_2\text{O}$ , and its absolute configuration has been determined as shown in Figure 18 (32).

For the present chiral complexes, three sources of  $\underline{d}$ -

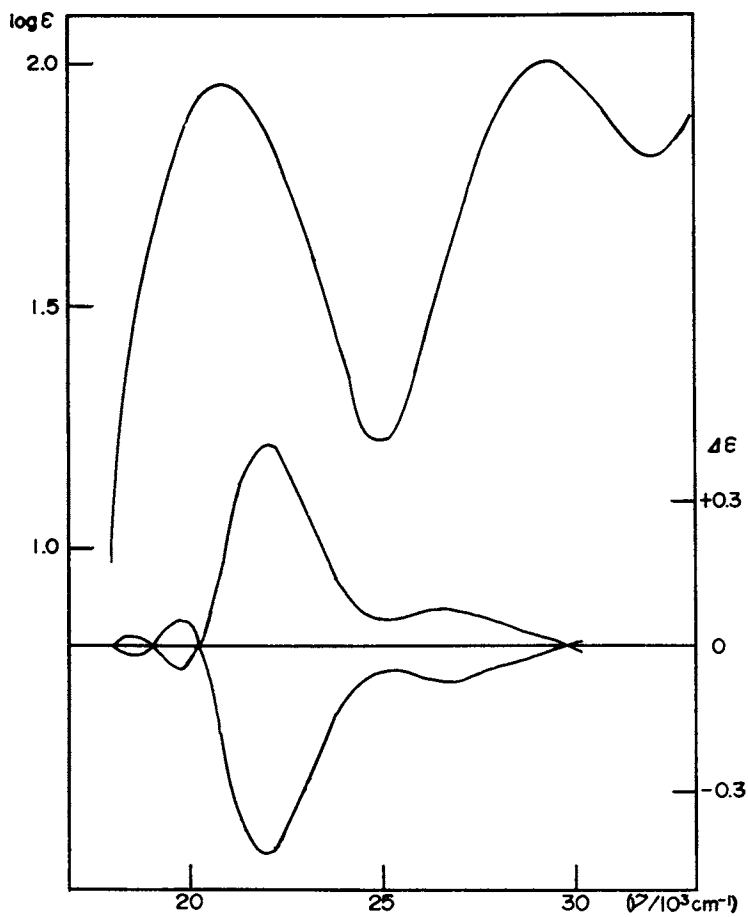


Figure 13. Absorption and CD spectra of enantiomers of  $[\text{Co}(\text{gly})(\text{NH}_3)(\text{tacn})]^{2+}$

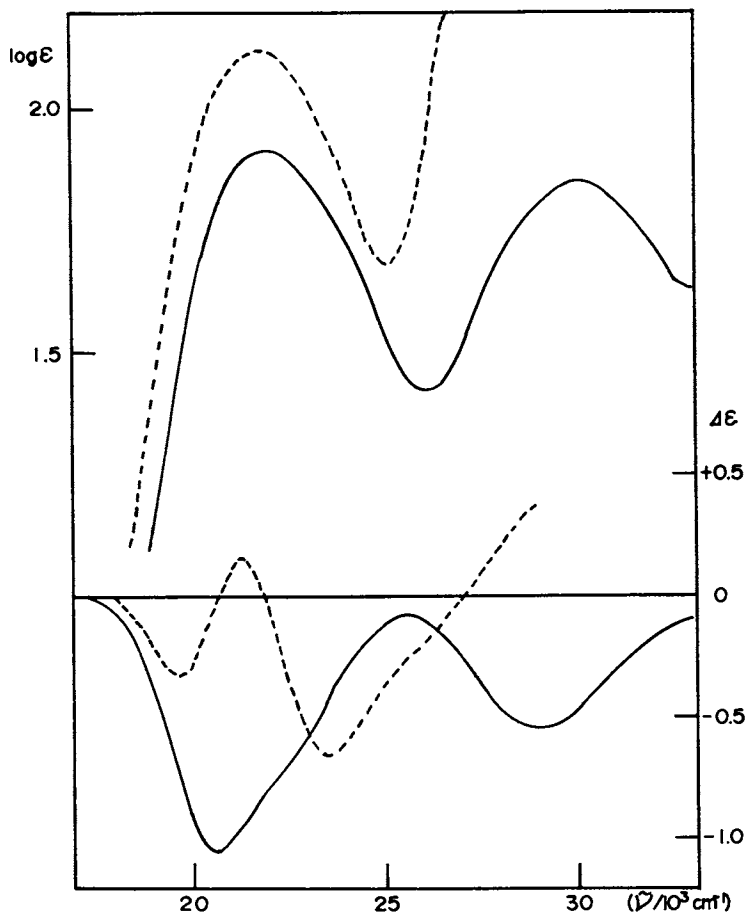


Figure 14. Absorption and CD spectra of  $(-)_598\text{-[Co(CN)(gly)(tacn)]}^+$  and  $(-)_589\text{-[Co(NO}_2\text{)(gly)(tacn)]}^+$

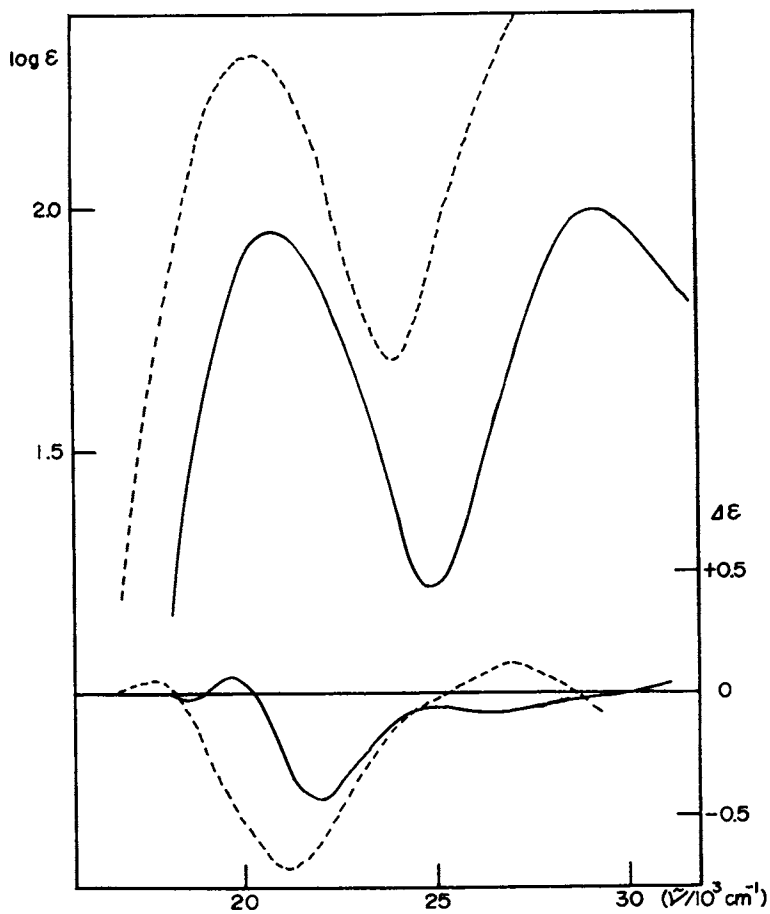


Figure 15. Absorption and CD spectra of (—)  $(-)_S_{89}[\text{Co}(\text{gly})(\text{NH}_3)(\text{tacn})]^{2+}$  and (---)  $(-)_S_{89}[\text{Co}(\text{NCS})(\text{gly})(\text{tacn})]^+$

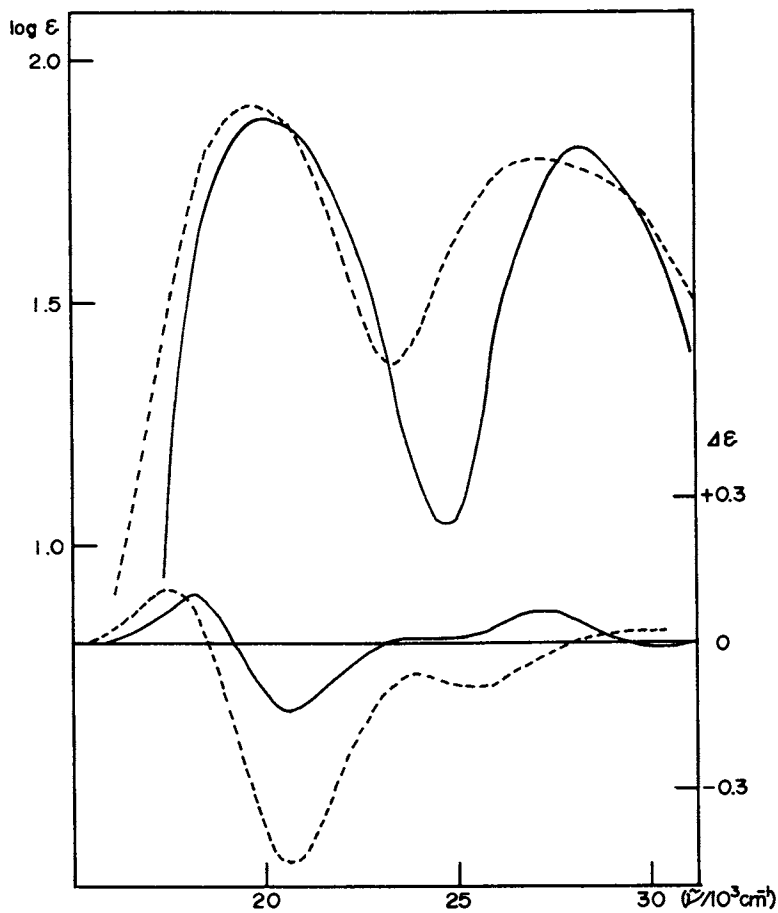


Figure 16. Absorption and CD spectra of  $(-)_S S S-[Co(gly)(tacn)(H_2O)]^{2+}$  and  $(-)_S S S-[Co(OH)(gly)(tacn)]^+$



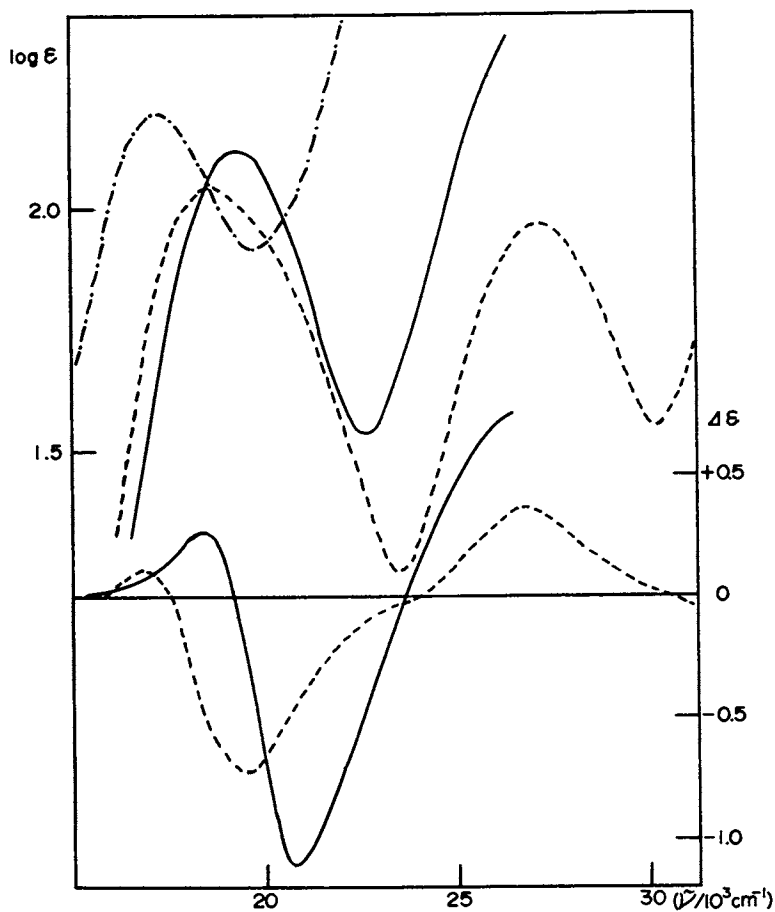
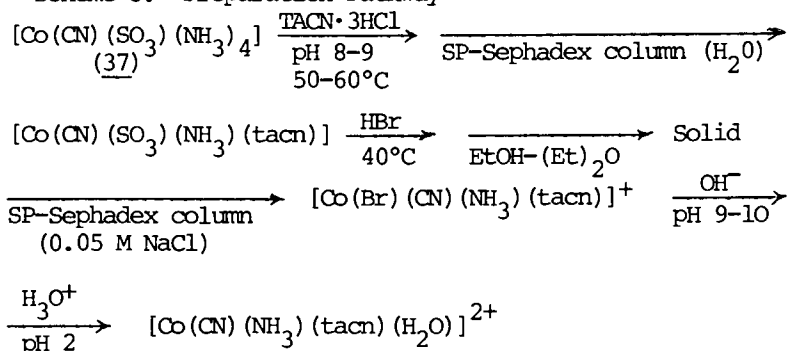


Figure 17. Absorption spectra of  $[\text{Co}(a)(\text{gly})(\text{tacn})]$ : (—),  $a = \text{N}_3$ ; (---), Cl; (- · - ·), I. CD spectra of (—),  $(+)_S$   $[\text{Co}(\text{N}_3)(\text{gly})(\text{tacn})]^+$  and (---),  $(-)_S$   $[\text{Co}(\text{Cl})(\text{gly})(\text{tacn})]^+$ .

electron optical activity must be considered. They are helical distribution of a glycinato ring and a  $-\text{NH}-\text{CH}_2-\text{CH}_2-\text{NH}-$  chelate ring of tacn, the conformation of the three chelate rings of tacn, and the arrangement of a glycinato ring and an unidentate. However, it is thought that the first and second sources have little effect on the solution CD spectrum on the basis of the following facts. The CD spectra of  $(-)^{589}-[\text{Co}(\text{gly})(\text{NH}_3)(\text{tacn})]^{2+}$  and  $(-)^{589}-[\text{Co}(\text{gly})(\text{NH}_3)(\text{tame})]^{2+}$  resemble well to each other in the shape and peak intensity; the  $\Delta\epsilon$  value for  $(-)^{589}-[\text{Co}(\text{gly})(\text{NH}_3)(\text{tacn})]^{2+}$ ,  $\Delta\epsilon=-0.42$ , corresponds well with that for  $(-)^{589}-[\text{Co}(\text{gly})(\text{NH}_3)(\text{tame})]^{2+}$ ,  $\Delta\epsilon=-0.44$  (27).

CD spectral studies on bis[R-2-methyl-1,4,7-triazacyclononane]cobalt(III),  $[\text{Co}(\text{R-metacn})_2]^{3+}$ , have been reported by Mason and Peacock (33) and later by Nonoyama (34). For this complex, nine geometrical isomers are possible and five isomers have been isolated by means of chromatography on SP-Sephadex (34). Each CD spectrum exhibited a very strong positive peak in the first absorption band region ( $\Delta\epsilon=+4.35$  to  $+4.72$ ), due to chiral puckering, with the  $\lambda$ -conformation, of each of the six chelate rings (33, 34). The crystal structure has been determined for a mixture of the three isomers (35). In this connection the present authors have found that when CD measurements were carried out for an aqueous solution of bis(1,4,7-triazacyclononane)cobalt(III),  $[\text{Co}(\text{tacn})_2]^{3+}$ , in the presence of  $[\text{Sb}_2(\text{d-tart})_2]^{2-}$ , a positive peak was observed in the first absorption band region, indicating preferential formation of a conformation (probably  $\lambda$ ) of the chelate rings. This observation suggests that the conformational contribution becomes appreciable if a conformation is advantageous for the tacn chelate rings. In other words, the observation supports a small contribution from a fixed conformation to the solution spectrum for the present  $[\text{Co}(\text{a})(\text{gly})(\text{tacn})]$  complex, even though the crystal structure of the complex reveals either  $\lambda\lambda\lambda$  or  $\delta\delta\delta$  ring conformation.

Scheme 3. Preparation Pathway



Complexes of [Coabc(tacn)]-type — At the present stage of the work two complexes,  $[\text{Co}(\text{Br})(\text{CN})(\text{NH}_3)(\text{tacn})]\text{Cl}$  and  $[\text{Co}(\text{CN})-$

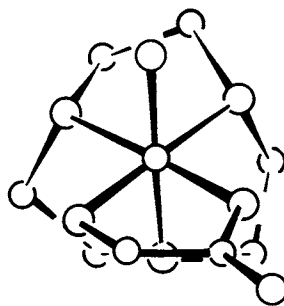


Figure 18. Absolute configuration of  $(-)_s{}_{89}\text{-}[\text{Co}(\text{gly})(\text{NH}_3)(\text{tacn})]^{2+}$

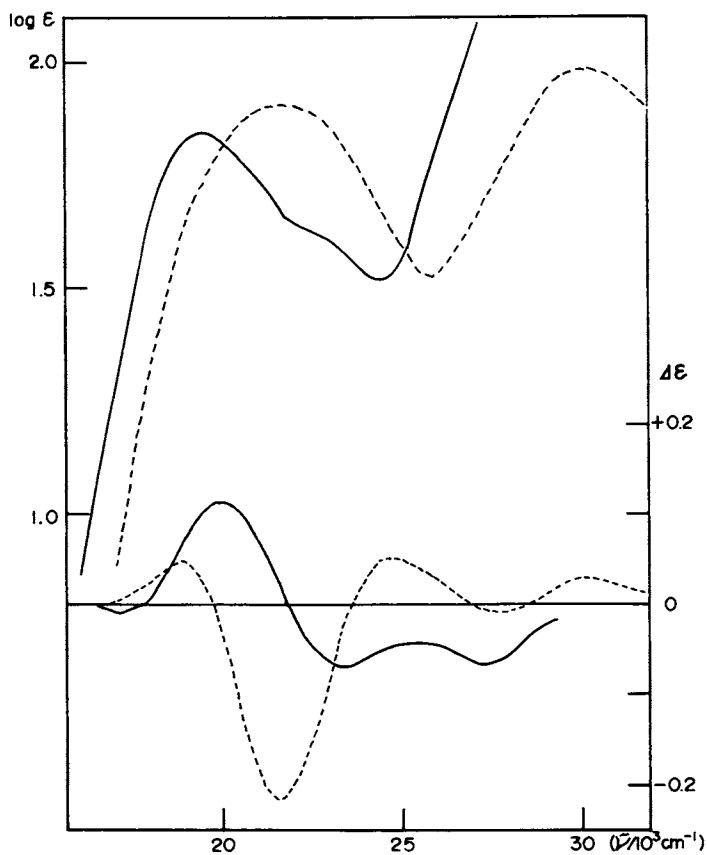


Figure 19. Absorption and CD spectra of (—),  $(+)_s{}_{89}\text{-}[\text{Co}(\text{CN})(\text{Br})(\text{NH}_3)(\text{tacn})]^{+}$  and (---),  $(+)_s{}_{46}\text{-}^{CD}\text{-}[\text{Co}(\text{CN})(\text{NH}_3)(\text{tacn})(\text{H}_2\text{O})]^{2+}$

$(\text{NH}_3)(\text{tacn})(\text{H}_2\text{O})](\text{ClO}_4)_2$ , have been prepared and resolved into their enantiomers (36)<sup>4,2</sup>. The preparation pathway is given in Scheme 3. Optical resolutions were carried out similarly to those for the  $[\text{Co}(\text{gly})(\text{tacn})]$ -type complexes (SP-Sephadex C-25 in  $\text{Na}^+$  form and  $[\text{Sb}_2(\text{d-tart})_2]^{2-}$  eluent). The absorption and CD spectra are shown in Figure 19.

#### Literature Cited

1. Nakamoto, K. and McCarthy, P. J. (eds.), "Spectroscopy and Structure of Metal Chelate Compounds." pp.156-215, John Wiley Sons, Inc., New York, 1968.
2. Hawkins, C. J., "Absolute Configuration of Metal Complexes," Wiley-Interscience, New York, 1971.
3. Ciardelli, F. and Salvadori, P. (eds.), "Fundamental Aspects and Recent Developments in Optical Rotatory Dispersion and Circular Dichroism." pp.196-239, Heyden Son Ltd., London, 1973.
4. Hawkins, C. J., Stark, J. A. and Wong, C. L., Aust. J. Chem., (1972), 25, 273.
5. Bailar, J. C., Jr. and Peppard, D. F., J. Am. Chem. Soc., (1940), 62, 105.
6. Ito, T. and Shibata, M., Inorg. Chem., (1977), 16, 108.
7. Shibata, M., Proc. Jpn. Acad., (1974), 50, 779.
8. Shibata, Y. and Maruki, T., J. Coll. Sci. Im. Univ. Tokyo, (1917), 41, Art. 2, 1.
9. Riesenfeld, E. and Klement, R., Z. Anorg. Chem., (1922), 124, 1.
10. Thomas, W., J. Chem. Soc., (1923), 123, 617.
11. Ray, B. C., J. Indian Chem. Soc., (1937), 14, 440.
12. Wells, A. F., Z. Kris., (A), (1936), 95, 74.
13. Gilinskaya, E. A., Ser. Fiz-Mat. i Estestven. Nauk, (1953), 3, 133.
14. Komiyama, Y., Bull. Chem. Soc. Jpn., (1953), 29, 300.
15. Komiyama, Y., Bull. Chem. Soc. Jpn., (1954), 30, 13.
16. Ito, T. and Shibata, M., Chem. Lett., 1975, 375.
17. McCaffery, A. J., Mason, S. F. and Norman, B. J., J. Chem. Soc., 1965, 5094.
18. Cahn, R. S., Ingold, C. K. and Prelog, V., Angew. Chem., Int. Ed. Engl., (1966), 5, 385.
19. Toriumi, K., Saito, S. and Saito, Y., Acta Cryst., (1977), B33, 1378.
20. Werner, A., Ber. Dtsch. Chem. Ges., (1919), 45, 1229.
21. Shintani, H., Sato, S. and Saito, Y., Acta Cryst., (1976), B32, 1184.
22. Enomoto, Y., Ito, T. and Shibata, M., Chem. Lett., 1974, 423.
23. Muramoto, S. and Shibata, M., Bull. Chem. Soc. Jpn., (1978), 51, 3505.
24. Mason, S. F., Mol. Phys., (1979), 37, 843.
25. Flynn, C. M., Jr. and Stucky, G. D., Inorg. Chem., (1969), 8, 178.

26. Flynn, C. M., Jr. and Stucky, G. D., Inorg. Chem., (1969), 8, 335.
27. Yamanari, K., Hidaka, J. and Shimura, Y., Bull. Chem. Soc. Jpn., (1975), 48, 1653.
28. Hosokawa, Y., Hidaka, J. and Shimura, Y., Bull. Chem. Soc. Jpn., (1975), 48, 3175.
29. Richman, J. E. and Atkins, T. J., J. Am. Chem. Soc., (1974), 96, 2268.
30. Kanazawa, S. and Shibata, M., Bull. Chem. Soc. Jpn., (1971), 48, 2424.
31. Gillard, R. D. and Maskill, R., J. Chem. Soc. (A), 1971, 2813.
32. Sato, S., Ohba, S., Shimba, S., Fujinami, S., Shibata, M. and Saito, Y., Acta Cryst., (1978), B35, in press.
33. Mason, S. F. and Peacock, R. D., Inorg. Chim. Acta, (1976), 19, 75.
34. Nonoyama, M., Inorg. Chim. Acta, (1978), 29, 211.
35. Mikami, M., Kuroda, R., Konno, M. and Saito, Y., Acta Cryst., (1977), B33, 1485.
36. Shimba, S., Fujinami, S. and Shibata, M., Chem. Lett., 1979, 783.
37. Siebert, V. H., Z. Anorg. Allg. Chem., (1964), 327, 63.

RECEIVED September 13, 1979.

# Optical Resolution of Facial and Meridional Tris(aminoacidato)cobalt(III) Chelates by *d*-Tartrate and by Antimony *d*-Tartrate

HAYAMI YONEDA, SHIGEO YAMAZAKI, and TOMOYO YUKIMOTO

Department of Chemistry, Faculty of Science, Hiroshima University,  
Hiroshima, Japan

It is not easy to obtain both enantiomers of non-charged chiral complexes in optically pure form. Chromatographic separation by the use of asymmetric adsorption on an optically active adsorbent (for example, quartz, starch and *d*-lactose *etc.*) has been regarded as almost the only means for this purpose. However, usually such procedures lead to partial separation of enantiomers. This is probably because asymmetric adsorption is very weak. To make matters worse, we do not know the stereochemistry of asymmetric adsorption, nor how to improve the efficiency of separation. We attempted to attack this problem by extending the technique and the ion association model for ion-exchange chromatography. Here, we describe the mechanism of chromatographic separation of enantiomers of facial and meridional tris(aminoacidato)cobalt(III) chelates (See Figure 1).

## Complete Resolution of *fac*-[Co( $\beta$ -ala)<sub>3</sub>]

The facial isomer of [Co( $\beta$ -ala)<sub>3</sub>] has three carboxyl oxygen atoms in a triangular face of an octahedron and three amino groups in the opposite triangular face. The expected large dipole moment causes fairly large adsorption on the adsorbent. Thus, chromatographic separation of enantiomers is expected with a suitable resolving agent. On the other hand, [Co(en)<sub>3</sub>]<sup>3+</sup> was reported to be resolved completely into enantiomers through a column packed with the Na form of SE-Sephadex cation-exchanger using an aqueous solution of Na<sub>2</sub> *d*-tartrate (1). As a part of the structural studies of optical resolution, we have determined the crystal structures of a series of diastereomeric salts,  $\Lambda$ -[Co(en)<sub>3</sub>]Br·*d*-tart·5H<sub>2</sub>O (2),  $\Lambda$ -Li[Cr(en)<sub>3</sub>](*d*-tart)<sub>2</sub>·3H<sub>2</sub>O (3) and  $\Lambda$ -H[Co(en)<sub>3</sub>](*d*-tart)<sub>2</sub>·3H<sub>2</sub>O (4). Although these crystals are quite different in chemical formula, cell dimension, and space group symmetry, they have a remarkable resemblance to each other in the face-to-face close contact mode of *d*-tart with  $\Lambda$ -[M(en)<sub>3</sub>]<sup>3+</sup>. This ion-pair structure is formed by the contact of the four oxygen atoms of *d*-tart and the three NH<sub>2</sub> groups of the complex. Therefore,

0-8412-0538-8/80/47-119-315\$05.00/0

© 1980 American Chemical Society

only one half of the complex is involved in this association. Since *fac*-[Co( $\beta$ -ala)<sub>3</sub>] has a similar triangular face of three NH<sub>2</sub> groups and shows the AB-type PMR signal of the NH<sub>2</sub> groups similar to that of [Co(en)<sub>3</sub>]<sup>3+</sup>, quite similar association of *d*-tart is expected for *fac*-[Co( $\beta$ -ala)<sub>3</sub>]. In fact, this complex was separated completely into enantiomers through the column packed with Na form of CM-Sephadex cation-exchanger by the use of Na<sub>2</sub>*d*-tart dissolved in ethanol-water mixed solvent (5).

Separation and Identification of Isomers of *fac*-[Co( $\alpha$ -AA)<sub>3-n</sub>( $\beta$ -AA)<sub>n</sub>] (6)

In order to obtain the detailed feature of optical resolution of *fac*-[Co(AA)<sub>3</sub>] where AA represents  $\alpha$ - or  $\beta$ -amino acid, a series of diastereomeric or enantiomeric mixtures of *fac*-[Co( $\alpha$ -AA)<sub>3-n</sub>( $\beta$ -AA)<sub>n</sub>] were prepared and each mixture was eluted by passing an aqueous solution of Na<sub>2</sub>*d*-tart through the column packed with TSK cation-exchange resin. For *fac*-[Co(gly)<sub>3-n</sub>( $\beta$ -ala)<sub>n</sub>], the retention volumes of the enantiomers were obtained in each chromatographic run. Thus, the ratio of the retention volumes of enantiomers, that is, the separation factor for  $\Lambda$  and  $\Delta$  pairs of [Co(gly)<sub>2</sub>( $\beta$ -ala)], [Co(gly)( $\beta$ -ala)<sub>2</sub>] and [Co( $\beta$ -ala)<sub>3</sub>] were obtained easily.

In case a chiral amino acid, L- or D-serine is involved in complex formation, the procedure to obtain the separation factors for enantiomeric pairs,  $\Lambda$ (L)- $\Lambda$ (D) and  $\Delta$ (D)- $\Delta$ (L) is complicated.

Facial complexes separated through the H<sup>+</sup> form of SP-Sephadex, [Co(L-ser)<sub>3</sub>], [Co(L-ser)<sub>2</sub>( $\beta$ -ala)] and [Co(L-ser)( $\beta$ -ala)<sub>2</sub>] contain the chiral ligand L-ser and are presumed to be the mixture of diastereomers,  $\Lambda$ (L) and  $\Delta$ (L). Separation of diastereomers is, in general, not so difficult as that of enantiomers. Each of these diastereomeric mixtures was chromatographed through the column of TSK ion-exchange resin using Na<sub>2</sub>SO<sub>4</sub> aqueous solution as eluent. Each elution curve consists of two peaks, a large first elution peak and a much smaller second elution peak. The problem is whether the first eluted isomer has the  $\Delta$  configuration or not. To determine this, the first and the second eluted fractions were collected, and the CD spectra of these fractions were measured.

Since the CD spectrum of the first eluted isomer of *fac*-[Co(L-ser)<sub>3</sub>] is quite similar to that of  $\Delta$ -*fac*-[Co(L-ala)<sub>3</sub>] whose absolute configuration is established (7), the first eluted isomer is concluded to have the  $\Delta$  configuration (Figure 2(a)). The second eluted isomer should be assigned to  $\Lambda$ . In the case of *fac*-[Co(L-ser)<sub>2</sub>( $\beta$ -ala)], the first eluted isomer shows the CD pattern similar to that of the first eluted isomer of *fac*-[Co(L-ser)<sub>3</sub>] in that the major CD band lies in the longer wavelength region (ca. 525 nm). Therefore, the first eluted isomer in this case is also assigned as  $\Delta$ . Here, a small CD component of opposite sign to the major peak appears at ca. 500 nm, as the result of substitution of  $\beta$ -ala for L-ser. This effect should be more marked in the CD

spectrum of *fac*-[Co(L-ser)( $\beta$ -ala)<sub>2</sub>]. In fact, in the CD spectrum of the first eluted isomer of *fac*-[Co(L-ser)( $\beta$ -ala)<sub>2</sub>], the component in the longer wavelength region diminishes, and the component at ca. 500 nm is enhanced (Figure 2(c)). Since the first eluted isomer in this case is also the major component of the diastereomeric mixture as it is in the first and second cases, it is natural to assign the first eluted isomer in the third complex to  $\Delta$ . *Facial*-[Co( $\beta$ -ala)<sub>3</sub>] is not separated into two peaks with Na<sub>2</sub>SO<sub>4</sub> solution. Here, the Na<sub>2</sub>*d*-tart solution is used instead of Na<sub>2</sub>SO<sub>4</sub>, and optical resolution was achieved. In Figure 2(d), the CD spectrum of the second eluted isomer is shown. The spectrum pattern is quite similar to that of the first eluted isomer of *fac*-[Co(L-ser)( $\beta$ -ala)<sub>2</sub>] (Figure 2(c)). Thus, it is safely concluded that the isomer of *fac*-[Co( $\beta$ -ala)<sub>3</sub>] eluted first with *d*-tart has the configuration  $\Lambda$ , and that the second eluted isomer has the configuration  $\Delta$ . This assignment coincides with the assignment made by analogy with the case of  $\Lambda$ -[Co(en)<sub>3</sub>]<sup>3+</sup>-*d*-tart.

The CD spectra of the second eluted isomers of three complexes, [Co(L-ser)<sub>3-n</sub>( $\beta$ -ala)<sub>n</sub>](n=0,1 and 2) are not exactly the same with but quite similar to those of the corresponding first eluted isomers, except that the CD sign is opposite. From these CD spectra, the CD spectra of  $\Delta$ - and  $\Lambda$ -[Co(D-ser)<sub>3-n</sub>( $\beta$ -ala)<sub>n</sub>] are estimated. They could not be measured directly because only a small amount of D-serine complexes was available. When eluted with Na<sub>2</sub>SO<sub>4</sub> solution, the elution curve of *fac*-[Co(D-ser)<sub>3-n</sub>( $\beta$ -ala)<sub>n</sub>] is the same as that of the corresponding L-serine complexes. Thus, the configuration of the first eluted isomer in the D-serine complexes must be  $\Lambda$ . In this way, we have obtained two series of the retention volumes of diastereomeric pairs,  $\Delta$ (major peak) and  $\Lambda$ (minor peak) for L-serine complexes and  $\Lambda$ (major peak) and  $\Delta$ (minor peak) for D-serine complexes. When eluted with Na<sub>2</sub>SO<sub>4</sub> solution, the ratio for each enantiomeric pair is always quite close to unity, which means that they are certainly enantiomeric pairs.

As stated before, the CD spectrum of *fac*-[Co(L-ser)<sub>2-n</sub>( $\beta$ -ala)<sub>n</sub>] shows a gradual change with increasing number of  $\beta$ -ala. If we changed this assignment of the configuration of one of these complexes from  $\Delta$  to  $\Lambda$ , this gradual change in the CD spectrum pattern would be broken. In addition,  $\Delta$ -*fac*-[Co(L-ala)<sub>3</sub>] is fairly soluble in water, while  $\Lambda$ -*fac*-[Co(L-ala)<sub>3</sub>] is insoluble. Therefore, it is natural to assign the configuration of the more soluble diastereomer to  $\Delta$ (L) or  $\Delta$ (D). Since the second eluted isomer  $\Lambda$ (L) or  $\Delta$ (D) has very low solubility, most of it is presumed to be removed at the filtration stage of the preparation, giving a much smaller quantity of this isomer.

#### Trend of the Separation Factors of Enantiomeric Pairs Eluted with *d*-Tart

The separation of each diastereomeric pair was complete when



0.1M Na<sub>2</sub>*d*-tart aqueous solution was used in place of Na<sub>2</sub>SO<sub>4</sub> solution. The procedure to obtain the separation factor( $\alpha$ ) of the enantiomeric pair is the same with that eluted with Na<sub>2</sub>SO<sub>4</sub>. The results are shown in Table I.

Table I. The Separation Factor of Enantiomeric Pairs Eluted with *d*-Tart

| Samples   | $\alpha$ |
|---|----------|
| ( I ) $\begin{matrix} fac-\Delta[Co(D-ser)_3] \\ fac-\Delta[Co(L-ser)_3] \end{matrix}$                          | 1.007    |
| ( II ) $\begin{matrix} fac-\Delta[Co(D-ser)_3] \\ fac-\Lambda[Co(L-ser)_3] \end{matrix}$                        | 1.007    |
| ( III ) $\begin{matrix} fac-\Lambda[Co(D-ser)_2(\beta-ala)] \\ fac-\Delta[Co(L-ser)_2(\beta-ala)] \end{matrix}$ | 1.033    |
| ( IV ) $\begin{matrix} fac-\Delta[Co(D-ser)_2(\beta-ala)] \\ fac-\Lambda[Co(L-ser)_2(\beta-ala)] \end{matrix}$  | 1.032    |
| ( V ) $\begin{matrix} fac-\Lambda[Co(D-ser)(\beta-ala)_2] \\ fac-\Delta[Co(L-ser)(\beta-ala)_2] \end{matrix}$   | 1.090    |
| ( VI ) $\begin{matrix} fac-\Delta[Co(D-ser)(\beta-ala)_2] \\ fac-\Lambda[Co(L-ser)(\beta-ala)_2] \end{matrix}$  | 1.005    |
| ( VII ) $\begin{matrix} fac-\Delta[Co(\beta-ala)_3] \\ fac-\Lambda[Co(\beta-ala)_3] \end{matrix}$               | 1.060    |
| ( VIII ) $\begin{matrix} fac-\Delta[Co(gly)(\beta-ala)_2] \\ fac-\Lambda[Co(gly)(\beta-ala)_2] \end{matrix}$    | 1.047    |
| ( IX ) $\begin{matrix} fac-\Delta[Co(gly)_2(\beta-ala)] \\ fac-\Lambda[Co(gly)_2(\beta-ala)] \end{matrix}$      | 1.022    |

Inspection of these separation factors reveal that the enantiomeric separation is most efficient for  $fac-[Co(\beta-ala)_3]$  which contains three six-membered chelate rings, and that the separation efficiency decreases with increasing number of five-membered chelate rings. For  $fac-[Co(ser)_3]$ , little separation of enantiomers with *d*-tart takes place. Here, it must be noted that the separation factors for the pair,  $\Delta-fac-[Co(D-ser)(\beta-ala)_2] - \Lambda-fac-[Co(L-ser)(\beta-ala)_2]$ , and the pair,  $\Delta-fac-[Co(L-ser)(\beta-ala)_2] - \Lambda-fac-[Co(D-ser)(\beta-ala)_2]$  are quite different from each other, the former is exceedingly high, and the latter exceedingly low. However, the average comes close to the value of  $fac-[Co(gly)(\beta-ala)_2]$ .

Association Model for Discrimination

As to the mechanism of optical resolution of  $[\text{Co}(\text{en})_3]^{3+}$ , a face-to-face close contact model was proposed, in which the *d*-tart anion approaches along the three-fold axis of the complex toward the triangular face formed by the three  $\text{NH}_2$  groups of the complex (See, Figure 3). Here three N-H bonds serve for hydrogen bonding with three oxygen atoms of *d*-tart to strengthen the association. We consider that the existence of the fourth oxygen atom of *d*-tart plays a decisive role for discrimination of the  $\Lambda$  isomer from the  $\Delta$ . The fourth oxygen fits in the space between two en chelate rings in the ion-pair,  $\Lambda\text{-}[\text{Co}(\text{en})_3]^{3+}\text{-}d\text{-tart}$  (See Figure 3). However, if the complex is replaced by the  $\Delta$  enantiomer, the fourth oxygen will touch the shoulder of the chelate ring, so that the structure of the ion-pair will not be intimate. Anyway, for discrimination of enantiomers, association assisted by hydrogen bonding is necessary. Therefore, it is natural to assume that the direction of the N-H bond is important for *d*-tart to form hydrogen bonds. Since the  $\text{NH}_2$  group of  $[\text{Co}(\text{en})_3]^{3+}$  has axial and equatorial N-H bonds, the association of *d*-tart along the three-fold axis of the complex is presumed to be assisted by hydrogen bonding using the axial N-H bonds. The facial complex  $[\text{Co}(\beta\text{-ala})_3]$  also has axial and equatorial N-H bonds. Thus, quite similar discrimination mechanism can be presumed for *fac*- $[\text{Co}(\beta\text{-ala})_3]$ . However, the situation will change for *fac*- $[\text{Co}(\alpha\text{-AA})_3]$ . As is well known, the  $\alpha$ -aminoacidato ligand forms a five-membered chelate ring which is almost planar (8). Thus, two N-H bonds of a chelate ring are directed upward and downward from this plane with equal angles. Therefore, looking at the complex, for example, *fac*- $[\text{Co}(\text{L-ser})_3]$  along its three-fold axis, the two N-H bonds of a chelate ring are directed like a letter "V". There is no difference between the two N-H bonds as axial and equatorial in the  $\beta$ -ala chelate ring (9). Consequently, the oxygen atoms of *d*-tart have two possibilities to make hydrogen bonding with either one of these two N-H bonds. This situation may work unfavorably for *d*-tart to discriminate the  $\Lambda$  from the  $\Delta$ . The small separation factor of *fac*- $[\text{Co}(\text{ser})_3]$  can be thus understood.

Trend of the Separation Factors of Enantiomeric Pairs Eluted with Antimony *d*-Tart

The separation of each diastereomeric pair was also complete for 0.1M  $\text{Na}_2\text{Sb } d\text{-tart}$  aqueous solution as eluent. The procedure to obtain the separation factor ( $\alpha$ ) was the same as for *d*-tart. The results are shown in Table II. As seen from these figures, the separation factor decreases with increasing number of  $\beta$ -ala ligands. This trend is just the reverse to the trend in the case of *d*-tart. Therefore, the discrimination mechanism for Sb *d*-tart is presumed to be quite different from that for *d*-tart.

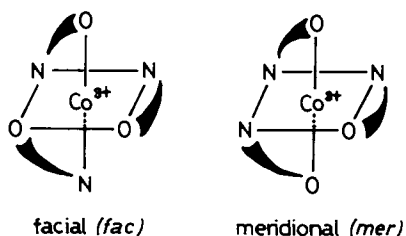


Figure 1. Geometrical isomers of tris-(aminoacidato)cobalt(III)

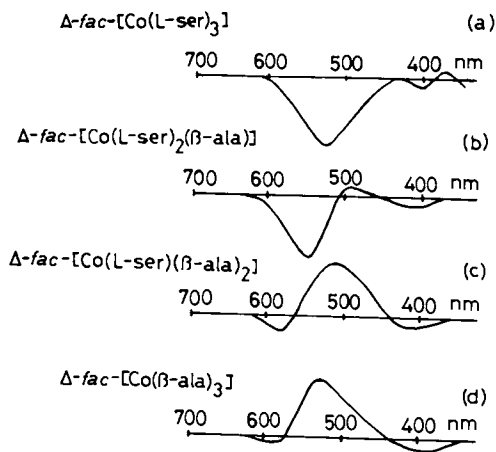
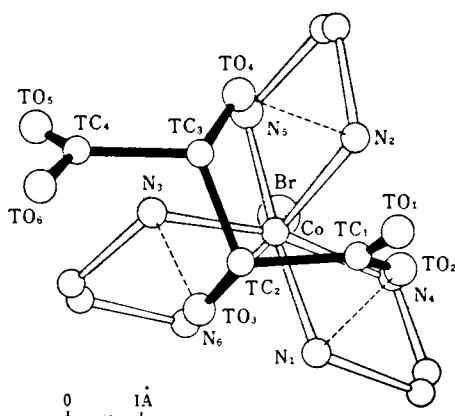


Figure 2. CD spectra of the first-eluted isomers (6)



Chemistry Letters

Figure 3. Face-to-face close contact between  $\Lambda$ -[Co(en)<sub>3</sub>]<sup>3+</sup> and d-tart<sup>2-</sup> in  $\Lambda$ -[Co(en)<sub>3</sub>]·Br·d-tart·5H<sub>2</sub>O (2)

Table II. The Separation Factor of Enantiomeric Pairs Eluted with Sb *d*-tart

| Samples |   | $\alpha$ |
|---------|---|----------|
| ( I )   | $fac-\Lambda[\text{Co}(\text{D-ser})_3]$<br>$fac-\Delta[\text{Co}(\text{L-ser})_3]$                                     | 1.702    |
| ( II )  | $fac-\Delta[\text{Co}(\text{D-ser})_3]$<br>$fac-\Lambda[\text{Co}(\text{L-ser})_3]$                                     | 1.510    |
| ( III ) | $fac-\Lambda[\text{Co}(\text{D-ser})_2(\beta\text{-ala})]$<br>$fac-\Delta[\text{Co}(\text{L-ser})_2(\beta\text{-ala})]$ | 1.349    |
| ( IV )  | $fac-\Delta[\text{Co}(\text{D-ser})_2(\beta\text{-ala})]$<br>$fac-\Lambda[\text{Co}(\text{L-ser})_2(\beta\text{-ala})]$ | 1.193    |
| ( V )   | $fac-\Lambda[\text{Co}(\text{D-ser})(\beta\text{-ala})_2]$<br>$fac-\Delta[\text{Co}(\text{L-ser})(\beta\text{-ala})_2]$ | 1.060    |
| ( VI )  | $fac-\Delta[\text{Co}(\text{D-ser})(\beta\text{-ala})_2]$<br>$fac-\Lambda[\text{Co}(\text{L-ser})(\beta\text{-ala})_2]$ | 1.189    |
| ( VII ) | $fac-\Delta[\text{Co}(\beta\text{-ala})_3]$<br>$fac-\Lambda[\text{Co}(\beta\text{-ala})_3]$                             | 1.060    |

Association Model of Sb *d*-Tart (10)

Since the trend in the separation factor for  $fac-[\text{Co}(\text{D- or L-ser})_{3-n}(\beta\text{-ala})_n]$  is reversed between *d*-tart and Sb *d*-tart, discrimination of enantiomers by Sb *d*-tart is presumed to take place with the association in the direction other than along the three-fold axis of the complex. Figure 4 shows the schematic representations of the  $\Lambda$  and  $\Delta$  tris-chelate complexes. As seen in this figure, the  $\Lambda$  and  $\Delta$  configurations are characterized by the mode of coordination of three chelate rings as well as by the shape of the space between chelate rings. The space formed by the chelate rings of the  $\Lambda$  configuration has an "L" shape and is called an L-shaped channel. The space between chelate rings of the  $\Delta$  configuration has a "J" shape and is called a J-shaped channel. As to the mechanism of discrimination of enantiomers of  $[\text{Co}(\text{en})_3]^{3+}$  and its related complexes, we proposed the key-and-lock association model between Sb *d*-tart and the L-shaped channel of the  $\Lambda$ -complex. According to this model, the  $\Lambda$  enantiomer of  $fac-[\text{Co}(\text{AA})_3]$  is eluted first with Sb *d*-tart, as observed. The trend of the separation factor with increasing number of  $\beta\text{-ala}$  (six-membered chelate ring) is not definitely explained with this model, but probably the six-membered chelate rings may obscure the L-shaped channel

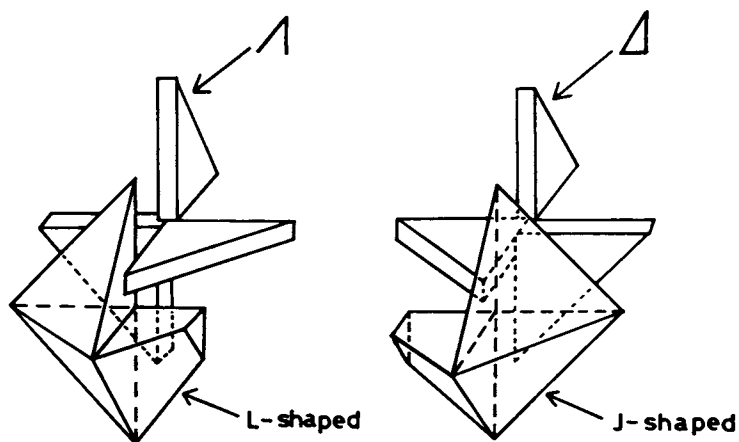


Figure 4. A model proposed for the association of  $Sb_2(d\text{-tart})_2^{2-}$  with tris(chelate)-cobalt(III) compounds

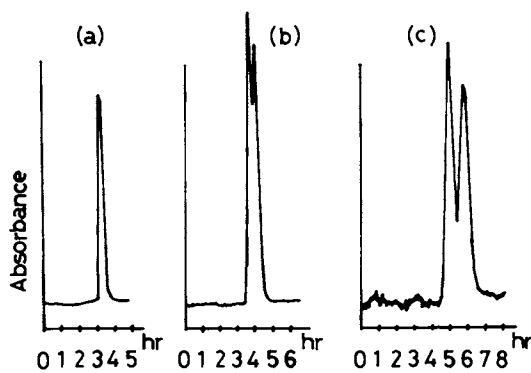


Figure 5. Effect of alcohol on the chromatographic separation of mer- $[Co(\beta\text{-ala})_3]$  enantiomers

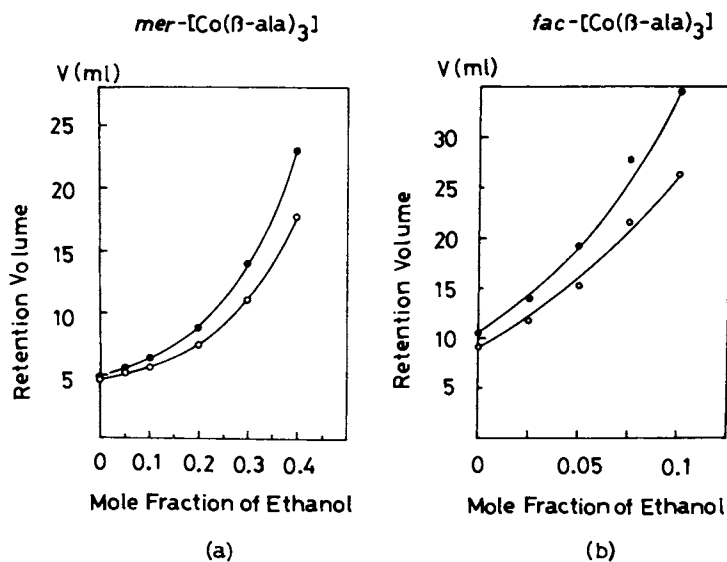


Figure 6. The plots of retention volume,  $V_{adj}$ , against the mole fraction of ethanol in eluent, in the chromatographic resolution of *mer*- and *fac*-[Co(β-ala)<sub>3</sub>]

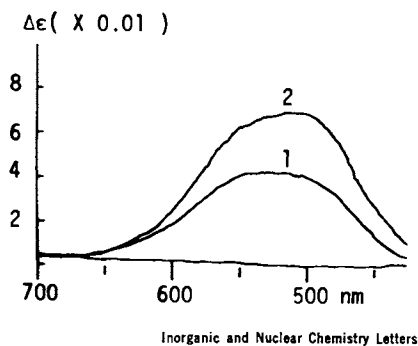


Figure 7. Induced CD spectra of *mer*-[Co(β-ala)<sub>3</sub>] (0.01M) in the presence of *Li*<sub>2</sub>*Sb*<sub>2</sub>-*d*-*tart*<sub>2</sub> (0.1M) in: (1) pure water; (2) 20% ethanol-water (1).

character.

### Resolution of *mer*-[Co( $\beta$ -ala)<sub>3</sub>] (11)

The meridional isomer of [Co( $\beta$ -ala)<sub>3</sub>] also has L-shaped channels. Therefore, this complex should also be separated into enantiomers with Sb *d*-tart. We attempted to chromatograph *mer*-[Co( $\beta$ -ala)<sub>3</sub>] with Sb *d*-tart solution. However, the complex passes through the column with too short a retention time to allow the separation of enantiomers. Thus, we had the idea to place Sb *d*-tart in the resin phase. That is, Sb *d*-tart is loaded on an anion-exchange resin, and through this resin the complex is eluted with water. The elution curve is shown in Figure 5(a). There is a slight splitting of the elution peak. The separation was improved with the addition of ethanol as shown in Figure 5(b) and (c). Figure 6(a) shows the variation of the retention volumes of both enantiomers with increasing mole fraction of ethanol in the eluent. The retention volumes of the both enantiomers increase with increasing amount of ethanol, and the separation factor is improved with addition of ethanol. This is valid also in the case of facial complexes, as shown in Figure 6(b). The effect of ethanol can be explained as the dehydration effect of ethanol from the solvation sphere of associating species. The induced CD spectrum of *mer*-[Co( $\beta$ -ala)<sub>3</sub>] dissolved in Sb *d*-tart solution is enhanced by the addition of ethanol (See Figure 7). This indicates that dehydration enhances close contact between the complex and Sb *d*-tart. Chromatographic resolution of enantiomers using an anion-exchange resin loaded with Sb *d*-tart (resolving agent) has two merits.

- 1) Higher concentration of Sb *d*-tart (resolving agent) can be used, therefore, higher efficiency is expected than the Sb *d*-tart solution as eluent.
- 2) The eluate contains only the sample enantiomer. Thus a large scale preparation of enantiomers is possible.

### Literature Cited

1. Yoshikawa, Y.; Yamasaki, K. Inorg. Nucl. Chem. Lett., 1976, 6, 523.
2. Kushi, Y.; Kuramoto, M.; Yoneda, H. Chem. Lett., 1976, 135.
3. Kushi, Y.; Kuramoto, M.; Yoneda, H. ibid., 1976, 339.
4. Tada, T.; Kushi, Y.; Yoneda, H. ibid., 1977, 379.
5. Yoneda, H.; Yoshizawa, T. ibid., 1976, 707.
6. Yamazaki, S.; Yukimoto, T.; Yoneda, H. J. Chromatogr., 1979, 175, 317.
7. Denning, G. R.; Piper, T. S. Inorg. Chem., 1966, 5, 1056.
8. Freeman, H. C. Adv. Protein Chem., 1967, 22, 257.
9. Soling, H. Acta Chim. Scand., 1978, A32, 361.
10. Nakazawa, H.; Yoneda, H. J. Chromatogr., 1978, 160, 89.
11. Yamazaki, S.; Yoneda, H. Inorg. Nucl. Chem. Lett., 1979, 15, 195.

RECEIVED September 13, 1979.

# Stereoselective Synthesis of Quadridentate Ligands Utilizing a Template Reaction of Metal Complexes

M. SABURI, T. MAKINO, K. HATA, K. MIYAMURA, and S. YOSHIKAWA

Department of Synthetic Chemistry, Faculty of Engineering,  
The University of Tokyo, Hongo, Bunkyo-ku, Tokyo 113, Japan

Curtis and coworkers first reported the amine-imine linkage formation of the type shown in Figure 1 by condensation of two molecules of acetone with ethylenediamines in the presence of nickel(II) or copper(II) ions (1, 2, 3). It was also shown that this type of reaction generally occurs with several carbonyl compounds (4, 5). Later, the mechanism of the linkage formation and the stereoisomerism and some reactions of the metal complexes with macrocycles were investigated in detail (5, 6, 7).

Further, it should be noted that the same macrocycle as in Figure 1 could be obtained by using condensation dimers of acetone, such as diacetone alcohol or mesityl oxide (8). It was also found that several kinds of  $\alpha,\beta$ -unsaturated ketones and  $\beta$ -hydroxyketones may be used to prepare macrocyclic diamino-diimines (8). This observation is very important, because by using suitable ketones it becomes possible to introduce desired substituent(s) into the three carbon atom linkage. In fact, a variety of diamino-diimine macrocycles has been prepared and used as ligands in recent years (9 - 14). However, almost all of the macrocycles were synthesized under reaction conditions not requiring metal ions such as nickel(II).

The use of substituted 1,2-diamines in place of ethylenediamine gave another possibility to increase the variety of macrocycles. Studies by some researchers, using racemic (3, 15) or optically active (15, 16) propylenediamine produced macrocyclic and open-chain ligands, as shown in Figure 2. However, this is the only example which succeeded in formation of this linkage, using chiral diamines. An attempt to use butane-2,3-diamine or stilbenediamine was reported to be unsuccessful (3).

On the other hand, some amine compounds have been found to give open-chain quadridentate ligands by reaction with acetone (3, 17, 18, 19, 20). It is noteworthy that the copper(II) complex of *N*-hydroxyethylethylenediamine, which has a primary and a secondary amino group, gives a single-bridged ligand by reaction with acetone (19, 20). This observation is of much

0-8412-0538-8/80/47-119-325\$05.00/0

© 1980 American Chemical Society



importance because it seems to support the view that some N-monosubstituted 1,2-diamines will give rise to the corresponding open-chain triamino-imines by condensation reactions with ketones in the presence of metal ions.

In Table I are listed the structures and abbreviations of the chiral N-substituted 1,2-diamines and the ketones used in this report. Our investigation started with the expectation that only the primary amino group of these diamines would be involved in the condensation reactions with the ketones used.

Reactions of Ni(S-ampr)<sub>3</sub><sup>2+</sup> Ion with Ketones (21). Initially, the reactions of tris(2(S)-aminomethylpyrrolidine)nickel(II) (Ni(S-ampr)<sub>3</sub><sup>2+</sup>) with MVK and HBO were examined. The condensation reactions were carried out in methanol under the conditions indicated in Table II, and reaction products were separated from other compounds by SP-Sephadex cation exchange chromatography. The products were collected and purified as tetraphenylborate or tetrachlorozincate salts. The separation and purification procedures are almost the same throughout the several reactions will be described here.

In this way, two kinds of nickel(II) complexes were obtained from reaction mixtures with either MVK or HBO (See Scheme 1). The structures of these complexes (Figure 3) are most effectively distinguished by IR measurements, the details of which will be reported elsewhere (21).

A few interesting matters are noticed from the results in Table II. The first is that in addition to the expected complex in which amine-imine linkages connect pairs of primary amino groups (type C in Figure 3), those in which the linkage connects a primary and a secondary amino group (type A or B) are produced. If only the primary amino group were involved in these reactions, the type C complex might be the sole product. The reason for the formation of type A and B complexes will be discussed later.

The second important matter is that the distribution of the products is different between reactions with MVK and HBO. In the MVK reaction, linkage formation takes place exclusively between primary and secondary amino groups, while in the HBO reaction such selectivity is not observed.

Further, it should be noted that in the reaction with HBO, no macrocyclic complex was formed, despite the fact that the type B complex was actually obtained. It was readily confirmed that the B complex (R<sub>1</sub>, R<sub>2</sub> = H), after being isolated, could be converted to the macrocycle A (R<sub>1</sub>, R<sub>2</sub> = H) by reaction with MVK. Therefore, the difference in reactivity between MVK and HBO is obvious.

Table II also includes the results of the reactions of Ni(S-ampr)<sub>3</sub><sup>2+</sup> with some other ketones; i.e., MNPk, HPO, MOX, and DAA. It is interesting that with these ketones the amine-imine linkage connects selectively the primary amino groups of two diamines. Linkage formation between a primary and a secondary amino group no longer occurs. It should be noted that these

Table I. Structures and Abbreviations of Chiral 1,2-Diamines and Ketones

| Name                           | Structure  | Abbreviation |
|--------------------------------|--|--------------|
| 2(S)-2-aminomethyl-pyrrolidine |  | S-ampr       |
| 2(R)-2-aminomethyl-piperidine  |  | R-ampi       |
| 3(S)-3-amino-piperidine        |  | S-apip       |
| 3(S)-3-amino-hexahydroazepine  |  | S-ahaz       |
| diacetone alcohol              | $(\text{CH}_3)_2\text{C}(\text{OH})\text{CH}_2\text{C}(\text{O})\text{CH}_3$               | DAA          |
| mesityl oxide                  | $(\text{CH}_3)_2\text{C}=\text{CH}-\text{C}(\text{O})\text{CH}_3$                          | MOX          |
| methyl vinyl ketone            | $\text{CH}_2=\text{CH}-\text{C}(\text{O})\text{CH}_3$                                      | MVK          |
| 4-hydroxy-2-butanone           | $\text{HO}-\text{CH}_2\text{CH}_2-\text{C}(\text{O})\text{CH}_3$                           | HBO          |
| methyl n-propenyl-ketone       | $\text{CH}_3-\text{CH}=\text{CH}-\text{C}(\text{O})\text{CH}_3$ <sup>°1</sup>              | MNPK         |
| 4-hydroxy-2-pentanone          | $\text{CH}_3-\text{CH}(\text{OH})-\text{CH}_2-\text{C}(\text{O})\text{CH}_3$ <sup>°2</sup> | HPO          |

°1 Mixture of cis and trans isomers

°2 The racemic mixture



four ketones have at least one methyl group on the carbon atom  $\beta$  to the carbonyl group. So it can be anticipated that some steric effect is at work in the linkage-forming reaction.

Reactions of  $\text{Cu}(\text{S-ampr})_2^+$  Ion with MVK and DAA. (22)

Similar linkage formation reactions took place for copper(II) complex of S-ampr. In Table II are shown the results with MVK and DAA. Again in the case of DAA, only the type C complex was formed; that is, only the primary amino groups were concerned in the condensation. On the other hand, all three complexes generated in the MVK reaction. Among these complexes, the macrocycle (A) was the main product, and the yields of the others (B and C) were very low. Thus, in the MVK reaction, linkage formation seems to occur chiefly between a primary and a secondary amino group, as in case of the nickel(II) complex.

The stereoselectivity among A, B and/or C observed in the linkage formation reactions of S-ampr complexes is explained essentially as follows, taking some steric factors into consideration. There are two possible gauche conformations in which the S-ampr may coordinate to a metal ion, namely the  $\delta$  and the  $\lambda$  conformers. As shown in Figure 4, the substituents on the N and C atoms have different orientations from one another in these  $\delta$  and  $\lambda$  conformations. From a stereochemical view, the  $\delta$  conformation will be more preferable than the  $\lambda$ . Figure 4 also shows two modes of linking two molecules of S-ampr. In the case where both the primary amino groups are connected (Figure 4-b), no serious steric repulsions are found, even if  $R_1$  and/or  $R_2$  are methyl groups. However, in the case in which the linkage connects a primary and a secondary amino group (Figure 4-a), steric repulsion occurs between C-substituents at the linkage and the pyrrolidine ring of S-ampr, if the substituent  $R_1$  is a methyl group. Therefore, if both  $R_1$  and  $R_2$  in Figure 4-a are protons, a linkage connecting a primary and a secondary amino group will be favored. In these terms, the results given in Table II are reasonable because only with MVK or HBO can the amine-imine bridge occur between primary and secondary amines; with other bridging reagents, complexes having such structures are not formed at all.

Reactions of  $\text{Cu}(\text{II})$  Complexes of S-apip and S-ahaz. (22, 23)

Experimental results on linkage formation, which were obtained by using S-apip and S-ahaz as diamines, give further information about this kind of condensation. Both diamines, S-apip and S-ahaz, can act as bidentate ligands when amino group at 3 position of the ring takes the axial orientation.

Further, an interesting feature of these diamines as ligands for the copper(II) ion has been recognized (24). As illustrated in Figure 5, there are two geometrical ways of coordination; cis and trans. In the cis form, where the primary and secondary amino groups take positions cis to one another, the two apical position on the copper(II) ion are considered to be blocked from the coordination because of the presence of the diamine skeleton,

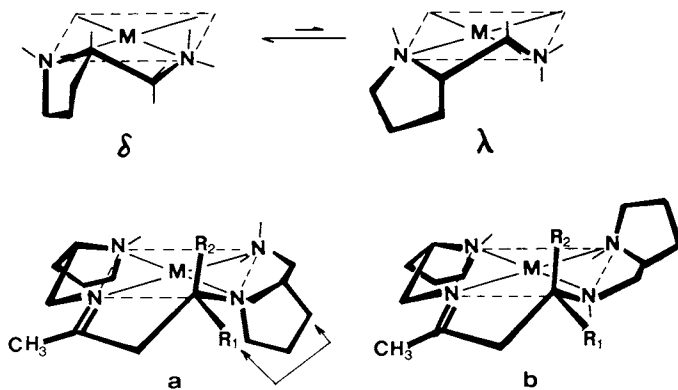


Figure 4. Possible conformations of coordinated *S*-ampr ( $\delta$  and  $\lambda$ ) and the structure of condensation products with the single linkage (*a* and *b*)

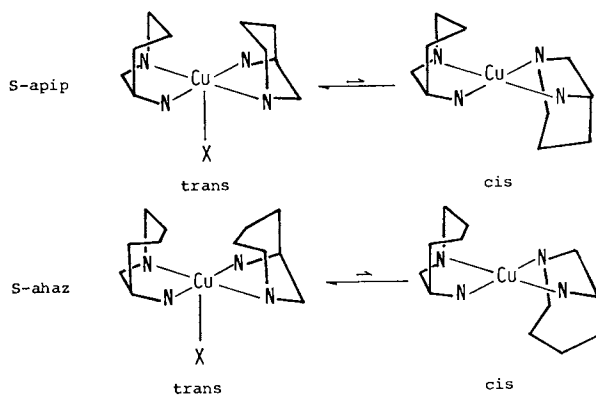


Figure 5. Geometrical isomers (*trans* and *cis*) of Cu(II) complexes of *S*-apip and *S*-ahaz

so that the complex will have a four-coordinated structure. In the trans form, one of the apical position of copper(II) is open for coordination with such ligands as halides or solvents. On the basis of spectroscopic and conductivity measurements, some evidence has been obtained supporting this suggestion that the copper(II) complexes of these diamines preferably take this five coordination structure, even though a very small amount of the cis structure is probably present at equilibrium (24). Therefore, it is expected that if the five-coordinated structure is maintained during linkage formation with ketones, the main products will have structures in which primary and secondary amines are connected regardless of the particular ketones used. This is because steric repulsions found in the condensation reactions between S-ampr and ketones other than MVK and HBO, seems not to occur in these diamine complexes.

The results of the condensation reactions for S-apip and S-ahaz Cu(II) complexes are summarized in Table III. The structures of products, A, B, and C in Table III are illustrated in Figure 6 for the case of S-apip.

A few interesting facts are recognized from these data. As far as S-apip and S-ahaz are concerned, products with less crowded ketones such as MVK, HBO, MNPK, or HPO have, without exception, the amine-imine linkage formed between primary and secondary amines. Hence, the products are either A or B, or sometimes both of them, as in the case of S-apip-MNPK and S-ahaz-MVK. Further, the yields are not so bad. Therefore it is very probable that linkage formation takes place, almost exclusively, on the five-coordinated structure of copper(II), as expected above. Such selectivity due to the coordination mode about copper(II) ion will not work well in the case of the S-ampr complex, because of its structure, so that a small amount of type C is obtained.

Remarkable differences are found between the results for MOX or DAA and other ketones. With these acetone dimers, no macrocyclic product was obtained. In the case of S-apip and S-ahaz, the yield of other products (B and C) are also very low. This probably indicates the effects of some steric factors, which reduce the reactivity. The steric factor will be due chiefly to repulsions brought about by two methyl groups in ketones. The repulsion works in the transition state for formation of both B and C, so that the yield of each for S-apip and S-ahaz is lowered.

The formation of type C products for S-apip and S-ahaz is rather surprising, because these substances should be generated through the four-coordinated-copper(II) complexes. The four-coordinated species are considered to be present in only a small ratio compared with the five-coordinated species, as discussed earlier. Therefore, the formation of C for these diamines (S-apip and S-ahaz) seems to suggest the low reactivity of acetone dimers towards their five-coordination complexes.



Further, type C complexes of S-apip and S-ahaz should have a severe steric repulsion between the methyl group at the linkage and the six- or seven-membered ring axially substituted to the five-membered chelate rings. Thus, they might have some distorted structures, such as a *cis*- $\beta$  form, instead of the planar structure, although the possibility has not been confirmed as yet.

Another important stereochemical factor working in linkage formation is the effect of the direction of the N-H bond on the secondary nitrogen. For all of the diamines described so far; i.e. S-ampr, S-apip, and S-ahaz, the N-H bond is equatorial in character, as shown in Figure 7.

2(R)-2-Aminomethylpiperidine (R-ampi), another *N*-substituted chiral 1,2-diamine, has a very similar structure to the S-ampr, but the N-H bond for the coordinated R-ampi should preferably have an axial direction. It is possible to suppose a coordination structure having an equatorial N-H bond, as illustrated in Figure 7. However, such a structure will be less stable than that with the axial N-H bond.

In fact, by a reaction of its copper(II) complex with MVK, R-ampi gave two open chain products, which correspond to those indicated as Figure 3-B and C for the case of S-ampr complex. The yields were very low. Furthermore, in this case the formation of the macrocyclic product was too small to be isolated, even if it were formed. This is in contrast to the observation that macrocycles were the main products for the other diamines upon reactions with MVK.

Thus, the reactivity of R-ampi is obviously much lower than that of S-ampr toward MVK in the presence of copper(II) ion. The difference in results between these diamines could not be explained, if the effect of the N-H bond direction were not taken into consideration. This is one of rare examples which show that the difference in the orientation of the N-H bond, equatorial or axial, will decide its reactivity in metal complex reactions.

### Summary

This report is concerned with the stereoselectivity of the condensation reactions of some chiral *N*-substituted 1,2-diamines with  $\alpha,\beta$ -unsaturated ketones or  $\beta$ -hydroxyketones using nickel(II) or copper(II) ions as the templates. Through the reactions, steric repulsions between the substituents of diamines and those on ketones affect mainly the selectivity of linkage formation. In the case of the copper(II)-template reaction, the influence of coordination modes of the diamines around the metal ion is also observed. The importance of the direction of the N-H bond at the coordinated secondary nitrogen is recognized; the equatorial N-H bond is sufficiently reactive for reaction with ketones, while the axial N-H seems to be almost unreactive.



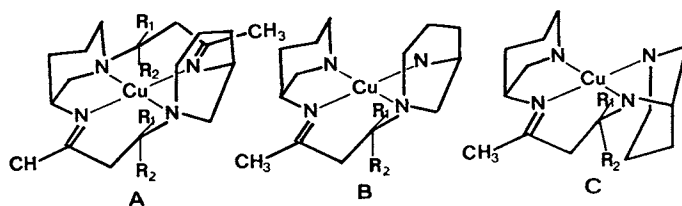


Figure 6. Products for condensation reaction of  $\text{Cu}(\text{S-apip})_2^{2+}$  with some ketones

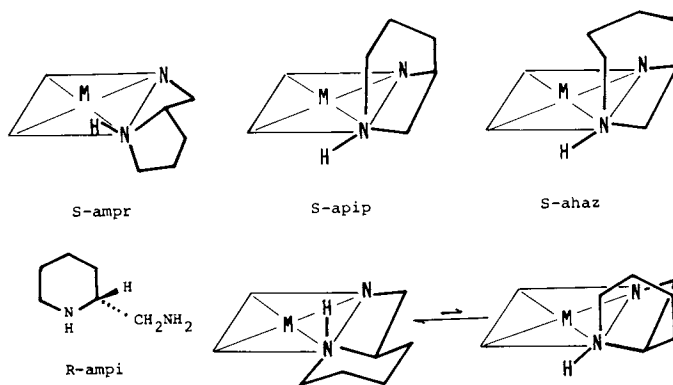


Figure 7. Conformations of coordinated N-substituted chiral 1,2-diamines

Literature Cited

1. Curtis, N.F., *J. Chem. Soc.*, (1960) 4409
2. Curtis, N.F., and House, D.A., *Chem. and Ind.*, (1961) 1708
3. Blight, M.M., and Curtis, N.F., *J. Chem. Soc.*, (1962) 3016
4. House, D.A., and Curtis, N.F., *J. Am. Chem. Soc.*, (1964) 86, 1331
5. Curtis, N.F., *Coord. Chem. Rev.*, (1968) 3, 3
6. Curtis, N.F., *J. Chem. Soc. Dalton*, (1972) 1357
7. Lindoy, L.F., and Busch, D.H., *Prep. Inorg. Reac.*, (1971) 6, 1
8. MacDarmott, T.E., and Busch, D.H., *J. Am. Chem. Soc.*, (1964) 89, 5780
9. Curtis, N.F., and Hay, R.W., *Chem. Commun.*, (1966) 524
10. Kolinski, R.A., and Korybut-Daszkiewicz, B., *Inorg. Chem. Acta*, (1975) 14, 273
11. Hay, R.W., and Lawrence, G.A., *J. Chem. Soc. Dalton*, (1975) 1466
12. Hay, R.W., and Jerahg, B., *J. Chem. Soc. Dalton*, (1977) 1261
13. Hay, R.W., Piplani, D.P., and Jeragh, B., *J. Chem. Soc. Dalton*, (1977) 1951
14. Cook, D.F., Curtis, N.F., and Hay, R.W., *J. Chem. Soc. Dalton*, (1973) 1160
15. Curtis, N.F., *J. Chem. Soc. Dalton*, (1973) 863
16. Ito, H., and Fujita, J., *Bull. Chem. Soc. Jpn.*, (1971) 44 741
17. Patel, V.C., and Curtis, N.F., *J. Chem. Soc. (A)*, (1968) 1265
18. Curtis, N.F., *J. Chem. Soc. Dalton*, (1975) 91
19. Patel, V.C., and Curtis, N.F., *J. Chem. Soc. (A)*, (1969) 1607
20. Hughes, M.N., Underhill, M., and Rutt, K.J., *J. Chem. Soc. Dalton*, (1972) 1219
21. Makino, T., Saburi, M., and Yoshikawa, S., to be submitted.
22. Miyamura, K., Makino, T., Hata, K., Saburi, M., and Yoshikawa, S., to be submitted.
23. Makino, T., Hata, K., Saburi, M., and Yoshikawa, S., 287 *Chem. Lett.*, (1979)
24. Morita, M., Mizoguchi, Y., Saburi, M., and Yoshikawa, S., to be submitted.

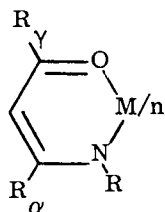
RECEIVED October 4, 1979.

## Stereochemistry of Cobalt(III) $\beta$ -Ketoaminates and Some Mixed-Ligand Analogues

CHARLES J HINRICHSSEN and ROBERT C. FAY

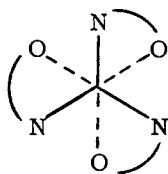
Department of Chemistry, Cornell University, Ithaca, NY 14853

In recent years there has been considerable interest in the complexes of transition metals with  $\alpha, \beta$ -unsaturated  $\beta$ -ketoamines (1),  $\frac{1}{2}$ ,

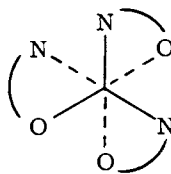


1

especially in their stereochemical properties (2, 3, 4, 5). Because the  $\beta$ -ketoaminate ligand is unsymmetrical, metal tris( $\beta$ -ketoaminates) may exist as fac and mer isomers. Previous studies of V(III)



facial



meridional

and Cr(III) tris( $\beta$ -ketoaminates) (5, 6) have revealed the presence of only one stereoisomer, which can be assigned the mer-configuration on the basis of NMR studies of the paramagnetic V(III) complexes (5). Evidently the fac-isomer is destabilized by steric interactions between the three N-alkyl or N-aryl groups, which project, in the fac-isomer, from a single octahedral face (5, 6). A similar situation obtains for tris(N-R-salicylaldimine) and tris(N-R-pyrrole-2-aldimine) complexes; these complexes also exist exclusively as the

0-8412-0538-8/80/47-119-337\$05.00/0

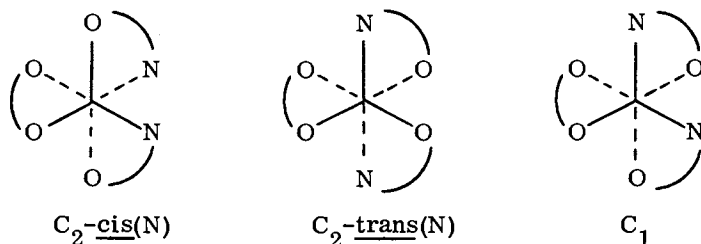
© 1980 American Chemical Society

mer-stereoisomer (5, 7).

When  $R = H$ , steric interactions should not be a problem and both geometric isomers should exist. Indeed, in some unpublished work about 15 years ago, one of us (R. C. F.) prepared the tris-(acetylacetonate imine) chelate of Co(III) (1,  $R = H$ ,  $R_\alpha = R_\gamma = CH_3$ ,  $M = Co$ ) and obtained evidence for the existence of both fac- and mer-isomers. However, it was not possible to characterize these complexes properly because they are relatively insoluble in organic solvents. More recently, Srivastava and co-workers (8, 9) have prepared acetylacetonate imine complexes of several trivalent metals, including Co(III), but they have ignored the possibility of fac-mer isomerism.

We wish to report that the  $\beta$ -ketoamine 5-amino-2,2-dimethylhex-4-en-3-one (Hadmh) gives soluble Co(III) complexes,  $Co(admh)_3$  (1,  $R = H$ ,  $R_\alpha = CH_3$ ,  $R_\gamma = C(CH_3)_3$ ,  $M = Co$ ), which can be separated into fac- and mer-isomers and can be characterized by a variety of physical methods. The marked increase in solubility is due to introduction of the tert-butyl group.

We have also prepared and characterized the mixed-ligand analogues,  $Co(admh)_2(acac)$  and  $Co(admh)(acac)_2$  ( $acac = acetylacetonate$ ).  $Co(admh)_2(acac)$  may exist as three geometrical isomers, two having  $C_2$  symmetry ( $C_2$ -cis(N) and  $C_2$ -trans(N)) and one having no sym-



metry ( $C_1$ ). The two isomers having cis-nitrogen atoms have been isolated; no evidence was found for the  $C_2$ -trans(N) isomer.  $Co(admh)(acac)_2$  exists as a single stereoisomer and has no symmetry. Reported herein are (1) NMR, electronic, and CD spectra and dipole moment measurements for all of the  $Co(admh)_n(acac)_{3-n}$  complexes, and (2) kinetic and equilibrium data for fac-mer isomerization of  $Co(admh)_3$ .

### Experimental Section

fac- and mer-Tris(5-amino-2,2-dimethylhex-4-en-3-onato)cobalt(III). Under a dry nitrogen atmosphere potassium tert-butoxide (5.7 g, 51 mmol) was dissolved in 100 ml of dry tert-butanol, and the solution was heated to reflux. Hadmh (6.35 g, 45.0 mmol) was added,

and after 40 min of stirring at reflux temperature,  $[(C_2H_5)_4N]_2[CoCl_4]$  (6.89 g, 14.9 mmol) was added. The resulting dark green solution was allowed to reflux for  $\sim 6$  h with vigorous stirring while oxygen gas was bubbled through the solution at a rate of  $\sim 5$  bubbles/sec. The mixture was then stirred overnight at room temperature with bubbling of oxygen being continued. After the solution was filtered to remove insoluble matter, the tert-butanol was removed in vacuo. The residue was dissolved in hexane and the solution was passed through a short column of neutral alumina (15 x 3.0 cm o.d.) to remove impurities. Because the  $Co(admh)_n(acac)_{3-n}$  complexes tend to decompose on activated alumina, the alumina employed in this work was treated with 3-10% water (by weight) prior to use. Vacuum distillation of the hexane afforded 6.0 g of  $Co(admh)_3$  (84% theoretical).

The fac- and mer-isomers were separated by chromatography ( $\sim 2$  g sample) on a 35 x 3.8 cm o.d. column of neutral alumina/3-10% water using 4:1 (v/v) hexane-benzene as the eluent. The mer-isomer (green band) is eluted first, followed by the fac-isomer (red band). After the solvent was removed in vacuo, the complexes were sublimed at 100°C (0.005 Torr) to remove benzene of crystallization; mp 131-135°C (mer), 133-135°C (fac). Anal. Calcd for  $Co(C_8H_{14}NO)_3$ : C, 60.11; H, 8.83; Co, 12.29; N, 8.76; mol wt 480. Found (mer): C, 59.92; H, 8.57; Co, 11.92; N, 8.95; mol wt 474. Found (fac): C, 60.05; H, 8.87; Co, 12.47; N, 9.01; mol wt 456.

#### Preparation of Mixed-Ligand Complexes. General Procedure.

All of the  $Co(admh)_n(acac)_{3-n}$  complexes were prepared under dry nitrogen using dried solvents. The product was purified by removing the solvent in vacuo, dissolving the residue in benzene, and passing the resulting solution through a short column of neutral alumina/10% water. The molar ratios of the reactants were adjusted to give the desired stereoisomer as the major product. However, other  $Co(admh)_n(acac)_{3-n}$  complexes were formed as well, and so the desired complex had to be separated from the others by chromatography. A 40 x 3.8 cm o.d. column of neutral alumina/10% water was used with hexane-benzene mixtures as the eluent. The elution order, ranging from first-eluted to last-eluted, is as follows: mer- $Co(admh)_3$  (green), fac- $Co(admh)_3$  (red),  $C_2$ -cis(N)- $Co(admh)_2(acac)$  (light violet),  $C_1$ - $Co(admh)_2(acac)$  (light brown),  $Co(admh)(acac)_2$  (dark brown),  $Co(acac)_3$  (green). Upon completing a chromatographic separation, the column was regenerated by washing it with 1:4 (v/v) benzene-ether.

$C_2$ -cis(N)-Bis(5-amino-2,2-dimethylhex-4-en-3-onato)(2,4-pentanedionato)cobalt(III). Acetylacetonone (4.4 g, 44 mmol) was added to a solution of potassium tert-butoxide (7.1 g, 63 mmol) in 100 ml of

freshly distilled tert-butanol, and the solution was heated to  $\sim 60^\circ$  with stirring. This was followed by addition of Hadmh (2.07 g, 14.7 mmol) and, after 30 min,  $[(C_2H_5)_4N]_2[CoCl_4]$  (6.70 g, 14.5 mmol). Oxygen was then bubbled into the solution for 4 h at  $\sim 60^\circ$  and then overnight at  $\sim 40^\circ$ . The  $C_2$ -cis(N) isomer was separated from the other  $Co(admh)_n(acac)_{3-n}$  complexes by chromatography on alumina using 3:2 (v/v) hexane-benzene as the eluent. Benzene of crystallization was removed by subliming the compound at  $100^\circ C$ . Yield, 1.0 g (31%); mp  $119-121^\circ C$ . Anal. Calcd for  $Co(C_8H_{14}NO)_2(C_5H_7O_2)_2$ : C, 57.53; H, 8.05; Co, 13.44; N, 6.39; mol wt 438. Found: C, 57.56; H, 8.19; Co, 13.62; N, 6.42; mol wt 431.

$C_1$ -Bis(5-amino-2,2-dimethylhex-4-en-3-onato)(2,4-pentanedionato)cobalt(III). Hadmh (5.80 g, 41.1 mmol) and then potassium tert-butoxide were added to a solution of  $Co(acac)_2$  (6.00 g, 23.3 mmol) in 130 ml of dry benzene. The reaction mixture was stirred for 3 h at room temperature while oxygen was bubbled through the solution. The yield of crude product was 7.0 g (78%); about half of this proved to be the  $C_2$  isomer after chromatographic separation on alumina using 4:1 (v/v) benzene-hexane as the eluent. Benzene of crystallization could not be removed by pumping in vacuo, nor by sublimation; the  $C_2$  isomer does not sublime below its melting point, and the sublimate obtained above the melting point was a mixture of  $C_1$ - and  $C_2$ - $Co(admh)_2(acac)$ , as well as  $Co(admh)(acac)_2$  and fac- and mer- $Co(admh)_3$ . The benzene was removed by chromatography on a short alumina column using first hexane and then dichloromethane as the eluent. After pumping off the solvents, the solid was dried in vacuo for several hours until the NMR spectrum showed that the product was free of hexane and dichloromethane; mp  $117-119^\circ C$ . Anal. Calcd for  $Co(C_8H_{14}NO)_2(C_5H_7O_2)_2$ : C, 57.53; H, 8.05; Co, 13.44; N, 6.39; mol wt 438. Found: C, 57.65; H, 8.49; Co, 13.44; N, 6.08; mol wt 447.

(5-Amino-2,2-dimethylhex-4-en-3-onato)bis(2,4-pentanedionato)cobalt(III). This complex was prepared by the same procedure as that employed for synthesis of  $C_1$ - $Co(admh)_2(acac)$ . The following amounts of reactants were used:  $Co(acac)_2$ , 12.85 g, 50.0 mmol; Hadmh, 5.7 g, 40 mmol; potassium tert-butoxide, 2.0 g, 18 mmol; benzene,  $\sim 150$  ml. The yield of crude product was 14 g (87%). The product was chromatographed in 2-3 g portions on alumina and was eluted first with 3:2 hexane-benzene to remove the  $Co(admh)_3$  and  $Co(admh)_2(acac)$  bands. The polarity of the eluent was then increased (1:1, 2:1, 5:1 (v/v) benzene-hexane) while the dark brown band of  $Co(admh)(acac)_2$  was eluted, leaving  $Co(acac)_3$  on the column. The product was freed of benzene by sublimation at  $100^\circ C$ . The complex darkens when heat-

ed to  $\sim 138^\circ$  and melts at  $151\text{--}154^\circ$ . Anal. Calcd for  $\text{Co}(\text{C}_8\text{H}_{14}\text{NO})\text{--}(\text{C}_5\text{H}_7\text{O}_2)_2$ : C, 54.41; H, 7.10; Co, 14.83; N, 3.52; mol wt 397. Found: C, 54.84; H, 7.22; Co, 14.53; N, 3.41; mol wt 396.

Partial Resolution of Optical Isomers.  $\text{Co}(\text{admh})(\text{acac})_2$  was resolved partially on a previously described  $230 \times 3.9$  cm o.d. column of D-(+)-lactose (10). In two separate chromatograms, 130 mg of sample dissolved in 1.5 ml of benzene was placed on the column and eluted with 1:1 benzene-hexane. The entire eluted solution was collected in two parts. The first fractions from each chromatogram were combined and evaporated to dryness. The enantiomer in excess was then concentrated by extracting the residue with 1 ml of hexane.

The fac- and mer- $\text{Co}(\text{admh})_3$  and  $\text{C}_1$ - and  $\text{C}_2$ - $\text{Co}(\text{admh})_2(\text{acac})$  complexes could not be resolved by the above method, but these complexes were resolved partially by a low-temperature chromatographic method (11) using a  $60 \times 1.3$  cm o.d. column of D-(+)-lactose (18 g) absorbed on neutral alumina (40 g). The column was equipped with an insulated glass jacket (2.8 cm o.d.) which permitted it to be cooled with the vapor from a Dewar of boiling liquid nitrogen; the temperature of the column was kept at  $-95$  to  $-125^\circ\text{C}$ . Approximately 70 mg of sample dissolved in 5 ml of isopentane-ether was placed on the column and eluted with the same solvent. The ratio of isopentane to ether was 8:1 (v/v) for fac- and mer- $\text{Co}(\text{admh})_3$ , 7:1 (v/v) for  $\text{C}_1$ - $\text{Co}(\text{admh})_2(\text{acac})$ , and 5:1 (v/v) for  $\text{C}_2$ - $\text{Co}(\text{admh})_2(\text{acac})$ . A total of four separate chromatograms were run for each compound. The first fractions were combined, and the resultant mixture was divided in half. Each half was then chromatographed separately. The first fractions from these two chromatograms were then combined and chromatographed. The first fraction from this final chromatogram was evaporated, and the enantiomer in excess was concentrated by extracting the residue with  $\sim 1$  ml of cold ( $\sim -120^\circ$ ) Freon 22 (chlorodifluoromethane).

Physical Measurements. Molecular weights were determined in  $\sim 0.07$  M benzene solutions at  $37^\circ\text{C}$  by vapor pressure osmometry. Dipole moments were measured in dilute benzene solution at  $25.00 \pm 0.05^\circ\text{C}$  using a previously described method (12). Values of the atomic polarization,  ${}_A P_2$ , for the admh and acac ligands were estimated from the total polarization,  ${}_T P_2$ , of trans- $\text{Pd}(\text{admh})_2$  (13) and  $\text{Co}(\text{acac})_3$ . Assuming that  $\text{Co}(\text{acac})_3$  and trans- $\text{Pd}(\text{admh})_2$  have  $D_3$  and  $\text{C}_{2h}$  symmetry, respectively, the orientation molar polarizations,  ${}_O P_2$ , should be zero for both complexes. For  $\text{Co}(\text{acac})_3$ ,  ${}_T P_2 = 134 \pm 8 \text{ cm}^3$  and  ${}_E P_2 = 99 \pm 7 \text{ cm}^3$ ; therefore  ${}_A P_2 = {}_T P_2 - {}_E P_2 = 35 \pm 6 \text{ cm}^3$  ( $11.7 \pm 2 \text{ cm}^3$  per acac ligand). Similarly, for trans- $\text{Pd}(\text{admh})_2$  (13),  ${}_T P_2 = 126.9 \pm 9.9$  and  ${}_E P_2 = 104.1 \pm 9.2 \text{ cm}^3$ ;

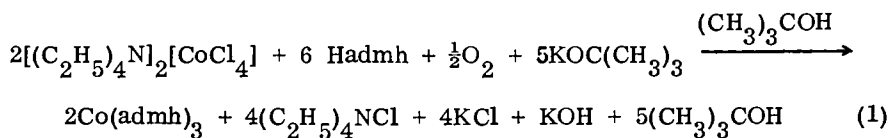
therefore,  $A_{P_2} = 22.8 \pm 4.1 \text{ cm}^3$  ( $11.4 \pm 2.1 \text{ cm}^3$  per admh ligand).

Proton NMR spectra were obtained at ambient temperature (39°) with a Varian A-60A spectrometer. For determination of chemical shifts and coupling constants, the magnetic field sweep width was calibrated with a standard sample of chloroform and tetramethylsilane in carbon tetrachloride. Three to five spectra were recorded and the reported values of chemical shifts and coupling constants are average values. Electronic spectra were recorded with a Cary model 14 recording spectrophotometer. ORD and CD spectra were obtained with a Cary model 60 spectropolarimeter or a JASCO ORD/UV-5.

Kinetic and Equilibrium Studies. Rates and equilibrium constants for fac-mer isomerization of  $\text{Co(admh)}_3$  were determined in chlorobenzene solution in the temperature ranges 97.2 - 115.2°C and 97.2 - 120.1°C, respectively. The sample solutions, sealed in NMR tubes, were placed in a constant temperature bath ( $\pm 0.1^\circ$ ) for an appropriate length of time and the isomerization reaction was then quenched. Relative concentrations of the fac- and mer-isomers were determined by integration of the tert-butyl region of proton NMR spectra, which was recorded in quadruplicate at ambient temperature with a Varian A-60A spectrometer at a sweep width of 50 Hz. Representative spectra are shown in Figure 1. The second lowest-field peak is due to the three equivalent tert-butyl groups of the fac-isomer. Hence, the mole fraction of the fac-isomer was calculated by subtracting half the area of the two high-field peaks from the area of the two low-field peaks and dividing the result by the total area of all four peaks. All kinetic runs began with the fac-isomer and, in general, they were followed for 2-3 half-lives. In the determination of equilibrium constants, the equilibrium was approached at each temperature from the fac- and the mer-sides.

## Results and Discussion

Preparation and Properties. The  $\text{Co(admh)}_3$  complexes were prepared in good yield by a nonaqueous chelation procedure, similar to that employed by Holm *et al.* (14), involving reaction in tert-butanol of  $\text{CoCl}_4^{2-}$  with the  $\beta$ -ketoamine and oxygen in the presence of potassium tert-butoxide (eq 1). The oxygen serves to oxidize the cobalt,

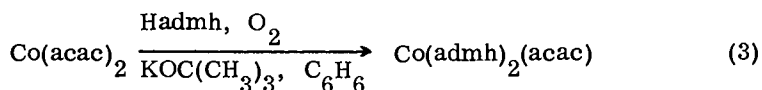
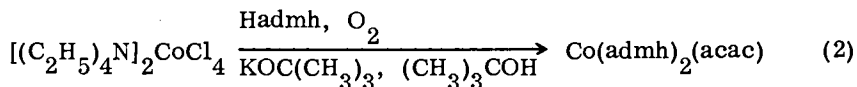


and the tert-butoxide picks up the proton from the weakly acidic  $\beta$ -ketoamine. The fac- and mer-isomers were subsequently separated



by column chromatography on neutral alumina using 4:1 hexane-benzene as the eluent.

Co(admh)<sub>2</sub>(acac) was prepared by an analogous procedure, using a mixture of Hadmh and Hacac (eq 2). Alternatively, Co(admh)<sub>2</sub>(acac) may be obtained by reaction of Co(acac)<sub>2</sub> with Hadmh and oxygen (eq 3). These reactions give a mixture of products, including Co-



(admh)<sub>3</sub> and Co(admh)(acac)<sub>2</sub> as well as geometric isomers of Co(admh)<sub>2</sub>(acac). Reaction 2 affords C<sub>2</sub>-cis(N)-Co(admh)<sub>2</sub>(acac) as the major product, while reaction 3 gives mainly the C<sub>1</sub> isomer. Co(admh)(acac)<sub>2</sub> was prepared by reaction 3, using a lower ratio of Hadmh to Co(acac)<sub>2</sub>.

The mixtures of products obtained by reactions 2 and 3 were separated by chromatography on neutral alumina. The complexes are more easily eluted, the greater the number of admh ligands (Table I).

Table I. Column Chromatography on Alumina

| Band | Hexane/benzene<br>eluent | Color   | Mp, °C  | Compound   |
|------|--------------------------|---------|---------|--|
| 1    | 4:1                      | green   | 131-134 | <u>mer</u> -Co(admh) <sub>3</sub>                            |
| 2    | 4:1                      | red     | 133-135 | <u>fac</u> -Co(admh) <sub>3</sub>                            |
| 3    | 3:2                      | lt. vl. | 119-121 | C <sub>2</sub> - <u>cis</u> (N)-Co(admh) <sub>2</sub> (acac) |
| 4    | 1:4                      | lt. bn. | 117-119 | C <sub>1</sub> -Co(admh) <sub>2</sub> (acac)                 |
| 5    | 1:1 → 1:5                | dk. bn. | 151-154 | Co(admh)(acac) <sub>2</sub>                                  |
| 6    | benzene/ether            | green   | 204-206 | Co(acac) <sub>3</sub>  |

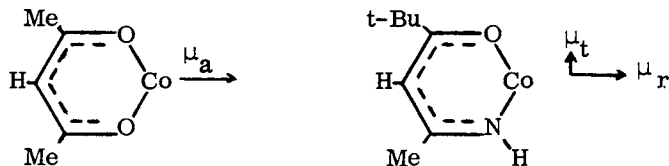
The elution order parallels increasing solubility in saturated hydrocarbons and increasing ease of sublimation as one goes from Co(acac)<sub>3</sub> to Co(admh)<sub>3</sub>. These trends seem to be related to the presence of tert-butyl groups in the admh ligands since tris(acetylacetonate imine)cobalt(III) complexes are only sparingly soluble in organic solvents. The elution orders fac-Co(admh)<sub>3</sub> after mer-Co(admh)<sub>3</sub> and C<sub>1</sub>-Co(admh)<sub>2</sub>(acac) after C<sub>2</sub>-cis(N)-Co(admh)<sub>2</sub>(acac) are in accord with the greater dipole moments of the cis and the C<sub>1</sub> isomers (vide infra). The progress of the chromatograms can be followed easily because all of the complexes have different colors. All of the Co(admh)<sub>n</sub>(acac)<sub>3-n</sub> (n = 1, 2, 3) complexes are new. All are monomeric in benzene and nonelectrolytes in nitrobenzene; molar con-

ductances of  $10^{-3}M$  solutions at  $25^{\circ}C$  are less than  $0.026 \text{ ohm}^{-1}\text{cm}^2 \text{ mol}^{-1}$ .

Only two of the three possible isomers of  $\text{Co}(\text{admh})_2(\text{acac})$  have been isolated, the  $C_1$  isomer and one of the two  $C_2$  isomers ( $C_2$ -cis(N), (vide infra). Attempts to find the missing  $C_2$ -trans(N) isomer by isomerization of the  $C_1$  and the  $C_2$ -cis(N) isomers gave mixtures of all of the compounds listed in Table I, but NMR and chromatographic analysis of these mixtures afforded no evidence for the  $C_2$ -trans(N) isomer.

**Stereochemistry.** The stereochemistries of the  $\text{Co}(\text{admh})_n(\text{acac})_{3-n}$  complexes have been assigned on the basis of NMR spectra, electronic spectra, and dipole moment measurements. Proton chemical shifts and coupling constants are presented in Table II. The first-eluted, green isomer of  $\text{Co}(\text{admh})_3$  exhibits three tert-butyl, three methyl, and three ring proton resonances, indicative of the mer-structure, which has no symmetry, while the second-eluted, red isomer gives just a single resonance for each type of group, consistent with the fac-configuration, of  $C_3$  symmetry. The less easily eluted, light-brown  $\text{Co}(\text{admh})_2(\text{acac})$  complex can be assigned the  $C_1$  structure on the basis of the two admh resonances and the two acac methyl resonances. A single resonance line for each of the various protons of the more easily eluted, violet  $\text{Co}(\text{admh})_2(\text{acac})$  complex is indicative of  $C_2$  symmetry, but the NMR spectra do not distinguish between the  $C_2$ -cis(N) and the  $C_2$ -trans(N) configurations. All of the admh methyl resonances are split by  $\sim 1$  Hz, and the ring proton resonances by  $\sim 2.5$  Hz, owing to spin coupling between these protons and the neighboring NH proton.

Dipole moment measurements (Table III) confirm the stereochemical assignments for fac- and mer- $\text{Co}(\text{admh})_3$  and  $C_1$ - $\text{Co}(\text{admh})_2(\text{acac})$  but, unfortunately, these measurements also do not distinguish between the  $C_2$ -cis(N)- and  $C_2$ -trans(N)- $\text{Co}(\text{admh})_2(\text{acac})$  isomers. The molecular dipole moments may be resolved into a Co-acac group moment,  $\mu_a$ , and radial and transverse Co-admh group moments,  $\mu_r$  and  $\mu_t$ , respectively. Assuming that the complexes have octahedral geometry, one obtains the expressions in the second column of Table



III for the molecular dipole moments. The observed moments for fac- and mer- $\text{Co}(\text{admh})_3$  and the pair of compounds  $C_1$ - $\text{Co}(\text{admh})_2(\text{acac})$  and  $\text{Co}(\text{admh})(\text{acac})_2$  afford an average value of  $1.68 \pm 0.13$  D

Table II. Proton Chemical Shift<sup>a</sup> and Coupling Constant<sup>b</sup> Data

| Compound   | admh                       |                  |                | acac                        |                    |                |                |
|--|----------------------------|------------------|----------------|-----------------------------|--------------------|----------------|----------------|
|  | $-\text{C}(\text{CH}_3)_3$ | $-\text{CH}_3^c$ | $-\text{CH}^c$ | $J^d \text{CH}_3\text{-NH}$ | $J^d \text{CH-NH}$ | $-\text{CH}_3$ | $-\text{CH}^c$ |
| $\overline{\text{mer}}\text{-Co}(\text{admh})_3$   | -1.10                      | -2.23            | -4.90          | 1.10                        | 2.55               |                |                |
|  | -0.93 <sup>d</sup>         | -2.15            | -4.86          | 0.92                        | 2.50               |                |                |
|  | -0.93 <sup>d</sup>         | -2.09            | -4.83          | 0.92                        | 2.47               |                |                |
| $\overline{\text{fac}}\text{-Co}(\text{admh})_3$   | -1.10                      | -2.02            | -4.88          | 0.67                        | 2.16               |                |                |
| $\text{C}_2\text{-Co}(\text{admh})_2(\text{acac})$ | -1.05                      | -2.18            | -4.99          | 0.93                        | 2.40               | -2.04          | -5.33          |
| $\text{C}_1\text{-Co}(\text{admh})_2(\text{acac})$ | -1.21                      | -2.25            | -5.02          | 0.89                        | 2.43               | -2.15          | -5.35          |
|  | -0.95                      | -2.08            | -4.95          | 0.73                        | 2.35               | -1.79          |                |
| $\text{Co}(\text{admh})(\text{acac})_2$            | -1.09                      | -2.32            | -5.10          | 0.93                        | 2.41               | -2.30          | -5.44          |
|  |                            |                  |                |                             |                    | -2.09          | -5.41          |
|  |                            |                  |                |                             |                    | -2.04          |                |
|  |                            |                  |                |                             |                    | -1.91          |                |
| $\text{Co}(\text{acac})_3$                         |                            |                  |                |                             |                    | -2.19          | -5.53          |

<sup>a</sup>  $\delta$ -Ppm ( $\pm 0.01$ ), in  $\text{CDCl}_3$  solution, relative to an internal reference of tetramethylsilane (1% by volume). Temperature is 39°C. Concentration of compounds is 70-100 mg/ml of solvent. <sup>b</sup>In Hz ( $\pm 0.05$ ) at 39°C.

<sup>c</sup> Midpoint of doublet. <sup>d</sup> These resonances coincide in  $\text{CDCl}_3$ , but they are resolved in chlorobenzene (see Figure 1).

Table III. Dipole Moment Data

| Compound   | $\mu$  | Calcd $\mu$ , D | Obsd $\mu$ , D |
|--|--|-----------------|----------------|
| <u>mer</u> -Co(admh) <sub>3</sub>                              | $\sqrt{2}\mu_t$                                | 2.38            | 2.57 ± 0.08    |
| <u>fac</u> -Co(admh) <sub>3</sub>                              | $\sqrt{6}\mu_t$                                | 4.12            | 4.07 ± 0.05    |
| C <sub>2</sub> - <u>cis</u> (N)-Co(admh) <sub>2</sub> (acac)   | $\mu_t - (\mu_a - \mu_r)$                      | 1.68            | 1.70 ± 0.16    |
| C <sub>2</sub> - <u>trans</u> (N)-Co(admh) <sub>2</sub> (acac) | $\mu_t + (\mu_a - \mu_r)$                      | 1.68            |                |
| C <sub>1</sub> -Co(admh) <sub>2</sub> (acac)                   | $[3\mu_t^2 + (\mu_a - \mu_r)^2]^{\frac{1}{2}}$ | 2.91            | 2.73 ± 0.07    |
| Co(admh)(acac) <sub>2</sub>                                    | $[\mu_t^2 + (\mu_a - \mu_r)^2]^{\frac{1}{2}}$  | 1.68            | 1.61 ± 0.11    |

for the transverse component of the Co-admh group moment. Combining this value of  $\mu_t$  with the molecular moment of Co(admh)(acac)<sub>2</sub>, 1.61 ± 0.11 D, gives a value of approximately zero for  $(\mu_a - \mu_r)$ . Because the calculated moments for the C<sub>2</sub>-cis(N) and C<sub>2</sub>-trans(N) isomers differ by only twice  $(\mu_a - \mu_r)$ , these isomers cannot be distinguished on the basis of the observed moment for the C<sub>2</sub> isomer that we have isolated. The average agreement of ~4% between the observed and calculated moments (Table III) is remarkably good and confirms the validity of this type of analysis.

The stereochemical assignments are further confirmed and the geometry of C<sub>2</sub>-Co(admh)<sub>2</sub>(acac) is established by electronic absorption spectra (Figures 2-4 and Table IV). Spectra of fac- and mer-Co(admh)<sub>3</sub> (Figure 2) exhibit significant differences in the region of the first ligand field band (<sup>1</sup>A<sub>1g</sub> → <sup>1</sup>T<sub>1g</sub> in O<sub>h</sub>). The fac-isomer gives a single, relatively sharp band at 19,100 cm<sup>-1</sup>, while the corresponding band of the mer-isomer is weaker and split into two components at 16,900 and ~19,600 cm<sup>-1</sup>. These differences are in accord with the fact that the fac-isomer has higher symmetry and is farther from being centrosymmetric than the mer-isomer.

Absorption spectra of the Co(admh)<sub>2</sub>(acac) complexes (Figure 3) exhibit similar differences in the region of the first ligand field band. The higher symmetry C<sub>2</sub> isomer shows a single band at 18,000 cm<sup>-1</sup>; the corresponding band of the C<sub>1</sub> isomer is split into two components ~15,600 and 19,000 cm<sup>-1</sup>. If the C<sub>2</sub> isomer had a trans-arrangement of N atoms, the coordination group would have approximate D<sub>4h</sub> symmetry and one would expect a large splitting of the first ligand field band (15, 16). Since the C<sub>2</sub> isomer exhibits less splitting than the C<sub>1</sub> isomer, the C<sub>2</sub> isomer can be assigned the C<sub>2</sub>-cis(N) structure.

Figure 4 compares the electronic spectra of complexes having different numbers of admh ligands: Co(acac)<sub>3</sub>, Co(admh)(acac)<sub>2</sub>, which exhibits a fairly large (3300 cm<sup>-1</sup>) splitting of the first ligand field band, C<sub>2</sub>-Co(admh)<sub>2</sub>(acac), and fac-Co(admh)<sub>3</sub>. As the number of admh ligands increases, there is a monotonic increase in the energy

Table IV. Absorption and CD Spectral Data<sup>a</sup>

| Compound  | $\nu_{\max} \times 10^{-3},$<br>cm <sup>-1</sup> | Log $\epsilon$ | $\nu \times 10^{-3},$<br>cm <sup>-1</sup> | $\epsilon_l - \epsilon_r$ |
|---|--|----------------|---|---------------------------|
| <u>fac</u> -Co(admh) <sub>3</sub>                                 |  |                | 16.8                                      | 0.20                      |
|   | 19.1   | 2.51           | 19.5                                      | -0.52                     |
|   | 23.4 (sh) <sup>b</sup>                           | 2.72           | 26.7                                      | 0.71                      |
|   | 29.8   | 3.96           | 31.8                                      | 1.0                       |
|   | 42.5   | 4.59           | 40.0                                      | (-3.8) <sup>c</sup>       |
|   |  |                | 46.3                                      | (1.9)                     |
| <u>mer</u> -Co(admh) <sub>3</sub>                                 | 16.9   | 2.16           | 15.6                                      | 0.046                     |
|   | 19.6 (sh)  | 2.25           | 18.5                                      | -0.050                    |
|   | 23.5 (sh)  | 2.77           |   |                           |
|   | 30.3   | 3.85           |   |                           |
|   | 40.5   | 4.50           |   |                           |
| C <sub>2</sub> - <u>cis</u> (N)-Co(admh) <sub>2</sub> -<br>(acac) |  |                | 16.5                                      | 0.089                     |
|   | 18.0   | 2.36           | 18.9                                      | -0.042                    |
|   | 23.3 (sh)  | 2.56           |   |                           |
|   | 30.2   | 3.84           |   |                           |
|   | 40.5   | 4.55           |   |                           |
| C <sub>1</sub> -Co(admh) <sub>2</sub> (acac)                      | 15.6 (sh)  | 1.9            | 15.2                                      | 0.038                     |
|   | 19.0   | 2.33           | 18.9                                      | -0.040                    |
|   | 23.0 (sh)  | 2.6            | 24  | (0.02)                    |
|   | 30.3   | 3.83           |   |                           |
|   | 40.4   | 4.47           |   |                           |
|   | 44.4   | 4.44           |   |                           |
| Co(admh)(acac) <sub>2</sub>                                       | 15.2 (sh)  | 1.87           | 15.2                                      | -0.48                     |
|   | 18.5   | 2.21           | 18.0                                      | 0.72                      |
|   | 22.5 (sh)  | 2.4            | 24.1                                      | -0.67                     |
|   | 31.2   | 3.88           | 30.4                                      | -4.9                      |
|   | 40.0   | 4.55           | 38.5                                      | 12.5                      |
|   | 44.4   | 4.52           | 45.0                                      | (-4.7)                    |

<sup>a</sup>Spectra were recorded in absolute ethanol. CD data refer to the first-eluted fraction. <sup>b</sup>Shoulder. <sup>c</sup>Parentheses indicate an approximate value.

American Chemical  
Society Library  
1155 16th St. N. W.

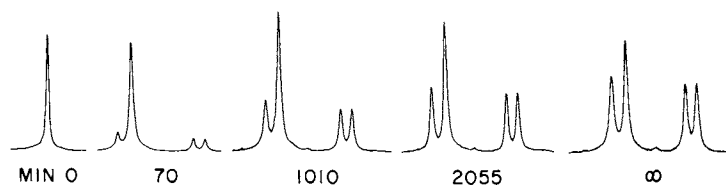


Figure 1. The tert-butyl region of the proton NMR spectra at a sweep width of 50 Hz for  $\text{Co(admh)}_3$  in chlorobenzene after heating a 0.302M solution of the fac-isomer for various numbers of minutes at  $108.1^\circ\text{C}$

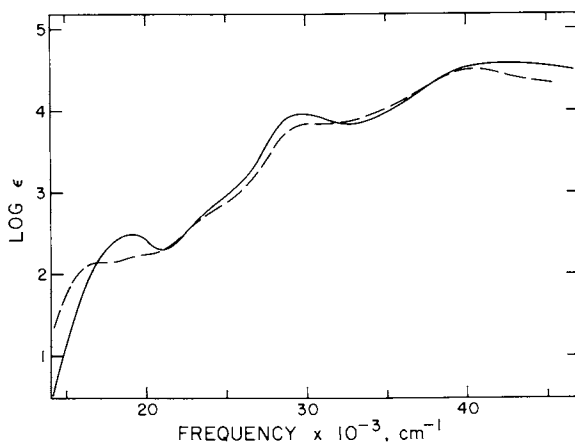


Figure 2. Electronic spectra of  $\text{fac-Co(admh)}_3$  (—) and  $\text{mer-Co(admh)}_3$  (---) in absolute ethanol

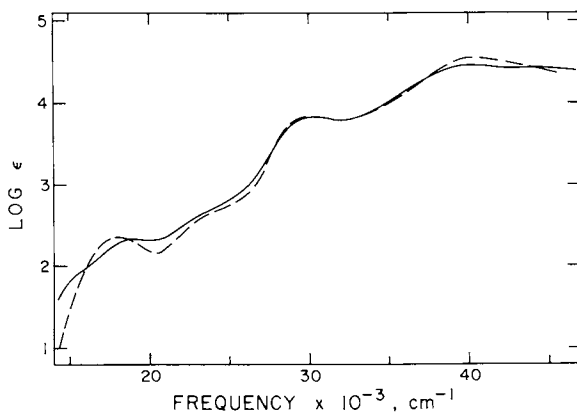


Figure 3. Electronic spectra of  $C_2$ -cis(N)-Co(admh)<sub>2</sub>(acac) (—) and  $C_1$ -Co(admh)<sub>2</sub>(acac) (---) in absolute ethanol.

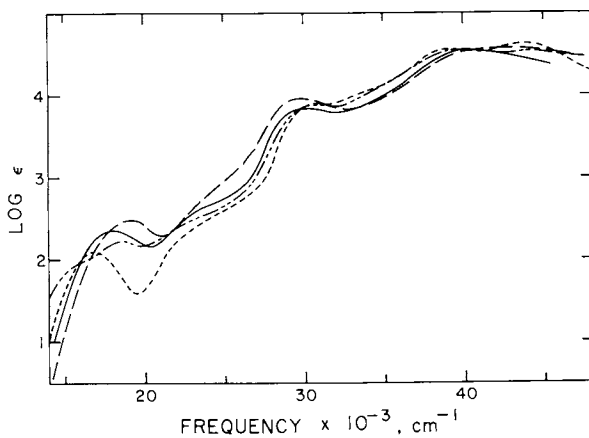


Figure 4. Electronic spectra of fac-Co(admh)<sub>3</sub> (—),  $C_2$ -cis(N)-Co(admh)<sub>2</sub>(acac) (---), Co(admh)(acac)<sub>2</sub> (— · —), and Co(acac)<sub>3</sub> (····) in absolute ethanol.

of the first ligand field band, from 16,800  $\text{cm}^{-1}$  in  $\text{Co}(\text{acac})_3$  to 19,100  $\text{cm}^{-1}$  in  $\text{fac-Co}(\text{admh})_3$ . This is in accord with the greater ligand field strength of the N-containing admh ligand. The intensity of the ligand field band also increases monotonically on going from  $\text{Co}(\text{acac})_3$  to  $\text{fac-Co}(\text{admh})_3$ , in accord with the increasing departure from a center of symmetry.

Partial Resolution and Absolute Configurations. Partial resolution of the  $\text{Co}(\text{admh})_n(\text{acac})_{3-n}$  complexes was effected by column chromatography on D-(+)-lactose.  $\text{Co}(\text{admh})(\text{acac})_2$  was resolved partially at room temperature using a 230-cm column that we have employed previously for partial resolution of metal  $\beta$ -diketonates (10). However, this procedure did not work for the bis- and tris-admh complexes. The bis and tris complexes were resolved partially, with much greater difficulty, by a low-temperature procedure that employed D-(+)-lactose on alumina as the adsorbent, isopentane-ether as the eluent, and temperatures of  $-95$  to  $-125^\circ\text{C}$ . After chromatography, the eluent was evaporated and the enantiomer in excess was concentrated by extracting the solid with chlorodifluoromethane at  $-120^\circ\text{C}$ . The values of  $\epsilon_\ell - \epsilon_r$  for the  $\text{Co}(\text{admh})_n(\text{acac})_{3-n}$  complexes (Table IV) are very small compared with  $\epsilon_\ell - \epsilon_r$  for partially resolved  $\text{Co}(\text{acac})_3$  (17), indicating that resolution was incomplete in all cases.

The absolute configurations of the  $\text{Co}(\text{admh})_n(\text{acac})_{3-n}$  complexes have been assigned by comparison of their CD spectra with the CD spectrum of  $(-)_546\text{-Co}(\text{acac})_3$  (17), the first-eluted enantiomer from D-(+)-lactose, which has been shown by X-ray diffraction to have the  $\Lambda$  absolute configuration (17). In the region of the first ligand field band, this enantiomer exhibits a negative  $A_2$  component at 15,500  $\text{cm}^{-1}$  and a more intense, positive E component at 17,500  $\text{cm}^{-1}$ , in accord with Mason's empirical rule (18, 19, 20). The signs of the E and  $A_2$  components of the exciton-split  $\pi-\pi^*$  transition are also in agreement with the  $\Lambda$  configuration (21); the E component at 38,200  $\text{cm}^{-1}$  is positive and the  $A_2$  component at 44,400  $\text{cm}$  is negative (17).

The CD spectrum of the first-eluted fraction of  $\text{Co}(\text{admh})(\text{acac})_2$  (Figure 5) is qualitatively identical to the CD of  $\Lambda(-)_546\text{-Co}(\text{acac})_3$ . Replacement of one diketonate oxygen atom with an  $\text{NH}$  group seems to have relatively little effect on the CD, except for an 800- $\text{cm}^{-1}$  increase in the splitting of the two components ( $A_2$  and E in  $D_3$ ) of the ligand field band. The signs of the CD bands indicate that the first-eluted enantiomer has the  $\Lambda$  configuration.

The CD spectrum of the first-eluted fraction of  $\text{fac-Co}(\text{admh})_3$  (Figure 6) is qualitatively similar, but enantiomeric in sign, to CD spectra of the first-eluted fractions of  $\text{Co}(\text{acac})_3$  and  $\text{Co}(\text{admh})(\text{acac})_2$ . The  $\text{mer-Co}(\text{admh})_3$ ,  $C_2\text{-cis(N)-Co}(\text{admh})_2(\text{acac})$ , and  $C_1\text{-Co}(\text{admh})_2(\text{acac})$  complexes could not be resolved well enough to obtain reliable



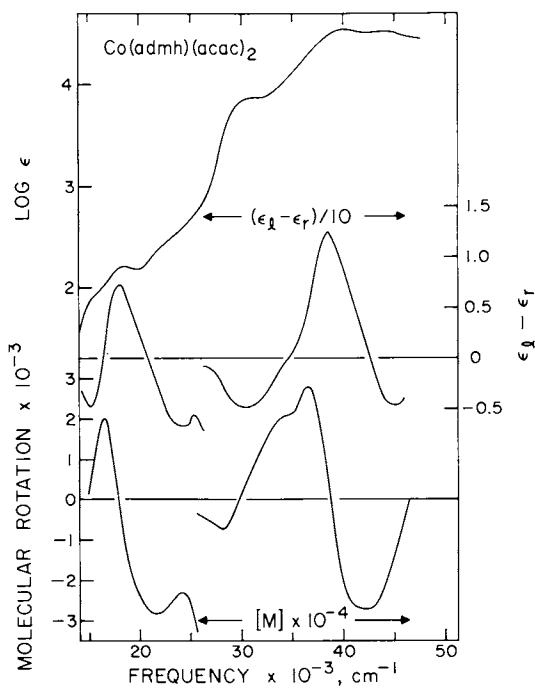


Figure 5. Absorption spectrum, CD, and optical rotatory dispersion for partially resolved  $\Lambda$ - $(-)$ <sub>4,46</sub>-Co(admh)(acac)<sub>2</sub> in absolute ethanol; first-eluted fraction from D-(+)-lactose.

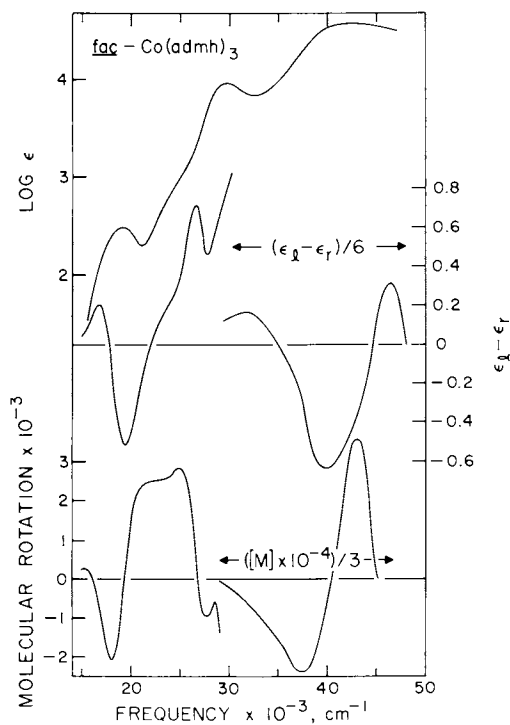


Figure 6. Absorption spectrum, CD, and optical rotatory dispersion for partially resolved  $\Delta(-)_{346}\text{-fac-Co(admh)}_3$  in absolute ethanol; first-eluted fraction from  $D(+)$ -lactose-alumina.

CD spectra in the ultraviolet, but in the region of the first ligand field band the first-eluted fractions of these complexes, like fac-Co(admh)<sub>3</sub>, exhibit positive and negative components of A<sub>2</sub> and E parcentage, respectively (cf. Table IV). It appears, therefore, that whereas the first-eluted enantiomers of Co(acac)<sub>3</sub> and Co(admh)(acac)<sub>2</sub> have the  $\Lambda$  configuration, the first-eluted enantiomers of the bis- and tris-admh complexes have the  $\Delta$  configuration. This interesting reversal in elution order may be due to a change in the site of interaction with the D-(+)-lactose as an increasing number of admh tert-butyl groups shield the polar carbonyl groups. For example, Co(acac)<sub>3</sub> presumably uses its carbonyl oxygen atoms to interact with the D-(+)-lactose, while Co(admh)<sub>3</sub> may have to use its NH groups because the oxygen atoms are shielded by the neighboring tert-butyl groups. Such shielding could also explain, at least in part, why the bis- and tris-admh complexes are so much more difficult to resolve.

Isomerization of fac-Co(admh)<sub>3</sub>. The kinetics of fac-mer isomerization of Co(admh)<sub>3</sub> have been studied by following the time dependence of the integrated intensities of the tert-butyl proton resonances (cf. Figure 1). Rate constants for fac to mer isomerization,  $k_{fm}$ , and equilibrium constants for mer to fac isomerization,  $K_{mf}$  are set out in Table V. The isomerization is first-order in the

Table V. Rate Constants and Equilibrium Constants for Geometrical Isomerization of Co(admh)<sub>3</sub> in Chlorobenzene Solution<sup>a</sup>

| Temp, °C | Concn, mol/l | $k_{fm} \times 10^6, \text{sec}^{-1}$ | $K_{mf}$          |
|----------|--------------|---------------------------------------|-------------------|
| 97.2     | 0.230        | 0.769 $\pm$ 0.022                     | 0.538 $\pm$ 0.010 |
| 97.35    | 0.276        | 0.766 $\pm$ 0.018                     |                   |
| 104.4    | 0.254        | 1.88 $\pm$ 0.04                       | 0.538 $\pm$ 0.010 |
| 104.45   | 0.285        | 1.90 $\pm$ 0.05                       |                   |
| 108.1    | 0.302        | 2.86 $\pm$ 0.07                       | 0.526 $\pm$ 0.011 |
| 111.2    | 0.329        | 4.67 $\pm$ 0.20                       | 0.510 $\pm$ 0.011 |
| 111.2    | 0.365        | 4.86 $\pm$ 0.13                       |                   |
| 115.2    | 0.304        | 7.72 $\pm$ 0.28                       | 0.581 $\pm$ 0.016 |
| 120.1    | 0.338        |                                       | 0.561 $\pm$ 0.018 |

<sup>a</sup>All errors are estimated at the 95% confidence level.

complex with rate constants ranging from  $8 \times 10^{-7}$  to  $8 \times 10^{-6} \text{sec}^{-1}$  in the temperature range 97 to 115°C. Equilibrium constants for mer to fac isomerization are larger than the statistical value of 1/3 and

are essentially independent of temperature.

Arrhenius and Eyring activation parameters were obtained in the usual way from least-squares plots of  $\log k$  vs.  $1/T$  and  $\log(k/T)$  vs.  $1/T$ , respectively. Activation parameters and rate constants at a common temperature for  $\text{Co}(\text{admh})_3$  and the related  $\beta$ -diketonate complexes,  $\text{Co}(\text{acac})_3$  and  $\text{Co}(\text{bzac})_3$  ( $\text{bzac}$  = benzoylacetate), are compared in Table VI.  $\text{Co}(\text{admh})_3$  rearranges more slowly (by a factor of

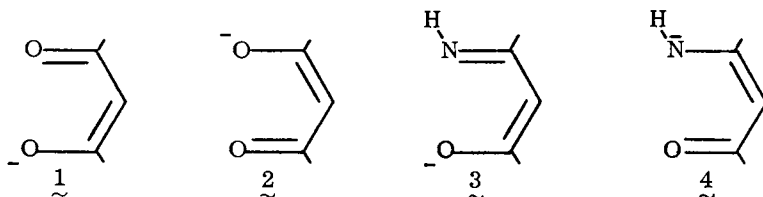
Table VI. Rate Constants and Activation Parameters for Rearrangement of  $\text{Co}(\text{admh})_3$ ,  $\text{Co}(\text{acac})_3$ , and  $\text{Co}(\text{bzac})_3$  in Chlorobenzene Solution

|   | $\text{Co}(\text{admh})_3^{\text{a}}$ | $\text{Co}(\text{acac})_3^{\text{b}}$ | $\text{Co}(\text{bzac})_3^{\text{c}}$ |
|---|---------------------------------------|---------------------------------------|---------------------------------------|
| $k_{97.3} \times 10^6, \text{sec}^{-1}$ | $0.77 \pm 0.02^{\text{d}}$            | $71.9 \pm 0.5$                        | $205 \pm 7$                           |
| $E_a, \text{kcal/mol}$                  | $36.9 \pm 1.9$                        | $34.8 \pm 0.6$                        | $32.7 \pm 0.5$                        |
| Log A                                   | $15.6 \pm 1.1$                        | $16.4 \pm 0.3$                        | $15.6 \pm 0.3$                        |
| $\Delta H^*, \text{kcal/mol}$           | $36.1 \pm 1.9$                        | $34.1 \pm 0.6$                        | $32.0 \pm 0.5$                        |
| $\Delta S^*, \text{eu}$                 | $11 \pm 5$                            | $14 \pm 2$                            | $11 \pm 1$                            |

<sup>a</sup> Fac-mer isomerization (this work). <sup>b</sup> Optical inversion (ref 10). <sup>c</sup> Fac-mer isomerization (ref 23). <sup>d</sup> All errors are estimated at the 95% confidence level.

100-300) and has a higher activation enthalpy (by 2-4 kcal); the activation entropies are essentially identical. The mechanism of inversion and isomerization of cobalt  $\beta$ -diketonates has been shown to involve chelate ring opening via rupture of one Co-O bond (22, 23), and in view of the similarity in the activation parameters in Table VI, it seems likely that  $\text{Co}(\text{admh})_3$  rearranges by an analogous mechanism. Co-N bond rupture is ruled out by the slower rate of rearrangement of  $\text{Co}(\text{admh})_3$  in comparison with  $\text{Co}(\text{acac})_3$  and  $\text{Co}(\text{bzac})_3$ ; if the Co-N bond in  $\text{Co}(\text{admh})_3$  broke more easily than the Co-O bond,  $\text{Co}(\text{admh})_3$  would be expected to rearrange more rapidly than cobalt  $\beta$ -diketonates.

The higher activation enthalpy for  $\text{Co}(\text{admh})_3$  can be rationalized in terms of valence bond resonance structures 1 - 4. In metal  $\beta$ -diketonates 1 and 2 contribute equally, while in  $\beta$ -ketoamine com-



plexes, 3 should predominate over 4 because oxygen is more electro-negative than nitrogen. Consequently, the metal-oxygen bond should be stronger in metal  $\beta$ -ketoaminoates, thus increasing the barrier to stereochemical rearrangements.

Acknowledgment. The support of this research by National Science Foundation Grant CHE-7620300 is gratefully acknowledged.

#### Literature Cited

1. Holm, R. H.; Everett, Jr., G. W.; Chakravorty, A. Prog. Inorg. Chem., (1966), 7, 83.
2. Holm, R. H. Acc. Chem. Res., (1969), 2, 307.
3. Everett, Jr., G. W.; Holm, R. H. J. Am. Chem. Soc., (1965), 87, 2117.
4. Everett, Jr., G. W.; Holm, R. H. J. Am. Chem. Soc., (1966), 88, 2442.
5. Röhrscheid, F.; Ernst, R. E.; Holm, R. H. Inorg. Chem., (1967), 6, 1607.
6. Collman, J. P.; Kittleman, E. T. Inorg. Chem., (1962), 1, 499.
7. Chakravorty, A.; Holm, R. H. Inorg. Chem., (1964), 3, 1521.
8. Srivastava, A. K.; Rana, V. B.; Mohan, M. J. Inorg. Nucl. Chem., (1974), 36, 3864.
9. Srivastava, A. K.; Rana, V. B.; Mohan, M.; Swami, M. P.; Jain, P. C. J. Inorg. Nucl. Chem., (1975), 37, 723.
10. Fay, R. C.; Girgis, A. Y.; Klabunde, U. J. Am. Chem. Soc., (1970), 92, 7056.
11. Norden, B.; Jonas, I. Inorg. Nucl. Chem. Letters, (1976), 12, 33.
12. Serpone, N.; Fay, R. C. Inorg. Chem., (1969), 8, 2379.
13. Howie, J. K. Ph.D. Thesis, Cornell University, (1977).
14. Holm, R. H.; Röhrscheid, F.; Everett, Jr., G. W.; Inorg. Syn., (1968), 11, 72.
15. Matsuoka, N.; Hidaka, J.; Shimura, Y. Bull. Chem. Soc. Japan, (1967), 40, 1868.
16. Matsuoka, N.; Hidaka, J.; Shimura, Y. Inorg. Chem., (1970), 9, 719.
17. VonDreele, R. B.; Fay, R. C. J. Am. Chem. Soc., (1971), 93, 4936.
18. Ballard, R. E.; McCaffrey, A. J.; Mason, S. F. Proc. Chem. Soc. London, (1962), 331.
19. McCaffrey, A. J.; Mason, S. F. Mol. Phys., (1963), 6, 359.
20. McCaffrey, A. J.; Mason, S. F.; Ballard, R. E. J. Chem. Soc., (1965), 2883.

21. Larsen, E.; Mason, S. F.; Searle, G. H. Acta Chem. Scand., (1966), 20, 191.
22. Gordon, II, J. G.; Holm, R. H. J. Am. Chem. Soc., (1970), 92, 5319.
23. Girgis, A. Y.; Fay, R. C. J. Am. Chem. Soc., (1970), 92, 7061.

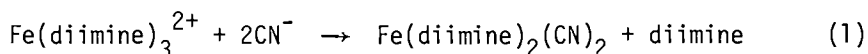
RECEIVED September 13, 1979.

## Absolute Configurations from Solution Reactions: The Tris(diimine)iron(II)/Cyanide Inversion Reaction

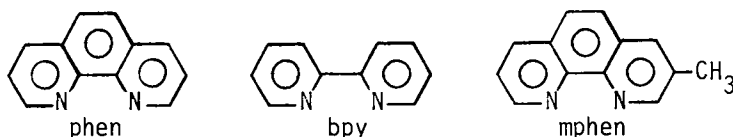
RONALD D. ARCHER and CHRISTOPHER J. HARDIMAN

Department of Chemistry, University of Massachusetts, Amherst, MA 01003

The reaction of aqueous cyanide with a tris(diimine)iron(II) chelate



shows interesting stereochemical changes, especially when the diimine is 1,10-phenanthroline, phen. The reaction produces an



optical inversion throughout the visible (charge transfer) and ultraviolet ( $\pi-\pi^*$ ) spectral regions (1) as shown in Figure 1.

The reaction of aqueous cyanide with such tris(diimine)iron(II) chelates was originally of interest because of the apparent bimolecular nature of the reaction (2,3,4). Initial stereochemical interest in the cyanide reaction (1) was based on the observation (5,6,7) that stereochemical changes in substitution reactions of  $d^6$  octahedral complexes show an inverse correlation to ligand field spectrochemical splittings provided that both the reactant and the product(s) are spin-paired; i.e., inert to further stereochemical reactions which would mask the initial stereochemistry. The cobalt(III) Bailar inversion reactions (8,9,10) are the classical examples of such changes and occur only for cobalt(III) chelates with four nitrogen donors plus two weaker donors. The iron(II) diimines appeared ideal for investigation because iron(II) requires all six ligands to be spectrochemically as strong as the nitrogen donors of the diimines for inertness to be obtained. The stronger cyanide ligand stabilizes the product so that stereochemical observations are possible.

0-8412-0538-8/80/47-119-357\$05.00/0

© 1980 American Chemical Society

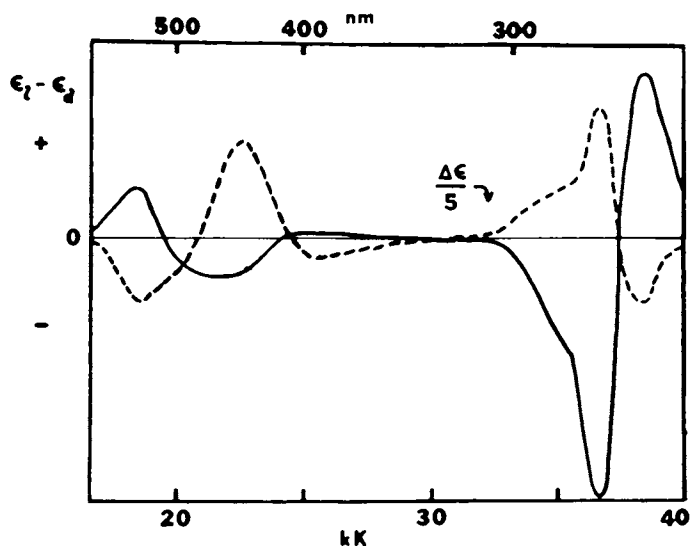


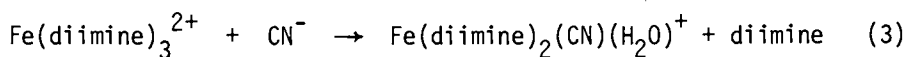
Figure 1. CD of  $\Delta\text{-Fe}(\text{phen})_3^{2+}$  (—) and the  $\text{Fe}(\text{phen})_2(\text{CN})_2$  product (---) (1)



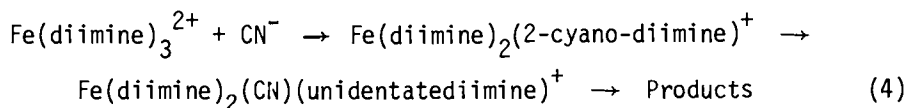
Also, the nucleophilicity of cyanide overpowers the nucleophile independent dissociation and intramolecular racemization reactions, which had been well studied many years ago (11-16).

$$\frac{-d[\Lambda\text{-Fe}(\text{diimine})_3^{2+}]}{dt} = \{k_d + k_i + k_1[\text{CN}^-]\}[\Lambda\text{-Fe}(\text{diimine})_3^{2+}] \quad (2)$$

where  $k_d$  is the dissociative rate constant,  $k_i$  is the intramolecular racemization rate constant, and together they constitute  $k_0$ , the total nucleophile-independent rate constant. Both terms contribute racemic products. Following Margerum (2), the rate constant which is first order in cyanide is designated as  $k_1$ . No cyanoaqua intermediate can be observed; therefore the rate determining step is normally considered to be



Because cyanide can act as a nucleophile on aromatic rings, the alternate possibility (17)



cannot be eliminated. This mechanism predicts retained or racemic products as the unidentate diimine is replaced by a second cyanide ligand.

Although one investigator was unable to observe the  $\text{Fe}(\text{phen})_3^{2+}$ /cyanide inversion reaction (18) and subsequently stated at an international conference that our results were wrong, Gillard, Hughes, Kane-Maguire, and Williams (19) have found our optical inversion results to be correct to within experimental error. The question of the handedness of the product was raised by the latter group, which favors reaction 4 for the reaction in question.

### Handedness

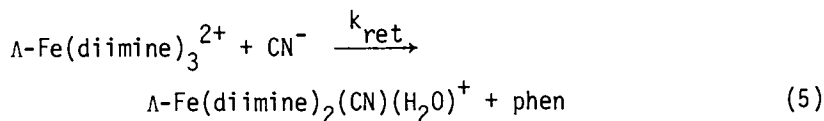
The question of whether the optical inversion is a true chemical inversion has been of concern to us (1,20,21) for some time, too. The rationale of a chemical inversion being associated with the optical inversion is based on the "nonempirical" analysis of the  $\pi\text{-}\pi^*$  electronic transitions of the tris and bis chelates (22-27). The long-axis  $\pi\text{-}\pi^*$  head-to-head  $A_2$  and B levels of the tris and bis chelates, respectively, are expected to be at higher energies than the long-axis head-to-tail E and A levels of the tris and bis chelates, respectively. For  $\Lambda$  isomers, the head-to-head transitions should have negative rotatory strengths and the head-to-tail ones should be positive. Therefore, retention

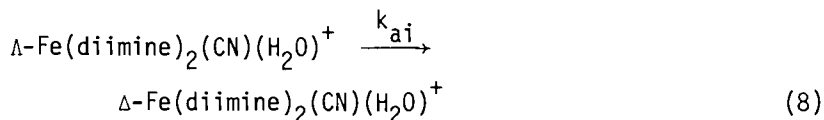
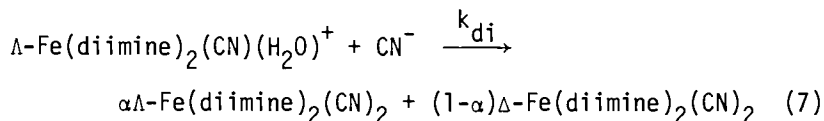
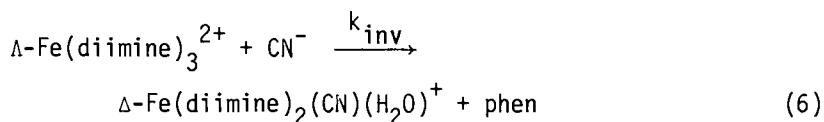
reactions should produce rotational spectral similarities as in the reaction of  $\text{Fe}(\text{bpy})_3^{2+}$  with cyanide, where the product exhibits the same optical chirality as the reactant complex (21). Shifts in such energy levels could make the chirality assignments incorrect (28,29), although molecular orbital calculations by Sanders (30,31) as well as the intermediate exciton coupling calculations by Mason (26,27) show agreement with simple exciton assignments. The absolute configuration of the  $\text{Fe}(\text{phen})_3^{2+}$  ion (32) is in agreement with the simple exciton assignment detailed above. We have observed no spectral shifts of the type anticipated for assignment problems. Furthermore, the activation parameters for the reactions of aqueous cyanide with  $\text{Fe}(\text{phen})_3^{2+}$  and  $\text{Fe}(\text{bpy})_3^{2+}$  are consistent with opposite chiralities for the two products (20,21), which is consistent with the circular dichroism spectra of the products. Even so, we decided to get a geometrical isomer handle on the reaction as well.

The rotatory strengths for the bis chelate  $\pi-\pi^*$  transitions are theoretically one-half those of the tris chelates, although experimentally the values are sometimes even less. We have assumed a 1:2 ratio in all of our studies, but other values would not invalidate our conclusions.

#### Activation Parameter Separation Through Stereochemical Results

Kinetics studies allowed us to evaluate  $k_0$  and  $k_1$  for the  $\text{Fe}(\text{phen})_3^{2+}$ /cyanide reaction in relation to the stereochemistry of the  $\text{Fe}(\text{phen})_2(\text{CN})_2$  product (1). Although it is evident that the optically active product comes from the cyanide dependent  $k_1$  path, the percent of optically inverted  $\text{Fe}(\text{phen})_2(\text{CN})_2$  product is not directly related to the percent which reacts by the cyanide-dependent path. (To illustrate, at 0.4 M cyanide almost 90% of the reaction proceeds through the cyanide dependent path but the optical activity is only about one-third of the optical activity observed for the 2.0 M cyanide reaction product.) On the other hand, a linear relationship does exist for a plot of (% by  $k_1$  path)/(% optically active product) vs.  $1/[\text{CN}^-]$ , where the % by the  $k_1$  path is determined from  $k_1[\text{CN}^-]/(k_0+k_1[\text{CN}^-])$ . Several possible mechanisms have been considered for the reaction, but the simplest mechanism considered which agreed with the results allowed a separation of retention and inversion paths. The strange linear relationship can be fit to the reaction scheme:





although the "aqua inversion" reaction (equation 8) was treated as a racemization in the earlier papers and called  $k_{\text{ar}}$ . The consideration of this reaction (equation 8) as an inversion of the cyanoaqua ion is predicated by the strong nucleophilicity of cyanide and geometrical arguments which show that a movement of either end of either chelate ring produces the inverted configuration from that prior to the movement. The lack of trans products or other side products (TLC experiments herein) substantiates this conclusion. The two specific rate constants are related as follows:

$$k_{\text{ar}} = 2k_{\text{ai}} \quad (9)$$

i.e., each inversion produces 2 racemic molecules so that the apparent rate of racemization is twice the rate of inversion. The mechanism provides a rationale for the linear (% by  $k_1$ )/(% optically active) vs.  $1/[\text{CN}^-]$  plot, which has an

$$\text{intercept} = k_1/(k_{\text{inv}} - k_{\text{ret}}) \quad (10)$$

and a

$$\text{slope} = 2k_1k_{\text{ai}}/k_{\text{di}}(k_{\text{inv}} - k_{\text{ret}}) \quad (11)$$

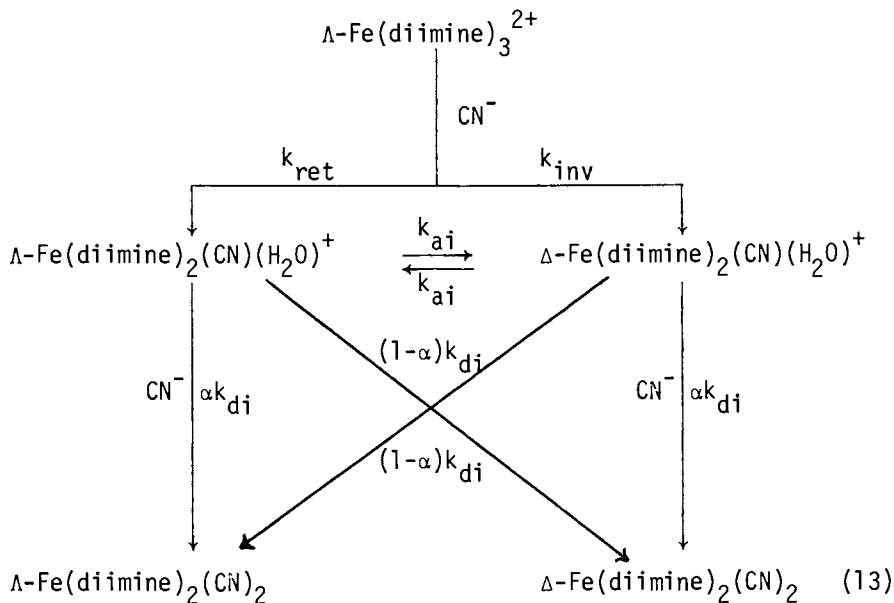
for the mechanism produced by reactions 5 - 8 with 5 and 6 as slow steps, so that the observed

$$k_1 = k_{\text{inv}} + k_{\text{ret}} \quad (12)$$

The derivation of these expressions has been published previously (20).

Molecular models and chemical intuition provide the logic behind this mechanism as detailed previously (20). Cyanide entry "trans" to a displaced diimine produces a situation in which the remaining diimines must rearrange. Because trans bis chelates with ligands of this type and low-spin iron(II) are unlikely because of hydrogen-hydrogen repulsions, only inversion can occur. Conversely, if cyanide enters adjacent to a displaced diimine, retention is logical.

Overall this reaction scheme for a symmetrical diimine is



where an excellent fit of data for both  $\text{Fe}(\text{phen})_3^{2+}$  and  $\text{Fe}(\text{bpy})_3^{2+}$  have been obtained assuming  $\alpha = 1$ . The above mentioned plot gives good linearity over the temperature range 0 to 15° and is consistent with  $k_{\text{inv}} > k_{\text{ret}}$  for  $\text{Fe}(\text{phen})_3^{2+}$  and  $k_{\text{ret}} > k_{\text{inv}}$  for  $\text{Fe}(\text{bpy})_3^{2+}$ . Table 1 shows the activation parameters and other relevant data for the two reactions. Note that for the  $\text{Fe}(\text{phen})_3^{2+}$  reaction, in which inversion predominates, a negative temperature factor occurs in terms of the percent of optically active product. For  $\text{Fe}(\text{bpy})_3^{2+}$ , retention and a positive temperature factor are observed. The activation parameters are consistent with a mechanism in which cyanide approach perturbs the low-spin  $d^6$  complex sufficiently for an electron to enter one of the  $e_g(\sigma^*)$  orbitals. A consideration of possible perturbations (1) makes the ligand across from the perturbing cyanide loosened by the  $\sigma^*$  electron. One end of each of the adjacent ligands is also loosened by this perturbation and these can move as cyanide enters the

Table I<sup>a</sup>  
 The Fe(phen)<sub>3</sub><sup>2+</sup>/CN<sup>-</sup> and Fe(bpy)<sub>3</sub><sup>2+</sup>/CN<sup>-</sup> Reactions

| Complex                             | Temp., °C | Maximum % Activity <sup>b</sup> | k <sub>ret</sub> × 10 <sup>5</sup> | k <sub>inv</sub> × 10 <sup>5</sup> |
|-------------------------------------|-----------|---------------------------------|------------------------------------|------------------------------------|
| Fe(bpy) <sub>3</sub> <sup>2+</sup>  | 0.0       | +17.4(0.5)                      | 6.0(0.4)                           | 3.0(0.4)                           |
|                                     | 8.0       | +24.4(1.0)                      | 20.3(0.6)                          | 10.2(0.6)                          |
|                                     | 15.0      | +27.0(1.4)                      | 58.2(2.0)                          | 27.0(2.0)                          |
|                                     |           | ΔH <sup>‡</sup> (kJ/mole)       | = 96.7(1.2)                        | 92.9(0.9)                          |
|                                     |           | ΔS <sup>‡</sup> (J/mole deg)    | = 28 (4)                           | 10 (3)                             |
| Fe(phen) <sub>3</sub> <sup>2+</sup> | 0.5       | -14.9(0.4)                      | 6.9(0.4)                           | 11.6(0.4)                          |
|                                     | 8.0       | -13.3(0.4)                      | 22.4(1.4)                          | 34.1(1.3)                          |
|                                     | 15.0      | -11.6(0.8)                      | 66.4(5.9)                          | 99.6(5.6)                          |
|                                     |           | ΔH <sup>‡</sup> (kJ/mole)       | = 100.0(1.2)                       | 94.6(3.2)                          |
|                                     |           | ΔS <sup>‡</sup> (J/mole deg)    | 41 (4)                             | 26 (11)                            |

<sup>a</sup>Standard deviations given in parentheses; k's in M<sup>-1</sup> sec<sup>-1</sup>.

<sup>b</sup>Observed retention and inversion at infinite time for 1.99 M [CN<sup>-</sup>] assuming R(tris) = 2R(bis); a negative sign on the activity means the product has a reversed optical chirality.

coordination sphere. This is path a in Figure 2. Alternatively, the other end of an adjacent ligand might move to make room for the very nucleophilic cyanide (path b in Figure 2). In either case inversion results because of the steric prohibition on the trans isomer. If an adjacent ligand is lost retention occurs (path c in Figure 2). As we have detailed before (21), the possibility of one end detachments with bpy and the fact that one end of the adjacent ligands would be loosened by a σ\* electron (1), easily accounts for the change from inversion to retention for the change from the rigid phen ligand to the more flexible bpy. The activation parameters are consistent with these arguments; that is, the inversion path in which both ends of the leaving ligand has been loosened has a lower activation energy than the retention path even for the bpy reaction where the retention path predominates. The lower entropy of activation for the inversion path reflects the lower frequency factor associated with the concerted process necessary for this path.

#### Unsymmetrical Diimine Potential

Whereas all of the inversion reaction products with symmetrical chelates produce one isomer, the potential information available from unsymmetrical chelates is shown in Table II. From the table the value of the Δ-fac-Fe(mphen)<sub>3</sub><sup>2+</sup> ion for detecting the stereochemical changes in the cyanide reaction is obvious.

Table II

| Reaction Stereochemistry <sup>a</sup>  |  |  |                       |
|--|--|--|-----------------------|
| Fe(diimine) <sub>3</sub> <sup>2+</sup> | Fe(diimine) <sub>2</sub> (CN)(H <sub>2</sub> O) <sup>+</sup> |  |                       |
|  | Path a <sup>b</sup>  | Path b   | Path c                |
| Λ(symmetrical)                         | Δ  | Δ  | Λ                     |
| Λ-facial                               | Δ-C <sub>1</sub>   | Δ-C <sub>2</sub> ( <u>trans</u> ); Δ-C <sub>2</sub> ( <u>cis</u> ) | Λ-C <sub>1</sub>      |
| Λ-meridional                           | Δ(1:1:1) <sup>c</sup>  | Δ(1:4:1) <sup>c</sup>  | Λ(1:1:1) <sup>c</sup> |

<sup>a</sup>For isomer designations see Figure 3.

<sup>b</sup>Path designations are from Figure 2.

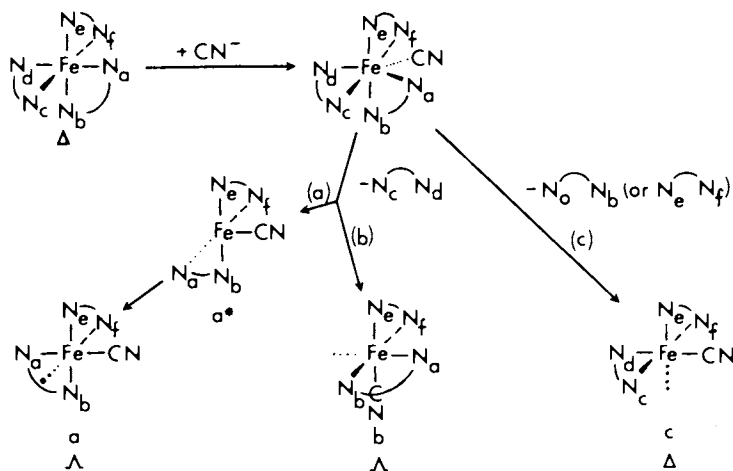
<sup>c</sup>Ratios of C<sub>2</sub>(trans):C<sub>1</sub>:C<sub>2</sub>(cis).

### Experimental Section

3-Methyl-1,10-phenanthroline. Initially the ligand was prepared according to the Skraup procedure of Case (33), but the low yield (6%) led us to employ another method used for the corresponding ethyl derivative by Case, Jacobs, Cook, and Dickstein (34). The latter procedure involves a Skraup synthesis between 3-methyl-8-aminoquinoline (33) and glycerol (rather than 8-aminoquinoline and methacrolein). By using dry glycerol and recycling unreacted amine, the product was obtained in high yield (92%).

Λ-fac-Tris(3-methyl-1,10-phenanthroline)iron(II) Diantimony-ditartrate. The Fe(mphen)<sub>3</sub><sup>2+</sup> ion was prepared and resolved analogous to the method of Dwyer and Gyarfás (35). The reaction was carried out under nitrogen in the presence of iron filings to avoid oxidation of the iron(II) prior to chelation. The reactions were performed on a 0.4 g scale and precipitation was induced by rotary evaporation under reduced pressure and the precipitate was washed with cold water. The strong circular dichroism spectrum indicates that a Λ-Fe(mphen)<sub>3</sub><sup>2+</sup> diastereomer has been formed.

Λ-fac-Tris(3-methyl-1,10-phenanthroline)iron(II) Perchlorate. The metathesis synthesis of the perchlorate salt from the diantimonyditartrate salt (classically thought to be two antimonyl tartrate anions) was performed analogous to that of Dwyer and Gyarfás (35) with two added diethyl ether washes prior to air drying. The <sup>1</sup>H NMR spectrum shows a single sharp methyl resonance indicative of the fac isomer.



## Inorganic Chemistry

Figure 2. Proposed inversion paths (a) and (b) together with retention path (c) for cyanide acting as a nucleophile on an iron(II)-tris(diimine) complex with rigid ligands such as  $\text{Fe}(\text{phen})_3^{2+}$ . Intermediates a, b, and c are assumed to add water and cyanide in the vacant octahedral position ( $\cdots$ ) without further stereochange, although reinversion of the aquocyno complex appears to compete with anation.

$\text{N}_a$  of  $a^*$  cannot bond because of steric factors (20).

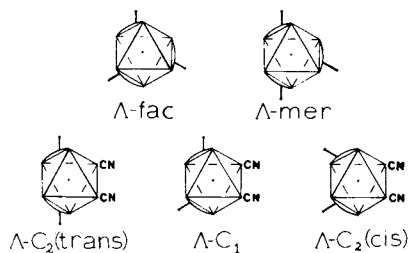


Figure 3. The  $\Lambda$  geometrical isomers for equivalent unsymmetrical phen-type ligands; e.g.,  $\text{Fe}(\text{mphen})_3^{2+}$  and  $\text{Fe}(\text{mphen})_2(\text{CN})_2$ . The analogous  $\Delta$  isomers should be obvious. Only the cis-dicyano possibilities shown are sterically feasible, so the cis and trans designations refer to the relative orientations of the methyl groups in the two  $\text{C}_2$  isomers of  $\text{Fe}(\text{mphen})_2(\text{CN})_2$ .

Cyanide Reaction. The reaction of  $\text{Fe(mphen)}_3^{2+}$  with cyanide was conducted with either the perchlorate salt or directly with the diastereomer immediately after decomposition of the diantimonytartrate ion with base under nitrogen at  $0^\circ$ , the conditions of the cyanide reaction. The product of the reaction was extracted into chloroform, the volume was reduced to dryness with rotary evaporation, the free ligand was extracted with benzene, and spectral measurements made.

Thin Layer Chromatographic Isomer Separation. The geometrical isomers were separated by spotting a chloroform solution of the product on a silica gel plate and eluting with a 15:1 v/v chloroform/methanol solution. The spots or bands were dissolved in methanol and the solutions were evaporated to dryness.

Spectral Determinations. The circular dichroism spectra were obtained on a Cary 60 modified as reported previously (20). The spectra were obtained with aqueous solutions. The 1:1 v/v  $\text{CD}_3\text{OD}/\text{CD}_2\text{Cl}_2$   $^1\text{H}$  NMR spectra were obtained with a Perkin Elmer R-12 spectrometer. The ultraviolet/visible electronic spectra in water or chloroform were obtained with a Cary 14 spectrophotometer with matched one cm Supracil cells.

## Results and Discussion

The circular dichroism spectrum of the isomer designated as  $\Lambda$ -fac- $\text{Fe(mphen)}_3^{2+}$  is shown in Figure 4. The facial designation is based on the sharp  $^1\text{H}$  NMR signal observed for the resolved complex relative to the broader signal observed for the synthetic mixture of fac and mer isomers. The shielding is analogous for all protons, thus only a small difference is observed. Thus the absolute purity of the facial isomer cannot be assured.

The circular dichroism spectra of the thin layer chromatographed product of a fairly concentrated  $\text{Fe(mphen)}_3^{2+}$  sample in 2 M aqueous cyanide, for which both a precipitate and a solution were obtained, is presented in Figure 5. The spot labelled 1 has a  $^1\text{H}$  NMR signal at about 2.5 ppm downfield from tetramethylsilane, spot 2 has a doublet at 2.5 and 1.9 ppm, and spot 3 has a singlet at 1.9 ppm. A molecular model shows the considerable shielding available to the  $\text{C}_2$ (cis) methyl groups and one of the methyl groups on the  $\text{C}_1$  isomer. Thus the spots are assigned as

|   |                               |
|---|-------------------------------|
| 1 | $\text{C}_2$ ( <u>trans</u> ) |
| 2 | $\text{C}_1$                  |
| 3 | $\text{C}_2$ ( <u>cis</u> )   |

consistent with the NMR spectra. All have identical absorption spectra and no other iron residues can be observed. Hence the entire coordination product appears to be the three neutral  $\text{Fe(mphen)}_2(\text{CN})_2$  isomers.



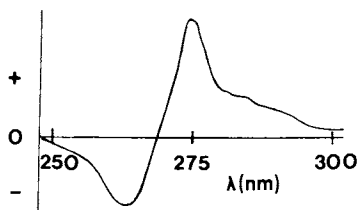


Figure 4. The CD spectrum of  $\Delta$ -fac- $\text{Fe}(\text{mphen})_3^{2+}$  in water

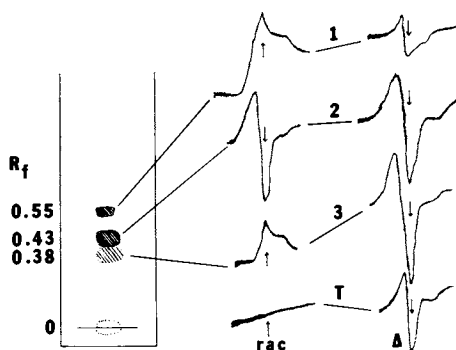


Figure 5. A thin-layer chromatogram of the product of  $\Delta$ - $\text{Fe}(\text{mphen})_3^{2+}$  plus 2M aqueous cyanide under concentration conditions where both a racemic (*rac*) precipitate and an optically active ( $\Delta$ ) solution result. The CD spectrum of the total (*T*) fraction and each spot is presented with an arrow indicating the low energy  $\pi$ - $\pi^*$  transition at 275 nm. Energy increases to the left on each spectrum in this figure.

To obtain quantitative results more dilute solutions were prepared. Under these conditions the reaction solution remained homogeneous throughout the reaction. The results are tabulated in Table III.

Table III

Isomer Percentages for the  $\text{Fe}(\text{mphen})_2(\text{CN})_2$  Products of the  $\Lambda$ -fac- $\text{Fe}(\text{mphen})_3^{2+}$  plus Aqueous Cyanide Reaction

|  | [CN <sup>-</sup> ] |           |          |           |          |           |          |           |
|--|--------------------|-----------|----------|-----------|----------|-----------|----------|-----------|
|  | 1.66 M             |           | 0.83 M   |           | 0.66 M   |           | 0.49 M   |           |
| $\text{Fe}(\text{mphen})_2(\text{CN})_2$ | $\Delta$           | $\Lambda$ | $\Delta$ | $\Lambda$ | $\Delta$ | $\Lambda$ | $\Delta$ | $\Lambda$ |
| $\text{C}_2(\text{trans})$               | 13.9               | 14.1      | 14.9     | 15.1      | 12.4     | 12.6      | 14.4     | 14.6      |
| $\text{C}_1$                             | 27.3               | 21.7      | 25.7     | 22.3      | 27.0     | 25.0      | 25.9     | 24.1      |
| $\text{C}_2(\text{cis})^a$               | 11.5               | 11.5      | 11.0     | 11.0      | 11.5     | 11.5      | 11.0     | 11.0      |

<sup>a</sup>Overlap between  $\text{C}_1$  and  $\text{C}_2(\text{cis})$  may have negated a small activity for the  $\text{C}_2(\text{cis})$  isomer. A separate sample at 5.0 M CN<sup>-</sup> indicated 11.8%  $\Delta$  and 12.2%  $\Lambda$   $\text{C}_2(\text{cis})$  isomers as well as 15.4%  $\Delta$  and 15.6%  $\Lambda$   $\text{C}_2(\text{trans})$ , and 27.2%  $\Delta$  and 17.8%  $\Lambda$   $\text{C}_1$  isomers.

The percentage of each geometrical isomer ( $\Delta + \Lambda$ ) was only estimated in whole percents from the absorption spectral intensities of the spots extracted from the TLC plates. The differences in the two optical isomers of each geometrical isomer were determined from the circular dichroism spectra assuming theoretical rotatory strengths. Thus, the actual numbers are less accurate than the overall trends. Note that the  $\text{C}_1$  isomer activity increases by a factor of about five over the cyanide concentration range measured, whereas the  $\text{C}_2(\text{trans})$  isomer activity remains virtually unchanged throughout. [Unfortunately the overlap in spots 2 and 3 precluded accurate measurements for the  $\text{C}_2(\text{cis})$  isomer.]

Mechanisms which predict parallel increases in the activity of the isomers do not appear tenable. However, realizing that the second step ( $k_{dj}$ ) competes with isomerizations ( $k_{aj}$ ) and that once the very nucleophilic cyanide is attached to the iron center, it is even more tenacious than the mphen ligand, the  $k_{aj}$  path stereochemistry can be summarized as shown in Table IV.

The  $k_{dj}$  path gives  $\alpha$  retention plus  $(1-\alpha)$  of the same products indicated in Table IV. Using the rate constants from the unsubstituted  $\text{Fe}(\text{phen})_3^{2+}/\text{CN}^-$  reaction, which assumes  $\alpha=1$ , the stereochemistry for the first step of the  $\text{Fe}(\text{mphen})_3^{2+}/\text{CN}^-$  reaction can be calculated. The results for three concentrations (from two different  $\Lambda$ -fac reactant preparations) are listed in Table V.

Table IV

The "Aqua Inversion" Reaction Stereochemistry<sup>a</sup>

| $\text{Fe(mphen)}_2(\text{CN})(\text{H}_2\text{O})^+$ | $\xrightarrow{k_{ai}}$ | $\text{Fe(mphen)}_2(\text{CN})(\text{H}_2\text{O})^+$               |
|---|------------------------|---|
| $\Delta\text{-C}_2(\text{trans})$                     | $\longrightarrow$      | $\Lambda\text{-C}_1$  |
| $2\Delta\text{-C}_1$                                  | $\longrightarrow$      | $\Lambda\text{-C}_2(\text{trans}) + \Lambda\text{-C}_2(\text{cis})$ |
| $\Delta\text{-C}_2(\text{cis})$                       | $\longrightarrow$      | $\Lambda\text{-C}_1$  |

<sup>a</sup>If the cyanide stays in place, the only rearrangements of the two mphen ligands which can occur through aqua displacement are those given; analogous changes occur for the  $\Lambda$  isomer.

Table V

Calculated Isomer Percentages for the  $\Lambda\text{-fac-Fe(mphen)}_3^{2+}$   
to  $\text{Fe(mphen)}_2(\text{CN})(\text{H}_2\text{O})^+$  Reaction<sup>a</sup>

| $\text{Fe(mphen)}_2(\text{CN})(\text{H}_2\text{O})^+$ | 5.0 M $\text{CN}^-$ |           | 1.66 M $\text{CN}^-$ |           | 0.49 M $\text{CN}^-$ |           |
|---|---------------------|-----------|----------------------|-----------|----------------------|-----------|
|   | $\Delta$            | $\Lambda$ | $\Delta$             | $\Lambda$ | $\Delta$             | $\Lambda$ |
| $\text{C}_2(\text{trans})$                            | 16.3                | 15.8      | 15.0                 | 14.1      | 17.4                 | 16.0      |
| $\text{C}_1$  | 27.1                | 16.4      | 28.0                 | 20.2      | 26.4                 | 22.2      |
| $\text{C}_2(\text{cis})$                              | 12.3                | 12.1      | 11.9                 | 10.9      | 11.0                 | 10.2      |

<sup>a</sup>These values are based on the calculated second step stereochemistry found for  $\text{Fe(phen)}_3^{2+}$  (20); i.e., the same  $k_{ar}/k_{di}$  ratio with  $\alpha=1$ , which transforms as about 1 inverted product molecules to 2.5 retained product molecules for the second step. The inverted second step products are assumed to follow Table IV stereochemistry.

The stereochemical results are dependent on similar reaction stereochemistry and rates for the mphen and phen chelates. The calculations are also valid if the retention:inversion ratio for the second step is simply due to  $\alpha k_{di}$  and  $(1-\alpha) k_{di}$ ; i.e.,  $k_{di} \gg k_{ai}$ . Clearly, the  $\Delta$  configuration is formed in the first step, but the  $\text{C}_1$  isomer clearly predominates in the optical activity. The slight  $\Lambda$  activity of the  $\text{C}_2(\text{trans})\text{-Fe(mphen)}_2(\text{CN})_2$  isomer appears to be due to the large amount of  $\Delta\text{-C}_1\text{-Fe(mphen)}_2\text{-}(\text{CN})(\text{H}_2\text{O})^+$  produced in the first step. Some reinverts either through the  $1-\alpha$  part of  $k_{di}$  path and/or the  $k_{ai}$  path.

For all three geometrical isomers of  $\text{Fe}(\text{mphen})_2(\text{CN})(\text{H}_2\text{O})^+$  to exhibit  $\Delta$  predominance from the  $\Lambda$ -fac- $\text{Fe}(\text{mphen})_3^{2+}$  ion chemical inversion must take place. See Table II. Both the a and b paths of Figure 2 appear to be involved in the formation of inverted products.

A sizeable part of the racemic background of all isomers may be due to the cyano ligand activation envisioned by Gillard (17,19). If the ligand is removed prior to the addition of cyanide, the high-spin bis chelate could undergo numerous rearrangements prior to cyanide returning it to a low-spin state. We have not been able to explain the isomer results and the activation parameters by any mechanism which does not consider an inversion reaction as part of the mechanism. A recent suggestion that the mechanism of cyanide reactions with the tris(diimine)iron(II) ions is dissociative (36) was based on similar  $\Delta V^\ddagger$  values for cyanide and hydroxide reactions. That suggestion ignores both reaction stereochemistry and other activation parameters.

### Conclusion

The synthesis of the unsymmetrical 3-methyl-1,10-phenanthroline (mphen) and the resolution of the facial isomer of  $\text{Fe}(\text{mphen})_3^{2+}$  has allowed us to investigate the stereochemistry associated with the optical inversion reaction previously observed for the corresponding unmethylated  $\text{Fe}(\text{phen})_3^{2+}$  ion with cyanide. We conclude that the  $\Lambda$ -fac- $\text{Fe}(\text{mphen})_3^{2+}$  isomer produces an excess of all three  $\Delta$ - $\text{Fe}(\text{mphen})_2(\text{CN})(\text{H}_2\text{O})^+$  isomers when the  $\Lambda$ -fac isomer reacts with cyanide, even though the final  $\text{Fe}(\text{mphen})_2(\text{CN})_2$  product has only one strongly  $\Delta$  isomer. Thus the optical inversion is a chemical inversion as well.

### Acknowledgements

Taken in part from the Honors Thesis submitted by Mr. Hardiman to Hampshire College, December 1978. The work was done at the University of Massachusetts and was supported through funds provided by the University of Massachusetts.

### Addendum

Burgess (37) allows for inversion through the Gillard mechanism (17) by considering activation by the 2-cyano derivative, but loss of another diimine as the cyano group is transferred to the metal; cf. Blandamer, Burges and Wellings (38) for hydroxide analogy. However, the rationale for a predominance of inversion would appear to require a triplet excited state indistinguishable from the one we have chosen. Also, Twigg and coworkers (39) find that 6-adducts (rather than 2-adducts) occur for 5-nitro-1,10-phenanthroline. (The 2-adducts are important in the development of the Gillard mechanism.) Thus, we conclude that while addition

compounds may be important in bpy complex retention reactions and in overall racemization reactions, direct cyanide attack appears to be the best explanation for the inversion reactions.

#### Literature Cited

1. Archer, R.D.; Suydam, L.J.; Dollberg, D.D. J. Am. Chem. Soc. (1971), 93, 6837.
2. Margerum, D.W. J. Am. Chem. Soc. (1957), 79, 2728.
3. Margerum, D.W.; Morganthaler, L.P. "Advances in the Chemistry of Coordination Chemistry", Kirschner, S., Editor, p. 481, Macmillan, N.Y., 1961.
4. Margerum, D.W.; Morganthaler, L.P., J. Am. Chem. Soc. (1962), 84, 705.
5. Archer, R.D. Coord. Chem. Rev. (1969), 4, 243.
6. Basolo, F. Advan. Chem. Ser. No. 62 (1967), 408.
7. Archer, R.D. Proc. Int. Conf. Coord. Chem. (1964), 8, 111.
8. Bailar, J.C., Jr.; Auten, R.W. J. Am. Chem. Soc., (1934), 56 774.
9. Bailar, J.C., Jr. Rev. Pure Appl. Chem. (1966), 16, 91.
10. Archer, R.D. "Coordination Chemistry", Kirschner, S., Editor, p. 18, Plenum Press, N.Y., 1969.
11. Lee, T.S.; Kolthoff, I.M.; Leussing, D.L. J. Am. Chem. Soc. (1948), 70, 3596.
12. Basolo, F.; Hayes, J.C.; Neumann, H.M. J. Am. Chem. Soc. (1954), 76, 3807.
13. Dickens, J.E.; Basolo, F.; Neumann, H.M. J. Am. Chem. Soc. (1957), 79, 1286.
14. Sieden, L.; Basolo, F.; Neumann, H.M. J. Am. Chem. Soc. (1959), 81, 3809.
15. Burgess, J. J. Chem. Soc., A (1968), 1085.
16. Burgess, J. J. Chem. Soc., A (1969), 1899.
17. Gillard, R.D. Coord. Chem. Rev. (1975), 16, 67.

18. Nord, G. Acta Chem. Scand. (1973), 37, 743.
19. Gillard, R.D.; Hughes, C.T.; Kane-Maguire, L.A.P.; Williams, P.A. Transition Metal Chem. (1976), 1, 114.
20. Archer, R.D.; Dollberg, D.D. Inorg. Chem. (1974), 13, 1551.
21. Dollberg, D.D.; Archer, R.D. Inorg. Chem. (1975), 14, 1888.
22. Bosnich, B. Accts. Chem. Res. (1969), 2, 266.
23. Mason, S.F. Inorg. Chim. Acta Rev. (1968), 2, 89.
24. Bosnich, B. Inorg. Chem. (1968), 7, 178.
25. Hanazaki, I.; Nagakura, S. Inorg. Chem. (1969), 8, 654.
26. Mason, S.F.; Peart, B.J.; Waddell, R.E. J. Chem. Soc., Dalton Trans. (1973), 944.
27. Mason, S.F.; Peart, B.J. J. Chem. Soc., Dalton Trans. (1973), 949.
28. Ferguson, J.; Hawkins, C.J.; Kane-Maguire, N.A.P.; Lip, H. Inorg. Chem. (1969), 8, 771.
29. Bray, R.G.; Ferguson, J.; Hawkins, C.J. Austr. J. Chem. (1969), 22, 2091.
30. Sanders, N. J. Chem. Soc., A (1971), 1563.
31. Sanders, N. J. Chem. Soc., Dalton Trans. (1972), 345.
32. Zalkin, A.; Templeton, D.H.; Veki, T. Inorg. Chem. (1973), 12, 1641.
33. Case, F.H. J. Am. Chem. Soc. (1948), 70, 3994.
34. Case, F.H.; Jacobs, Z.B.; Cook, R.S.; Dickstein, J. J. Org. Chem. (1957), 22, 390.
35. Dwyer, F.P.; Gyarfás, E.C. J. Proc. Roy. Soc. N. S. Wales (1949), 83, 263.
36. Lawrance, G.A.; Stranks, D.R.; Suvachittanont, S. Inorg. Chem. (1979), 18, 82.
37. Burgess, J., Private discussions at Second International Symposium on the Mechanisms of Reactions in Solution, Canterbury, England, July 1979.

38. Blandamer, M.J.; Burgess, J.; Wellings, P. *Transition Metal Chem.* (1979), 4, 95.
39. Anderson, D.W.W.; Roberts, P.; Twigg, M.V.; Williams, M.B. *Inorg. Chim. Acta* (1979), 34, L281.

RECEIVED September 13, 1979.

## Photoacoustic Detection of Natural Circular Dichroism in Crystalline Transition Metal Complexes

RICHARD ALAN PALMER, JOSEPH C. ROARK, and JAMES C. ROBINSON

P. M. Gross Chemical Laboratory, Duke University, Durham, NC 27706

The advantages of using crystalline solids (particularly single crystals) for optical absorption and linear dichroism measurements are well known (1). Less widely appreciated perhaps are the advantages (and limitations) of extending this technique to the measurement of optical activity. Although many of the points below apply equally well to magnetically induced "optical activity", the primary emphasis of our work has been on the measurement of "natural" optical activity as a technique for studying conformation and absolute configuration. These data can serve as important bench marks since independent (X-ray) determination of absolute configuration and conformation is frequently possible (2). The relatively low dipole strengths of  $d-d$  and certain other low lying, highly forbidden electronic transitions makes solid state optical activity measurements particularly applicable to transition metal ion complexes.

For intrinsically chiral species that are inert enough to be resolved conventionally, the measurement of natural optical activity in crystals has the same advantages as single crystal absorption measurements. In addition, however, it also affords the opportunity to determine rotational strengths of species which do not exhibit optical activity in solution. There are two classes of such materials: 1) intrinsically achiral chromophores which crystallize in enantiomorphous space groups, and 2) intrinsically chiral but labile chromophores which spontaneously resolve on crystallization.

The measurement of optical activity in single crystals has been studied most extensively by transmission techniques, although recent development of emission methods has also been reported (3,4). Transmission methods are limited to those compounds which can be obtained in suitably large and perfect single crystals. In addition, only in non-biaxial crystals can the complications of linear birefringence be avoided easily. (However, a two-angle method for cancelling these effects has

0-8412-0538-8/80/47-119-375\$05.25/0

© 1980 American Chemical Society



been recently proposed (5.) Generally, of the two possible experiments, circular dichroism (CD) is the choice over optical rotatory dispersion (ORD) due to the relative insensitivity of the former to crystal imperfection and strain. However, the most serious limitation on single crystal optical activity measurement is high absorptivity, since, as is generally the case, absorbance  $A = \epsilon cl (= \beta \ell)$  must be  $\ll 1$ . (Note that if  $\epsilon = 100 \text{ l mol}^{-1} \text{ cm}^{-1}$  and  $c = 5 \text{ mol l}^{-1}$ , then the crystal must be only 0.02 mm thick for  $A = 1$ ). Unless doping into a colorless host crystal is possible, the difficulties of cutting and polishing a crystal with  $\epsilon > 50$  (of appropriate thickness) while retaining a macrosized window are obvious. The use of micro equipment is a viable approach in some cases, whereas diffuse transmission spectra of mulls is another possible solution. However, transmission CD of mulls is particularly sensitive to scattering depolarization. For those chiral systems which radiatively decay after electronic excitation, circularly polarized luminescence (CPL) (optical activity of the excited state) and fluorescence detected circular dichroism (FD CD) (detection of optical activity of the ground state by measurement of radiative decay) are useful probes of conformation in the solid state (3,4).

The recent revival of interest in the photoacoustic effect in condensed media (6,7) led us to consider the possibility of detecting natural circular dichroism photoacoustically. Certain aspects of the photoacoustic effect suggest that this technique might be generally applicable to all chiral solids regardless of crystal class, size or perfection, or strength of absorption. Although subsequent theoretical developments and experimental results have caused us to limit considerably the predicted scope of this method, nevertheless, it is possible now to say clearly that the experiment does work and offers prospects for unique results. In this paper we review briefly the nature of the theory and practice of condensed phase photoacoustic spectroscopy and its extension to the measurement of natural circular dichroism, and present initial results for single crystals and powders.

#### The Nature of the Condensed Phase Photoacoustic Effect

The photoacoustic effect in solids and liquids was first described by Bell almost 100 years ago (8). Recent interest in photoacoustic detection has centered around the possibilities of applying it to the measurement of the absorption spectra of highly absorbing and/or light scattering materials of both physical and biochemical interest (7). In the conventional photoacoustic spectroscopy (PAS) experiment a sample is enclosed in a small air-tight cell and illuminated with intensity-modulated monochromatic light. Absorption of the radiation followed by non-radiative decay results in a periodic heat flow within the sample, which upon reaching the sample surface, causes a cyclic thermal expansion of the layer of gas

at the surface. This produces pressure pulses in the gas which are detected by a sensitive microphone placed in the cell. A plot of the microphone signal as a function of wavelength  $\lambda$ , in principle, represents a non-radiative decay excitation spectrum analogous to the radiative decay excitation spectrum measured for luminescent materials.

The characteristics of the photoacoustic signal may be summarized briefly as follows:

1. Transmission of the light is not necessary; only absorption and (some) non-radiative decay.
2. The strength of the signal is proportional, not only to the intensity of the incident radiation, but also to its energy. (More heat will result from a UV transition than from an IR transition).
3. The strength of the signal will also depend inversely on the modulation frequency of the incident radiation. (Short pulses of the same intensity have less power than long ones.)
4. Scattering is not a serious problem and, in fact, the more surface area in contact with the energy transfer gas, the better. That is, powders should give stronger signals than massive pieces of the same material.
5. The signal has phase  $\phi$  as well as amplitude  $q$ , the phase being related to the time required for the heat to reach the surface and the sound to reach the microphone. The phase will depend on the absorptivity  $\beta(\text{cm}^{-1})$ , the thermal diffusivity  $\alpha_s(\text{cm}^2\text{s}^{-1})$  and the non-radiative decay lifetime ( $\tau$ ).
6. The linear dependence of the signal strength on  $\beta$  is limited to regions of the spectrum where  $\beta/\alpha_s < 1$ . ( $\alpha_s = (2\alpha_s/\omega)^{1/2}$ ) (see below). Near and above this limit the variation of  $q$  with  $\beta$  approaches zero.

The above statements of the nature of the photoacoustic effect are drawn primarily from the conclusions of the theory developed by Rosencwaig and Gersho (R-G) (9), based on a one-dimensional thermal piston model. Since this is the starting point for extending the theory of photoacoustic spectroscopy (PAS) to include photoacoustic circular dichroism (PACD), a brief survey of the salient factors and important parameters of that treatment follows.

According to the R-G theory the central parameters of the mathematical model of the photoacoustic effect are: 1) the optical absorption coefficient  $\beta(\text{cm}^{-1})$ ; 2) the optical absorption length  $\mu_\beta = 1/\beta(\text{cm})$ ; 3) the thermal conduction coefficient  $\alpha_s = (2\alpha_s/\omega)^{1/2}$ ; 4) the angular frequency of modulation  $\omega(\text{rad s}^{-1})$ ; 5) the thermal diffusivity  $\alpha_s(\text{cm}^2\text{s}^{-1})$ ; and 6) the thermal diffusion length  $\mu_s = (1/\alpha_s)$ . The signal is also dependent on various constants which are defined in the original paper (9), including the source intensity. Assuming various

limiting conditions of sample thickness and absorptivity, the R-G theory may be shown to yield several more simplified results (see below).

An important difference between PAS and conventional transmission spectroscopy is that the PAS signal depends both on the sample's thermal and optical properties. Only light absorbed within one thermal diffusion length ( $\mu_S$ ) of the surface contributes to the signal. If the absorption coefficient is large enough so that  $\mu_B < \mu_S$ , (or  $\beta/a_S > 1$ ) the PAS signal becomes independent of changes in  $\beta$ . This "saturation" condition may be alleviated somewhat by increasing the modulation frequency  $\omega$ , (thus effectively shortening the thermal diffusion length so that  $\mu_B > \mu_S$ ). However, since the signal strength is also shown to depend on  $\omega^{-n}$  (where  $n = 1.5$  for  $\beta/a_S < 1$ ), the sensitivity of the system limits the utility of this technique for avoiding saturation effects. The incidence of saturation is a serious impediment to the quantitative application of PAS. Various sampling techniques such as co-grinding with MgO have been proposed as solutions to this problem (10). In addition, the use of the phase angle of the signal ( $\phi$ ) has been shown to permit quantitative determination of  $\beta$  free of many of the uncertainties of conventional amplitude ( $q$ ) measurements, even in the region of initial saturation (11).

From the results of the R-G theory it would appear that detection of circular dichroism photoacoustically would have the following potential applications:

1) Crystalline (or non-crystalline) powders and turbid suspensions. This potential results from the lack of dependence on the detection of transmitted light. This would permit the averaging of linear birefringence effects in biaxial crystals, measurements on crystals with poor growth characteristics, and on compounds too labile to grow large crystals even though they are resolvable by rapid precipitation of diastereomers. Turbid biological specimens, suspensions, gels, etc., might also be probed for optical activity by such a technique.

2) Single crystals too thick or too highly absorbing to permit sufficient transmission of light for conventional measurements of optical activity.

It has been the goal of this work to develop the theory and techniques to test these propositions. Obviously PACD will not be completely immune to the depolarization effects of scattering, and when  $q$  no longer varies with  $\beta$  (because of saturation)  $\Delta q (=q_L - q_R)$  must approach zero. The initial evaluation of the extent of these problems is the subject of this paper.

#### The PACD Experiment

Due to the unique way in which the photoacoustic signal is generated, there are two possible ways of performing the PACD experiment (Figure 1). The Type 1 experiment involves only circular polarization at modulation frequency  $\omega_C$ . If  $\beta_L \neq \beta_R$ ,

a photoacoustic signal will be generated which is proportional to  $\Delta\beta$ . If  $\beta_L = \beta_R$ , no photoacoustic signal can result because there is no intensity modulation of the heat distribution in the solid. This experiment has been applied successfully to detect MCD and LD by the photoacoustic technique (12). If the light is also intensity modulated at frequency  $\omega_p \gg \omega_c$ , then the Type II experiment is obtained. Type II differs from Type I in that a photoacoustic signal is also generated at  $\omega_p$ . The signal detected at  $\omega_p$  then varies in intensity at frequency  $\omega_c$  when circular dichroism is present. (One may draw an analogy to AM radio with  $\omega_p$  being the carrier frequency and  $\omega_c$  providing the amplitude modulation.) The PACD signal may be obtained by the following sequence: 1) demodulation of the signal at  $\omega_p$  (phase-sensitive detection (PSD) with a time constant  $\tau \ll 1/\omega_c$ ), and 2) PSD of the demodulated signal using  $\omega_c$  as the reference frequency. Since the photoacoustic signal (proportional to  $\beta$ ) can be obtained by low-pass filtering the output of PSD#1, and the PACD signal (proportional to  $\Delta\beta$ ) is obtained at the output of PSD#2, the ratio of the outputs ( $Q_{\text{PSD2}}/Q_{\text{PSD1}}$ ) should be proportional to  $\Delta\beta/\beta = g$ .

The sign of the CD is obtained from the phase angle of the PACD signal, with (+)CD giving a phase  $180^\circ$  from that of (-)CD (Figure 2). Since the phase angle is a function of the absorptivity (11), vector-tracking lock-in amplifiers must be used, and since the vector magnitude is always positive, the sign information must be obtained from the phase angle. The experimental phase angle is a relative quantity which includes contributions from the modulation source, cell and microphone responses, and electronics. Although it is possible to determine the relation of the phase angle to the CD sign by measuring the PACD of a known pair of enantiomers, this calibration may not be consistent due to the dependence of the phase angle on the above parameters.

#### PAS Theory

Using the R-G photoacoustic theory (9), the pressure variations in the cell may be written as:

$$\Delta P(t) = q \cos(\omega t - \pi/4 - \phi) \quad (1)$$

where  $q$  is the vector magnitude of the complex sinusoidal pressure variation  $Q = Q_1 + iQ_2$ . The general form of  $Q$ , given by equation 21 of Ref. (9), is quite complicated but can be simplified for several special cases. For the particular case of optically and thermally thick samples (R-G Case 2c, i.e.,  $\mu_B \ll \lambda_S$  and  $\mu_S \ll \lambda_S$ ),  $Q$  is given by

$$Q = K \left[ \frac{\beta(r-1)}{(\beta^2 - \sigma_s^2)} \right] \quad (2)$$



where  $r = (1-i)/2a_s$ ,  $\sigma_s = (1-i)a_s$ , and where the constant parameters for a given experiment have been grouped in  $K = (\gamma I_0 P_0 / 2\sqrt{2} k_s l g a T_0)$ . The photoacoustic phase angle is then given by (11)

$$\phi = \tan^{-1} \frac{\text{Im}(Q)}{\text{Re}(Q)} = -\tan^{-1}(2a_s/\beta + 1). \quad (3)$$

### PACD Theory

The photoacoustic-CD experiment may be treated as a superposition of two photoacoustic experiments (Figure 2) (12,13), one using left circularly polarized light and the other using right circularly polarized light, but 180° out-of-phase:

$$\begin{aligned} \Delta P(t) &= q_l \cos(\omega_c t - \pi/4 - \phi_c) + q_r \cos(\omega_c t - \pi/4 - \phi_c - \pi) \\ &= (q_l - q_r) \cos(\omega_c t - \pi/4 - \phi_c) \end{aligned} \quad (4)$$

Equation 4 is applicable to the Type I experiment where there is circular polarization modulation at  $\omega_c$ . The relation between  $\Delta q$  and the sample's absorptivity and thermal properties is seen in Figure 3. A linear dependence on  $\beta$  and thus on  $g$  is found for  $\beta < a_s$  ( $\nu_B > \nu_s$ ). At  $\beta > a_s$  ( $\nu_B < \nu_s$ ) saturation occurs and the PACD magnitude decreases as the absorptivity increases. Thus photoacoustic saturation will lead to anomalously low  $g$  values, since the photoacoustic magnitude approaches a constant value for  $\beta > a_s$  (14). The PACD phase angle (Figure 4) is a function of  $a_s$  and  $\beta$  and varies from -90° ( $\beta \ll a_s$ ) to 0° ( $\beta \gg a_s$ ).

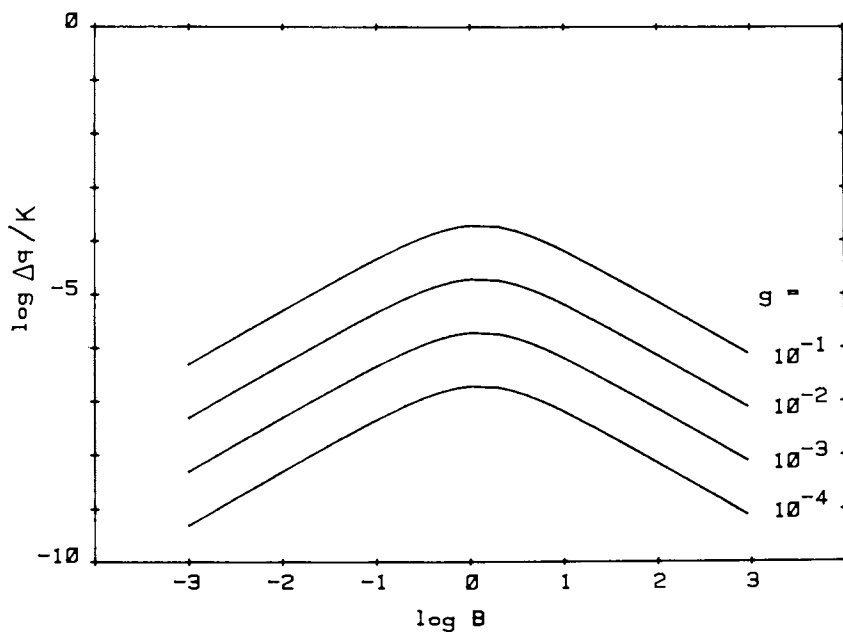
In the Type II experiment with light chopping at frequency  $\omega_p$ , the total pressure variations are given by

$$\begin{aligned} \Delta P(t) &= 1/2[q_l \cos(\omega_p t - \pi/4 - \phi_l) \cos(\omega_c t - \pi/4 - \phi_c) \\ &\quad + q_r \cos(\omega_p t - \pi/4 - \phi_r) \cos(\omega_c t - \pi/4 - \phi_c - \pi)] \end{aligned} \quad (5)$$

where the factor of 1/2 enters due to the 50% duty cycle of the light chopper. Demodulation of the signal at the chopping frequency  $\omega_p$  leads to the following equation, which describes the signal at the demodulator output:

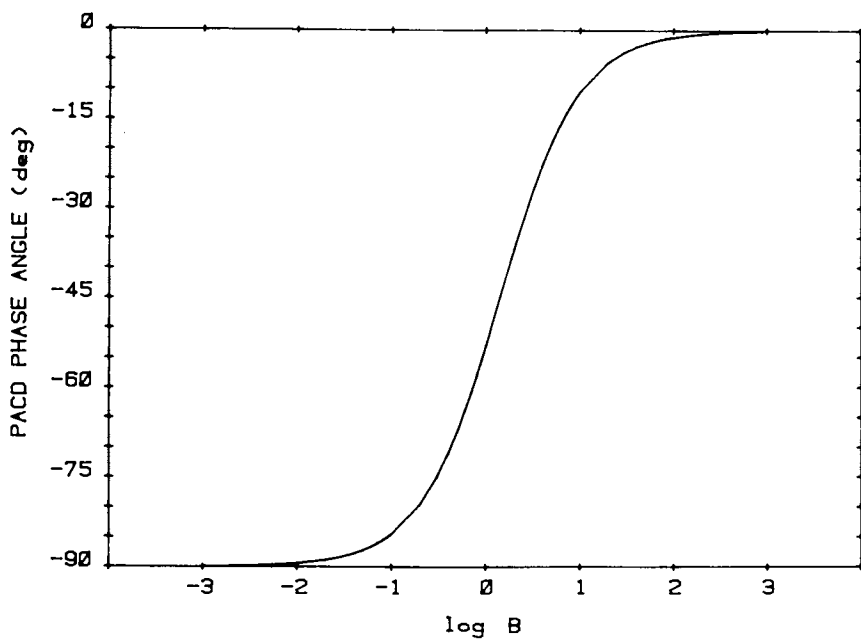
$$Q_{PAS} = 1/2[q_l \cos(\omega_c t - \phi_c') + q_r \cos(\omega_c t - \phi_c' - \pi)], \quad (6)$$

where we note that the phase information contained in  $\phi_c$  is lost in the process of demodulation at  $\omega_p$ . Filtering out the  $\omega_c$  components via a low pass filter leaves the PAS magnitude signal



Optical Society of America

Figure 3. A log-log plot of the PACD magnitude normalized to the coefficient  $K$  of Equation 2 vs.  $\log B$ , where  $B \equiv \beta/a_s$ .  $\beta$  is the optical absorption coefficient ( $\text{cm}^{-1}$ ) and  $a_s$  is the thermal conduction coefficients ( $\text{cm}^{-1}$ ). The onset of photo-acoustic saturation occurs at  $\log B = 0$ .  $B = \beta/a_s$ ;  $a_s = 100 \text{ cm}^{-1}$  (19).



Optical Society of America

Figure 4. Plot of the PACD phase angle ( $\phi_c$ ) vs.  $\log B$ . See Figure 3 caption for definitions. (All  $g$  values.)  $B = \beta/a_s$ ;  $a_s = 100 \text{ cm}^{-1}$  (19).



$$Q_{\text{PAS}} = 1/2[q_{\ell} + q_r] = q. \quad (7)$$

Further PSD of the demodulated signal, but this time using a lock-in referenced to the CD modulation  $\omega_c$ , yields

$$Q_{\text{PACD}} = 1/2[q_{\ell} - q_r] = 1/2 \Delta q. \quad (8)$$

The functional form of the PACD magnitude is the same for both Types I and II, but an important difference between the two is that  $q_{\ell}$  and  $q_r$  are governed by the photoacoustic rather than the CD modulation frequency. In both Type I and II, enantiomers will give phase angles  $180^\circ$  apart:

$$\phi_{(+)\text{CD}} = \phi_{(-)\text{CD}} + 180^\circ \quad (9)$$

### Experimental

**Materials:** Photoacoustic measurements were made on a component-assembled PAS spectrometer consisting of a 9W argon ion laser (Spectra Physics), a 0.5 cc internal volume PAS cell equipped with a sensitive electret microphone (Radio Shack, 3.2 mV/Pa). Circular polarization modulation was achieved with a special low frequency (220 Hz) photoelastic modulator (15) (Hinds International). Signals were detected and processed with a vector tracking lock-in amplifier (PAR model 5204), and intensity modulation was done with a 30-slot blade mechanical chopper (Ortec). Syntheses of all compounds were by well established literature methods.

The components as described above were assembled to perform the Type I PACD experiment (Figure 5). This experiment was chosen because it is the simplest and most direct approach to obtaining PACD. An argon ion laser was chosen because of its high intensity monochromatic output and because strong lines were available at regions of absorption for several samples of interest. Photoelastic modulation was used instead of Pockels' cell modulation because of the wide acceptance angle and low voltage required. Two of the samples,  $\text{Ni(en)}_3(\text{NO}_3)_2$  and  $\text{Na}(\text{UO}_2)(\text{OAc})_3$ , are examples of compounds which are optically active in the solid state only.  $\text{Ni(en)}_3(\text{NO}_3)_2$  racemizes in solution, but spontaneously resolves on crystallization (space group  $P6_322$ ) (16).  $\text{NaUO}_2(\text{OAc})_3$  is intrinsically achiral but crystallizes in the cubic, enantiomorphous space group ( $P2_13$ ) (17).

Experimentally, light from the laser was polarized vertically and passed  $45^\circ$  to the stress axes of the photoelastic modulators producing alternately left and right circularly polarized light at 220 Hz. Three types of measurements were made: 1) PAS magnitude spectra at the modulation frequency were recorded by inserting the mechanical chopper and using

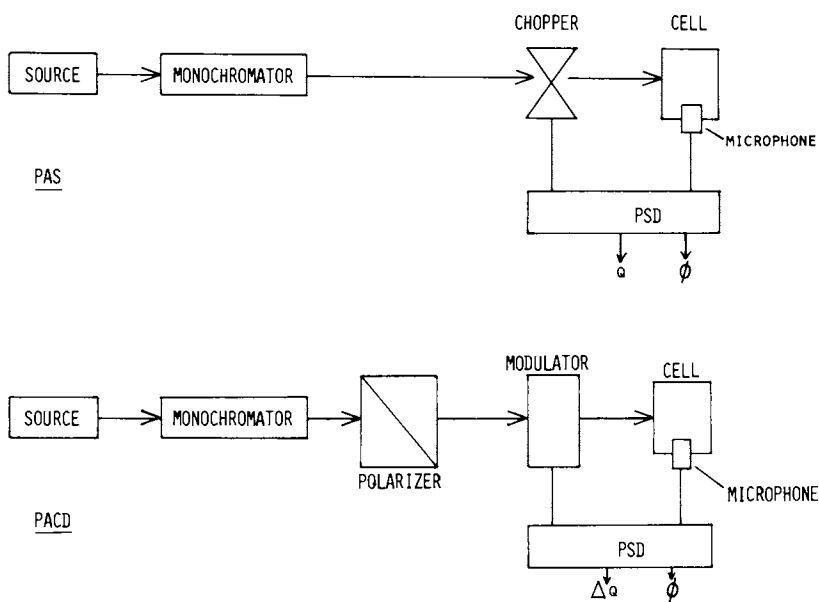


Figure 5. A block diagram of a single-beam PAS experiment (top) and a single-beam (Type I) PACD experiment (bottom)

its reference frequency at the lock-in; 2) PACD measurements were made without the chopper by taking the 220 Hz photoelastic modulation signal as the lock-in reference; and 3) noise measurements were made by blocking the light beam and detecting background signals at the modulation frequency, thus allowing measurement of laser and acoustic noise, as well as providing a quantitative measure of cell acoustic integrity. Noise levels for PACD were generally  $\pm 10$  nV for  $\Delta Q$  and  $\pm 5^\circ$  for  $\phi$ . Background noise was  $10 \pm 10$  nV. Light intensity was normalized by adjusting the laser power to a common level for all lines with the exception of the 457.9 nm line, which was limited to only 100 mW.

### Results

Conventional transmission absorption and CD spectra of the samples are given in Figures 6-8, where the positions of the laser lines relative to the absorption and CD bands are shown. Experimental data (for the compounds used) are given in Tables 1-5. Included in the tables are PAS magnitudes ( $Q$ ), PACD values ( $\Delta Q$ ), photoacoustically determined  $g$  values ( $g_{PA}$ ) and the phases of the  $\Delta Q$  signals ( $\phi$ ). Also included for comparison are the transmission  $\epsilon$ ,  $\Delta\epsilon$ , and  $g$  values.

### Discussion

As predicted by theory, differences in phase angles for enantiomers are ca.  $180^\circ$ . In addition, the results are in qualitative agreement with the transmission data in that  $\Delta Q$  and  $g_{PA}$  values follow the trends of  $\Delta\epsilon$  and  $g$ .

The values of  $g_{PA}$  obtained for crystals are invariably larger than the values for powders, but both are lower than the transmission values. For example, in  $Ni(en)_3(NO_3)_2$  the crystal  $\Delta Q$  values are ten times greater than the powder  $\Delta Q$  values. Theory predicts that powders should give stronger PAS signals because of their greater surface area. This is observed for the PAS magnitudes but not for PACD signals. In these experiments, powders give  $g_{PA}$  values 100 times smaller than those determined by transmission and crystals give  $g$  values ten times smaller than transmission  $g$  values. It is likely that light scattering and surface depolarization, especially in the case of powders, are degrading the PACD signal. Although saturation would also lead to low  $g$  values, the low  $\beta$  values for the absorption bands studied clearly indicate that saturation effects should not be present.

Another source of error in  $g_{PA}$  values may be background signals. In  $Na(UO_2)(OAc)_3$ , for example, it was possible to make one measurement in a region where  $\epsilon = 0$ . A coherent background signal was obtained, probably from cell wall absorption of scattered light (18). Background signal correction may help to quantify results. For this reason, however, comparisons between PAS and transmission measurements should be made between  $\Delta Q$  and  $\Delta\epsilon$  instead of the respective  $g$  values, since the background effects cancel in  $\Delta Q$ .

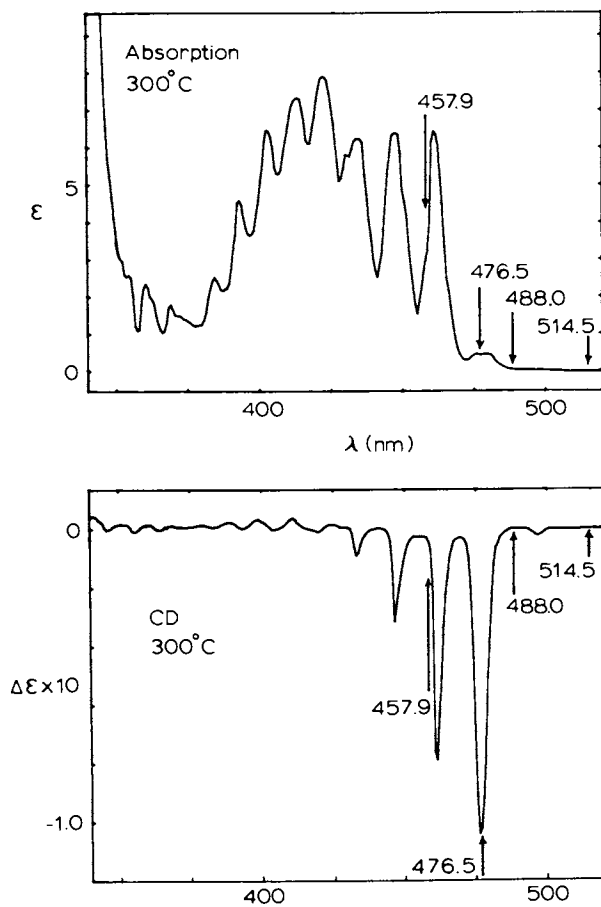


Figure 6. Single crystal absorption and CD spectra of  $\text{NaUO}_2(\text{OAc})_3$  at room temperature showing positions of pertinent  $\text{Ar}^+$  laser lines

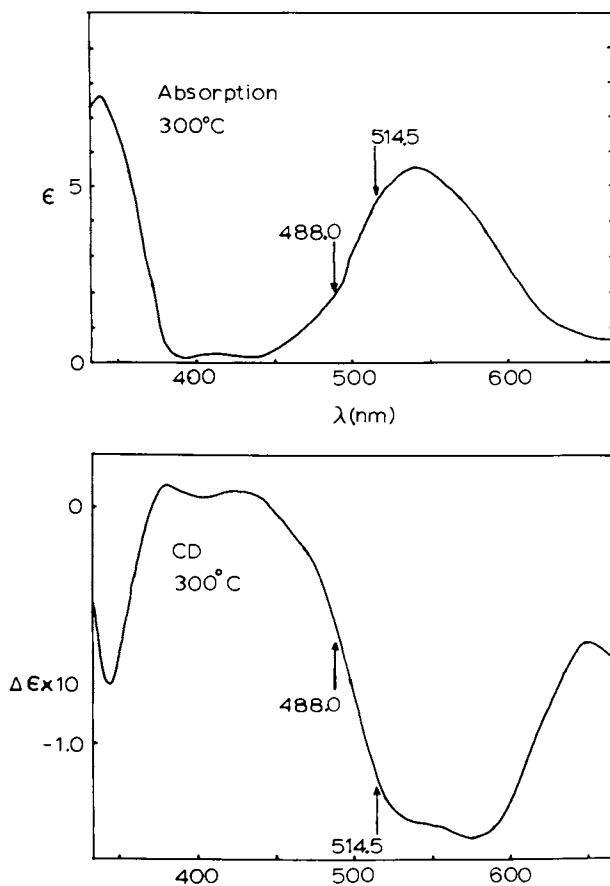


Figure 7. Axial single-crystal absorption and CD spectra of  $\text{Ni}(\text{en})_3(\text{NO}_3)_2$  at room temperature showing positions of pertinent Ar<sup>+</sup> laser lines

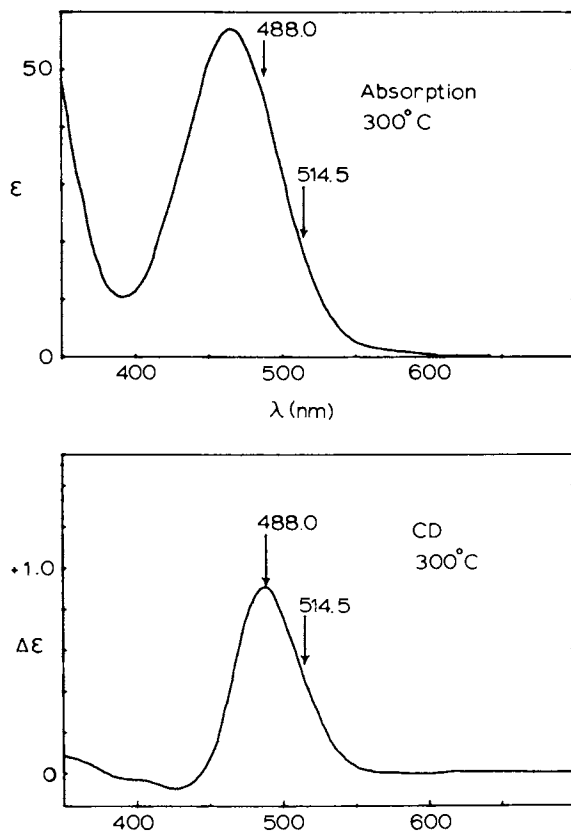


Figure 8.  $H_2O$  solution absorption and CD spectra of  $Co(en)_3I_3$  at room temperature showing positions of pertinent Ar<sup>+</sup> laser lines

Table I. Single crystal PAS, PACD and transmission measurements of  $\text{NaUO}_2(\text{OAc})_3$ .

| $\lambda$<br>(Å) | PAS*                   |  |                            | TRANSMISSION  |   |                      |
|------------------|------------------------|--|----------------------------|---|---|----------------------|
|                  | Q<br>( $\mu\text{V}$ ) | $\Delta Q$ <sup>†</sup><br>( $\mu\text{V}$ ) | $\phi$ <sup>‡</sup><br>(°) | $\epsilon$ mole <sup>-1</sup> cm <sup>-1</sup><br>( $\lambda$ mole <sup>-1</sup> cm <sup>-1</sup> ) | $\Delta\epsilon$ mole <sup>-1</sup> cm <sup>-1</sup><br>( $\lambda$ mole <sup>-1</sup> cm <sup>-1</sup> ) | g                    |
| 5145             | 2.7                    | 0  |                            |   |   |                      |
| 4880             | 3.4                    | 0  |                            | 0.42  | $+1.0 \times 10^{-1}$   | $2.5 \times 10^{-1}$ |
| 4765             | 6.5                    | 0.300  | 12                         | 5.51  | $+4.1 \times 10^{-3}$   | $7.5 \times 10^{-4}$ |
| 4579             | 39.0                   | 0  |                            |   |   |                      |
| 5145             | 4.3                    | 0  |                            |   |   |                      |
| 4880             | 5.9                    | 0  |                            | 0.42  | $-1.0 \times 10^{-1}$   | $2.5 \times 10^{-1}$ |
| 4765             | 9.5                    | 0.310  | -145                       | 5.51  | $-4.1 \times 10^{-3}$   | $7.5 \times 10^{-4}$ |
| 4579             | 43.0                   | 0  |                            |   |   |                      |

\* Normalized to 200 mW Laser Power

†  $\pm 0.010 \mu\text{V}$ ‡  $\pm 10^\circ$

Table II. Axial single crystal PAS, PACD and transmission measurements of  $\text{Ni(en)}_3(\text{NO}_3)_2 \cdot$ 

| $\lambda_0$<br>(Å) | PAS*                   |                                 |                      |                        | TRANSMISSION                                   |  |                       |
|--------------------|------------------------|---------------------------------|----------------------|------------------------|--|--|-----------------------|
|                    | Q<br>( $\mu\text{V}$ ) | $\Delta Q$<br>( $\mu\text{V}$ ) | $\rho_{\text{PA}}$   | $\phi$<br>( $^\circ$ ) | $(\epsilon \text{ mole}^{-1} \text{ cm}^{-1})$ | $(\epsilon \text{ mole}^{-1} \text{ cm}^{-1})$ | g                     |
| 5145               | 67                     | 0.300                           | $4.5 \times 10^{-3}$ | 50                     | 4.50   | +0.133   | $2.95 \times 10^{-2}$ |
| 4880               | 47                     | 0.165                           | $3.5 \times 10^{-3}$ | 50                     | 1.94   | +0.065   | $3.35 \times 10^{-2}$ |
| 5145               | 90                     | 0.200                           | $2.2 \times 10^{-3}$ | -130                   | 4.50   | -0.133   | $2.95 \times 10^{-2}$ |
| 4880               | 60                     | 0.090                           | $1.5 \times 10^{-3}$ | -135                   | 1.94   | -0.065   | $3.35 \times 10^{-2}$ |

\* Normalized to 600 mW Laser Power



Table III. Powder PAS and PACD measurements of  $\text{NaUO}_2(\text{OAC})_3$ .

| $\lambda$<br>(Å) | Q<br>( $\mu\text{V}$ ) | $\Delta Q^{\dagger}$<br>( $\mu\text{V}$ ) | $g_{\text{PA}}$       | $\phi^{\ddagger}$<br>( $^{\circ}$ ) |
|------------------|------------------------|---|-----------------------|-------------------------------------|
| 5145             | 58                     | 0   |                       |                                     |
| 4880             | 82                     | 0   |                       |                                     |
| 4765             | 114                    | 0.500                                     | $+4.4 \times 10^{-3}$ | 45                                  |
| 5145             | 15                     | 0   |                       |                                     |
| 4880             | 28                     | 0   |                       |                                     |
| 4765             | 53                     | 0.500                                     | $-9.4 \times 10^{-3}$ | -120                                |

\* 200 mW laser power

 $\dagger \pm 0.10 \mu\text{V}$  $\ddagger \pm 5^{\circ}$ Table IV. Powder PAS and PACD measurements of  $\text{Ni}(\text{en})_3(\text{NO}_3)_2$ .

| $\lambda$<br>(Å) | Q<br>( $\mu\text{V}$ ) | $\Delta Q^{\dagger}$<br>( $\mu\text{V}$ ) | g                  | $\phi^{\ddagger}$<br>( $^{\circ}$ ) |
|------------------|------------------------|---|--------------------|-------------------------------------|
| 5145             | 370                    | 0.070                                     | $2 \times 10^{-4}$ | 75                                  |
| 4880             | 320                    | 0.040                                     | $1 \times 10^{-4}$ | 70                                  |
| 5145             | 440                    | 0.040                                     | $9 \times 10^{-5}$ | -75                                 |
| 4880             | 300                    | 0.030                                     | $1 \times 10^{-4}$ | -90                                 |

\* Normalized to 600 mW laser power

 $\dagger \pm 0.010 \mu\text{V}$  $\ddagger \pm 10^{\circ}$

Table V. Powder PAS, PACD and solution transmission measurements of 5% Co(en)<sub>3</sub>Cl<sub>3</sub> in Rh(en)<sub>3</sub>Cl<sub>3</sub>.

| $\lambda$<br>(Å) | POWDER PAS*     |                                       |                            | SOLUTION TRANSMISSION                                 |   |                      |
|------------------|-----------------|---------------------------------------|----------------------------|---|---|----------------------|
|                  | Q<br>( $\mu$ V) | $\Delta Q$ <sup>†</sup><br>( $\mu$ V) | $\phi$ <sup>‡</sup><br>(°) | $\epsilon$<br>( $\text{l mole}^{-1} \text{cm}^{-1}$ ) | $\Delta\epsilon$<br>( $\text{l mole}^{-1} \text{cm}^{-1}$ ) | g                    |
| 5145             | 320             | 0.075                                 | $2.3 \times 10^{-4}$       | 18.2  | +0.539  | $6.6 \times 10^{-2}$ |
| 4880             | 780             | 0.100                                 | $1.3 \times 10^{-4}$       | 45.1  | -0.902  | $2.0 \times 10^{-2}$ |
| 5145             | 420             | 0.035                                 | $8.3 \times 10^{-5}$       | 18.2  | +0.539  | $6.6 \times 10^{-2}$ |
| 4880             | 710             | 0.100                                 | $1.4 \times 10^{-4}$       | 45.1  | -0.902  | $2.0 \times 10^{-2}$ |

\* Normalized to 600 mW Laser Power

\*\*  $\pm 20^\circ$ †  $\pm 0.010 \mu\text{V}$ ‡  $\pm 10^\circ$

### Conclusions

The photoacoustic detection of natural circular dichroism has been demonstrated successfully. Preliminary results at several fixed wavelengths on a limited number of samples show qualitative agreement with corresponding transmission data. In spite of the small signal levels involved, reproducibility is good. It appears that powders suffer scattering depolarization effects, which also occur with diffuse transmission measurements.

Sensitivity with regard to  $g$  values is difficult to estimate. Although experimental  $g$  values of  $10^{-1}$  to  $10^{-5}$  (representing pressure changes of  $10^{-8}$  to  $10^{-9}$  atm) were obtained, they did not correspond directly to transmission  $g$  values.

The experiments reported here were designed to demonstrate the feasibility of the measurement and to provide an initial test of the theory. As single beam experiments, the results are laser noise limited. Planned elaboration of the equipment to make double beam measurements should provide an increase in sensitivity. Other modifications which may improve detectability are: cell design changes to reduce cell wall absorptions while maintaining minimal cell volume, laser output feed-back control, and signal averaging. With improved sensitivity the use of lower power tunable laser excitation will be feasible. Eventual improvement of sensitivity to the level required for use of continuum sources is at present doubtful.

Continuing work is directed toward extension of these measurements to other compounds, improvement of sensitivity and reliability, and exploration of the possibilities of variable modulation (Type II) measurements to reduce saturation effects, and of PACD depth profiling.

### Acknowledgements

The authors gratefully acknowledge the support of the work by the National Science Foundation, the National Institutes of Health and the Duke University Biomedical Research Support Grant. We acknowledge also C. S. Johnson (U.N.C.) and A. F. Schreiner (N.C.S.U) for use of laser facilities, F. S. Richardson for communication of results in advance of publication and for helpful discussions, and J. L. Howell and A. F. Kirby for valuable experimental assistance.

### Literature Cited

1. Hush, N. S.; Hobbs, R. J. Progr. Inorg. Chem., (1968), 10, 259.
2. Bijovet, A. F.; Peerdeman, A. F.; van Bommel, A. J. Nature, (1951), 168, 271.
3. Tinoco, I. Jr.; Turner, D. H. J. Am. Chem. Soc., (1976), 98, 6453; and reference cited within.
4. Richardson, F. S.; Riehl, J. P. Chem. Rev., (1977), 77, 773; and references within.

5. Perekalina, Z. B.; Kaldybaev, K. A.; Konstantinova, A. F.; Belyaev, L. M. Soviet Physics-Cryst., (1977), 22, 262.
6. Rosencwaig, A. Anal. Chem., (1975), 47, 592A.
7. Somoano, R. B. Agnew. Chem. Intern. Ed., (1978), 17, 238.
8. Bell, A. G. Am. J. Sci., (1880), 20, 305.
9. Rosencwaig, A.; Gersho, A. J. Appl. Phys., (1976), 47, 64.
10. Noonan, J. A.; Reichard, H. S. Pittsburgh Conf. on Anal. Chem. and Appl. Spectr., (1979), Abstr. #186.
11. Roark, J. C.; Palmer, R. A.; Hutchison, J. S. Chem. Phys. Lett., (1978), 60, 112.
12. Fournier, D.; Boccara, A. C.; Badoz, J. J. Appl. Phys. Lett., (1978), 32, 640.
13. Saxe, J. D.; Faulkner, T. R.; Richardson, F. S. J. Appl. Phys., in press.
14. McClelland, J. F.; Kniseley, R. N. Appl. Optics, (1976), 15, 2658.
15. Kemp., J. C.; private communication.
16. Swink, L. N.; Atoji, M. Acta Cryst., (1960), 13, 630.
17. Zachariasen, W. H.; Plettinger, H. A. Acta Cryst., (1959), 12, 526.
18. McClelland, J. F.; Knisely, R. N. Appl. Optics, (1976), 15, 2967.
19. Topical Meeting on Photoacoustic Spectroscopy, Technical Digest, Optical Society of America, 1979, paper Th A3. Reproduced with permission.

RECEIVED September 13, 1979.

## Stereochemical Description and Notation for Coordination Systems

THOMAS E. SLOAN<sup>1</sup>

Chemical Abstracts Service, P.O. Box 3012, Columbus, OH 43210

DARYLE H. BUSCH

Department of Chemistry, The Ohio State University, Columbus, OH 43210

The terminology and notation that have been used to describe coordination compounds have been derived with one notable exception from the terms and symbols developed to describe the stereochemistry of carbon compounds. The terms *cis*, *trans*; *endo*, *exo*; *dextro*, *d*, *D*, (+); and *levo*, *l*, *L* (-) all have been used to describe the stereochemistry of coordination compounds in a close analogy with organic compounds (see Figure 1). As the descriptions of the chemistry and structures of coordination systems have become more varied and complex, the meanings of these terms have become less precise, as in the example of a *cis* or *trans* tricarbonyl octahedral compound (see Figure 2). The terms *fac* and *mer* were coined to indicate the facial and meridional disposition of substituted octahedral structures.

Geometric isomers of linear quadridentate ligands on octahedral compounds are recognized to exist in one *trans* and two *cis* forms (see Figure 3). The *cis* compounds are generally referred to as the  $\alpha$  and  $\beta$  forms. In these examples we can see that the terminology developed to denote the relatively simple tetrahedral and planar carbon stereochemistry is not adequate when applied to the stereochemistry of octahedral compounds. And when we consider that there are eighteen well-defined geometries of mononuclear complexes for coordination numbers 4 to 9 with literally tens of thousands of possible isomeric configurations, then it is not difficult to comprehend the need for notations that are systematic and developed within the basic requirements and boundary limits that are unique to coordination chemistry.

The first systematic designation of the stereochemistry of coordination compounds was developed by Werner. Werner numbered the ligand sites on the coordination polyhedra as shown in Figure 4.

<sup>1</sup> To whom correspondence should be addressed.

0-8412-0538-8/80/47-119-397\$05.50/0

© 1980 American Chemical Society

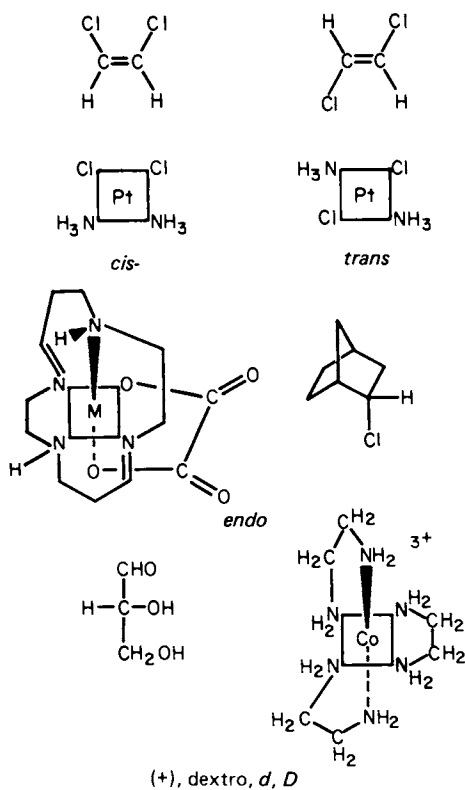


Figure 1. The commonly used stereochemical terms and symbols in inorganic and organic chemistry

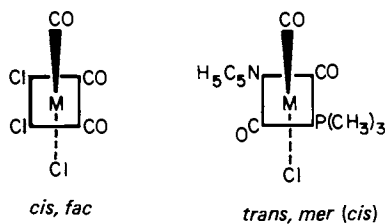


Figure 2. Stereochemical terms for tris-(unidentate) octahedral complexes

Muetterties and Wright have suggested numbering schemes for coordination polyhedra with up to 20 coordination sites (1). IUPAC adopted a polyhedral numbering system that was first suggested by McDonnell and Pasternack (2, 3) (see Figure 4). The McDonnell method for polyhedral numbering substitutes lower case Roman characters to designate the coordination positions. This was done to eliminate any confusion that would occur between the substitution numbering within a ligand and the numbering of the coordination position. McDonnell also suggested the adoption of a class symbol for use in cipher coding to indicate the geometry of the central atom coordination site. All methods for numbering of coordination polyhedra are similar and do provide unambiguous nomenclature that is structurally exact, providing the geometry of the central atom coordination sphere is either readily apparent or remembered.

Locant numbering conventions share similar handicaps. These handicaps become apparent when the locants are put to use (see Table I below).

Table I. Stereochemical numbering for diamminebis(ethylenediamine) platinum

*ab*-diammine-*cf,de*-bis(ethylenediamine)platinum  
*ab*-diammine-*cd,ef*-bis(ethylenediamine)platinum  
(+)*x*-*ab*-diammine-*cd,ef*-bis(ethylenediamine)platinum  
*rac-ab*-diammine-*cd,ef*-bis(ethylenediamine)platinum

The most significant handicaps associated with directionally specific locants are the inability to distinguish enantiomeric pairs of compounds directly from the notation and the arbitrary and often complicated hierarchical rules to determine what ligands are to be associated with which locants. Another complexity of locant notations that is sometimes overlooked is the need for additional symbols or other notation to indicate that there is less information meant than is expressed in the name with locants. Often the geometric configuration of a compound is known but not the absolute configuration. Thus the *X* in the third name is necessary in the locant notation because it is not possible to draw and number the *cis* chiral structure ambiguously. Similarly, *rac* is the recommended term to indicate a mixture of enantiomers.

The need for a rational stereochemical notation has become increasingly acute since the establishment of the first absolute configuration by Bijvoet in 1951 (4). The importance of the stereoconfiguration in living systems and the influence of stereochemical configuration on the course of reactions also

reinforces this position. The systematic notation that has gained the greatest acceptance is the notation proposed by Cahn, Ingold, and Prelog (5). The Cahn-Ingold-Prelog (CIP) notation is based on a priority ranking of ligands in a three-dimensional molecular representation. This ranking procedure is called the CIP Sequence Rule. The CIP Sequence Rule is used to specify the absolute configuration of tetrahedral carbon atoms in organic compounds, is the basis of the *E,Z* notation proposed by Blackwood *et al.* to specify the isomerism of the ligands about a double bond (6), and is the ranking employed by Brown *et al.* in the CHEMICAL ABSTRACTS notation that specifies the complete stereochemistry of coordination compounds (7, 8).

### Ligand Indexing

The CIP ranking of ligands is termed the CIP priority and is determined according to the subrules: 0) Nearer end of axis or side of plane precedes further. 1) Higher atomic number precedes lower. 2) Higher atomic mass precedes lower. 3) *Z* (seqcis) precedes *E* (seqtrans) (9). 4) Like pair (*R,R* or *S,S*) precedes unlike (*R,S* or *S,R*). 5) *R* precedes *S*.

The tin compound in Figure 5 illustrates the CIP priorities for ligands of different atomic number. Chlorine is atomic number 17, silicon 14, nitrogen 7, and carbon 6. Note, the higher the priority, the lower the CIP priority number. It is not uncommon to have ligating atoms of the same atomic number being compared as shown for the cobalt compound in Figure 6. For these structures the CIP method provides a formalism for exploring a ligand to determine the ligand of highest priority, second highest, third, etc.

In Table II the CIP exploration procedures are illustrated. The ligands are explored from the center of interest, atom by atom, until a determination is obtained on the basis of atomic number or the next appropriate criterion, in the order listed. Considering the two phenoxy ligands, the structures are represented with the atomic number at the atom positions with the double bonds expanded with replica atoms of atomic number 6 shown in curves. The determination of priority is made at the fifth level by comparing oxygen, atomic number 8, to carbon, atomic number 6, in the second branch of the exploration table.

For the pyridine ligand, replica atoms on the *ortho* carbon positions are atomic number (6.5). This results from the resonance of the double bonds to the pyridine nitrogen. The resonance is allowed for by averaging carbon + nitrogen on either side of the *ortho* carbons,  $\frac{6+7}{2} = 6.5$ . At the third level, the sequence 6.5, 6, 1 determines the pyridine priority when compared to the explorations of the remaining ligands.



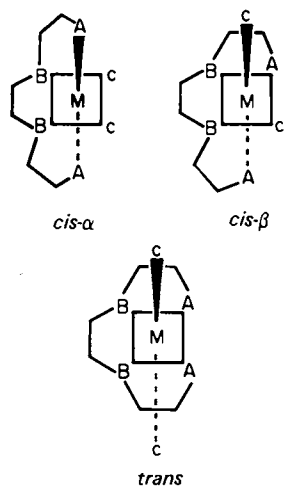


Figure 3. Geometric isomers of octahedral complexes with linear quadridentate ligands

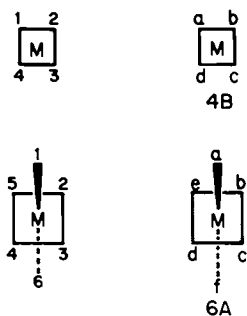


Figure 4. Werner and McDonnell numbering for square planar and octahedral structures

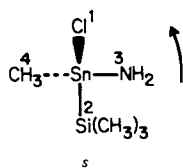


Figure 5. Cahn-Ingold-Prelog ligand relative priority determined by atomic number

Table II. Ligand CIP exploration table (by atomic number)

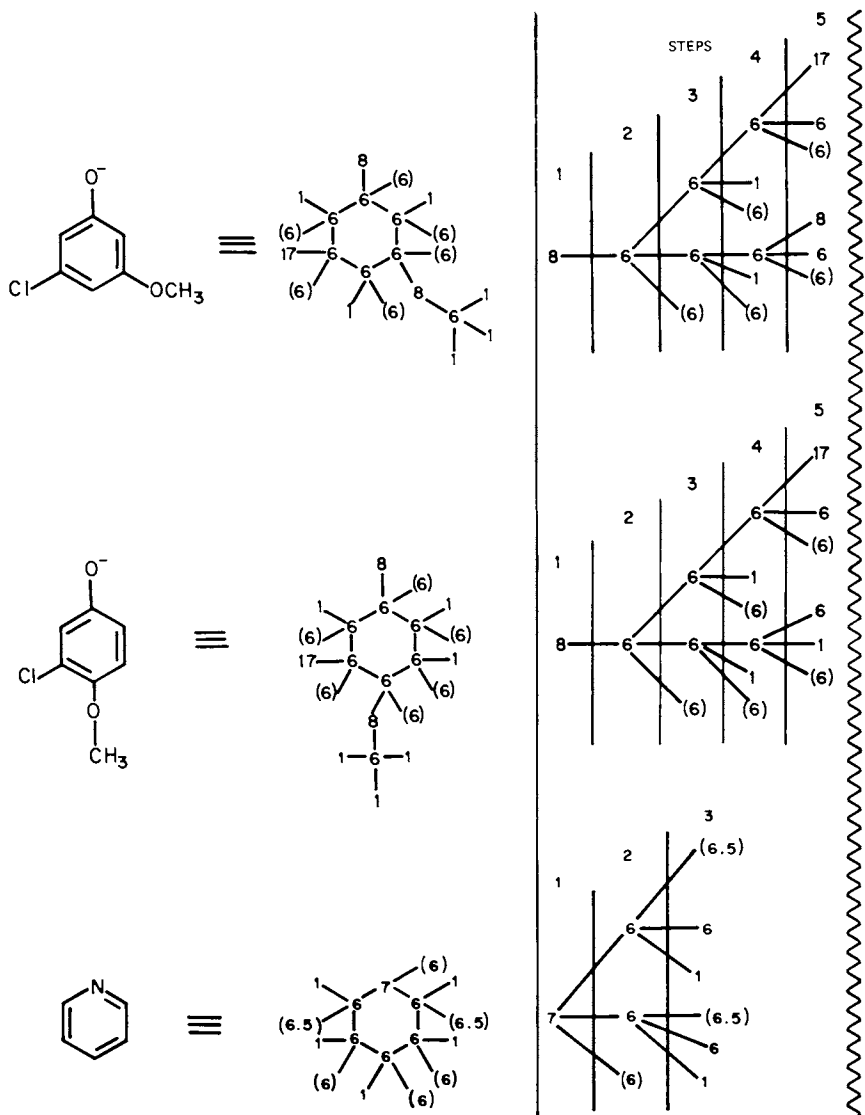
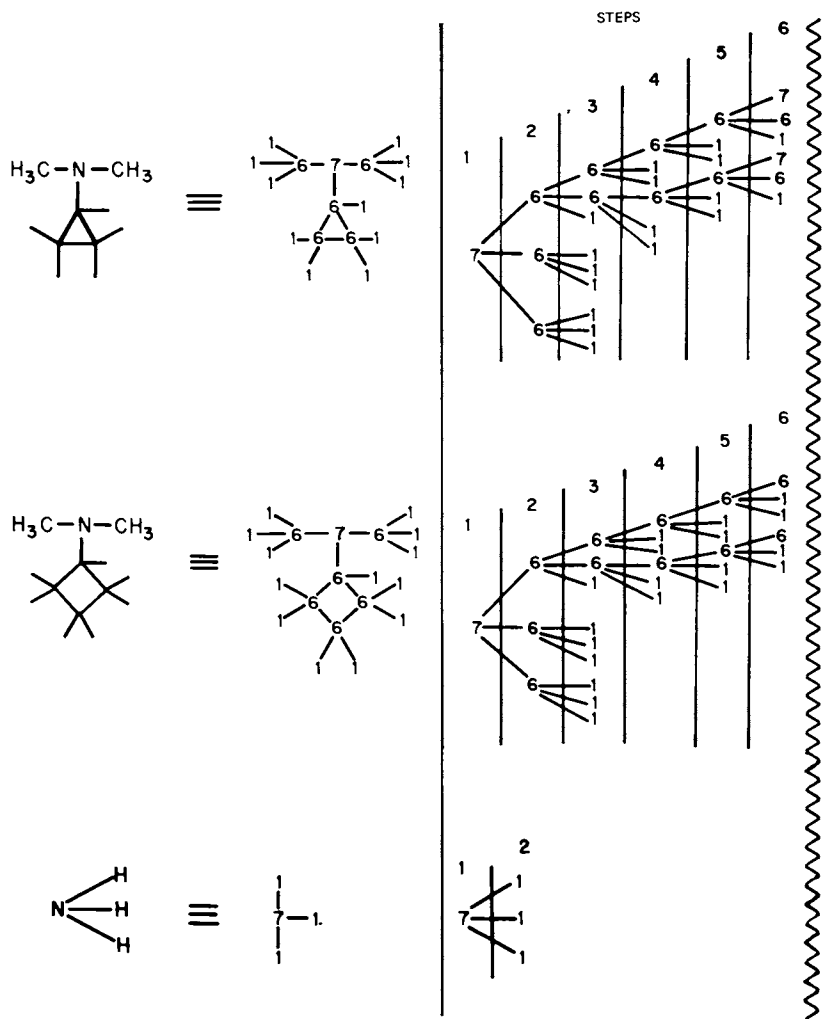


Table II. Continued



The comparison of the cyclopropyl and cyclobutyl amine ligands illustrate that it is not necessarily the size of the group being compared but the nature of the path. Thus the cyclopropyl group results in the preferred path at the sixth level of comparison when it returns to the amine nitrogen before the cyclobutyl group. The exploration of the ammonia is illustrated at the bottom of Table II.

Now, returning to the structure of the cobalt complex, we have derived the rankings as shown in Figure 7. One might agree that these are highly stylized and schematic procedures and the formalism leads to some results not intuitively anticipated. However, at Chemical Abstracts Service, we have accumulated a vast amount of experience with the CIP system with hundreds of thousands of compounds, both organic and coordination, and we find very few cases in which the CIP formalism completely breaks down.

The CIP formalism is not the only method that has been developed to rank constitutionally different ligands. Professor Ugi and his co-workers have been investigating the computer-assisted solutions to various problems in chemistry and chemical documentation (10). In their studies they have developed an algorithm they call the CANON algorithm that will number the atoms of a molecule based on the graph connectivity of the molecule. The canonical numbering thus derived has the property that it always gives the same connectivity list. This algorithm is similar to the Morgan algorithm that is the basis of the Chemical Abstracts Service Chemical Registry System (11) but differs in two fundamental respects. The CANON algorithm retains information regarding the constitutional symmetry of the molecule and has been specifically designed to give a relative ranking to ligands that is the same as the CIP relative ranking for most compounds. The CANON algorithm is based on the graph priorities of the molecular formula and thus does not consider formalisms such as bond order or resonance.

The CANON algorithm derives a ligand ranking by assigning an atomic index based on the atomic number, *e.g.*, the higher the atomic number, the lower the atomic index (see Figure 8). An atomic descriptor is then derived by listing the atomic index of the atom being considered followed by the atomic indexes of the  $\alpha$  or adjacent atoms. The  $\alpha$  atomic index numbers are listed in increasing numerical sequence. The atomic descriptors are now compared number by number, left to right, and the atoms are ordered in increasing sequence by atomic descriptor to give: a>h,i>b,c>j,k>d>e,f>g>n,v>l,r,p,u>nn,oo>x,ee>mm,ii>aa,bb,cc,dd>m,o,q,e,t,w,jj,kk,ll>y,z,ff,gg,hh>H's. In this first repetition of the algorithm, the relative priorities of two ligands -- pyridine and ammonia -- are established and the remaining four are grouped in two sets, the two phenoxy and alkyl amine ligands. The next two iterations of

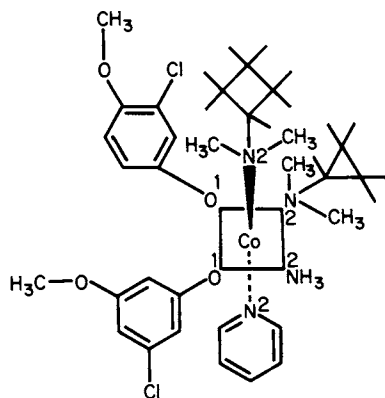


Figure 6. Assignment of CIP priority numbers for ligands with donor atoms of the same atomic number

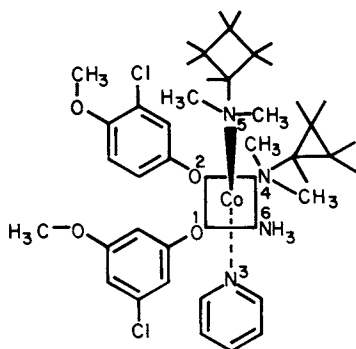


Figure 7. CIP relative priority numbers by ligand exploration

the CANON program are illustrated in Figures 9 and 10. Continuing for four more repetitions, the algorithm provides a constitutional numbering as shown in Figure 11. Comparing the cobalt ligating atoms b=4, c=5, d=8, e=9, f=10, and g=11 gives the relative ordering of the cobalt coordinating ligands, b>c>d e>f>g. This is the same order derived from CIP explorations, but not the same absolute value for ligand atom index numbers *vis-a-vis* the CIP priority numbers.

The CANON algorithm does provide a constitutionally-based structural numbering which in most cases gives the same relative priorities as the CIP priorities without considering either bonding formalism, resonance, or other theoretical conventions.

The relative ranking of ligands for the description of the stereochemical properties of a molecule is the most utilized and accepted principle throughout stereochemical nomenclature. This is not yet the practice, however, in discussing the stereochemistry in coordination and inorganic chemistry. In the context of coordination and inorganic chemistry, stereochemical information is either presented in the more traditional terminology, or more often by means of a stereospecific structural representation.

Now let us consider those properties unique to coordination compound structures that must be defined to give a unique, unambiguous notation system to describe the stereoconfiguration. First, the geometry of the central atom must be indicated. The geometric distribution of ligands within the basic structure should be denoted specifically. This can mean anywhere from the 15 possible position isomers of an octahedral complex with six differing ligands to over 10,000 postulated isomers for the 8 coordinate square-faced bicapped trigonal prismatic structures. Lastly, the chirality of the structure, both the central atom and ligand chiralities, must be represented.

#### Chemical Abstracts Service Stereochemical Notation

Conforming to these principles, Chemical Abstracts Service has devised a stereochemical notation which was first introduced into the Chemical Abstracts Service Chemical Registry System and CA Indexes in 1972 (7) and was extended to higher coordination numbers in 1977 (8).

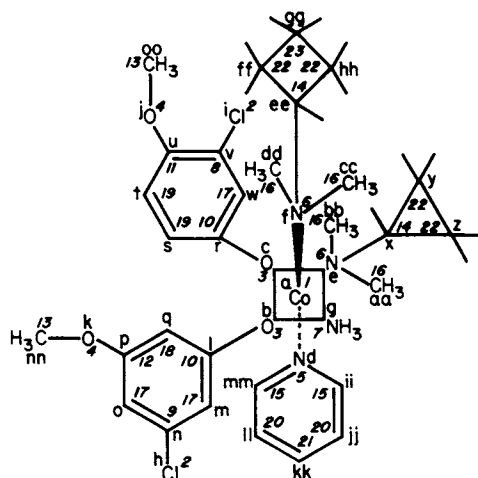
The CHEMICAL ABSTRACTS stereochemical notation system is composed of four parts: the site symmetry term, the configuration number, the chirality label, and the ligand stereochemical label.

The site symmetry term indicates the idealized geometry of the central atom and is a letter code derived from the geometric terms used to describe the coordination polygon. The coordination number is given to define further the site symmetry









|                             |                        |
|-----------------------------|------------------------|
| a = 1:3.3.5.6.6.7           | o = 17:9.12.29         |
| i = 2:8                     | q = 18:10.12.29        |
| h = 2:9                     | s = 19:10.19.29        |
| b,c = 3:1.10                | t = 19:11.19.29        |
| j = 4:11.13                 | jj,ll = 20:15.21.29    |
| k = 4:12.13                 | kk = 21:20.20.29       |
| d = 5:1.15.15               | y,z = 22:14.22.30.30   |
| e,f = 6:1.14.14.16.16       | ff,hh = 22:14.23.30.30 |
| g = 7:1.24.24.24            | gg = 23:22.22.30.30    |
| v = 8:2.11.17               | Hg = 24:7              |
| n = 9:2.17.17               | Hnn,oo = 25:13         |
| l = 10:3.17.18              | Hx,ee = 26:14          |
| r = 10:3.17.19              | Hmm,ii = 27:15         |
| u = 11:4.8.19               | Haa,bb,cc,dd = 28:16   |
| p = 12:4.17.18              | Hw,m,o = 29:17         |
| nn,oo = 13:4.25.25.25       | Hq = 29:18             |
| x,ee = 14:6.22.22.26        | Hs,t = 29:19           |
| mm,ii = 15:5.20.27          | Hjj,ll = 29:20         |
| aa,bb,cc,dd = 16:6.28.28.28 | Hkk = 29:21            |
| w = 17:8.10.29              | Hy,z,ff,hh = 30:22     |
| m = 17:9.10.29              | Hgg = 30:23            |

a>i>h>b,c>j>k>d>e,f>g>v>n>l>r>u>p>nn,oo>x,ee>mm,ii>aa,bb,cc,dd>

1 2 3 4 5 6 7 8 9 10 11 12 13 14 15 16 17 18 19

w>m>o>q>s>t>jj,ll>kk>y,z>ff,hh>gg>Hg>Hnn,oo>Hx,ee>Hmm,ii>Haa,bb,cc,dd>

20 21 22 23 24 25 26 27 28 29 30 31 32 33 34 35

Hw,m,o>Hq>Hs,t>Hjj,ll>Hkk>Hy,z,ff,hh>Hgg

36 37 38 39 40 41 42

Figure 10. CANON ligand priority assignment, third iteration

term. The site symmetry terms for the more common central atom polyhedra are shown in Table III.

The configuration number is a one- to nine-digit number used to identify atoms on symmetry elements of a structure and in this way distinguish geometric isomers. Configuration numbers are derived from priority numbers assigned by application of the CIP Sequence Rule. The degeneracy resulting from the identity of coordinating atoms or groups (giving identical CIP priority numbers) is resolved by observing the following principles.

Trans Maximum Difference Subrule for Coordination Numbers Four to Six. The same relative priority numbers are assigned to all constitutionally equivalent atoms. For example, in the system  $Ma_2b_2c_2$  (where M is a central atom and a, b, and c represent monodentate ligands), the relative priority numbers are 1, 1, 2, 2, 3, 3. Whenever a choice exists in distinguishing between constitutionally equivalent donor atoms, the preference is given to the donor atom trans to the donor of highest CIP priority number. In this way configuration numbers can be chosen based on the symmetry characteristics of a particular geometry to distinguish between the position isomers of any geometry through coordination six by giving a number no more than three digits in length.

Priming Subrule a. When there are two or more equivalent bidentate or tridentate ligands, *e.g.*,  $M(AA)_3$ ,  $M(AB)_3$ , and  $M(BAB)_2$  (where M is a central atom and AA, AB, and BAB represent multidentate chelating ligands) and the same priority numbers thus occur in equivalent ligands, the ties are broken by identically priming, double priming, etc., all the CIP priority numbers of ligating atoms within a ligand to determine both the configuration number and the chirality symbol.

Priming Subrule b. In the cases of symmetrical quadridentate, quinquedentate, and sexidentate ligands, ties between equivalent ligating atoms are broken, where necessary, by priming ligating atom priority numbers in half of the ligand. When two or more nonequivalent tie-breaking choices exist, the tie is broken by application of the trans maximum difference subrule. Primed ligating atom priority numbers are less preferred (higher value) than those which are unprimed but are of the same absolute value; doubly primed priority numbers are less preferred than primed, etc. The primes are not included in the configuration number except when absolutely necessary, *e.g.*, for octahedral complexes containing two identical tridentate ligands and trigonal-prismatic complexes containing two or more identical multidentate ligands.

Three different chirality labels are used to indicate the chirality at the coordination center. Although these symbols

Table III. Symmetry site terms

|              |   |
|--------------|---|
|              | <u>Four-Coordinate Polyhedra</u>        |
| <i>T-4</i>   | tetrahedron                             |
| <i>SP-4</i>  | square plane                            |
|              | <u>Five-Coordinate Polyhedra</u>        |
| <i>TB-5</i>  | trigonal bipyramid                      |
| <i>SP-5</i>  | square pyramid                          |
|              | <u>Six-Coordinate Polyhedra</u>         |
| <i>OC-6</i>  | octahedron                              |
| <i>TP-6</i>  | trigonal prism                          |
|              | <u>Seven-Coordinate Polyhedra</u>       |
| <i>PB-7</i>  | pentagonal bipyramid                    |
| <i>OCF-7</i> | octahedron face monocapped              |
| <i>TPS-7</i> | trigonal prism square face monocapped   |
|              | <u>Eight-Coordinate Polyhedra</u>       |
| <i>CU-8</i>  | cube                                    |
| <i>SA-8</i>  | square antiprism                        |
| <i>DD-8</i>  | dodecahedron                            |
| <i>HB-8</i>  | hexagonal bipyramid                     |
| <i>OCT-8</i> | octahedron trans-bicapped               |
| <i>TPT-8</i> | trigonal prism triangular face bicapped |
| <i>TPS-8</i> | trigonal prism square face bicapped     |
|              | <u>Nine-Coordinate Polyhedra</u>        |
| <i>TPS-9</i> | trigonal prism square face tricapped    |
| <i>HB-9</i>  | heptagonal bipyramid                    |

all indicate essentially the same thing, *R*, *C*, and  $\Delta$  indicate right-handed or clockwise, and *S*, *A*, and  $\Lambda$  indicate left-handed or anticlockwise; the assignment definition of right- and left-handed are different for each set of symbols. Because of the differing assignment definitions there is no exact translation of *R* to *C* or *C* to  $\Delta$ . For this reason we have chosen to use the three different sets of chirality symbols to emphasize the different underlying assignment definitions. Briefly, *R* and *S* are used for tetrahedral centers exactly as defined by Cahn, Ingold, and Prelog (5).  $\Delta$  and  $\Lambda$  indicate the chirality as defined by the helical chelation in bis and tris bidentate octahedral complexes (12). *C* and *A* are the chirality symbols used for all the other central atom geometries, coordination numbers, and chelating configurations (7).

The configurations of centers or other stereoelements in a ligand such as the configuration of an amino acid ligand are noted after the chirality symbol of the central atoms.

The indication of chirality would seem to be the simplest of the stereochemical properties to indicate, requiring only a binary set of symbols indicating either the right- or left-handed chirality. As is the case with many other seemingly simple problems, there is much more to be considered and more will be presented on this aspect at the end of the paper.

The utility of the CAS notation to describe the stereochemistry of coordination compounds is illustrated in the following examples. The first example of the complete notation is the cobalt compound to which the CIP priority numbers have been assigned previously (see Figure 12). The cobalt is an octahedral-six coordinate; thus, the site symmetry term is *OC*-6. The configuration number is determined by defining an axis containing the highest priority ligand and giving the priority number of the ligating atom *trans* to this highest priority atom on this axis. The next number is the priority number of the ligand in the perpendicular plane *trans* to the ligand of highest priority in this plane. This gives a configuration number of 46. By making use of the *trans* relationships of the ligands in an octahedral complex, only a two digit configuration number is required to differentiate all 15 possible position isomers of this complex. The chirality symbol is determined by viewing the plane from the ligand of highest priority, ligand of CIP priority 1, and noting the direction of the increasing progression of the priority numbers. The direction is anticlockwise or left and is noted by the *A* chirality symbol.

The next example (see Figure 13) is the tris(ethylenediamine)cobalt(III) complex. The site symmetry term is octahedral, six coordinate or *OC*-6, and the configuration number is 11. The nitrogen atoms are all equivalent, and the chelation defines a right-handed or  $\Delta$  helix to give the complete notation *OC*-6-11- $\Delta$ . I have indicated the primes on the chelating ligands in this structure to illustrate how to determine the

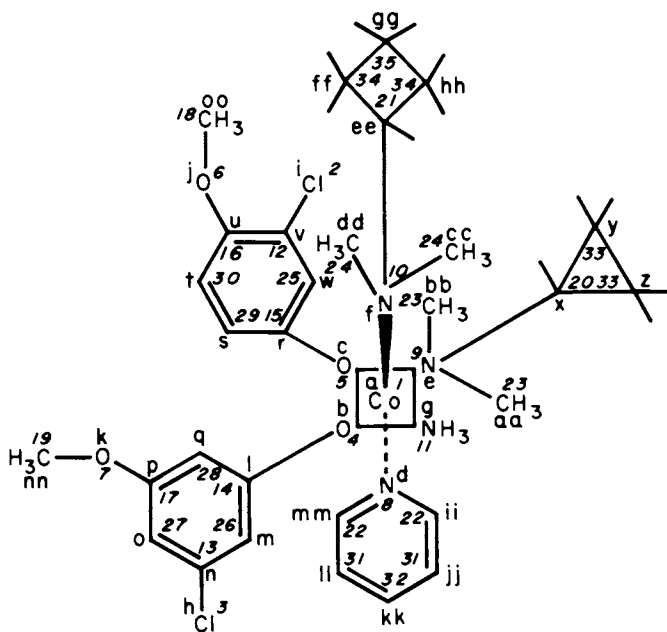
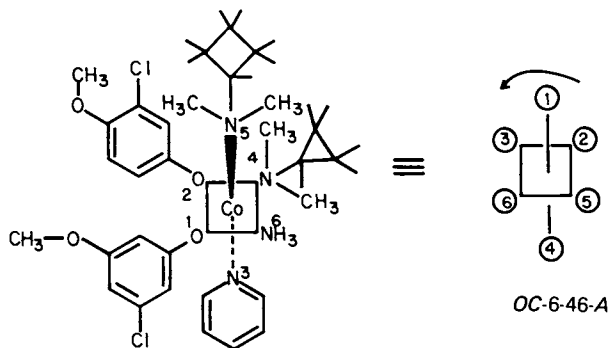


Figure 11. CANON constitutional numbering

Figure 12.  $[\text{CoNH}_3[(\text{C}_6\text{H}_7)(\text{CH}_3)_2\text{N}][3\text{Cl-4}(\text{CH}_3\text{O})\text{C}_6\text{H}_3\text{O}][3\text{Cl-5}(\text{CH}_3\text{O})\text{-C}_6\text{H}_3\text{O}][(\text{CH}_3)_2(\text{C}_6\text{H}_5)\text{N}](\text{C}_5\text{H}_5\text{N})]$

chirality for chelating situations other than bis or tris bidentate ligands. The priming is accomplished such that the axis is defined as having the largest possible difference, in this example 1" is *trans* to 1. The structure is now viewed from the ligating atom of priority 1 on the axis and the progression in the plan is 1,1',1',1" or anticlockwise.

The next example, Figure 14, is the (*N,N'*-ethylenebis-(glycinato))(oxalato) cobaltate complex. The oxalate oxygens are CIP priority 1, the glycine oxygens are CIP priority 2, and the nitrogens are priority 3. The ethylenebis(glycine)=quadridentate ligand is primed to give the maximum difference on the axis. The complex is octahedral-six coordinate, *OC*-6, the configuration number is 33, and the chirality is *C*. The other position isomer (*β-cis*) would be 32.

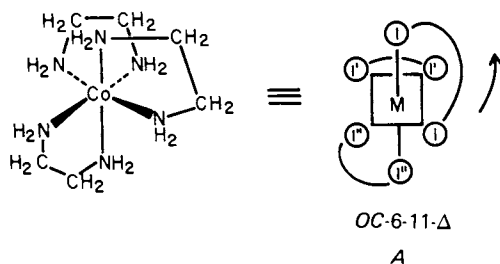
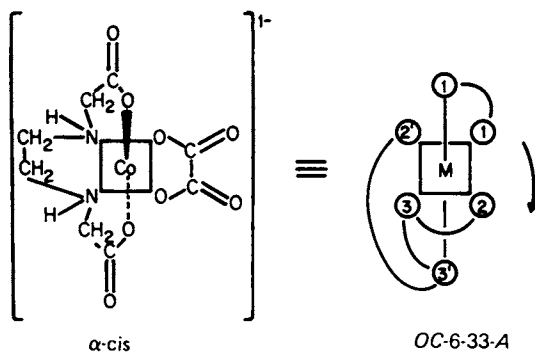
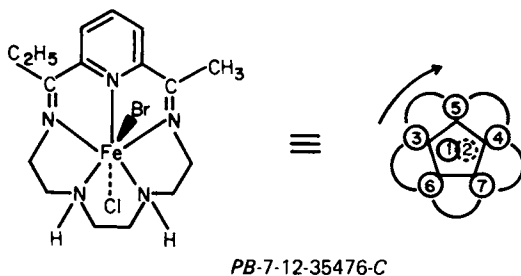
The last example, Figure 15, is a bromo chloro macrocyclic iron complex. Bromine is CIP priority 1, chlorine is 2, the imine nitrogens 3 and 4, the pyridine nitrogen 5, and the amine nitrogens 6 and 7. The complex is pentagonal bipyramidal-seven coordinate, *PB*-7, the atoms on the axis are priority numbers 12- and the priority numbers for the atom in the plane are given in lowest sequential order, 35476. This clockwise order is symbolized as *C*.

The development and use of the commonly used terminology of coordination compound stereochemistry have been outlined and indicate some of the recent developments in the assignment of ligand indexing priorities. The application of ligand indexing in the CHEMICAL ABSTRACTS stereochemical notation has also been introduced. The CA stereochemical notation provides a unique and unambiguous description for all the possible isomers of the 18 central atom geometries commonly reported for coordination compounds. These are significant and needed additions to the nomenclature of the stereochemistry of coordination compounds, but what other coordination systems remain to be described?

It was indicated earlier that use of binary symbols to describe asymmetric centers in molecules is not always as simple as it might appear. In compounds with several asymmetric centers, the situation to be described becomes more complex. With two asymmetric centers, there are four possible configurations. Using the descriptors developed for carbon chemistry, the four isomers are *RR*, *SS*, *RS*, and *SR*. For three chiral centers we can have 2<sup>3</sup> or 8 isomers, *RRR*, *SSS*, *SRS*, *RSR*, *RSS*, *SSR*, *RRS*, *SRR*. The center-by-center notation works well for a limited number of chiral centers. However, binary symbolism becomes more cumbersome the more centers there are to be described.

### More Complex Stereochemical Systems

Another approach to a notation for these more complicated structures has been suggested in various forms. Essentially,

Figure 13.  $[\text{Co}(\text{en})_3]^{3+}$ Figure 14.  $[\text{Co}[(\text{CH}_2)_2[\text{NH}(\text{C}_2\text{H}_2\text{O}_2)]_2(\text{C}_2\text{O}_4)]$ Figure 15.  $[\text{FeBrCl}(\text{C}_{16}\text{H}_{25}\text{N}_5)]$

this alternate approach involves definition of a standard isomer of the structure to be described, much the same as in the present IUPAC recommendations (13), and then relating all other isomers to the standard form. For compounds with many chiral centers and/or more complicated chiral elements, this form of notation is being investigated actively. This standard or permutational isomer notation (14) does require an extensive dictionary of reference structures with the standard numbering indicated. It also has the same difficulties as mentioned earlier in relating the relative configurations of the various centers within a structure when the absolute stereochemistry is not known. In carbon chemistry relating the chirality of several centers is presently accomplished with notations such as the  $\alpha, \beta$  notation in steroid stereochemistry and the relative notation used at Chemical Abstracts Service termed the  $R^*S^*$  notation (15).

The asymmetric cluster in Figure 16 is representative of the structures in which the chirality properties of the structure are not associated with any atomic site in the molecule. Metalloborane clusters with this type of symmetry properties have also been reported. The stereochemical notation for asymmetric clusters will have to specify cluster chirality. And when clusters with more complex ligand substitution patterns and chiral ligands are prepared, the configurations of all metal centers and the chiralities of the associated ligands must be given.

The molybdenum atom in Figure 17 is pseudotetrahedrally coordinated with trihapto and pentahapto ligands. There are many chiral polyhapto coordinated compounds. In these compounds the structures as a whole can be chiral, they can be similar to clusters, the metal centers can be asymmetric (as is the molybdenum atom in this structure), the ligands can have asymmetric centers, and the substitution on the ligands can generate chiral elements such as the 1,2 or 1,3 disubstitution of nonidentical groups on the cyclopentadienyl ring.

The polynuclear compound in Figure 18 anticipates the linking of two different central atom geometries in one molecule. For these structures the site symmetry designator must be associated with the correct center, all the position isomers of each center must be described, and the absolute and relative chiral relationships at each center and within the ligands must be interrelated and described. The phosphorus compound in Figure 19 illustrates just such a compound with both a tetrahedral and a trigonal bipyramidal center in the same molecule. This relatively simple molecule has 10 possible position isomers at the phosphorus center, each of which is chiral. And with a chiral carbon adjacent to the oxygen atom in the ring 19b, there are a total of 40 possible isomers.



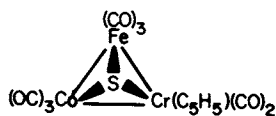


Figure 16.  $[[Cr(CO)_2(\eta^5-C_5H_5)][Fe(CO)_3][Co(CO)_3]-\mu_S-S]$  (16)

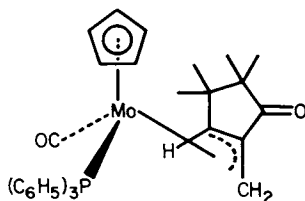


Figure 17.  $[Mo(CO)(\eta^5-C_5H_5)(\eta^3-(2-CH_2C_5H_5O))][P(C_6H_5)_3]$  (17)

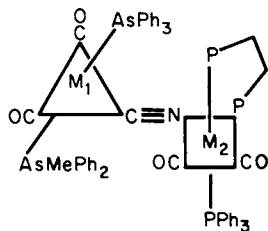
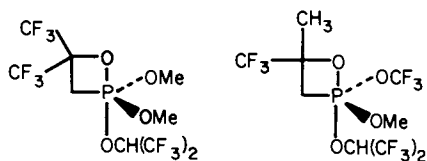


Figure 18. A polynuclear complex with two different central atom geometries



[37006-43-6]

40 Isomers

a

b

Figure 19. 1,2-Oxaphosphatane isomers

## Conclusion

The subject of coordination compound stereochemistry remains complex and challenging. The nomenclature and notation developed to describe the stereochemistry of coordination compounds have been derived from those terms used to describe organic compounds.

The concept of ligand ranking, which has been used for over a decade in the stereochemical nomenclature of carbon compounds, has been applied successfully to the description of coordination compounds. Of the two approaches to ligand ranking that we presented, the Cahn-Ingold-Prelog (CIP) notation has gained the most acceptance. The Chemical Abstracts Service Registry stereonotation which is based on the CIP ligand ranking has proven particularly useful for describing the common geometries of coordination numbers four through nine.

The last four examples that we have provided illustrate that while a good start has been made toward a rational nomenclature for coordination compound stereochemistry, many challenges still remain.

## Abstract

A brief summary of the stereodescriptive terms *cis*, *trans*, *fac*, *mer*, *endo*, *exo*, etc., currently employed in the chemical literature is presented with a discussion of their limitations. The development of ligand index numbering of skeletal positions and its relationship to the IUPAC system of locant designators is outlined. The extension of the Cahn-Ingold-Prelog (CIP) priorities to tetracoordinate through nonacoordinate systems, introduced into the Indexes to CHEMICAL ABSTRACTS (CA), is given with a comparison to the ligand indexing systems. The stereochemical relationships of more complex coordination compounds are considered, including (a) mononuclear complexes with two or more chiral centers (relative and absolute stereochemical descriptors); (b) organic systems with other than tetrahedral atoms; (c) the stereochemical notation problems of *hapto* systems, and (d) polynuclear coordination compounds. These systems are presented with illustrative examples and some of the apparent advantages and shortcomings of the CIP priority designators and ligand index notations are discussed.

## Literature Cited

\* To whom correspondence should be addressed.

1. Muetterties, E. L.; Wright, C. M. Q. Rev., Chem. Soc., (1967) 21, 109.

2. "IUPAC Nomenclature of Inorganic Chemistry," 2nd ed., Butterworths: London, 1971.
3. McDonnell, P. M.; Pasternack, R. F. J. Chem. Doc., (1965) 5, 56.
4. Bijvoet, J. M.; Peerdeman, N. F.; von Bommel, A. J. Nature, (1951) 168, 271.
5. Cahn, R. S.; Ingold, C.; Prelog, V. Angew. Chem. Int. Engl., (1966) 5, 385.
6. Blackwood, J. E.; Gladys, C. L.; Loening, K. L.; Petrarca, A. E.; and Rush, J. E. J. Am. Chem. Soc., (1968) 90, 509.
7. Brown, M. F.; Cook, B. R.; Sloan, T. E. Inorg. Chem., (1975) 14, 1273.
8. Brown, M. F.; Cook, B. R.; Sloan, T. E. Inorg. Chem., (1978), 17, 1563.
9. When comparing ligands having geometrical differences, the ligand with the *Z* configuration is preferred to the ligand with the *E* configuration. When the geometrical difference is not due to the presence of a double bond, the *seqcis* arrangement is preferred to the *seqtrans* arrangement as defined by Cahn, Ingold, and Prelog.
10. Schubert, W.; Ugi, I. J. Chem. Soc., (1978) 100, 37 and private communication.
11. Morgan, H. L. J. Chem. Doc., (1965) 5, 107.
12. "IUPAC Nomenclature of Inorganic Chemistry," 2nd ed., Butterworths: London, 1971. Rule 7.8.
13. Ibid. Rule 7.5 and Rule 7.6.
14. Ugi, I. Private communication.
15. Blackwood, J. E.; Giles, Jr., P. M. J. Chem. Inf. Comput. Sci., (1975) 15, 67.
16. Richter, F.; Vahrenkamp, H. Angew. Chem. Int. Ed. Engl., (1978) 17, 864.
17. Collin, J.; Roustan, J.; Codiot, P. C.R. Hebd. Seances Acad. Sci. Ser. C. (1978) 286-C, 529-31.

RECEIVED September 13, 1979.

# INDEX

## A

|   |                     |
|---|---------------------|
| $A_1$   |                     |
| → ( $A_2 + E$ )*e transitions, CD spectra for           | 28f, 30f, 69f, 70f  |
| charge transfer transitions                             | 228                 |
| symmetry  | 228                 |
| $A_2$ symmetry  | 228                 |
| $^1A_{1g} \rightarrow ^1E_g$ transition                 | 228                 |
| $^1A_{1g} \rightarrow ^1T_{1g}$ absorption band         | 228, 232<br>221–225 |
| $^4A_2$   |                     |
| → $^4A_2$ ( $A_1$ ) transitions                         | 139                 |
| → $^4E$ ( $E_b$ ) transitions                           | 139                 |
| → $^4T_1$ transition                                    | 139                 |
| $^4A_{2g} \rightarrow ^4T_{1g}$ transition              | 139                 |
| AA-CPA-Zn, absorption spectra of                        | 199f                |
| AA-CPA-Zn, CD spectra of                                | 199f                |
| Absolute configuration (s)                              | 14, 269, 400        |
| from the CD spectrum for tris(catecholato)chromate(III) | 158                 |
| of chiral metal complexes, determination of             | 73                  |
| by x-ray scattering                                     | 43                  |
| of $Co(admh)_n(acac)_{3-n}$ complexes                   | 350                 |
| of Co, CD spectra for                                   | 292–301             |
| of $(-)^{589-}[Co(gly)(NH_3)(tacn)]^{2+}$               | 312f                |
| of $(-)^{589-}Co(NO_2)_2(ox)(NH_3)_2$                   | 299f                |
| of complexes in Pfeiffer systems                        | 245t                |
| of $Cr(men)_3$ isomers                                  | 139                 |
| determination of  | 81                  |
| and equilibrium displacement                            | 242–246             |
| of iron(III) enterobactin                               | 161                 |
| of metal coordination compounds                         | 43                  |
| of N-C-C-P*   | 208                 |
| of $n_2 \eta$ -olefins                                  | 91                  |
| from solution reactions                                 | 357–373             |
| of <i>l</i> -stien                                      | 262                 |
| of transition metal catecholates                        | 158                 |
| of transition metal complexes                           | 13–39               |
| Absorption  |                     |
| $^1A_{1g} \rightarrow ^1T_{1g}$ band(s)                 | 228, 232<br>221–225 |
| $^1A_{1g} \rightarrow ^1T_{1g}$ charge transfer         | 224                 |
| <i>d-d</i>  | 224                 |
| of chromium(III) deferriferrioxamine B isomers          | 150f                |
| of $[Coa(gly(tacn))] complexes$                         | 305–311             |

## Absorption (continued)

|   |               |
|---|---------------|
| of <i>cis-cis</i> and <i>cis-cis-cis</i> cobalt complexes   | 294f          |
| of $[Co(ox)(NH_3)_2(H_2O)_2]^+$ data                        | 300f<br>347t  |
| CD spectra of cobalt-aminophosphine complexes               | 210–218       |
| intensities, <i>d-d</i> spectrum(a)                         | 77            |
| of AA-CPA-Zn  | 199f          |
| of bis(acetylacetonato)cobalt(III)-aminophosphine complexes | 214f          |
| of the bis(acetylacetonato)ethylenediamine complexes        | 213           |
| of azonaphthol ligands                                      | 201f          |
| of azophenol ligands  | 201f          |
| of $\Lambda$ -tris(benzohydroximato)cobaltate(III) ion      | 143f          |
| of tris(benzohydroxamato)iron(III)                          | 145f          |
| $c_2-Co(admh)_2(acac)$ electronic                           | 346           |
| of $(+)^{546-}[Co(CN)(NH_3)(tacn)(H_2O)]^{2+}$              | 312f          |
| of chromic deferriferrichrome                               | 147f          |
| of chromium(III) aerobactin                                 | 152f          |
| of the $Co(admh)_2(acac)$ complexes                         | 346           |
| of $[Co(a)(gly)(tacn)]$                                     | 310f          |
| of $Co(III)$ -azophenolate complexes                        | 200           |
| of <i>s-cis</i> - $Co(III)$ complexes                       | 260f          |
| for $(+)^{546} Co(III)$ isomers                             | 265f          |
| $[CoCl_2(aminophosphine)_2](ClO_4)$ complexes               | 210           |
| of <i>cis</i> - $[CoCl_2(NH_3)_2(en)]^+$ isomer             | 290f          |
| of $(+)^{589-}[Co(CN)(Br)(NH_3)(tacn)]^+$                   | 312f          |
| $(-)^{589-}[Co(CN)(gly)(tacn)]^+$                           | 307f          |
| of $[Co(CO_3)(ox)(NH_3)_2]^-$                               | 300f          |
| $Co(III)$ (edda) (AA-CPA-Zn)                                | 203–205, 204f |
| <i>s-cis</i> $[Co(edda)(l-stien)]^+$                        | 266f          |
| of $Co(en)_3I_3$ , solution                                 | 389f          |
| of $(-)^{589-}[Co(gly)(NH_3)(tacn)]^{2+}$                   | 308f          |
| of $[Co(gly)(NH_3)(tacn)]^{2+}$ enantiomers                 | 306f          |
| of $(-)^{589-}[Co(gly)(tacn)(H_2O)]^{2+}$                   | 309f          |

|  |               |
|--|---------------|
| Absorption ( <i>continued</i> )  |               |
| of $(-)\text{-}_{589}\text{-[Co(NCS)(gly)-}$<br>$(\text{tacn})]^+$ .....   | 308f          |
| of $(-)\text{-}_{589}\text{-Co(NO}_2\text{)(gly)-}$<br>$(\text{tacn})^+$ .....   | 307f          |
| of $(-)\text{-}_{589}\text{-Co(OH)(gly)(tacn)^+$   | 309f          |
| of $\text{Cr}(\text{benz})_3$ .....  | 141f          |
| of $\text{Cr}(\text{men})_3$ .....   | 141f          |
| of <i>trans</i> -dichloro $\text{CO(III)-}$<br>aminophosphine complexes  | 211f          |
| of ferric complex of rhodo-<br>torulic acid .....  | 151f          |
| of Ferrichrome A .....   | 146f          |
| for ferric siderophores .....  | 134           |
| of $\Delta\text{-K}_3\text{Rh}(\text{catecholate})_3$ .....  | 160f          |
| of $\text{K}_3[\text{Rh}(\text{ent})_3]$ .....   | 162f          |
| of $\text{NaUO}_2(\text{OAc})_3$ , single-crystal  | 397f          |
| of $\text{Ni}(\text{en})_3(\text{NO}_3)_2$ , axial single-<br>crystal .....  | 388f          |
| of pentaammine $\{(S)\text{-2-chloro-}$<br>propionato} cobalt(III) tetra-<br>raphenylborate solvent<br>effect on ..... | 229f          |
| of $\Delta\text{-Rh}(\text{catecholate})_3$ .....  | 160f          |
| of tris(thiobenzohydroxamate)-<br>chromium .....   | 156f          |
| of tris(thiobenzohydroxamate)-<br>iron(III) .....  | 157f          |
| Acetic acid complexes, substituted<br>dibenzylethylene-diaminedi- .....  | 269           |
| Achiral chromophore .....  | 82, 85, 88-90 |
| inducibility of .....  | 84-85         |
| octahedral symmetry of .....   | 89            |
| Achiral metal-ligating atom chromo-<br>phore .....   | 75-77         |
| Activation parameter separation<br>through stereochemical results  | 360-363       |
| Additivity   |               |
| of CD contributions .....  | 255-257       |
| of CD of <i>d-d</i> transitions .....  | 273-286       |
| rule(s) .....  | 90            |
| of the vicinal contributions .....   | 310           |
| of the configurational contribu-<br>tions .....  | 310           |
| Adsorption of quartz ground .....  | 6             |
| Aerobactin .....   | 149           |
| CD spectra of iron(III) .....  | 149           |
| iron(III) .....  | 149           |
| structure of .....   | 151f          |
| Alanine .....  | 116           |
| vicinal effect for $\beta_1$ bound   | 284f          |
| Aldehyde condensation structures,<br>regio- .....  | 127           |
| Aldehyde condensation structures,<br>stereospecific .....  | 127           |
| Algorithm, CANON .....   | 404           |
| Algorithm, Morgan .....  | 404           |
| C-Alkyl substitution on rotational<br>strength, effect of .....  | 269           |
| Amide linkages of iron(III) entero-<br>bactin, hydrolysis of .....   | 154           |
| Amido ion addition to chelated<br>maleate, orientations for .....  | 122f          |
| Aminates   |               |
| Co(III) $\beta$ -keto- .....   | 337           |
| Cr(III) tris $\beta$ -keto- .....  | 337           |
| V(III) tris $\beta$ -keto- .....   | 337           |
| Amine(s)   |               |
| to CD spectra, contribution of<br>stilbenedi- .....  | 262-268       |
| complexes  |               |
| with acetone, condensation reac-<br>tion of metal(II)-ethylene-<br>di- .....   | 328f          |
| with acetone, condensation<br>reaction of metal(II)-<br>propylenedi- .....   | 328f          |
| conformations of coordinated N-<br>substituted chiral 1,2-di- .....  | 334f          |
| -imine linkage .....   | 326, 331      |
| formation condensation reaction ..   | 325           |
| S-1-phenylethyl- .....   | 99            |
| S-propylenedi- .....   | 255           |
| S,S-stilbenedi- .....  | 269           |
| structures and abbreviations of<br>chiral 1,2-di- .....  | 237t          |
| systems, divalent metal ion .....  | 123           |
| Amino<br>acid  |               |
| 2-bromoethyl- .....  | 118           |
| chelate systems, bis(ethylenedi-<br>amine) .....   | 116           |
| complex(es)  |               |
| CD spectra of R & S .....  | 274           |
| ions, optically .....  | 255           |
| parameters of the Gaussian<br>components for the CD<br>spectra of .....  | 279           |
| substituted triethylenetetra-<br>amine cobalt(III)- .....  | 275f          |
| triethylenetetraaminacobalt-<br>(III)- .....   | 273           |
| vicinal effect in a homologous<br>series triethylenetetra-<br>aminacobalt(III)- .....                                  | 273-286       |
| esters, coordinated .....  | 117           |
| vicinal effect of .....  | 274           |
| nitriles .....   | 117           |
| $\alpha$ -Aminoethylaryl diphenylphos-<br>phines .....   | 177           |
| Ammonia with <i>levo</i> - $[\text{Co}(\text{en})_2\text{Cl}]\text{Cl}$ ,<br>reaction of .....                         | 4t            |
| Anilines, 4-substituted .....  | 92            |
| Anion effect .....   | 89            |
| Anisotropic perturbing groups .....  | 268           |
| Antimony   |               |
| tartrate ion with tris(chelate)-<br>cobalt(III) compounds .....  | 322f          |

- Antimony (*continued*)  
 tartrate, lithium ..... 323f  
*d*-tartrate, association model of ..... 321  
*d*-tartrate-eluted enantiomeric  
 pairs, separation factors of 319–321t  
 Aqua inversion reaction stereochem-  
 istry ..... 369t  
 Arsanilazotyrosine 248 carboxy-  
 peptidase ..... 198f  
 Aryl-substitution ..... 175  
 Aspartate ester complex ..... 119  
 Asymmetric  
 catalysis ..... 169  
 clusters, stereochemical notation for 415  
 hydrogenation ..... 169–192  
 of CH<sub>2</sub>=CXY, optical yield of ..... 35t  
 mechanism of ..... 176  
 mechanistic studies on ..... 172–175  
 by 7-member chelate ring bi-  
 phosphines, catalytic ..... 185  
 structural study of ..... 35–37  
 of  $\alpha,\beta$ -unsaturated carboxylic  
 ligand DI OXOP, enamide hydro-  
 genation by ..... 191  
 nitrogens to CD spectra, contri-  
 butions of ..... 268  
 nitrogens, electronic effects on ..... 269  
 Avidin ..... 187  
 Axis system, definition of ..... 87f  
 Azepine, geometrical isomers of  
 Cu(II) complexes of 3(*S*)-3-  
 aminomethylpiperidine and  
 3(*S*)-aminohexahydro- ..... 334f  
 Azepine, reactions of Cu(II) com-  
 plexes of 3(*S*)-3-aminopeperi-  
 dine and 3(*S*)-3-aminohexa-  
 hydro- ..... 329–333  
 Azohistidines ..... 205  
 Azoligand Co(III) complexes, prepa-  
 ration of model ..... 197–200  
 Azoligands, model ..... 198f  
 Azonaphthol  
 Co(III)–EDDA complexes, CD  
 spectra of ..... 202f  
 complexes, CD properties of ..... 200–203  
 ligands, absorption spectra of ..... 201f  
 Azophenol  
 chelation of metal ions ..... 195–197  
 Co(III)–EDDA complexes, CD  
 spectra of ..... 202f  
 complexes, CD properties of ..... 200–203  
 ligands, absorption spectra of ..... 201f  
 Azophenolate complexes, absorption  
 spectra of Co(III)– ..... 200  
 Azoproteins, CD as probe of metal  
 ion interaction with ..... 195–205  
 Azoprotein derivatives, characteriza-  
 tion of Co(III) ..... 197–200  
*Azobacter vinelandii* ..... 154  
 Azotyrosine in protein, CD of Co(III)  
 chelation by ..... 203–205
- B**
- Bacillus subtilis* ..... 154  
 Bacteria, enteric ..... 154  
 Bailar inversion reactions, cobalt(III) 357  
 tris(Bidentate) complexes ..... 73–90  
 Bidentate complex ions, tris- ..... 19  
 Binary symbols ..... 413  
 Binding  
 of enamides by 6-membered chelate  
 ring rhodium complexes ..... 177  
 by 5-membered chelate ring biphos-  
 phine rhodium complexes ..... 157–177  
 by 7-membered chelate ring biphos-  
 phine rhodium complexes ..... 177  
 to rhodium, unsaturated carboxylic  
 acid ..... 191  
 selectivity in enamide ..... 184f  
 Biphosphines  
 catalytic asymmetric hydrogenation  
 by 7-member chelate ring ..... 185  
 chelating chiral ..... 169  
 complex(es)  
 chair and twist-boat conforma-  
 tions in a 7-member chelate  
 ring ..... 184f  
 chiral conformations in 5-member  
 chelate ring ..... 184f  
 conformational isomerism in a  
 6-member chelate ring ..... 184f  
 ferrocene-derived ..... 187  
 hydroxyproline-derived ..... 183  
 rhodium complexes  
 binding by 5-membered chelate  
 ring ..... 175–177  
 binding by 7-membered chelate  
 ring ..... 177  
 catalysis by 5-membered chelate  
 ring ..... 175–177  
 catalysis by 7-membered chelate  
 ring ..... 177  
 with larger-ring chelates of  
 chiral ..... 187
- Bonding  
 geometries of *trans*-tris(benzo-  
 hydroxamato)chromium(III),  
 octahedral ..... 138f  
 geometries of *cis*-tris(benzohy-  
 droxamato)iron(III) octa-  
 hedral ..... 138f  
 and Pfeiffer effect, hydrogen ..... 246–253  
 Born–Oppenheimer adiabatic  
 approximation ..... 44–45  
 Boron<sub>1</sub> charge transfer transitions ..... 228  
 Boron<sub>1</sub> symmetry ..... 228

|  |      |  |                   |
|--|------|--|-------------------|
| Boron <sub>2</sub> symmetry .....                                  | 228  | CAS ( <i>see</i> Chemical Abstracts Service)               |                   |
| Bovine serum albumin .....   | 205  | Catalysis  |                   |
| Butene   |      | asymmetric .....   | 169               |
| <i>cis</i> -2-   | 107  | homogeneous .....  | 172               |
| in <i>trans</i> ( <i>N</i> ,//)-[PtCl(L-proline)-                  |      | by 5-membered chelate ring biphos-                         |                   |
| ( <i>S,S-trans</i> -2-butene, [ <sup>3</sup> H]),                  |      | phine rhodium complexes .....                              | 175-177           |
| second-order rate constants of                                     |      | by 7-membered chelate ring biphos-                         |                   |
| 2-   | 106t | phine rhodium complexes .....                              | 177               |
| [PtCl <sub>3</sub> ( <i>S,S-trans</i> -2-butene[ <sup>3</sup> H]), |      | by 6-membered chelate ring rho-                            |                   |
| second-order rate constants for                                    |      | dium complexes .....                                       | 177               |
| the substitution of <i>trans</i> -2-                               | 107t | Catalytic influence of decolorizing                        |                   |
| <i>S</i> -2-methyl-2- (mbn) .....                                  | 92   | carbon .....   | 6                 |
| <i>S,S-trans</i> -2-   | 92   | Catecholate(s)   |                   |
| <i>trans</i> -2-   |      | chromate(III), absolute configura-                         |                   |
| tbn .....  | 92   | tion from the CD spectrum for                              |                   |
| change in CD spectrum of .....                                     | 110f | tris-  | 158               |
|  |      | complexes, model .....                                     | 158               |
|  |      | with Fe(III), reaction of .....                            | 135f              |
|  |      | siderophore complexes .....                                | 154-158           |
|  |      | CD ( <i>see</i> Circular dichroism)                        |                   |
|  |      | Charge transfer  |                   |
|  |      | absorption bands .....                                     | 224               |
|  |      | chromophore moment products .....                          | 79                |
|  |      | intermediate states .....                                  | 85                |
|  |      | states, electric moments of .....                          | 79                |
|  |      | transition(s) .....  | 224-225, 228, 232 |
|  |      | A <sub>1</sub> .....                                       | 228               |
|  |      | B <sub>1</sub> .....                                       | 228               |
|  |      | CD of (σ) <sub>L</sub> → d <sub>z</sub> <sup>2</sup> ..... | 78-81             |
|  |      | sigma(σ) <sub>L</sub> → d <sub>z</sub> <sup>2</sup> .....  | 228-232           |
|  |      | Chelate(s)   |                   |
|  |      | biphosphine complexes, chiral con-                         |                   |
|  |      | formations in 5-member ring .....                          | 184               |
|  |      | of chiral biphosphines, rhodium                            |                   |
|  |      | complexes with larger-ring .....                           | 187               |
|  |      | chromophore system (B), per-                               |                   |
|  |      | turbating .....  | 77-78             |
|  |      | complex, geometrical isomers of a                          |                   |
|  |      | tris-  | 135f              |
|  |      | complex, optical isomers of tris-                          | 135f              |
|  |      | directed, stereospecificity .....                          | 123-124           |
|  |      | imine formation in coordinated .....                       | 123               |
|  |      | 5-membered .....   | 115               |
|  |      | ring(s)  |                   |
|  |      | arrangements of the residual                               |                   |
|  |      | electron density peaks with                                |                   |
|  |      | a five-membered .....                                      | 33f               |
|  |      | for tris-bidentate complexes,                              |                   |
|  |      | planar projections of a .....                              | 25f               |
|  |      | bisphosphine(s)  |                   |
|  |      | catalytic asymmetric hydro-                                |                   |
|  |      | genation by 7-member .....                                 | 185               |
|  |      | complex, chair and twist-boat                              |                   |
|  |      | conformations in a   |                   |
|  |      | 7-member .....   | 184               |
|  |      | complex, conformational                                    |                   |
|  |      | isomerism in a 6-member ..                                 | 184               |

## C

## Cahn-Ingold-Prelog (CIP)

|                                 |           |
|---------------------------------|-----------|
| exploration, ligand .....       | 402f-403f |
| exploration procedures .....    | 400       |
| formalism .....                 | 404       |
| ligand relative priority .....  | 40f       |
| notation .....                  | 400       |
| priority .....                  | 400       |
| numbers for ligands .....       | 405       |
| relative priority numbers ..... | 405f      |
| Sequence Rule .....             | 400, 409  |

## CANON

|                                  |           |
|----------------------------------|-----------|
| algorithm .....                  | 404       |
| constitutional numbering .....   | 412f      |
| ligand priority assignment ..... | 407f-408f |

## Carbinolamine formation, stereo-

|                |         |
|----------------|---------|
| specific ..... | 126-127 |
|----------------|---------|

## Carbon

|  |      |
|--|------|
| catalytic influence of decolorizing ..                                       | 6    |
| compounds, nomenclature of stereo-   |      |
| chemistry of .....   | 397  |
| -NMR spectrum of <i>trans</i> -dichloro                                      |      |
| cobalt-amino-phosphine .....   | 211f |
| Carbon <sub>2</sub> - <i>cis</i> ( <i>N</i> )-Co-(admh) <sub>2</sub> (acac), |      |
| electronic spectra of .....  | 349f |

|                                    |          |
|------------------------------------|----------|
| Carbon <sub>2</sub> symmetry ..... | 177, 181 |
|------------------------------------|----------|

Carboxylates, solvent-dependent CD  
of pentaamine-cobalt(III)

|                           |         |
|---------------------------|---------|
| complexes of chiral ..... | 226-236 |
|---------------------------|---------|

## Carboxylic acid(s)

|                                       |     |
|---------------------------------------|-----|
| asymmetric hydrogenation of α,β-      |     |
| unsaturated .....                     | 185 |
| binding to rhodium, unsaturated ..... | 191 |
| CD spectra of 2-chloro-               |     |
| in rhodium biphosphine com-           |     |
| plexes, coordination of un-           |     |
| saturated .....                       | 187 |

- Chelate(s) (*continued*)  
 ring(s) (*continued*)  
 biphosphine(s) (*continued*)  
 rhodium complexes, binding  
   by 5-membered ..... 175-177  
 dependence of isomer formation  
   on conformation of ..... 7  
 enamide binding to 6-member ..... 180f  
 geometry in  $[\text{Co}(\text{tmd})_3]^{3+}$  ..... 20t  
 5-membered ..... 13-17  
   effect on, separation efficiency of ..... 318  
 6-membered ..... 17-20  
   effect on separation factor ..... 321  
   rhodium complexes, binding  
     of enamides by ..... 177  
   rhodium complexes, catalysis  
     by ..... 177  
 7-membered ..... 20-22  
 systems, conformations effects in ..... 115  
 systems, steric effects in ..... 115  
 sarcosinate ion ..... 115-116  
 systems, bis(ethylenediamine)  
   amino acid ..... 116  
   systems, tris- ..... 115  
 $\pi$ - $\pi^*$  transitions of the tris and  
   bis ..... 359-360
- Chelated maleate, orientations for  
 amido ion addition to ..... 122f
- Chelating chiral biphosphine ..... 169
- Chelating ligand ..... 9
- Chelation by azotyrosine in protein,  
 CD of Co(III) ..... 203-205
- Chelation of metal ions, azophenol 195-197
- Chemical Abstracts Service (CAS)  
 stereochemical notation ..... 406-413  
 examples ..... 411-413
- Chiral  
 aminophosphine chelate ligands,  
   CD spectra of cobalt(III)  
   complexes containing ..... 207-218  
 biphosphine, chelating ..... 169  
 biphosphines, rhodium complexes  
   with larger-ring chelates of ..... 187  
 carboxylates, solvent-dependent  
   CD of pentaamminecobalt(III)  
   complexes of ..... 226-236  
 conformations in 5-member chelate  
   ring biphosphine complexes ..... 184  
 diamines, solvent dependence of  
   CD of complexes of ..... 222  
 1,2-diamines, conformations of  
   coordinated *N*-substituted ..... 334f  
 1,2-diamines, structures and  
   abbreviations of ..... 327t  
 ketones, structures and abbrevia-  
   tions of ..... 327t
- Chiral (*continued*)  
 ligand, chemical shifts of N-H  
   protons of ..... 222  
 ligand, stereoselective solvation  
   of ..... 221-223  
 metal  
   complexes, CD intensities in  
     vibronic transitions of ..... 43-71  
   complexes, determination of  
     absolute configurations of ..... 73  
     by x-ray scattering ..... 43  
   ion cages ..... 128-130  
 transition metal complexes,  
   quantum mechanical theory  
   of optical activity in ..... 43-44  
 trigonal dihedral ( $D_3$ ) metal  
   complex, CD of a ..... 67
- Chirality  
 assignments ..... 360  
 cluster ..... 415  
 conformational ..... 14  
 designation configurational ..... 13-14  
 induction in coordination  
   complexes ..... 115-130  
 label(s) ..... 406-408, 409-411
- Chiroptical properties of optically  
 active transition metal complexes 43
- Chromate (III)  
 absolute configuration from the CD  
   spectrum for tris(catecholato)-  
   *trans*-tris(benzohydroximato)- ..... 140f  
   optical isomers of tris(catecholato)-  
   tris(thiobenzohydroximato)- ..... 155f  
   trianions, tris(benzohydroximato) .. 139
- Chromic deferriferriochrome, absorp-  
 tion spectra of ..... 147f
- Chromic deferriferriochrome, CD  
 spectra of ..... 147f
- Chromium  
 absorption spectrum of tris(thio-  
   benzohydroxamate)- ..... 156f  
 -(benz)<sub>3</sub>, absorption spectra of ..... 141f  
 -(benz)<sub>3</sub> isomers ..... 142  
 -(cat)<sub>3</sub>, CD spectra of  $\Delta$ - ..... 159f  
 -(cat)<sub>3</sub>, CD spectra of  $\Delta$ -K<sub>3</sub>- ..... 159f  
 -(C<sub>2</sub>O<sub>4</sub>)<sub>3</sub><sup>3-</sup>, optical rotatory dis-  
   persion of (+)<sub>D</sub> ..... 241f  
 -(C<sub>2</sub>O<sub>4</sub>)<sub>3</sub><sup>3-</sup>, racemization of (+)<sub>D</sub>  
   enantiomer of ..... 244f  
 -(ent), CD spectra of  $[\text{NH}_4]_3$ - ..... 163f  
 -(ent)<sup>-3</sup>, CD spectra of ..... 161  
 -(men)<sub>3</sub>, absorption spectra of ..... 141f  
 -(men)<sub>3</sub>, CD spectra of ..... 141f  
 -(men)<sub>3</sub> isomers ..... 139
- Chromium(III)  
 aerobactin, absorption spectra of ..... 152f  
 aerobactin, CD spectra of ..... 152f



- Chromium(III) (*continued*)
- trans*-tris(benzohydroxamato)- ..... 137f
  - complexes ..... 144
  - tris(hydroxamato)- ..... 134
  - CD spectra of tris(thiobenzo-  
hydroxamato)- ..... 156f
  - deferriferrioxamine B isomers,  
absorption of ..... 150f
  - tris( $\beta$ -diketonato)- ..... 142
  - enterobactin ..... 164f
  - isomers, tris(benzohydroxamato)- .. 136
  - tris( $\beta$ -ketoaminates) ..... 337
  - octahedral bonding geometries of  
*trans*-tris(benzohydroxamato)- 138f
  - tris(oxalato)- ..... 142
  - rhodotorulic acid ..... 149
- Chromophore
- achiral ..... 82, 85, 88-90, 273
  - inducibility* of ..... 84
  - metal-ligating atom ..... 75-77
  - octahedral symmetry of ..... 89
  - azo ..... 197
  - definitions ..... 74-78
  - models, separable ..... 74-75
  - moment products, CT ..... 79
  - system (B), perturbing chelate ..... 77-78
  - tetragonal ..... 224
- Chymotrypsin ..... 205
- CH<sub>2</sub>=CXY, optical yield of asym-  
metric hydrogenation of ..... 35f
- CIP (*see* Cahn-Ingold-Prelog)
- Circular dichroic
- intensities in vibronic transitions of  
chiral metal complexes ..... 43-71
  - properties of azonaphthol  
complexes ..... 200-203
  - properties of azophenol ..... 200-203
  - spectra
    - of AA-CPA-Zn ..... 199f
    - of azonaphthol Co(III)-EDDA  
complexes ..... 202f
    - of azophenol Co(III)-EDDA  
complexes ..... 202f
    - of (*S*)-2-chlorovaleric acid ..... 227
    - of Co(III)(EDDA)  
(AA-CPA-Zn) ..... 204f
- Circular dichroism (CD) ..... 19
- associate-induced (AIDC) theory .. 273
  - between two complexes of *trans*-  
(*N*,//)-[PtCl(L-aminocar-  
boxylate)(ethylene) type,  
difference in ..... 105f
  - calculations ..... 66-71
  - of charge-transfer transitions ..... 78-81
  - stereochemical correlations in ..... 73-90
  - of a chiral trigonal dihedral (*D*<sub>3</sub>)  
metal complex ..... 67
- Circular dichroism (*continued*)
- of Co(III) chelation by azotyro-  
sine in protein ..... 203-205
  - of complexes of chiral diamines,  
solvent dependence of ..... 222
  - contributions, additivity of ..... 255-257
  - in crystalline transition metal com-  
plexes, photoacoustic detection  
of natural ..... 375-394
  - curve(s)
    - of bis(acetylacetonato)-cobalt-  
(III) aminophosphine  
complexes ..... 217f-218f
    - $\Delta\epsilon$ [Co(DBEDDA)en<sup>+</sup>- $\Delta\epsilon$ -Co-  
(dmedda)en<sup>+</sup>, difference ..... 265f
    - $\Delta\epsilon$ [Co(EDDA)en<sup>+</sup>- $\Delta\epsilon$ -Co-  
(dmedda)en<sup>+</sup>, difference ..... 265f
    - for Co(en)<sub>2</sub>S-pala<sup>+</sup> isomers ..... 256f
    - of (-)<sub>589</sub>-[Co(gly)(NH<sub>3</sub>)-  
(tame)]-Cl<sub>2</sub>3H<sub>2</sub>O ..... 302f
    - for [Co(l-pn)<sub>2</sub>en<sup>3+</sup> isomers ..... 258f
  - of the *d-d* transitions ..... 81
  - additivity of ..... 273-286
  - stereochemical correlations in ..... 73-90
  - dispersion-induced ..... 82
  - of Fe(phen)<sub>2</sub>(CN)<sub>2</sub> product ..... 365f
  - of  $\Delta$ -Fe(phen)<sub>3</sub><sup>2+</sup> product ..... 365f
  - fluorescence-detected (FDCD) ..... 376
  - insensitivity to crystal imperfection  
and strain ..... 376
  - intensities ..... 81
  - of EDDA complexes, substituent  
effect ..... 257-262
  - ion association effect on ..... 225
  - magnitude of *d-d* ..... 86
  - of metal complexes, solvent  
effect on ..... 221-236
  - for partially resolved  $\Lambda$ -(-)  
546-Co(admh)(acac)<sub>2</sub>,  
absorption spectrum ..... 315f
  - for partially resolved  $\Delta$ -(-)<sub>546</sub>-fac-  
Co(admh)<sub>3</sub>, absorption spec-  
trum ..... 352f
  - pattern of platinum(II) complexes ..... 92
  - pattern of rhodium(I) complexes .. 92
  - of pentaaminocobalt(III) com-  
plexes of chiral carboxylates,  
solvent-dependent ..... 226-236
  - Pfeiffer ..... 242
  - photoacoustic (PACD) ..... 377
  - as probe of metal ion interaction  
with azoproteins ..... 195-205
  - spectrum(a) ..... 276f
  - for the A<sub>1</sub> → (A<sub>2</sub> + E)\*e  
transitions ..... 69f-70f
  - for absolute configuration of  
cobalt ..... 292-301

- Circular dichroism (*continued*)  
 spectrum(a) (*continued*)  
 of bis(acetylacetonato)cobalt-  
 (III)-aminophosphine ..... 216f  
 of amino acid complexes, paramet-  
 ers of the Gaussian com-  
 ponents for ..... 279t  
 of tris(benzohydroxamato)-  
 iron(III) ..... 145f  
 of  $\Delta$ -tris(benzohydroximato)-  
 cobaltate(III) ion ..... 143f  
 for tris(catecholato)chromate-  
 (III), absolute configuration  
 from ..... 158  
 of 2-chloro-carboxylic acids ..... 227  
 of chromic deferriferrichrome ..... 147f  
 [Coa(gly)(tacn)] complexes 305-311  
 of mer-[Co( $\beta$ -ala)<sub>3</sub>], induced ..... 323f  
 of Co-aminophosphine com-  
 plexes ..... 210-218  
 of Co(admh)(acac)<sub>2</sub> ..... 350  
 of (-)<sub>589</sub><sup>-</sup>[Co(Cl)(gly)(tacn)]<sup>+</sup> ..... 310f  
 of cis[CoCl<sub>2</sub>(NH<sub>3</sub>)<sub>2</sub>(en)]<sup>+</sup> isomer ..... 293f  
 of (+)<sub>589</sub><sup>-</sup>[Co(CN)(Br)(NH<sub>3</sub>)-  
 (tacn)]<sup>+</sup> ..... 312f  
 of (-)<sub>589</sub><sup>-</sup>[Co(CN)<sub>2</sub>(CO<sub>3</sub>)-  
 (En)]<sup>-</sup> ..... 295f  
 of (-)<sub>589</sub><sup>-</sup>[Co(CN)<sub>2</sub>(en)-  
 (H<sub>2</sub>O)<sub>2</sub>]<sup>+</sup> ..... 295f  
 of (-)<sub>589</sub><sup>-</sup>[Co(CN)(gly)-  
 (tacn)]<sup>+</sup> ..... 307f  
 of (+)<sub>546</sub><sup>CD</sup>[Co(CN)(NH<sub>3</sub>)-  
 (tacn)(H<sub>2</sub>O)]<sup>2+</sup> ..... 312f  
 of (+)<sub>589</sub><sup>-</sup>[Co(CN)<sub>2</sub>(ox)(en)]<sup>-</sup> ..... 295f  
 of cis-cis and cis-cis-cis Co  
 complexes ..... 294f  
 of s-cis Co(III) complexes ..... 260f  
 Co(III) complexes containing  
 chiral aminophosphine  
 chelate ligands ..... 207-218  
 of Co(III) complexes ethylene-  
 diamine-*N,N'*-diacetate  
 ion ..... 255-271  
 of Co(II) complexes with opti-  
 cal activity due to uniden-  
 tate ligand arrangement ..... 289-313  
 of [Co(CO<sub>3</sub>)(ox)(NH<sub>3</sub>)<sub>2</sub>]<sup>-</sup> ..... 300f  
 of s-cis-[Co(edda)(l-stein)]<sup>+</sup>  
 isomers, s-cis ..... 266f  
 of Co(en)<sub>3</sub>I<sub>3</sub> ..... 389f  
 of (-)<sub>589</sub><sup>-</sup>[Co(gly)(NH<sub>3</sub>)-  
 (tacn)]<sup>2+</sup> ..... 308f  
 of [Co(gly)(NH<sub>3</sub>)(tacn)]<sup>2+</sup>  
 enantiomers ..... 306f  
 of (-)<sub>589</sub><sup>-</sup>[Co(gly)(tacn)-  
 (H<sub>2</sub>O)]<sup>2+</sup> ..... 309f  
 for (+)<sub>546</sub><sup>-</sup>Co(III) isomers ..... 265f
- Circular dichroism (*continued*)  
 spectrum(a) (*continued*)  
 of (+)<sub>589</sub><sup>-</sup>[Co(N<sub>3</sub>)(gly)-  
 (tacn)]<sup>+</sup> ..... 310f  
 of (+)<sub>546</sub><sup>CD</sup>[Co(Nb<sub>6</sub>O<sub>19</sub>)  
 (gly)(H<sub>2</sub>O)]<sup>6-</sup> ..... 304f  
 of (+)<sub>546</sub><sup>CD</sup>[Co(Nb<sub>6</sub>O<sub>19</sub>)  
 (gly)(NH<sub>3</sub>)]<sup>6-</sup> ..... 304f  
 of (-)<sub>589</sub><sup>-</sup>[Co(NCS)(gly)  
 (tacn)]<sup>+</sup> ..... 308f  
 of (+)<sub>589</sub><sup>-</sup>[Co(NO<sub>2</sub>)<sub>2</sub>(CO<sub>3</sub>)  
 (en)]<sup>-</sup> ..... 299f  
 of (-)<sub>589</sub><sup>-</sup>[Co(NO<sub>2</sub>)<sub>2</sub>(CO<sub>3</sub>)-  
 (NH<sub>3</sub>)<sub>2</sub>]<sup>-</sup> ..... 298f  
 of (+)<sub>589</sub><sup>-</sup>[Co(NO<sub>2</sub>)<sub>2</sub>(en)  
 (H<sub>2</sub>O)<sub>2</sub>]<sup>+</sup> ..... 299f  
 of (-)<sub>589</sub><sup>-</sup>[Co(NO<sub>2</sub>)(gly)  
 (tacn)]<sup>+</sup> ..... 307f  
 of (+)<sub>589</sub><sup>-</sup>[Co(NO<sub>2</sub>)<sub>2</sub>(mal)-  
 (NH<sub>3</sub>)<sub>2</sub>]<sup>-</sup> ..... 298f  
 of (+)<sub>589</sub><sup>-</sup>[Co(NO<sub>2</sub>)<sub>2</sub>(NH<sub>3</sub>)<sub>2</sub>-  
 (H<sub>2</sub>O)<sub>2</sub>]<sup>+</sup> ..... 298f  
 of (+)<sub>598</sub><sup>-</sup>[Co(NO<sub>2</sub>)<sub>2</sub>(ox)  
 (en)]<sup>-</sup> ..... 299f  
 of (+)<sub>589</sub><sup>-</sup>[Co(NO<sub>2</sub>)<sub>2</sub>(ox)  
 (en)]<sup>-</sup> ..... 299f  
 of (+)<sub>589</sub><sup>-</sup>[Co(NO<sub>2</sub>)<sub>2</sub>(ox)  
 (NH<sub>3</sub>)<sub>2</sub>]<sup>-</sup> ..... 298f  
 of (-)<sub>589</sub><sup>-</sup>[Co(OH)(gly)-  
 (tacn)]<sup>+</sup> ..... 309f  
 of [Co(ox)(NH<sub>3</sub>)<sub>2</sub>(H<sub>2</sub>O)<sub>2</sub>]<sup>+</sup> ..... 300f  
 of *trans*-[Co{(R)-pn}<sub>2</sub>Cl<sub>2</sub>]BPH<sub>4</sub>  
 in various solvents ..... 223f  
 of [Co(D-ser)<sub>3-n</sub>( $\beta$ -ala-  
 nine)<sub>n</sub>] isomers ..... 317  
 of [Cobalt(L-ser)<sub>3-n</sub>( $\beta$ -ala-  
 nine)<sub>n</sub>] isomers ..... 317  
 of fac-[Co(L-ser)( $\beta$ -ala)<sub>2</sub>] ..... 317  
 of cobalt-1,4,7-triazacyclo-  
 nonane complexes ..... 303-313  
 for cis-cis complexes ..... 292-301  
 contributions of asymmetric  
 nitrogens to ..... 268  
 contributions of stibenediamine  
 to ..... 262-268  
 correlation of stereochemistry  
 and ..... 268-269  
 of  $\Delta$ -[Cr(cat)<sub>3</sub>] ..... 159f  
 of [Cr(enterobactin)]<sup>-3</sup> ..... 161  
 of Cr(men)<sub>3</sub> ..... 141f  
 of Cr(III) aerobactin ..... 152f  
 determinations ..... 366  
 of tris-diamine cobalt(III)  
 complexes ..... 19, 22  
 of diastereomeric pairs of  
 Co(acac)<sub>2</sub>-aminophosphine  
 complexes ..... 217f

|   |  |
|---|--|
| Circular dichroism ( <i>continued</i> )   | Circular dichroism ( <i>continued</i> )                                      |
| spectrum(a) ( <i>continued</i> )  | spectrum(a) ( <i>continued</i> )   |
| of <i>trans</i> -dichloro cobalt(III)-  | spectral data ..... 347 <i>t</i>   |
| aminophosphine complexes .. 212 <i>f</i>  | spectral features, influence of  |
| of Fe(mphen) <sub>3</sub> <sup>3+</sup> ..... 366                                   | vibronic coupling on ..... 68  |
| of Fe(III) aerobactin ..... 149, 152 <i>f</i>                                       | transition for <i>s</i> -cis-  |
| of Fe(III) hydroxamate ..... 149  | [Co(DBEDDA)en] <sup>+</sup> ..... 268-269                                    |
| of $\Delta$ -fac-Fe(mphen) <sub>3</sub> <sup>2+</sup> ..... 367 <i>f</i>            | Cluster(s)   |
| of Ferrichrome A ..... 146 <i>f</i>   | chirality ..... 415  |
| of ferric complex of rhodotorulic   | modes ..... 47   |
| acid ..... 151 <i>f</i>   | stereochemical notation for asym-  |
| for ferric siderophores ..... 134   | metric ..... 415   |
| of first-eluted isomers ..... 320 <i>f</i>  | [Coa(gly)(tacn)] complexes,  |
| influence of Jahn-Teller inter-   | absorption of ..... 305-311  |
| actions on the ..... 46   | [Coa(gly)(tacn)] complexes, CD   |
| influence of pseudo Jahn-Teller   | spectra of ..... 305-311   |
| interactions on ..... 46  | [Coabc(tacn)], complexes of ..... 311-313                                    |
| of <i>cis</i> -isomers ..... 136  | Cobaloxime moiety electronic   |
| of <i>trans</i> -isomers ..... 136  | structure ..... 34   |
| of $\Delta$ -K <sub>3</sub> [Cr(cat) <sub>3</sub> ] ..... 159 <i>f</i>              | Cobalt   |
| of $\Delta$ -K <sub>3</sub> Rh (catecholate) <sub>3</sub> ..... 160 <i>f</i>        | -(acac) <sub>2</sub> aminophosphine  |
| of $\Delta$ - <i>cis</i> -K <sub>3</sub> [Rh(ent) <sub>3</sub> ] ..... 162 <i>f</i> | complexes, structures of   |
| of NaUO <sub>2</sub> (OAc) <sub>3</sub> , single-crystal .. 397 <i>f</i>            | $\Delta$ (S)- and $\Delta$ (S)- ..... 216 <i>f</i>                           |
| of [NH <sub>4</sub> ] <sub>3</sub> [Cr(ent)] ..... 163 <i>f</i>                     | -(admh) <sub>3</sub> , <i>tert</i> -butyl region of the                      |
| of Ni(en) <sub>3</sub> (NO <sub>3</sub> ) <sub>2</sub> , axial single               | proton NMR spectra for ..... 348 <i>f</i>                                    |
| crystal ..... 388 <i>f</i>  | -(admh) <sub>3</sub> complexes, preparation                                  |
| of $\eta^2$ -olefin complexes of plati-   | and properties ..... 342   |
| num(II), peaks in ..... 98 <i>t</i>   | -(admh) <sub>n</sub> (acac) <sub>3-n</sub> complexes,                        |
| of palladium-aminophosphine   | partial resolution of ..... 350  |
| complexes ..... 209 <i>f</i>  | -(admh) <sub>n</sub> (acac) <sub>3-n</sub> complexes,                        |
| of pentaammine{(S)-2-chloro-  | preparation of ..... 339   |
| propionato}cobalt(III) } ..... 226  | -(admh) <sub>n</sub> (acac) <sub>3-n</sub> complexes,                        |
| solvent effect on ..... 231 <i>f</i>  | stereochemistries of ..... 344   |
| of pentaammine{(S)-2-chloro-  | -(aminodimethylhex-4-en-3-one)-  |
| propionato-cobalt(III)  | 2(acetylacetonate), prepara-   |
| tetraphenylborate, tempera-   | tion by ..... 343-344  |
| ture effect on ..... 234 <i>f</i>   | -(L-alaine) <sub>3</sub> isomers, solubility of .. 317                       |
| of <i>trans</i> (N, //)-[PtCl(N-me-L-   | -aminophosphine, C-NMR spec-   |
| pro)(ethylene)], change in 110 <i>f</i>   | spectrum of <i>trans</i> -dichloro ..... 211 <i>f</i>                        |
| of $\Delta$ -Rh(catecholate) <sub>3</sub> ..... 160 <i>f</i>                        | -aminophosphine complexes,   |
| of [Rh(enterobactin)] <sup>-3</sup> ..... 161                                       | preparation of ..... 208-210   |
| of R & S amino acid complexes .... 274  | CD spectra for absolute configura-   |
| of S-alaninepentaaminecobalt-   | tion of ..... 292-301  |
| (III)-aminophosphine,   | -(chxn) <sub>3</sub> ] <sup>3+</sup> , difference synthesis .... 34 <i>f</i> |
| solvent effect on ..... 233 <i>f</i>  | Cl <sub>2</sub> (aminophosphine) <sub>2</sub> ] (ClO <sub>4</sub> ),         |
| of square planar complexes con-   | structure of ..... 210   |
| taining prochiral olefins   | complexes  |
| stereoselective olefin  | absorption of <i>cis</i> - <i>cis</i> and <i>cis</i> -                       |
| exchange ..... 91   | <i>cis</i> - <i>cis</i> ..... 294 <i>f</i>                                   |
| -structure correlation studies  | enzyme-like activity of ..... 2  |
| using ..... 65  | with <i>cis</i> - <i>cis</i> unidentate distribut-                           |
| of tbn, change in ..... 110 <i>f</i>  | tion, syntheses of ..... 289-292   |
| of tris(thiobenzohydroxa-   | -(dien) <sub>2</sub> ] <sup>3+</sup> , geometries of mer- ..... 27 <i>t</i>  |
| mato)Cr(III) ..... 156 <i>f</i>   | $\beta$ -diketonates, mechanism of inver-                                    |
| of tris(thiobenzohydroxa-   | sion and isomerization of ..... 354  |
| mato)Fe(III) ..... 157 <i>f</i>   | -(ed3a)NO <sub>2</sub> <sup>-</sup>  |
| of transition metal complexes,  | EDDA   |
| influence of vibronic inter-  | -(EDDA)en <sup>+</sup> , $\Delta$ - ..... 268                                |
| actions on ..... 46   | -(EDDA)-(1-stien) <sup>+</sup> ..... 262, 269                                |

Cobalt (*continued*)

|  |         |
|--|---------|
| - (EDDA) $X_2$ isomers, structures of ..   | 260f    |
| - (EDTA) .....   | 269     |
| - (en)(1-pn) $_2^{3+}$ isomers .....   | 255-256 |
| - (en)(pn)(NO $_2$ ) $_2^+$ , isomers <i>cis</i> - .....   | 7       |
| - (en) $_2$ (C $_2$ O $_4$ ) $^{1-}$ .....   | 123     |
| - (en) $_2$ Cl $_2$ ]Cl, reaction of ammonia<br>with <i>levo</i> - .....   | 4t      |
| - (en) $_3$ I $_3$ , solution absorption of .....  | 389f    |
| - (en) $_3^{3+}$ .....   | 46      |
| - (en) $_3$ ] $^{1+3}$ , isomers .....   | 142     |
| - (en) $_3$ ] $^{3+}$ isomers, stabilities of .....  | 15      |
| - (NH $_3$ ) $_5$ OOCCH=CHCOOR $^{2+}$ .....   | 119     |
| - (1,3-PDTA) .....   | 269     |
| - {(R)-pn $_2$ Cl $_2^+$ , <i>trans</i> - .....  | 221-222 |
| - (R,R-ptn) $_3$ ] $^{3+}$ , (+) $_{546}$ .....  | 20      |
| - (1-SDDA)en $^+$ .....  | 269     |
| - (1-SDTA), stereospecificity of .....   | 269     |
| - (tmd) $_3$ ] $^{3+}$ , chelate ring, geometry<br>in .....  | 20t     |
| - 1,4,7-triazacyclononane com-<br>plexes, synthesis of .....   | 303-313 |
| - (trien)Cl $_2$ ] $^+$ , $\alpha$ - .....   | 127     |
| <i>cis</i> -[Cobalt chlorine $_2$ (NH $_3$ ) $_2$ (en)] $^+$<br>isomer, absorption of <i>cis</i> - .....                                     | 293f    |
| <i>fac</i> -Cobalt( $\alpha$ -amino acid) $_3$ - $_n$ ( $\beta$ -<br>amino acid) $_n$ ] isomers, separa-<br>tion and identification of ..... | 316-317 |
| <i>fac</i> -Cobalt(L-serine)( $\beta$ alanine) $_2$<br>isomer, CD spectra of .....   | 317     |
| <i>mer</i> -[Cobalt( $\beta$ -alanine) $_3$ ], chro-<br>matographic resolution .....   | 323f    |
| <i>mer</i> -[Cobalt( $\beta$ -alanine) $_3$ ], enantio-<br>mers, effect of alcohol on chro-<br>matographic separation of .....               | 322f    |
| <i>mer</i> -[Cobalt( $\beta$ -alanine) $_3$ ], induced<br>CD spectra of .....  | 323f    |
| <i>mer</i> -[Cobalt( $\beta$ -alanine) $_3$ ], resolu-<br>tion of .....  | 324     |
| $\Delta\epsilon$ [Cobalt(EDDA)en $^+$ ]- $\Delta\epsilon$ [Co-<br>(dmedda)en] $^+$ , difference CD<br>curves .....                           | 265f    |
| (+)-[Cobalt(en) $_3$ ] $^{3+}$ .....   | 43      |

## Cobalt III

|                                   |            |
|-----------------------------------|------------|
| acetatopentaammine-               | 228        |
| amine systems .....               | 123        |
| -amino acid complexes             |            |
| substituted triethylenetetraamine | 275f       |
| algebra in calculation of vicinal |            |
| effects .....                     | 277f       |
| average vicinal effects .....     | 277f       |
| CD glycine complexes .....        | 278f       |
| CD spectrum (a) of .....          | 276f, 283f |
| component Gaussians .....         | 276f       |
| configurational effects .....     | 280f-281f  |
| reaction scheme .....             | 275        |
| vicinal effect(s) .....           | 280f-281f  |
| vicinal effect for prochiral      |            |
| amino acid .....                  | 283f       |

Cobalt(III) (*continued*)

|   |           |
|---|-----------|
| -amino acid complexes ( <i>continued</i> )  |           |
| triethylenetetraamine-  | 273       |
| vicinal effect in a homologous  |           |
| series triethylenetetra-  |           |
| amine- .....  | 273-286   |
| -aminophosphine, CD spectra of  |           |
| bis(acetylacetonato) .....  | 216f      |
| -aminophosphine complexes   |           |
| absorption spectra of bis(acetyl-   |           |
| acetonato) .....  | 214f      |
| absorption spectra of <i>trans</i> -  |           |
| dichloro .....  | 211f      |
| CD curves of bis(acetyl-  |           |
| acetonato)- .....   | 211f-218f |
| CD spectra of <i>trans</i> -dichloro .....  | 212f      |
| -azophenolate complexes, absorp-<br>tion spectra of .....   | 200       |
| azoprotein derivatives, characteri-<br>zation of .....  | 197-200   |
| Bailar inversion reactions .....  | 357       |
| tris(benzohydroxamato)- .....   | 142       |
| carboxylate complexes, penta-<br>amine- .....   | 229f      |
| CD spectrum of pentaammine  |           |
| {(S)-2-chloro-propionato} .....   | 226       |
| chelates by <i>d</i> -tartrate resolving<br>agents optical resolution of<br>facial and meridional tris-<br>(aminoacidato) ..... | 315-324   |
| chelation by azotyrosine in protein,<br>circular dichroism of .....   | 203-205   |
| complex(es)   |           |
| absorption spectra of <i>s-cis</i> - .....  | 260f      |
| band of tris-diamine .....  | 20t       |
| CD spectra  |           |
| of <i>s-cis</i> - .....   | 260f      |
| of tris-diamine .....   | 19, 22    |
| containing chiral aminophos-<br>phine chelate ligands .....   | 207-218   |
| ethylenediamine- <i>N,N'</i> -<br>diacetate ion .....   | 255-271   |
| with optical activity due to<br>unidentate ligand arrange-<br>ment .....  | 289-313   |
| of chiral carboxylates, solvent-<br>dependent CD of penta-<br>amine- .....  | 226-236   |
| tris(diamine)- .....  | 225       |
| energy level diagram .....  | 50f       |
| ethylenediamine- <i>N,N'</i> - <i>diacetate</i> .....   |           |
| ion, phenyl substituent   |           |
| contributions .....   | 255-271   |
| octahedral .....  | 207       |
| preparation of model azo-<br>ligand .....   | 197-200   |
| rotatory strengths of tris-<br>(diamine) .....  | 24t       |
| trigonal dihedral .....   | 57        |

|   |               |   |                   |
|---|---------------|---|-------------------|
| Cobalt(III) ( <i>continued</i> )                    |               | Complex(es)   |                   |
| complex(es) ( <i>continued</i> )                    |               | $\pi^-$ .....   | 38f               |
| of trigonal dihedral symmetry .....                 | 64            | $\sigma^-$ .....  | 38f               |
| compounds, <i>cis</i> - <i>trans</i> rearrange-     |               | with a cyclic terdentate .....  | 27-31             |
| ments of .....                                      | 2             | planar projections of a chelate   |                   |
| <i>cis</i> -dichloro- <i>cis</i> -diammineethylene- |               | ring for tris-bidentate .....   | 25f               |
| diamine- .....                                      | 6             | Concanavalin A .....  | 205               |
| (EDDA)  |               | Condensation products with the  |                   |
| (AA-CPA-Zn) absorption                              |               | single linkage, structure of .....  | 330f              |
| spectrum .....                                      | 203-205, 204f | Configuration(s)  |                   |
| (AA-CPA-Zn), CD spectra of ..                       | 204f          | absolute .....  | 14, 269, 375, 400 |
| (azo dye) complexes .....                           | 200           | of chiral metal complexes,  |                   |
| complexes .....                                     | 201f, 269     | determination of .....  | 73                |
| CD spectra of azonaphthol .....                     | 202f          | of Co(admh) <sub>n</sub> (acac) <sub>3-n</sub>  |                   |
| CD spectra of azophenol .....                       | 202f          | complexes .....   | 350               |
| geometrical isomers of tris(amino-                  |               | of cobalt, CD spectra for .....   | 292-301           |
| acidato)- .....                                     | 320f          | of <i>cis</i> -[CoCl <sub>2</sub> (NH <sub>3</sub> ) <sub>2</sub> (en)] <sup>+</sup> isomer | 294f              |
| incorporation .....                                 | 198f          | of (+) <sub>589</sub> -[Co(CN) <sub>2</sub> (mal)-  |                   |
| into enzymes method .....                           | 196f          | (NH <sub>3</sub> ) <sub>2</sub> ] <sup>-</sup> .....  | 298f              |
| into hormones method .....                          | 196f          | of (-) <sub>589</sub> -[Co(gly)(NH <sub>3</sub> )-  |                   |
| ion, pyruvato imine bis(ethylene-                   |               | (tacn)] <sup>2+</sup> .....   | 312f              |
| diamine) .....                                      | 124           | of (-) <sub>589</sub> -[Co(NO <sub>2</sub> ) <sub>2</sub> (OX)-                             |                   |
| isomers, absorption spectra for (+)                 | 265f          | (NH <sub>3</sub> ) <sub>2</sub> ] <sup>-</sup> .....  | 299f              |
| isomers, CD spectra for (+) <sub>546</sub> .....    | 265f          | of complexes in Pfeiffer systems ..   | 245f              |
| $\beta$ -ketoaminates .....                         | 337           | determination of .....  | 81                |
| modification of enzymes with .....                  | 195           | and equilibrium displacement  | 242-246           |
| modification of hormones with .....                 | 195           | of Fe(III) enterobactin .....   | 161               |
| pentaammine {(S)-2-chloro-                          |               | of Fe(phen) <sub>3</sub> <sup>2+</sup> .....  | 360               |
| propionato} .....                                   | 228, 229f     | of metal coordination compounds   | 43                |
| rotational strength of pentaammine                  |               | of N-C-C-P* .....   | 208               |
| {(S)-2-chloropropionato} .....                      | 233f          | of $\eta_2$ -olefins .....  | 91                |
| (S)-alaninepentaammine- .....                       | 232           | from solution reactions .....   | 357-373           |
| solvent effect on CD spectrum of                    |               | of l-stein .....  | 262               |
| pentaammine {(S)-2-chloro-                          |               | of transition metal complexes .....   | 13-39             |
| propionato}- .....                                  | 231f          | <i>d</i> <sup>5</sup> .....   | 134               |
| solvent effect on CD spectrum of                    |               | number .....  | 406-408           |
| (S)-alaninepentaammine- .....                       | 233f          | temperature dependence of product   | 3                 |
| synthesis (5-amino-2,2-dimethyl-                    |               | of transition metal catecholates .....  | 158               |
| hex-4-en-3-onato)                                   |               | $\Lambda$ - <i>cis</i> Configuration, ferrichrome .....                                     | 144               |
| synthesis, <i>fac</i> - and <i>mer</i> -tris .....  | 338-339       | $\Lambda$ - <i>cis</i> Configuration, ferrichrysin .....                                    | 144               |
| bis (2,4-pentanedionato)- .....                     | 340-341       | Configurational   |                   |
| C <sub>2</sub> - <i>cis</i> (N)-bis(2,4-pentane-    |               | chirality, designation .....  | 13-14             |
| dionato) .....                                      | 339-340       | contributions, additivity rule of .....   | 301               |
| C <sub>1</sub> -bis(2,4-pentanedionato) .....       | 340           | curves  |                   |
| systems .....                                       | 49-51         | Co(L-ala)(NH <sub>3</sub> )(tame) <sup>2+</sup> .....                                       | 302               |
| tetraphenylborate, temperature                      |               | Co(L-ileu)(NH <sub>3</sub> )(tame) <sup>2+</sup> .....                                      | 302f              |
| effect on CD spectrum of                            |               | Co(L-val)(NH <sub>3</sub> )(tame) <sup>2+</sup> .....                                       | 302f              |
| pentaammine-{(S)-2-chloro-                          |               | dissymmetry .....   | 273               |
| propionato}- .....                                  | 234f          | effect(s) .....   | 273               |
| tetraphenylborate solvent effect on                 |               | curves for [Co(l-pn) <sub>2</sub> en] <sup>3+</sup>   |                   |
| absorption spectrum of penta-                       |               | isomers .....   | 259f              |
| ammine-{(S)-2-chloropro-                            |               | of optically active ligands .....   | 268               |
| pionato} .....                                      | 230f          | isomerism .....   | 13                |
| Cobaltate(III) ion, absorption                      |               | Conformation(s) .....   | 375               |
| spectra of $\Lambda$ -tris(benzohydroxi-            |               | boat .....  | 185               |
| mato)- .....  | 143f          | of chelate ring, dependence of  |                   |
| Cobaltate(III) ion, CD spectra of                   |               | isomer formation on .....   | 7                 |
| $\Lambda$ -tris(benzohydroximato)- .....            | 143f          | of coordinated N-substituted chiral   |                   |
| coe (see Cyclooctene)                               |               | 1,2-diamines .....  | 334f              |

- Conformation(s) (*continued*)  
of coordinated *S*-aminomethyl  
pyrrolidine, possible ..... 330*f*  
of cycloheptane ..... 181  
designation ..... 14  
effects in chelate ring systems ..... 115  
in a 7-member chelate ring biphos-  
phine complex, chair and  
twist-boat ..... 184  
in 5-member chelate ring biphos-  
phine complexes, chiral ..... 184  
of a 6-membered metal trimeth-  
ylenediamine ring ..... 17
- Conformational  
chirality ..... 14  
dissymmetry ..... 273  
effect ..... 273  
of optically active ligands ..... 268  
energy ..... 14  
difference ..... 225  
isomerism ..... 13  
in a 6-member chelate ring  
biphosphine complex ..... 184
- Conformer(s)  
population change ..... 225–226  
strain energies for  $[\text{Co}(\pm\text{chxn})_3]^{3+}$  ..... 17  
strain energies for  $[\text{M}(\text{cn})_3]$  ..... 16*t*
- Coordinated amino acid esters ..... 117
- Coordinated chelates, imine forma-  
tion in ..... 123
- Coordination  
complexes, chirality induction  
in ..... 115–130  
compounds  
absolute configuration of metal .. 43  
historical review, stereochemistry  
of ..... 1–10  
separation of isomers of ..... 13  
stereoselective syntheses of ..... 8  
modes of ..... 29  
numbers four to six, priming sub-  
rule a, trans maximum differ-  
ence subrule for ..... 409  
numbers four to six, priming sub-  
rule b, trans maximum differ-  
ence subrule for ..... 409  
systems, stereochemical descrip-  
tion and notation for ..... 397–417
- Copper (*S*-ampr) $_2^{2+}$  with methyl vinyl  
ketone and di acetone alcohol,  
reactions of ..... 329
- Copper (*S*-apip) $_2^{2+}$  with ketones, prod-  
ucts for condensation reaction of 334*f*
- Copper(II)  
complexes of *S*-apip and *S*-ahaz,  
geometrical isomers of ..... 330*f*  
complexes of *S*-apip and *S*-ahaz,  
reactions of ..... 329–333
- Copper(II) (*continued*)  
–3-(*S*)-3-aminohexahydroazepine,  
products distribution for reac-  
tions of ..... 332*t*  
–*S*-aminomethylpyrrolidine com-  
plexes with several ketones,  
products distribution for reac-  
tions of ..... 332*t*  
–3(*S*)-3-aminopiperidine, prod-  
ucts distribution for reactions  
of ..... 332*t*  
Cotton ..... 255  
Coupled-oscillator contribution ..... 79
- Coupling(s)  
( $A_2 + E$ )\**e*  
( $A_2 + E$ )\*( $a_1 + 2e$ ), trigonally  
distorted systems ..... 56  
on CD spectral features, influence  
of vibronic ..... 68  
constant data ..... 345*t*  
constants, equations, linear ..... 54  
effects, vibronic ..... 58  
interchelate ..... 77  
linear ( $A_2 + E$ )\**e* pseudo  
Jahn–Teller ..... 56  
model, dynamic ..... 26  
 $T_{1g}^*(t_{2g} e_g)$  ..... 51  
 $(T_{1g} + T_{1u})*(T_{1u} + t_{2u})$  ..... 58–64  
vibronic ..... 45–46
- CPA (*see* Carboxypeptidase A)
- CPL (circularly polarized lumi-  
nescence) ..... 376
- Cryptates ..... 128
- Crystal field model ..... 26
- CT (*see* Charge-transfer)
- Cyanide inversion reaction, tris-  
(diimine)iron(II)– ..... 357–373
- Cyanide ion at a chelated imine,  
stereospecific addition of ..... 124–126
- Cyclic terdentate, complexes with ..... 27–31
- Cycloctene (coe) ..... 92
- D**
- $d-\pi^*$  (ethylene) transition ..... 104–106
- $D_3$   
complexes, electron density dis-  
tribution in ..... 31–32  
molecular point symmetry ..... 158  
symmetry ..... 75, 139, 161  
systems ..... 86
- $D_{3d}$  symmetry ..... 76–79
- $d^3$  configuration ..... 134
- $d-d$   
absorption bands ..... 224  
absorption intensities ..... 77  
CD, magnitude of ..... 86  
rotatory strengths, influence of  
vibronic interactions on ..... 47



- Equilibrium  
 constants for geometrical isomerization of  $\text{Co}(\text{admh})_3$ , rate and ..... 353*t*  
 displacement, absolute configuration and ..... 242–246  
 displacement mechanism for Pfeiffer effect in inorganic chemistry ..... 239–253  
 geometries of the  $\text{lel}_3$  isomers ..... 16  
 Esters, coordinated amino acid ..... 117  
 Ethylenediamine  
 amino acid chelate systems, bis- ..... 116  
 Co(III) ion, pyruvato imine bis-complexes, absorption spectra of the *bis*(acetylacetonato) ..... 213  
 -*N, N'*-diacetate (EDDA)  
 complexes, substituent effect, CD intensities of ..... 257–262  
 ion, CD spectra of Co(III) complexes ..... 255–271  
 ion, phenyl substituent contributions in Co(III) complexes ..... 255–271  
 tris(Ethylenediamine) ..... 128–130  
 Exciton assignments ..... 360
- F**
- Fac (*see* Isomer(*s*), fac)  
*u*-Facial-isomers ..... 26  
 FD CD (fluorescence-detected circular dichroism) ..... 376  
 Ferric enterobactin ..... 164*f*  
 Ferrichrome(*s*) ..... 133  
 A ..... 144  
 absorption spectra of ..... 146*f*  
 CD spectra of ..... 146*f*  
 $\Lambda$ -cis configuration ..... 144  
 structure of ..... 148*f*  
 Ferrichrysin  $\Lambda$ -cis configuration ..... 144  
 Ferrioxamine(*s*) ..... 149  
 E ..... 149  
 structure of linear ..... 150*f*  
 Fumarate, methyl ..... 118*f*
- G**
- Gaussians, component ..... 276*f*  
 Geometrical isomers of a tris(chelate) complex ..... 135*f*  
 Geometries  
 of  $[\text{Co}(\text{en})_3]^{3+}$  ..... 15*t*  
 of  $[\text{Cr}(\text{en})_3]^{3+}$  ..... 15*t*  
 of the  $\text{lel}_3$  isomers, equilibrium ..... 16  
 of mer- $[\text{Co}(\text{dien})_2]^{3+}$  ..... 27*t*  
 Gerade components ..... 57  
 Glucagon ..... 205
- H**
- Hamiltonian equation(*s*)  
 harmonic oscillator ..... 54  
 perturbation ..... 49  
 vibronic ..... 48, 51–52  
 Hamiltonian, harmonic oscillator ..... 52  
 Harmonic oscillator Hamiltonian equations ..... 54  
 Heptadiene, bicyclo- ..... 181  
 Heptane, conformations of cyclo- ..... 181  
 Herzberg–Teller (perturbative) formalism for vibronic interactions .. 46  
 Herzberg–Teller (HT) vibronic theory ..... 58  
 Hexadecapole moment, electric ..... 23  
 Hexahydroazepine, products distribution for reactions of Cu(II)-3(*S*)-3-amino- ..... 332*t*  
 Hexene, hydrogenation of cyclo- ..... 173  
 Histidines ..... 195, 197  
 Homogeneous catalysis ..... 172  
 Hormones method, Co(III) incorporation into ..... 196*f*  
 Hydration of olefins, stereospecific ..... 117–123  
 Hydrogen bonding mechanism  
 Pfeiffer effect ..... 248*f*  
 Hydrogen bonding and Pfeiffer effect ..... 246–253  
 Hydrogenation  
 asymmetric ..... 169–192  
 ligand DI OXOP, enamide ..... 191  
 of  $\text{CH}_2=\text{CXY}$ , optical yield of ..... 35*t*  
 mechanism of ..... 176  
 mechanistic studies on ..... 172–175  
 by 7-member chelate ring biphosphines, catalytic ..... 185  
 of olefins by optically active transition metal catalysis ..... 36*f*  
 structural study of ..... 35–37  
 of  $\alpha, \beta$ -unsaturated carboxylic acids ..... 185  
 of cyclohexene ..... 173  
 of  $\alpha$ -ethylstyrene ..... 185  
 homogeneous ..... 171  
 of prochiral olefins ..... 169  
 Hydroxamate  
 CD spectra of iron(III) ..... 149  
 complexes ..... 142  
 model ..... 134–144  
 siderophore ..... 134, 144–149  
 with Fe(III), reaction of ..... 135*f*  
 Hyperpolarizability term ..... 85
- I**
- Imine  
 formation in coordinated chelates .. 123  
 linkage, amine- ..... 326, 331  
 formation, condensation reaction 325



|  |           |
|--|-----------|
| Imine ( <i>continued</i> )   |           |
| stereospecific addition of cyanide   |           |
| ion at a chelated .....  | 124       |
| Inducibility of achiral chromophore .....  | 84-85     |
| Inducing power .....   | 84-88     |
| Inherent dissymmetry .....   | 273       |
| Inorganic isomers .....  | 1         |
| Insulin .....  | 205       |
| International union of pure and applied chemistry (IUPAC) .....  | 399, 415  |
| polyhedral numbering system .....  | 399       |
| Intrinsic rotatory strength .....  | 22-23     |
| Inversion  |           |
| optical .....  | 3, 359    |
| paths for iron(II)-tris(diimine)-complex, proposed .....   | 365f      |
| reaction   |           |
| aqua .....   | 361       |
| stereochemistry .....  | 369t      |
| Co(III) Bailar .....   | 357       |
| tris(diimine)Fe(II)-cyanide .....  | 357-373   |
| Ion association effect on CD .....   | 225       |
| Ions, tris-bidentate complex .....   | 19        |
| Iron   |           |
| (benz) <sub>3</sub> isomers .....  | 144       |
| (bpy) <sub>3</sub> <sup>2+</sup> /CN <sup>-</sup> reactions .....  | 363t      |
| complexes .....  | 91        |
| (dipy) <sub>3</sub> <sup>2+</sup> .....  | 81        |
| (mphen) <sub>2</sub>   |           |
| (CN)(H <sub>2</sub> O) <sup>+</sup> isomers .....  | 370       |
| (CN)(H <sub>2</sub> O) <sup>+</sup> reaction, isomer percentages for $\Lambda$ -fac-Fe-(mphen) <sub>3</sub> <sup>2+</sup> to ..... | 369       |
| (CN) <sub>2</sub> products, isomer percentages for .....   | 368t      |
| (mphen) <sub>3</sub> <sup>2+</sup>   |           |
| CD spectra of .....  | 366       |
| CD spectrum of $\Lambda$ -fac-cyanide product, thin-layer chromatogram .....   | 367f      |
| with cyanide, reaction of .....  | 366, 368t |
| to Fe(mphen) <sub>2</sub> (CN)(H <sub>2</sub> O) <sup>+</sup> reaction, isomer percentages for $\Lambda$ -fac- .....               | 369t      |
| (phen) <sub>2</sub> (CN) <sub>2</sub> product, CD of .....   | 358f      |
| (phen) <sub>3</sub> <sup>2+</sup>  |           |
| absolute configuration of .....  | 360       |
| CD of $\Delta$ - .....   | 365f      |
| /CN <sup>-</sup> reactions .....   | 363t      |
| transport compounds, stereochemistry of microbial .....  | 133-165   |
| Iron(II)   |           |
| aerobactin, CD spectra of .....  | 149       |
| diantimony-ditartrate synthesis, $\Lambda$ -fac-tris(3-methyl-1,10-phenanthroline)- .....  | 364       |
| -tris(diimine)   |           |
| -cyanide inversion reaction .....  | 357-373   |
| Iron(II) ( <i>continued</i> )  |           |
| -tris(diimine) ( <i>continued</i> )  |           |
| complex, proposed inversion path for .....   | 365f      |
| complex, retention path for .....  | 365f      |
| perchlorate synthesis, $\Lambda$ -fac-tris(3-methyl-1,10-phenanthroline) .....   | 364       |
| Iron(III)  |           |
| absorption spectrum of tris(benzohydroxamato)- .....   | 145f      |
| absorption spectrum of tris(thio-benzohydroxamato)- .....  | 157f      |
| aerobactin .....   | 149       |
| CD spectrum of .....   | 152f      |
| tris(benzohydroxamato)- .....  | 142       |
| CD spectra of .....  | 145f      |
| CD spectra of tris(thiobenzohydroxamato)- .....  | 157f      |
| complexes .....  | 144       |
| d <sup>5</sup> .....   | 134       |
| enterobactin, absolute configuration of .....  | 161       |
| enterobactin, hydrolysis of the amide linkages of .....  | 154       |
| hydroxamate, CD spectra of .....   | 149       |
| hydroxamate complexes .....  | 142       |
| octahedral bonding geometries of <i>cis</i> -tris-(benzohydroxamato)- ..   | 138f      |
| thiohydroxamate complexes .....  | 142       |
| Isomer(s)  |           |
| CD spectra of <i>cis</i> - .....   | 136       |
| CD spectra of <i>trans</i> - .....   | 136       |
| [Co(en) <sub>3</sub> ] <sup>3+</sup> .....   | 142       |
| of coordination compounds, separation of .....   | 13        |
| Cr(benz) <sub>3</sub>  |           |
| 2,4-diaminopentane .....   | 19        |
| equilibrium geometries of the <i>lel</i> <sub>3</sub> .....  | 16        |
| <i>u</i> -facial .....   | 26        |
| formation on conformation of chelate ring, dependence of .....   | 7         |
| Fe(benz) <sub>3</sub> .....  | 144       |
| <i>fac</i> - <i>mer</i> .....  | 337       |
| inorganic .....  | 1         |
| <i>levo</i> - $\beta$ - .....  | 4         |
| <i>mer</i> - .....   | 26        |
| notation, permutational .....  | 415       |
| Pt(NH <sub>3</sub> ) <sub>2</sub> Cl <sub>2</sub> Br <sub>2</sub> .....  | 5         |
| separation, geometrical .....  | 366       |
| stabilities of [Co(en) <sub>3</sub> ] <sup>3+</sup> .....  | 15        |
| strain energies of the <i>lel</i> <sub>3</sub> .....   | 16        |
| structure of stable .....  | 122f      |
| Isomerism  |           |
| configurational .....  | 13        |
| conformational .....   | 13        |
| in a 6-member chelate ring   |           |
| biphosphine complex .....  | 184       |

- Isomerization of  $\text{Co}(\text{admh})_3$   
 fac- ..... 353  
 kinetic studies for fac-mer ..... 342  
 rate and equilibrium constants  
 for geometrical ..... 353*t*
- IUPAC (*see* International union of  
 pure and applied chemistry)
- J**
- Jahn-Teller  
 distortion(s) ..... 46, 51  
 effect (JT) ..... 45  
 pseudo (PJT) ..... 45  
 interactions on the CD spectra,  
 influence of pseudo ..... 46  
 interactions on the CD spectra,  
 influence of ..... 46
- JT (*see* Jahn-Teller effect)
- K**
- Ketones, structures and abbrevia-  
 tions of chiral ..... 327*t*
- Kirkwood-Kuhn contribution ..... 79
- L**
- LD (Linear dichroism) ..... 81  
 Lel (*see parallel*)  
 Leuteinizing hormone-releasing  
 hormone ..... 205
- Ligand(s)  
 arrangement, CD spectra of  
 cobalt(III) complexes with  
 optical activity due to uniden-  
 tate ..... 289-313  
 associated spectral changes, deter-  
 mination by ..... 195-197  
 asymmetric influence, trans- ..... 99-106  
 chelating ..... 9  
 CIP exploration ..... 402*f*-403*f*  
 CIP priority numbers for ..... 405*f*  
 diamino-diimine macrocycles  
 use as ..... 325  
 DI OXOP, enamide hydrogenation  
 by the asymmetric ..... 191  
 exploration ..... 405*f*  
 -field bands of ammine complexes .. 224  
 field effects ..... 46  
 importance of the cis ..... 92-99  
 indexing ..... 400-406  
 geometric isomers of octahedral  
 complexes with linear  
 quadridentate ..... 401*f*  
 model azo ..... 198*f*  
 open-chain quadridentate ..... 325  
 relative priority, CIP ..... 401  
 resolution of racemic potential ..... 8
- Ligands (*continued*)  
 solvation of nonchiral ..... 224-225  
 stereochemical label ..... 406-408  
 stereoselective solvation of  
 chiral ..... 221-223  
 using template reaction of metal  
 complexes, stereoselective  
 synthesis of quadridentate ..... 325-334  
 Linear coupling constants, equations .. 54  
 Linear dichroism (LD) ..... 81  
 Lithium antimony tartrate ..... 323*f*  
 Locant number conventions ..... 399
- M**
- Mbn (Methyl-2-butene) ..... 92  
 $[\text{M}(\text{catecholate})_3]^{3-}$  anions ..... 159*f*  
 MD (*see* Magnetic dipole)  
 Macrocycles use as ligands,  
 diamino-diimine ..... 325  
 Magnetic dipole transition(s)  
 allowed ..... 82-84  
 forbidden ..... 81-82  
 selection rules for ..... 49  
 moments equations ..... 60  
 Magnetic transition moment ..... 23, 76  
 Maleate, methyl ..... 118*f*  
 Maleate, orientations for amido ion  
 addition to chelated ..... 122*f*  
 Maleato dianion, monodentate ..... 120  
 Maleatoester complexes, pentaammine 119  
 Mapping of strain energy surfaces ..... 15  
 trans Maximum difference subrule for  
 coordination numbers four to six,  
 priming subrule a ..... 409  
 trans Maximum difference subrule for  
 coordination numbers four to six,  
 priming subrule b ..... 409  
 6-Membered chelate rings ..... 17-20  
 biphosphine complex, conforma-  
 tional isomerism in ..... 184  
 effect on separation factor ..... 321  
 enamide binding to ..... 180*f*  
 rhodium complexes, catalysis by .... 177  
 5-Membered chelate ring biphosphine  
 complexes ..... 13-17  
 chiral conformations in ..... 184  
 rhodium, binding by ..... 175-177  
 rhodium, catalysis by ..... 175-177  
 7-Membered chelate ring(s)  
 biphosphine(s)  
 catalytic asymmetric hydro-  
 genation by ..... 185  
 complex, chair and twist-boat  
 conformations in ..... 184  
 rhodium complexes, binding by ..... 177  
 rhodium complexes, catalysis by .... 177  
 6-Membered metal trimethylene ring,  
 conformations of ..... 17

American Chemical  
 Society Library

1155 16th St. N. W.

In Stereochemistry of Optically Active Transition Metal Compounds; Douglas, B., et al.;  
 ACS Symposium Series 200, American Chemical Society, Washington, DC, 1980.

Washington, D. C. 20036

|  |              |
|--|--------------|
| Mer ( <i>see</i> Isomers, Mer)   |              |
| Metal  |              |
| atom, effective charge on central  | 31 <i>t</i>  |
| catalysis, asymmetric hydrogenation of olefins by optically active transition  | 36 <i>f</i>  |
| catecholates, absolute configuration of transition   | 158          |
| complex(es)  |              |
| absolute configuration of transition   | 13–39        |
| CD of a chiral trigonal dihedral ( $D_3$ )   | 67           |
| intensities in vibronic transitions of chiral  | 43–71        |
| determination of absolute configurations of chiral   | 73           |
| six-coordinate trigonal dihedral ( $D_3$ )   | 47–49        |
| solvent effect on CD of  | 221–236      |
| sources of dissymmetry in optically active   | 273          |
| stereoselective synthesis of quadridentate ligands using template reaction of  | 325–334      |
| transition   |              |
| influence of vibronic interactions on CD spectra of ..   | 46           |
| octahedral   | 58           |
| photoacoustic detection of natural CD in crystalline   | 375–394      |
| quantum mechanical theory of optical activity in chiral  | 43–44        |
| rotational strength of optically active  | 255          |
| by x-ray scattering, determination of absolute configuration of a chiral   | 43           |
| coordination compounds, absolute configuration of ion(s)   | 43           |
| amine systems, divalent  | 123          |
| azophenol chelation of   | 195–197      |
| cages, chiral  | 128–130      |
| interaction with azoproteins, CD as probe of   | 195          |
| -olefin complexation, stereo-selection in  | 170–172      |
| -siderophore complex   | 133          |
| system, tris(diamine)  | 13           |
| trimethylenediamine ring, conformations of a six-membered ..   | 17           |
| Metal(II)-ethylenediamine complexes with acetone, condensation reaction of   | 328 <i>f</i> |
| Metal(II)-propylenediamine complexes with acetone, condensation reaction of  | 328 <i>f</i> |
| Methyl   |              |
| -2-butene (mbn)  | 92           |
| fumarate   | 118 <i>f</i> |
| maleate  | 118 <i>f</i> |
| Microbial iron transport compounds, stereochemistry of   | 133–165      |
| Model, dynamic coupling  | 26           |
| Moment(s)  |              |
| of CT states, electric   | 79           |
| data, dipole   | 346 <i>t</i> |
| definition of perturbation expansions  | 76           |
| effective dipole   | 77           |
| electric hexadecapole  | 23           |
| representations  | 76–77        |
| transition   | 76, 86       |
| electric   | 81           |
| dipole   | 82           |
| magnetic   | 76           |
| Monodentate maleato dianion  | 120          |
| Morgan algorithm   | 404          |
| <b>N</b>   |              |
| Nickel   |              |
| (en) $_3$ (NO $_3$ ) $_2$  |              |
| axial single-crystal   |              |
| absorption spectra of  | 388 <i>f</i> |
| CD spectra of  | 388 <i>f</i> |
| PACD measurements of   | 391 <i>t</i> |
| PAS measurements of  | 391 <i>t</i> |
| transmission measurements of ..  | 391 <i>t</i> |
| powder PACD measurements of ..   | 392 <i>t</i> |
| powder PAS measurements of   | 392 <i>t</i> |
| ( <i>o</i> -phenanthroline) $_3$ Cl $_2$ , Pfeiffer effect and racemization of   | 243 <i>t</i> |
| ( <i>o</i> -phenanthroline) $_3$ $2^+$ system, Pfeiffer rotation   | 242          |
| ( <i>S</i> -ampr) $_3$ $2^+$ with ketones, reactions of  | 326–329      |
| ( <i>S</i> -ampr) $_3$ (ClO $_4$ ) $_2$ with ketones, reactions of   | 332          |
| Nickel(II)-Cu(II)- <i>S</i> -aminomethylpyrrolidine complexes with several ketones, products distribution for reactions of | 332 <i>t</i> |
| Nitriles, amino  | 117          |
| Nitrogen(s)  |              |
| to CD spectra, contributions of asymmetric   | 268          |
| electronic effects on asymmetric   | 269          |
| $\pi^*$ transition   | 226–228      |
| NMR spectra  | 172          |
| Nomenclature of stereochemistry of carbon compounds  | 397          |
| Notation   |              |
| for asymmetric clusters, stereochemical  | 415          |
| CAS stereochemical   | 406–413      |

- Notation (*continued*)  
 for coordination systems, stereochemical description and ..... 397-417  
 examples, stereochemical ..... 412f-416f  
 permutational isomer ..... 415
- Nucleophile independent dissociation reactions ..... 359
- Numbering  
 CANON constitutional ..... 412f  
 conventions, locant ..... 399  
 for diamminebis(ethylenediamine) platinum, stereochemical ..... 402f-403f  
 for octahedral structures ..... 401f  
 for square planar structures ..... 401f  
 system, IUPAC polyhedral ..... 399
- O**
- Oblique (ob) ..... 14
- Octadiene, cyclo- ..... 181
- Octahedral  
 bonding geometries of *cis*-tris(benzohydroxamato)chromium (III) ..... 138f  
 complexes  
 with linear quadridentate ligands, geometric isomers of ..... 401f  
 preparation of ..... 5  
 substitution reactions of  $d^6$  ..... 357
- modes  
 $Q_3(t_{1u})$  ..... 48, 59  
 $Q_4(t_{1u})$  ..... 59  
 $Q_6(t_{1u})$  ..... 59
- structures, numbering for ..... 401f  
 symmetry ..... 78  
 of achiral chromophore ..... 89  
 transition metal complexes ..... 58
- Octene, *S,S*-*trans*-cyclo- ..... 92
- Olefin(s) (*continued*)  
 absolute configuration of  $\eta^2$ - ..... 91  
 absorption data of platinum(II) complexes containing  $\eta^2$  ..... 95t  
 absorption data of rhodium(I) complexes containing  $\eta^2$ - ..... 95t  
 complexation, stereoselection in metal- ..... 170-172  
 complexes of platinum(II), peaks in CD spectra of  $\eta^2$  ..... 98t  
 complexes, square planar rhodium-exchange  
 CD spectra of square planar complexes containing prochiral olefins stereoselective .. 91  
 induction of asymmetry on ..... 109  
 in platinum(II) complexes ..... 91  
 stereoselectivity on ..... 106  
 hydrogenation of prochiral ..... 169  
 -platinum complexes, stereoselection in ..... 171
- Olefin(s) (*continued*)  
*R,R*-configuration of prochiral ..... 93f  
*S,S*-configuration of prochiral ..... 93f  
 stereoselective olefin exchange, CD spectra of square planar complexes containing prochiral ..... 91  
 stereospecific hydration of ..... 117-123
- One-electron theory of molecular optical activity ..... 44
- Optical activity  
 in chiral transition metal complexes, quantum mechanical theory of ..... 43-44  
 due to unidentate ligand arrangement, CD spectra of cobalt(II) complexes with .. 289-313  
 measurement of natural ..... 375  
 one-electron theory of molecular ..... 44  
 in single crystals by transmission techniques, measurement of ... 375  
 sources of *d*-electron ..... 305-311
- inversion ..... 3, 359  
 pH dependence of ..... 3
- isomers  
 of tris(catecholato)chromate(III) ..... 158  
 of tris(catecholato)rhodate(III) ..... 158  
 of a tris(chelate) ..... 135f  
 partial resolution of ..... 341
- resolution(s)  
 of cobalt complexes with *cis*-*cis* unidentate distribution .. 289-292  
 of  $[\text{Co}(\text{en})_3]^{3+}$  complex, mechanism of ..... 319  
 of facial and meridional tris(aminoacidato)cobalt(III) chelates by *d*-tartrate resolving agents ..... 315-324
- rotation, specific optical rotation and molar optical rotation, observed ..... 329  
 rotatory dispersion (ORD) ..... 240  
 of  $(+)_B\text{-}[\text{Cr}(\text{C}_2\text{O}_4)_3]^{3-}$  for partially resolved  $\Lambda\text{-}(-)_{546}\text{-Co}(\text{admh})_2(\text{acac})_2$ , absorption spectrum ..... 351f  
 for partially resolved  $\Lambda\text{-}(-)_{546}\text{-fac-Co}(\text{admh})_3$ , absorption spectrum ..... 352f  
 rotatory strength ..... 26
- Optically active  
 amino acid complex ions ..... 255  
 complexes of transition metals, rotational strength of ..... 255  
 transition metal complexes, chiroptical properties of ..... 43



- Photoacoustic (*continued*)  
 spectroscopy (*continued*)  
 experiment, diagram of ..... 385f  
 measurements  
 of  $\text{NaUO}_2(\text{OAC})_3$ , single-crystal ..... 391t  
 of  $\text{Ni}(\text{en})_3(\text{NO}_3)_2$ , axial single-crystal ..... 391t  
 powder  
 of 5%  $\text{Co}(\text{en})_3\text{Cl}_3$  in  $\text{Rh}(\text{en})_3\text{Cl}_3$  ..... 393t  
 of  $\text{NaUO}_2(\text{OAC})_3$  ..... 392t  
 of  $\text{Ni}(\text{en})_3(\text{NO}_3)_2$  ..... 392t  
 signals, strength of in powders ..... 386  
 theory ..... 379-381  
 transmission spectroscopy, difference between ..... 378
- Piperidine  
 products distribution for reactions  
 of  $\text{Cu}(\text{II})$ -3(S)-3-amino ..... 332t  
 and 3(S)-aminohexahydroazepine, geometrical isomers of  $\text{Cu}(\text{II})$  complexes of 3(S)-3-aminomethyl- ..... 330f  
 and 3(S)-3-aminohexahydroazepine, reactions of  $\text{Cu}(\text{II})$  complexes of 3(S)-3-amino- ..... 329-333
- Platinum  
 $\text{Cl}(\text{acac})(\text{C}_2\text{H}_4)$  ..... 106  
 $\text{Cl}(\text{L-am})(\text{ethylene})$ , *trans*(*N, //*)- ..... 99-109  
 $\text{Cl}(\text{L-am})(\text{ethylene})$ , CD spectra of *trans*(*N, //*)- ..... 103f  
 $\text{Cl}(\text{L-am})(\text{ethylene})$ ] type, difference in CD between two complexes of *trans*(*N, //*)- ..... 105f  
 $\text{Cl}(\text{L-am})(\text{ethylene})$ , UV absorption ..... 103f  
 $\text{Cl}(\text{L-am})(\text{olefin})$ , kinetic thermodynamic optical yields of *trans*(*N, //*)- ..... 111t  
 $\text{Cl}(\text{L-pro})(\text{ethylene})$  *cis*(*N, //*)- ..... 106  
 $\text{Cl}(\text{L-proethylene})$ , CD spectra of *cis*(*N, //*)- ..... 108f  
 $\text{Cl}(\text{L-proethylene})$ , UV absorption of *cis*(*N, //*)- ..... 108f  
 $\text{Cl}(\text{L-pro-trans-2-butene})$ , CD spectra of ..... 94f  
 $\text{Cl}(\text{L-pro-trans-2-butene})$ , UV absorption spectra of ..... 94f  
 $\text{Cl}(\text{L-prolinate})$ -(*S, S-trans-2-butene*), CD spectra of *cis*(*N, //*)- ..... 97f  
 $\text{Cl}(\text{L-prolinate})$ -(*S, S-trans-2-butene*), CD spectra of *trans*(*N, //*)- ..... 97f  
 $\text{Cl}(\text{L-prolinate})(\text{S, S-trans-2-butene}(3H1))$ , second-order rate constants in *trans*(*N, //*)- ..... 106t  
 $\text{Cl}(\text{L-prolinate})(\text{S, S-tbn})$  ..... 92  
 $\text{Cl}(\text{L-pro})(\text{S, S-tbn})$ , *trans*(*N, //*)- ..... 107  
 $\text{Cl}(\text{N-alkyl-L-pro})(\text{ethylene})$ , *trans*(*N, //*)- ..... 104  
 $\text{Cl}(\text{N-bz-L-val})(\text{ethylene})$ , *trans*(*N, //*)- ..... 104  
 $\text{Cl}(\text{N-me-L-pro})(\text{ethylene})$ , change in CD spectrum of ..... 110f  
 $\text{Cl}(\text{o-phenyl-enediamine})(\text{S-mbn})$  ..... 92  
 $\text{Cl}_3(\text{S, S-trans-2-butene}_3\text{H})$ , second-order rate constants for the substitution of *trans-2-butene* ..... 107t  
 $\text{Cl}_3(\text{S, S-trans-cyclooctene})$ - ..... 107  
 $\text{Cl}_2(\text{S-mbn})(\text{4-substituted-pyridine})$ , *trans*- ..... 99  
 $\text{Cl}_3(\text{S, S-tbn})$ - ..... 107  
 transition states on the nucleophilic attack of tbn upon ..... 108f  
 $(\text{NH}_3)_2\text{Cl}_2$ , *cis-trans*- ..... 2  
 $(\text{NH}_3)_2\text{Cl}_2\text{Br}_2$  isomers ..... 5  
 complexes, stereoselection in olefin- ..... 171  
 stereochemical numbering for diamminebis(ethylenediamine) ..... 402f-403f
- Platinum(II) complexes ..... 91  
 CD pattern of ..... 92  
 CD spectra of ..... 100f, 101f, 102f  
 containing  
 coe  
 CD spectra of ..... 95f  
 CD spectra binuclear  
 UV absorption binuclear ..... 96f  
 $\eta^2$ -olefins, absorption data of ..... 95t  
 tbn, CD spectra of ..... 95f  
 olefin exchanges in ..... 91  
 peaks in CD spectra of  $\eta^2$ -olefin ..... 98t  
 square planar ..... 170  
 UV absorption ..... 100f
- Platinum(II), *trans*-dichlorodiamine- ..... 10  
 Platinum(IV), attachment of a tridentate amine to ..... 9  
 Polyhedral numbering system, IUPAC ..... 399  
 Priming subrule a, *trans* maximum difference subrule for coordination numbers four to six ..... 409  
 Priming subrule b, *trans* maximum difference subrule for coordination numbers four to six ..... 409  
 Prochiral olefins, hydrogenation of ..... 169  
 Prochiral olefins stereoselective olefin exchange, circular dichroism spectra of square planar complexes containing ..... 91  
 Product configuration, temperature dependence of ..... 3  
 Prolinate ..... 99  
 N-benzyl-L- ..... 104

|   |      |  |         |
|---|------|--|---------|
| Proline                                 |      | Rate constants ( <i>continued</i> )              |         |
| complex, CD of B <sub>2</sub> -S-       | 285f | in <i>trans</i> (N, //)-[PtCl(L-prolinate)-      |         |
| S-                                      | 286  | (S,S- <i>trans</i> -2-butene) <sub>3</sub> H1],  |         |
| vicinal effect for β <sub>2</sub> -S-   | 284f | second-order                                     | 106t    |
| Prolinato, L-hydroxyprolinate,          |      | for the substitution of <i>trans</i> -2-         |         |
| <i>N</i> -methyl-L-hydroxy-             | 104  | butene [PtCl <sub>2</sub> (S,S- <i>trans</i> -2- |         |
| Prolinato, <i>N</i> -methyl-L-          | 104  | butene) <sub>3</sub> H1], second-order           | 107t    |
| hydroxyprolinate L-hydroxy-             | 104  | Rhodate(III), optical isomers of                 |         |
| Propane, 1,2-diamino-                   | 115  | tris(catecholato)-                               | 158     |
| Propionic acid, rotamers of 2-sub-      |      | [Rhodium(ent) <sub>3</sub> ], absorption spec-   |         |
| stituted                                | 229f | trum K <sub>3</sub> -                            | 162f    |
| Proton chemical shift data              | 345t | [Rhodium(ent) <sub>3</sub> ], CD spectrum of     |         |
| PSD (phase-sensitive detection)         | 379  | Δ- <i>cis</i> -K <sub>3</sub> -                  | 162f    |
| Pseudo Jahn-Teller couplings, linear    |      | [Rhodium(enterobactin)] <sup>3-</sup> , CD       |         |
| (A <sub>2</sub> + E)*e                  | 56   | spectra of                                       | 161     |
| Pseudo Jahn-Teller distortions          | 51   | Rhodium  |         |
| Puckering motion                        | 16   | biphosphine complexes                            | 188f    |
| Pyridines, 4-substituted                | 92   | binding by 5-membered chelate                    |         |
| Pyrrolidine complexes                   |      | ring   | 175-177 |
| with ketones, reaction products of      |      | binding by 7-membered chelate                    |         |
| S-aminomethyl                           | 328f | ring   | 177     |
| with several ketones, products dis-     |      | catalysis by 5-membered chelate                  |         |
| tribution for reaction of               |      | ring   | 175-177 |
| Cu(II)-S-aminomethyl-                   | 332t | catalysis by 7-membered chelate                  |         |
| with several ketones, products dis-     |      | ring   | 177     |
| tribution for reactions of              |      | coordination of unsaturated                      |         |
| Ni(II)-S-aminomethyl-                   | 332t | carboxylic acids in                              | 187     |
| Pyrrolidine, possible conformations     |      | with larger-ring chelates of chiral              | 187     |
| of coordinated S-aminomethyl            | 330f | (catecholate) <sub>3</sub> , absorption spectra  |         |
| Pyruvato imine <i>bis</i> (ethylene-di- |      | of Δ-K <sub>3</sub> -                            | 160f    |
| amine)cobalt(III) ion                   | 124  | (catecholate) <sub>3</sub> , CD spectra of Δ-    | 160f    |
|   |      | complexes  | 185     |
|   |      | binding of enamides by 6-mem-                    |         |
|   |      | bered chelate ring                               | 177     |
|   |      | catalysis by 6-membered chelate                  |         |
|   |      | ring   | 177     |
|   |      | enamide  | 174f    |
|   |      | -olefin, square planar                           | 187     |
|   |      | phosphine  | 172     |
|   |      | unsaturated carboxylic acid                      |         |
|   |      | binding to                                       | 191     |
|   |      | Rhodium(I) complexes                             | 169     |
|   |      | absorption spectra of                            | 93f     |
|   |      | CD pattern of                                    | 92      |
|   |      | containing                                       |         |
|   |      | coe  |         |
|   |      | CD spectra of                                    | 95f     |
|   |      | CD spectra binuclear of                          | 96f     |
|   |      | UV absorption binuclear                          | 96f     |
|   |      | γ <sup>2</sup> -olefins, absorption data of      | 95t     |
|   |      | tbn, CD spectra of                               | 95f     |
|   |      | Rhodotorulic acid (RA)                           | 149     |
|   |      | absorption spectra of ferric                     |         |
|   |      | complex of                                       | 151f    |
|   |      | CD spectra of ferric complex of                  | 151f    |
|   |      | chromium(III)                                    | 149     |
|   |      | structure of                                     | 151f    |
|   |      | Regio-aldehyde condensation struc-               |         |
|   |      | tures  | 127     |
|   |      | Resolution(s)                                    |         |

- Resolution(s) (*continued*)  
of Co(admh)<sub>n</sub>(acac)<sub>3-n</sub> complexes, partial ..... 350  
of fac-[Co(β-ala)<sub>3</sub>] ..... 315-316  
of fac-[Co(β-ala)<sub>3</sub>], chromatographic ..... 323f  
of mer-[Co(β-ala)<sub>3</sub>] ..... 324  
of mer-[Co(β-ala)<sub>3</sub>], chromatographic ..... 323f  
of Co complexes with cis-cis unidentate distribution, optical ..... 289-292  
of the dichloro complex ..... 3  
of facial and meridional tris(aminoacidato)-cobalt(III) chelates by *d*-tartrate resolving agents, optical ..... 315-324  
of optical isomers, partial ..... 341  
Resolving agents, optical resolution of facial and meridional tris(aminoacidato) cobalt(III) chelates by *d*-tartrate ..... 315-324  
Retention path for iron(II)-tris(dimine) complex, proposed ..... 365f  
Rotamers (*see also* Conformers) ..... 226  
of 2-substituted propionic acid ..... 229f  
Rotation, equations, Pfeiffer ..... 239  
Rotation D,L-[Ni(*o*-phen)<sub>3</sub>]<sup>2+</sup> system, Pfeiffer ..... 242  
Rotational strength ..... 226, 228  
decrease in ..... 301  
effect of *C*-alkyl substitution on ..... 269  
effect on *N*-substitution on ..... 269  
of optically active complexes of transition metals ..... 255  
of pentaammine {(*S*)-2-chloropropionato}cobalt(III) ..... 233f  
Rotatory dispersion  
of D,L-[Cr(C<sub>2</sub>O<sub>4</sub>)<sub>3</sub>]<sup>3-</sup>, Pfeiffer ..... 241f  
of (+)<sub>D</sub>-[Cr(C<sub>2</sub>O<sub>4</sub>)<sub>3</sub>]<sup>3-</sup>, optical ..... 241f  
optical (ORD) ..... 240  
Pfeiffer ..... 242  
Rotatory strength(s) ..... 359-360  
definition, vibronic ..... 44  
of tris(diamine)cobalt(II) complexes ..... 24f  
electronic ..... 44-45  
equations ..... 44-45, 55, 57, 60  
vibronic ..... 61-64  
optical ..... 26  
vibronic ..... 45, 47
- S**
- Sarcosinate ion chelates ..... 115-116  
of Co(admh)<sub>n</sub>(acac)<sub>3-n</sub> complexes ..... 344  
and CD spectra, correlation of stereochemistry ..... 268-269  
Second-order perturbation theory ..... 83  
Selectivity on olefin exchange, stereo- 106  
Siderophore(s)  
absorption spectra for ferric ..... 134  
CD spectra for ferric ..... 134  
complex(es)  
catecholate ..... 154-158  
hydroxamate ..... 134, 144-149  
metal-  
thiohydroxamate ..... 149-154  
properties ..... 133  
Sigma-complex(III) ..... 34  
Sigma(σ)<sub>1</sub> → d<sub>z<sup>2</sup></sub> charge transfer transitions ..... 228-232  
Site symmetry designator ..... 415  
Site symmetry term ..... 406-408, 410t  
Six-coordinate trigonal dihedral (D<sub>3</sub>) metal complexes ..... 47-49  
Sodium *d*-tartrate ..... 316  
Sodium UO<sub>2</sub>(OAC)<sub>3</sub>  
powder PACD measurements of ..... 392t  
powder PAS measurements of ..... 392t  
single-crystal  
absorption spectra of ..... 397f  
CD spectra of ..... 387f  
measurements of  
PACD ..... 390t  
PAS ..... 390t  
transmission ..... 390t  
Solvation  
of chiral ligand, stereoselective ..... 221-223  
at NH<sub>2</sub> groups of diamine or amino alcohol complex, degree of stereoselective ..... 222  
of nonchiral ligand ..... 224-225  
Solvent  
dependence of CD of complexes of chiral diamines ..... 222  
-dependent CD of pentaamminecobalt(III) complexes of chiral carboxylates ..... 226-236  
effect  
on absorption spectrum of pentaammine {(*S*)-2-chloropropionato}cobalt(III) tetraphenylborate ..... 230f  
on CD of metal complexes ..... 221-236  
on CD spectrum of pentaammine{(*S*)-2-chloropropionato}-cobalt(III) ..... 231f  
on CD spectrum of (*S*)-alanine-pentaamminecobalt(III) ..... 233f  
Spectra of tris(diamine)cobalt(III) complexes, CD ..... 22  
Square planar complexes  
containing prochiral olefins stereoselective olefin exchange, circular dichroism spectra of ..... 91  
platinum(II) ..... 170  
projection of ..... 105f  
rhodium-olefin ..... 187  
Square planar structures numbering ..... 401f





- Temperature dependence of product configuration ..... 3
- Temperature effect on CD spectrum of pentaammine ((S)-2-chloropropionato)-cobalt(III) tetraphenylborate ..... 234f
- Terdentate, complexes with a cyclic ..... 27-31
- Thermal piston model, one-dimensional ..... 377
- Thiohydroxamates with Fe(III), reaction of ..... 135f
- Thiohydroxamate siderophore complexes ..... 149-154
- Transition(s)
- d-d* ..... 228
- $^1A_{1g} \rightarrow ^1E_g$  ..... 228
- additivity of CD of *d-d* transitions ..... 273-286
- CD of the *d-d* ..... 81
- charge transfer ..... 228, 232
- $\pi-\pi^*$  of the tris and bis chelates ..... 359-360
- dipole moment ..... 23
- energy ..... 76
- magnetic dipole allowed ..... 82-84
- magnetic dipole forbidden ..... 81-82
- metal(s)
- catalysis, asymmetric hydrogenation of olefins by optically active ..... 36f
- catecholates, absolute configuration of ..... 158
- complexes
- absolute configuration of ..... 13-39
- chiroptical properties of optically active ..... 43
- influence of vibronic interactions on CD spectra of ..... 46
- photoacoustic detection of natural CD crystalline ..... 375-394
- quantum mechanical theory of optical activity in chiral ..... 43-44
- rotational strength of optically active complexes of ..... 255
- moment(s) ..... 76, 86
- electric ..... 81
- magnetic ..... 23, 76
- $n \rightarrow \pi^*$  ..... 226-228
- sigma ( $\sigma$ )<sub>L</sub>  $\rightarrow$   $d_z^2$  charge transfer ..... 228-232
- states on the nucleophilic attack of tbn upon [PtCl<sub>3</sub>(S,S-tbn)] ..... 108f
- Transmission
- measurements
- of 5% Co(en)<sub>3</sub>Cl<sub>3</sub> in Rh(en)<sub>3</sub>Cl<sub>3</sub> solution ..... 393t
- of NaUO<sub>2</sub>(OAc)<sub>3</sub>, single crystal ..... 390t
- of Ni(en)<sub>3</sub>(NO<sub>3</sub>)<sub>2</sub>, axial single-crystal ..... 391t
- Transmission (*continued*)
- spectroscopy, difference between Pas and ..... 378
- techniques, measurement of optical activity in single crystals by ..... 375
- 1,4,7-Triazacyclononane complexes, CD spectra of cobalt- ..... 303-313
- 1,4,7-Triazacyclononane complexes, synthesis of cobalt- ..... 303-313
- Tridentate amine to platinum(IV), attachment of ..... 9
- Trigonal
- dihedral
- Co(II) ..... 57
- (D<sub>3</sub>) metal complex, CD of a chiral ..... 67
- (D<sub>3</sub>) metal complexes, six-coordinate ..... 47-49
- symmetry, cobalt(III) complexes of ..... 64
- e-type modes ..... 58
- modes, Q<sub>3a</sub>(a<sub>2</sub>) ..... 48
- modes, Q<sub>3e</sub>(e) ..... 48
- Trigonally distorted systems coupling (A<sub>2</sub> + E)\* (a<sub>1</sub> + 2e) ..... 56
- Trimethylenediamine ring, conformations of a six-membered metal ..... 17
- Tyrosine(s) ..... 195, 197
- U**
- tris Unidentate octahedral complexes, stereochemical terms for .. 398f
- V**
- Valeric acid, CD spectrum of (S)-2-chloro- ..... 227
- Valinate, N-benzyl-L- ..... 104
- Valine ..... 116
- Vanadium (III) (tris  $\beta$ -ketoaminates) ..... 337
- Vibrational
- amplitude functions ..... 52, 54
- integral equations ..... 62
- modes ..... 47
- Q<sub>2</sub> ..... 52
- Q<sub>5e</sub> ..... 52
- Q<sub>3</sub>(t<sub>1u</sub>) ..... 51
- Q<sub>4</sub>(t<sub>1u</sub>) ..... 51
- Q<sub>6</sub>(t<sub>2u</sub>) ..... 51
- ungerade ..... 58
- wave functions ..... 55
- Vibronic
- coupling ..... 45-46
- on CD spectral features, influence of ..... 68
- effects ..... 58
- energy levels ..... 52
- Hamiltonian equation ..... 48, 51-52

|  |        |   |         |
|--|--------|---|---------|
| Vibronic ( <i>continued</i> )            |        | Vicinal ( <i>continued</i> )            |         |
| interactions .....                       | 59     | effects ( <i>continued</i> )            |         |
| on CD spectra of transition metal        |        | definition .....                        | 255     |
| complexes, influence of .....            | 46     | in a homologous series triethyl-        |         |
| energies .....                           | 46     | enetetraaminocobalt(III)-               |         |
| Herzberg-Teller (perturbative)           |        | amino acid complexes .....              | 273-286 |
| formalism for .....                      | 46     | of optically active ligands .....       | 268     |
| on <i>d-d</i> rotatory strengths, influ- |        | for $\beta_2$ -S-proline .....          | 284f    |
| ence of .....                            | 47     |   |         |
| levels .....                             | 55     | <b>W</b>                                |         |
| rotatory strength(s) .....               | 45, 57 | Wave functions .....                    | 76      |
| definition .....                         | 44     | electronic .....                        | 55      |
| equations .....                          | 61-64  | equations, perturbed .....              | 59      |
| theory, Herzberg-Teller (HT) .....       | 58     | vibrational .....                       | 55-56   |
| transitions of chiral metal com-         |        | vibronic .....                          | 45      |
| plexes, CD intensities in .....          | 43-71  | ( $A_2 + E$ )*e coupled excited         |         |
| wave function(s) .....                   | 45     | states .....                            | 67      |
| ( $A_2 + E$ )*e coupled excited          |        | equations .....                         | 49      |
| states .....                             | 67     | for $T_{1g}^*(t_{2g} + e_g)$ .....      | 52      |
| equations .....                          | 49     | Werner .....                            | 397     |
| for $T_{1g}^*(t_{2g} + e_g)$ .....       | 52     |   |         |
| coupled system .....                     | 55     | <b>X</b>                                |         |
| Vicinal                                  |        | X-ray diffraction powder patterns ..... | 32      |
| contributions, additivity rule of .....  | 301    |   |         |
| dissymmetry .....                        | 273    | <b>Z</b>                                |         |
| effect(s) .....                          | 273    | Zero-order electronic Hamiltonian       |         |
| algebra in calculation of .....          | 277f   | equation .....                          | 48      |
| of amino acid .....                      | 274    |   |         |
| average .....                            | 277f   |   |         |
| for $\beta_1$ bound alanine .....        | 284f   |   |         |